VNIVERSITAT DE VALÈNCIA

Desintegraciones hadrónicas y radiativas del leptón tau: $\tau^- \to (PPP)^-\nu_\tau$, $\tau^- \to P^-\gamma\nu_\tau$

Pablo Roig Garcés

IFIC, Departament de Física Teòrica

Tesis doctoral

Director: Jorge Portolés Ibáñez

València, a 15 de Noviembre de 2010

JORGE PORTOLÉS IBÁÑEZ, Científico Titular del Instituto de Física Corpuscular de València,

CERTIFICA

Que la presente memoria "Desintegraciones hadrónicas y radiativas del leptón tau" ha sido realizada bajo su dirección en el Departament de Física Teòrica de la Universitat de València, por PABLO ROIG GARCÉS y constituye su Tesis para optar al grado de Doctor en Física.

Y para que así conste, en cumplimiento de la legislación vigente, presenta en el Departament de Física Teòrica de la Universitat de València la referida Tesis Doctoral, y firma el presente certificado.

València, a 4 d'Octubre de 2010.

Jorge Portolés Ibáñez

A mi madre, por todo y por siempre;
y a Maru, por aguantarme durante
la redacción de esta Tesis.

Índice general

Capítulo 1

Introducción

1.1. Introducción general al problema

Esta Tesis Doctoral estudia las desintegraciones del leptón τ que incluyen algún mesón entre las partículas finales, llamadas por ello desintegraciones hadrónicas o semileptónicas. Al contrario de lo que sucede con el resto de leptones (electrón, e^- y muón, μ^-) su masa ($M_\tau \sim 1{,}8$ GeV) es suficientemente elevada como para permitir este tipo de desintegraciones incluyendo mesones ligeros (piones -π-, kaones -K- y etas -η, η'-). Estos procesos incluyen además el correspondiente neutrino del tau, ν_τ, y pueden incluir (en los llamados procesos radiativos) múltiples fotones, γ. Si bien es cinemáticamente posible producir otros mesones ligeros cuyas masas sean menores que la del tau, el tiempo de vida característico de estas partículas (resonancias) es excesivamente corto como para que sean detectadas. No obstante, como veremos, el efecto de su intercambio es importante para entender estas desintegraciones. Aunque $M_\tau \sim 2M_p$, donde M_p es la masa del protón, debido a que es algo inferior en realidad ($M_\tau = 1,777$ GeV y $2M_p = 1,876$ GeV) y a la conservación del número bariónico (que exigiría producirlos en pares barión-antibarión, siendo el más ligero protón-antiprotón) las desintegraciones del τ a bariones están prohibidas.

Las desintegraciones puramente leptónicas del τ son procesos debidos a la interacción electrodébil, que a día de hoy quedan adecuadamente descritos en el marco del Modelo Estándar de Física de Partículas (SM) [1]. En las desintegraciones hadrónicas del tau interviene, adicionalmente, la interacción fuerte. Aunque es bien conocido que la Cromodinámica Cuántica (Quantum Chromodynamics, QCD) es la teoría [2] que la describe, no somos capaces todavía de resolver el problema que nos ocupa utilizando el Lagrangiano de QCD únicamente, como explicaremos.

Las dos dificultades señaladas anteriormente -que las resonancias no sean estados asintóticos en el sentido de que sea posible su detección y que no seamos capaces de resolver QCD para hallar una solución al problema- nos dan la clave del interés de las desintegraciones semileptónicas del tau: proporcionan por un lado un entorno limpio en el que estudiar la interacción fuerte a energías bajas e intermedias, ya que la mitad electrodébil del proceso es limpia y está bajo control desde el punto de vista teórico; por otra parte, dado el intervalo de energías del sistema hadrónico

que cubren estas desintegraciones (esencialmente desde el umbral de producción de $\pi \sim 0{,}14$ GeV hasta M_τ), las resonancias más ligeras se pueden intercambiar en capa másica (*on-shell*), de modo que sus efectos son notables y se puede así proceder al estudio de sus propiedades.

La interacción nuclear fuerte fue descubierta en el experimento clásico de Rutherford, que probó la existencia del núcleo atómico: era una fuerza de gran intensidad y muy corto alcance. Pronto dicha fuerza comenzó a estudiarse en procesos de dispersión entre hadrones -las partículas que experimentan la interacción fuerte- (que se creían elementales) en lugar de núcleos atómicos. El gran número de hadrones descubierto en los años 50 y 60 con el advenimiento de los primeros aceleradores de partículas sugería que dichas partículas no fuesen fundamentales, a imagen de lo sucedido con los elementos químicos, al fin constituidos por protones y neutrones en sus núcleos. Para completar la analogía, la sistematización de las propiedades de los hadrones (en este contexto íntimamente ligadas a sus números cuánticos y en concreto a las simetrías aproximadas de sabor) ayudó a entender su subestructura y Gell-Mann comprendió que los hadrones debían estar constituidos por los llamados quarks, con un número cuántico adicional -de color- que resolvía los problemas de adecuación del espín de las partículas observadas a la estadística cuántica que obedecían.

Ahora bien, mientras que es posible desligar protones o neutrones de un núcleo -bien sea a través de radiactividad natural o artificialmente- no se ha conseguido hasta la fecha extraer quark constituyente alguno del hadrón en que se halle. Esta propiedad se conoce como confinamiento y, aunque existen razones teóricas que apuntan a dicho fenómeno no existe una explicación del mismo. Este hecho impone una dificultad a la hora de entender los procesos mediados por interacción fuerte: mientras que se produce entre quarks y gluones (los bosones intermediarios de la QCD, que también tienen autointeracciones), nuestros detectores registran únicamente hadrones, pues los quarks, antiquarks y gluones producidos forman inmediatamente objetos con carga de color total nula: hadronizan. Al contrario del resto de fuerzas conocidas (electromagnética, débil y gravitatoria), en la QCD la fuerza no disminuye con la distancia sino que aumenta -aunque sea muy corto su alcance-.

Aunque después se abundará en esta cuestión, baste decir por el momento que aunque QCD es la teoría de la interacción fuerte, no sabemos cómo manejarla en su régimen no perturbativo y, por ello, a efectos computacionales, su Lagrangiano sólo permite abordar analíticamente procesos inclusivos y a energías elevadas ($E > 2$ GeV típicamente) donde un tratamiento en términos de quarks, antiquarks y gluones tiene sentido. A las energías menores en que sucede nuestro problema deberemos buscar un camino alternativo. Como sucede siempre en Física, una elección adecuada de los grados de libertad simplifica (o incluso permite) la resolución. En nuestro estudio exclusivo de determinados canales de desintegración del tau es evidente que serán los mesones y resonancias más ligeras los grados de libertad adecuados para abordar el problema. El método más conveniente y riguroso de hacerlo es el uso de las Teorías de Campo Efectivas ($EFTs$), que preservan las simetrías de la teoría

fundamental y están escritas en términos de los grados de libertad relevantes en una región de energías dada. Como las desintegraciones del τ suceden alrededor de una escala típica de energías densamente poblada por resonancias, no será suficiente emplear Teoría de Perturbaciones Quiral (χPT) [3, 4, 5] que incluye sólo los mesones pseudoescalares más ligeros (π, K, η), sino que será necesario, además, incorporar a las resonancias como grados de libertad activos para extender a energías superiores la teoría: la Teoría Quiral de Resonancias ($R\chi T$) [6, 7] es una herramienta que permite este desarrollo.

En lo que resta de Introducción elaboraremos con mayor detalle sobre aspectos relevantes de la física de taus no abordados en capítulos posteriores y sobre QCD y nuestras limitaciones a la hora de implementar sus soluciones en física hadrónica a energías bajas e intermedias. Después avanzaremos algunas de las ideas capitales subyacentes a nuestro marco teórico en referencia a las teorias efectivas, la teoría quiral de perturbaciones, el límite de gran número de colores de QCD y la propia teoría quiral de resonancias. Finalizaremos con una enumeración de los distintos capítulos de la Tesis.

1.2. La Física del τ

Comenzamos con una introducción somera a la física del tau que permitirá contextualizar adecuadamente este trabajo: El leptón τ es un miembro de la tercera generación que se desintegra a partículas que incluyen los sabores ligeros pertenecientes a las dos primeras, junto al ν_τ. Por ello, la física de taus podría darnos pistas que permitieran entender por qué existe una serie de (al menos tres) copias de leptones y quarks que sólo se diferencian por su masa [8] (Tabla 1.1):

Parece lógico que sean los fermiones más pesados los más sensibles a la generación de masa fermiónica. Al ser el quark top demasiado pesado como para hadronizar antes de desintegrarse, la física de quarks b y leptones τ es prometedora en este sentido. Aunque el valor de M_τ no permite desintegraciones a mesones encantados (con quark c), es el τ el único leptón suficientemente pesado como para desintegrarse en hadrones y así, relacionar de algún modo los sectores de quarks (ligeros) y leptones.

El grupo liderado por M. L. Perl [10] descubrió el τ en 1975, lo que constituyó el primer indicio experimental a favor de la existencia de la tercera generación de partículas y, consiguientemente, también la primera indicación de que era inteligible dentro del SM la violación de CP [11] ya observada [12] en el sistema de kaones neutros, a través de la matriz de mezcla de Cabibbo, Kobayashi y Maskawa [11, 13]. De todos modos, esta explicación no es suficiente como para entender la enorme preponderancia observada en nuestro Universo de materia sobre antimateria [9, 14, 15], lo que representa una de las claras indicaciones de la existencia de algún tipo de

Generación	quarks	m_q	leptones	m_l
1	d	3,5 $\leftrightarrow$ 6,0 MeV	e^-	$\sim$ 0,5110 MeV
	u	1,5 $\leftrightarrow$ 3,3 MeV	ν_e	$<$ 2 eV
2	s	70 $\leftrightarrow$ 130 MeV	μ^-	$\sim$ 105,7 MeV
	c	1,16 $\leftrightarrow$ 1,34 GeV	ν_μ	$<$ 0,19 MeV
3	b	4,13 $\leftrightarrow$ 4,37 GeV	τ^-	$\sim$ 1,777 GeV
	t	169 $\leftrightarrow$ 175 GeV	ν_τ	$<$ 18,2 MeV

Cuadro 1.1: Contenido de materia del SM. Las masas de quarks corresponden al esquema $\overline{MS}$ con la escala de renormalización $\mu = m_q$ para los quarks pesados (c, b) y $\mu = 2$ GeV para los ligeros. Para estos últimos el valor de m_q dado es una estimación de la masa corriente (*current quark mass*). En el caso del quark t se emplea un promedio de las medidas en Tevatron pero no el reciente ajuste global del $TEVEWWG$, véase [8]. Las masas de los neutrinos son las masas "efectivas": $m^{2\,eff}_{\nu_k} = \sum_i |U_{ki}|^2 m^2_{\nu_i}$. Sin embargo, a partir de datos cosmológicos es posible determinar [9] $\sum_k (m_{\nu_k}) < 0{,}67$ eV.

nueva física más allá del SM [1]. Los números cuánticos del τ quedaron establecidos [20] de modo casi simultáneo al descubrimiento de la siguiente partícula de su generación, el quark b [21]. La partícula más pesada conocida hasta la fecha, el quark top, no fue detectado hasta 1995 [22, 23].

Resumiré a continuación brevemente la Física que podemos aprender de las desintegraciones del τ [24, 25, 26, 27, 28, 29].

En primer lugar, estas desintegraciones permiten verificar la universalidad de las corrientes electrodébiles, tanto cargadas como neutras. Dentro del SM, las desintegraciones leptónicas más sencillas del τ vienen descritas por la correspondiente anchura parcial, cuya expresión es [30, 31, 32]:

$$\Gamma(\tau^- \rightarrow \nu_\tau\, l^-\, \overline{\nu}_l) \;=\; \frac{G_F^2\, M_\tau^5}{192\,\pi^3}\, f\left(\frac{m_l^2}{M_\tau^2}\right)\, r_{EW}, \tag{1.1}$$

donde $f(x) = 1 - 8x + 8x^3 - x^4 - 12x^2 \log x$ y r_{EW} incluye las correcciones radiativas electrodébiles no incorporadas en la constante de Fermi, G_F, y la estructura no local del propagador del W, $r_{EW} \sim 0{,}9960$. Por tanto, el cociente

$$\frac{\mathcal{B}(\tau \rightarrow e)}{\mathcal{B}(\tau \rightarrow \mu)} \;=\; \frac{f\left(\frac{m_e^2}{M_\tau^2}\right)}{f\left(\frac{m_\mu^2}{M_\tau^2}\right)} \tag{1.2}$$

está fijado y permite verificar la universalidad de las corrientes cargadas electrodébiles. Las restricciones resultantes son bastante fuertes: $\sim 0{,}20\,\%$ para el cociente e/μ

[1] Los recientes resultados experimentales relativos a la razón entre flujos extragalácticos de materia y antimateria [16, 17, 18, 19] no tienen -por el momento- una explicación unánimemente aceptada.

y $\sim 0{,}22\,\%$ para las razones que incluyen al τ. Los errores asociados provienen de la indeterminación actual de $\sim 0{,}3$ MeV en M_τ. Esta incertidumbre es todavía mayor [33, 34] en la relación entre la tasa de desintegración (*branching ratio*, BR) a leptones y la vida media del tau -fijada utilizando el valor de la constante de Fermi proviniente de la desintegración del μ- (aparece elevada a la quinta potencia en la ec. (1.1)), que se mejorará notablemente en $BES-III$ y $KEDR$ próximamente [35]. $KEDR$ prevé alcanzar un error total de 0,15 MeV y $BES-III$ de sólo 0,10 MeV. No trataremos aquí la determinación de la masa del τ cerca de su umbral de producción [35].

En el SM, todos los leptones con la misma carga eléctrica tienen acoplos idénticos al bosón Z, tal y como se ha venido comprobando en LEP y SLC durante años. La precisión alcanzada para los acoplamientos axial-vectores de corriente neutra es aún mayor que para los vectoriales [36]:

$$\frac{a_\mu}{a_e} = 1{,}0001(14), \quad \frac{v_\mu}{v_e} = 0{,}981(82); \quad \frac{a_\tau}{a_e} = 1{,}0019(15), \quad \frac{v_\tau}{v_e} = 0{,}964(32). \tag{1.3}$$

A partir de $\tau^- \rightarrow \nu_\tau\, l^-\, \overline{\nu}_l$ se ha obtenido también un límite superior para los acoplos estándar y no estándar [37, 38, 39, 40, 41, 42] entre corrientes fermiónicas levógiras/dextrógiras (left/right-handed: L/R) : RR, LR , RL, LL; escalares, vectoriales y tensoriales (S, V, T). Es destacable que los límites actuales no permitan concluir que la transición es del tipo predicho: $V-A$ [43]. Tanto estas cotas como las de los '*Michel parameters*' [37] [2] mejorarán ostensiblemente en $BES-III$ [35, 44].

En el SM mínimo con neutrinos sin masa, existe un número leptónico aditivo que se conserva separadamente para cada generación (el llamado número leptónico de sabor, *lepton flavour number*). Sin embargo, y tras la evidencia de la oscilación de neutrinos $\nu_\mu \rightarrow \nu_e$ anunciada por $LSND$ [45, 46], la confirmación a través de las medidas de oscilaciones publicada por SNO [47, 48] y Super-Kamiokande [49, 50] descarta la anterior hipótesis del SM mínimo. Está claro por tanto que dicho número cuántico de familia se viola en procesos que involucran neutrinos. Aunque sería lo más natural que esto sucediera también en procesos con e, μ, τ, todos los datos actuales son consistentes con tal ley de conservación es ese subsector leptónico. A pesar de que los límites en violación de número cuántico leptónico de sabor a través de desintegraciones de τ están mejorando día a día ($BR \leq 10^{-7}$) [51, 52, 53, 54, 55, 56, 57, 59, 58, 60, 61, 62, 63, 64, 65, 66] , están lejos todavía de los límites existentes en las desintegraciones de μ con análoga violación [25].

El laboratorio de $FERMILAB$ en Chicago ha resultado una herramienta fundamental para el descubrimiento de los otros miembros de la tercera generación. Allí -como ya se comentó- el quark b fue descubierto en 1977, el top en 1994-5 (con la ayuda inestimable de la profecía de LEP, tal y como comentaré) y, finalmente, el experimento $DONUT$ [67] consiguió detectar la partícula restante, el neutrino tauónico, en 2000. De hecho, los mejores límites directos sobre la masa del neutrino, m_{ν_τ}, vienen de las desintegraciones hadrónicas del τ [68]: $\tau^- \rightarrow \nu_\tau\, X^-$, donde

[2] Estos parámetros describen la distribución del espacio fásico en las desintegraciones leptónicas de μ, τ.

$X^- = (\pi\,\pi\,\pi)^-, (2K\,\pi)^-, (5\pi)^-$. Aunque -según ya se indicó- quedan ampliamente rebasados por las cotas provenientes de estudios cosmológicos, nuestro estudio podría mejorar los límites directos.

Además, las desintegraciones semileptónicas del τ son el marco ideal para estudiar efectos de interacción fuerte en condiciones realmente muy limpias, ya que la mitad electrodébil de la desintegración está por completo bajo control y no se ve afectada por la hadronización que ensucia sobremanera el proceso. Estas desintegraciones sondean el elemento de matriz de la corriente cargada levógira entre el vacío de QCD y el estado final hadrónico, tal y como se representa en la Figura 1.1. Se dedicará más atención a este tema -central en la Tesis- a lo largo del trabajo.

Una comprobación directa de QCD [69] se puede realizar a partir del cociente

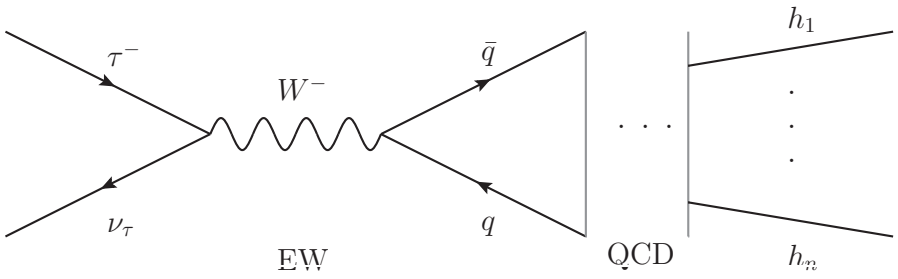

Figura 1.1: Diagrama de Feynman para la contribución al orden dominante a una desintegración hadrónica genérica del leptón τ.

$$R_\tau \equiv \frac{\Gamma(\tau^- \to \nu_\tau \,\text{hadrones}\,(\gamma))}{\Gamma(\tau^- \to \nu_\tau\, e^-\, \nu_e\,(\gamma))} = R_{\tau,V} + R_{\tau,A} + R_{\tau,S}\,, \tag{1.4}$$

que separa las contribuciones de las corrientes vectorial (V) y axial-vector (A) que corresponden a un número par/impar de piones en estado final de aquellas con un número impar de kaones (S es una abreviatura de procesos con cambio de extrañeza). Determinados canales (como $KK\pi$) no pueden ser asociados *a priori* a corriente V o A. En este caso, es especialmente importante un estudio como el que realizamos para saber cuánto contribuye cada una a la anchura parcial de dicho canal.

La predicción teórica requiere las funciones de correlación de dos puntos de las corrientes levógiras de quarks: $L^\mu_{ij} = \bar{\psi}_j \gamma^\mu (1-\gamma_5)\psi_i$, $(i,j = u,d,s)$:

$$\Pi^{\mu\nu}_{ij}(q) \equiv i \int d^4x\, e^{iqx}\, \langle 0|T(L^\mu_{ij}(x) L^\nu_{ij}(0)^\dagger)|0\rangle = \left(-g^{\mu\nu}q^2 + q^\mu q^\nu\right)\, \Pi^{(1)}_{ij}(q^2) + q^\mu q^\nu\, \Pi^{(0)}_{ij}(q^2)\,. \tag{1.5}$$

Utilizando la propiedad de analiticidad, R_τ se puede escribir como una integral de contorno en el plano de s compleja, donde el circuito se recorre en sentido antihorario alrededor del círculo de radio $|s| = M_\tau^2$ centrado en el origen:

$$R_\tau = 6\pi i \oint_{|s|=M_\tau^2} \frac{ds}{M_\tau^2} \left(1 - \frac{s}{M_\tau^2}\right)^2 \left[\left(1 + 2\frac{s}{M_\tau^2}\right)\Pi^{(0+1)}(s) - 2\frac{s}{M_\tau^2}\Pi^{(0)}(s)\right]\,, \tag{1.6}$$

donde $\Pi^{(J)}(s) \equiv |V_{ud}|^2\,\Pi^{(J)}_{ud}(s) + |V_{us}|^2\,\Pi^{(J)}_{us}(s)$. En (1.6) sólo hace falta conocer los correladores para s complejo $\sim M_\tau^2$, que es notablemente mayor que la escala asociada con efectos no perturbativos. Utilizando la expansión en producto de operadores (*Operator Product Expansion*, OPE [70, 71, 72]) para evaluar la integral de contorno, R_τ se puede escribir como una expansión en potencias de $1/M_\tau^2$.

Así, la predicción teórica de $R_{\tau,V+A}$ se puede expresar como sigue [73]:

$$R_{\tau,V+A} \;=\; N_C\,|V_{ud}|^2\,S_{EW}\,(1 \,+\, \delta'_{EW} \,+\, \delta_P \,+\, \delta_{NP})\,, \tag{1.7}$$

donde $N_C \,=\, 3$ es el número de colores posibles de cada quark. S_{EW} y δ'_{EW} contienen las correcciones electrodébiles conocidas a los órdenes dominante y subdominante en la aproximación logarítmica. Las correcciones no perturbativas puede demostrarse (y comprobarse) que son pequeñas [73] . La corrección dominante ($\sim 20\,\%$) proviene de la contribución de QCD puramente perturbativa, δ_P, que ya se conoce hasta $\mathcal{O}\,(\alpha_S^4)$ [73, 74] e incluye una resumación de los efectos más relevantes a órdenes superiores [30, 31, 32, 74, 75, 76, 77]. El resultado final [29, 78, 79, 80] resulta ser extremadamente sensible al valor de $\alpha_s(M_\tau^2)$, y permite una determinación muy fina del acoplamiento de QCD que -en el esquema $\overline{MS}$- es [81] [3]:

$$\alpha_s(M_\tau^2) \;=\; 0{,}342 \pm 0{,}012\,. \tag{1.8}$$

Al usar las ecuaciones del grupo de renormalización (Renormalization Group Equations, RGE) para hacer evolucionar este valor hasta la escala del Z [82] uno encuentra que:

$$\alpha_s(M_Z^2) \;=\; 0{,}1213 \pm 0{,}0014\,, \tag{1.9}$$

mientras que el valor obtenido en desintegraciones hadrónicas del bosón Z [8] es

$$\alpha_s(M_Z^2) \;=\; 0{,}1176 \pm 0{,}0020\,, \tag{1.10}$$

por lo que hay acuerdo entre el valor extraído de desintegraciones hadrónicas de taus y la medida directa realizada en el pico del Z, con mejor precisión incluso en el primer caso. Esto proporciona una bella comprobación del cambio con la escala del valor del acoplamiento de QCD, esto es, una comprobación experimental realmente significativa de *libertad asintótica*.

Es pertinente un comentario respecto a la fiabilidad de los errores en el resultado (1.8). Dicho estudio asume que se da la dualidad quark-hadrón [83]. Las violaciones de ésta [84] y el error inducido en análisis que la utilizan -como la determinación anterior de α_S- ha sido un tema de investigación reactivado [85, 86, 87, 88, 89] recientemente, después de que durante muchos años se ignorara sistemáticamente. Aunque los últimos análisis abogan porque esta violación se haya subestimado, de modo que los errores serían mayores, lo cierto es que la cuestión no está clara todavía y se necesitará por un lado modelos más realistas (esencialmente se usa un único modelo basado en resonancias y con menos frecuencia otro basado en instantones;

[3] Véase en esta referencia los trabajos utilizados en la determinación.

ambos debidos a Shifman [84]) para parametrizar tales violaciones, y por otro datos experimentales de mayor calidad para poder cuantificar este efecto con precisión.

La medida separada de las anchuras de desintegración de procesos con $|\Delta S| = 0$ y con $|\Delta S| = 1$ nos brinda la oportunidad de ser sensibles al efecto de ruptura de la simetría $SU(3)$ de sabor inducida por la masa del quark extraño. Concretamente, esto sucede a través de las diferencias

$$\delta R_\tau^{kl} = \frac{R_{\tau,V+A}^{kl}}{|V_{ud}|^2} - \frac{R_{\tau,S}^{kl}}{|V_{us}|^2} \approx 24\frac{m_s^2(M_\tau^2)}{M_\tau^2}\Delta_{kl}(\alpha_S) - 48\pi^2\frac{\delta O_4}{M_\tau^4}Q_{kl}(\alpha_S)\,, \tag{1.11}$$

donde se ha introducido los momentos espectrales R_τ^{kl}:

$$R_\tau^{kl} = \int_0^{M_\tau^2} \mathrm{d}s \left(1 - \frac{s}{M_\tau^2}\right)^k \left(\frac{s}{M_\tau^2}\right)^l \frac{dR_\tau}{ds}\,. \tag{1.12}$$

Las correcciones perturbativas $\Delta_{kl}(\alpha_S)$ y $Q_{kl}(\alpha_S)$ se conocen a $\mathcal{O}(\alpha_S^3)$ y $\mathcal{O}(\alpha_S^2)$, respectivamente [90, 91, 92] y δO_4, proporcional a la ruptura de simetría $SU(3)$ -ya que lo es a la diferencia entre el condensados de quarks s y u- está bien determinado [93]. Aunque en un futuro, con datos de excepcional calidad, sería posible determinar tanto $m_s(M_\tau)$ como $|V_{us}|$ simultáneamente analizando el conjunto de momentos espectrales, en la determinación más reciente [94] se fija:

$$m_s(2\,\mathrm{GeV}) \;=\; 94 \pm 6\,\mathrm{MeV}\,, \tag{1.13}$$

-obtenida con las últimas determinaciones de simulaciones en el retículo (*lattice*) y utilizando reglas de suma de QCD- de modo que el momento con mayor sensibilidad a $|V_{us}|$, con $kl = 00$, permite extraer [95]:

$$|V_{us}| = 0{,}2208 \pm 0{,}0033_{\mathrm{exp}} \pm 0{,}0009_{\mathrm{th}} \;=\; 0{,}2208 \pm 0{,}0034\,, \tag{1.14}$$

que puede competir en precisión con la extracción estándar de $|V_{us}|$ de desintegraciones K_{e3} [96] y con las nuevas propuestas realizadas para tal determinación. Más aún, el error asociado a esta determinación de $|V_{us}|$ se puede reducir en el futuro ya que está dominado por la incertidumbre experimental que disminuirá notablemente en años venideros gracias a los datos de factorías de mesones B. Como se sugirió, otra mejora realizable consistirá en el ajuste simultáneo de $|V_{us}|$ y m_s a un conjunto de momentos de la distribución de masa invariante de las desintegraciones hadrónicas del tau, que proporcionará todavía más precisión en la determinación de ambos parámetros.

Hoy por hoy, todos los resultados experimentales sobre el leptón τ son consistentes con el SM. Sin embargo, el análisis de datos ya recogidos en fábricas de mesones B como $BaBar$ y $Belle$ -y futuros experimentos en esta última- o instalaciones dedicadas a la producción de $\tau - c$ como BES resultan prometedores para obtener verificaciones cada vez más exigentes del SM y explorar la Física más allá del mismo [4].

[4] En el capítulo 5 se explica la importancia de las desintegraciones de taus para conocer el sector escalar y para determinar la masa de un Higgs ligero.

1.3. QCD: la teoría de la interacción fuerte

A continuación introducimos brevemente QCD con el fin de explicar por qué es a día de hoy imposible resolver problemas como los que nos planteamos de modo analítico y completo.

Los experimentos de dispersión profundamente inelástica en $SLAC$ [97, 98] permitieron concluir que los protones no eran partículas puntuales, sino que tenían una subestructura en términos de partículas de carga eléctrica fraccionaria (*quarks*). A pesar de que estos quarks habían sido predichos teóricamente al intentar encontrar un esquema de clasificación de la gran cantidad de mesones observados durante los '60 -primero [99, 100]- y al tratar de entender cómo se aplicaba las estadísticas cuánticas a todas estas partículas y en especial a los bariones de espín 3/2 -después [101]-, no estaba clara su existencia más allá del ente matemático y todos los experimentos subsiguientes fallaron en su intento de aislar estos constituyentes como partículas libres. Las dos características principales de la interacción fuerte se habían manifestado: libertad asintótica a altas energías y confinamiento de los quarks en hadrones a bajas energías.

Diversos estudios teóricos de teorías gauge no abelianas [102, 103] demostraron que el distinto comportamiento UV e IR de esta teoría podía explicarse en base a un álgebra no conmutativa. Más tarde, la evidencia de que el barión Δ^{++} existía llevó a concluir que debía haber un número cuántico adicional -llamado de color- a través de la conservación del teorema de Conexión Espín-Estadística, y motivó un trabajo de la comunidad teórica que acabaría dando como resultado la explicación simultánea de todos estos fenómenos a través del cuadro presentado por Fritzsch, Gell-Mann y Leutwyler [2], quienes identificaron $SU(3)$ -donde 3 es el número de colores diferentes que un quark puede tener- como el grupo de gauge base para la construcción de la QCD. Es decir, la teoría permanece invariante bajo transformaciones locales del grupo $SU(3)$ de color. Existe toda una serie de evidencias teóricas y experimentales de que esto es así [104].

La simetría gauge no-abeliana local $SU(N_C)$ para n_f (número de sabores) campos de materia de quarks [5] determina el Lagrangiano de QCD que directamente incorpora la interacción de éstos con los campos de gauge gluónicos y las autointeracciones de estos gluones. El Lagrangiano de QCD es:

$$\begin{aligned}
&\mathcal{L}_{QCD} = \overline{q}\,(i\not{D} - \mathcal{M})\,q - \frac{1}{4}G^a_{\mu\nu}G^{\mu\nu}_a + \mathcal{L}_{\mathcal{GF}+\mathcal{FP}}\,,\\
&D_\mu = \partial_\mu - ig_s G^a_\mu \frac{\lambda_a}{2}\,,\\
&G^a_{\mu\nu} = \partial_\mu G^a_\nu - \partial_\nu G^a_\mu + g_s f^{abc} G^b_\mu G^c_\nu,
\end{aligned} \tag{1.15}$$

donde $a = 1, \ldots, 8$, G^a_μ son los campos de gluones y g_s es la constante de acoplamiento fuerte. El campo de quark q es un vector columna con n_f componentes en

[5] El grupo de gauge fija el contenido en bosones -partículas mediadoras- de la teoría, pero no así los campos de materia: su representación y número de copias es algo que debe inferirse de los datos experimentales.

espacio de sabor, $\mathcal{M}$ representa la matriz de masas de los quarks es espacio de sabor y viene dada por $\mathcal{M} = \text{diag}\left(m_1, \ldots, m_{n_f}\right)$, donde m_i son las diferentes masas de los quarks: m_u, m_d, m_c, m_s, m_t, m_b para $n_f = 6$ dentro del SM, parámetros a cuyo valor la simetría no impone ninguna restricción. Como vemos, la simetría gauge prohíbe que los gluones tengan masa y sus acoplos son iguales para todos los sabores de quark. Las matrices $\frac{\lambda^a}{2}$ son los generadores de $SU(3)$ en la representación fundamental y quedan normalizadas mediante $\text{Tr}\left(\frac{\lambda^a}{2}\frac{\lambda^b}{2}\right) = \frac{1}{2}\delta_{ab}$ y f^{abc} son las constantes de estructura del grupo de gauge, $SU(N_C)$. Finalmente, el término de Fadeev-Popov [105], $\mathcal{L}_{\mathcal{GF}+\mathcal{FP}}$, incluye el Lagrangiano anti-hermítico que introduce los campos de fantasmas y el término que fija el gauge:

$$\begin{aligned}
\mathcal{L}_{\mathcal{GF}} &= -\frac{1}{2\xi}\left(\partial^\mu G^a_\mu\right)\left(\partial_\nu G^\nu_a\right), \\
\mathcal{L}_{\mathcal{FP}} &= -\partial_\mu\overline{\phi}_a D^\mu\phi^a\,, \;\; D^\mu\phi^a \equiv \partial^\mu\phi^a - g_s f^{abc}\phi_b\, G^\mu_c\,,
\end{aligned} \tag{1.16}$$

donde ξ es el llamado parámetro de gauge, y $\overline{\phi}^a$ (a = 1, ... , N_C^2-1) es un conjunto de campos escalares, hermíticos, sin masa y que anticonmutan entre sí. La derivada covariante, $D^\mu\phi^a$, contiene el acoplamiento necesario entre campos de fantasmas y gluónicos y $\mathcal{L}_{\mathcal{FP}}$ es obligatoriamente anti-hermítico para introducir una violación explícita de unitariedad que cancele las probabilidades no-físicas correspondientes a las polarizaciones longitudinales de los gluones y devolver así la propiedad fundamental de unitariedad a los observables físicos que se obtiene finalmente. Una explicación muy pedagógica sobre estos términos se puede encontrar en [104]. No discutimos aquí el llamado término θ [106], invariante bajo $SU(N_C)$ y que viola CP si no hay ningún quark sin masa. A día de hoy los experimentos más precisos no indican ninguna violación de CP en procesos fuertes. Esta presunta violación se manifestaría, por ejemplo, en un momento dipolar eléctrico no nulo del neutrón. La cota experimental [8] es nueve órdenes de magnitud inferior al valor natural teórico.

La evolución de la constante de acoplo con la energía está detrás de la propiedad de libertad asintótica y parece apuntar al confinamiento como una consecuencia natural. El acoplamiento g_s que aparece en el Lagrangiano de QCD (1.15) recibe correcciones cuánticas [104] que, a primer orden en la expansión en el número de lazos (*loops*), vienen dadas por los diagramas de la Figura 1.2.

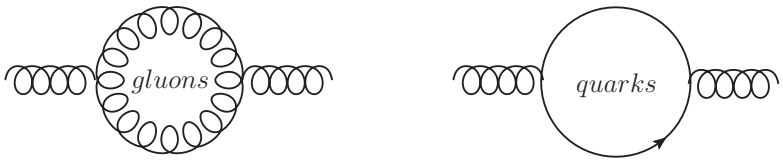

Figura 1.2: Diagramas de Feynman para la contribución a un lazo a la función β_{QCD}.

La función β_{QCD} se define a través del uso de las ecuaciones del grupo de renor-

malización, (Renormalization Group Equations, RGE [6]). A un lazo viene dada por [113, 114, 115, 116, 117]:

$$\beta_{QCD} = \mu\frac{\partial g_s}{\partial \mu} = -\left(11 - \frac{2n_f}{3}\right)\frac{g_s^3}{16\pi^2}\,, \tag{1.17}$$

por consiguiente -a este orden en la expansión-, es negativo para $n_f \leq 16$. Las RGE implican que el acoplamiento renormalizado varíe con la escala de energías, el llamado *running coupling*. Al ser $\beta_{QCD} \leq 0$, si resolvemos (1.17), esta desigualdad comportará que el acoplamiento renormalizado, g_s^R, decrezca al aumentar la energía; en otras palabras, llevará a la libertad asintótica de la interacción.

Hemos supuesto implícitamente que el cálculo a un lazo nos da una aproximación razonablemente buena, al menos cualitativamente. Cabe decir que, al hablar de libertad asintótica es este el caso, valga recordar (1.8), (1.10). De hecho, los cálculos a los órdenes subdominantes, $NNNLO$, [118, 119] apoyan este razonamiento.

Al integrar la ecuación (1.17) obtenemos que:

$$\alpha_s(q^2) = \frac{12\pi}{(33 - 2n_f)\log(q^2/\Lambda_{QCD}^2)}\,, \tag{1.18}$$

donde se ha definido $\alpha_s \equiv g_s^2/4\pi$. Esta ecuación ilustra cómo el acoplamiento (renormalizado) fuerte depende únicamente de la escala característica de QCD, Λ_{QCD}, definida en función del valor acoplo renormalizado a una determinada escala de renormalización, μ, y de μ mismo mediante:

$$\log(\Lambda_{QCD}^2) = \log\mu^2 - \frac{12\pi}{\alpha_s(\mu^2)(33 - 2n_f)}\,. \tag{1.19}$$

Las RGE y sus verificaciones experimentales -como por ejemplo el par de ecuaciones (1.8), (1.10)- parecen estar en perfecto acuerdo con una interacción cuya carga es el grado de libertad de color muy intensa a bajas energías (i.e. largas distancias), lo que provocaría el confinamiento. Una imagen intuitiva de este fenómeno es sencilla: al separar dos cargas eléctricas, la intensidad de la interacción entre ellas queda reducida (*apantallada*) por la creación de dipolos entre ambas. Este efecto corresponde al término con $-2n_f$ en la ecuación (1.18). En el caso de las cargas de color, el diferente comportamiento es debido al término con el 33 en dicha ecuación. Las autointeracciones de gluones hacen que haya *antiapantallamiento* y llega un momento en que no es posible seguir separando el par quark-antiquark ya que es energéticamente más favorable crear un nuevo par. Salvando las diferencias y para completar una analogía intuitiva, se puede decir que sería como sucede con los

[6] Las RGE [107, 108, 109, 110, 111, 112] se deducen al requerir que un observable no pueda depender de la escala de renormalización escogida arbitrariamente y que la física sea invariante de escala. Esto último conlleva que las funciones de Green tengan un comportamiento bien definido bajo reescalado de los momentos que aparecen en ellas. Esto permite relacionar los valores de las cantidades renormalizadas a energías distintas y también calcular las dimensiones anómalas, que modifican la evolución con la energía deducida sólo con análisis dimensional debido a efectos cuánticos.

imanes. Al romper uno, siempre nos encontramos con un nuevo imán, con dos polos opuestos. Es imposible aislar el monopolo magnético como lo es aislar una carga de color.

De un modo algo más técnico, la fase confinante se define en términos del comportamiento de la acción del llamado lazo de Wilson (*Wilson loop*) [120], que corresponde al camino descrito en cuatro dimensiones por un par quark-antiquark entre sus puntos de creación y aniquilación. En una teoría no confinante, la acción de este lazo sería proporcional a su perímetro. Sin embargo, en una teoría confinante, la acción del lazo iría como el área. Como el perímetro de dos líneas abiertas es igual a la suma, mientras que el área se hace infinita, en la teoría no confinante sería posible separar el par; mientras que en la confinante no lo sería. Aunque los lazos de Wilson fueron introducidos para tener una formulación no perturbativa de la QCD y resolver el problema de confinamiento, esto no ha sido posible todavía. Su influencia -como la de tantas ideas surgidas intentando entender QCD- ha sido no obstante muy grande, ya que condujeron a Polyakov [121] a la formulación moderna de las teorías de cuerdas (*string theories*).

A pesar de lo que se ha dicho existe un modo de acercarse experimentalmente al confinamiento. Hasta ahora se ha considerado siempre teoría de campos a temperatura y densidad finitas. En el origen del Universo ambas fueron tan elevadas que la simetría quiral estaría rota y los quarks y gluones no tendrían tiempo de hadronizar debido a sus interacciones constantes. En experimentos con iones pesados se está investigando este marco para intentar arrojar más luz sobre el problema de confinamiento.

En resumen, las correcciones cuánticas provocan que la intensidad de la interacción cambie con la energía. En el caso de QCD es muy intensa a bajas energías, por lo que no podremos hacer una expansión perturbativa en potencias de la constante de acoplo y realizar cálculos útiles así, ya que no convergerán al no cumplirse $\alpha_S \ll 1$. Adicionalmente, y debido al confinamiento, habrá que encontrar el modo de relacionar la teoría fundamental con grados de libertad quark, antiquark y gluón con los mesones producidos en las desintegraciones de taus. Veremos en los siguientes apartados y capítulos que la solución a ambos problemas viene de la mano, pues el encontrar los grados de libertad adecuados nos permitirá entender cómo construir un cálculo fiable.

1.4. Las Teorías Cuánticas de Campos Efectivas

La Historia de la Física es una historia de entendimiento de fenómenos cada vez más numerosos y diversos. En muchos casos, la comprensión de los nuevos no invalida la descripción de los antiguos, que se obtiene como un caso particular de las nuevas teorías, de mayor alcance. En ocasiones, la vieja teoría puede verse como una teoría efectiva de la nueva en un determinado rango de aplicación de ésta.

Algunos ejemplos pueden resultar ilustrativos: a principios del S. XIX se tenía

una descripción correcta de la electrostática. Diversos experimentos debidos a Ørsted, Ampère, Ohm y Faraday -entre otros- aumentaron el conjunto de fenómenos a describir simultáneamente incluyendo la electrodinámica y el magnetismo con flujos variables con el tiempo. El conjunto de todos ellos se podía explicar coherentemente a través de las ecuaciones de Maxwell. En ellas se describía la naturaleza ondulatoria de la luz, mostrándola como una onda electromagnética que se propagaba a una velocidad, c, constante universal de la teoría. En el límite $c \to \infty$, se pierde la corriente de desplazamiento de Maxwell. Por tanto, la teoría antigua (ley de Ampère) se podía ver como caso límite de la moderna (ecuaciones de Maxwell) cuando se consideraba un determinado parámetro pequeño ($1/c$). La ley de Ampère puede considerarse el primer orden en la expansión en $1/c$ de la llamada ley de Ampère generalizada que se obtiene de las ecuaciones de Maxwell. Es pues una teoría efectiva de la primera. En fenómenos estáticos, un tratamiento basado en las ecuaciones completas de Maxwell es innecesario y bastan las ecuaciones de Coulomb o Ampère, obviamente.

La Mecánica Newtoniana es válida en gran número de sucesos de nuestra vida diaria. Sin embargo no lo es en el mundo de lo extraordinariamente pequeño o de lo enormemente veloz. La Mecánica Cuántica la generaliza en el primer caso y la Relatividad Especial en el segundo. Una de las hipótesis fundamentales de la teoría cuántica es que la acción está cuantizada en múltiplos enteros de la constante de Planck ($\hbar$), lo que permite explicar el espectro de emisión de los cuerpos negros, por ejemplo. El valor de esta constante es tan pequeño que en los sucesos macroscópicos es irrelevante. Es por ello lógico que el límite $\hbar \to 0$ de la teoría cuántica nos devuelva a la teoría clásica que es así una teoría efectiva de aquélla. Nadie recurriría a la Mecánica Cuántica para resolver un problema macroscópico salvo que fuera para ilustrar una lección de introducción a la Cuántica.

Puede verse también que la electrodinámica clásica de Maxwell es la teoría efectiva de la electrodinámica cuántica en el límite $\hbar \to 0$. La que desde un punto de vista era antes teoría fundamental, desde otro es efectiva de la siguiente fundamental. De nuevo parece innecesario resolver el problema de la trayectoria de un cuerpo macroscópico cargado sometido a un campo electromagnético utilizando la teoría cuántica. Queda claro que las teorías efectivas son más útiles (de ahí su otra posible traducción como *eficaces*) que las fundamentales en los subsectores en que se aplican.

Salvo que trabajemos con una teoría *del todo* nuestra teoría será siempre efectiva, y además mejor que lo sea. El adjetivo debe verse como algo positivo, ya que evitamos complicar el problema innecesariamente y escogemos las variables adecuadas para describirlo. Queda justificar que sea una teoría cuántica de campos (*Quantum Field Theory*, QFT).

El método habitual de estudio de las $QFTs$ se basa en el empleo de teoría de perturbaciones en potencias de la constante de acoplo, que debe ser pequeña para que cada término contribuya menos que el anterior y podamos cortar nuestra expansión a un orden dado, debido a que la serie de perturbaciones no es sumable exactamente. Tal expansión no tiene sentido en nuestro caso de las desintegraciones hadrónicas del τ, por el valor de $\alpha_S \sim \mathcal{O}(1)$ por lo que debemos buscar una vía

alternativa.

De todas formas, es conveniente no renunciar a las $QFTs$, ya que su formalismo nos garantiza que los observables cumplan todos los requisitos de una teoría cuántica relativista (como debe ser la que describa nuestra física de partículas): microcausalidad (si dos puntos espacio-temporales están separados espacialmente cualesquiera operadores definidos en ellos tienen relaciones de conmutación o anticonmutación -según su estadística- triviales), unitariedad (la suma de probabilidades de todos los sucesos posibles es la unidad), analiticidad (las funciones de los campos deben ser complejo-diferenciables en el entorno de cada punto de su dominio), invariancia Poincaré (el grupo de simetría de la Relatividad), teorema de conexión espín-estadística (estadística de Fermi-Dirac para partículas de espín semientero y de Bose-Einstein para partículas de espín entero) y descomposición en núcleos, *clusters* (asegura la localidad de la teoría, ya que regiones suficientemente separadas se comportan independientemente).

Convencidos ya de que las técnicas de las $QFTs$ son altamente deseables hay que reconocer que no son, por sí mismas, suficientes, ya que si uno se restringe a estos principios tan generales necesitaría muchísima información experimental para poder caracterizar una teoría y así hacer predicciones. Según hemos visto antes, es conveniente utilizar las $EFTs$. Así pues, será natural y adecuado emplear las teorías cuánticas de campos efectivas en nuestro problema.

Para formularlas necesitamos identificar los grados de libertad relevantes y el parámetro de la expansión, lo que en general sucederá simultáneamente, como veremos en las secciones siguientes. Habrá una escala típica, Λ, que separará los grados de libertad activos de los pasivos. Se considerará en la acción las partículas con $m \ll \Lambda$, mientras que se procederá a la integración funcional de la acción de las variables pesadas con $M \gg \Lambda$. Consideraremos las interacciones entre los estados ligeros que organizaremos en serie de potencias en $1/\Lambda$. Como $m/\Lambda \ll 1$ el efecto de cada término sucesivo será menor que el del anterior y podremos cortar la expansión a un orden dado. Además, tendremos control sobre el error cometido estimando la contribución del primer término omitido a partir del parámetro de expansión y los términos conocidos.

Finalizaremos esta sección con la formulación de las $EFTs$ cuánticas à la Weinberg [3]: si -para unos grados de libertad dados- aplicamos teoría de perturbaciones con el Lagrangiano más general posible consistente con las simetrías asumidas de la teoría obtendremos los elementos de matriz S -y por tanto los observables que de ella se derivan- más generales posibles consistentes con analiticidad, unitariedad perturbativa, descomposición en núcleos y las simetrías asumidas.

Obsérvese que respecto a la formulación más general que antes se introdujo aquí se añade el comprometerse con una elección de grados de libertad y suponer unas simetrías de la teoría subyacente, pero nada más. Esta aproximación se revisará más tarde, pues quizá pueda ser deseable una aproximación más elaborada en la que se incluya más contenido dinámico de la teoría subyacente.

1.5. Teoría Quiral de Perturbaciones

Se acaba de poner de relieve el concepto de simetría. Las simetrías han sido siempre la clave para la comprensión de los fenómenos físicos. Por un lado se expresan en términos del mayor rigor matemático y por otro permiten -en ciertos casos- las aproximaciones, base de prácticamente cualquier cálculo realista.

¿Cuál será la simetría que podremos emplear para construir nuestra teoría efectiva? La respuesta no es sencilla ni inmediata. Uno pensaría en alguna propiedad relacionada directamente con el grupo de gauge de la teoría, con la propiedad de color. Debido a la hadronización, las estructuras posibles con carga total de color nula quedan inmediatamente fijadas por las reglas para el producto de representaciones de la teoría de grupos, ya que conocemos las representaciones de los campos de gauge (adjunta) y hemos fijado las de materia (triplete y antitriplete para quarks y antiquarks, respectivamente). En lo que nos ocupa comprobamos que los mesones cumplen esta condición, pero no obtenemos nada útil para desarrollar nuestra teoría efectiva. De hecho, asumiendo confinamiento, observamos que dejar libre N_C es la única posibilidad que nos queda, la trataremos en el siguiente apartado.

No será pues una simetría gauge local la que nos permita construir la teoría efectiva. Veamos qué simetrías globales tiene la interacción fuerte. Pensemos en primer lugar que en los procesos examinados en esta Tesis vamos a producir los mesones más ligeros: piones, kaones y etas. Es intuitivo que los quarks más pesados no serán activos. Examinemos por tanto el Lagrangiano de QCD únicamente para los sabores ligeros: u, d, s, $n_f = 3$ en (1.15). Si en primera aproximación despreciamos las masas de estos quarks $m_u \sim m_d \sim m_s \sim 0$, el Lagrangiano de QCD es invariante bajo transformaciones separadas de las componentes dextrógira y levógira de los quarks, transformaciones globales del grupo $G \equiv SU(n_f)_L \otimes SU(n_f)_R$, el llamado grupo de simetría quiral.

Sabemos que las simetrías locales determinan la interacción -como en (1.15)-. Para las simetrías globales hay dos posibilidades: Si tanto el Lagrangiano como el vacío son invariantes bajo el grupo de transformaciones G entonces la simetría se manifiesta en el espectro de partículas. Sin embargo, si aunque el Lagrangiano sea invariante bajo transformaciones pertenecientes a G el vacío de la teoría no lo es, entonces el espectro reflejará las simetrías de un cierto subgrupo H del grupo G, donde tanto el Lagrangiano como el vacío serán simétricos bajo transformaciones de H, pero sólo el Lagrangiano será invariante bajo todo el grupo G. Se habla en este caso de que ha habido ruptura espontánea de la simetría $G \to H$. Sabemos además que tendremos tantas partículas de masa nula (bosones de Goldstone [122]) como generadores rotos. Es decir, el número de bosones de Goldstone será igual a la diferencia entre el número de generadores de G y de H.

Si recurrimos a la fenomenología observamos que los mesones más ligeros se pueden clasificar en multipletes ($n_f = 3$) de igual espín (J) y paridad intrínseca (P), lo que corresponde a las representaciones de $SU(3)_V$. También vemos que los multipletes con paridad opuesta no tienen la misma masa: el multiplete de vectores ($J^P = 1^-$) es más ligero que el de axial-vectores (1^+). Y el de mesones pseudoes-

calares (0^-) es mucho más ligero que el de escalares (0^+) o que las partículas de espín 1 [7]. En el capítulo 3 se muestra cómo estas observaciones conducen a concluir que el patrón de ruptura espontánea de simetría es $SU(3)_L \otimes SU(3)_R \to SU(3)_V$. El número de generadores rotos es $n_f^2 - 1 = 8$, que sería el número de bosones de Goldstone que deberíamos observar. En realidad, como las masas de los quarks ligeros son pequeñas comparadas con el parámetro típico de hadronización, $\Lambda_{\chi SB} \sim 1\text{GeV}$, pero no nulas, se tiene junto a la ruptura espontánea de la simetría quiral una ruptura explícita de la misma por ser $m_l \neq 0$, $m_l = m_u$, m_d, m_s. Por este motivo observamos 8 partículas con masa pequeña pero no nula a las que llamamos pseudo-bosones de Goldstone (en razón a su origen en la ruptura espontánea de la simetría y a su masa en la ruptura explícita de la misma). Éstos son los piones, kaones y etas detectados en nuestras desintegraciones de taus: $\pi^\pm, \pi^0, \eta, K^\pm, K^0, \bar{K}^0$.

Ahora que ya tenemos la simetría y los grados de libertad debemos preocuparnos de construir el Lagrangiano efectivo que los incluya adecuadamente. El teorema de Weinberg nos asegura que una vez hecho esto, el tratamiento perturbativo del mismo nos conducirá a los elementos de matriz S más generales posibles en un tratamiento consistente. El formalismo que permite construir Lagrangianos efectivos en base a grupos de simetría con ruptura espontánea de la misma se debe a Callan, Coleman, Wess y Zumino [123, 124]. Su aplicación a QCD a bajas energías nos permitirá escribir una EFT que describa la interacción de estos pseudo-bosones de Goldstone. Además, como hay un intervalo de energía razonable entre estas partículas y las siguiente más pesadas, el efectos de estos modos pesados será pequeño y permitirá construir una teoría efectiva que contenga sólo estos modos, la Teoría Quiral de Perturbaciones, χPT [4, 5].
Veremos más adelante que esta teoría presenta un parámetro de expansión natural en el cociente entre las masas o momentos de los pseudo-bosones de Golstones sobre la escala $\Lambda_{\chi SB}$, que será bastante menor que la unidad. Hemos resuelto por tanto todos los problemas que nos planteábamos: χPT es una EFT construida en base a las simetrías de QCD en cierto subsector de la misma (el de sabores ligeros en procesos a baja energía donde sólo se producen pseudo-bosones de Goldstone y la simetría quiral de QCD es una buena aproximación) y con un parámetro de expansión que permite desarrollar teoría de perturbaciones. Ahora bien, debido al valor de la masa del tau, entorno a 1,8 GeV, las resonancias podrán ser grados de libertad activos en algunas regiones del espectro de desintegración, por lo que deberemos extender χPT a energías superiores e incluir nuevos grados de libertad. Desafortunadamente, en este caso será mucho más complicado cumplimentar los pasos anteriores de cara a la construcción de la teoría, como ahora veremos.

[7] Llamaremos genéricamente resonancias a todas estas partículas que contienen sabores ligeros más pesadas que el multiplete más ligero de partículas 0^-.

1.6. El límite de gran número de colores de QCD

Al incorporar partículas más pesadas se rompe el contaje de la teoría, ya que las masas y momentos de estos nuevos grados de libertad son del mismo orden o superior a $\Lambda_{\chi SB}$, de modo que su cociente ya no es un buen parámetro de expansión de la teoría. Se añade otra dificultad: ya no existe un intervalo grande y bien definido de energías que separe las partículas que serán grados de libertad activos de nuestra teoría de las que serán integradas de la acción por no serlo. Veremos que una solución a ambos problemas puede venir de considerar el límite de gran número de colores de QCD [125, 126, 127]. En cualquier caso, hay que destacar que contrariamente a lo que sucede en el sector de muy bajas energías con χPT no se conoce cómo construir una EFT dual a QCD en el régimen de energías intermedias. El límite $N_C \to \infty$ es una herramienta que permitirá entender qué contribuciones son más importantes -de todas las permitidas por las simetrías- en nuestro Lagrangiano.

't Hooft sugirió considerar el límite de QCD cuando el número de colores posibles del grupo de gauge tendía a infinito [125]. Su motivación era conseguir una teoría más simple que guardara semejanza con la original y de la que se pudiera deducir propiedades cualitativas -y con suerte cuantitativas- de la subyacente. En el límite de gran N_C QCD es exactamente soluble en dos dimensiones [126], pero no en las cuatro habituales. Sin embargo, si asumimos que la teoría es confinante se pueden derivar toda una serie de características experimentales de QCD, lo que sugiere que esta construcción es una buena aproximación a la naturaleza. Entre ellas adelantamos por el momento que:
- En el límite estricto $N_C \to \infty$ los mesones son libres, estables (no se desintegran) y no interaccionan entre ellos. Las masas de los mesones tienen límites suaves y hay infinidad de ellos: toda una torre de excitaciones por cada conjunto de números cuánticos.
- A primer orden en la expansión en $1/N_C$ la dinámica de los mesones queda descrita por diagramas a orden árbol obtenidos con un Lagrangiano efectivo local cuyos grados de libertad son mesones, tal y como se ha considerado antes en el enfoque de las $EFTs$ à la Weinberg de χPT.

Llegados a este punto uno observa que hay una cierta contradicción interna entre la construcción de $EFTs$ à la Weinberg y la expansión en $1/N_C$ de QCD que habrá que resolver de algún modo: por un lado el enfoque à la Weinberg nos dice que definamos el contenido de partículas y las simetrías y luego construyamos el Lagrangiano más general posible consistente con las simetrías asumidas de la teoría garantizando que obtendremos a través de una aproximación perturbativa los resultados más generales compatibles con propiedades generales de la QFT y las simetrías de partida. El problema es que al introducir resonancias el parámetro de expansión que nos funcionaba en χPT deja de hacerlo.

Por otra parte, cuando pensamos que el límite de gran número de colores de QCD puede servirnos para organizar una expansión en $1/N_C$ que nos saque del atolladero observamos que contradice las ideas enunciadas en el anterior párrafo, ya que una de sus conclusiones a primer orden es que no podemos fijar a priori el contenido

de partículas de la EFT, por consistencia de la expansión habrá infinitas copias de cada tipo de resonancia.

Es por ello que tenemos dos posibilidades:
- O bien olvidamos el requisito de la formulación à la Weinberg de hacer una elección de grados de libertad adecuada al rango de energías en que sucede nuestro proceso y por tanto a los grados de libertad activos e incluimos el espectro necesario que pide el límite $N_C \to \infty$.
- O bien incluimos el espectro fenomenológico y nos desviamos del contaje en $1/N_C$.

Se podría pensar que incorporando los efectos subdominantes en $1/N_C$ podremos llegar al espectro medido. Esta idea no se puede concretar por el momento debido a la naturaleza de la expansión en $1/N_C$ de QCD. Si bien a un orden en α_S hay un número determinado de diagramas, y éstos se pueden calcular y sus efectos resumar, no sucede lo mismo en $1/N_C$: en cada orden intervienen infinitos diagramas, y nadie ha sido todavía capaz de idear algún mecanismo que nos permita estudiar esta cuestión. En el marco de las teorías efectivas basadas en esta expansión sí existen estudios a orden subdominante en $1/N_C$, como veremos.

Adicionalmente, cabe recordar que el enfoque à la Weinberg no incluye ningún tipo de información dinámica sobre la teoría subyacente: es el precio a pagar por su generalidad. En nuestro caso veremos que una teoría con grados de libertad pseudo-bosones de Goldstone y resonancias, que respeta la simetrías de QCD a bajas energías, y por tanto reproduce χPT a bajos momentos, y basada en el límite $N_C \to \infty$ no es compatible con el comportamiento conocido de QCD a altas energías. Como nuestra teoría debe funcionar hasta $E \sim 2$ GeV y a esas energías la QCD perturbativa ya es fiable, esto no debe suceder. Así pues la teoría que necesitamos precisará de la adición de información dinámica de QCD -lo que permitirá que enlace los regímenes quiral y perturbativo en el sector mesónico de sabores ligeros- y de, o bien renunciar a la elección de estados físicos como grados de libertad, o bien modelizar la expansión en $1/N_C$. Éstas son las cuestiones que se discute en el siguiente apartado.

1.7. La Teoría Quiral de Resonancias

La Teoría Quiral de Resonancias, $R\chi T$ [6, 7], incluye los pseudo-bosones de Goldstone y las resonancias como grados de libertad activos de la teoría y requiere las propiedades generales de las $QFTs$ y la invariancia bajo C y P de QCD. Sus características fundamentales se tratan a continuación.

El límite a bajas energías de $R\chi T$ debe ser χPT. Esta propiedad se ha utilizado para predecir sistemáticamente las $LECs$ de χPT en términos de las masas y acoplamientos de las resonancias al integrar éstas de la acción, a los órdenes quirales $\mathcal{O}(p^4)$ [6] y $\mathcal{O}(p^6)$ [128] en el sector de paridad intrínseca positiva, con $N_C \to \infty$ y exigiendo el comportamiento dictado por QCD a altas energías.

El Lagrangiano de χPT incluye el octete de pseudo-bosones de Goldstone. En

su extensión, el de $R\chi T$ incorpora a las resonancias como grados de libertad, que se incluyen en nonetes debido a que octetes y singletes de un grupo $SU(N_C = 3)$ se funden en un nonete para $N_C \to \infty$. El Lagrangiano de χPT se construye en base a la simetría quiral aproximada de QCD sin masas. Después se incorporan las rupturas espontánea y explícita de la simetría del mismo modo que sucede en QCD. Los nonetes de resonancias se añaden exigiendo las propiedades generales e invariancias bajo C y P y la estructura de los operadores viene dada por simetría quiral. A primer orden en la expansión en $1/N_C$ los términos con más de una traza y los lazos están suprimidos. La primera propiedad permite postergar ciertos términos permitidos por las simetrías del Lagrangiano y la segunda justifica su uso a nivel árbol como se explicó antes.

Según ya se dijo la teoría determinada por las simetrías no posee algunas propiedades conocidas de QCD a altas energías. Por ello se debe proceder al empalme con QCD asintótica a nivel de funciones de Green y/o factores de forma. La aplicación de estas propiedades determina una serie de relaciones entre los acoplamientos de la teoría que permiten que con un menor número de datos experimentales de partida la teoría sea capaz de predecir otras. En concreto en esta Tesis obtenemos relaciones de este tipo sobre los factores de forma en dos tipos de procesos que confrontaremos a las halladas en funciones de Green de dos y tres puntos donde intervienen los mismos acoplamientos [8]. El buen comportamiento ultravioleta prohíbe términos con muchas derivadas, lo que nos ayuda a delimitar el número de operadores que intervienen en el Lagrangiano ya que el contaje que a tal efecto servía en χPT ahora está roto. La situación no es tan sencilla, como se comentará después, pues condiciones de consistencia pueden requerir introducir operadores con más derivadas y con alguna relación no trivial entre sus acoplos. En general, no se incluye términos con un número excesivo de derivadas ya que se precisarían relaciones ajustadas muy finamente (*fine tuning*) para asegurar las cancelaciones necesarias a altos momentos. En muchos casos no es sino el éxito fenomenológico la comprobación de que la construcción seguida es adecuada.

Respecto a la inconsistencia entre la aproximación à la Weinberg y el límite estricto $N_C \to \infty$ debemos decir que no se conoce ningún modo de implementar la torre infinita de resonancias sin modelización. Por tanto, parece razonable comenzar estudiando procesos sencillos con el menor número de grados de libertad posible involucrados. A medida que se tenga mayor control de la teoría en esta aproximación será posible ir incluyendo más estados del espectro de resonancias. Esta aproximación no es sólo práctica desde el punto de vista de ir estimando progresivamente los distintos coeficientes de la teoría, sino que es la base de la buena descripción física, siempre en términos del menor número posible de parámetros compatible con la información experimental. El mayor grado de precisión progresivo de ésta acabará exigiéndonos una descripción más elaborada, pero mientras no sea preciso no será deseable tampoco.

Finalmente, nuestro estudio fenomenológico no puede evitar introducir algunas

[8] No existen cálculos en $R\chi T$ de funciones de Green de cuatro puntos, cuyas relaciones de comportamiento asintótico pudiéramos confrontar a las de las desintegraciones hadrónicas del tau.

propiedades que resultan ser efectos al orden siguiente en el desarrollo en $1/N_C$. En el intervalo de energías en que se desintegran los taus las resonancias alcanzan su capa másica y además tienen un comportamiento resonante debido a su anchura típicamente menor que su masa. Las anchuras son un efecto a orden subdominante que incluiremos de modo consistente en $R\chi T$, como veremos.

1.8. Organización de la Tesis

Como se ha dicho, nuestro estudio adopta el enfoque de las $EFTs$. Se realiza por tanto una introducción a sus fundamentos en el Capítulo 3. Tres son los pilares teóricos de nuestro trabajo: por un lado el asegurar el límite correcto a bajas energías, dictado por χPT. Por otro, el límite de gran número de colores (N_C) de QCD aplicado a teorías efectivas con grados de libertad hadrónicos, en nuestro caso $R\chi T$. Y finalmente, el garantizar un comportamiento acorde al dictado por QCD a altas energías para los distintos factores de forma. La primera y la segunda cuestión son abordadas en los Capítulos 3 y 4, respectivamente, mientras que la tercera se introduce en la Sección 4.5 y se pone en práctica en cada aplicación particular de la teoría en los siguientes capítulos, a los que precede un breve resumen de los estudios teóricos más significativos y un repaso de las características esenciales de las desintegraciones hadrónicas exclusivas del tau (capítulo 5). Las aplicaciones consideradas son: las desintegraciones hadrónicas con tres piones (capítulo 6) y con dos kaones y un pión (Capítulo 7). También se incluyen las desintegraciones con mesones η (capítulo 8) y las desintegraciones radiativas del tau con un único mesón $\tau \to P^- \gamma \nu_\tau$, donde $P = \pi$, K, en el Capítulo 9 . Con todas ellas mejoramos excepcionalmente el control de los parámetros del Lagrangiano de resonancias que participa en los procesos señalados, tanto en la corriente vectorial como en la axialvector y, por tanto, conocemos mejor cómo describir de un modo teóricamente sólido basado en las $EFTs$ y las simetrías de QCD estas desintegraciones del τ. Podremos explotar estas adquisiciones en un futuro, aplicándolas a procesos más complejos. La Tesis acaba con las conclusiones generales del trabajo realizado.

Chapter 2

Introduction

2.1 General introduction to the problem

This Thesis studies those decays of the τ lepton including mesons among the final state particles, that are called, for this reason, hadron or semileptonic decays. Contrary to what happens to the other leptons (electron, e^- and muon, μ^-) its mass ($M_\tau \sim 1.8$ GeV) is large enough to allow this kind of decays including light mesons (pions -π-, kaons -K- and etas -η, η'-). These processes include, in addition, the corresponding tau neutrino, ν_τ, and may include (in the so-called radiative processes) multiple photons, γ. Although it is kinematically possible to produce other light mesons whose masses are lighter than M_τ, the characteristic lifetime of these particles (resonances) is way too short to allow their detection. Notwithstanding, as we will see, the effect of their exchange is important in order to understand these decays. Although $M_\tau \sim 2M_p$, where M_p is the proton mass, since it is a bit smaller actually ($M_\tau = 1,777$ GeV and $2M_p = 1,876$ GeV) and to the conservation of baryon number (that would require producing them in baryon-antibaryon pairs, the lighter being proton-antiproton) τ decays into baryons are forbidden.

Purely leptonic decays of the τ are processes mediated by the electroweak interaction, that today is adequately described in the framework of the Standard Model of Particle Physics (SM) [1]. In hadron decays of the tau, the strong interactions acts, additionally. Although it is common lore that Quantum Chromodynamics, QCD is the theory [2] that describes it, we are not yet able to solve the problem at hand using only the QCD Lagrangian, as we will explain.

Both difficulties mentioned above -the fact that the resonances are not asymptotic states, so that it is not possible to detect them, and our current inability to solve QCD to find a solution to the problem- are telling us how interesting can the semileptonic tau decays be: the provide a clean environment where to study the strong interaction at low and intermediate energies, because the electroweak part of the process is clean and under theoretical control; on the other side, given the range of energies the hadron system can span (essentially from the threshold for pion production, $\pi \sim 0.14$ GeV, to M_τ), the lightest resonances can be exchanged on-mass-shell (or simply on-shell, in what follows), in such a way that their effects

are sizable and one can thus study their properties.

The strong interaction was discovered in the classic Rutherford's experiment, proving the existence of the atomic nucleus: it was a force of amazing strength and very short range. Soon after, this force started to be studied in scattering experiments between hadrons -as the particles experiencing strong interactions are called- (they were believed to be elementary then) instead of atomic nuclei. The large number of hadrons that was discovered in the '50s and '60s with the advent of the first particle accelerators suggested that these particles were not fundamental, analogously to what happened with the chemical elements, in the end constituted by protons and neutrons tighten in their nuclei. In order to complete the analogy, the systematics attached to the hadron properties (in this context intimately related to the quantum numbers and specifically to the approximate flavour symmetries) helped to understand their substructure and Gell-Mann comprehended that hadrons had to be constituted by the so-called quarks, possessing an additional quantum number -christened as color- that solved all problems of adequacy of the observed spin and the quantum statistics obeyed by the particles.

However, whereas it is possible to unbind protons or neutrons from the nucleus -either through natural radioactivity or artificially- it has been impossible so far to free any constituent quark from the hadron to which it belongs. This property is known as confinement and, though there are theoretical reasons pointing to this phenomenon there is not yet any explanation of it. This fact imposes a difficulty when understanding the processes mediated by strong interaction: while it is produced between quarks and gluons (the intermediary QCD bosons, that also autointeract), our detectors are recording only (in this context) hadron events, since quarks, antiquarks and gluons cluster immediately after they are produced into objects with vanishing total color charge: they hadronize. Contrary to the remaining known forces (electromagnetic, weak and gravitational), in QCD the force does not diminish as the distance increases, but just the opposite -even though its range is very short-.

Although we will dwell into this later on, let it be enough for the moment saying that even though QCD is the theory of strong interactions, we can not handle it in its non-perturbative regime and, therefore, computationally, its Lagrangian only allows to tackle analytically inclusive processes at high energies ($E > 2$ GeV typically) where a treatment in terms of quarks, antiquarks and gluons is meaningful. At the lower energies where our problem occurs we must search an alternative way. As it uses to happen in Physics, an appropriate choice of the degrees of freedom simplifies (or even allows) the solution. In our study of several exclusive tau decay channels it is evident that they will be the lighter mesons and resonances. The most convenient and rigorous way to do it is the use of Effective Field Theories ($EFTs$), that preserve the symmetries of the fundamental theory and are written in terms of the relevant degrees of freedom in a given energy range. As τ decays typically happen in an energy scale densely populated by resonances, it would not be enough to employ Chiral Perturbation Theory (χPT) [3, 4, 5] that includes only the lightest pseudoescalar mesons (π, K, η). Instead, it will be necessary to incorporate

the resonances as active degrees of freedom to extend the theory to higher energies: Resonance Chiral Theory ($R\chi T$) [6, 7] is the tool allowing these developments.

In the remainder of the Introduction we will elaborate in greater detail on the relevant aspects of tau Physics that are not treated in later chapters and on QCD and our limitations when implementing its solutions in Hadron Physics at low and intermediate energies. After that, we will summarize some of the capital ideas underlying out theoretical framework concerning $EFTs$, Chiral Perturbation Theory, the large number of colours limit of QCD and Resonance Chiral Theory itself. We will finish by enumerating the different chapters of this Thesis.

2.2 τ Physics

We begin with a short introduction to tau physics that will allow us to contextualize adequately this work: The τ lepton is a member of the third generation which decays into particles belonging to the first two and including light flavours, in addition to its neutrino, ν_τ. This is the reason why tau physics could give us useful hints in order to understand why there are (at least three) lepton and quark copies that only differ by their masses [8] (Table 2.2):

Generation	quarks	m_q	leptons	m_l
1	d	$3.5 \leftrightarrow 6.0$ MeV	e^-	~ 0.5110 MeV
	u	$1.5 \leftrightarrow 3.3$ MeV	ν_e	< 2 eV
2	s	$70 \leftrightarrow 130$ MeV	μ^-	~ 105.7 MeV
	c	$1.16 \leftrightarrow 1.34$ GeV	ν_μ	< 0.19 MeV
3	b	$4.13 \leftrightarrow 4.37$ GeV	τ^-	~ 1.777 GeV
	t	$169 \leftrightarrow 175$ GeV	ν_τ	< 18.2 MeV

Table 2.1: Matter content of the SM. Quark masses correspond to the $\overline{MS}$ scheme with renormalization scale $\mu = m_q$ for heavy quarks (c, b) and $\mu = 2$ GeV for light quarks. For the latter the given value of m_q is an estimate for the so-called current quark mass. In the case of the t quark it comes from averaging Tevatron measurement but it does not include the recent global fit by $TEVEWWG$, see [8]. Neutrino masses are the so-called "effective masses": $m_{\nu_k}^{2\,eff} = \sum_i |U_{ki}|^2 m_{\nu_i}^2$. However, cosmological data allows to set a much lower bound [9] $\sum_k (m_{\nu_k}) < 0.67$ eV.

It seems reasonable that the heavier fermions will be more sensitive to the generation of fermion masses. Being the top quark too heavy to hadronize before decaying, b quark and τ lepton physics seems promising in this respect. Although the value of M_τ does not allow for decays into charmed mesons (containing a c quark), the τ is the only lepton massive enough to decay into hadrons and thus relate somehow

the (light) quark and lepton sectors.

The group led by M. L. Perl [10] discovered the τ in 1975. This constituted the first experimental evidence in favor of the existence of third generation particles and, consequently, the first indication that it was possible to accommodate within the SM CP violation [11], that had already been observed [12] in the neutral kaon system, through the Cabibbo, Kobayashi and Maskawa [11, 13] mixing matrix. Anyhow, this explanation is not enough to understand the enormous observed abundance of matter over antimatter in our Universe [9, 14, 15], which represents one of the indications for the existence of some type of new physics beyond the SM [1]. τ quantum numbers were established [20] almost simultaneously to the discovery of the next particle of its generation, the b quark [21]. The heaviest particle known so far, the top quark, was not detected until 1995 [22, 23].

In the following, I will summarize briefly the Physics one can learn from τ decays [24, 25, 26, 27, 28, 29].

First of all, these decays allow to verify the universality of electroweak currents, both neutral and charged. Within the SM, the easiest lepton τ decays are described by the following partial width [30, 31, 32]:

$$\Gamma(\tau^- \rightarrow \nu_\tau \, l^- \, \overline{\nu}_l) \, = \, \frac{G_F^2 \, M_\tau^5}{192 \, \pi^3} \, f\left(\frac{m_l^2}{M_\tau^2}\right) \, r_{EW}, \tag{2.1}$$

where $f(x) = 1 - 8x + 8x^3 - x^4 - 12x^2 \log x$ and r_{EW} includes the electroweak radiative corrections not incorporated in the Fermi constant, G_F, and the non-local structure of the W propagator, $r_{EW} \sim 0.9960$. Therefore, the ratio

$$\frac{\mathcal{B}(\tau \rightarrow e)}{\mathcal{B}(\tau \rightarrow \mu)} \, = \, \frac{f\left(\frac{m_e^2}{M_\tau^2}\right)}{f\left(\frac{m_\mu^2}{M_\tau^2}\right)} \tag{2.2}$$

is fixed and allows to verify the universality of the charged electroweak currents. The resulting restrictions are rather strong: $\sim 0.20\%$ for the e/μ ratio and $\sim 0.22\%$ for the ratios including the τ. The associated errors come from the current indetermination of ~ 0.3 MeV in M_τ. This uncertainty is even larger [33, 34] in the ratio among the branching ratio, BR, to leptons and the tau lifetime -that is fixed using the value for the Fermi constant extracted from the μ decay- (it appeared to the fifth power in. (2.1)), that will be improved substantially in $BES-III$ and $KEDR$ soon [35]. $KEDR$ foresees to reach a total error of 0.15 MeV and $BES-III$ of only 0.10 MeV. We will not discuss here the determination of the τ mass close to its production threshold [35].

In the SM, all leptons with the same electric charge have identical couplings to the Z boson. This has been verified at LEP and SLC for years. The precision

[1] The recent experimental results concerning the ratio of matter and antimatter galactic and extragalactic fluxes [16, 17, 18, 19] do not have -for the moment- an explanation universally accepted.

reached for the neutral current axial-vector couplings is even better than for the vectors [36]:

$$\frac{a_\mu}{a_e} = 1.0001(14), \quad \frac{v_\mu}{v_e} = 0.981(82); \quad \frac{a_\tau}{a_e} = 1.0019(15), \quad \frac{v_\tau}{v_e} = 0.964(32). \tag{2.3}$$

From $\tau^- \rightarrow \nu_\tau\, l^-\, \overline{\nu}_l$ it was also obtained an upper limit for the standard and non-standard couplings [37, 38, 39, 40, 41, 42] between left/right-handed (L/R) fermion currents: RR, LR , RL, LL; scalars, vectors and tensors (S, V, T). It is remarkable that the current limits do not allow to conclude that the transition is of the predicted type: $V - A$ [43]. Both these bounds and thoss on the '*Michel parameters*' [37] [2] will improve sizably in $BES - III$ [35, 44].

In the minimal SM with massless neutrinos, there is an additive lepton number that is conserved separately for each generation (the so-called lepton flavour number). Notwithstanding, and after the evidence of the neutrino oscillation $\nu_\mu \rightarrow \nu_e$ announced by $LSND$ [45, 46], the confirmation through the oscillation measurements published by SNO [47, 48] and Super-Kamiokande [49, 50] discards the former hypothesis of the minimal SM. There is therefore no doubt that this generation quantum number conservation is violated in processes involving neutrinos. Though the most natural thing would be that this also happens in processes with e, μ, τ, all current data are consistent with that conservation law in this lepton subsector. Despite the limits on lepton flavour violation coming from τ decays are improving every day ($br \leq 10^{-7}$) [51, 52, 53, 54, 55, 56, 57, 59, 58, 60, 61, 62, 63, 64, 65, 66] , they are still far than the existing limits in μ decays with analogous violation [25].

$FERMILAB$ in Chicago became a fundamental tool in the discovery of the other members of the third generation. There, the b quark was discovered in 1977, the top quark in 1994-5 (with the help of the valuable LEP prophecy, as I will explain) and, finally, the $DONUT$ experiment [67] succeeded in the discovery of the remaining particle, the tau neutrino, in 2000. In fact, the best direct limits on the neutrino mass, m_{ν_τ}, come from hadron τ decays [68]: $\tau^- \rightarrow \nu_\tau\, X^-$, where $X^- = (\pi\,\pi\,\pi)^-, (2K\,\pi)^-, (5\pi)^-$. Although -as it was already written- they are clearly superseded by the bounds coming from cosmological observations, our study might be able to improve the direct limits.

Besides, semileptonic τ decays are the ideal benchmark to study strong interaction effects in very clean conditions, since the electroweak part of the decay is controlled theoretically -to much more precision than the hadron uncertainties even taking the LO contribution- and it does not get polluted by the hadronization that the process involves. These decays probe the hadron matrix element of the left-handed charged current between the QCD vacuum and the final state hadrons, as it is represented in Figure 1.1. We will devote more attention to this topic, central in the Thesis, throughout the work.

[2] These parameters describe the phase-space distribution in the μ and τ lepton decays.

A direct test of QCD [69] can be made through the ratio

$$R_\tau \equiv \frac{\Gamma(\tau^- \to \nu_\tau \,\text{hadrones}\,(\gamma))}{\Gamma(\tau^- \to \nu_\tau\, e^-\, \nu_e\,(\gamma))} = R_{\tau,V} + R_{\tau,A} + R_{\tau,S}\,, \tag{2.4}$$

that splits the contributions from vector (V) and axial-vector (A) currents corresponding to an even/odd number of final-state pions from those with an odd number of kaons (S is short for strangeness changing processes). Given channels (like $KK\pi$) can not be associated *a priori* to V or A current. In this case, it is specially important to consider a study as ours in order to know the relative contributions of each one to the partial width of that channel.

The theoretical prediction requires the appropriate two-point correlation functions of left-handed (LH) quark currents: $L^\mu_{ij} = \bar\psi_j \gamma^\mu (1-\gamma_5)\psi_i$, $(i,j = u,d,s)$:

$$\Pi^{\mu\nu}_{ij}(q) \equiv i \int d^4x\, e^{iqx}\, \langle 0|T(L^\mu_{ij}(x) L^\nu_{ij}(0)^\dagger)|0\rangle = \left(-g^{\mu\nu}q^2 + q^\mu q^\nu\right)\, \Pi^{(1)}_{ij}(q^2) + q^\mu q^\nu\, \Pi^{(0)}_{ij}(q^2)\,. \tag{2.5}$$

Using the property of analyticity, R_τ can be written as a contour integral in the complex s-plane, where the circuit is followed counterclockwise around a circle of radius $|s| = M_\tau^2$ centered at the origin:

$$R_\tau = 6\pi i \oint_{|s|=M_\tau^2} \frac{ds}{M_\tau^2} \left(1 - \frac{s}{M_\tau^2}\right)^2 \left[\left(1 + 2\frac{s}{M_\tau^2}\right)\Pi^{(0+1)}(s) - 2\frac{s}{M_\tau^2}\Pi^{(0)}(s)\right]\,, \tag{2.6}$$

where $\Pi^{(J)}(s) \equiv |V_{ud}|^2\, \Pi^{(J)}_{ud}(s) + |V_{us}|^2\, \Pi^{(J)}_{us}(s)$. In (2.6) one needs to know the correlators for complex $s \sim M_\tau^2$ only, that is larger than the scale associated to non-perturbative effects. Using the Operator Product Expansion, OPE [70, 71, 72]) to evaluate the contour integral, R_τ can be written as an expansion in powers of $1/M_\tau^2$.

Therefore, the theoretical prediction of $R_{\tau,V+A}$ can be written as follows [73]:

$$R_{\tau,V+A} = N_C\, |V_{ud}|^2\, S_{EW}\, (1 + \delta'_{EW} + \delta_P + \delta_{NP})\,, \tag{2.7}$$

where $N_C = 3$ is the number of colours. S_{EW} and δ'_{EW} contain the known electroweak corrections to leading and subleading orders in the logarithmic approximation. One can show and check that the non-perturbative corrections are small [73]. The leading correction ($\sim 20\%$) comes from the purely perturbative QCD correction, δ_P, that is known up to $\mathcal{O}\,(\alpha_S^4)$ [73, 74] and includes a resummation of the most relevant effects at higher orders [30, 31, 32, 74, 75, 76, 77]. The final result [29, 78, 79, 80] turns out to be extremely sensitive to the $\alpha_s(M_\tau^2)$ value, allowing to determine very precisely the QCD coupling that - in the $\overline{MS}$ scheme- is [81] [3]:

$$\alpha_s(M_\tau^2) = 0.342 \pm 0.012\,. \tag{2.8}$$

When one uses the Renormalization Group Equations, RGE, to run this value up to the Z scale [82] one gets:

$$\alpha_s(M_Z^2) = 0.1213 \pm 0.0014\,, \tag{2.9}$$

[3] See in this reference all works employed in this determination.

while the value obtained in hadronic Z-boson decays [8] is

$$\alpha_s(M_Z^2) \,=\, 0.1176 \pm 0.0020\,. \tag{2.10}$$

Therefore, there is agreement between the extraction from hadron tau decays and the direct measurement at the Z peak, even with better precision in the first case. This provides a beautiful test of the change of the QCD coupling with the scale, that is, a significant experimental test of *asymptotic freedom*.

A comment with respect to the reliability of the errors in the result (2.8) is in order. This study assumes that the quark-hadron duality [83] is realized. Its violations [84] and the error induced in the analysis that rely on it -like the determination of α_S- is being an active area of research [85, 86, 87, 88, 89] recently, after being ignored systematically for years. Although the last works point to an understimation of the error induced, this issue is not clear yet and one would need on one hand more realistic theoretical models to estimate these violations (essentially only one is used that is based on resonances and less frequently, another one that is instanton based; both developed by Shifman [84]) , and on the other hand more quality experimental data to quantify precisely this effect.

The separate measurement of the decay widths of $|\Delta S| = 0$ and $|\Delta S| = 1$ processes gives us the opportunity to be sensitive to the effect of $SU(3)$ flavour symmetry breaking induced by the strange quark mass. Specifically, this happens through the differences

$$\delta R_\tau^{kl} = \frac{R_{\tau,V+A}^{kl}}{|V_{ud}|^2} - \frac{R_{\tau,S}^{kl}}{|V_{us}|^2} \approx 24\frac{m_s^2(M_\tau^2)}{M_\tau^2}\Delta_{kl}(\alpha_S) - 48\pi^2\frac{\delta O_4}{M_\tau^4}Q_{kl}(\alpha_S)\,, \tag{2.11}$$

where the spectral moments R_τ^{kl} were introduced:

$$R_\tau^{kl} = \int_0^{M_\tau^2} \mathrm{d}s \left(1-\frac{s}{M_\tau^2}\right)^k \left(\frac{s}{M_\tau^2}\right)^l \frac{dR_\tau}{ds}\,. \tag{2.12}$$

The perturbative corrections $\Delta_{kl}(\alpha_S)$ and $Q_{kl}(\alpha_S)$ are known to $\mathcal{O}(\alpha_S^3)$ and $\mathcal{O}(\alpha_S^2)$, respectively [90, 91, 92] and δO_4, proportional to the $SU(3)$ breaking- since it is to the difference of the s and u quark condensates- are well determined [93]. Although in the future, with exceptional quality data, it would be possible to determine both $m_s(M_\tau)$ and $|V_{us}|$ simultaneously analizing the whole set of spectral moments, in the most recent determination [94] one fixes:

$$m_s(2\,\mathrm{GeV}) \,=\, 94 \pm 6\,\mathrm{MeV}\,, \tag{2.13}$$

-obtained with the latest lattice determinations and using QCD sum rules- in such a way that the more sensitive moment to $|V_{us}|$, with $kl = 00$, allows to extract [95]:

$$|V_{us}| = 0.2208 \pm 0.0033_{\mathrm{exp}} \pm 0.0009_{\mathrm{th}} \,=\, 0.2208 \pm 0.0034\,, \tag{2.14}$$

that can be competitive with the standard extraction of $|V_{us}|$ from K_{e3} decays [96] and with the new proposals made for this determination. Moreover, the error associated to this determination of $|V_{us}|$ can be reduced in the future since it is dominated

by the experimental uncertainty that would be reduced notably in forthcoming years thanks to B-factory data. As suggested, another improvement that one could make would consist in fitting simultaneously $|V_{us}|$ and m_s to a set of moments of the invariant mass distribution in hadron tau decays, that would provide even more precision in the extraction of both parameters.

Up to now, all experimental results on the τ are consistent with the SM. However, the analysis of B-factories data from $BaBar$ and $Belle$ -and future experiments in the latter- or facilities dedicated to $\tau - c$ production, as BES are promising in order to obtain more and more stringent verifications of the SM and explore the physics beyond it [4].

2.3 QCD: The theory of strong interaction

Next we will introduce briefly QCD in order to explain why it is not possible to solve the problems we deal with analytically and completely.

Deep inelastic scattering experiments at $SLAC$ [97, 98] allowed to conclude that the protons were not punctual particles. Instead, they have substructure made up of particles with fractional electric charge (*quarks*). Although these quarks had been predicted theoretically while trying to find a scheme to clasify the large amount of mesons observed during the '60s -first [99, 100]- and when trying to understand how to apply the quantum statistics to all of them, and especially to the spin 3/2 baryons -later on [101]-, it was not clear that their existence went beyond a mathematical concept and all subsequent experiments failed in their attempt to isolate them as free particles. The two main features of strong interaction had manifested: asymptotic freedom at high energies and confinement of quarks in hadrons at low energies.

Different formal studies of non-abelian gauge theories [102, 103] showed the different UV and IR behaviours of this theory could be explained in terms of a non-conmuting algebra. Later on, the evidence that the baryon Δ^{++} existed led to the conclusion that there had to exist an additional quantum number -called colour- through the conservation of the Spin-Statistics theorem, and motivated the effort of the Scientific community that finally brought as a result the simultaneous explanation of all abovementioned phenomena through the picture presented by Fritzsch, Gell-Mann and Leutwyler [2], who identified $SU(3)$ - 3 being the number of different colours a quark can have- as the gauge group, basis for the construction of QCD. The theory remains thus invariant under local transformations of the $SU(3)$ colour group. There are a number of theoretical and experimental evidences supporting this picture [104].

The local non-abelian gauge symmetry $SU(N_C)$ for n_f (number of flavours) quark

[4] In the Chapter 5 we explain the importance of hadron τ decays in order to find out what the scalar sector of the SM is and eventually to determine the mass of a light Higgs.

matter fields [5] determines the QCD Lagrangian, directly incorporating the interaction of these with the gluon gauge fields and the selfinteractions among these gluons. The QCD Lagrangian is:

$$\begin{aligned}
&\mathcal{L}_{QCD} = \overline{q}\,(i\not{D} - \mathcal{M})\,q - \frac{1}{4}G^a_{\mu\nu}G^{\mu\nu}_a + \mathcal{L}_{\mathcal{GF}+\mathcal{FP}}\,,\\
&D_\mu = \partial_\mu - ig_s G^a_\mu \frac{\lambda_a}{2}\,,\\
&G^a_{\mu\nu} = \partial_\mu G^a_\nu - \partial_\nu G^a_\mu + g_s f^{abc} G^b_\mu G^c_\nu,
\end{aligned} \tag{2.15}$$

where $a = 1, \ldots, 8$, G^a_μ are the gluon fields and g_s is the strong coupling constant. The quark field q is a column vector with n_f components in flavour space, $\mathcal{M}$ represents the quark mass matrix in flavour space and it is given by $\mathcal{M} = \text{diag}\left(m_1, \ldots, m_{n_f}\right)$, where m_i are the different quark masses: m_u, m_d, m_c, m_s, m_t, m_b for $n_f = 6$ within the SM, parameters whose value is not restricted by symmetry. As we see, the gauge symmetry forbides a non-vanishing mass for the gluons and their couplings are universal, irrespective of flavour. The matrices $\frac{\lambda^a}{2}$ are the $SU(3)$ generators in the fundamental representation, normalized as $\text{Tr}\left(\frac{\lambda^a}{2}\frac{\lambda^b}{2}\right) = \frac{1}{2}\delta_{ab}$ and f^{abc} are the structure constants of the gauge group, $SU(N_C)$. Finally, the Fadeev-Popov term [105], $\mathcal{L}_{\mathcal{GF}+\mathcal{FP}}$, includes the anti-hermitian Lagrangian introducing the ghost fields and the gauge-fixing term:

$$\begin{aligned}
&\mathcal{L}_{\mathcal{GF}} = -\frac{1}{2\xi}\,(\partial^\mu G^a_\mu)(\partial_\nu G^\nu_a)\,,\\
&\mathcal{L}_{\mathcal{FP}} = -\partial_\mu\overline{\phi}_a D^\mu\phi^a\,,\;\; D^\mu\phi^a \equiv \partial^\mu\phi^a - g_s f^{abc}\phi_b\,G^\mu_c\,,
\end{aligned} \tag{2.16}$$

where ξ is the gauge parameter, and $\overline{\phi}^a$ (a = 1, ... , N_C^2-1) is a set of scalar, hermitian, massless and anticonmuting fields. The covariant derivative, $D^\mu\phi^a$, contains the needed coupling between ghost and gluon fields and $\mathcal{L}_{\mathcal{FP}}$ is antihermitian, as it must, in order to introduce a explicit unitarity violation cancelling the non-physical probabilities corresponding to the longitudinal polarizations of gluons and restore the fundamental property of unitarity to the physical observables that are finally obtained. A very pedagogical explanation of this can be found in Ref. [104]. We do not discuss here the so-called θ term [106], invariant under $SU(N_C)$ and CP violating if there is not any massless quark. The most precise experiments do not indicate any CP violation in strong interaction processes. This allegged violation would manifest, for instance, in a non-vanishing neutron dipole electric moment. The experimental bound [8] is nine orders of magnitude smaller than a natural theoretical value.

The running of the coupling constant with the energy is behind the property of asymptotic freedom and seems to point to confinement as a natural consequence.

[5] The gauge group fixes the bosons content -mediators of the theory- but it does not for the matter fields: its representation and number of copies is something that must be inferred from experimental data.

The coupling g_s that appears in the QCD Lagrangian (2.15) receives quantum corrections [104] that, at one loop, are given by the diagrams in Fig. 1.2.

The β_{QCD} function is defined through the use of the Renormalization Group Equations, RGE [6]). At one loop they are given by [113, 114, 115, 116, 117]:

$$\beta_{QCD} \,=\, \mu\frac{\partial g_s}{\partial \mu} \,=\, -\left(11-\frac{2n_f}{3}\right)\frac{g_s^3}{16\pi^2}\,, \tag{2.17}$$

so that -at this order in the expansion-, is negative for $n_f \leq 16$. RGE imply that the renormalized coupling varies with the energy, so-called *running coupling*. Being $\beta_{QCD} \leq 0$, this will result in the decreasing of the renormalized coupling, g_s^R, when increasing the energy; that is, in asymptotic freedom.

We have implicitly assumed that the one-loop computation gives a reliable approach. When speaking about asymptotic behaviour this is the case, just remember (2.8), (2.10). In fact, the computations at (N)NNLO [118, 119] support this reasoning.

Integrating the equation (2.17) we find:

$$\alpha_s(q^2) \,=\, \frac{12\pi}{(33-2n_f)\log(q^2/\Lambda^2_{QCD})}\,, \tag{2.18}$$

where $\alpha_s \,\equiv\, g_s/4\pi$ has been defined. This equation depicts how the strong (renormalized) coupling running depends just on the QCD-scale, Λ_{QCD}, defined in terms of the renormalized coupling value at some renormalization scale, μ, and μ itself by:

$$\log(\Lambda^2_{QCD}) \,=\, \log\mu^2 \,-\, \frac{12\pi}{\alpha_s(\mu^2)(33-2n_f)}\,. \tag{2.19}$$

RGE and the experimental tests of them seem -(2.8), (2.10)- to be in agreement with a very strong color interaction at low energies that can cause confinement. There is an easy intuitive picture of this phenomenon: when splitting two electric charges, the strength of the mutual interaction decreases (is screened) by the creation of dipoles between them. This effect corresponds to the term with $-2n_f$ in Eq. (2.17). In the case of colour charges, the different behaviour comes from the term including the 33 in that equation. Gluon selfinteractions cause anti-screening and finally, it is not possible to keep on separating the quark-antiquark pair since it is energetically favoured to create a new pair. In order to complete the intuitive analogy, one could compare this with magnets. When breaking one, there will always appear new ones, with oposed poles. It is impossible to isolate the magnetic monopole as it is isolating a colour charge.

[6] RGE [107, 108, 109, 110, 111, 112] are derived from the requirement that an observable can not depend on the arbitrary chosen renormalization scale and that the physics must be scale invariant. The last property implies that the Green functions have a well-defined behaviour under rescaling of the momenta appearing in them. This allows to relate the values of the renormalized quantities at different energies and also to calculate the anomalous dimensions, that modify the evolution with energy derived on dimensional grounds because of quantum effects.

More technically, the confining phase is defined in terms of the behaviour of the action of the Wilson loop [120], that corresponds to the path followed by a quark-antiquark pair in four dimensions between its creation and annihilation points. In a non-confining theory, the action of this loop would be proportional to its perimeter. However, in a confining theory, the loop action would grow with the area. Since the perimeter of two open lines is equal to its sum, while the area goes to infinity, in a non-confining theory it would be possible to split the pair; while in the confining it would not be so. Although Wilson loops were introduced in order to have a non-perturbative formulation of QCD and solve confinement, this has not been possible so far. Its influence -like many ideas that emerged trying to understand QCD- has been great, since it lead Polyakov [121] to formulate string theories in a modern way.

Despite of what has been said, there could be an experimental way to come close to confinement. So far we have always considered field theories at finite temperature and density. At the begining of the Universe both were so high that chiral symmetry would be broken there and quarks and gluons would not have the time to hadronize because of their incessant interactions. This framework is being investigated in heavy ion experiments to try shed some light on the problem of confinement.

In summary, quantum corrections make the strength of the interaction to change with the energy. In the case of QCD, it is very strong at low energies, so we will not be able to make a perturbative expansion in powers of the coupling constant and make useful computations in this way, because they will not converge since $\alpha_S \sim 1$. Aditionally, and due to confinement, one should find the way to relate the fundamental theory with quark, antiquark and gluon degrees of freedom with the mesons produced in hadron tau decays. In the next sections and chapters we will see that the solution to both problems comes together: when one finds the appropriate degrees of freedom, we will understand how to build a reliable and useful computation.

2.4 Quantum Effective Field Theories

The history of Physics is a history of the understanding of more and more numerous and diverse phenomena. In many cases, the understanding of the new does not invalidate the description of the already-known, that is obtained as a particular limiting case of the new theories, whose range is larger. Sometimes, the old theory can be regarded as en effective theory of the new one in a determined range of application of it.

Some examples can illustrate this: at the beginning of the XIX century a correct description of electrostatics was already achieved. Diverse experiments due to Ørsted, Ampère, Ohm and Faraday -among others- increased the number of phenomena to describe simultaneously including electrodynamics and magnetism with time-dependent fluxes. The whole set could be explained coherently through Maxwell equations. In them, the wave nature of light was described, showing it as an electromagnetic wave propagating at a given speed, c, that was a universal

constant of the theory. In the limit $c \to \infty$, one loses the Maxwell's displacement current. As a consequence, the old theory (Ampère's law) could be seen as a limiting case of the new one (Maxwell equations) when the appropriate parameter $(1/c)$ was considered to be small. Ampère's law can be considered as the first order in the expansion in $1/c$ of the so-called generalized Ampère's law that could be obtained from the Maxwell equations. It is thus an EFT of the former. In static phenomena a similar treatment, based on the complete Maxwell equations is unnecessary and Coulomb or Ampère's laws are enough, obviously.

Newtonian mechanics is valid for a large number of situations in our everyday life. Notwithstanding this is not the case in the world of the infinitely small or enormously fast. Quantum Mechanics generalizes it in the first case and Especial Relativity does it in the second. One of the fundamental hypothesis of the quantum theory is that the action is quantized in integer multiples of the Planck's constant $(\hbar)$, which allows to explain the emission blackbody spectra, for instance. The value of this constant in IS units is so small that it becomes macroscopically irrelevant. For this reason it makes sense that the limit $\hbar \to 0$ of the quantum theory will bring us back to the classical theory that is this way and EFT of the former. Nobody would resort to Quantum Mechanics to solve a macroscopic problem unless it is to illustrate an introductory lesson to the topic.

It can also be seen that classical Maxwell's electrodynamics is an EFT of Quantum Electrodynamics, QED, appropriate in the limit $\hbar \to 0$. The theory that we have seen before as fundamental, it is from this point of view an EFT of the next more fundamental theory. Again it is not necessary to solve the equation of motion of a macroscopic charged body in presence of an EM field using the quantum theory. From the practical point of view, $EFTs$ are more useful than the fundamental in its subsectors of applicability.

But for the case that we work for a theory *of everything* our theory will always be effective, and it will be better this way since one avoids complicating the problem without any need and the choice of variables is suitable to its description. We still need to justify that this effective theory would be a quantum field theory, (QFT).

The most common method of study of $QFTs$ is based in the use of perturbation theory in powers of the coupling constant, that must be small for every term in the expansion to be smaller than the previous one so that we can cut our expansion at a given order, because the perturbative series is not exactly summable. Such an expansion does not make sense in our case of hadron τ decays, for the value $\alpha_S \sim \mathcal{O}(1)$. Then, one has to find an alternative way to proceed.

In any case, it is convenient not to abandon $QFTs$, since their formalism guarranties that the observables will fulfill all requirements of a relativistic quantum theory (as it must be the theory describing the Physics of our elementary particles): microcausality (if two space-time points are separated spatially, whatsoever operators defined in them satisfy trivial commutation or anticommutation rules -depending on their statistics-), unitarity (the sum of all possible events is unity), analyticity (the functions of the fields must be complex-differentiable in the vicinity of every point of its domain) , Poincaré invariance (the symmetry group of Rel-

ativity), spin-statistics connexion theorem (Fermi-Dirac statistics for half-integer spin and Bose-Einstein for particles with integer spin) and cluster decomposition (ensuring the locality of the theory, since sufficiently far away regions behave independently).

Although we have seen that the techniques of $QFTs$ are highly desirable we must admit that they are not enough on their own, because if one incorporates these very general principles into the theory one would need a lot of experimental information to characterize a theory and therefore make predictions. As we have seen before it is convenient to use $EFTs$. Therefore, it will be natural and adequate to employ quantum $EFTs$ in our problem.

In order to formulate them we need to identify the relevant degrees of freedom and the expansion parameter. Both things will happen generally at the same time, as we will see. There will be a typical scale, Λ, separating active and passive degrees of freedom. Particles with $m \ll \Lambda$ will be kept in the action while the heavy fields with $M \gg \Lambda$ will be functionally integrated out. We will consider the interactions among the lightest states that will be organized in a power series in $1/\Lambda$. Since $m/\Lambda \ll 1$ the effect of every consecutive term will be less than the previous one and we will be able to cut the expansion at a given order. Besides, we will be able to control the error introduced estimating the contribution of the first omitted term from the expansion parameter and the known terms.

We will close the section stating Weinberg's definition of $EFTs$ [3]: if -for a given set of degrees of freedom- we apply perturbation theory with the most general Lagrangian consistent with the assumed symmetries we will obtain the most general S matrix elements -and therefore the observables that are obtained from them- that are consistent with analyticity, perturbative unitarity, cluster decomposition and the assumed symmetries.

We note that with respect to the most general formulation introduced before we are adding here the compromise with a choice of degrees of freedom and the assumption of the symmetries of the underlying theory. This approach will be reviewed later on, because it may be desirable to make a more elaborated approach including dynamical content of the underlying theory.

2.5 Chiral Perturbation Theory

We have highlighted the concept of symmetry. Symmetries have always been the key to understand physical phenomena. On one hand they are expressed with the greatest mathematical rigour, on the other end they allow -in some cases- approximations, that are at the core of almost any realistic computation.

Which is the symmetry that we can employ to build our effective theory? The answer is neither easy nor immediate. One could think in some property directly related to the gauge group of the theory, with the property of colour. Due to hadronization, the possible structures with vanishing total colour charge are im-

mediately fixed by the product of representations in group theory, since we know the representations of the gauge group (adjoint) and we have fixed that of matter (triplet and antitriplet for quarks and antiquarks, respectively). We can check that the mesons fulfill this condition, but we do not obtain anything useful in order to develop our EFT. Indeed, assuming confinement, we observe that letting N_C free is the only remaining possibility that we will consider next.

It will not be then a local gauge symmetry the one allowing us to built the EFT. Let us see which global symmetries has the strong interaction. We think first that in this Thesis we study processes that produce the lightest mesons: pions, kaons and etas. It is intuitive that the heavier quarks will not be active. Therefore, we consider the QCD Lagrangian for light flavours: u, d, s, $n_f = 3$ in (2.15). If we neglect in first approximation the masses of these quarks $m_u \sim m_d \sim m_s \sim 0$, the QCD Lagrangian is invariant under separate transformations of the RH and LH components of the quark fields, global transformations of the group $G \equiv SU(n_f)_L \otimes SU(n_f)_R$, the so-called chiral symmetry group.

Local symmetries determine the interaction -as in (2.15)-. There are two possibilities for globals symmetries: If both the Lagrangian and the vacuum are invariant under the group of transformations G then the symmetry is manifest in the particles spectrum. However, even if the Lagrangian is invariant under transformations belonging to G, the vacuum is not, then the spectra will reflect the symmetries of a certain subgroup H of G, where both the Lagrangian and the vacuum will be symmetric under transformations of H, but only the Lagrangian will be invariant under all the group G. One speaks in this case of spontaneous symmetry breakdown of the symmetry $G \to H$. We also know that we will have as many massless scalar particles (Goldstone bosons [122]) as broken generators. That is, the number of Goldstone bosons equals the difference between the number of generators in G and H.

If we restore to phenomenology we observe that the lightest mesons can be classified in multiplets ($n_f = 3$) of equal spin (J) and intrinsic parity (P), which corresponds to the representations of the group $SU(3)_V$. we also see that multiplets with opposite parity do not share mass: the vector multiplet ($J^P = 1^-$) is lighter than that of axial-vectors (1^+). and that of pseudoscalar mesons (0^-) is much lighter than the scalars (0^+) or than the spin 1 particles [7]. In Chapter 3 it is explained how these observations lead to the pattern of spontaneous breaking of the symmetry is $SU(3)_L \otimes SU(3)_R \to SU(3)_V$. There are $n_f^2 - 1 = 8$ broken generators, that would be the number of Goldstone bosons that we should observe. In fact, since the masses of the light quarks are small compared to the typical hadronization parameter, $\Lambda_{\chi SB} \sim 1$GeV, but not zero, we have in addition to the spontaneous breaking of the symmetry a explicit breaking of it because $m_l \neq 0$, $m_l = m_u$, m_d, m_s. That is why we observe 8 particles with small but nonvanishing mass that we call pseudo-Goldstone bosons, *pGbs*, (for his origin in the spontaneous breaking of the symmetry and his mass in the explicit breaking of it). These are the pions, kaons and etas

[7] We will call resonances all light-flavoured particles heavier than those belonging to the lightest multiplet 0^-.

detected in our semileptonic tau decays: $\pi^{\pm}, \pi^0, \eta, K^{\pm}, K^0, \bar{K^0}$.

Now that we have the symmetry and our choice of degrees of freedom we have to worry about building the EFT Lagrangian that contains them conveniently. Weinberg's theorem ensures that having done that, the perturbative treatment of it will lead to the most general S-matrix elements in a consistent way. The formalism that allows to build effective Lagrangians for symmetry groups that have been broken spontaneously is due to Callan, Coleman, Wess and Zumino [123, 124]. Its application to low-energy QCD will allow us to write an EFT describing the interaction among pseudo-Goldstone bosons. Moreover, since there is an energy gap between these particles and the next heavier ones, the effect of these heavier modes will be small and will allow to build an EFT containing only these modes, Chiral Perturbation Theory, χPT [4, 5].

This theory has a natural expansion parameter in the ratio between masses or momenta of the pseudo-Goldstone bosons over the scale $\Lambda_{\chi SB}$, that will be much less than unity. All the initial problems are thus solved: χPT is an EFT built upon symmetries of QCD in a specific subset of it (light flavours in low-energy processes where the only products are *pGbs* and chiral symmetry is a good approximation) and with a expansion parameter that permits to do perturbation theory. Since, $M_\tau \sim 1.8$ GeV, the resonances could be active degrees of freedom, so that we will have to enlarge χPT to higher energies and include new degrees of freedom. Unfortunately, in this case it will be more complicated to proceed through the previous steps to build the theory, as we will see.

2.6 QCD in the limit of a large number of coulours

When we incorporate heavier particles the counting is broken, since the masses and momenta of these new degrees of freedom are of the same or higher order than $\Lambda_{\chi SB}$, in such a way that its ratio is no longer a good expansion parameter of the theory. We have another difficulty: there is no longer a large and well-defined energy gap separating the particles that are active degrees of freedom of the theory from those who will be integrated out because they are not. We will see that a solution to both problems can arrive from considering the large number of colours limit of QCD [125, 126, 127]. Anyhow, we should point out that as opposed to the low-energy sector with χPT, it is not known how to build an EFT dual to QCD in the intermediate energy range. The limit $N_C \to \infty$ is a tool that will allow to understand which are the dominant contributions and which are not important -among all allowed by symmetries- in our Lagrangian.

't Hooft suggested considering QCD in the limit when the number of colours of the gauge group goes to infinity [125]. His motivation was achieving a simpler theory that still kept some resemblance with the original one and from which one could derive qualitative properties -hopefully also quantitative- of the underlying one. In this limit QCD is exactly soluble in two dimensions [126], but not in four. Still, if

we assume that the theory is confining, a number of experimental features of QCD can be derived, which suggests that this construction is a good approximation to nature. Among them we will highlight for the moment that:
- In the $N_C \to \infty$ limit mesons are free, stable (they do not decay) and do not interact among themselves. Meson masses have a smooth limit and there are infinite: a tower of excitations per each set of quantum numbers.
- At first order in the expansion in $1/N_C$ meson dynamics described by tree level diagrams obtained with an effective local Lagrangian whose degrees of freedom are mesons, as it was discussed in the Weinberg's view of χPT.

At this point one can observe that there is a certain internal contradiction between the construction of $EFTs$ à la Weinberg and the expansion in $1/N_C$ for QCD that should be solved in some way: on the one hand Weinberg's view is to define the particle content and the symmetries and then to build the most general Lagrangian consistent with the assumed symmetries and it guarantees that we will obtain the most general results through a perturbative approach. The problem is that the introduction of the resonances invalidates the former expansion parameter, that was successful for χPT .

On the other side, the large number of colours limit of QCD can help us to organize an expansion in $1/N_C$, but it contradicts the ideas in the previous paragraph since one of its conclusions at lowest order is that we can not fix a priori the particle content of the EFT, for the consistency of the expansion we have to have infinite copies of every type of resonance.

Because of that we have two possibilities:
- Either we forget the requirement for the Weinberg's formulation of making a suitable choice of degrees of freedom for the energy range we are considering and we include the spectra demanded by the limit $N_C \to \infty$.
- Or we include the phenomenological spectra and depart from the $1/N_C$ counting.

One could think that incorporating subleading effects in $1/N_C$ we may be able to get the measured spectra. This idea can not become a reality for the moment because of the nature of the $1/N_C$ expansion in QCD. It is true that a given order in α_S there is a definite number of diagrams, and that they can be computed and their effects resummed, but this is not at all the case in $1/N_C$: at every order there are infinite diagrams, and nobody has been able to think of a mechanism able to study this question. In the framework of $EFTs$ based on this expansion there are studies investigating the NLO in $1/N_C$.

Additionally, one can recall that the Weinberg's approach does not include any type of dynamical information on the underlying theory: this is the price to pay for its generality. In our case we will see that a theory with pseudo-Goldstone degrees of freedom and resonances, that respects the symmetries of low-energy QCD, and therefore reproduces χPT at low momenta, based in the limit $N_C \to \infty$, is not compatible with the known asymptotic behaviour of QCD at high-energies. Since we want our theory to work up to some $E \sim 2$ GeV and at these energies perturbative QCD is already reliable, this must not happen. Then, the theory we need will require dynamical information from QCD -this will allow it lo link the chiral and

perturbative regimes in the sector of light-flavoured mesons- and, either renounce to the choice of the physical final states as degrees of freedom or to model the expansion in $1/N_C$. This is discussed in the next section.

2.7 Resonance Chiral Theory

Resonance Chiral Theory, $R\chi T$ [6, 7], includes the pseudo-Goldstone bosons and the resonances as active degrees of freedom of the theory and requires general properties of $QFTs$ and the invariance under C and P QCD has. Their fundamental features are sketched in the following.

The low-energy limit of $R\chi T$ must be χPT. This property has been used to predict systematically the $LECs$ of χPT in terms of masses and couplings of the resonances when integrating these ones out of the action, at the chiral orders $\mathcal{O}(p^4)$ [6] and $\mathcal{O}(p^6)$ [128] in the even-intrinsic parity sector, with $N_C \to \infty$ and requiring the QCD high-energy behaviour.

The χPT Lagrangian includes the octet of pseudo-Goldstone bosons. When extending χPT, $R\chi T$ incorporates the resonances as active degrees of freedom that are included in nonets, since octet and singlet of a $SU(N_C = 3)$ group merge into a nonet for $N_C \to \infty$. The χPT Lagrangian is built using the approximate chiral symmetry of massless QCD. After that, the spontaneous and explicit symmetry breaking is incorporated in exactly the same way as it happens in QCD. The nonets of resonances are added requiring the general properties and invariance under C and P and the structure of the operators is determined by chiral symmetry. At first order in the expansion in $1/N_C$ the terms with more than a trace and the loops are suppressed. The first property permits to postpone some terms allowed by the symmetries of the Lagrangian and the second one its use at tree level, as it was already explained.

We remark that the theory determined by symmetries does not share yet some of the known properties of QCD at high energies yet. Therefore, one must match the theory with asymptotic QCD at the level of Green functions and/or form factors. The application of these properties determines a series of relations between the couplings of the theory that allows it to be predictive with less experimental information than otherwise. In this Thesis we obtain relations of this type on the form factors in two different type of processes that we will confront to those found in two- and three-point Green functions where the same couplings appear [8]. The nice UV behaviour forbids terms with a lot of derivatives, what helps us to limit the number of operators in the Lagrangian, since the counting that worked in χPT is now broken. The situation is not that easy, as we will comment later on, because consistency conditions may require the introduction of operators with more derivatives and some non-trivial relations among their couplings. Generally speaking, we

[8] There are not computations within $R\chi T$ of four-point Green functions, whose short-distance relations we could confront to ours.

do not include terms with a lot of derivatives because this would require fine-tuned relations to ensure the required cancellations needed at large momenta. In many cases the phenomenological success is the support of our approach.

There is an inconsistency between Weinberg's approach and the strict limit $N_C \to \infty$, but to our knowledge, there is no known way of implementing the infinite tower of resonances in a model independent way. Then, it seems reasonable to start studying easy processes with the minimum number of degrees of freedom involved. As we get more and more control in this approximation (or the data get more and more precise) we will be able to include more states if needed. This approach is practical in order to estimate the different coefficients of the theory and it also respects the goal of a good physical description, trying to do it in terms of the least number of variables.

Finally, our phenomenological study can not avoid introducing some properties that are higher orders in the $1/N_C$ expansion. In the energy range where the taus decay, resonances reach their on-mass condition and do indeed resonate due to their width, typically lower than its mass. Widths are a subleading effect. We will include them consistently within $R\chi T$, as we will see.

2.8 Organization of the Thesis

As it has been said, our study adopts the approach of $EFTs$. For this reason we introduce its basics in Chapter 3. Three are the cornerstones of our work on the theory side: on the hand ensuring the right limit at low energies, ruled by χPT. On the other, the large number of colours (N_C) limit of QCD applied to EFT with hadron degrees of freedom, in our case $R\chi T$. And finally, to warrant a behaviour at high energies in agreement with QCD for the different form factors. The first and second question are considered in Chapters 3 and 4, respectively, whereas the third one is introduced in Section 4.5 and applied in any particular application of the theory considered in later chapters, that are preceded by a brief summary of the theoretical studies undertaken and an overview on the essentials of exclusive hadron tau decays (Chapter 5). The applications that we consider are: hadron decays into three pions (Chapter 6) and with two kaons and a pion (Chapter 7). We also include the decays including η mesons (Chapter 8) and the radiative decays of the tau with a single meson $\tau \to P^- \gamma \nu_\tau$, where $P = \pi$, K, in Chapter 9. With all of them we will improve exceptionally the control on the parameters of the resonance Lagrangian participating in the considered processes, both in the vector and in the axial-vector current and, therefore we know better how to describe, in a theoretically sound way based on $EFTs$ and the symmetries of QCD, these τ decays. We will be able to take advantage of all these findings in the future, applying them to more complex processes. The thesis ends with the general conclusions on the work done.

Chapter 3

Effective Field Theories: Chiral Perturbation Theory

3.1 Introduction

Effective Field Theories are built upon two seemingly contradictory deep roots: the idea of symmetry and the usefulness of making justified approximations. That is because symmetry is linked to the mathematical structure behind and appears to be fundamental, while an approximation implicitly seems to assume some deviations from Nature. We will clarify in which context -that of $EFTs$- both concepts join together in a rigorous approximation.

It is not true that if one had the exact solution to the complete theory, no one would use the EFT instead. The EFT is more convenient in its domain of applicability because it uses the right variables and exploits the hierarchy of the problem. We will be more specific about this point later on.

Although the precise formulation of $EFTs$ has been reached in the last thirty years, the two main ideas named above are, in a sense, living within Physics for long. It is common lore that the choice of variables can make the problem easier. If not exactly realized in Nature symmetries are sometimes given at a quite approximate level and allow for a parameterization of the problem that exploits that and renders the computation doable (it is advisable to use cylindrical coordinates to solve the Laplace Equation in a tube-shaped cavity, for instance). At the same time, either analytically or numerically, one can work corrections to this exact solution by including the symmetry breaking as it happens in reality, or faithfully modeling it. We will see quite generally how these ideas of symmetry and approximation apply.

One of the longstanding motivations in Physics has been that of pursuing the so-called *theory of everything*. This theory would be almost useless because the energy scales involved would be orders of magnitude higher than the ones we can probe experimentally. That would be the situation for any theory that unifies Gravity with other forces, since its characteristic energy scale, the so-called Planck Mass ($M_{Pl} = (8\pi G)^{-1/2} \sim 10^{18}$ GeV), is outside our reach. Thus, this unification would be useless but from the point of view of the likely mathematical beauty. An EFT

description using just the active degrees of freedom in any specific setting is in order.

On the other hand, if we leave gravity aside, the situation changes: If there was exact unification of the SM gauge groups [129] -with maybe some others [130], adding extra particles [131], using small additional dimensions to reduce $E \sim M_{Pl}$ [132, 133, 134], etc.- at some energy scale ever accessible to experiments, then we would reaffirm our understanding on SM, gain more insight on some kind of Physics beyond it (BSM) discovered by that time and get a number of predictions testable in experiments.

Let us use the very well-known example of the hydrogen atom to explain how the relevant degrees of freedom arise naturally. A first description of the system is achieved by using the Schrödinger equation for the electron bounded to a proton by Coulomb's law. The only properties that count at this stage are the electron mass and charge (or, equivalently, the fine structure constant, $\alpha \equiv e^2/(4\pi) \sim 1/137$). It does not essentially matter that the proton mass is not infinite, because it is much heavier than the electron one. The spin 1/2 of the electron does not affect yet either. If one counts the mass scales that appear in the problem, one sees they are m_e and M_P, being $m_e/M_P \sim 5 \cdot 10^{-4}$. Any effect of $m_e/M_P \neq 0$ will be a $\sim 10^{-3}$ correction, at most. One can see that the leading interaction involving spin (between the electron spin and the electrons' orbital angular momentum) are also suppressed with respect to the leading Coulombic interaction. The general feature we may extract is that the characteristic energy scale of the problem (Λ) is set by the electron mass and the strength of the interaction: $\Lambda \sim m_e\alpha$, the typical momentum (or inverse of length scale, the familiar Bohr radius) of the system. Therefore, the relevant degrees of freedom will correspond to particles with energies much lower than this one ($m, E \ll \Lambda$): ultrasoft photons with energy of the order of $m_e\alpha^2$, that sets the scale of energy splittings between levels, the Rydberg (or inverse of characteristic times). On the other hand, particles with much higher energies ($M \gg \Lambda$) will influence tinily the spectrum and thus can be integrated out from the action. This will be the case of the proton or soft and hard photons. But also of the W-boson, what justifies that electroweak corrections to this QED bound state are marginal.

One has then the possibility of constructing the most general Lagrangian consistent with QED symmetries including interactions among the lightest states and one will be able to organize them efficiently as an expansion in powers of E/Λ. We have found through this example the general rules for building $EFTs$: identifying the relevant energy scale of the problem, integrating out the heavier modes and building the most general Lagrangian consistent with symmetries involving the light modes: a tower of interactions that one will conveniently organize in powers of E/Λ. The procedure rests on Weinberg's Theorem, that will be discussed in Section 3.2.

The fact that the heavier states can be integrated out (as explained in Section 3.3) does not mean that they do not leave any mark in the low-energy Physics. The effect of these states on the EFT is double: on the one side they pose symmetry requirements on the EFT [1], on the other hand they correct the values of the con-

[1]For instance, in the non-relativistic $EFTs$ the relativistic invariance of the fundamental theory implies relations between the $LECs$ in the EFT that are valid to all orders in the coupling constant.

stants specifying the dynamics of the low-Energy theory ($LECs$), that are different in the full and in the effective theory in case they enter in both [2], see Section 3.4.

If the underlying theory is weakly coupled at the scale Λ one is able to compute explicitly the values of the $LECs$. Otherwise, one must rely in lattice evaluations or fix them phenomenologically as discussed in Section 3.6. In the first case, the same coupling constant will serve as an expansion parameter to apply the perturbative techniques, while in the second one it may be difficult to find such a parameter.

One important feature of $EFTs$ mentioned above was that there is an infinite number of interacting terms in the EFT, which makes the theory non-renormalizable in the classical sense. However, this is not a problem once we understand that $EFTs$ add to the general characteristics of renormalizable theories the need of having a rule in order to estimate the size of these non-renormalizable terms. This will allow us to stop the expansion once we reach some desired maximum error associated to our computation. We will classify the terms in the Lagrangian according to some counting scheme that makes explicit the organization of all allowed interaction terms in powers of the expansion parameter. Then, at a given order, one will have infinites that will be renormalized by redefining the $LECs$ appearing at the next order in the expansion. If one regularizes using Dimensional Regularization (that preserves all symmetries of the theory in the renormalization procedure), renormalizability is assured since every infinite will be the coefficient of an operator respecting the symmetries and therefore already present in the effective Lagrangian at a higher order, determining an order-by-order renormalization. At the practical level, $EFTs$ are as renormalizable as those classically called that way. For a given asked accuracy we have to take into account terms in the expansion up to some order, that includes a finite number of terms, as in any renormalizable theory.

A general remark before closing this introductory section: It seems that $EFTs$ are the tool that solves everything and that is not true. The Hydrogen atom is a system with a well-defined hierarchy of scales and a non-relativistic nature. Then, the ratios E/Λ and v/c are two small magnitudes that work extremely well in the setting described above. Moreover, most of Particle Physics systems fulfill the non-trivial characteristic that there is a small number of quantities playing a role in the problem with some scaling among them. This allows (and suggests) an EFT approach. Even in the cases where the scaling is not so well defined or the expansion parameter is not that small it is an advisable tool. However, in Chemistry (or even more in Biology) there appear an enormous amount of unrelated energy scales of comparable magnitude. Then even the extremely simple approach applied to the Hydrogen atom as first step will lead in an EFT study to too cumbersome expressions to make any sense out of them. We are lucky that these techniques can be applied in Physics.

In the remainder of the chapter we will be more precise on the ideas sketched above. We have made extensive use of Refs. [135, 136, 137, 138, 139, 140, 141, 142] in order to prepare this part.

[2] This does not happen when the degrees of freedom are different in the fundamental and effective theory.

3.2 Validity of $EFTs$: Weinberg's Theorem

We will precise now the formulation of $EFTs$ à la Weinberg. It can be stated as a theorem [3]:

For a given set of asymptotic states, perturbation theory with the most general Lagrangian containing all terms allowed by the assumed symmetries will yield the most general S matrix elements consistent with analyticity, perturbative unitarity, cluster decomposition and the assumed symmetries.

$EFTs$ describe the physics at low energies, this defined with respect to some energy scale, Λ, characteristic of higher energy processes. Heavier states with $M \gtrsim \Lambda$ are integrated out from the action and the relevant degrees of freedom are those with masses $m << \Lambda$. There is a well defined ordering in powers of E/Λ for the infinite interactions among the light states one gets.

The view on renormalizability of $QFTs$ has changed through the years. For much time, it was claimed that for a QFT to be renormalizable one needed that the Lagrangian contained only terms with dimension less or equal than that of the space-time, D. If operators of any dimension were allowed, one would need an infinite number of counterterms to absorb all the infinites and consequently an infinite number of unknown parameters condemning the theory to have no predictive power. Since the EFT has an infinite number of terms ($\mathcal{L}_{eff} = \mathcal{L}_{\leq D} + \mathcal{L}_{D+1} + ...$, where only the first one is renormalizable in the classical sense) the conclusion seems devastating.

We have explained at the end of the previous section that the infinite number of terms in the EFT will not cause any problem with respect to the renormalization of the theory. For a definite number of powers in the (E/Λ) expansion, the symmetries of the EFT allow only a finite number of operators in the Lagrangian. Consequently, there will be a finite number of counterterms that renormalize the theory at this order.

In addition to the problem of no predictivity, one could think that as the energy of the process increases this tower of classically non-renormalizable interactions will give rise to a wild violation of unitarity at high energies. To clarify that this is not the case, we will classify the Quantum Field Theories according to their sensitivity to high energy [143]:

1. Asymptotically free theories: Nothing in them signals a limiting energy beyond which they can no longer be employed.

2. Ultraviolet unstable theories: The theories themselves report about a limit energy range of applicability. This statement will be illustrated with several examples in section 3.5.

$EFTs$ belong to the second group. The main difference with respect to the first ones comes from the appearance of new $LECs$ at every order in the perturbative

expansion -that is not simply an expansion in the number of loops, as we will see-. It makes no sense to go further and further in this expansion indefinitely. Every new order in the series in (E/Λ) is intended to achieve a more detailed description. The accuracy reached with every new term goes as $\epsilon \lesssim \left(\frac{E}{\Lambda}\right)^{D_i^{max}-4}$, where D_i^{max} is the highest dimension of all operators included [3]. Once we demand a limited precision, we know at which order in the expansion we can stop. Moreover, if we desire to enlarge the applicability of the EFT to higher energy physics the way out is not to include operators of higher and higher dimension, because as soon as $E \sim M_1$ -being M_1 the mass of the lightest initially integrated out particle- the Weinberg's theorem tells that the right procedure is to include it in the Lagrangian as an active field. This happens usually, and there is a formal way to deal with this successive incorporation of particles, that we will describe in the next section.

In QCD, confinement forbids quarks and gluons to be asymptotic states. Weinberg's theorem guarantees that writing out the most general Lagrangian in terms of hadrons -that can be thought as active degrees of freedom in a given subset of energies- consistent with the needed symmetries and respecting all the other stated conditions will bring us the most general observables consistent with the assumed symmetries and general properties of $QFTs$.

3.3 Integrating out the heavy modes

We will explain here more formally the integration of heavy modes from the action that has been anticipated in the previous sections. We will use the path integral formalism and assume that the theory at high energies is known. The effective action Γ_{eff}, will be written only in terms of the light modes and encodes all the information at low energies, where it yields the same S matrix elements than the fundamental theory by construction. S_{eff} reads

$$e^{i\,S_{\text{eff}}[\Phi_l]} \;=\; \int [\mathrm{d}\Phi_h]\; e^{iS[\Phi_l,\Phi_h]}\,, \tag{3.1}$$

where Φ_l and Φ_h refer to the light and heavy fields respectively and $S[\Phi_l,\Phi_h]$ is the action of the underlying theory where both modes are dynamical. The effective Lagrangian gets defined through

$$S_{\text{eff}}[\Phi_l] \;=\; \int \mathrm{d}^4x\; \mathcal{L}_{\text{eff}}[\Phi_l]\,. \tag{3.2}$$

The effective action $S_{\text{eff}}[\Phi_l]$ can be computed using the saddle point technique. The heavy field Φ_h is expanded around some field configuration $\overline{\Phi}_h$ as follows ($\Delta\Phi_h(x) \equiv$

[3] There will be quantum corrections to this estimate, that most of the time will be irrelevant. Anyway, the moral is that the error is essentially under control, as one would ask any theory for.

$\Phi_h(x) - \overline{\Phi}_h)$

$$S[\Phi_l,\Phi_h] = S[\Phi_l,\overline{\Phi}_h] + \int \mathrm{d}^4x \left.\frac{\delta S}{\delta\Phi_h(x)}\right|_{\Phi_h=\overline{\Phi}_h} \Delta\Phi_h(x) + \frac{1}{2}\int \mathrm{d}^4x\,\mathrm{d}^4y \left.\frac{\delta^2 S}{\delta\Phi_h(x)\delta\Phi_h(y)}\right|_{\Phi_h=\overline{\Phi}_h} \Delta\Phi_h(x)\Delta\Phi_h(y) + \dots . \quad (3.3)$$

$\overline{\Phi}_h$ is chosen so that the second term in the RHS of Eq. (3.3) vanishes to allow a (formal) Gaussian integration

$$\left.\frac{\delta S[\Phi_l,\Phi_h]}{\delta\Phi_h(x)}\right|_{\Phi_h=\overline{\Phi}_h} = 0\,. \quad (3.4)$$

With this choice Eq. (3.1) is

$$e^{i\,S_{\rm eff}[\Phi_l]} = e^{i\,S[\Phi_l,\overline{\Phi}_h]} \int [\mathrm{d}\Phi_h]\, e^{i\int \mathrm{d}^4x\,\mathrm{d}^4y\left\{\frac{1}{2}\Delta\Phi_h(x)\,A(x,y)\,\Delta\Phi_h(y)+\dots\right\}}\,, \quad (3.5)$$

where

$$A\,(x,y) \equiv \left.\frac{\delta^2 S}{\delta\Phi_h(x)\delta\Phi_h(y)}\right|_{\Phi_h=\overline{\Phi}_h}\,. \quad (3.6)$$

We see from Eq. (3.5) that the first term corresponds to a tree level integration of the heavy field Φ_h. The power counting of the EFT will determine how the expansion is realized, as we will see in the case of χPT in Chapter 2.

Two comments are in order: The procedure is iterative; one can have a pair of $\{EFT$-fundamental theory$\}$ valid up to some energy scale Λ. Then, for $E > \Lambda$, some other mode may become active and the fundamental theory in the previous step will become the EFT in the next one. The other remark concerns the actual use of that integration. The general procedure outlined above can involve complicated or unfeasible calculations. This may happen because the degrees of freedom are different in both theories and there is no unambiguous way of relating both, or because a perturbative treatment is not applicable. In these situations one may restore to phenomenology or lattice evaluations to do the computations. In any case, it is always possible to obtain some information on $e^{i\,S_{\rm eff}[\Phi_l]}$ from symmetry constraints stemming from the fundamental theory.

3.4 Effect of heavy modes on low-energy Physics

We have stated in Section 3.1 that although the heavy modes are non-dynamical at low energies they have an impact in the $LECs$ of the theory when integrating them out following the method in Sect. 3.3 in going from the the fundamental theory to the effective one. We will see this general property at work in the case of χPT. There is again a theorem expressing this notion precisely, due to Appelquist and

Carazzone [144]:

For a given renormalizable theory whose particles belong to different energy scales, that does not suffer Spontaneous Symmetry Breaking and does not have chiral fermions; the only effects of the heavy particles of characteristic mass M in the physics of the light particles of masses around m at low energies either appear suppressed by inverse powers of M or through renormalization.

The question is immediate: Does it apply in general? Does it to QCD?

QCD is renormalizable [145, 146, 147, 148] and we have discussed in the introduction that there are six quarks with masses spanning four orders of magnitude. This suggests that one could very likely have hadrons belonging to different energy scales, and also dynamical gluons with very different energy-momentum. In principle, the first condition of the theorem does not seem impossible to meet, although one should revise this assumption in any particular scenario. Moreover there is no spontaneous symmetry breaking associated to the QCD vacuum. Finally its fermions are not chiral: left-handed and right-handed fermions do not couple differently to the gauge color group. All conditions of the Appelquist-Carazzone theorem are *a priori* fulfilled.

3.5 Example

We will introduce an example of $EFTs$ in order to help us illustrate some general characteristics of $EFTs$ that have already been discussed and will be of use in the next sections. We will see how:

- An EFT indicates its border of applicability by itself.
- $EFTs$ help to understand the physics involved giving us some hints that point to the more fundamental theory to be scrutinized in future experiments.

Inspired by the coupling of the electromagnetic current to photons, Fermi [149] proposed as the basis of a theory of weak interactions a local current $\times$ current interaction among fermions that we can write -just for the lightest species- now as:

$$\mathcal{L} \,=\, -\frac{4G_F}{\sqrt{2}}\,\left[V_{us}V_{ud}^{*}\,\left(\overline{u}\gamma^{\mu}P_L s\right)\,\left(\overline{d}\gamma_{\mu}P_L u\right)\,+\,\left(\overline{e}\gamma^{\mu}P_L\nu_e\right)\,\left(\overline{\nu}_{\mu}\gamma_{\mu}P_L\mu\right)\right]\,+\,\mathcal{O}\left(\frac{1}{M_W^4}\right)\,, \tag{3.7}$$

where P_L is the projector over left-handed states.

Eq. (3.7) and dimensional analysis imply that $\sigma\left(\nu_{\mu}\,e^{-}\,\rightarrow\,\mu^{-}\,\nu_e\right)$ must diverge in the ultraviolet as $G_F^2\,s$, which signals again a more general theory, the SM.

Is this the end of the story? Coming back to the hierarchy problem, see Table 1, there is a dimension five operator (thus, suppressed at low energies by the high-energy scale) that respects all gauge symmetries of the SM and that will give mass to Majorana neutrinos [150]:

$$-\,\frac{1}{2\Lambda}\left(\widetilde{\overline{\ell}}_L\,\varphi\right)\,F\,\left(\widetilde{\varphi}^{\dagger}\,\ell_L\right)\,+\,\text{h.c.} \tag{3.8}$$

through diagonalization of the mass-term [4]. Thus, $M^{\rm Majorana} \equiv \frac{v^2}{\Lambda} F$, where v^2 is related to the electroweak scale and Λ to the new Physics scale. The important lesson we learn from this particular example is that regarding the SM as an EFT we can go on learning about a more fundamental theory. To mention a recent example, let us note that these ideas have also been applied under the hypothesis of minimal flavor violation [151].

The same physical predictions in the full and effective theories should be expected around the heavy-threshold region. Thus, both descriptions are related through a so-called matching condition: the two theories (with and without the heavy field) should give the same S matrix elements for processes involving light particles.

Until the matching conditions have not been taken into account, one is not dealing with the effective field theory, that is, the matching procedure is a fundamental step to develop effective approaches. We will illustrate how this works with the Fermi theory, see Eq. (3.7).

When the W-boson momentum is small compared to its mass, its propagator can be Taylor-expanded to give:

$$\frac{1}{p^2 \, - \, M_W^2} \, = \, -\frac{1}{M_W^2} \left(1 \, + \, \frac{p^2}{M_W^2} \, + \, \frac{p^4}{M_W^4} \, + \, \ldots \right) , \tag{3.9}$$

and the lowest order in this expansion can be applied to the SM tree-level result for $u\,s \, \to \, d\,u$ in the unitary gauge:

$$\mathcal{A} \, = \, \left(\frac{i\,g}{\sqrt{2}} \right)^2 \, V_{us} V_{ud}^* \, \left(\overline{u} \gamma^\mu P_L s \right) \, \left(\overline{d} \gamma^\nu P_L u \right) \, \left(\frac{-i\,g_{\mu\nu}}{p^2 - M_W^2} \right) , \tag{3.10}$$

to give:

$$\mathcal{A} \, = \, \left(\frac{i}{M_W^2} \right) \, \left(\frac{i\,g}{\sqrt{2}} \right)^2 \, V_{us} V_{ud}^* \, \left(\overline{u} \gamma^\mu P_L s \right) \, \left(\overline{d} \gamma_\mu P_L u \right) \, + \, \mathcal{O} \left(\frac{1}{M_W^4} \right) . \tag{3.11}$$

Comparing this to the amplitude obtained with Eq. (3.7) we can match both theories up to $\mathcal{O}\left(\frac{1}{M_W^4}\right)$ corrections by relating the corresponding coupling constants through the W mass:

$$\frac{G_F}{\sqrt{2}} \, = \, \frac{g^2}{8 M_W^2} \, . \tag{3.12}$$

Going further in the expansion of Eq. (3.9) will require to include additional higher-dimension operators in Eq. (3.7).

[4] Left-handed leptons are collected in the ℓs, φs include the Higgs field and F is, in general , non-diagonal in flavour space.

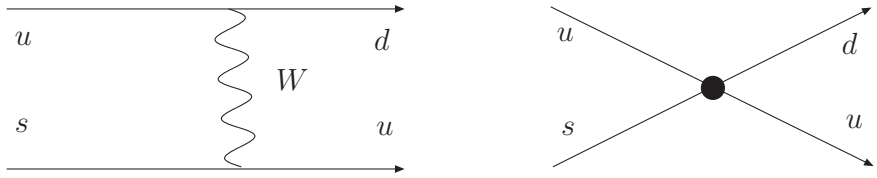

Figure 3.1: Feynman diagrams for the flavour changing charged current process $us \to du$ at lowest order: within the fundamental electroweak theory through W-exchange (left) and using Fermi's EFT (right). The effective local vertex is represented by the thick dot.

In this particular example the tree level matching is not trivial because the $|\Delta S| = 1$ processes are allowed without loops. For $|\Delta S| = 2$, the LO non-trivial contribution comes from the loop box diagram.

In the Fermi theory it has been possible to compute the $LECs$ in the EFT from the fundamental theory. In our case, when studying low and intermediate energy QCD, it will not be possible to derive from QCD the couplings of $R\chi T$, the matching conditions in this case will apply when demanding asymptotic QCD behaviour to the Green functions and form factors obtained within $R\chi T$. That will impose some restrictions on the effective couplings of the theory, as we will see.

3.6 Weakly and strongly coupled theories

A weakly coupled theory is one in which perturbation theory applies in a given energy range, whereas it is strongly coupled in some energy interval if the couplings are there comparable to (or even greater than) unity and any ordering for the perturbation series makes no sense. One might try to understand why asymptotic states differ from interacting states for these strongly coupled theories as a consequence of this property. In practice, and apart from very few realistic exceptions (like, for instance, Bethe-Salpeter equation [152, 153, 154] for bound states in QFT) we are only able to get rid of physical problems in QFT by using perturbative methods: Either belonging to the original theory or to an EFT (in fact, the naming non- perturbative methods has been generalized for this last case); so, it is clear that our inability for dealing with such kind of mathematical problems makes $EFTs$ even more necessary.

Finally, another consequence for weakly/strongly coupled theories is that in them the naïf dimensional analysis is not/is modified by anomalous dimensions [5]. Anomalous dimensions (together with a non-abelian gauge group) can explain how a theory can share ultraviolet freedom and infrared confinement, as it is the case for

[5]The anomalous dimensions are quantum corrections to the classical operator dimensions. Their importance at different energy scales can be evaluated by using the so-called Renormalization Group Equations.

QCD. Ref. [155] gives an easy and illustrative example of this. We recall its main features in the following: Let us consider the two-dimensional Thirring model [156] for a fermionic field whose Lagrangian is

$$\mathcal{L} = \overline{\psi}\left(i\partial\!\!\!/ - m\right)\psi - \frac{1}{2}g\left(\overline{\psi}\gamma^{\mu}\psi\right)^{2} . \tag{3.13}$$

It can be shown that it is dual to the sine-Gordon model for a fundamental scalar field, with the Lagrangian:

$$\mathcal{L} = \frac{1}{2}\partial_{\mu}\phi\partial^{\mu}\phi + \frac{\alpha}{\beta^{2}}\cos\beta\phi\,, \tag{3.14}$$

where the couplings g and β are related by means of:

$$\frac{\beta^{2}}{4\pi} = \frac{1}{1 + g/\pi}\,, \tag{3.15}$$

that indeed shows us that sine-Gordon strongly coupled model with $\beta^{2} \approx 4\pi$ can be studied with the weakly coupled Thirring model ($g \approx 0$). Then, we have two -equally valid and quite different- alternatives for describing the same theory (this happens because of the big anomalous dimensions that appear within strongly coupled theories at some scale. They can change drastically the behaviour of the different operators entering the *EFT* when considering them at different energies). At a given energy scale, we can choose between a strongly coupled theory involving bosons that has big anomalous dimensions and a weakly coupled theory whose degrees of freedom are fermions with little anomalous dimensions. From the purely formal point of view, there is no reason to prefer one alternative to the other one, but in order to compute it is clear that the second option -that has a smooth perturbative behaviour- is more comfortable.

This example emphasizes again the importance of making a right selection of degrees of freedom. A theory that can be really involved at some energies (sine-Gordon model, that is strongly coupled) can be studied by means of another one, which is easier (Thirring model).

The parallelism with *QCD* is tempting. The strongly coupled low-energy *QCD* can be treated by means of a weakly coupled theory written in terms of bosons, and this will be much easier than if we would have tried to solve it using quarks and gluons as the relevant fields.

3.7 Precise low-energy Physics as a probe for New Physics

Under the conditions of the Appelquist-Carazzone Theorem one sees that the effect of integrating out the heavy particles is to modify the values of the *LECs* and

impose symmetry restrictions. We enumerated how all conditions of the theorem (but for maybe the energy gap between particles in some regions of the spectrum) were accomplished for the theory of strong interactions. However one can have $EFTs$ applicable to sectors of the rest of the SM that may not fulfill the theorem and bring valuable information about the Physics at higher energies by analyzing with precision the low-energy experiments because in this case the effect of heavy modes in low-energy Physics will not be that mild. This is indeed the case for the electroweak (EW) sector of the SM, where spontaneous symmetry breaking affects the EW vacuum and fermions are chiral in the sense defined above.

Thus, we understand that when extremely precise LEP data were analyzed and compared to theoretical computations including many quantum corrections, the Z width [157], and its decay into a b-$\overline{b}$ pair [158, 159], were shown to be so sensitive to the yet-undiscovered top quark, through m_t, that it indicated where to find it at $FERMILAB$, as we told in the introduction. This is a clear and historically interesting example of how immensely precise low-energy experiments can give us clues about where physics beyond our model waits hidden.

We will add two related examples of current interest: an electroweak precision test (measurement of the weak mixing angle) and the anomalous magnetic moment of the muon. We will be very schematic here just in order to highlight the point we wish to make, for a detailed analysis one can consult recent reviews on the topic [160, 161], or Ref. [162].

Precision tests of the SM are promising places to look for physics BSM. An accurate measurement must be supplemented by very precise input parameters and higher order radiative corrections. At first sight it is striking that the measurement with finest precision is the main source of uncertainty in the end. That highest precision number is that of the fine structure constant, α, determined from the measurement of the anomalous magnetic moment of the electron [163], with amazing accuracy: $g_e/2 = 1.00115965218073(28) \Rightarrow \alpha^{-1} = 137.035999084(51)$, relying on perturbative QED as summarized in Ref.[164]. However, physics at higher energies is not described by this α measured at zero momentum transfer but for the one incorporating the quantum running. The shift of the fine structure constant from the Thompson limit to high energies involves necessarily a low-energy region in which non-perturbative hadron effects spoil that astonishing precision. In particular, the effective fine structure constant at the Z pole plays an important role in EW precision tests, like the weak mixing angle, θ_W, related to α, the Fermi constant, G_F, and M_Z through [165, 166, 167]:

$$\sin^2\theta_W \cos^2\theta_W = \frac{\pi\alpha}{\sqrt{2}G_F M_Z^2(1-\Delta r)}\,, \tag{3.16}$$

where Δr incorporates the universal correction $\Delta\alpha(M_Z)$, the quadratic dependence on m_t and all remaining quantum effects. In the SM, Δr depends on various physical parameters including the mass of the Higgs Boson, M_H, still unknown. This way, the measurements of $\sin^2\theta_W$ can help to put indirect bounds on M_H [168, 169, 170]. The error on $\Delta\alpha(M_Z)$ dominates the theoretical prediction. Here and in the case of

the muon magnetic anomaly the source of the uncertainty is similar, and it depends on $R(s)$, defined as follows:

$$R(s) = \frac{\sigma\left(e^+e^- \to \text{had}(\gamma)\right)}{\sigma\left(e^+e^- \to \mu^+\mu^-(\gamma)\right)}\,. \tag{3.17}$$

Specifically, the hadron contribution $\Delta\alpha^{(5)}_{\text{had}}(M_Z)$ of the five quarks lighter than the Z boson can be related to Eq. (3.17) via [171]:

$$\Delta\alpha^{(5)}_{\text{had}}(M_Z) = -\left(\frac{\alpha M_Z^2}{3\pi}\right)\Re e\int_{m_\pi^2}^{\infty}\mathrm{d}s\frac{R(s)}{s(s-M_Z^2-i\epsilon)}\,, \tag{3.18}$$

where

$$R(s) = \frac{\sigma^0_{\text{had}}(s)}{4\pi\alpha^2/(3s)}\,, \tag{3.19}$$

and $\sigma^0_{\text{had}}(s)$ is the total cross section for the annihilation into any hadron with vacuum polarization and initial state QED corrections subtracted off. As discussed extensively in the introduction, we are lacking a way of using the QCD Lagrangian that allows to compute Eq. (3.19) with enough accuracy to discriminate if there is new physics associated to the measurement of $\sin^2\theta$. The strategy is to use experimental data on the e^+e^- annihilation into any hadron state from threshold up to some energy ($\sim$ 2 GeV) where we can already rely on perturbative QCD supplemented by a motivated description of the lineshape of the many resonances appearing as sharp peaks in the hadron cross section. Therefore, the theoretical prediction of $R(s)$ -and of the observables that depend on it- includes experimental information.

The current accuracy of this dispersion integral is at the level of 1% and it is dominated by the measurements in the region below a few GeV [172, 173, 174, 175, 176, 177, 178, 179, 180, 181, 182, 183].

As in the case of the fine-structure constant at the Z scale we have just considered, the theoretical (in the sense commented above) prediction of the anomalous magnetic moment of the muon is dominated by the error on the hadron vacuum polarization effects at non-perturbative energies. Using analyticity and unitarity it was shown [184] that it could be computed from the dispersion integral:

$$a_\mu^{had,LO} = \frac{1}{4\pi^3}\int_{4m_\pi^2}^{\infty}\mathrm{d}sK(s)\sigma^0(s) = \frac{\alpha^2}{3\pi^2}\int_{4m_\pi^2}^{\infty}\frac{\mathrm{d}s}{s}K(s)R(s)\,, \tag{3.20}$$

where the kernel $K(s) \sim 1/s$ is further enhancing the low-energy contributions. In particular, the dominant part is given by the two-pion vector form-factor ($F_V^{\pi\pi}(s)$):

$$a_\mu^{had,\pi\pi} = \left(\frac{\alpha m_\mu}{6\pi}\right)^2\int_{4m_\pi^2}^{\Lambda}\frac{\mathrm{d}s}{s}\sigma_\pi^3|F_V^{\pi\pi}(s)|^2K(s)\,, \tag{3.21}$$

where σ_π is defined immediately above Eq. (C.7) and Λ is the scale up to which we consider experimental data instead of the theoretical perturbative QCD prediction.

A recent compilation of e^+e^- $BaBar$ data gives [185] $a_\mu^{had,LO} = (695.5 \pm 4.1) \cdot 10^{-10}$, with similar results obtained by other groups [160, 161, 183, 186]. The current prediction is [185, 187] $a_\mu^{SM} = 116591834(49) \cdot 10^{-11}$, to be compared to the experimental average $a_\mu^{exp} = 116592080(63) \cdot 10^{-11}$, that yields for the difference $exp - SM$ $\Delta a_\mu = 246(80) \cdot 10^{-11}$, 3.1 standard deviations. This would seem an indication for new physics [188]. However, given the facts that:

- There have been discrepancies [189, 190] in the shape of $R(s)$ (not that much in the integrated value) in the region of interest between the different experiments $KLOE$, $CMD2$, SND and $BaBar$ that seemed to hint to underestimated systematical errors in the unfolding of the data. An increase of precision in the experimental measurement and a revision of the estimated uncertainties in the treatment of radiative corrections could help settle this issue.

- One should have an independent way of extracting $a_\mu^{had,LO}$ using R_τ -Eq. (2.4)- after an isospin rotation. This way one would have a theory prediction using τ data instead of e^+e^- data. The results obtained with τ data seem to be closer to the SM ones (1.9 σ away, [191]).

- A common treatment of radiative correction (including maybe more than one Monte Carlo generator) by the different collaborations would be desirable.

One should conclude that it is still early to claim for this BSM physics.

The purpose of this section has been to show a few selected physical observables that allow for precision measurements at low energies that were sensitive to new physics at higher energies. The SM would be the EFT of the one describing all phenomena at this higher scale. In all cases that was possible because the EW sector of the SM did not fulfill the conditions of the Appelquist-Carazzone theorem, and thus the effect of heavier modes was not only in modifying the values of the $LECs$ and imposing additional symmetry properties. It is also instructive to see how in the cases of both $\sin\theta_W$ and a_μ this probe of BSM physics is polluted by the hadron uncertainty imposed by low-energy QCD, some aspects of which we are discussing through this Thesis.

3.8 Summary of EFTs

We conclude the first block of the chapter with a recapitulation on the main features of EFTs. They are the following ones:

- Dynamics at low energies does not depend on details of physics at high energies.

- One includes in the action only the relevant degrees of freedom according to the physics scale considered and to the particle masses. If there are large

energy gaps, we can decouple the different energy scales, that is:

$$0 \leftarrow m \ll E \ll M \rightarrow \infty\,.$$

There is a well-defined perturbative way of incorporating finite corrections induced by these scales.

- Exchanges mediated by heavy particles have been replaced by a set of local (non-renormalizable) operators involving only the light modes.

- The EFT-Lagrangian is a sum of operators, $\mathcal{L} = \sum_i c_i O_i$, whose coefficients scale as $c_i \rightarrow E^{d_i-\gamma_i}\, c_i$. Here, d_i comes from dimensional analysis and γ_i is the anomalous dimension. Provided we have chosen the right degrees of freedom, anomalous dimensions are small and the leading behaviour at low energies is given by the lowest dimension operators. Then, going further in the expansion we improve our accuracy: to include all corrections up to order $1/E^p$, one should include all operators with dimension $\leq d_i - \gamma_i + p$, i.e., all terms with coefficients of dimension $\geq -p$. The number of operators to be considered at each order is finite.

- Although $EFTs$ are not renormalizable in the classical sense -they are ultraviolet unstable-, they are order-by-order renormalizable for a given asked accuracy.

- $EFTs$ have the same infrared behaviour than the underlying theory. On the contrary, $EFTs$ do not possess the same ultraviolet behaviour than the fundamental one, so we need to perform a matching procedure to ensure that they are equivalent at a given intermediate (matching) scale.

- Whenever we respect symmetry principles for building the EFT, we will get the right theory written in terms of the variables we have chosen (*Weinberg's theorem*).

- Under some conditions, Sect. 3.4, the only remnants of the high-energy dynamics are in the $LECs$ and in the symmetries of the EFT (*Decoupling theorem*).

3.9 Introduction to Chiral Perturbation Theory

In this section we will introduce a paradigm of $EFTs$, χPT. We will need it to build the $R\chi T$ Lagrangian. The remainder of the chapter will be devoted to it.

We have seen in the Introduction, Eq. (1.17), how the strong coupling evolves to smaller values with increasing energy and the converse in the other end of energies: it increases its value as the energy gets smaller and smaller. A look to Figure 3.2 could be instructive.

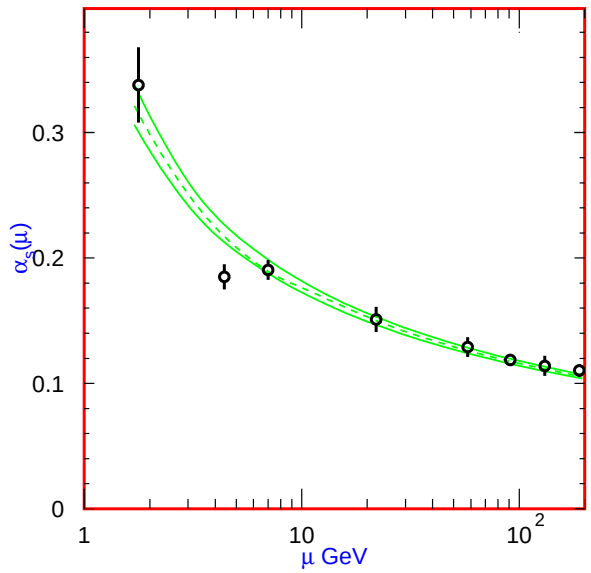

Figure 3.2: Summary of the values of $\alpha_S(\mu)$ at the values of μ where they are measured. The lines show the central values and the $\pm 1\sigma$ limits of the PDG [8] average. The figure clearly shows the decrease in α_S when increasing μ. The data correspond to -as μ increases- τ width, Υ decays, deep inelastic scattering, e^+e^- event shapes at 22 GeV from the $JADE$ data, shapes at $TRISTAN$ at 58 GeV, Z width, and e^+e^- event shapes at 135 and 189 GeV.

One sees that at $\mu \sim 2$ GeV the value of $\alpha_S(\mu)$ is not yet that big to prevent a meaningful perturbative expansion in terms of it. Following the RGE to extrapolate to lower values of μ it is found that at a typical hadron scale $\mu \sim M_\rho, M_P$ one can have $\alpha_S(\mu) \geq 0.5$ that jeopardizes that approach. Since hadron decays of the τ span the range $0.14 - 1.78$ GeV, one should find a way out that starts from QCD. One rigorous alternative is to simulate on the lattice the QCD action. We will not report about this option here. Although it has proved to be very successful in many non-perturbative strong-interaction problems, the processes we study here have not been addressed by the lattice community yet. One can also construct models that keep this or that feature of QCD, but we do not find this alternative satisfactory. Finally, one can build an EFT of QCD for this subset of energies using as variables the active degrees of freedom as we will describe next.

In order to discuss the global symmetries of the QCD Lagrangian, Eq. (1.15), we will restrict ourselves to the so-called light sector of QCD, with n_f light flavours. In our case, $n_f = 3$: u, d, s, that are much lighter than the so-called heavy quarks c, b, t. The characteristic hadron scale lies in between both regimes. Therefore, integrating out these three heavy quarks we go from [6] $QCD^{n_f=6}$ to $QCD^{n_f=3}$. The Lagrangian of $QCD^{n_f=3}$ in the limit of massless light quarks (so-called chiral limit)

[6] The effective strong coupling in the two theories are related by a matching condition, introduced in Sect. 3.5. This is discussed in Ref. [192], for instance.

is:

$$\mathcal{L}^0_{QCD} \,=\, i\,\overline{q}_L \not{D}\, q_L \,+\, i\,\overline{q}_R \not{D}\, q_R \,-\, \frac{1}{4} G^a_{\mu\nu} G^{\mu\nu}_a \,, \tag{3.22}$$

where the upper-index zero reminds us the limit taken, and we have employed the usual notation for the left(right)-handed spinors $q_L(q_R)$ and projectors: $q_L \equiv P_L q$ ($q_R \equiv P_R q$).

The Lagrangian, Eq. (3.22), is invariant under global transformations belonging to $SU(n_f)_L \otimes SU(n_f)_R \otimes U(1)_V \otimes U(1)_A$. $U(1)_V$ is trivially realized in the meson sector but it gives rise to baryon number conservation, $U(1)_A$ gets broken by anomalies and explains why the η' is heavier than the η or the kaons. Finally, it remains $SU(n_f)_L \otimes SU(n_f)_R$, the so-called chiral group of transformations in flavour space, that acts on the chiral projections of the quark fields in the following way:

$$\begin{aligned} q_L \;&\longrightarrow\; q_L{}' \,=\, g_L q_L \,, \\ q_R \;&\longrightarrow\; q_R{}' \,=\, g_R q_R \,, \end{aligned} \tag{3.23}$$

where $g_{L,R} \in SU(n_f)_{L,R}$.

This chiral symmetry, which should be approximately valid in the light quark sector (u, d, s), is however not seen in the meson spectrum (Table 3.1):

J^P	Particle	m (MeV)	J^P	Particle	m (MeV)
0^-	π^0	~ 135.0	0^+	a_0	~ 985
	$\pi^\pm$	~ 139.6		$\mathrm{a}_0^\pm$	~ 985
	η, η'	~ 547.9, (957.8)		f_0	~ 980
	$K^\pm$	~ 493.7		$K^{*\pm}$	~ 800
	$K^0, \overline{K}^0$	~ 497.7		$K^{*0}, \overline{K}^{*0}$	~ 800
1^-	ρ^0	~ 775.8	1^+	a_1^0	~ 1230
	$\rho^\pm$	~ 775.5		$\mathrm{a}_1^\pm$	~ 1230
	ω, ϕ	~ 782.7, (1019.5)		h_1, f_1	~ 1170, (1281.8)
	$K^{*\pm}$	~ 892.0		$K_1^{*\pm}$	~ 1273
	$K^{*0}, \overline{K}^{*0}$	~ 891.7		$K_1^{*0}, \overline{K}_1^{*0}$	~ 1273

Table 3.1: Spectrum of the lightest mesons [8]. The $f_0(600)$ or σ [193, 194] is not included in the Table.

The conclusions we draw are the following ones:

- Mesons are nicely classified into $SU(3)_V$ representations.
- Reversing intrinsic parity changes drastically the spectrum (just compare the masses of the octet of $J^P = 0^-$ versus that with $J^P = 0^+$, or $J^P = 1^-$ vs. $J^P = 1^+$). Thus, a transformation involving γ_5 is not a symmetry of the

spectrum. Chiral transformations seem not to be a symmetry of low-energy QCD.

- The octet of $J^P = 0^-$ stands out being its members much lighter than the ones in other octets.

Although chiral symmetry changes the parity of a given multiplet, the previous spectrum is not contradictory with it. We shall recall that there exist two ways of realizing a global symmetry: In the Wigner-Weyl way all the symmetries of the Lagrangian are shared by the vacuum of the theory and then they are manifest in the spectrum. In the Nambu-Goldstone way, there is a so-called spontaneous breakdown of the symmetry that makes compatible the observed spectrum with the underlying approximate symmetry.

There are two fundamental theorems concerning spontaneous symmetry breaking: Goldstone theorem [122, 195], which is devoted to global continuous symmetries and Higgs-Kibble theorem [196, 197, 198, 199, 200], that worries about local gauge symmetries.

Chiral symmetry is a global symmetry, then Goldstone theorem is the one applied here. We can state it in the following way: *Given a global continuous symmetry of the Lagrangian: either the vacuum shares the symmetry of the Hamiltonian; or there appear spin zero massless particles as a display of Spontaneous Symmetry Breaking. In the last case, for every spontaneously broken generator, the theory must contain a massless particle, the so-called Goldstone boson.*

Vafa and Witten showed [201] that the ground state of the theory must be invariant under vector transformations, so that Spontaneous Symmetry Breaking cannot affect the vector part of the chiral subgroup ($V^a_\mu \equiv R^a_\mu + L^a_\mu$), but the axial one ($A^a_\mu \equiv R^a_\mu - L^a_\mu$).

Let us consider [202, 203] a Noether charge Q, and assume the existence of an operator $\mathcal{O}$ that satisfies

$$\langle\, 0|[Q, \mathcal{O}]|0\,\rangle \neq 0\,; \tag{3.24}$$

the only possibility for this to be valid is that $Q|0\,\rangle \neq 0$. Goldstone theorem states there exists a massless state $|G\,\rangle$ such that

$$\langle\, 0|J^0|G\,\rangle\langle\, G|\mathcal{O}|0\,\rangle \neq 0\,. \tag{3.25}$$

It is important to notice that the quantum numbers of the Goldstone boson are dictated by those of J^0 and $\mathcal{O}$. The quantity in the left-hand side of Eq. (3.24) is called the order parameter of SSB.

Considering that $U(1)_A$ is affected by anomalies, only $SU(n_f)_A$ can be concerned with the Goldstone theorem. Then, for $n_f = 3$ and for the lightest quark flavours (u, d, s) we end up with eight broken axial generators of the chiral group and, correspondingly, eight pseudoscalar Goldstone states $|G^a\,\rangle$, which can be identified with the eight lightest hadrons (three πs, four Ks and the η, see Table 3.1), their (relatively) small masses being generated by the explicit breaking of chiral symmetry

induced by the quark mass matrix entering the QCD Lagrangian. The corresponding operators, $\mathcal{O}^a$, must be pseudoscalars. The simplest possibility is $\mathcal{O}^a = \overline{q}\gamma_5\lambda^a q$, which satisfies

$$\langle\, 0|[Q_A^a, \overline{q}\gamma_5\lambda^b q]|0\,\rangle \;=\; -\frac{1}{2}\,\langle\, 0|\overline{q}\left\{\lambda^a, \lambda^b\right\} q|0\,\rangle \;= -\frac{2}{3}\,\delta^{ab}\,\langle\, 0|\overline{q}q|0\,\rangle\,. \tag{3.26}$$

The quark condensates

$$\langle\, 0|\overline{u}u|0\,\rangle \;=\; \langle\, 0|\overline{d}d|0\,\rangle \;=\; \langle\, 0|\overline{s}s|0\,\rangle \;\neq\; 0 \tag{3.27}$$

are then the natural order parameters of Spontaneous Chiral Symmetry Breaking ($S\chi SB$).

3.10 Different representations for the Goldstone fields

Based on the previous reasoning, our basic assumption is the pattern of $S\chi SB$:

$$G \;\equiv\; SU(3)_L \otimes\; SU(3)_R \;\overrightarrow{S\chi SB}\; H \;\equiv\; SU(3)_V. \tag{3.28}$$

Since there is a mass gap between the lightest multiplet of pseudoscalar particles and the rest of the spectrum, we can easily apply the Weinberg's approach and formulate an EFT dealing only with these modes.

The general formalism for EFT-Lagrangians with SSB was worked out by Callan, Coleman, Wess and Zumino ($CCWZ$) [123, 124]. A very clear explanation can be found in Ref. [136].

Consider a theory in which a global symmetry group G is spontaneously broken down to one of its subgroups, H. The vacuum manifold is the coset space G/H.

The set of coordinates we choose has to be able to describe the local orientation of the vacuum for small fluctuations around the standard vacuum configuration. Let $\Xi(x) \in G$ be the rotation matrix that transforms the standard vacuum configuration to the local field one. Due to the invariance of the vacuum under H transformations, Ξ happens to be not unique; namely, $\Xi(x)\,h(x)$ -where $h \in H$- gives the same configuration. In the present case, $\Xi(x) \in O(N)$ and we can parameterize any vector ϕ by means of the suitable Ξ matrix:

$$\phi(x) \;=\; \Xi(x) \begin{pmatrix} 0 \\ 0 \\ . \\ . \\ . \\ 0 \\ v \end{pmatrix}. \tag{3.29}$$

The same configuration $\phi(x)$ can also be described by $\Xi(x)\,h(x)$. In our example, $h(x)$ is a matrix of the form:

$$h(x) \,=\, \begin{pmatrix} h'(x) & 0 \\ 0 & 1 \end{pmatrix}\,, \tag{3.30}$$

with $h'(x)$ is an arbitrary $O(N-1)$ matrix, since:

$$\begin{pmatrix} h'(x) & 0 \\ 0 & 1 \end{pmatrix} \begin{pmatrix} 0 \\ 0 \\ . \\ . \\ . \\ 0 \\ v \end{pmatrix} = \begin{pmatrix} 0 \\ 0 \\ . \\ . \\ . \\ 0 \\ v \end{pmatrix}\,. \tag{3.31}$$

The $CCWZ$ prescription is to pick a set of broken generators X, and choose

$$\Xi(x) \,=\, e^{i\,X\cdot\pi(x)}\,, \tag{3.32}$$

where $\pi(x)$ describes the Goldstone modes.

Under a global transformation g, the matrix $\Xi(x)$ changes to a new matrix $g\;\Xi(x)$ for $\phi(x) \,\rightarrow\, g\phi(x)$, that it is not in the standard form of Eq. (3.32), but can be written as

$$g\,\Xi \,=\, \Xi'\,h\,, \tag{3.33}$$

that is usually turned into

$$\Xi(x) \,\longrightarrow\, g\,\Xi(x)\,h^{-1}(g,\,\Xi(x))\,. \tag{3.34}$$

$CCWZ$ formalism is characterized by equations (3.32) and (3.34) for the pseudo-Goldstone boson (pG) fields and their transformation law. The transformation h appearing there is non-trivial because the Goldstone boson manifold is curved. Any other choice gives the same results as $CCWZ$ formalism for all observables, such as the S matrix, but does not give the same off-shell Green functions.

The $CCWZ$ prescription in Eq. (3.32) says nothing about which set of broken generators we would better choose. Depending on our choice, we will have a different base. There are two that have become standard in order to write the QCD chiral Lagrangian, the so-called ξ-basis and the Σ-basis [136]. Each of them brings us a different equivalent parameterization (commonly called U and u, respectively).

There are many simplifications that occur for QCD because the coset space G/H is isomorphic to a Lie group.

Let $X^a \,=\, T^a_L \,+\, T^a_R$ be our choice of broken generators.

An element $g \in G$ can be written as:

$$g \,=\, \begin{pmatrix} L & 0 \\ 0 & R \end{pmatrix}\,, \tag{3.35}$$

where $L(R) \in SU(3)_{L(R)}$. The unbroken transformations are of the form (3.35), with $L = R = U$,

$$g = \begin{pmatrix} U & 0 \\ 0 & U \end{pmatrix} . \tag{3.36}$$

Now, using the $CCWZ$ recipe, Eq. (3.32):

$$\Xi(x) = e^{\,i\,X\cdot\pi(x)} = exp \begin{pmatrix} i\,T\cdot\pi & 0 \\ 0 & -i\,T\cdot\pi \end{pmatrix} = \begin{pmatrix} \xi(x) & 0 \\ 0 & \xi^\dagger(x) \end{pmatrix} , \tag{3.37}$$

where

$$\xi = e^{\,i\,X\cdot\pi} \tag{3.38}$$

stands for the upper block of $\Xi(x)$. The transformation rule Eq. (3.34) gives

$$\begin{pmatrix} \xi(x) & 0 \\ 0 & \xi^\dagger(x) \end{pmatrix} \to \begin{pmatrix} L & 0 \\ 0 & R \end{pmatrix} \begin{pmatrix} \xi(x) & 0 \\ 0 & \xi^\dagger(x) \end{pmatrix} \begin{pmatrix} U^{-1}(x) & 0 \\ 0 & U^{-1}(x) \end{pmatrix} , \tag{3.39}$$

and, consequently, the transformation rule for ξ,

$$\xi(x) \longrightarrow L\,\xi(x)\,U^{-1}(x) = U(x)\,\xi(x)\,R^\dagger , \tag{3.40}$$

which defines U in terms of L (R) and ξ. If we choose $X^a = T^a_L$ as the basis for broken generators, we will have $U = R$, and

$$\Sigma(x) \longrightarrow L\,\Sigma(x)\,R^\dagger . \tag{3.41}$$

Finally, comparing Eqs. (3.40) and (3.41), one concludes that Σ and ξ are related by

$$\Sigma(x) = \xi^2(x) . \tag{3.42}$$

In the context of χPT, everybody writes $U(x)$ instead of $\Sigma(x)$ and $u(x)$ substitutes $\xi(x)$. It is also more common to employ $\Phi(x)$ for the coordinates of the Goldstone fields. We will follow this notation from now on.

The Goldstone boson nature restricts these fields to be angular variables, thus dimensionless. It is convenient to work with boson fields of mass dimension one, which motivates the standard choice:

$$u = e^{i\,T\cdot\,\Phi/F}, \;\; U = u^2 \tag{3.43}$$

where $F \sim 92.4$ MeV is the pion decay constant.

$$\Phi(x) = \sqrt{2}\,T_a\Phi^a(x) = \frac{1}{\sqrt{2}}\sum_{a=1}^{8}\lambda_a\Phi^a = \begin{pmatrix} \frac{1}{\sqrt{2}}\pi^0 + \frac{1}{\sqrt{6}}\eta_8 & \pi^+ & K^+ \\ \pi^- & -\frac{1}{\sqrt{2}}\pi^0 + \frac{1}{\sqrt{6}}\eta_8 & K^0 \\ K^- & \overline{K}^0 & -\frac{2}{\sqrt{6}}\eta_8 \end{pmatrix} , \tag{3.44}$$

where the Gell-Mann matrices in flavour space, λ_a, -which are the fundamental representation of $SU(3)$- have been introduced with the same normalization as for

$SU(N_C)$ generators of QCD.

Notice that $U(\Phi)$ transforms linearly under the chiral group, but the induced transformation on the pG fields is highly non-linear.

There is abundant good literature available on this topic and its specific application to χPT [143, 202, 203, 204, 205, 206].

3.11 Lowest order Lagrangian. Method of external currents

In order to obtain an EFT realization of QCD at low energies for the light quark sector, we should write the most general Lagrangian involving the matrix $U(\Phi)$ (or $u(\Phi)$), which respects chiral symmetry. The Lagrangian can be organized in terms of increasing powers of momentum or, equivalently, of derivatives (the subindex $2n$ refers to that):

$$\mathcal{L}_{\chi PT} \,=\, \sum_{n=1}^{\infty} \mathcal{L}_{2n}\,, \tag{3.45}$$

being the dominant behaviour at low energies given by the terms with the least number of derivatives. Unitarity of U obliges two derivatives to be present for having a non-trivial interaction. At lowest order, the effective chiral Lagrangian in the U-formalism is uniquely given by the term:

$$\mathcal{L}_2 \,=\, \frac{F^2}{4} \langle\, \partial_\mu U^\dagger \partial^\mu U \,\rangle\,. \tag{3.46}$$

where $\langle\, A \,\rangle$ is short for trace in flavour space of the matrix A.

Expanding the matrix that exponentiates the pG fields in a power series in Φ, we get the Goldstone kinetic terms plus a tower of interactions increasing in the number of pseudoscalars. It is a capital fact that all interactions among the Goldstones can be predicted in terms of a single coupling, F. The non-linearity of the EFT-Lagrangian relates the amplitudes of processes involving a different number of pGs, allowing for absolute predictions in terms of F. This sector was thoroughly studied by Weinberg [3, 207, 208, 209].

But the lightest mesons do not interact solely due to elastic scattering among themselves. In addition to the strong interaction, they also experience electromagnetic and (semileptonic) electroweak interactions and this has to be taken into account. In order to compute the associated Green functions, we will follow the procedure employed by Gasser and Leutwyler, who developed χPT consistently to one loop ([4, 5, 210]). We extend the chiral invariant QCD massless Lagrangian, Eq. (3.22), by coupling the quarks to external Hermitian matrix fields v_μ, a_μ, s, p [7]:

$$\mathcal{L}_{QCD} \,=\, \mathcal{L}^0_{QCD} \,+\, \overline{q}\gamma^\mu \left(v_\mu + \gamma_5 a_\mu\right) q \,-\, \overline{q}\left(s - i\gamma_5 p\right) q\,. \tag{3.47}$$

[7] We do not include the tensor source [211].

External photons and W boson fields are among the gauge fields and (pseudo)scalar fields provide a very convenient way of incorporating explicit χSB through the quark masses (see Eq. (3.56), where $\mathcal{M}$ is defined.):

$$\begin{aligned} r_\mu &\to r_\mu + e\mathcal{Q}A_\mu\,, \\ \ell_\mu &\to \ell_\mu + e\mathcal{Q}A_\mu + \frac{2\,e}{\sqrt{2}\sin\theta_W}\left(W^\dagger T_+ + h.c.\right)\,, \\ s &\to s + \mathcal{M}\,, \end{aligned} \tag{3.48}$$

being

$$\mathcal{Q} = \begin{pmatrix} \frac{2}{3} & 0 & 0 \\ 0 & -\frac{1}{3} & 0 \\ 0 & 0 & -\frac{1}{3} \end{pmatrix} \;,\; T_+ = \begin{pmatrix} 0 & V_{ud} & V_{us} \\ 0 & 0 & 0 \\ 0 & 0 & 0 \end{pmatrix}. \tag{3.49}$$

Inclusion of external fields promotes the global chiral symmetry to a local one:

$$\begin{aligned} q &\to g_R\, q_R + g_L\, q_L\,, \\ s + ip &\to g_R\,(s + ip)\, g_L^\dagger\,, \\ \ell_\mu &\to g_L\,\ell_\mu\, g_L^\dagger + i g_L\,\partial_\mu\, g_L^\dagger\,, \\ r_\mu &\to g_R\, r_\mu\, g_R^\dagger + i g_R\,\partial_\mu\, g_R^\dagger\,. \end{aligned} \tag{3.50}$$

where we have introduced the definitions $r_\mu \equiv v_\mu + a_\mu$ and $\ell_\mu \equiv v_\mu - a_\mu$; and requires the introduction of a covariant derivative, $D_\mu U$, and associated non-Abelian field-strength tensors, $F_{L,R}^{\mu\nu}$:

$$\begin{aligned} D_\mu U &= \partial_\mu U - i r_\mu U + i U \ell_\mu \;,\; D_\mu U \to g_R\, D_\mu\, U\, g_L^{-1}, \\ F_x^{\mu\nu} &= \partial^\mu\, x^\nu - \partial^\nu\, x^\mu - i\,[x^\mu,\, x^\nu] \;,\; x = r,\, \ell. \end{aligned} \tag{3.51}$$

The transformations of the external sources under the discrete symmetries $P//C$ are as follows:

$$\begin{aligned} s + ip &\to s - ip\,//\,(s - ip)^\top, \\ \ell_\mu &\to r^\mu\,//\,-r_\mu^\top, \\ r_\mu &\to \ell^\mu\,//\,-\ell_\mu^\top. \end{aligned}$$

The power of the external field technique is exhibited when computing chiral Noether currents. Green functions are obtained as functional derivatives of the generating functional, $Z\,[v^\mu,\, a^\mu,\, s,\, p]$, defined via the path-integral formula

$$\exp\{iZ\} = \int \mathcal{D}q\,\mathcal{D}\overline{q}\,\mathcal{D}G_\mu \exp\left\{i\int \mathrm{d}^4x\,\mathcal{L}_{\mathcal{QCD}}\right\} = \int \mathcal{D}U \exp\left\{i\int \mathrm{d}^4x\,\mathcal{L}_{\text{eff}}\right\}. \tag{3.52}$$

At lowest order in momenta, Z reduces to the classical action, $S_2 = \int \mathrm{d}^4x\,\mathcal{L}_2$, and the currents can be trivially computed by taking suitable derivatives with respect

to the external fields. In particular, one realizes the physical meaning of the pion decay constant, F, defined as

$$\langle\, 0|(J_A^\mu)^{12}|\pi^+(p)\,\rangle \;\equiv\; i\sqrt{2}F\,p^\mu\,. \tag{3.53}$$

The locally chiral invariant Lagrangian of lowest order describing the strong, electromagnetic and semileptonic weak interactions of mesons was given by Gasser and Leutwyler [4, 5]:

$$\mathcal{L}_2 \;=\; \frac{F^2}{4}\,\langle\, D_\mu U D^\mu U^\dagger \,+\, \chi U^\dagger \,+\, \chi^\dagger U\,\rangle\,,\;\; \chi \,=\, 2B(s\,+\,ip). \tag{3.54}$$

The two $LECs$ that characterize completely the $\mathcal{O}(p^2)$-chiral Lagrangian are related to the pion decay constant and to the quark condensate in the chiral limit:

$$\begin{aligned} F_\pi \;&=\; F\,[1\,+\,\mathcal{O}(m_q)] \;=\; 92.4\,\mathrm{MeV}\,, \\ \langle\, 0|\overline{u}u|0\,\rangle \;&=\; -F^2\,B\,[1\,+\,\mathcal{O}(m_q)]\,. \end{aligned} \tag{3.55}$$

A consistent chiral counting must be developed to organize the infinite allowed terms in the Lagrangian. Depending on the actual relation of these two $LECs$ one could have different $EFTs$ for low-energy QCD. This illustrates the fact that the Weinberg's approach to $EFTs$ does only rely on symmetries but does not have dynamical content incorporated. This issue is studied in the next section.

3.12 Weinberg's power counting rule

Chiral Lagrangians were originally organized in a derivative expansion based on the following chiral counting rules (see Table 3.2).

Using Eqs. (3.43, 3.44) and setting the external scalar field equal to the quark

Operator	$\mathcal{O}$
U	p^0
$D_\mu U$, v_μ, a_μ	p
$F_{L,R}^{\mu\nu}$	p^2
s, p	p^2

Table 3.2: Chiral counting in Standard χPT.

mass matrix -that is, explicitly breaking chiral symmetry in the same way it happens in QCD-,

$$s \,=\, \mathcal{M}_q \,=\, \begin{pmatrix} m_u & 0 & 0 \\ 0 & m_d & 0 \\ 0 & 0 & m_s \end{pmatrix}\,, \tag{3.56}$$

one can straightforwardly read off from Eq. (3.54) the pseudoscalar meson masses to leading order in m_q:

$$\begin{aligned} m^2_{\pi^\pm} &= 2\widehat{m}B\,, \\ m^2_{\pi^0} &= 2\widehat{m}B - \varepsilon + \mathcal{O}(\varepsilon^2), \\ m^2_{K^\pm} &= (m_u + m_s)B\,, \\ m^2_{\overline{K}^0, K^0} &= (m_d + m_s)B\,, \\ m^2_{\eta_8} &= \frac{2}{3}(\widehat{m} + 2m_s)B + \varepsilon + \mathcal{O}(\varepsilon^2), \end{aligned} \tag{3.57}$$

where [202]

$$\widehat{m} = \frac{1}{2}(m_u + m_d)\,, \quad \varepsilon = \frac{B}{4}\frac{(m_u - m_d)^2}{(m_s - \widehat{m})}\,. \tag{3.58}$$

With the quark condensate assumed to be non-vanishing in the chiral limit ($B \neq 0$), these relations explain the chiral counting rule in Table 3.2.

Up to this point, χPT is a very elegant way of understanding the phenomenological successes obtained in the pre-QCD era. The well-known relations already obtained with current algebra techniques are recovered using Eqs. (3.54) and (3.56):

$$F^2\, m^2_\pi = -2\widehat{m}\,\langle\, 0|\overline{q}\, q|0\,\rangle \quad [212] \tag{3.59}$$

$$B = \frac{m^2_\pi}{2\widehat{m}} = \frac{m^2_{K^+}}{m_s + m_u} = \frac{m^2_{K^0}}{m_s + m_d} \quad [212]\,,\ [213] \tag{3.60}$$

$$3m^2_{\eta_8} = 4m^2_K - m^2_\pi \quad [214]\,,\ [215], \tag{3.61}$$

but the real power of χPT -as an EFT- lies in the fact that it gives a perfectly defined way of taking into account the next orders in the chiral expansion and the quantum corrections.

χPT is based on a two-fold expansion: as a low-energy effective theory, it is an expansion in small momenta. On the other hand, it is also an expansion in the quark masses, m_q, around the chiral limit. In full generality, the Lagrangian is:

$$\mathcal{L}_{\chi PT} = \sum_{i,j} \mathcal{L}_{ij}\,, \quad \mathcal{L}_{ij} = \mathcal{O}(p^i\, m_q^j)\,. \tag{3.62}$$

The two expansions become related by Eq. (3.57). If the quark condensate is non-vanishing in the chiral limit, meson masses squared start out linear in m_q. Assuming the linear terms to give the dominant behaviour there, we end up with the standard chiral counting with $m_q \sim \mathcal{O}(p^2)$ and

$$\mathcal{L}_{eff} = \sum_d \mathcal{L}_d\,, \quad \mathcal{L}_d = \sum_{i\,+\,2j\,=\,d} \mathcal{L}_{ij}\,. \tag{3.63}$$

In short, Eq. (3.54) has two $LECs$: F and B. χPT assumes B to be big compared to F and organizes the chiral counting according to that assumption. Generalized

χPT [216, 217, 218] was developed as a scheme adapted for much smaller values of B, a picture that is not supported by lattice evaluations of the condensate [219, 220, 221, 222, 223, 224, 225, 226] or estimations based on sum rules [227, 228, 229, 230, 231, 232, 233]. Another issue that is still unsolved concerns the possible instabilities due to vacuum fluctuations of sea $q-\bar{q}$ pairs, as the number n_f of light fermions increases [234, 235, 236, 237, 238, 239, 240].

In order to build higher orders in the chiral expansion it is better to use the chiral tensor formalism that uses u instead of U as the exponential non-linear realization of the pGs. This is so because the building blocks in the U-formalism (U, $F_{L,R}^{\mu,\nu}$, χ) do not transform in the same way under the chiral group. While this is not an issue for dealing with the lowest order Lagrangians, in can make very difficult to determine the minimal setting of independent operators at higher chiral orders.

The Lagrangian must be chiral symmetric, hermitian, and Lorentz, parity (P) and charge conjugation (C) invariant. In the u-formulation one uses traces of chiral tensors either transforming as

$$X \;\rightarrow\; h(g,\,\Phi)\,X\,h(g,\,\Phi)^{\dagger}\,, \tag{3.64}$$

or being chiral invariant.

With this purpose, we define the chiral tensors:

$$\begin{aligned} u_{\mu} &= i\left\{u^{\dagger}\left(\partial_{\mu}-ir_{\mu}\right)u-u\left(\partial_{\mu}-il_{\mu}\right)u^{\dagger}\right\}\,,\\ \chi_{\pm} &= u^{\dagger}\,\chi\,u^{\dagger}\pm u\,\chi^{\dagger}\,u\,, \end{aligned} \tag{3.65}$$

The lowest order chiral Lagrangian that can be written respecting also all other symmetries is then

$$\mathcal{L}_2 \;=\; \frac{F^2}{4}\langle\, u_{\mu}\,u^{\mu}\;+\;\chi_{+}\,\rangle\,. \tag{3.66}$$

Explicit χSB is incorporated through χ_+, where χ is given by Eq. (3.54). Then, in the isospin limit,

$$\chi \;=\; 2\,B\,s \;=\; \begin{pmatrix} m_{\pi}^2 & 0 & 0\\ 0 & m_{\pi}^2 & 0\\ 0 & 0 & 2m_K^2-m_{\pi}^2 \end{pmatrix}\,. \tag{3.67}$$

The content of Eqs. (3.54) and (3.66) is exactly the same.

Now we will explain why the expansion in an EFT may not be simply an expansion in the number of loops. This is indeed what happens in χPT.

Consider an arbitrary complex Feynman diagram involving just pGs. We recall the expansion in χPT, Eq. (3.45). The LO Lagrangian supplies $\mathcal{O}(p^2)$ vertices, the NLO one $\mathcal{O}(p^4)$ couplings, and so on and so forth. Using N_d to denote the number of vertices obtained employing the Lagrangian of order $\mathcal{O}(p^d)$, remembering that pG fields have mass dimension one and that any momentum running inside a loop is to

be integrated over four dimensions -after proper renormalization-, one may conclude that for this generic diagram all powers of momentum will fulfill the relation:

$$D \,=\, 4L \,-\, 2B_I \,+\, \sum_d N_d\, d\,, \tag{3.68}$$

being L the number of loops and B_I the number of internal boson lines, respectively.

Moreover, there is a topological relation for any connected Feynman diagram

$$L \,=\, B_I \,-\, \left(\sum_d N_d \,-\, 1\right) \tag{3.69}$$

that one can use to erase B_I from Eq. (3.68) to end up with Weinberg′s power counting rule [3]:

$$D \,=\, 2L \,+\, 2 \,+\, \sum_d N_d(d-2)\,. \tag{3.70}$$

It is straightforward to read off from (3.70) the exact ordering of the chiral expansion:

- $D = 2$ corresponds to $L = 0$ and $N_2 = 1$, i.e., tree level contributions obtained using Eq. (3.54) -or (3.66)-. This makes sense: we recover the predictions of old current algebra as the dominant very low-energy behaviour in χPT.

- $D = 4$ is obtained either with $L = 0$ and $N_4 = 1$, or with $L = 1$ and arbitrary insertions of N_2. Tree level contributions coming from $\mathcal{L}_4$ are to be balanced with one-loop diagrams formed with $\mathcal{L}_2$. And so on. This is in agreement with the order-by-order renormalization of χPT: the divergences generated at a given chiral order are renormalized by the appropriate counterterms appearing at the next order.

However, this is not the whole story. For χPT to be dual to QCD at low energies it must satisfy classical symmetries slightly modified by quantum properties. Classical symmetries can be swapped away by anomalies, which are long-distance non-perturbative effects. And this is what happens with $U(1)_A$ for the massless QCD Lagrangian, Eq. (3.22). To ensure the duality, every aspect of low-energy QCD must be realized in the same way in χPT and, particularly, one must add a term that reproduces this anomaly, as it is discussed in the next section. Moreover, it is not possible to write a generating functional for massless QCD that is simultaneously invariant under the subsets of V and A transformations of the chiral group. It is mandatory to include a term that mimics this behaviour whose degrees of freedom are pGs. This task was carried out by Wess, Zumino and Witten [241, 242], who wrote such a kind of functional, $WZWf$. It happens to start contributing at $\mathcal{O}(p^4)$. Therefore, three contributions shape NLO chiral expansion that are, schematically: $L = 0$ with $N_4 = 1$, $L = 1\ \forall\ N_2$, and $WZWf$.

3.13 NLO in the chiral expansion

The lowest order Lagrangian is $\mathcal{O}(p^2)$ (Eq. (3.66)) for even intrinsic parity and $\mathcal{O}(p^4)$ (the $WZWf$) in the odd-intrinsic parity sector.

There is a new operator that enters the $\mathcal{O}(p^4)$ Lagrangian in the u-formalism:

$$f_\pm^{\mu\nu} \;=\; u\,F_L^{\mu\nu}\,u^\dagger \pm u^\dagger\,F_R^{\mu\nu}\,u\,, \tag{3.71}$$

that collects the left(right)-handed field-strength tensors presented in Eq. (3.51). The covariant derivative in this formalism reads:

$$\nabla_\mu X \;=\; \partial_\mu X \,+\, [\Gamma_\mu,\, X]\,, \tag{3.72}$$

defined in terms of the chiral connection

$$\Gamma_\mu \;=\; \frac{1}{2}\left\{u^\dagger\left(\partial_\mu \,-\, ir_\mu\right)u \,+\, u\left(\partial_\mu \,-\, il_\mu\right)u^\dagger\right\}\,, \tag{3.73}$$

for the covariant derivative to be transformed in the same way as X does, Eq. (3.64).

It easy to check that $(\nabla_\mu X)^\dagger \;=\; \nabla_\mu(X^\dagger)$. The connection does not transform covariantly as X. It will be useful when introducing the chiral multiplets of resonances in $R\chi T$, which transform in the same fashion. With Γ_μ one may also build the covariant tensor

$$\Gamma_{\mu\nu} \;=\; \partial_\mu\Gamma_\nu \,-\, \partial_\nu\Gamma_\mu \,+\, [\Gamma_\mu, \Gamma_\nu]\,. \tag{3.74}$$

The other $\mathcal{O}(p^2)$ operators transforming covariantly, Eq. (3.64) are:

$$\begin{aligned} & u_\mu u_\nu\,, \\ h_{\mu\nu} \;=\; & \nabla_\mu u_\nu \,+\, \nabla_\nu u_\mu\,, \end{aligned} \tag{3.75}$$

where it has been used that u_μ can be written as

$$u_\mu \;=\; i\,u^\dagger D_\mu U u^\dagger \;=\; -i\,u D_\mu U^\dagger \;=\; u_\mu^\dagger, \tag{3.76}$$

and is traceless.

The relevant transformation properties of chiral tensors in this formalism are shown in Table 3.3. Taking these into account, we achieve the most general $\mathcal{O}(p^4)$ chiral Lagrangian written in terms of them:

$$\begin{aligned} \mathcal{L}_4 \;=\; & L_1\langle\, u_\mu u^\mu\,\rangle^2 \,+\, L_2\langle\, u_\mu u^\nu\,\rangle\langle\, u^\mu u_\nu\,\rangle \,+\, L_3\langle\, u_\mu u^\mu u_\nu u^\nu\,\rangle \,+\, L_4\langle\, u_\mu u^\mu\,\rangle\langle\,\chi_+\,\rangle \\ & + L_5\langle\, u_\mu u^\mu \chi_+\,\rangle \,+\, L_6\langle\,\chi_+\,\rangle^2 \,+\, L_7\langle\,\chi_-\,\rangle^2 \,+\, L_8/2\,\langle\,\chi_+^2 + \chi_-^2\,\rangle \\ & - i\,L_9\langle\, f_+^{\mu\nu} u_\mu u_\nu\,\rangle \,+\, L_{10}/4\,\langle\, f_{+\mu\nu} f_+^{\mu\nu} - f_{-\mu\nu} f_-^{\mu\nu}\,\rangle \\ & + i\,L_{11}\langle\,\chi_-(\nabla_\mu u^\mu + i/2\,\chi_-)\,\rangle \,-\, L_{12}\langle\,(\nabla_\mu u^\mu + i/2\,\chi_-)^2\,\rangle \\ & + H_1/2\,\langle\, f_{+\mu\nu} f_+^{\mu\nu} + f_{-\mu\nu} f_-^{\mu\nu}\,\rangle \,+\, H_2/4\,\langle\,\chi_+^2 - \chi_-^2\,\rangle\,, \end{aligned} \tag{3.77}$$

where the terms whose coefficients are L_{11} and L_{12} do vanish considering the equations of motion (EOM) of $\mathcal{O}(p^2)$. The EOM for $\mathcal{L}_2$ is:

$$\mathcal{O}_2^{EOM}(u) \;=\; \nabla_\mu u^\mu \,-\, \frac{i}{2}\left(\chi_- - \frac{1}{n_f}\langle\,\chi_-\,\rangle\right) \;=\; 0; \tag{3.78}$$

L_{11} and L_{12} can now be skipped at $\mathcal{O}(p^4)$ using that:

$$\mathcal{L}_4^{\text{off-shell}} \;=\; L_{11}\langle\, \chi_- \mathcal{O}_2^{EOM}(u)\,\rangle \;-\; L_{12}\langle\, \mathcal{O}_2^{EOM}(u)\mathcal{O}_2^{EOM}(u)^\dagger\,\rangle. \tag{3.79}$$

The terms with coefficients H_1 and H_2 are contact terms relevant for the renormalization of χPT.

The renormalization of χPT needed to work at $\mathcal{O}(p^4)$ was accomplished in Refs.

Operador	P	C	h.c.	χ order
u_μ	$-u^\mu$	u_μ^T	u_μ	p
$\chi_\pm$	$\pm\chi_\pm$	$\chi_\pm^T$	$\pm\chi_\pm$	p^2
$f_{\mu\nu\,\pm}$	$\pm f_\pm^{\mu\nu}$	$\mp f_{\mu\nu\,\pm}^T$	$f_{\mu\nu\,\pm}$	p^2
Φ	-Φ	Φ^T	Φ	1
u	$u^\dagger$	u^T	$u^\dagger$	1
Γ^μ	Γ_μ	-$\Gamma^{\mu\,T}$	-Γ^μ	p
$u_{\mu\nu}$	$-u^{\mu\nu\,\dagger}$	$u_{\mu\nu}^T$	$u_{\mu\nu}^\dagger$	p^2
$\nabla_\mu u_\nu$	-$\nabla^\mu u^\nu$	$(\nabla_\mu u_\nu)^T$	$\nabla_\mu u_\nu$	p^2

Table 3.3: Transformation properties under C, P and hermitian conjugation of the chiral tensors and other useful structures in the u-formalism. T means transposed.

[4, 5]. The divergences that arise using $\mathcal{L}_2$ at one-loop, divergences are of order $\mathcal{O}(p^4)$ and are renormalized with the $LECs$ of $\mathcal{L}_4$:

$$\begin{aligned} L_i &= L_i^r(\mu) + \Gamma_i \frac{\mu^{D-4}}{32\pi^2}\left\{\frac{2}{D-4} + C\right\}, \\ H_i &= H_i^r(\mu) + \tilde{\Gamma}_i \frac{\mu^{D-4}}{32\pi^2}\left\{\frac{2}{D-4} + C\right\}, \end{aligned} \tag{3.80}$$

where D is the space-time dimension and C is a constant defining the renormalization scheme.

The renormalized couplings, $L_i^r(\mu)$ do depend on the arbitrary renormalization scale μ. This dependence cannot survive in any physical observable. As it had to happen, it is canceled out with that coming from the loop in any physically meaningful quantity.

As we said, the odd-intrinsic parity sector starts at $\mathcal{O}(p^4)$. Its appearance is due to one of the anomalies affecting the chiral group $U(3)_L \otimes U(3)_R$. On the one hand there is the anomaly which makes that the classical symmetry $U(1)_A$ is lost at the quantum level. Apart from group color factor, it is identical to the case of the axial anomaly of QED, discovered perturbatively in one-loop computations [243, 244] by Adler, Bell and Jackiw. Later on, the proof that this result does not receive radiative corrections [245] by Adler and Bardeen insinuated that anomalies

could have a non-perturbative nature, as it was shown by Fujikawa, using the path-integral formalism [246, 247].

On the other hand, there is an anomaly that affects the whole $U(3) \otimes U(3)$ symmetry group that has its origin in the fact that it is not possible to preserve the simultaneous invariance of the generating functional under vector and axial-vector transformations. Wess and Zumino [241] were the first to obtain a functional generating this anomaly that affects chiral transformations written in terms of *pGs*. Operatively, it is more useful the one derived later by Witten [242], that I will present here following the discussion in [248].

The fermionic determinant does not allow for a chiral invariant regularization. Given the transformations

$$g_R \,=\, 1 \,+\, i(\alpha(x) + \beta(x))\,,\; g_L \,=\, 1 \,+\, i(\alpha(x) - \beta(x)), \tag{3.81}$$

the conventions in the definition of the fermionic determinant may be chosen to preserve the invariance of the generating functional, Z, either under V transformations, or under the A ones; but not both simultaneously. Choosing to preserve invariance under the transformations generated by the vector current, the change in Z only involves the difference $\beta(x)$ between g_R and g_L.

$$\begin{aligned}
\delta Z &= -\int \mathrm{d}x \langle\, \beta(x)\Omega(x)\,\rangle\,, && (3.82)\\
\Omega(x) &= \frac{N_C}{16\pi^2}\varepsilon^{\alpha\beta\mu\nu}\left[v_{\alpha\beta}\, v_{\mu\nu} \,+\, \frac{4}{3}\, D_\alpha\, a_\beta\, D_\mu a_\nu \,+\, \frac{2i}{3}\,\{\, v_{\alpha\beta},\, a_\mu\, a_\nu\}\right.\\
&\qquad \left. +\, \frac{8i}{3}\, a_\mu\, v_{\alpha\beta}\, a_\nu \,+\, \frac{4}{3}\, a_\alpha a_\beta\, a_\mu\, a_\nu\right]\,, && (3.83)\\
v_{\alpha\beta} &= \partial_\alpha\, v_\beta \,-\, \partial_\beta v_\alpha \,-\, i\,[v_\alpha,\, v_\beta]\,, && (3.84)\\
D_\alpha\, a_\beta &= \partial_\alpha\, a_\beta \,-\, i\,[v_\alpha,\, a_\beta]\,. && (3.85)
\end{aligned}$$

Notice that Ω only depends on the external fields, v_μ and a_μ, and that the quark masses do not occur.

The explicit form for the functional $Z\,[U, \ell, r]$ that reproduces the chiral anomaly

given by Witten [242] is:

$$
\begin{aligned}
Z\,[U,\,\ell,\,r]_{\rm WZW} \;&=\; -\frac{i\,N_C}{240\pi^2}\int_{M^5} {\rm d}^5x\varepsilon^{ijklm}\langle\,\Sigma_i^L\,\Sigma_j^L\,\Sigma_k^L\,\Sigma_l^L\,\Sigma_m^L\,\rangle \qquad (3.86)\\
&\quad -\frac{iN_C}{48\pi^2}\int {\rm d}^4x\varepsilon_{\mu\nu\alpha\beta}\left(W(U,\,\ell,\,r)^{\mu\nu\alpha\beta}\,-\,W(\mathbf{1},\,\ell,\,r)^{\mu\nu\alpha\beta}\right)\\
W(U,\,\ell,\,r)_{\mu\nu\alpha\beta} \;&=\; \langle\,U\,\ell_\mu\,\ell_\nu\,\ell_\alpha\,U^\dagger\,r_\beta\,+\,\frac{1}{4}\,U\,\ell_\mu\,U^\dagger\,r_\nu\,U\,\ell_\alpha\,U^\dagger\,r_\beta\,+\,i\,U\,\partial_\mu\,\ell_\nu\,\ell_\alpha\,U^\dagger\,r_\beta\\
&\quad +i\,\partial_\mu\,r_\nu\,U\,\ell_\alpha\,U^\dagger\,r_\beta\,-\,i\,\Sigma_\mu^L\,\ell_\nu\,U^\dagger\,r_\alpha\,U\,\ell_\beta\,+\,\Sigma_\mu^L\,U^\dagger\,\partial_\nu\,r_\alpha\,U\,\ell_\beta\\
&\quad -\Sigma_\mu^L\,\Sigma_\nu^L\,U^\dagger\,r_\alpha\,U\,l_\beta\,+\,\Sigma_\mu^L\,l_\nu\,\partial_\alpha\,l_\beta\,+\,\Sigma_\mu^L\,\partial_\nu\,l_\alpha\,l_\beta\\
&\quad -i\,\Sigma_\mu^L\,\ell_\nu\,\ell_\alpha\,\ell_\beta\,+\,\frac{1}{2}\,\Sigma_\mu^L\,\ell_\nu\,\Sigma_\alpha^L\,\ell_\beta\,-\,i\,\Sigma_\mu^L\,\Sigma_\nu^L\,\Sigma_\alpha^L\,\ell_\beta\,\rangle\\
&\quad -(L\,\longleftrightarrow\,R)\;,\;N_C\,=\,3\,,\\
&\quad \Sigma_\mu^L\,=\,U^\dagger\,\partial_\mu\,U\;,\;\Sigma_\mu^R\,=\,U\,\partial_\mu\,U^\dagger\,, \qquad (3.87)
\end{aligned}
$$

where $(L\,\longleftrightarrow\,R)$ stands for the exchange

$$
U\,\longleftrightarrow\,U^\dagger\;,\quad \ell_\mu\,\longleftrightarrow\,r_\mu\;,\quad \Sigma_\mu^L\,\longleftrightarrow\,\Sigma_\mu^R\,. \qquad (3.88)
$$

The first term in Eq. (3.86) bears the mark of the anomaly: It is a local action in five dimensions that can not be written as a finite polynomial in U and $D_\mu U$ in four dimensions. This term involves at least five pseudoscalar fields and will not contribute either to the hadron three meson decays of the τ or to its radiative decays with one meson in the final state. Eqs. (3.86) and (3.87) contain all the anomalous contributions to electromagnetic and semileptonic weak meson decays: $\pi^0\,\to\,\gamma\gamma$, $\pi\,\to\,e\nu_e\gamma$, etc. For further discussions on this topic see also Ref. [249].

3.14 NNLO overview and scale over which the chiral expansion is defined

χPT is an expansion in powers of momentum over a typical hadronic scale that we can understand in two equivalent ways:

- pGs stand out due to $S\chi SB$. This generates -through quantum effects-, the $S\chi SB$-scale, Λ_χ, as a natural parameter over which the chiral expansion is defined.

- Decoupling theorem told us that one of the effects of heavy integrated-out particles in the physics of light modes appears in inverse powers of these larger masses. Then, we expect typical masses of the lowest-lying resonances to provide this scale, as well.

I will start considering the appearance of that scale through loops. For this, let us consider scattering among pGs at $\mathcal{O}(p^4)$. Apart from the tree level contribution of $\mathcal{L}_4$, there will be that given by $\mathcal{L}_2$ at one-loop, whose amplitude is of order

$$I \sim \int \frac{\mathrm{d}^4 p}{(2\pi)^4} \frac{p^2}{F^2} \frac{p^2}{F^2} \frac{1}{p^4}\,, \tag{3.89}$$

where $1/p^4$ comes from the internal boson propagators and each interacting vertex of $\mathcal{L}_2$ gives -after expanding the LO Lagrangian up to terms with four powers of Φ, that is, four pGs- a factor $(p/F)^2$ [8]. One can estimate this integral as

$$I \sim \frac{q^4}{16\pi^2} \frac{1}{F^4} \log \mu\,, \tag{3.90}$$

where μ is the renormalization scale. On the other hand, the tree level interaction given by $\mathcal{L}_4$ has the shape $L_i^r\,(q/F)^4$. We know the total amplitude is scale independent which implies that a shift in the scale μ has to be balanced by that of the tree level $\mathcal{L}_4$ contribution. The loop-related factor $1/16\,\pi^2$ must be also in $\mathcal{L}_4$.

We can write the $\mathcal{L}_{eff}$ as:

$$\mathcal{L} = \frac{F^2}{4}\left[\widetilde{\mathcal{L}}_2 + \frac{\widetilde{\mathcal{L}}_4}{\Lambda_\chi^2} + \frac{\widetilde{\mathcal{L}}_6}{\Lambda_\chi^4}\ldots\right], \tag{3.91}$$

where $1/\Lambda_\chi$ gives the expansion of the EFT-Lagrangian in powers of q/Λ_χ. It is straightforward to check that this also happens as the chiral order in the expansion is increased. Taking into account the loop-related factor, we estimate

$$\Lambda_\chi \sim 4\pi F \sim 1\,\mathrm{GeV}\,. \tag{3.92}$$

This dimensional analysis suggests that the $n-pGs$ vertex will receive a contribution from the $\mathcal{O}(p^m)$ Lagrangian that will go as

$$F^2\Lambda_\chi^2 \left(\frac{\Phi}{F}\right)^n \left(\frac{\partial}{\Lambda_\chi}\right)^m, \tag{3.93}$$

and, consequently, the $LECs$ in the Lagrangian will be of order

$$\frac{F^2}{\Lambda_\chi^{m-2}} \sim \frac{F^{4-m}}{(4\pi)^{m-2}}\,. \tag{3.94}$$

On should be aware that $\Lambda_\chi \sim 1$ GeV does not mean χPT can be applied up to this energy. The complementary point of view explained at the beginning helps to understand this. $M_\rho \sim 0.8$ GeV sentences all χPT attempts to explain physics from this region on to failure unless one explicitly incorporates resonances as active

[8] All vertices will have some momentum p, but other external ones too. The q below intends to represent these ones.

degrees of freedom, as $R\chi T$ does.

$M_\rho \sim 0.8$ GeV is to be regarded as a clear upper bound for the validity of χPT and corresponds to the typical size of the counterterm corrections. On the other hand, $4\pi F \simeq 1.2$ GeV is the scale associated to quantum effects through loop corrections.

There is still one more reason for using $R\chi T$ when we go over 0.5 GeV, or so. The lowest order contributions in the chiral expansion lose importance continuously and we are forced to go further and further in the expansion to reach the same accuracy. Two $LECs$ specify the $\mathcal{O}(p^2)$ Lagrangian , 10 appear at $\mathcal{O}(p^4)$ but 90 are challenging us and the number of different experimental data we can collect to fix them at $\mathcal{O}(p^6)$. Although not all of them enter a given process, the description becomes pretty much easier when resonances become active variables, as we will see. The $\mathcal{O}\left(p^6\right)$ χPT Lagrangian was developed and the renormalization program was accomplished in Refs. [250, 251, 252, 253].

Chapter 4

The Large N_C limit and Resonance Chiral Theory

4.1 Introduction

We finished the last Chapter by recalling some of the motivations for enlarging χPT and extend it to higher energies. The problem is that as soon as we try to do it the chiral counting gets broken because the momentum of the pGs can get comparable to Λ_χ or M_ρ. Thus, there is no immediate parameter to build the expansion upon.

In many other instances in QCD, this difficulty does not occur. QCD is perturbative at high energies, so the same strong coupling is a useful expansion parameter in that energy region. There can be a double expansion (in α_S and $1/M_Q$) because pole masses are good parameters for a quick convergence of the perturbative series when studying heavy quarks: Heavy Quark Effective Theory ($HQET$) -for just one heavy quark- [254, 255, 256, 257, 258, 259] , or (potential) Non-Relativistic QCD ($(p)NRQCD$) -if both quarks are heavy- [260, 261, 262, 263, 264, 265, 266, 267, 268].

In addition to the lack of a natural expansion parameter in the region where the light-flavoured resonances pop up, there is some thinking in χPT, that might guide the strategy to follow. While in the $EFTs$ listed in the previous paragraph the expansion parameters are quantities appearing in the QCD Lagrangian, this is not the case for χPT: the expansion involves the momenta and masses of the pGs and Λ_χ (not the quarks and gluons and Λ_{QCD}).

The proposed expansion parameter, $1/N_C$, will indeed be useful to describe the physics of light-flavoured mesons. Moreover, it can be used to understand qualitatively some results in χPT in terms of a quantity that defines the gauge group of the strong interactions in QCD.

4.2 $1/N_C$ expansion for QCD

't Hooft [125] had the seminal idea of generalizing QCD from a theory of three colours to the case with N_C colours. Though a priori this can be regarded as an unnecessary artifact that will make things even more difficult, this is not -at all- the case, and QCD gets simplified in the large-N_C limit becoming even solvable in one spatial plus one time dimension [126].

Later on, many papers appeared guided by 't Hooft's idea, Ref. [127] is the capital one, but see also Refs. [269, 270, 271]. This part of the chapter is mainly based on them and on Refs. [272, 273, 274, 275].

As we will see, there are many phenomenological facts that find their only explanation on large-N_C arguments. This is, at the end of the day, the strongest support the $1/N_C$ expansion for QCD has.

Recall the QCD Lagrangian, (1.15). From it, we can read off the Feynman rules obtained for all QCD vertices and see how the coupling of a fermionic line to a gluon is $\mathcal{O}(g_s)$, exactly as the three gluon vertex. The four gluon interaction is $\mathcal{O}(g_s^2)$, each quark loop runs over three colours and each gluon loop over eight possibilities, corresponding to the number of generators of $SU(3)_C$. Eight is not so much greater than three, but in the large-N_C limit, the number of gluon states (N_C^2-1) is really huge compared to that of quarks (N_C). It is also reasonable to approximate N_C^2-1 by N_C^2, that is, to consider $U(N_C)$ instead of $SU(N_C)$. The first ingredient of the large-N_C limit of QCD is to take into account that gluon states are more important than quark states. The second one comes from asking a finite behaviour in this limit for the quantum corrections and happens to modify the usual counting in powers of g_s for the vertices reminded before.

Prior to that, it is useful to introduce in this context the double line notation for the gluon lines. This way we represent each gluon as a quark-antiquark pair, an approximation that becomes exact in the large-N_C limit. For the gluon selfenergy, we will have the diagrams displayed in Fig. 4.1.

Within the new notation, each line represents a given colour propagating. After fixing external colour indices, there is no remaining freedom in the quark-loop contribution, but there is still an inner loop in the purely gluon contribution over which N_C colours can run.

If we now use the Feynman rules obtained from Eq. (1.15), we perceive that the second diagram in Figure 4.1 behaves, in the large-N_C limit, as g_s^2, while the first one diverges: it goes as $g_s^2\, N_C$. As we want gluon self-energy (and the β-function) to be finite in the limit $N_C \to \infty$, we are led to redefine g_s as $\tilde{g}_s \equiv \frac{g_s}{\sqrt{N_C}}$. This also modifies the Feynman rules. Now, gluon coupling to a fermionic current or three gluon vertex will be of $\mathcal{O}\left(\frac{1}{\sqrt{N_C}}\right)$; and four gluon local interaction of $\mathcal{O}\left(\frac{1}{N_C}\right)$. This way, the beta function reads:

$$\mu \frac{\mathrm{d}\tilde{g}_s}{\mathrm{d}\mu} \;=\; -\left(11 - 2\frac{n_f}{N_C}\right)\, \frac{\tilde{g}_s^2}{48\pi^2}\,, \tag{4.1}$$

Figure 4.1: Feynman diagrams for the *LO* contribution to the gluon self-energy: using the usual notation (left), and with the double line one (right).

and we keep the hadronization scale Λ_{QCD} independent of the number colours when it is taken to be large. One can see from Eq.(4.1) that quark loops are suppresed with respect to gluon loops in the large-N_C limit.

Let us consider now the diagrams of Figure 4.2.

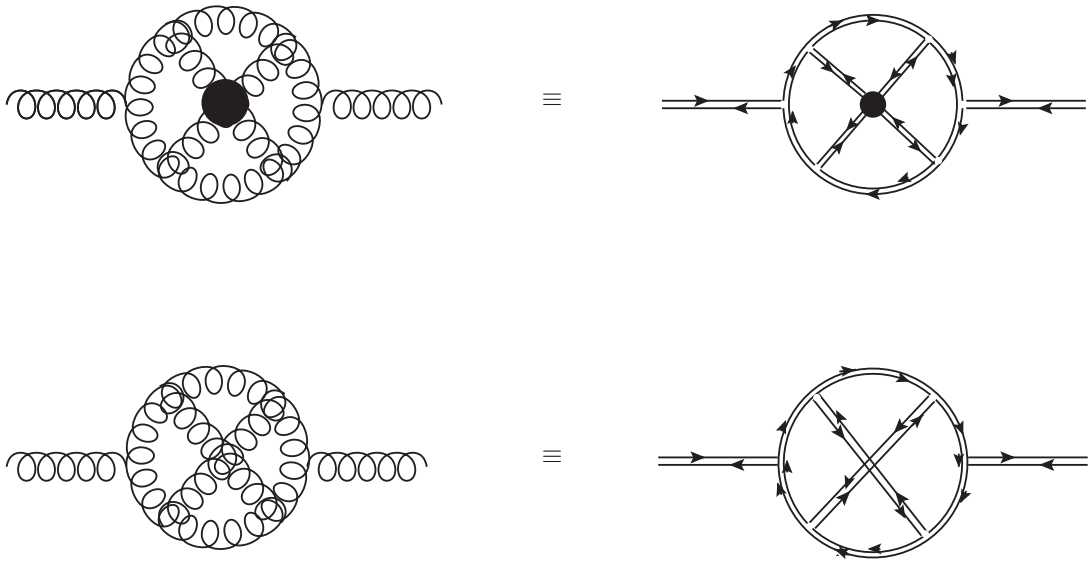

Figure 4.2: Comparison between planar and non-planar diagrams for gluon self-energy. The four-gluon vertex is depicted by a thick dot. Other superpositions of two gluon lines correspond to crossings and not to intersections.

The upper diagram in Figure 4.2 is planar -all superposition of lines correspond to intersections- , while the lower one is not -some of them are just crossings-. For the first one, the counting is $\left(\frac{1}{\sqrt{N_C}}\right)^6 \frac{1}{N_C} N_C^4 = 1$, of the same order than the purely

gluon contribution in Figure 4.1.

For the lower one, we have $\left(\frac{1}{\sqrt{N_C}}\right)^6 N_C = \frac{1}{N_C^2}$. This is because the diagram is non-planar and the number of colour loops has decreased from four to one and the central vertex has disappeared.

We have seen explicitly how, in the easiest examples, two selection rules arise:

- Non-planar diagrams are suppressed by the factor $\frac{1}{N_C^2}$.
- Internal quark loops are suppressed by the factor $\frac{1}{N_C}$.

Planar diagrams, with arbitrary exchanged gluons do dominate (and the obliged external quark loop to be a meson).

To see that all this is always true it is convenient to rescale fermion and gluon fields:

$$\tilde{G}^a_\mu = \frac{\tilde{g}_S}{\sqrt{N_C}} G^a_\mu \,, \tag{4.2}$$

$$\tilde{q} = \frac{1}{\sqrt{N_C}} q \,, \tag{4.3}$$

whence

$$\mathcal{L}_{QCD} = N_C \left[\bar{\tilde{q}} \left(i\tilde{\not{D}} - \mathcal{M} \right) \tilde{q} - \frac{1}{4\tilde{g}_S^2} \tilde{G}^a_{\mu\nu} \tilde{G}^{\mu\nu}_a \right] , \tag{4.4}$$

and all the counting is simply in powers of $\frac{1}{N_C}$. It can be seen [273] that the order in this expansion for any connected vacuum diagram is related to a topological invariant, the Euler-Poincaré characteristics, which allows to demonstrate the above properties in full generality independently of the number of exchanged gluons. The conclusion we draw is clear: In the large-N_C limit, Feynman diagrams are planar and without internal quark loops.

It is worth to stress that $\frac{1}{N_C}$-expansion for QCD has to be regarded in a different way than usual expansions in perturbation theory. Expanding in powers of the coupling constant gives us Feynman diagrams and, at any given order, there are a finite number of them contributing to a process. Looking at the commented equivalence among diagrams belonging to Figure 4.1, which is clearly the LO Feynman diagram, and to Figure 4.2; a general fact is enlightened: In order to obtain a given order in $\frac{1}{N_C}$, we need an infinite number of Feynman diagrams. The diagrams collected in Figure 4.3 are both of LO in $1/N_C$ and one could think of much more complicated ones.

4.3 N_C counting rules for correlation functions

Two related basic assumptions are made for studying meson dynamics in the large-N_C limit:

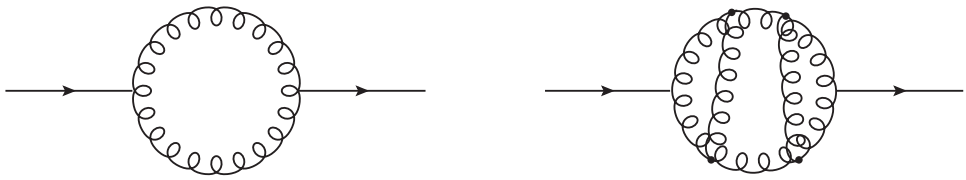

Figure 4.3: Two *LO* contributions in $1/N_C$ to gluon self-energy. Gluon vertices are highlighted by a thick dot.

- QCD remains to be a confining theory for $N_C \to \infty$.
- Therefore, the sum of the dominant planar diagrams is responsible of confinement in this limit.

We will consider quark and gluon composite operators whose quantum numbers are able to create a meson [1] (they must be color-singlet thus). The aim is to understand some salient features of meson phenomenology by looking to gauge invariant operators that cannot be splitted into separate gauge invariant pieces. For the quark operators, [2] the suitable bilinears are named according to the same spin-parity assignments used for mesons: scalars ($\overline{q}\,q$), pseudoscalars ($\overline{q}\,\gamma_5\,q$), vectors ($\overline{q}\,\gamma^\mu\,q$), or axial-vectors ($\overline{q}\gamma^\mu\,\gamma_5 q$). We will represent them generically as $\tilde{\mathcal{O}}_i(x)$. We will use again the method of external sources (or currents, $J_i(x)$) coupled to them. In order to be consistent with the counting for the rescaled fields introduced in Eq. (4.2), the right expression to add will be [273] $N_C\, J_i(x)\, \tilde{\mathcal{O}}_i(x)$ that will keep all the selection rules told before. Correlations functions are obtained functionally differentiating the generating functional $W(J)$ with respect to the sources:

$$\langle\, \tilde{\mathcal{O}}_1\, \tilde{\mathcal{O}}_2 \ldots \tilde{\mathcal{O}}_z\, \rangle_C \;=\; \frac{1}{iN_C}\,\frac{\partial}{\partial J_1}\,\frac{1}{iN_C}\,\frac{\partial}{\partial J_2}\cdots\frac{1}{iN_C}\,\frac{\partial}{\partial J_z} W(J)|_{J=0}\,, \tag{4.5}$$

and each additional functional differentiation (*i.e.* each source insertion) is weighted by a factor $\sim \frac{1}{N_C}$. It can be shown that $\mathcal{O}(N_C^2)$ contributions stem from planar vacuum-like diagrams only with gluon lines. They can contribute to correlation functions of purely gluon operators. n-point Green function of purely gluon operators will be of $\mathcal{O}(N_C^{2-n})$. An r-meson vertex is of order $N_C^{1-r/2}$. Quark bilinear operators start contributing at $\mathcal{O}(N_C)$ -which corresponds to a quark loop in the outermost border-, being $\mathcal{O}(N_C^{1-n})$ the corresponding n-point Green function.

Considering that with $N_C = 3$ the symmetric wave-function in colour space of a meson is written as

$$M \;=\; \frac{1}{\sqrt{3}}\,\sum_{i=1}^{3}\overline{q}_i\,q_i\,, \tag{4.6}$$

[1] The large-N_C limit is also useful to understand some properties of baryons. For a review on this topic, see Refs.[273, 276, 277, 278].

[2] Symmetries also allow mixed operators composed by quarks and gluons and glueballs made up of gluons only.

in the large-N_C limit this will be

$$M \;=\; \frac{1}{\sqrt{N_C}} \sum_{i=1}^{N_C} \overline{q}_i \, q_i \,, \tag{4.7}$$

providing an amplitude for creating a meson that is -as it should be- independent of N_C. This property applies also for glueballs.

For any arbitrary number of currents, the dominant contribution will be

$$\langle \, T \, (J_1 \ldots J_n) \, \rangle \;\sim\; \mathcal{O}(N_C) \,, \tag{4.8}$$

given by diagrams with one external quark loop and arbitrary insertions of gluon lines that do not spoil the planarity of the diagram.

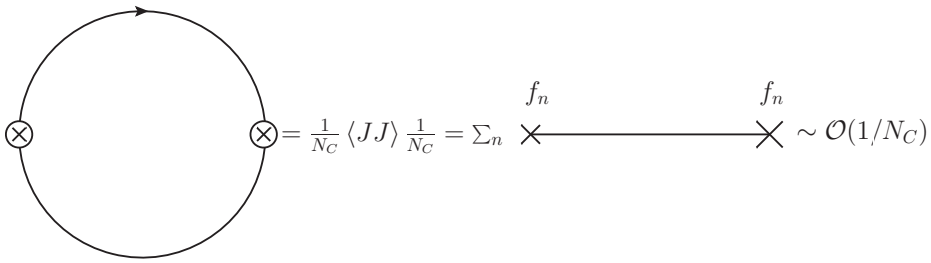

Figure 4.4: Basic diagram for the 2-point correlator and representation as a sum of tree-level diagrams with meson exchange.

In Ref. [273], it is shown that the action of $J(x)$ over the vacuum will create only one-meson states in the large-N_C limit. Taking this into account, the two-current correlator is of the form:

$$\langle \, J(k) \, J(-k) \, \rangle \;=\; \sum_n \frac{f_n^2}{k^2 - m_n^2} \,, \tag{4.9}$$

where the sum extends over infinite meson states of mass m_n and decay constant f_n defined through $f_n \;=\; \langle \, 0 | J | n \, \rangle$. This is a capital result from which we can derive most of meson phenomenology in this limit:

- Being $\langle \, JJ \, \rangle \sim \mathcal{O}(N_C)$, $f_n \;\sim\; \mathcal{O}(\sqrt{N_C})$ because k^2 has nothing to do with the N_C-counting. Meson decay constants are $\mathcal{O}(\sqrt{N_C})$.

- Moreover, the whole denominator must be $\mathcal{O}(1)$, whence $m_n \;\sim\; \mathcal{O}(1)$, too. Meson masses are said to have smooth large-N_C limit.

- $\langle \, J(k) \, J(-k) \, \rangle$ is known to have a logarithmic behaviour at large momentum [279, 280, 281, 282], k. Therefore, if we are to obtain these logarithms adding terms going as $1/k^2$, we will need an infinite number of them. Despite seeming quite surprising at first, the conclusion is clear: There are infinite mesons in the large-N_C limit.

- The poles of (4.9) are all in the real axis. Because the instability of a particle is translated into an imaginary part in its propagator that has to do with its decay width, we deduce that mesons are stable for $N_C \to \infty$.

To sum up, the two-point correlator is reduced in the large-N_C limit to the addition of tree-level diagrams in which $J(-k)$ creates a meson with amplitude f_n that propagates according to $\frac{1}{k^2-m_n^2}$ being annihilated by $J(k)$ with the same amplitude.

It is straightforward to generalize this result for an arbitrary number of currents. It can be shown that, in the large-N_C limit [274]:

- n-point Green functions are given by sums of tree level diagrams obtained by using a phenomenological Lagrangian written in terms of freely propagating mesons that accounts for local effective interactions among $m \leq n$ of them.

- Mesons do not interact, because both the m-meson vertex and the matrix element creating m mesons from the vacuum are $\mathcal{O}(N_C^{1-m/2})$, suppressed in this limit.

- The same can be applied for gluon states by considering gluon currents, $J_G = \langle\, G^{\mu\nu\, a}\, G_{\mu\nu\, a}\,\rangle$. The n-point Green function is $\mathcal{O}(N_C^2)$ and a g-gluon operator vertex is $\mathcal{O}(N_C^{2-g})$; so gluon states are also free, stable and non-interacting in the strict limit.

- The mixed correlator with m quark-bilinears and g gluon operators is $\mathcal{O}(N_C)$, but the local vertex among all them is $\mathcal{O}(N_C^{1-g-m/2})$, that is suppressed, too. Gluon and meson states do decouple in the large-N_C limit, being their ensemble suppressed by $1/\sqrt{N_C}$.

All this discussion is portrayed by Figure 4.5 where the counting in $1/N_C$ is given.

When considering the different Green functions, one wants to guarantee that all the poles are originated by the tree-level diagrams obtained from an EFT-Lagrangian. To show this, one needs to restore to unitarity and crossing symmetry. Crossing means that every pole appearing in a given channel will manifest in all others related to the previous one by crossing. Unitarity guarantees that every appearance of a pole in a given diagram will reappear each time this particular topology will occur as a subdiagram in a higher-order Green function. All amplitudes are thus produced by tree level exchanges with vertices given in an EFT-Lagrangian.

Some might raise an objection about the convergence of a series in $1/N_C$ that ends up being $1/3$ in the real world. QED is known to have a well-behaved perturbative expansion in powers of $\frac{\alpha_{\rm em}}{4\pi} = \frac{e^2}{(4\pi)^2} \sim 5 \cdot 10^{-4}$, but the electric charge unit is not that small, $e \sim 1/3 \sim 1/N_C$. In any case, in QCD the expansion is not in powers of $1/N_C^2$, although many times the corrections to LO in $1/N_C$ happen to be of this order. In spite of this, $1/N_C$ is a good expansion parameter for QCD, attending to the phenomenological successes in meson dynamics and also to the corroborated predictions large-N_C limit gives both for χPT and for $R\chi T$. All these reasons seem

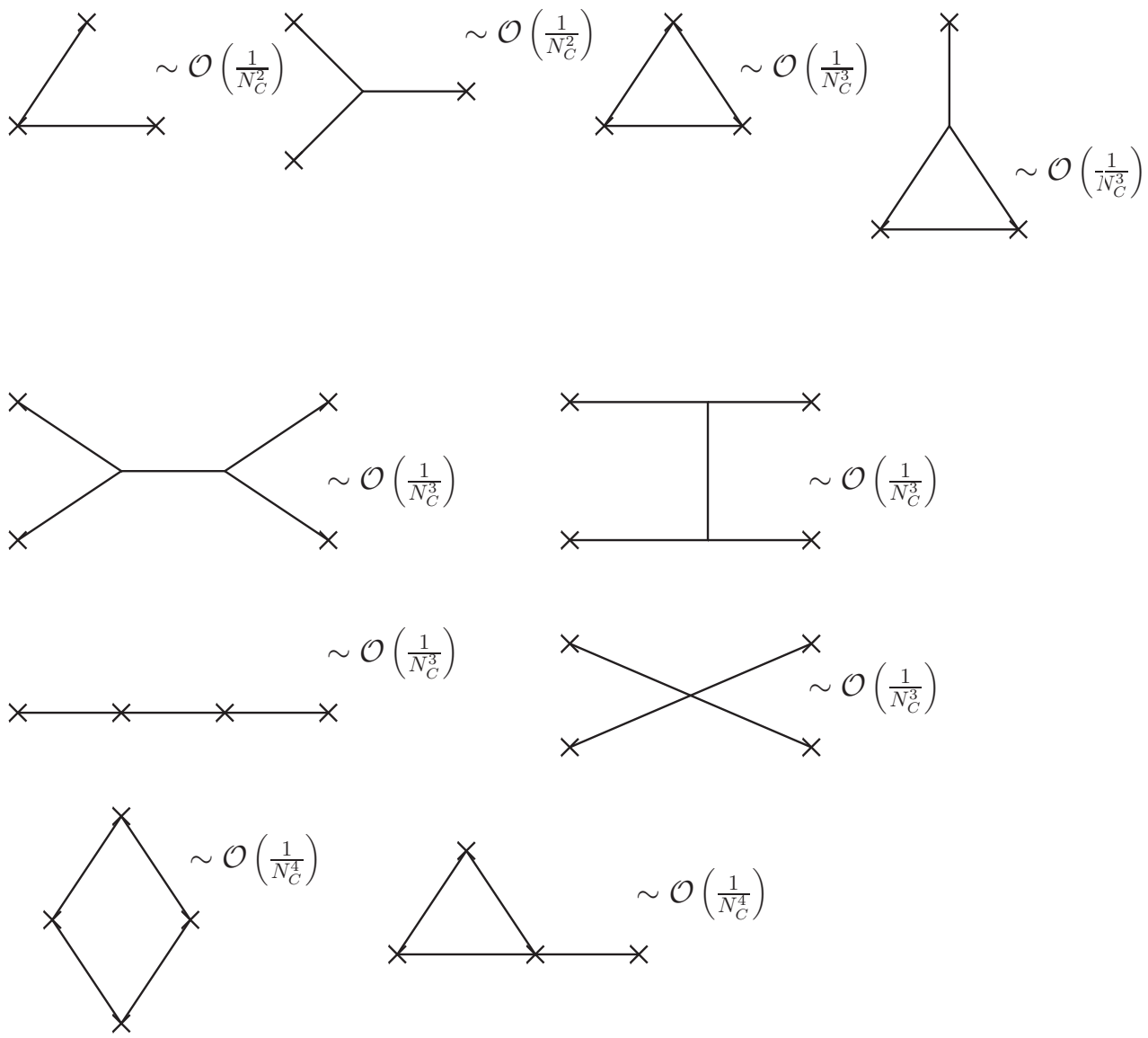

Figure 4.5: 3 and 4-point correlators given by meson exchanges: Tree-level diagrams are dominant and every quark loop is suppressed by one power of $1/N_C$. The counting in $1/N_C$ is given for all of them taking into account that every source brings in a $1/N_C$ factor and that r-meson vertices introduce the factor $N_C^{1-r/2}$.

to suggest that some factor comes to complement $1/N_C$ for the expansion parameter to be lowered. Unfortunately, we cannot check this explicitly. As it was told in the introduction to this chapter, an infinite number of Feynman diagrams contribute to each order in $1/N_C$ and nobody has achieved the formidable task of computing them by some clever resummation. For the moment, it is impossible to be more precise defining the expansion parameter of the large-N_C limit of QCD, but the reason lies in the different nature this expansion has compared to usual perturbative expansions

in powers of the coupling constant.

4.4 Resonance Chiral Theory

Our methodology stands on the construction of an action, with the relevant degrees of freedom (Weinberg's approach), led by the chiral symmetry and the known asymptotic behaviour of form factors and Green functions driven by large-N_C QCD. The large-N_C expansion of $SU(N_C)$ QCD implies that, in the $N_C \to \infty$ limit, the study of Green functions of QCD currents can be carried out through the tree level diagrams of a Lagrangian theory that includes an infinite spectrum of non-decaying states. Hence the study of the resonance energy region can be performed by constructing such a Lagrangian theory. The problem is that we do not know how to implement an infinite spectrum in a model independent way. However, it is well known from the phenomenology that the main role is always played by the lightest resonances. Accordingly it was suggested in Refs. [6, 7] that one can construct a suitable Lagrangian involving the lightest nonets of resonances and the octet of Goldstone bosons states (π, K and η). This is indeed an appropriate tool to handle the hadron decays of the tau lepton. The guiding principle in the construction of such a Lagrangian is chiral symmetry. When resonances are integrated out from the theory, i.e. one tries to describe the energy region below such states ($E \ll M_\rho$), the remaining setting is that of χPT, that was described in Chapter one and in the previous section in the context of the large-N_C limit. Then, $R\chi T$ is a link between the chiral and asymptotic regimes of QCD and a very useful tool to understand intermediate-energy QCD dynamics.

The path-integral formalism is adequate to explain what we are doing. Starting from the generating functional, Z, of QCD, one obtains the different Green functions taking the suitable functional derivatives of Z. Depending on up to which energy we consider the interesting physics scale to be, the heavier integrated-out degrees of freedom will be all meson resonances (χPT), or just the charmed -and even heavier- mesons ($R\chi T$). That is,

$$\begin{aligned} e^{\,i\,Z} &= \int \mathcal{D}q\,\mathcal{D}\overline{q}\,\mathcal{D}G_\mu\, e^{\,i\int \mathrm{d}^4x\,\mathcal{L}_{QCD}} \\ &= \int \mathcal{D}u \prod_{i=1}^{\infty}\mathcal{D}V_i \prod_{j=1}^{\infty}\mathcal{D}A_j \prod_{k=1}^{\infty}\mathcal{D}S_k \prod_{m=1}^{\infty}\mathcal{D}P_m\, e^{\,i\int \mathrm{d}^4x\mathcal{L}_{R\chi T}(u,V_i,A_j,S_k,P_m)} \\ &= \int \mathcal{D}u\, e^{\,i\int \mathrm{d}^4x\mathcal{L}_{\chi PT}(u)}\,, \end{aligned} \tag{4.10}$$

where V, A, S, P designates the type of resonance: vector (1^{--}), axial-vector (1^{++}), scalar (0^{++}) and pseudoscalar (0^{-+}). Integrating the resonances out of the action reproduces χPT-pGs interaction simply modifying the χPT-$LECs$. In Eq. (4.10) an infinite number of resonances have been considered per each set of quantum numbers, as $N_C \to \infty$ tells. There are two approaches to this: the single resonance

approximation (*sra*) considers that the lowest-lying multiplets are able to collect the bulk of the dynamical information and these are the only resonant degrees of freedom kept active in the action. Since there is an infinite number of Green functions, it is obviously impossible to satisfy all matching conditions with asymptotic QCD with these few resonances. The minimal hadronic approximation (*mha*) generalizes the *sra* by including into the action the minimal number of resonances that allows fulfilling the QCD short-distance constraints in the considered amplitude.

$R\chi T$ includes explicitly the χPT at $\mathcal{O}(p^2)$ but, instead of adding to it the next order in the chiral expansion, that piece is supplemented with a Lagrangian describing interactions among *pGs* and resonances. The more convenient chiral tensor formalism in terms of $u(x)$ and all the other structures introduced in (3.71) for the external sources and the *pGs* (3.43), (3.44), (3.65) whose transformation properties under C, P and Hermitian conjugation were collected in Table 3.3 are employed to write:

$$\mathcal{L}_{R\chi T}(u,V,A,S,P) \,=\, \mathcal{L}^{(2)}_{\chi PT}(u) \,+\, \mathcal{L}_R(u,V,A,S,P)\,. \tag{4.11}$$

For the resonance fields, the observed multiplets tell us that only octets and singlets in flavour space occur; so reffering to them as R and R_1, respectively, the non-linear realization of the chiral group G, will be given by [3]

$$R \,\to\, h(g,\,\Phi)\, R\, h(g,\,\Phi)^\dagger\,, \qquad R_1 \,\to\, R_1\,. \tag{4.12}$$

For the first vector nonet [4], we will have:

$$\begin{aligned} V_{\mu\nu} \;&=\; \frac{1}{\sqrt{2}}\sum_{a=0}^{8}\lambda_a V^a_{\mu\nu} \qquad\qquad (4.13)\\ &=\; \begin{pmatrix} \frac{1}{\sqrt{2}}\rho^0+\frac{1}{\sqrt{6}}\omega_8+\frac{1}{\sqrt{3}}\omega_1 & \rho^+ & K^{*+} \\ \rho^- & -\frac{1}{\sqrt{2}}\rho^0+\frac{1}{\sqrt{6}}\omega_8+\frac{1}{\sqrt{3}}\omega_1 & K^{*0} \\ K^{*-} & \overline{K}^{*0} & -\frac{2}{\sqrt{6}}\omega_8+\frac{1}{\sqrt{3}}\omega_1 \end{pmatrix}_{\mu\nu}\,, \end{aligned}$$

where it has been introduced the antisymmetric tensor formulation for vector fields instead of that due to Proca, that may be more familiar [5]. With this description one is able to collect, upon integration of resonances, the bulk of the low-energy couplings at $\mathcal{O}(p^4)$ in χPT without the inclusion of additional local terms [7]. In fact it is necessary to use this representation if one does not include the $\mathcal{L}^{(4)}_{\chi PT}$ in the Lagrangian theory. Though analogous studies at higher chiral orders have not been carried out, we will assume that no $\mathcal{L}^{(n)}_{\chi PT}$ with $n = 4, 6, ...$ in the even-intrinsic-parity and $n = 6, 8, ...$ in the odd-intrinsic-parity sectors need to be included in the theory.

[3] There are many possible ways to transform the resonance fields that lead to the same transformation under the vector group and it can be shown that they are all equivalent after a field redefinition. Since we are working in the u-basis the most convenient choice is the one in Eq. (4.12).

[4] In the $N_C \to \infty$ limit octet and singlet converge to a nonet.

[5] The appendix E is specially devoted to this topic.

Operador	P	C	h.c.
$V_{\mu\nu}$	$V^{\mu\nu}$	$-V_{\mu\nu}^T$	$V_{\mu\nu}$
$A_{\mu\nu}$	$-A^{\mu\nu}$	$A_{\mu\nu}^T$	$A_{\mu\nu}$
S	S	S^T	S
P	$-P$	P^T	P

Table 4.1: Transformation properties of resonances under P, C and Hermitian conjugation.

I write the axial-vector octet since it is also of major importance in the processes considered in this Thesis:

$$\begin{aligned} A_{\mu\nu} &= \frac{1}{\sqrt{2}}\sum_{a=0}^{8}\lambda_a A_{\mu\nu}^a \qquad (4.14)\\ &= \begin{pmatrix} \frac{1}{\sqrt{2}}\mathrm{a}_1^0+\frac{1}{\sqrt{6}}h_1+\frac{1}{\sqrt{3}}f_1 & \mathrm{a}_1^+ & K_{1A}^{*+} \\ \mathrm{a}_1^- & -\frac{1}{\sqrt{2}}\mathrm{a}_1^0+\frac{1}{\sqrt{6}}h_1+\frac{1}{\sqrt{3}}f_1 & K_{1A}^{*0} \\ K_{1A}^{*-} & \overline{K}_{1A}^{*0} & -\frac{2}{\sqrt{6}}h_1+\frac{1}{\sqrt{3}}f_1 \end{pmatrix}_{\mu\nu}. \end{aligned}$$

One can proceed analogously for S and P-multiplets [6] and for the particles with $J^{PC}=1^{+-}$ [283].

The formulation of a Lagrangian theory that includes both the octet of Goldstone mesons and $U(3)$ nonets of resonances is carried out through the construction of a phenomenological Lagrangian [123, 124] where chiral symmetry determines the structure of the operators. In order to construct the relevant Lagrangians, we need to introduce the covariant derivative (3.72), dictated by the local nature of the non-linear realization of G in R (4.12), in such a way that

$$\nabla_\mu R \to h(g,\,\Phi)\,\nabla_\mu R\,h(g,\,\Phi)^\dagger\,. \qquad (4.15)$$

The transformation properties of resonance fields under P, C and Hermitian conjugation that are needed to write the Effective Lagrangian are collected in Table 4.1. For other structures appearing in the later extensions of the original Lagrangian and their transformation properties, see Section 4.6.

We have to build the most general Lagrangian involving all the pieces that respect the assumed symmetries. This means considering $\mathcal{O}(p^2)$-pG tensors together with one resonance field. If we think about $\pi\,\pi$-scattering again, this amounts to consider as the first correction to the tree level amplitude not only the one-loop diagrams obtained with arbitrary insertions of $\mathcal{L}_2$ vertices, but also meson-resonance exchange amid both pairs of pions.

For the kinetic terms, bilinears in the meson fields are considered including the covariant derivative [6] and incorporating by hand the corresponding mass of the

[6] It reduces to the ordinary one in the case of singlets.

octet or singlet. The pattern of preserved $SU(3)_V$ justifies the same mass for all members of the representation of the symmetry group and it cannot be determined from first principles, but fitted to the experiment. The discrepancy among resonance masses within the same multiplet has two sources: on the one hand it corresponds to $SU(3)_V$ breaking operators and on the other hand to NLO corrections in $1/N_C$.

The construction of the interaction terms involving resonance and Goldstone fields is driven by chiral and discrete symmetries with a generic structure given by

$$\mathcal{O}_i \sim \left\langle R_1 R_2 ... R_j \chi^{(n)}(\phi) \right\rangle , \tag{4.16}$$

where $\chi^{(n)}(\phi)$ is a chiral tensor that includes only Goldstone and auxiliary fields. It transforms like R in Eq. (4.12) and has chiral counting n in the frame of χPT. This counting is relevant in the setting of the theory because, though the resonance theory itself has no perturbative expansion, higher values of n may originate violations of the proper asymptotic behaviour of form factors or Green functions. As a guide we will include at least those operators that, contributing to our processes, are leading when integrating out the resonances. In addition we do not include operators with higher-order chiral tensors, $\chi^{(n)}(\phi)$, that would violate the QCD asymptotic behaviour unless their couplings are severely fine tuned to ensure the needed cancellations of large momenta.

Guided by these principles and considering only one resonance field, the Lagrangian that was obtained in Ref. [6] is

$$\mathcal{L}_R = \sum_{R=V,\,A,\,S,\,P} \{ \mathcal{L}_{\rm kin}(R) + \mathcal{L}_2(R) \} , \tag{4.17}$$

where the kinetic term [7] is

$$\begin{aligned} \mathcal{L}_{\rm kin}(R) &= -\frac{1}{2}\langle \nabla^\lambda R_{\lambda\mu} \nabla_\nu R^{\nu\mu} - \frac{1}{2} M_R^2 R_{\mu\nu} R^{\mu\nu} \rangle , \quad R = V, A \quad , \\ \mathcal{L}_{\rm kin}(R) &= \frac{1}{2}\langle \nabla^\mu R \nabla_\mu R - M_R^2 R^2 \rangle , \quad R = S, P \quad , \end{aligned} \tag{4.18}$$

and M_R stands for the nonet mass in the chiral limit. The purely interacting term, $\mathcal{L}_2(R)$, is given by

$$\begin{aligned} \mathcal{L}_2[V(1^{--})] &= \frac{F_V}{2\sqrt{2}} \langle V_{\mu\nu} f_+^{\mu\nu} \rangle + \frac{i\, G_V}{2\sqrt{2}} \langle V_{\mu\nu} [u^\mu, u^\nu] \rangle , \\ \mathcal{L}_2[A(1^{++})] &= \frac{F_A}{2\sqrt{2}} \langle A_{\mu\nu} f_-^{\mu\nu} \rangle , \\ \mathcal{L}_2[S(0^{++})] &= c_d \langle S\, u_\mu u^\mu \rangle + c_m \langle S\, \chi_+ \rangle + \tilde{c}_d\, S_1 \langle u_\mu u^\mu \rangle + \tilde{c}_m\, S_1 \langle \chi_+ \rangle , \\ \mathcal{L}_2[P(0^{-+})] &= i\, d_m \langle P \chi_- \rangle + i \tilde{d}_m\, P_1 \langle \chi_- \rangle , \end{aligned} \tag{4.19}$$

where all couplings are real and it has been considered only the octet for V and A, because $\langle f_\pm^{\mu\nu} \rangle = \langle [u^\mu, u^\nu] \rangle = 0$ forbides couplings for V and A singlets at this

[7] This naming can be a little bit confusing because this term also includes interactions hidden in the covariant derivative part.

chiral order.

We also assume exact $SU(3)$ symmetry in the construction of the interacting terms, i.e. at level of couplings. Deviations from exact symmetry in hadron tau decays have been considered in [284]. However we do not include $SU(3)$ breaking couplings because we are neither considering next-to-leading corrections in the $1/N_C$ expansion. These corrections have already been considered within $R\chi T$ in Refs. [192, 285, 286, 287, 288, 289, 290, 291, 292, 293, 294].

4.5 Matching $R\chi T$ with QCD asymptotic behaviour

The long distance features of QCD [295, 296] have to be inherited by $R\chi T$ as made precise by the matching conditions. At high energies, $R\chi T$ must match the OPE, and this will impose some relations among its couplings. These relations will depend upon the Lagrangian we choose. Due to historical reasons we will explain here the results obtained with the kinetic pieces and the interactions terms in Eq. (4.19) restricting our attention to those that can be relevant in the processes we examine, namely the spin-one resonances.The number of relations that we obtain will influence decisively in the predictability of the theory. Working in the *sra*, we find [274]

- Vector Form Factor.
  At LO in $1/N_C$, the form factor of the pion is given within $R\chi T$ by

$$\mathcal{F}(q^2) \,=\, 1 \,+\, \frac{F_V\, G_V}{F^2}\frac{q^2}{M_V^2 - q^2}\,. \tag{4.20}$$

  and QCD short-distance behaviour [297] dictates $\Im\mathrm{m}\ \Pi_V(q^2) \,\to$ const. as $q^2 \to \infty$, which results [8] in a relation for the resonance couplings

$$F_V\, G_V \,=\, F^2\,. \tag{4.21}$$

- Axial Form Factor.
  We consider the axial form factor $G_A(t)$ governing the matrix element $\langle\gamma|A_\mu|\pi\rangle$ [4]. Extracting $G_A(t)$ from the $\langle VAP\rangle$ Green function by setting the pion massless, one finds

$$G_A(t) = \frac{F^2}{M_V^2}\,\frac{b_1 + b_3 t}{M_A^2 - t}\ . \tag{4.22}$$

  Demanding that the form factor $G_A(t)$ vanishes for large t [7, 281, 282, 298], we obtain

$$b_3 = 0\ . \tag{4.23}$$

[8] The imaginary part of the Vector-Vector correlator is given by the Vector form factor.

Using the $R\chi T$ Lagrangian, Eq. (4.19), under the hypothesis of single resonance exchange, one finds [7, 299]

$$G_A(t) = \frac{2F_V G_V - F_V^2}{M_V^2} + \frac{F_A^2}{M_A^2 - t} \ . \tag{4.24}$$

Requiring $G_A(t)$ to vanish for $t \to \infty$ implies the relation $F_V = 2G_V$, one version of the so-called KSFR relation [300, 301]. The inclusion of bilinear resonance couplings modifies the form factor as given in Eq. (4.22) [299] with $b_1 = M_A^2 - M_V^2,\ b_3 = 0$, and it induces a correction to the KSFR relation:

$$\frac{2F_V G_V - F_V^2}{2F^2} = 1 - \frac{F_V^2}{2F^2} = \frac{M_A^2 - 2M_V^2}{2(M_A^2 - M_V^2)} \ . \tag{4.25}$$

- Weinberg's sum rules.

  The two-point function of a vector correlator between left-handed and right-handed quarks defines the mixed correlator

$$\Pi_{LR}(q^2) \ = \ \frac{F^2}{q^2} \ + \ \frac{F_V^2}{M_V^2 - q^2} \ - \ \frac{F_A^2}{M_A^2 - q^2} \, . \tag{4.26}$$

  Gluon interactions safeguard chirality, so Π_{LR} must fulfill a non-subtracted dispersion relation. Moreover, it must vanish in the chiral limit faster than $1/(q^2)^2$ as $q^2 \to \infty$. This implies [302] the relation for the couplings:

$$F_V^2 - F_A^2 \ = \ F^2 \ , \qquad M_V^2 \, F_V^2 \ - \ M_A^2 \, F_A^2 \ = \ 0 \, . \tag{4.27}$$

Considering the above restrictions (4.21), (4.25)and (4.27), we are able to write all decay constants in terms of F and the resonance masses:

$$F_V^2 \ = \ F^2 \frac{M_A^2}{M_A^2 - M_V^2} \, , \quad F_A^2 \ = \ F^2 \frac{M_V^2}{M_A^2 - M_V^2} \, , \quad G_V^2 \ = \ F^2 \left(1 \ - \ \frac{M_V^2}{M_A^2} \right) . \tag{4.28}$$

Finally, we will see that applying the QCD-ruled short-distance behaviour to the decays $\tau^- \to P^- \gamma \nu_\tau$ computed using $R\chi T$ [303] allows to relate V and A masses

$$2 \, M_A^2 \ = \ 3 \, M_V^2 \, , \tag{4.29}$$

a result that reproduces the one obtained in Ref. [304] for the form-factor $\mathcal{F}_{\pi\gamma^*\gamma}$.

These relations guarantee the matching among QCD and its EFT, $R\chi T$, for the considered Green functions. Here it comes a caveat about phenomenology and QCD.

There are infinite Green functions both in QCD and also in its $EFTs$. In perturbative QCD, all of them are described in terms of a single coupling, α_s. In non-perturbative QCD this is clearly not the case. Then, the situation changes

and, unless we bear this in mind, we can arrive -or seem to arrive, to be precise-, to inconsistencies.

There is no difference between considering one set or another of Green functions in high-energy QCD. The situation is opposite in its low and intermediate-energy regime. For instance, we have seen that for a set consisting of vector, and axial-vector form factors of pGs and LR two-point correlators the relations (4.21), (4.25) and (4.27) ensure QCD asymptotic behaviour for the EFT working in the sra.

But, once we go further and study three-point correlators and form factors involving three particles in the final state it is likely that either the previous relations get modified *in some cases*, or -what it is preferable- we admit that the sra is a valid approach if we do not intend to describe all QCD Green functions at the same time [9]. Otherwise, we are forced to incorporate a second multiplet of resonances in the (axial-)vector case.

These discrepancies among QCD-asymptotic restrictions for the parameters entering $\mathcal{L}_R$ has already been found and discussed [299]. However, the understanding of this issue is evolving as more works are concluded. Our position towards this problem will get defined in later chapters concerning the practical applications of the theory. We will see that we will arrive to consistent relations for the radiative decays of the tau with one meson and for the three meson decays. However, it is very likely that they will not coincide with the relations one could find studying four-point Green functions. In any case, the study of the latter is a too involved task that we do not consider for the time being.

4.6 Extensions of the original Lagrangian

4.6.1 Even-intrinsic parity sector

We recall the purpose of the original paper were $R\chi T$ was borned [6], it was to build a sound theory including resonances within the chiral framework that respected all principles and symmetries governing light-flavoured QCD and that was able to reproduce the $\mathcal{O}(p^4)$ even-intrinsic parity chiral Lagrangian upon integration of the resonances.

In order to construct (4.17), (4.18), (4.19), $\mathcal{O}(p^2)$-pG tensors together with one resonance field were enough to accomplish that purpose.

One may wonder why we intend to extend the original Lagrangian in $R\chi T$, while for χPT the decision consists in going one order further in the chiral expansion. The nature of pGs is completely different to that of resonances. Whereas the first ones transform non-linearly under the vector subgroup, the second ones do it linearly. This results in a huge, fundamental difference. Processes involving different number of pGs are related. For instance, all $2n$-$pGs \to 2n$-pGs scattering processes are connected at a given order. As the easiest example, all of them are written in terms of

[9] The validity of these assumptions within large-N_C QCD is studied in Refs. [305, 306, 307, 308].

the pion decay constant at LO; but the divergence structure -before renormalizing- of say $12\,\pi \to 12\,\pi$ is given by that of the simplest process $2\,\pi \to 2\,\pi$, as well.

On the contrary, resonances are not free excitations (even in absence of χSB); so that any time we want to consider physics involving one more multiplet of resonances, we have to extend our Lagrangian to include it relying again on the same symmetry principles that guided the construction of the already existing pieces.

The analysis of $\tau^- \to (\pi\,\pi\,\pi)^-\,\nu_\tau$ within $R\chi T$ [309] could not ignore the relevance of the axial-vector a_1-resonance exchange within this decay. The contribution given by the chain $a_1 \to \rho\,\pi \to \pi\,\pi\,\pi$ driven by vector exchange was accounted for by going one step beyond the work in Ref. [6] including bilinear terms in the resonance fields that lead to a coupling $a_1\,\rho\,\pi$, hence only the generalization including one pseudoscalar was considered in the quoted paper.

The most general Lagrangian respecting all the assumed symmetries and including one $\mathcal{O}(p^2)$ chiral tensor, one vector and one axial-vector resonance fields can be written [309]

$$\mathcal{L}_2^{VAP} = \sum_{i=1}^{5} \lambda_i \mathcal{O}_{VAP}^i\,, \tag{4.30}$$

where λ_i are new unknown real adimensional couplings, and the operators $\mathcal{O}_{VAP}^i$ constitute the complete set of operators for building vertices with only one pseudoscalar [10] are given by

$$\begin{aligned}
\mathcal{O}_{VAP}^1 &= \langle\, [V^{\mu\nu},\, A_{\mu\nu}]\, \chi_-\,\rangle\,,\\
\mathcal{O}_{VAP}^2 &= i\langle\, [V^{\mu\nu},\, A_{\nu\alpha}]\, h_\mu^\alpha\,\rangle\,,\\
\mathcal{O}_{VAP}^3 &= i\langle\, [\nabla^\mu V_{\mu\nu},\, A^{\nu\alpha}]\, u_\alpha\,\rangle\,,\\
\mathcal{O}_{VAP}^4 &= i\langle\, [\nabla^\alpha V_{\mu\nu},\, A_\alpha{}^\nu]\, u^\mu\,\rangle\,,\\
\mathcal{O}_{VAP}^5 &= i\langle\, [\nabla^\alpha V_{\mu\nu},\, A^{\mu\nu}]\, u_\alpha\,\rangle\,,
\end{aligned} \tag{4.31}$$

where it has been used $h^{\mu\nu}$ defined in Eq. (3.75). As we are only interested in tree level diagrams, the $\mathcal{O}(p^2)$ χPT EOM, (3.78), has been used in $\mathcal{L}_2^{VAP}$ in order to eliminate one of the possible operators.

Explicit computation of the Feynman diagrams involved in this process -and in all applications studied in this Thesis- show that all the contributions coming from $\mathcal{L}_2^{VAP}$ can be written in terms of only three combinations of their couplings

$$\begin{aligned}
\lambda_0 &= -\frac{1}{\sqrt{2}}\left[4\lambda_1 + \lambda_2 + \frac{\lambda_4}{2} + \lambda_5\right]\,,\\
\lambda' &= \frac{1}{\sqrt{2}}\left[\lambda_2 - \lambda_3 + \frac{\lambda_4}{2} + \lambda_5\right]\,,\\
\lambda'' &= \frac{1}{\sqrt{2}}\left[\lambda_2 - \frac{\lambda_4}{2} - \lambda_5\right]\,.
\end{aligned} \tag{4.32}$$

[10] For a larger number of pGs, additional operators may emerge.

4.6.2 Odd-intrinsic parity sector

Now we turn to the WZW anomalous term, we recall that it is the LO contribution in the odd-intrinsic parity sector -$\mathcal{O}(p^4)$ in the chiral counting-. In Ref. [310], that is the fundamental reference for this section, a suitable Lagrangian was built and odd-intrinsic parity processes were examined within $R\chi T$. It is a common practice to assume that upon integrating the resonances in this Lagrangian one could saturate the values of the $\mathcal{O}(p^6)$ $LECs$ of χPT in the anomalous sector, analogously as it happens in the even parity sector.

This work has an added interest, because it gave rise to a set of works studying the behaviour of 3-point Green functions in $R\chi T$ [128, 299, 311].

Several authors [312, 313, 314, 315, 316] started to analyze systematically a set of QCD three-point functions that were free of perturbative contributions from QCD at short distances [11], a fact that made more reliable a smooth matching of the OPE result went down to low energies and the EFT description by a theory including resonances.

It was shown in Ref. [315] that while the ansatz derived from the lowest meson dominance approach to the large-N_C limit of QCD incorporates by construction the right short-distance behaviour ruled by QCD, the same Green functions as calculated with a resonance Lagrangian, in the vector field representation, are incompatible with the OPE outcome. The authors pointed out that these discrepancies cannot be repaired just by introducing the chiral Lagrangian of $\mathcal{O}(p^6)$ [12], [13]. New terms including resonance fields and higher-order derivatives are needed in this case in the vector-field representation, but the general procedure remains unknown.

This can be a serious drawback for any EFT involving resonances as active fields. Ref. [310] studies one class of Green functions analyzed in Ref. [315] in the odd-intrinsic parity sector with antisymmetric tensor formalism for the resonances. This required the introduction of an odd-intrinsic parity Lagrangian in the formulation of [6] containing all allowed interactions between two vector objects (either currents or resonances) and one pseudoscalar meson. I will introduce this extension of the original Lagrangian of $R\chi T$ in the following.

In principle, taking into account Weinberg's power counting rule and resonance exchange among vertices with pseudoscalar legs; at $\mathcal{O}(p^4)$ in the even-intrinsic parity sector one needs to treat on the same footing $\mathcal{L}_2$ at one loop, $\mathcal{L}_4$ at tree-level and $\mathcal{L}_2(R)$. In Ref. [7] it was shown that at this order in the chiral counting, the

[11] They vanish in absence of $S\chi SB$ for massless quarks.

[12] When one considers the pion form factor calculated within the Resonance Theory both in the vector and in the antisymmetric tensor formalisms [6], compatilibity with high-energy QCD constraints is found in the latter case without introducing $\mathcal{L}_{\chi PT}^{(4),\,\mathrm{even}}$. In the former case, the asymptotic behaviour is not good but upon introducing the $\mathcal{L}_{\chi PT}^{(4),\,\mathrm{even}}$ the required falloff is recovered. This possibility of including the Lagrangian at the next order in the chiral expansion does not yet yield the proper ultraviolet behaviour in the odd-intrinsic parity sector when working with the vector field formalism.

[13] We are not referring to the chiral counting in the framework of $R\chi T$, where this is known to be lost. We recall the remark in the paragraph including Eq. (4.16).

Effective Lagrangian $\mathcal{L}_{R\chi T} \equiv \mathcal{L}_2 + \mathcal{L}_R$ is enough to satisfy the high-energy QCD constraints.

Analogously, for the odd-intrinsic parity sector, three different sources might be considered:

- The WZW action [241, 242], which is $\mathcal{O}(p^4)$ and fulfills the chiral anomaly,
- Chiral invariant $\varepsilon_{\mu\nu\rho\sigma}$ terms involving vector mesons which, upon integration, will start to contribute at $\mathcal{O}(p^6)$ in the antisymmetric tensor formalism, and
- The relevant operators in the $\mathcal{O}(p^6)$ χPT Lagrangian.

The odd-intrinsic parity Lagrangians with resonances have already been studied in order to consider the equivalence for reproducing the one-loop divergencies of the WZW action among different representations for the resonance fields [312]. This procedure has also been thought to estimate the couplings appearing the $\mathcal{O}(p^6)$ chiral Lagrangian [317].

Within the antisymmetric tensor formalism, all the needed building blocks have already been introduced. Chiral invariance of the generating functional, together with Lorentz, Parity and Charge conjugation invariance and Hermiticity of the Lagrangian determine an independent set of operators for VVP and VJP Green functions to be [14]

• VJP terms:

$$\begin{aligned}
\mathcal{O}^1_{VJP} &= \varepsilon_{\mu\nu\rho\sigma} \langle \{V^{\mu\nu},\, f_+^{\rho\alpha}\} \nabla_\alpha u^\sigma \rangle\,, \\
\mathcal{O}^2_{VJP} &= \varepsilon_{\mu\nu\rho\sigma} \langle \{V^{\mu\alpha},\, f_+^{\rho\sigma}\} \nabla_\alpha u^\nu \rangle\,, \\
\mathcal{O}^3_{VJP} &= i\,\varepsilon_{\mu\nu\rho\sigma} \langle \{V^{\mu\nu},\, f_+^{\rho\sigma}\} \chi_- \rangle\,, \\
\mathcal{O}^4_{VJP} &= i\,\varepsilon_{\mu\nu\rho\sigma} \langle V^{\mu\nu}\, [f_-^{\rho\sigma},\, \chi_+] \rangle\,, \\
\mathcal{O}^5_{VJP} &= \varepsilon_{\mu\nu\rho\sigma} \langle \{\nabla_\alpha V^{\mu\nu},\, f_+^{\rho\alpha}\} u^\sigma \rangle\,, \\
\mathcal{O}^6_{VJP} &= \varepsilon_{\mu\nu\rho\sigma} \langle \{\nabla_\alpha V^{\mu\alpha},\, f_+^{\rho\sigma}\} u^\nu \rangle\,, \\
\mathcal{O}^7_{VJP} &= \varepsilon_{\mu\nu\rho\sigma} \langle \{\nabla^\sigma V^{\mu\nu},\, f_+^{\rho\alpha}\} u_\alpha \rangle\,.
\end{aligned} \tag{4.33}$$

• VVP terms:

$$\begin{aligned}
\mathcal{O}^1_{VVP} &= \varepsilon_{\mu\nu\rho\sigma} \langle \{V^{\mu\nu},\, V^{\rho\alpha}\} \nabla_\alpha u^\sigma \rangle\,, \\
\mathcal{O}^2_{VVP} &= i\,\varepsilon_{\mu\nu\rho\sigma} \langle \{V^{\mu\nu},\, V^{\rho\sigma}\} \chi_- \rangle\,, \\
\mathcal{O}^3_{VVP} &= \varepsilon_{\mu\nu\rho\sigma} \langle \{\nabla_\alpha V^{\mu\nu},\, V^{\rho\alpha}\} u^\sigma \rangle\,, \\
\mathcal{O}^4_{VVP} &= \varepsilon_{\mu\nu\rho\sigma} \langle \{\nabla^\sigma V^{\mu\nu},\, V^{\rho\alpha}\} u_\alpha \rangle\,.
\end{aligned} \tag{4.34}$$

The Schouten identity,

$$g_{\rho\sigma}\varepsilon_{\alpha\beta\mu\nu} + g_{\rho\alpha}\varepsilon_{\beta\mu\nu\sigma} + g_{\rho\beta}\varepsilon_{\mu\nu\sigma\alpha} + g_{\rho\mu}\varepsilon_{\nu\sigma\alpha\beta} + g_{\rho\nu}\varepsilon_{\sigma\alpha\beta\mu} = 0\,, \tag{4.35}$$

[14] The convention for the Levi-Civita density is $\varepsilon_{0123} = +1$ and J is short for external vector current.

has been employed to reduce the number of independent operators.

The authors of Ref. [312] also built VVP operators in the antisymmetric tensor formalism but applying the *LO EOM* to reduce the number of operators to three. This is a valid procedure provided one is only interested in on-shell degrees of freedom; but particles inside Green functions are not on their mass-shell. The resonance Lagrangian for the odd-intrinsic parity sector will thus be defined as

$$\begin{aligned} \mathcal{L}_V^{odd} &= \mathcal{L}_{VJP} + \mathcal{L}_{VVP}\,, \\ \mathcal{L}_{VJP} = \sum_{a=1}^{7} \frac{c_a}{M_V}\,\mathcal{O}_{VJP}^a \quad &, \qquad \mathcal{L}_{VVP} = \sum_{a=1}^{4} d_a\,\mathcal{O}_{VVP}^a\,; \end{aligned} \tag{4.36}$$

where the octet mass, M_V, has been introduced in $\mathcal{L}_{VJP}$, in order to define dimensionless c_a couplings. The set defined above is a complete basis for constructing vertices with only one-pseudoscalar; for a larger number of pseudoscalars additional operators may emerge.

As discussed, the $\mathcal{O}(p^6)$ χPT Lagrangian in the odd-intrinsic parity sector has to be considered, as well. Two operators may contribute at LO in $1/N_C$ to the $\langle\, VVP\,\rangle$ Green function:

$$\mathcal{L}_{\chi PT}^{(6),\,\mathrm{odd}} = i\,\varepsilon_{\mu\nu\alpha\beta}\left\{t_1\langle\,\chi_-\,f_+^{\mu\nu}\,f_+^{\alpha\beta}\,\rangle - i\,t_2\langle\,\nabla_\lambda f_+^{\lambda\mu}\left\{f_+^{\alpha\beta},\,u^\nu\right\}\rangle\right\}\,, \tag{4.37}$$

where the t_i $LECs$ are not fixed by symmetry requirements. The operators in Eq. (4.37) belong both to the EFT where resonances are still active fields and to that one where they have been integrated out. Hence in the latter case, we can split the couplings as $t_i = t_i^R + \hat{t}_i$, where t_i^R is generated by the integration of the resonances and $\hat{t}_i$ stands for the surviving $\mathcal{O}(p^6)$ χPT contribution when the resonances are still active. We will assume, as in the even-intrinsic parity sector, that $\hat{t}_i$ are negligible compared to the resonance contributions, the t_i are generated completely through interaction of vectors. Accordingly, we should not include $\mathcal{L}_{\chi PT}^{(6),\,\mathrm{odd}}$ in our study to avoid double counting of degrees of freedom. Then, the relevant effective resonance theory will be given by:

$$Z_{\mathrm{R}\chi\mathrm{T}}[v,\,a,\,s,\,p] = Z_{WZW}\,[v,\,a] + Z_{V\chi}^{\mathrm{odd}}[v,\,a,\,s,\,p]\,, \tag{4.38}$$

where $Z_{V\chi}^{\mathrm{odd}}$ is generated by $\mathcal{L}_\chi^2$ in (3.66), $\mathcal{L}_V$ in (4.17), (4.18), (4.19) and $\mathcal{L}_V^{\mathrm{odd}}$ in (4.36).

The VVP Green function is

$$(\Pi_{VVP})_{(\mu\nu)}^{(abc)}\,(p,\,q) = \int \mathrm{d}^4x \int \mathrm{d}^4y\, e^{i(p\cdot x\,+\,q\cdot y)}\,\langle\,0|T\left[V_\mu^a(x)\,V_\nu^b(y)\,P^c(0)\right]|0\,\rangle\,. \tag{4.39}$$

Provided a Green function is related to an order parameter of QCD, it vanishes in the chiral limit to all orders in perturbation theory, so that there is no term in the OPE expansion that goes with the identity. This is specially nice regarding the matching with the $R\chi T$ result, that will never include such a kind of term including

the identity. This is the case for $\langle\, VVP \,\rangle$ Green functions, and also for $\langle\, VPPP \,\rangle$ Green functions like those related to τ decays into three mesons but, for instance, it is no longer so in $\langle\, VVVV \,\rangle$ Green functions (like, for example, light-by-light scattering processes). It is conventionally written that we can rely on matching $R\chi T$ with the OPE at such low energies as $2\ GeV$ when there are order parameters involved. Otherwise, the matching becomes much more involved.

The $\langle\, VVP \,\rangle$ Green function is built within $R\chi T$ in [310]. When the limit of two momenta becoming large at the same time is taken, one finds compatibility with the QCD short-distance constraints, provided the following conditions among the $\mathcal{L}_V^{\rm odd}$ couplings hold

$$\begin{aligned}
&4c_3 \,+\, c_1 \,=\, 0\,,\\
&c_1 \,-\, c_2 \,+\, c_5 = 0\,,\\
&c_5 \,-\, c_6 = \frac{N_C}{64\pi^2}\,\frac{M_V}{\sqrt{2}F_V}\,,\\
&d_1 \,+\, 8d_2 = -\frac{N_C}{64\pi^2}\,\frac{M_V^2}{F_V^2} \,+\, \frac{F^2}{4F_V^2}\,,\\
&d_3 \,=\, -\frac{N_C}{64\pi^2}\,\frac{M_V^2}{F_V^2} \,+\, \frac{F^2}{8F_V^2}\,.
\end{aligned} \tag{4.40}$$

Being the couplings in the (odd-intrinsic parity) Effective Lagrangian independent of pG masses the result turns out to be general.

Now it comes the crucial point. The obtained $\langle\, VVP \,\rangle$ Green function reproduces the lowest meson dominance ansatz in [313]:

$$\Pi_{VVP}(p^2,\, q^2,\, (p+q)^2) \,=\, -\frac{\langle\, \overline{\psi}\psi \,\rangle_0}{2}\cdot\frac{(p^2+q^2+r^2) - \frac{N_C}{4\pi^2}\frac{M_V^4}{F^2}}{(p^2-M_V^2)(q^2-M_V^2)r^2}\,. \tag{4.41}$$

The previous ansatz (4.41) recovers the lowest meson dominance estimates for the $LECs$ derived in Ref. [315]. Their authors found impossible to reproduce them working with the vector representation for the resonances, not even paying the price of introducing local contributions from the $\mathcal{O}(p^6)$ chiral Lagrangian. They suggested that the problem could be due to the Effective Lagrangian approach and unlikely to be cured by using other representations for the resonance fields. The work undertaken in Ref. [310] contradicts this assertion for the $\langle\, VVP \,\rangle$ Green function in the odd-intrinsic parity sector.

The derived Lagrangian, Eq. (4.36), was tested through the computation of the decay width for the process $\omega \,\to\, \pi\,\gamma$ that was completely predicted thanks to the relations (4.40). This calculation pop up the question about the validity of Vector meson dominance-assumption [318, 319]. It was found that the direct vertex was larger than expected, even comparable to the ρ-mediated process. Anyway, these results agree with the large-N_C limit of $R\chi T$, in which both contributions are of the same order in the expansion. This feature was confirmed through the computation of other channels: In particular, $\omega \,\to\, 3\pi$ showed that Vector meson dominance

hypothesis was at variance with the experimental value for the decay width. This confirmed what was suggested before: that local $VPPP$ vertices in the odd-intrinsic parity sector are relevant.

We present here the last extension [320, 321] of the original Lagrangian that was first applied to study the $K\overline{K}\pi$ decay modes of the τ lepton. We have found that the most general $VPPP$ Lagrangian in the odd-intrinsic parity sector is

$$\mathcal{L}_{VPPP} = \sum_{i=1}^{5} \frac{g_i}{M_V} \mathcal{O}^i_{VPPP}\,, \tag{4.42}$$

where, in the chiral limit and using the Schouten identity, three new operators arise

$$\begin{aligned}
\mathcal{O}^1_{VPPP} &= i\,\varepsilon_{\mu\nu\alpha\beta}\,\left\langle V^{\mu\nu}\,\left(\,h^{\alpha\gamma}u_\gamma u^\beta - u^\beta u_\gamma h^{\alpha\gamma}\right)\right\rangle\,,\\
\mathcal{O}^2_{VPPP} &= i\,\varepsilon_{\mu\nu\alpha\beta}\,\left\langle V^{\mu\nu}\,\left(\,h^{\alpha\gamma}u^\beta u_\gamma - u_\gamma u^\beta h^{\alpha\gamma}\,\right)\right\rangle\,,\\
\mathcal{O}^3_{VPPP} &= i\,\varepsilon_{\mu\nu\alpha\beta}\,\left\langle V^{\mu\nu}\,\left(\,u_\gamma h^{\alpha\gamma}u^\beta - u^\beta h^{\alpha\gamma}u_\gamma\,\right)\right\rangle\,.
\end{aligned} \tag{4.43}$$

Apart from these ones, when the chiral limit is not taken, two new operators have to be taken into account

$$\begin{aligned}
\mathcal{O}^4_{VPPP} &= \varepsilon_{\mu\nu\alpha\beta}\,\left\langle\left\{\,V^{\mu\nu}\,,\,u^\alpha\,u^\beta\,\right\}\,\chi_-\right\rangle\,,\\
\mathcal{O}^5_{VPPP} &= \varepsilon_{\mu\nu\alpha\beta}\,\left\langle\,u^\alpha\,V^{\mu\nu}\,u^\beta\,\chi_-\right\rangle\,.
\end{aligned} \tag{4.44}$$

From the previous distinction, we can guess that matching at high energies will give us some information on the three couplings that survive in the chiral limit, but for the others it is likely that only phenomenological information will shed light on them.

Notice that we do not include analogous pieces to Eqs. (4.33) and (4.42) with an axial-vector resonance, that would contribute to the hadronization of the axial-vector current. This has been thoroughly studied in Ref. [309] (see also [322], this picture is supported by the conclusions in Chapter 6) in the description of the $\tau \to \pi\pi\pi\nu_\tau$ process and it is shown that no $\langle A\chi^{(4)}(\varphi)\rangle$ operators are needed to describe its hadronization. Therefore those operators are not included in our minimal description of the relevant form factors appearing in later chapters.

4.6.3 Concluding remarks

There are other extensions of the Lagrangian which will not be used in this Thesis. For the even-intrinsic parity sector, the reader can find in Ref. [128] the minimal set of operators corresponding to the coupling of a resonance and an $\mathcal{O}(p^4)$ chiral tensor, and trilinear resonance terms without any chiral tensor. For the odd-intrinsic parity part, in Ref. [323] there were written new pieces for the couplings among the two vector objects and a pG or a vector source: $\mathcal{O}_{V_1V_2P}$ and $\mathcal{O}_{V_1V_2J}$.

All the introduced extensions of the original Lagrangian will play a rôle in the three meson decays and one meson radiative decays of the τ examined in this Thesis. As we will see, the contribution of $VPPP$ vertices in the odd-intrinsic parity sector turns out to be fundamental for the decay $\omega \to 3\pi$. Therefore, apart from its own interest, we can take advantage of it to get additional restrictions on the new couplings introduced throughout this section. One of the targets of our work is to gain more control over the new couplings of the resonance Lagrangian introduced in this section and thus in improving our quantitative understanding of intermediate-energy meson dynamics.

Chapter 5

Hadron decays of the τ lepton

5.1 Introduction

In this chapter we want to set the model independent description of the hadron decays of the τ that we study. Using Lorentz invariance and general properties of QCD one can decompose any amplitude participating in a given process in terms of a set of scalar quantities that only depend on kinematical invariants, the so-called form factors. As explained in Appendix A, this description is equivalent to that in terms of structure functions.

Moreover, we also desire to explain the three different approaches to describe the the involved form factors and to illustrate others than ours. This will let appreciate better the improvements introduced by our study compared to previous approaches.

As we have discussed in previous chapters we still do not know a way to derive the form factors related to the hadronization of QCD currents in the intermediate energy region. In view of this, three major approaches have been developed to tackle these problems [324]:

- The first approach is the one motivated by the discussion in the previous chapters and followed in this Thesis. It consists in exploiting the power of the EFT framework à la Weinberg -Section 3.2- supplemented by some dynamical content of the problem at hand, namely the known short-distance behaviour of QCD -Section 4.5- and the large-N_C limit of QCD -Chapter 4-.

- The second approach is that of modeling phenomenological Lagrangians. Their actions are written in terms of hadron fields but employing ad-hoc assumptions whose link with QCD is not clear and which are introduced in order to get a simpler theory. As an example, we have the suggested Hidden Symmetry or Gauge Symmetry Lagrangians mentioned briefly in appendix F.

- Finally, we have another -more comfortable though less satisfactory- way of facing the problem. It is to propose dynamically driven parametrizations. They provide an amplitude suggested by the assumed dynamics: resonance dominance, pology, etc. The expressions one obtains are much easier than

those given by more based approaches, as we will see giving some examples later on. Numerical fit to data is quicker and the accordance between the theoretical expressions and the experiments are, often, remarkable. Notwithstanding, the connection between the ad-hoc parameters and QCD is missing. According to our understanding, the point is not just to get an impressive fit to the experimental points but to understand the hadronization of the QCD currents in these particular processes.

5.1.1 Breit-Wigner approach

As we want to compare our results to those obtained within the Breit-Wigner models, we describe their main features in this section.

Since long time ago, it is well-known that any hadronization process occurring in the resonance energy region will be dominated by the contribution of these resonance states. The application of this resonance dominance to hadron tau decays has a long history [325, 326, 327, 328]. A model based on these ideas that became very popular is due to Kühn and Santamaría [329].

In any of these cases the parametrization is accomplished by combining Breit-Wigner factors ($BW_R(Q^2)$) according to the expected resonance dominance in each channel [1], that is,

$$F(Q^2) \,=\, \mathcal{N}\; f\left(\alpha_i,\, \mathrm{BW}_{\mathrm{R_i}}(Q^2)\right)\,, \tag{5.1}$$

where $\mathcal{N}$ is a normalization and the former expression is not linear, in general, in the Breit-Wigner terms. Data are analyzed by fitting the α_i parameters and the masses and on-shell widths entering the Breit-Wigner factors. Two main models of parametrizations have been employed:

a) Kühn-Santamaría Model (KS)

The BW form factors are given by [325, 326, 327, 328, 329]

$$\mathrm{BW}^{\mathrm{KS}}_{\mathrm{R_i}}(Q^2) \,=\, \frac{M^2_{\mathrm{R_i}}}{M^2_{\mathrm{R_i}} - Q^2 - i\sqrt{Q^2}\Gamma_{\mathrm{R_i}}(Q^2)}\,, \tag{5.2}$$

that vanishes in the high-Q^2 region, as demanded by short-distance QCD.

b) Gounaris-Sakurai Model (GS)

It was originally developed to study the rôle of the $\rho(770)$ resonance in the vector form factor of the pion [330] still in the current algebra era. It has been applied over the years to other hadron resonances [331, 332, 333] by the experimental collaborations. The BW function now reads

[1] Consequently, they do not depend only on Q^2, the total hadron momenta, but also on other Lorentz invariants depending on the considered channel. The Q^2 in parenthesis intends to be a shorthand notation we will keep in the following.

$$\mathrm{BW}^{\mathrm{GS}}_{\mathrm{R_i}}(Q^2) \,=\, \frac{M^2_{\mathrm{R_i}} + f_{\mathrm{R_i}}(0)}{M^2_{\mathrm{R_i}} - Q^2 + f_{\mathrm{R_i}}(Q^2) - i\sqrt{Q^2}\Gamma_{\mathrm{R_i}}(Q^2)}\,, \tag{5.3}$$

where $f_{\mathrm{R_i}}(Q^2)$ encodes information of the off-shell behaviour of the considered resonance. For the particular case of the $\rho(770)$, it can be read off from Ref. [330].

In both models the normalization is fixed in order to reproduce the χPT $\mathcal{O}(p^2)$ behaviour at $Q^2 << M^2_\rho$. The experimental groups use to believe that the difference among the predictions of these two models gives an estimate of the theoretical error [2]. As we will see, this is a severe mistake, because the simplicity of these models is irrelevant if they fail to verify properties coming from QCD itself, as it happens to be the case, both in the three meson modes and the radiative decays with one meson. It is true that we learn things about the resonance structure using these models to fit the data, but it is not -as argued many times- that the (occasionally) little discrepancy among themselves in the observables (values of masses, on-shell widths and branching ratios and shape of the spectra and Dalitz plots) can be regarded as a proof of the rightness of both models.

5.1.2 Model independent description. General case

Within the Standard Model [3] the matrix amplitude for the exclusive hadron decays of the τ, $\tau^- \to H^-\nu_\tau$, is generically given by

$$\mathcal{M} \,=\, \frac{G_F}{\sqrt{2}} V^{ij}_{CKM}\, \overline{u}_{\nu_\tau}\, \gamma^\mu\, (1-\gamma_5)\, u_\tau\, \mathcal{H}_\mu\,, \tag{5.4}$$

where G_F is the Fermi constant, V^{ij}_{CKM} the corresponding element of the CKM matrix, and

$$\mathcal{H}_\mu \,=\, \langle\, H|(V_\mu - A_\mu)\, e^{i\mathcal{L}_{\mathrm{QCD}}}|0\,\rangle\,, \tag{5.5}$$

is the matrix element of the left-handed current that has to be evaluated in the presence of the strong QCD interactions.

Symmetries help us to decompose $\mathcal{H}_\mu$ in terms of the allowed Lorentz structures of implied momenta and a set of functions of Lorentz invariants, the hadron form factors, F_i, of QCD currents,

$$\mathcal{H}_\mu \,=\, \sum_i \underbrace{(\dots)^i_\mu}_{\text{Lorentz structure}} \quad F_i(Q^2, \dots)\,; \tag{5.6}$$

that are universal in the sense of being independent on the initial state, describing therefore the hadronization of QCD currents.

This decomposition is studied in detail in Appendix A, where it is also derived the equivalence among using form factors or structure functions to describe these

[2] In fact, Ref. [329] already used it with this purpose.

[3] A nice and short introductory description can be found in Refs. [334, 335].

hadron decays. We just recall for the moment that the decay width for a given channel is obtained by integrating over the n hadrons plus one neutrino differential phase space, the hadron and lepton tensors are defined from the following [4]

$$\overline{\sum}_{s,s'} \mathcal{M}\mathcal{M}^\dagger \equiv \left(\frac{1}{2\times\frac{1}{2}+1}\right)^2 \frac{G_F^2}{2} |V_{CKM}|^2 \, \mathcal{H}_{\mu\nu}\, \mathcal{L}^{\mu\nu} \,, \tag{5.7}$$

where $\mathcal{H}_\mu$ is the hadron current defined in Eq. (5.5), $\mathcal{L}^{\mu\nu}$ carries information on the lepton sector and d$\mathcal{PS}$ stands for the differential element for phase space integration:

$$\mathcal{H}_{\mu\nu} \equiv \mathcal{H}_\mu \mathcal{H}_\nu \;, \;\; \mathcal{L}^{\mu\nu} \;=\; \sum_{s,s'} \overline{u}_\tau(\ell,s)\gamma^\mu(1-\gamma_5)u_{\nu_\tau}(\ell',s')\gamma^\nu(1-\gamma_5)u_\tau(\ell,s)\,. \tag{5.8}$$

Then, one has

$$\mathrm{d}\Gamma \;=\; \frac{G_F^2}{4M_\tau} |V_{CKM}^{ij}|^2 \, \mathcal{L}_{\mu\nu}\, \mathcal{H}^\mu \, \mathcal{H}^{\nu\dagger} \, \mathrm{d}\mathcal{PS} \,, \tag{5.9}$$

with

$$\mathcal{L}_{\mu\nu}\, \mathcal{H}^\mu \, \mathcal{H}^{\nu\dagger} \;=\; \sum_X L_X \, W_X \,, \tag{5.10}$$

where W_X are the structure functions defined in the hadron rest frame.

The hadron structure functions, W_X, can be written in terms of the form factors and kinematical components and the study of spectral functions or angular distributions of data allow us to reconstruct them. Their number depends on the final state, being 4 in the case of two mesons and 16 for three. Either form factors or, equivalently, structure functions, are the target to achieve.

5.2 One meson radiative decays of the τ

5.2.1 Model independent description

For the decay modes with lowest multiplicity, $\tau \to P^-\nu : \tau$, $P = \pi, K$, the relevant matrix elements are already known from the measured decays $\pi^- \to \mu^-\nu_\mu$ and $K^- \to \mu^-\nu_\mu$. The corresponding τ decay widths can then be predicted rather accurately. These predictions are in good agreement with the measured values, and provide a quite precise test of chargedcurrent universality.

When one considers the emission of a photon things change and they provide dynamical information [336] about the hadron matrix elements of the $L_\mu = (V_\mu - A_\mu)$ current.

The process is $\tau^-(p_\tau) \to \nu_\tau(q) P^-(p)\gamma(k)$. The kinematics of this decay is equivalent to that of the radiative pion decay [337]. We will use $t := (p_\tau - q)^2 = (k+p)^2$.

[4] $\overline{\sum}_{s,s'}$ corresponds to the averaged sum over polarizations.

In complete analogy to the case of the radiative pion decay [338], the matrix element for the decay $\tau^- \to P^-\gamma\nu_\tau$ can be written as the sum of four contributions:

$$\mathcal{M}\left[\tau^-(p_\tau) \to \nu_\tau(q)P^-(p)\gamma(k)\right] = \mathcal{M}_{IB_\tau} + \mathcal{M}_{IB_P} + \mathcal{M}_V + \mathcal{M}_A\,, \tag{5.11}$$

with [5]

$$\begin{aligned}
i\mathcal{M}_{IB_\tau} &= G_F\, V_{CKM}^{ij}\, e\, F_P\, p_\mu\, \epsilon_\nu(k)\, L^{\mu\nu}\,,\\
i\mathcal{M}_{IB_P} &= G_F\, V_{CKM}^{ij}\, e\, F_P\, \epsilon^\nu(k)\, \left(\frac{2\,p_\nu\,(k\,+\,p)_\mu}{m_P^2\,-\,t}\,+\,g_{\mu\nu}\right)\, L^\mu\,,\\
i\mathcal{M}_V &= i\,G_F\, V_{CKM}^{ij}\, e\, F_V(t)\, \epsilon_{\mu\nu\rho\sigma}\epsilon^\nu(k)\, k^\rho\, p^\sigma\, L^\mu\,,\\
i\mathcal{M}_A &= G_F\, V_{CKM}^{ij}\, e\, F_A(t)\, \epsilon^\nu(k)\, \left[(t\,-\,2\,m_P^2)\, g_{\mu\nu}\,-\,2\,p_\nu k_\mu\right] L^\mu\,,
\end{aligned} \tag{5.12}$$

where e the electric charge and ϵ_ν the polarization vector of the photon. $F_V(t)$ and $F_A(t)$ are the so called structure dependent form factors. Finally L^μ and $L^{\mu\nu}$ are lepton currents defined by

$$\begin{aligned}
L^\mu &= \bar{u}_{\nu_\tau}(q)\gamma^\mu(1-\gamma_5)u_\tau(p_\tau)\,,\\
L^{\mu\nu} &= \bar{u}_{\nu_\tau}(q)\gamma^\mu(1-\gamma_5)\frac{\not{k}-\not{p}_\tau - M_\tau}{(k-p_\tau)^2 - M_\tau^2}\gamma^\nu u_\tau(p_\tau)\,.
\end{aligned} \tag{5.13}$$

The notation introduced for the independent amplitudes describes the four kinds of contributions: $\mathcal{M}_{IB_\tau}$ is the bremsstrahlung off the tau, (Figure 5.1(a)), $\mathcal{M}_{IB_P}$ is the sum of the pG bremsstrahlung (Figure 5.1(b)), and the seagull diagram (Figure 5.1(c)), $\mathcal{M}_V$ is the structure dependent vector (Figure 5.1(d)) and $\mathcal{M}_A$ the structure dependent axial-vector contribution (Figure 5.1(e)). Our ignorance of the exact mechanism of hadronization is parametrized in terms of the two form factors $F_A(t)$ and F_V(t). In fact, these form factors are the same functions of the momentum transfer t as those in the radiative pion decay, the only difference being that t now varies from 0 up to M_τ^2 rather than just up to m_π^2.

The two matrix elements $\mathcal{M}_{IB_\tau}$ and $\mathcal{M}_{IB_P}$ are not separately gauge invariant, but their sum, ie. the (total) matrix element for internal bremsstrahlung IB

$$\mathcal{M}_{IB} = \mathcal{M}_{IB_\tau} + \mathcal{M}_{IB_P}\,, \tag{5.14}$$

is indeed gauge invariant, as $\mathcal{M}_V$ and $\mathcal{M}_A$ are. We also define the (total) structure dependent radiation SD by

$$\mathcal{M}_{SD} = \mathcal{M}_V + \mathcal{M}_A\,. \tag{5.15}$$

[5] Notice that i and minus factors differ with respect to Ref. [336] (DF). Moreover, our form factors have dimension of inverse mass while theirs are dimensionless. In their work, this factor of $(\sqrt{2}m_\pi)^{-1}$ in the form factors is compensated by defining the sum over polarizations of the matrix element squared with an extra $2m_\pi^2$ factor. This should be taken into account to compare formulae in both works using that $F_V(t)^{DF} = \sqrt{2}m_\pi F_V(t)^{Our}$, $F_A(t)^{DF} = 2\sqrt{2}m_\pi F_A(t)^{Our}$.

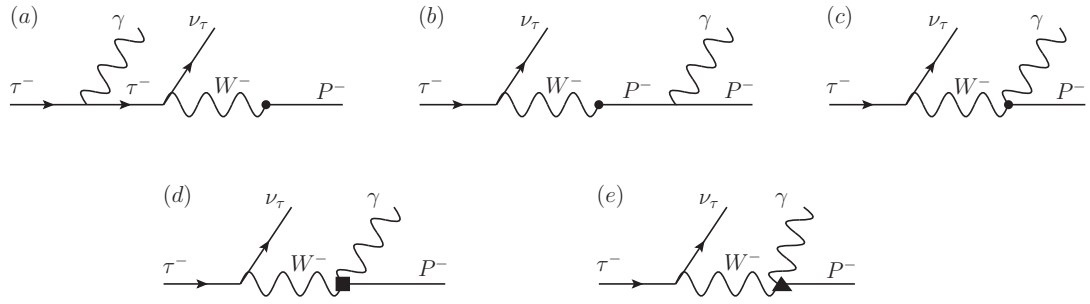

Figure 5.1: Feynman diagrams for the different kinds of contributions to the radiative decays of the tau including one meson, as explained in the main text. The dot indicates the hadronization of the QCD currents. The solid square represents the SD contribution mediated by the axial-vector current and the solid triangle the SD contribution via the vector current.

The spinor structure can be rearranged to give

$$\begin{aligned} i\mathcal{M}_{IB} &= G_F\, V_{ij}^{CKM}\, e\, F_P\, M_\tau \bar{u}_{\nu_\tau}(q)(1+\gamma_5)\left[\frac{p_\tau\cdot\epsilon}{p_\tau\cdot k}-\frac{p\cdot\epsilon}{p\cdot k}-\frac{\not{k}\not{\epsilon}}{2p_\tau\cdot k}\right]u_\tau(p_\tau)\,, \qquad (5.16)\\ i\mathcal{M}_{SD} &= G_F\, V_{ij}^{CKM}\, e\left\{i\epsilon_{\mu\nu\rho\sigma}L^\mu\epsilon^\nu k^\rho p^\sigma F_V(t)+\bar{u}_{\nu_\tau}(q)(1+\gamma_5)\left[(t-m_P^2)\not{\epsilon}-2(\epsilon\cdot p)\not{k}\right]u(p_\tau)F_A(t)\right\}. \end{aligned}$$

The square of the matrix element is then given by

$$\overline{|\mathcal{M}|^2}=\overline{|\mathcal{M}_{IB}|^2}+2\overline{\Re e(\mathcal{M}_{IB}\mathcal{M}_{SD}^\star)}+\overline{|\mathcal{M}_{SD}|^2}\,, \qquad (5.17)$$

where the bar denotes summing over the photon polarization and neutrino spin and averaging over the tau spin.

We follow Ref. [336] and divide the decay rate as follows: the internal bremsstrahlung part Γ_{IB} arising from $\overline{|\mathcal{M}_{IB}|^2}$, the structure dependent part Γ_{SD} coming from $\overline{|\mathcal{M}_{SD}|^2}$, and the interference part Γ_{INT} stemming from $2\overline{\Re e(\mathcal{M}_{IB}\mathcal{M}_{SD}^\star)}$. Furthermore Γ_{SD} is subdivided into the vector-vector (Γ_{VV}), the axial-vector—axial-vector (Γ_{AA}) and the vector—axial-vector interference term Γ_{VA}. Similarly Γ_{INT} gets splitted into the internal bremsstrahlung-vector interference Γ_{IB-V} and the internal bremsstrahlung–axial-vector interference Γ_{IB-A} parts. Thus, one has

$$\begin{aligned} \Gamma_{total} &= \Gamma_{IB}+\Gamma_{SD}+\Gamma_{INT}\,,\\ \Gamma_{SD} &= \Gamma_{VV}+\Gamma_{VA}+\Gamma_{AA}\,,\\ \Gamma_{INT} &= \Gamma_{IB-V}+\Gamma_{IB-A}\,. \end{aligned} \qquad (5.18)$$

It is convenient to introduce the dimensionless variables x and y:

$$x:=\frac{2p_\tau\cdot k}{M_\tau^2}\,,\qquad y:=\frac{2p_\tau\cdot p}{M_\tau^2}\,. \qquad (5.19)$$

In the tau rest frame x and y are the energies E_γ and E_π of the photon and the pion, respectively, expressed in units of $M_\tau/2$:

$$E_\gamma=\frac{M_\tau}{2}x\,,\qquad E_\pi=\frac{M_\tau}{2}y\,. \qquad (5.20)$$

Eq. (5.20) sets the scale for the photons to be considered as "hard" or "soft". This means that the formulae for internal bremsstrahlung should be similar for radiative tau and pion decay, once they are expressed in terms of x and y, as it is the case, albeit photons of comparable softness will have very different energies in both cases.

The kinematical boundaries for x and y are given by

$$0 \leq x \leq \ 1 - r_P^2\,, \qquad 1 - x + \tfrac{r_P^2}{1-x} \leq y \leq 1 + r_P^2\,, \tag{5.21}$$

where

$$r_P^2 := \left(\frac{m_P}{M_\tau}\right)^2 \sim_{0.077}^{0.006} \ll 1\,, \tag{5.22}$$

where the upper figure corresponds to $P = \pi$ and the lower one to $P = K$. It is also useful to note that

$$p \cdot k = \frac{M_\tau^2}{2}(x + y - 1 - r_P^2)\,, \qquad t := (p_\tau - q)^2 = (k + p)^2 = M_\tau^2(x + y - 1)\,. \tag{5.23}$$

The differential decay rate is given by [339]

$$d\Gamma(\tau^- \to \nu_\tau P^- \gamma) = \frac{1}{512\pi^5 E_\tau}\delta^{(4)}(k + p + q - p_\tau)\overline{|\mathcal{M}|^2}\frac{d^3\vec{k}d^3\vec{p}d^3\vec{q}}{E_\gamma E_\pi E_\nu}\,, \tag{5.24}$$

where the bar over the matrix element denotes summing over the photon polarization and neutrino spin and averaging over the tau spin. Choice of the tau rest frame, integration over the neutrino momentum, $\vec{p}$, and the remaining angles and introduction of x and y yield

$$\frac{d^2\Gamma}{dx\,dy} = \frac{m_\tau}{256\pi^3}\overline{|\mathcal{M}|^2}\,. \tag{5.25}$$

The integration over y yields the photon spectrum

$$\frac{\mathrm{d}\Gamma}{\mathrm{d}x} = \int_{1-x+\frac{r_P^2}{1-x}}^{1+r_P^2} \mathrm{d}y\,\frac{\mathrm{d}^2\Gamma}{\mathrm{d}x\,\mathrm{d}y}\,. \tag{5.26}$$

Because of the infrared divergence of the internal bremsstrahlung a low-energy cut must be introduced for the photon energy, by requiring $x \geq x_0$ one obtaines the integrated decay rate

$$\Gamma(x_0) = \Gamma(E_0) = \int_{x_0}^{1-r_P^2} \mathrm{d}x\frac{\mathrm{d}\Gamma}{\mathrm{d}x}\,, \tag{5.27}$$

that does depend on the photon energy cut-off ($E_0 = \frac{M_\tau}{2}x_0$). Instead of x and y one can use x and z, where z is the scaled momentum transfer squared:

$$z = \frac{t}{M_\tau^2} = x + y - 1\,, \tag{5.28}$$

whose kinematical boundaries are

$$z - r_P^2 \leq x \leq 1 - \frac{r_P^2}{z}\,, \qquad r_P^2 \leq z \leq 1\,. \tag{5.29}$$

Integration of $\frac{\mathrm{d}^2\Gamma}{\mathrm{d}x\,\mathrm{d}y}$ over x yields the spectrum in z, i. e. the spectrum in the invariant mass of the P-photon system:

$$\frac{\mathrm{d}\Gamma}{dz}(z) = \frac{\mathrm{d}\Gamma}{\mathrm{d}z}\left(\sqrt{t}\right) = \int_{z-r_P^2}^{1-r_P^2/z} \mathrm{d}x \frac{\mathrm{d}^2\Gamma}{\mathrm{d}x\,\mathrm{d}y}(x, y = z - x + 1)\,. \tag{5.30}$$

The integrated rate for events with $t \geq t_0$ is then given by

$$\Gamma(z_0) = \Gamma\left(\sqrt{t_0}\right) = \int_{z_0}^{1} \mathrm{d}z \frac{\mathrm{d}\Gamma}{\mathrm{d}z}(z)\,. \tag{5.31}$$

We note that z_0 is both an infrared and a collinear cut-off.

In terms of the quantities defined in Eq. (5.18) the differential decay rate is

$$\begin{aligned}
\frac{\mathrm{d}^2\Gamma_{IB}}{\mathrm{d}x\,\mathrm{d}y} &= \frac{\alpha}{2\pi} f_{IB}\left(x, y, r_P^2\right) \frac{\Gamma_{\tau^-\to\nu_\tau P^-}}{\left(1 - r_P^2\right)^2}\,, \\
\frac{\mathrm{d}^2\Gamma_{SD}}{\mathrm{d}x\,\mathrm{d}y} &= \frac{\alpha}{8\pi}\frac{M_\tau^4}{F_P^2}\left[|F_V(t)|^2 f_{VV}\left(x, y, r_P^2\right) + 4\Re e(F_V(t)F_A^\star(t)) f_{VA}\left(x, y, r_P^2\right) + \right. \\
&\quad \left. 4|F_A(t)|^2 f_{AA}(x, y, r_P^2)\right] \frac{\Gamma_{\tau^-\to\nu_\tau P^-}}{(1 - r_P^2)^2}\,, \\
\frac{\mathrm{d}^2\Gamma_{INT}}{\mathrm{d}x\,\mathrm{d}y} &= \frac{\alpha}{2\pi}\frac{M_\tau^2}{F_P}\left[f_{IB-V}\left(x, y, r_P^2\right)\Re e(F_V(t)) + 2 f_{IB-A}\left(x, y, r_P^2\right)\Re e(F_A(t))\right] \frac{\Gamma_{\tau^-\to\nu_\tau P^-}}{\left(1 - r_P^2\right)^2}\,,
\end{aligned} \tag{5.32}$$

where

$$\begin{aligned}
f_{IB}\left(x, y, r_P^2\right) &= \frac{\left[r_P^4(x+2) - 2r_P^2(x+y) + (x+y-1)\left(2 - 3x + x^2 + xy\right)\right]\left(r_P^2 - y + 1\right)}{\left(r_P^2 - x - y + 1\right)^2 x^2}\,, \\
f_{VV}\left(x, y, r_P^2\right) &= -[r_P^4(x+y) + 2r_P^2(1-y)(x+y) + (x+y-1)\left(-x + x^2 - y + y^2\right)]\,, \\
f_{AA}\left(x, y, r_P^2\right) &= f_{VV}\left(x, y, r_P^2\right)\,, \\
f_{VA}\left(x, y, r_P^2\right) &= -[r_P^2(x+y) + (1-x-y)(y-x)]\left(r_P^2 - x - y + 1\right)\,, \\
f_{IB-V}\left(x, y, r_P^2\right) &= -\frac{\left(r_P^2 - x - y + 1\right)\left(r_P^2 - y + 1\right)}{x}\,, \\
f_{IB-A}\left(x, y, r_P^2\right) &= -\frac{\left[r_P^4 - 2r_P^2(x+y) + (1-x+y)(x+y-1)\right]\left(r_P^2 - y + 1\right)}{\left(r_P^2 - x - y + 1\right) x}\,.
\end{aligned} \tag{5.33}$$

In the approximation $r_P^2 \approx 0$ (vanishing pion mass) these formulae simplify to

$$\begin{aligned}
f_{IB}(x,y,0) &= \frac{[1+(1-x)^2-x(1-y)](1-y)}{(x+y-1)x^2}\,,\\
f_{VV}(x,y,0) &= \left(x-x^2+y-y^2\right)(x+y-1)\,,\\
f_{VA}(x,y,0) &= (x+y-1)^2(x-y)\,,\\
f_{IB-V}(x,y,0) &= \frac{(x+y-1)(1-y)}{x}\,,\\
f_{IB-A}(x,y,0) &= \frac{(x-y-1)(1-y)}{x}\,.
\end{aligned} \tag{5.34}$$

We note that the radiative decay rate has been expressed in terms of the rate of the non-radiative decay ($\tau^- \to \nu_\tau P^-$):

$$\Gamma_{\tau^-\to\nu_\tau P^-} = \frac{G_F^2 |V_{CKM}^{ij}|^2 F_P^2}{8\pi} M_\tau^3 (1-r_P^2)^2\,. \tag{5.35}$$

We finish this section by presenting the analytical expressions for the invariant mass spectrum:

$$\begin{aligned}
\frac{\mathrm{d}\Gamma_{IB}}{\mathrm{d}z} &= \frac{\alpha}{2\pi}\left[r_P^4(1-z)+2r_P^2\left(z-z^2\right)-4z+5z^2-z^3+\right.\\
&\quad \left.+\left(r_P^4 z+2r_P^2 z-2z-2z^2+z^3\right)\ln z\right]\frac{1}{z^2-r_P^2 z}\frac{\Gamma_{\tau^-\to\nu_\tau P^-}}{\left(1-r_P^2\right)^2}\,,\\
\frac{\mathrm{d}\Gamma_{VV}}{\mathrm{d}z} &= \frac{\alpha}{24\pi}\frac{M_\tau^4}{F_P^2}\frac{(z-1)^2\left(z-r_P^2\right)^3(1+2z)}{z^2}|F_V(t)|^2\frac{\Gamma_{\tau^-\to\nu_\tau P^-}}{(1-r_P^2)^2}\,,\\
\frac{\mathrm{d}\Gamma_{VA}}{\mathrm{d}z} &= 0\,,\\
\frac{\mathrm{d}\Gamma_{AA}}{\mathrm{d}z} &= \frac{\alpha}{6\pi}\frac{M_\tau^4}{F_P^2}\frac{(z-1)^2\left(z-r_P^2\right)^3(1+2z)}{z^2}|F_A(t)|^2\frac{\Gamma_{\tau^-\to\nu_\tau P^-}}{\left(1-r_P^2\right)^2}\,,\\
\frac{\mathrm{d}\Gamma_{IB-V}}{\mathrm{d}z} &= \frac{\alpha}{2\pi}\frac{M_\tau^2}{F_P}\frac{(z-r_P^2)^2(1-z+z\ln z)}{z}\Re e(F_V(t))\frac{\Gamma_{\tau^-\to\nu_\tau P^-}}{\left(1-r_P^2\right)^2}\,,\\
\frac{\mathrm{d}\Gamma_{IB-A}}{\mathrm{d}z} &= -\frac{\alpha}{\pi}\frac{M_\tau^2}{F_P}\left[r_P^2(1-z)-1-z+2z^2+\right.\\
&\quad \left.+\left(r_P^2 z-2z-z^2\right)\ln z\right]\frac{z-r_P^2}{z}\Re e(F_A(t))\frac{\Gamma_{\tau^-\to\nu_\tau P^-}}{\left(1-r_P^2\right)^2}\,.
\end{aligned} \tag{5.36}$$

The interference terms $IB-V$ and $IB-A$ are now finite in the limit $z \to r_P^2$, which proves that their infrared divergencies are integrable.

Although the above formulae have been noted in Ref.[336], we independently calculate them [6] and explicitly give them here for completeness. Moreover we would

[6] Typoes in Refs. [336, 340, 341] have been detected through our calculation. The minus sign difference in the definition of the IB part has been taken into account.

like to point out that due to the fact that our definitions of the form-factors $F_V(t)$ and $F_A(t)$ differ from the ones given in Ref. [336], as we have mentioned before, there are some subtle differences in the above formulae between ours and theirs.

5.2.2 Breit-Wigner models

These processes where studied by Decker and Finkemeier in a series of papers [336, 342, 343, 344]. Their parametrization respected the chiral limit ($t = 0$) for the vector form factor, as given by the Wess-Zumino term. However, for the axial-vector form factor it was fixed to the value of $F_A(t = 0)$ in the radiative decay of the pion. This way, not only the value at threshold but also the low-t-dependence of the amplitude deviates from the QCD prediction, which is not satisfactory. Moreover, the off-shell widths employed for the vector resonances was just phase-space motivated, while the one for the axial-vector resonance a_1 employed the ad-hoc expression in the KS model. High-energy QCD behaviour of the form factors was properly implemented. Finally, the addendum to Ref. [336] change the relative sign between the IB and SD contributions, and this has not been confirmed by any later independent study, so this is another motivation for our work.

Our study, included in the next chapter intends to go beyond these approximations and provide a more based description of these decays. They are still undetected, a feature that makes them more interesting, as it is strange according to the estimations of the decay width of these processes. The decay modes reported by the PDG [8] are reviewed in Table 5.1.

5.3 Two meson decays of the τ

5.3.1 Model independent description

The vector form factor of the pion, $F_V^\pi(s)$ is defined through:

$$\left\langle \pi^+(p')\pi^-(p)\right|\frac{1}{\sqrt{2}}(\overline{u}\gamma^\mu u - \overline{d}\gamma^\mu d)\left|0\right\rangle \;=\; (p'-p)^\mu F_V^\pi(s)\,, \tag{5.37}$$

where $s = (p+p')^2$ (s will be defined analogously throughout this section), and the participating current is the third component of the vector one of the $SU(3)$ flavor symmetry of QCD. The matrix element of Eq. (5.37) is related by chiral symmetry to the one appearing in τ decays

$$\langle\, \pi^-(p_{\pi^-})\pi^0(p_{\pi^0})|\overline{d}\gamma^\mu u|0\,\rangle \;=\; \sqrt{2}(p_{\pi^-}-p_{\pi^0})^\mu F_V^\pi(s)\,. \tag{5.38}$$

n	Decay mode	BR(%)	n	Decay mode	BR(%)
0	$e^-\overline{\nu}_e$	17.85(5)		$\eta\overline{K}^0\pi^-$	$2.2(7)\cdot10^{-2}$
	$\mu^-\overline{\nu}_\mu$	17.36(5)		$\eta K^-\pi^0$	$1.8(9)\cdot10^{-2}$
	$e^-e^-e^+\overline{\nu}_e$	$2.8(1.5)\cdot10^{-3}$		$\pi^-2\eta$	$<1.1\cdot10^{-2}$ [a]
	$\mu^-e^-e^+\overline{\nu}_\mu$	$<3.6\cdot10^{-3}$ [b]		K^+2K^-	$1.58(18)\cdot10^{-3}$ [c]
1	π^-	10.91(7)		$\eta'\pi^-\pi^0$	$<8.0\cdot10^{-3}$ [b]
	K^-	$6.95(23)\cdot10^{-1}$	4	$\pi^+2\pi^-\pi^0$	4.59(7)
2	$\pi^-\pi^0$	25.52(10)		$\pi^-3\pi^0$	1.04(7)
	$\pi^-\overline{K}^0$	$8.4(0.4)\cdot10^{-1}$		$K^-\pi^+\pi^-\pi^0$	$1.35(14)\cdot10^{-1}$
	$K^-\pi^0$	$4.28(15)\cdot10^{-1}$		$K^-K^02\pi^0$	$<1.6\cdot10^{-2}$ [a]
	K^-K^0	$1.58(16)\cdot10^{-1}$		$K^-3\pi^0$	$4.7(2.1)\cdot10^{-2}$
	$K^-\eta$	$2.7(6)\cdot10^{-2}$		$\pi^-\pi^0K^0\overline{K}^0$	$3.1(2.3)\cdot10^{-2}$
	$\pi^-\eta$	$<1.4\cdot10^{-2}$ [a]		$\pi^-2\pi^0\overline{K}^0$	$2.6(2.4)\cdot10^{-2}$
	$\eta'\pi^-$	$<7.4\cdot10^{-3}$ [b]		$\eta2\pi^-\pi^+$	$2.3(5)\cdot10^{-2}$
3	$2\pi^-\pi^+$	9.32(7)		$\eta2\pi^0\pi^-$	$1.5(5)\cdot10^{-2}$
	$\pi^-2\pi^0$	9.27(12)		$2K^-K^+\pi^0$	$<4.8\cdot10^{-4}$ [b]
	$\pi^-\pi^+K^-$	$3.41(16)\cdot10^{-1}$		$2\eta\pi^-\pi^0$	$<2.0\cdot10^{-2}$
	$\pi^-\pi^0\overline{K}^0$	$3.9(4)\cdot10^{-1}$	5	$2\pi^-\pi^+2\pi^0$	$7.6(5)\cdot10^{-1}$
	$\pi^-\pi^0\eta$	$1.81(24)\cdot10^{-1}$		$\pi^-4\pi^0$	$7.6(5)\cdot10^{-1}$
	$\pi^-K^0\overline{K}^0$	$1.7(4)\cdot10^{-1}$		$K^-4\pi^0$	–
	$K^-K^0\pi^0$	$1.58(20)\cdot10^{-1}$	6	$2\pi^-\pi^+3\pi^0$	–
	$\pi^-K^+K^-$	$1.40(5)\cdot10^{-1}$		$3\pi^-2\pi^+\pi^0$	–
	$K^-2\pi^0$	$6.3(2.3)\cdot10^{-2}$			

Table 5.1: Decays of the τ according to the number of mesons, n, and the BR [8]. For the decay $\tau^- \to \nu_\tau X^-$, X^- is displayed in the table. [a]: with 95 % CL. [b]: with 90 % CL. [c]: However one should take into account the very recent measurement by the *Belle* collaboration [345] giving a BR of $(3.29 \pm 0.17^{+0.19}_{-0.20})\cdot10^{-5}$. –: The PDG does not give a bound for these channels.

The associated vector and scalar form factors entering the decay $\tau^- \to K^-\pi^0\nu_\tau$ are defined through:

$$\langle\, K^-(p_K)\pi^0(p_\pi)|\overline{s}\gamma^\mu u|0\,\rangle \;=\; \frac{1}{\sqrt{2}}\left[\left(p_K - p_\pi - \frac{\Delta_{K\pi}}{s}q\right)^\mu F_V^{K^-\pi^0}(s) + \frac{\Delta_{K\pi}}{s}q^\mu F_S^{K^-\pi^0}(s)\right]. \tag{5.39}$$

The different kaon and pion masses imply the appearance of the scalar form factor, $F_S^{K^-\pi^0}(s)$, that accounts for the non-conserving vector current part of the

decay, $q^\mu = (p_K + p_\pi)^\mu\,, s = q^2$ and

$$\Delta_{K\pi} = m_K^2 - m_\pi^2\,. \tag{5.40}$$

Chiral symmetry dictates then the structure of the process $\tau \to \bar{K}^0\pi^-\nu_\tau$: with the changes:

$$K^-\pi^0 \to \bar{K}^0\pi^-\,, \quad \overline{s}\gamma^\mu u \to \overline{u}\gamma^\mu s\,, \quad F_{V,S}^{K^-\pi^0}(s) \to \sqrt{2}\,F_{V,S}^{\bar{K}^0\pi^-}(s)\,. \tag{5.41}$$

An equivalent description is given in terms of the pseudoscalar ($F_0^{K\pi}(s) = -F_S^{K\pi}(s)$) and vector ($F_+^{K\pi}(s) = -F_+^{K\pi}(s)$) form factors. The vector form factor into two kaons is probed through $\tau^- \to K^-K^0\nu_\tau$:

$$\langle\, K^0(p_0)K^-(p_-)|\overline{d}\gamma^\mu u|0\,\rangle = \frac{1}{2}\,F_V^K(s)(p_0 - p_-)^\mu\,, \tag{5.42}$$

where, as in the case of the pion form factor, the vector current is conserved in the isospin limit.

The decay $\tau^- \to \eta\pi^-\nu_\tau$ can only be produced in the SM as an isospin violating effect [327], since it has opposite G-parity to the participating vector current. The coupling to the vector current occurs via an $\eta - \pi^0$ mixing. The related matrix element will exhibit the structure

$$\langle\, \eta(p_\eta)\pi^-(p_\pi)|\overline{d}\gamma^\mu u|0\,\rangle = \sqrt{\frac{2}{3}}\,F_V^{\pi\eta}(s)\frac{m_d - m_u}{m_d + m_u}\frac{m_\pi^2}{m_\eta^2 - m_\pi^2}(p_\pi - p_\eta)^\mu\,. \tag{5.43}$$

Finally, the $K^-\eta$ decay mode can be parametrized as follows

$$\langle\, K^-(p_K)\eta(p_\eta)|\overline{s}\gamma^\mu u|0\,\rangle = \sqrt{\frac{3}{2}}\,F_V^{K\eta}(s)(p_K - p_\eta)^\mu\,, \tag{5.44}$$

and the $\tau \to K^-\eta'\nu_\tau$ decay mode vanishes in the limit of ideal mixing for the η system, so that corrections to this approach will yield a suppressed branching fraction.

The differential decay rate for the process $\tau \to \nu_\tau h_1(p_1)h_2(p_2)$ is obtained from

$$d\Gamma(\tau \to \nu_\tau h_1 h_2) = \frac{1}{2M_\tau}\frac{G_F^2}{2}\,|V_{CKM}^{ij}|^2\,\{L_{\mu\nu}H^{\mu\nu}\}\,\mathrm{d}\mathcal{PS}^{(3)}\,. \tag{5.45}$$

In order to disentangle the angular dependence it is useful to introduce suitable linear combinations of density matrix elements of the hadron system [7]

$$L_{\mu\nu}H^{\mu\nu} = 2(M_\tau^2 - s)\,(\,\bar{L}_B W_B + \bar{L}_{SA}W_{SA} + \bar{L}_{SF}W_{SF} + \bar{L}_{SG}W_{SG}\,)\,, \tag{5.46}$$

We note that the most general decomposition of $L_{\mu\nu}H^{\mu\nu}$ (for two body decays) in terms of density matrix elements (or structure functions) W_X of the hadron system

[7] The general procedure is studied in Ref. [346], where it is shown that the angular dependencies can be isolated by introducing 16 combinations of defined symmetry.

has two additional terms $\bar{L}_A W_A + \bar{L}_E W_E$ [346]. However, W_A and W_E vanish in the case of tau decays into two pseudoscalar mesons. Nonvanishing W_A and W_E arise for example in decay modes with a vector and a pseudoscalar [347].

The hadron structure functions are related to the vector and scalar form factors as follows:

$$\begin{aligned} W_B(s) &= 4(\vec{p}_1)^2\,|F_V(s)|^2\,, \quad W_{SA}(s) = s\,|F_S(s)|^2\,, \\ W_{SF}(s) &= 4\sqrt{s}|\vec{p}_1|\,\Re e\,[F_V(s)F_S^*(s)]\,, \\ W_{SG}(s) &= -4\sqrt{s}|\vec{p}_1|\,\Im m\,[F_V(s)F_S^*(s)]\,, \end{aligned} \tag{5.47}$$

where $|\vec{p}_1| = p_1^z$ is the momentum of h_1 in the rest frame of the hadron system:

$$p_1^z = \frac{1}{2\sqrt{s}}\sqrt{[s - m_1^2 - m_2^2]^2 - 4m_1^2 m_2^2} \quad , \quad E_1^2 = (p_1^z)^2 + m_1^2\,. \tag{5.48}$$

The hadron structure functions $W_{B,\,SA,\,SF,\,SG}$ are linearly related to the density matrix elements of the hadron system:

$$W_B \,=\, H^{33}\,,\; W_{SA} \,=\, H^{00}\,, \quad W_{SF} \,=\, H^{03} + H^{30}\,,\; W_{SG} \,=\, -i(H^{03} - H^{30})\,. \tag{5.49}$$

Finally, the differential decay rate $d\Gamma/ds$ yields

$$\frac{d\Gamma}{ds} \;=\; \frac{G_F^2 |V_{CKM}^{ij}|}{2^8\pi^3} 2\frac{(M_\tau^2 - s)^2}{M_\tau^2 s^{3/2}}\;|p_1^z|\;\frac{2s + M_\tau^2}{3M_\tau^2}\left\{W_B(s) \,+\, \frac{3M_\tau^2}{2s + M_\tau^2}\,W_{SA}(s)\right\}. \tag{5.50}$$

5.3.2 Theoretical descriptions of the form factors

There is a great amount of data available on $F_V^\pi(s)$, Eq. (5.37), because it appears in the hadron matrix element entering the process $e^+e^- \to \pi^+\pi^-$ where there are many precise measurements [348, 349, 350, 351, 352, 353, 354] and, in the isospin limit, of the decay: $\tau^- \to \pi^-\pi^0\nu_\tau$, where the latest data was published by the *Belle* Collaboration [355]. $F_V^\pi(s)$ has been studied within χPT up to $\mathcal{O}(p^6)$ [210, 356, 357, 358], so the very-low energy description is really accurate.

The energies going from M_ρ to ~ 1.2 GeV are dominated by the ρ (770) so that this resonance can be characterized through the study of this form factor very well. Ref. [359] attempted to improve the $\mathcal{O}(p^4)$ χPT result by matching it at higher energies with an Omnès solution [360] of the dispersion relation satisfied by the vector form factor of the pion. This way, the description keeps its validity up to 1 GeV, approximately. Some years later, the unitarization approach was used [361] to obtain a good description of data in this region, as well. The KS-model [329] also parametrized this decay. We will discuss it in more detail along its description of the 3π channel in Section 5.4.3.

A model independent parametrization of this form factor built upon an Omnès solution for the dispersion relation has also been considered [362, 363, 364]. Combining this procedure with $R\chi T$ [362] improves the previous approach (it extends

now to ~ 1.3 GeV) if one includes information on the ρ' (1450) through $\pi\pi$ elastic phase-shift input in the Omnès solution.

It is clear that ρ' (1450) and ρ'' (1700) will play the main rôle in the energy region up to 2 GeV. However, the proposed parametrizations including both resonances only allow to quantify the relative strength of each one and the likely interference amid these resonances, the possible presence of a continuum component, etc. are completely lost with the most simple approaches. Within $R\chi T$, the ρ' (1450) was incorporated through a Dyson-Schwinger-like resummation [365], and the ideas of the $N_C \to \infty$ limit and vector meson dominance were used in Ref. [366], including a pattern of radial excitations expected from dual resonance models. They included the three lightest ρ resonances plus a tower of infinite number of zero-width higher-excited states in the spirit of large-N_C [367]. Using the hidden gauge formalism, Ref. [368] has emphasized the rôle of the $\rho-\omega-\phi$ mixing in this form factor. Using Padé approximants Refs. [369, 370] have studied all available space-like data on this form factor up to $Q^2 = 12$ GeV^2.

The last years have witnessed the discrepancy between $e^+e^- \to \pi^+\pi^-$ and $\tau^- \to \pi^-\pi^0\nu_\tau$ predictions [348, 349, 350, 351, 352, 353, 355] for $F_V^\pi(s)$. There have been some theoretical studies [191, 371, 372] of radiative corrections in the τ decay mode, but the difference is not fully accounted for yet.

There is also a large amount of good quality data on the $K\pi$ form factors. In addition to the e^+e^- data from $E865$ [373], $CLEO$ data appeared on τ decays [374], and two high-precision studies of the related τ decays were recently published by $BaBar$ [375] -for the charge channel $\tau^- \to K^-\pi^0\nu_\tau$- and $Belle$ [376]-$\tau^- \to K_S\pi^-\nu_\tau$-. A comparison of the newest experiments with the Monte Carlo expectations for the $\pi^-\pi^0$ and $(K\pi)^-$ meson modes is presented in Ref. [162].

The form factor $F_V^{K\pi}(s)$ was computed at $\mathcal{O}(p^4)$ in χPT in Ref. [210]. In Ref. [358] the χPT analysis is performed within the three flavour framework at next-to-next-to-leading order. This provides a good description of the very-low energy spectrum. In order to extend it to higher energies, in Ref. [377] the Linear sigma model, a quark-triangle model and Vector meson dominance have been used. The comparison to data [373] favours the last one. Simple Breit-Wigner models supplemented with vector meson dominance have also been used [378, 379]. They suffered the same problems explained in Section 5.2.2.

Both the vector and the scalar form factor have been reviewed recently. In Ref. [380], the distribution function for this decay has been obtained with the relevant vector and scalar form factors presented above computed within $R\chi T$ and taking into account additional constraints from dispersion relations and short-distances. The dynamically generated K_0^* (800) should be the resonance starring at the scalar form factor, whether K^* (1410) will modify a bit the more prominent contribution of K^* (892) to $F_V^{K\pi}(s)$, as the results confirm [381] when confronting it to Ref. [376]. In Ref. [382], the knowledge of $\mathcal{O}(p^6)$ chiral $LECs$ and of light quark masses has been improved studying $F_0^{K\pi}(s)$. These form factors have been studied using analyticity constraints and taking into account isospin violating corrections by Moussallam [284]. This strategy was also followed in Ref. [386] but sticking to the exact $SU(2)$

limit. The scalar form factor has also been studied [384, 385] matching χPT to a dispersive representation. Lately, it has been realized that there is anticorrelation in the parameters describing the vector form factor in $F_V^{K\pi}(s)$ from tau decays and $K_{\ell 3}$ decays [386, 387], which has allowed to reach smaller errors in the slope and curvature of this form factor.
The work [388] analyzed the two-kaon vector form factor, $F_V^K(s)$, in much the same way as done for two pions [359]. By that time, the experimental data [331, 389] were not in enough agreement with each other to check the proposed expression. New finer results have been published since then [390, 391], so a dedicated study of these modes within $R\chi T$ employing all present knowledge of $EFTs$, short-distance QCD, the large-N_C expansion, analyticity and unitarity would be desirable specially in light of forthcoming data from $BaBar$ and $Belle$.

We turn to the τ decays into η modes: the $\pi^-\eta^{(\prime)}$ channel has been observed recently for the first time [392], while for the $K^-\eta$ meson system there are recent measurements already published [393]. The smaller BR for the first one is consistent with the findings of Ref. [327] summarized before. A first description of this decay was attempted at the beginning of the eighties [394] and revisited recently [395] and the main features were already established few years later [327, 396]. The χPT result at $\mathcal{O}(p^4)$ [210] was extended to higher invariant masses of the hadron system in Ref. [397]. Even the isospin breaking corrections have been computed for this mode [398]. Again a study along the lines proposed in this Thesis would be interesting. The decay $\tau^- \to K^-\eta\nu_\tau$ has not been improved further than the χPT computation at $\mathcal{O}(p^4)$ [210].

5.4 Three meson decays of the τ

5.4.1 Model independent description

The hadron matrix element for the considered decays may be written as [346, 399]

$$\begin{aligned}\langle\,(PPP)^-|(V-A)^\mu|0\,\rangle &= V_1^\mu\,F_1^A(Q^2,\,s_1,\,s_2) + V_2^\mu\,F_2^A(Q^2,\,s_1,\,s_2) \\ &+ Q^\mu\,F_3^A(Q^2,\,s_1,\,s_2) + i\,V_3^\mu\,F_4^V(Q^2,\,s_1,\,s_2)\,,\end{aligned} \tag{5.51}$$

where

$$\begin{aligned}V_1^\mu &= \left(g^{\mu\nu} - \frac{Q^\mu Q^\nu}{Q^2}\right)(p_1-p_3)_\nu\ , \quad V_2^\mu = \left(g^{\mu\nu} - \frac{Q^\mu Q^\nu}{Q^2}\right)(p_2-p_3)_\nu\,, \\ V_3^\mu &= \varepsilon^{\mu\alpha\beta\gamma}\,p_{1\alpha}\,p_{2\beta}\,p_{3\gamma}\ , \quad Q^\mu = (p_1+p_2+p_3)^\mu\,, \quad s_i = (Q-p_i)^2\,,\end{aligned} \tag{5.52}$$

the upper indices on the form factors stand for the participating current, either the axial-vector (A), or the vector one (V) and not for the quantum numbers carried by them; notice that $F_3^A(Q^2,\,s_1,\,s_2)$ is the pseudoscalar form factor that accounts for a $J^P = 0^-$ transition. $F_1^A(Q^2,\,s_1,\,s_2)$ and $F_2^A(Q^2,\,s_1,\,s_2)$ are the axial-vector

form factors that carry $J^P = 1^+$ degrees of freedom. Finally, $F_4^V(Q^2, s_1, s_2)$ is the vector form factor, that has $J^P = 1^-$.

There are other properties that one can derive in full generality. For instance, due to the chiral Ward identity relating axial-vector and pseudoscalar currents, conservation of the first one in the chiral limit imposes that $F_3^A(Q^2, s_1, s_2)$ must vanish with the square of a pG mass and hence, its contribution may be suppressed. There are, of course, other constraints coming from $SU(2)$ or $SU(3)$ flavour symmetries for a given mode, like those stating that the form factors for the decays $\tau^- \to \pi^0\pi^0\pi^-\nu_\tau$ and $\tau^- \to \pi^-\pi^-\pi^+\nu_\tau$ are identical in the $SU(2)$ limit, as it happens for the form factors in the decays $\tau^- \to K^0\bar{K}^0\pi^-\nu_\tau$ and $\tau^- \to K^+K^-\pi^-\nu_\tau$. There are other symmetry requirements: in $\tau^- \to (3\pi)^-\nu_\tau$, Bose-Einstein symmetry implies that $F_2^A(Q^2, s_1, s_2) = F_1^A(Q^2, s_2, s_1)$ and G-parity forbids axial-vector current contributions to the decays of the τ into $\eta\pi^-\pi^0$ and $\eta\eta\pi^-$[327]. This kind of relations will be discussed and used in the following chapters.

We consider a general three meson decay of the τ: $\tau^-(\ell, s) \longrightarrow \nu_\tau(\ell', s') + h_1(p_1, z_1) + h_2(p_2, z_2) + h_3(p_3, z_3)$. The polarizations (s, s', z_1, z_2, z_3) will play no role in the following since we will assume the tau to be unpolarized. Then, the differential phase space for a generic channel is given by

$$\mathrm{d}\Gamma(\tau^- \longrightarrow (3h)^-\nu_\tau) = \frac{1}{2M_\tau}\frac{G_F^2}{2}|V_{ij}^{CKM}|^2 \mathcal{L}_{\mu\nu}H^{\mu\nu}\mathrm{d}\mathcal{PS}^{(4)}\,, \tag{5.53}$$

where the phase space-integration involves the three mesons and one neutrino in the final state:

$$\mathrm{d}\mathcal{PS}^{(4)} = (2\pi)^4\delta^4(\ell-\ell'-p_1-p_2-p_3)\frac{\mathrm{d}^3\overrightarrow{\ell'}}{(2\pi)^3 2E_\nu}\frac{\mathrm{d}^3\overrightarrow{p_1}}{(2\pi)^3 2E_1}\frac{\mathrm{d}^3\overrightarrow{p_2}}{(2\pi)^3 2E_2}\frac{\mathrm{d}^3\overrightarrow{p_3}}{(2\pi)^3 2E_3}\,. \tag{5.54}$$

In order to obtain the differential width as a function of Q^2 (the so-called spectral function), the integration over $\int \mathrm{d}\mathcal{PS}^{(4)}$ is carried out in two steps:

$$\mathrm{d}\Gamma = \prod_{i=1}^{3}\int \frac{\mathrm{d}^3\overrightarrow{\ell'}}{(2\pi)^3 2E_\nu}\frac{\mathrm{d}^3\overrightarrow{p_i}}{(2\pi)^3 2E_i}(2\pi)^4\delta\left(\ell-\ell'-\sum_{i=1}^{3}p_i\right)\overline{\sum}|\mathcal{M}|^2\,, \tag{5.55}$$

provided we use the Källen's trick to split the integrations by introducing a Dirac delta as follows:

$$\begin{aligned}\frac{\mathrm{d}\Gamma_{\tau^-\to(h_1h_2h_3)^-\nu_\tau}}{\mathrm{d}Q^2} &= \int \frac{\mathrm{d}^3\overrightarrow{p_\nu}}{(2\pi)^3 2E_\nu}\delta\left(Q^2-(p_\tau-p_\nu)^2\right)\times \\ &\int\prod_{i=1}^{3}\frac{\mathrm{d}^3\overrightarrow{p_i}}{(2\pi)^3 2E_i}(2\pi)^4\delta\left(Q-\sum_{i=1}^{3}p_i\right)\overline{\sum}|\mathcal{M}|^2\,.\end{aligned} \tag{5.56}$$

We have:

$$\int \frac{\mathrm{d}^3\overrightarrow{p_\nu}}{(2\pi)^3 2E_\nu}\delta\left(Q^2-(p_\tau-p_\nu)^2\right) = \int \frac{\mathrm{d}^3\overrightarrow{p_\nu}}{(2\pi)^3 2E_\nu}\delta\left(Q^2-M_\tau^2-m_\nu^2+2p_\tau p_\nu\right) =$$
$$= \frac{1}{(2\pi)^2}\int \frac{\mathrm{d}|\overrightarrow{p_\nu}||\overrightarrow{p_\nu}|^2}{E_\nu}\delta\left(Q^2-M_\tau^2-m_\nu^2+2M_\tau E_\nu\right) =$$
$$= \frac{1}{(2\pi)^2}\int \frac{\mathrm{d}|\overrightarrow{p_\nu}||\overrightarrow{p_\nu}|^2}{E_\nu}\frac{\delta\left(|\overrightarrow{p_\nu}|-|\widetilde{\overrightarrow{p_\nu}}|\right)}{2M_\tau\frac{|\overrightarrow{p_\nu}|}{E_\nu}} =$$
$$= \frac{1}{(2\pi)^2}\frac{1}{(2M_\tau)^2}|\widetilde{\overrightarrow{p_\nu}}| = \frac{1}{(2\pi)^2}\frac{\lambda^{1/2}(Q^2,M_\tau^2,m_\nu^2)}{4M_\tau^2}\,. \tag{5.57}$$

where it has been taken into account that decay widths are defined in the rest frame of the decaying particle, and $|\widetilde{\overrightarrow{p_\nu}}| = \frac{\lambda^{1/2}(Q^2,M_\tau^2,m_\nu^2)}{2M_\tau}$.
The integration over $\int \mathrm{d}\Pi_3$ is left involving the momenta p_i. It yields [339] (notice that a factor $(2\pi)^{-9}$ is not included in the definition of $\mathrm{d}\Pi_3$ immediately below):

$$\int \mathrm{d}\Pi_3 := \int \mathrm{d}s\,\mathrm{d}t\,\delta\left(s-(Q-p_3)^2\right)\,\delta\left(t-(Q-p_2)^2\right)\frac{\mathrm{d}\mathcal{PS}^{(3)}}{(2\pi)^4} = \frac{\pi^2}{4Q^2}\int \mathrm{d}s\,\mathrm{d}t\,, \tag{5.58}$$

where $s\equiv(p_1+p_2)^2\equiv s_{12}$, $t\equiv(p_1+p_3)^2\equiv s_{13}$, and $u\equiv(p_2+p_3)^2\equiv s_{23} = Q^2-s-t+m_1^2+m_2^2+m_3^2$. Using Eq. (5.58), one has:

$$\frac{\mathrm{d}\Gamma_{\tau^-\to(h_1h_2h_3)^-\nu_\tau}}{\mathrm{d}Q^2} = \frac{G_F^2|V_{ij}^{CKM}|^2}{128(2\pi)^5 M\tau}\frac{\lambda^{1/2}(Q^2,M_\tau^2,m_\nu^2)}{M_\tau^2}\frac{1}{Q^2}\times$$
$$\left\{\omega_{SA}(Q^2,s,t)\left(\Sigma_{\tau\nu}-\frac{\Delta_{\tau\nu}^2}{Q^2}\right)-\frac{1}{3}\frac{\overline{\omega}(Q^2,M_\tau^2,m_\nu^2)}{Q^2}\left(\omega_A(Q^2,s,t)+\omega_B(Q^2,s,t)\right)\right\}, \tag{5.59}$$

where there the integrated structure functions have been defined as follows:

$$\omega_{SA,\,A,\,B}(Q^2) = \int \mathrm{d}s\,\mathrm{d}t\,W_{SA,\,A,\,B}(Q^2,s,t)\,. \tag{5.60}$$

The other definitions employed include the so-called weak matrix element:
$\overline{\omega}(Q^2,M_\tau^2,m_\nu^2)\equiv(M_\tau^2-Q^2)(M_\tau^2+2Q^2)-m_\nu^2(2M_\tau^2-Q^2-m_\nu^2)$, and $\Sigma_{\tau\nu}\equiv M_\tau^2+m_\nu^2$, $\Delta_{\tau\nu}\equiv M_\tau^2-m_\nu^2$. $W_{SA,A,B}(Q^2,s,t)$ correspond to the structure functions in Ref. [346]. In terms of the form factors and set of independent vectors in Eqs. (5.51), (5.52) they are

$$\begin{aligned}
W_{SA} &= \left[Q^\mu\,F_3^A(Q^2,s_1,s_2)\right]\left[Q_\mu\,F_3^A(Q^2,s_1,s_2)\right]^* = Q^2\,|F_3^A(Q^2,s_1,s_2)|^2\,,\\
W_A &= -\left[V_1^\mu\,F_1^A(Q^2,s_1,s_2)+V_2^\mu\,F_2^A(Q^2,s_1,s_2)\right]\times\\
&\quad\left[V_{1\,\mu}\,F_1^A(Q^2,s_1,s_2)+V_{2\,\mu}\,F_2^A(Q^2,s_1,s_2)\right]\,,\\
W_B &= \left[V_{3\,\mu}\,F_4^V(Q^2,s_1,s_2)\right]\left[V_3^\mu\,F_4^V(Q^2,s_1,s_2)\right]^*\,.
\end{aligned} \tag{5.61}$$

In the excellent limit of vanishing neutrino mass, the Q^2-spectrum is simply given by:

$$\frac{d\,\Gamma}{d\,Q^2} \,=\, \frac{G_F^2\,|V_{ij}^{CKM}|^2}{128\,(2\pi)^5\,M_\tau}\,\left(\frac{M_\tau^2}{Q^2}-1\right)^2\,\int\,ds\,dt\,\left[W_{SA}+\frac{1}{3}\left(1+2\frac{Q^2}{M_\tau^2}\right)\,(W_A+W_B)\right]\,. \tag{5.62}$$

The limits of integration when obtaining the full width are the following ones:

$$\int_{Q^2_{min}}^{Q^{2\,max}} \mathrm{d}Q^2 \int_{s_{min}}^{s^{max}} \mathrm{d}s \int_{t_{min}}^{t^{max}} \mathrm{d}t\,, \tag{5.63}$$

$$t_{min}^{max}(Q^2,s) \,=\, \frac{1}{4s}\,\left\{\left(Q^2+m_1^2-m_2^2-m_3^2\right)^2-\left[\lambda^{1/2}\left(Q^2,s,m_3^2\right)\mp\lambda^{1/2}\left(m_1^2,m_2^2,s\right)\right]^2\right\}\,, \tag{5.64}$$

$$\begin{aligned} s_{min} \,&=\, (m_1+m_2)^2\,, \quad s^{max} \,=\, (\sqrt{Q^2}-m_3)^2\,\,; \\ Q^2_{min} \,&=\, (m_1+m_2+m_3)^2\,\,, \quad Q^{2\,max} \,=\, (M_\tau-m_\nu)^2\,. \end{aligned} \tag{5.65}$$

5.4.2 Recent experimental data

The *BaBar* [400] and *Belle* [345] collaborations have recently reported the measurement of the branching fractions of various particle combinations (any combination of pions and kaons) in the decay to three charged hadrons. The mass spectra have not been analysed yet. Previous studies of the mass spectra were done by the *CLEO* group [401], and the *ALEPH* [78], *DELPHI* [402] and *OPAL* [403] collaborations on the 3π mode. *CLEO* studied with detail also the $KK\pi$ modes [404, 405, 406]. The $3K$ modes have been observed by *Babar* [400] and *Belle* [407]. Recently, the *Belle* Collaboration performed a detailed study of various decays with the η meson in the final state [393].

5.4.3 Theoretical description of the form factors

Even before the discovery of the tau lepton, its mesonic decays and the relation between these ones and the hadron states produced in e^+e^- annihilation were studied [408, 409]. The late seventies witnessed the pioneering work of Fischer, Wess and Wagner [325], that employed the method of phenomenological Lagrangians to derive relations between different n-pion modes in terms of the pion decay constant, F. Ref. [410] used isospin invariance and measurements on e^+e^- annihilation to relate several channels. Ref. [411] attempted a Lagrangian description of the 3π decays including resonances and, explicitly, the a_1-π-ρ vertex [8]. However, the model was not consistent with χPT at $\mathcal{O}(p^4)$ and, moreover made the severe mistake of

[8] The a_1 dominance in heavy lepton decays was proposed in 1971 [408], 4 years before the tau lepton was actually discovered.

not including energy-dependent widths for these spin-one resonances. The model by Isgur, Morningstar and Reader [412] violated chiral symmetry. Braaten *et. al.* [413, 414] used an EFT approach, based on $U(3)_L \otimes U(3)_R$ for the vector resonances and respecting chiral symmetry up to $\mathcal{O}(p^2)$ for the pGs. However, it left aside the axial-vector mesons that happened to dominate these decays and assumed hidden local symmetry. Ref. [415] used the isobar model that violates 3-particle unitarity. In addition, the model did not respect chiral symmetry constraints. The works by B. A. Li [416, 417, 418, 419, 420] covered in a unified framework the most interesting decay channels. His theory was based on chiral symmetry for the pGs and the resonances were incorporated following $U(3)_L \otimes U(3)_R$. The author introduced an unjustified energy-dependent ρ-π-π vertex. Studies using old current algebra techniques were also undertaken by that time [421, 422].

The KS model [329] was a step forward, because in the zero-momentum limit it recovered the χPT results and, additionally, it provided more realistic off-shell widths for the involved resonances accounting both for vector and axial-vector states. However, as it was shown later, it was inconsistent with chiral symmetry [9] at $\mathcal{O}(p^4)$ [309, 423] [10]. Moreover, the proposed widths are only phase-space motivated. Although they work quite well, there is no dynamics in them, a feature that should not be satisfactory. The KS model was a major achievement in LEP times to understand τ data. Nowadays, the much more precise data samples and the finer understanding of the Lagrangian approach to the intermediate-energy meson dynamics demands the latter to be applied by the experimental community. We will report about its application to the three-meson decays modes of the tau in Chapters 6, 7 and 8. The recent study in Ref. [425] includes also the sigma contribution to this channel and reports that the a_1' effect is needed to improve significantly the agreement with the data. However, it violates chiral symmetry already at LO since it does not include the diagrams with pions in χPT at $\mathcal{O}(p^2)$.

Other three meson channels were studied following the KS model [378, 426, 427, 428]. In addition to the comments we made to the original work, several other issues enter in these cases [429, 430, 431, 432]: Some of the intermediate exchanged resonances in a given channel that are allowed by quantum numbers are not included in the model and, moreover, the treatment of spin-one resonances is inconsistent: the ρ (1450) has noticeable different mass and width in the axial-vector and vector current form factors and there are two multiplets of vector resonances in the axial-vector current while three in the vector current, a very unnatural phenomenon. It seems difficult to explain why the $\rho(1700)$ happens to be so important in the vector form factor, given its high mass. The KS model and its generalizations were implemented

[9] One could think that it is not that important to fulfill the NLO results in χPT while one is attempting a description in the GeV region. This is not true. The spectra are very sensitive to the normalization and low-energy dependence of the form factors that is carried on to the rest of the spectrum.

[10] The χPT result at $\mathcal{O}(p^4)$ [356] checked that χPT could only describe this decay in a tiny window of phase space. This low-energy part motivated also the study [424] aimed to find hints on the mechanism of dynamical chiral symmetry breaking.

in the famous *TAUOLA* library for tau decays [433, 434, 435, 436]. Later on, this parametrization of the hadron matrix elements was complemented by others based on experimental data by the *CLEO* [11] and Novosibirsk groups [438]. Currently, we are improving some of the proposed currents [439] using the results in this Thesis.

We end the section by quoting early studies that constructed the form factors using the chiral symmetry results at low energies and experimental information to extend it to the GeV-scale, on the $KK\pi$ [440] and $\eta\pi\pi$ modes [441, 442].

5.5 Decays of the τ including more mesons

5.5.1 Model independent description

As far as we know, there is no model independent description of the many-meson decay modes, for instance Ref. [443] builds the amplitude for the 4π decay assuming some decay chains and that the vertex functions are given by their on-shell structure and are transverse. This work was consequence of a previous study of $\tau \to \omega\pi^-\nu_\tau$ [347]. In Refs. [444, 445] isospin symmetry is used in order to determine that all decay channels $\tau^- \to (4\pi)^-\nu_\tau$ can be parametrized in terms of form factors that depend just on one quantity once the symmetries associated to relabeling the different 4π momenta have been used. Moreover, the form factors appearing in $e^+e^- \to (4\pi)^0$ can be obtained with the same single function. Isospin symmetry was systematically used for the first time in multimeson tau decays in Refs. [446, 447], where the meson channels $K\bar{K} + n\pi$, $n\pi$, $(2n+1)\pi$, $2n\pi$, and $K + n\pi$ were examined.

The decays with five mesons have been addressed in Ref. [448], but the proposed hadron matrix elements rely on the assumed substructure of the process.

5.5.2 Experimental data

Tau decays into four-meson modes have been measured very recently in the B-factories, and more data was collected from *ALEPH* [449] and *CLEO* [450, 451]. *BaBar* measured the BR for the mode $(K\pi)^0K^-\pi^0$ through $K^{*0}K^-\pi^0$ [452] and *Belle* for the mode $2\pi^-\pi^+\eta$ [453]. The five charged meson modes have been measured by *BaBar* [454] with much larger statistics than *CLEO* [455] achieved. Finally, the six-pion final state was studied also by the *CLEO* Collaboration [456].

5.5.3 Theoretical description of the form factors

In Ref. [457] comparisons of five- and six-pion τ decay data with the isospin relations indicates that the final states in these decays tend to involve an ω resonance.

[11] The *CLEO* parametrization was private, reserved for the use of the collaboration until published in [503] .

If the decay dynamics of the seven-pion τ decays are similar to the five- and six-pion decays, then isospin relations could explain a low branching ratio limit on the $\tau \to 4\pi^- 3\pi^+ \nu_\tau$ decay.

5.6 Hadron τ decays in Higgs physics at the LHC

In this section we will report briefly on the importance of mastering hadron decays of the tau in Higgs physics at the LHC. One of the main goals of the $ATLAS$ [458] and CMS [459] experiments at LHC is the search for the Higgs boson and the source of electroweak symmetry breaking. Both detectors are capable of doing that for any possible range of masses: 114.4 GeV -direct exclusion limit at 95% confidence level obtained by LEP [460] to 1 TeV [12] -there are many reasons to believe that the TeV scale is an upper limit for the Higgs mass, see for instance [462] and references therein-. In the low-mass region ($m_H < 130$ GeV) the decays of the Higgs boson into two photons or into two taus are the most promising for discovery. Irrespective of the value of m_H its decays into taus will be important to measure its couplings, spin and CP properties [463, 464, 465]. The production and decay of the τ leptons are well separated in space and time providing potential for unbiased measurements of the polarization, spin correlations, and the parity of the resonances decaying into τ leptons. The excellent knowledge of τ decay modes from low-energy experiments indeed makes this an ideal signature for observations of new physics. In the context of the Minimal Supersymmetric Standard Model ($MSSM$), the branching ratio of a $H \to \gamma\gamma$ decay is generally suppressed which makes the search for the decay $H \to \tau\tau$ very important. This section is mainly based in Refs. [458, 459, 466, 467].

In Figure 5.2 the branching fractions of the SM Higgs boson are shown as a function of m_H. Immediately after they are opened, the WW and ZZ decay modes dominate over all others ($t\bar{t}$ can barely reach 20%, as we can see from the curve appearing for $m_H \gtrsim 300$ GeV). All other fermionic modes are only relevant for the Higgs boson masses below $2(M_W - \Gamma_W)$. These modes show peculiar structures with a peak corresponding to both weak bosons being on-shell. We see also a valley in the WW corresponding to the peak in ZZ, since one is plotting the branching ratio. The decay $H \to b\bar{b}$ is dominating below 140 GeV. However, even though it was included as a possible channel that could help the Higgs discovery in the low-mass case up to 2005 [468], a re-evaluation of the QCD backgrounds swapped it away in later reports [458, 459]. Thus, the decays $H \to \tau\tau$ (with $br \sim 8\%$ for $120 < m_H < 140$ GeV) and $H \to \gamma\gamma$ ($br \sim 2 \cdot 10^{-3}$) would be the way to discover the Higgs boson in the low-mass case. In particular, the design of the detectors in the $ATLAS$ and CMS experiments makes –always attaching to this low-mass case–

[12] One should also note that the mass range $160 < m_H < 170$ GeV has also been excluded recently by a statistical combination of the direct searches performed by the Tevatron experiments, CDF and $D0$ [461]. Neither of these experiments has been able to reach any exclusion limit using only their own data yet.

the $H \to \tau\tau$ decay the most promising signature in the former and the $H \to \gamma\gamma$ in the latter.

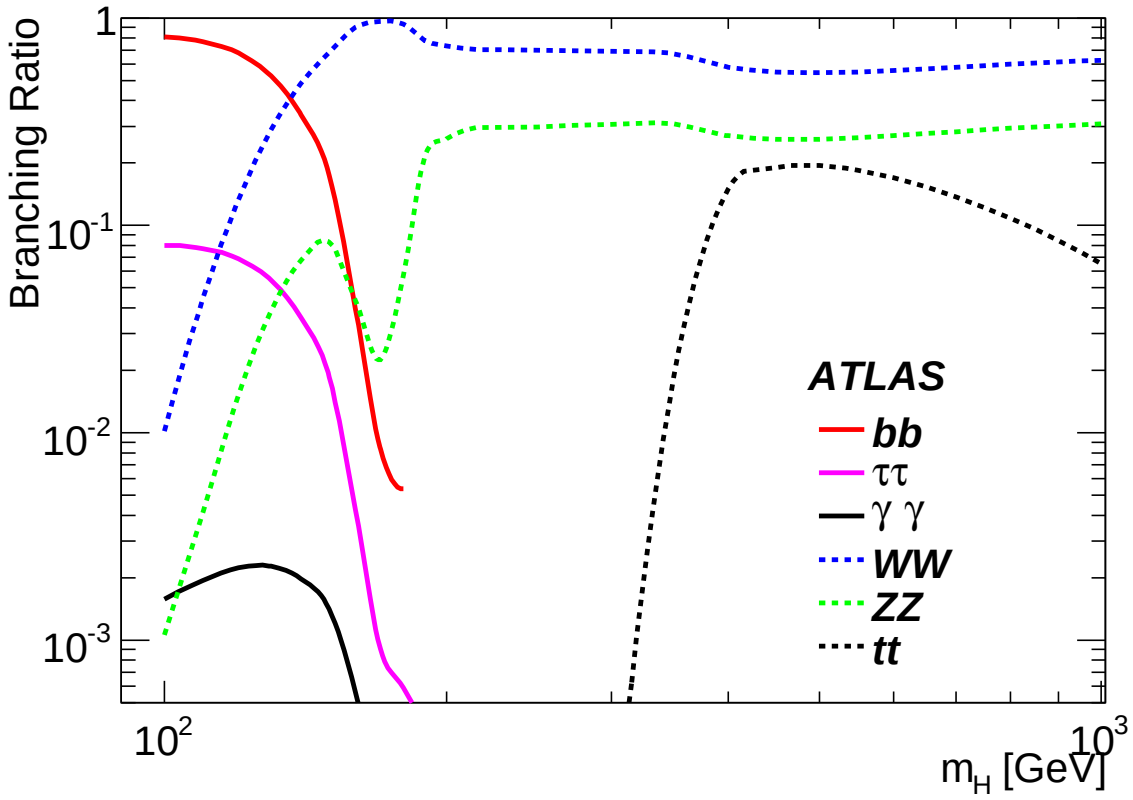

Figure 5.2: Branching ratio for the relevant decay modes of the *SM* Higgs boson as a function of its mass.

Although the reconstruction of τ leptons is usually understood as a reconstruction of the hadron decay modes, since it would be difficult to distinguish lepton modes from the primary electrons and muons, a dedicated effort has been devoted to electron and muon vetoing to reduce their background, so that all possible decays of a $\tau^+\tau^-$ pair: hadron-hadron (hh), lepton-lepton ($\ell\ell$) or mixed (ℓh) can be detected. The following nomenclature for τ decays is used from the detection point of view: single-prong means that exactly one charged meson (most frequently a π) is detected in the reconstructed decay, while three-prong means that there are three charged mesons detected. It is understood that one can generally tell a charged lepton from a charged meson and the small fraction (0.1%) of five-prong decays is usually too hard to detect in a jet environment. The transverse momentum range of interest at *LHC* spans from below 10 GeV to 500 GeV which makes necessary that at least two detection strategies are developed, as we will comment later on. As one can read from Table 5.1, τ leptons decay hadronically in 64.8% of the cases, while in 17.8%

(17.4%) of the cases they decay to an electron (muon). It is interesting to note that the $\tau \to \pi^{\pm}\nu_{\tau}$ decay represents only the 22.4% of single-prong decays hadron decays, so the detection of π^0 particles in $\tau \to n\pi^0\pi^{\pm}\nu_{\tau}$ is fundamental. For the three-prong τ decays, the $\tau \to 3\pi^{\pm}\nu_{\tau}$ decay contributes 61.6% and the $\tau \to n\pi^0 3\pi^{\pm}\nu_{\tau}$ only about one third. Although the decays containing only pions dominate, there is a small percentage of decays containing $K^{\pm}$ that can be identified as for states with $\pi^{\pm}$ from the detector point of view. A small percentage of states with K_S^0 cannot be easily classified as one- or three- prong decays since the K_S^0 decays significantly both to two charged and two neutral pions. In any study performed so far other multi-prong hadron modes have been neglected.

Three-prong decays of the τ (essentially $\tau \to n\pi^0 3\pi^{\pm}\nu_{\tau}$) have the additional interest of allowing for the reconstruction of the τ decay vertex. This is possible because $c\tau_{\tau} \sim 87\mu m$ that one can separate with the inner silicon detector tracking system. The transverse impact parameter of the $3\pi^{\pm}$ can be used to distinguish them from objects originated at the production vertex. As we stated before, this allows for a full treatment of spin effects. This has been done within the framework of the $ATLAS$ Monte Carlo simulation and events were generated using $PYTHIA$ 6.4 [469] interfaced with $TAUOLA$ [470, 504] [13]. Full spin correlations in production and decay of τ leptons were implemented. The associated spin properties in gauge boson, Higgs boson or $SUSY$ cascade decays carry information on the polarization of the decaying resonance: τ leptons from $W \to \tau\nu_{\tau}$ and $H^{\pm} \to \tau\nu_{\tau}$ will be completely longitudinally polarized, with $P_{\tau} = +1$ and $P_{\tau} = -1$, respectively. As a result, the charged to total visible energy distributions for one-prong decays will be different in these cases, permitting their differentiation unambiguously. At the LHC this effect can be used to suppress the background from the former and enhance observability of the latter [472]. The τ polarization could also be used to discriminate between $MSSM$ versus extra dimension scenarios [473]. On the contrary, τ leptons from neutral Higgs boson decays are effectively not polarized and those coming from Z decays obey a complicated function of the center-of-mass energy of the system and the angle of the decay products [474]. In the cleaner environment of a lepton collider, like the ILC, building variables sensitive to the longitudinal and transverse spin correlations may lead to a CP measurement of the Higgs boson [475, 476].

Two complementary algorithms for τ-identification and reconstruction have been studied:

- A track-based algorithm [477], which relies on tracks reconstructed in the inner detector and adopts an energy-flow approach based only on tracks and the energy in the hadronic calorimeter. It starts from seeds built from few (low multiplicity) high-quality tracks collimated around the leading one. It has been optimized for visible transverse energies in the range $10 - 80$ GeV, that corresponds to τ-decays from $W \to \tau\nu_{\tau}$ and $Z \to \tau\tau$ processes.

- A calorimeter-based algorithm [478], which relies on clusters reconstructed in the hadronic and electromagnetic calorimeters and builds the identification

[13] See also Sect. 7.1.

variables based on information from the tracker and the calorimeters. It has been optimized for visible transverse energies above 30 GeV, which corresponds to hadron τ-decays from heavy Higgs-boson production and decay.

Whereas the track-based algorithm has been tuned to preserve similar performance for single- and three-prong decays, the calorimeter-based algorithm has been tuned to provide the best possible rejection at medium-to-high energies and it is therefore more performant for single-prong decays than the track-based algorithm. Depending on the specific process and scenario under study, the trigger requirements are different, a complete description can be found in Ref. [458].

The Higgs-boson can be produced via four different mechanisms at hadron colliders. Although the largest production cross-section for $m_H \lesssim 1$ TeV is always that of gluon fusion, $gg \to H$, which is mediated at lowest order by a t-loop, the cleanest signal in the $H \to \tau\tau$ channel is due to the so-called Vector Boson Fusion (VBF) channel [479, 480], that is represented in Figure 5.3.

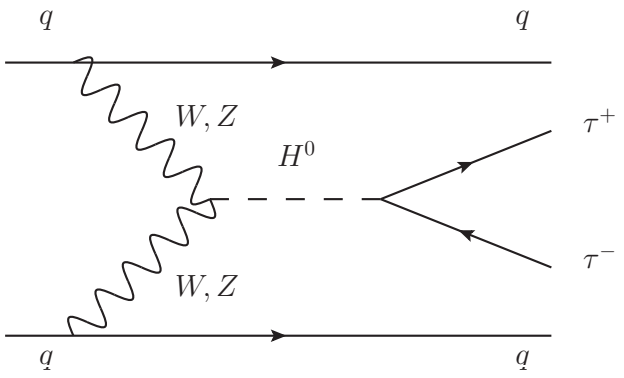

Figure 5.3: Feynman diagram for the lowest order Higgs production via VBF and subsequent decay $H^0 \to \tau^+\tau^-$.

The expected performance in the $ATLAS$ experiment will be adequate to extract τ signals in early LHC data from $W \to \tau\nu_\tau$ and $Z \to \tau\tau$ decays. These signals are important to establish and calibrate the τ identification performance with early data. The study of dijet events from QCD processes will allow a determination of τ fake rates. It is expected that such rates can be measured with a statistical precision at the percent level or better already with data corresponding to an integrated luminosity of 100 pb^{-1} [14]. In any case, despite the advances in theoretical tools and extraordinarily detailed simulation of the $ATLAS$ detector, it is preferable to

[14] We give some numbers to make easier this and subsequent figures: although the design luminosity of the LHC is $10^{34} cm^{-2} s^{-1}$, it is still a bit optimistic to count on $10^{32} cm^{-2} s^{-1}$ for the first year of operation. In this case, one could expect $\sim 30 fb^{-1}$ at the end of the first year. In fact the nominal luminosity is $66.2 fb^{-1}$/year, so $100\, pb^{-1} = 0.1 fb^{-1}$ would be achieved very early because the instantaneous luminosity for the very first measurements was expected to be at the level of $10^{31} cm^{-2} s^{-1}$.

estimate backgrounds from data rather than relying entirely on Monte Carlo simulations. All estimates can thus get sizable corrections as a result.

Once this first stage is completed, one would be ready to search for the $qqH \to qq\tau\tau$ decays via a Higgs boson produced in association with two jets. This analysis requires excellent performance from every $ATLAS$ detector subsystem; τ decays implies the presence of electrons, muons, pions and a few kaons, and missing transverse momentum, while the VBF process introduces jets that tend to be quite forward in the detector. Due to the small rate of signal production and large backgrounds, particle identification must be excellent and optimized specifically for this channel. Furthermore, triggering relies on the lowest energy lepton triggers or exceptionally challenging tau trigger signatures. The $ATLAS$ collaboration has estimated the sensitivity based on $\ell\ell$ and ℓh modes [458]. The hh channel has also been investigated and gives similar results for signal and non-QCD backgrounds as the other channels. However, due to the challenge of predicting the QCD background the estimated sensitivity for this mode was not reported.

The signal events are produced with significant transverse momenta, so the τ from the decay are boosted which causes their decay products being almost collinear in the lab frame. The di-tau invariant mass can be therefore reconstructed in the collinear approximation [15]. The mass resolution is ~ 10 GeV, leading to a $\sim 3.5\%$ precision on the mass measurement with $30fb^{-1}$ of data (one year of data taking). In the more recent analysis particular emphasis is put on data-driven background estimation strategies. Expected signal significance for several masses based on fitting the $m_{\tau\tau}$ spectrum is shown in Figure 5.4. The results obtained neglecting pileup effects indicate that a $\sim 5\sigma$ significance can be achieved for the Higgs boson mass in the range of special interest: $115 - 125$ GeV after collecting $30fb^{-1}$ of data and combining the $\ell\ell$ and ℓh channels. The effects induced by the event pile-up has not been fully addressed yet. As it is intuitive, the hadron decay gives more constraints, since there is only one neutrino that escapes detection, while two are unobserved in the lepton case. Unfortunately the QCD background prevents the usage of the hh mode for the moment, that could further improve the discovery potential in these decays. One can check in Figure 5.5 -note that this corresponds to one third of the luminosity taken as reference previously- that this is the gold-plated mode in the $ATLAS$ experiment for $m_H \lesssim 135$ GeV [16].

We will not cover in detail the relevance of hadron decays of the tau in Higgs searches in the context of the $MSSM$. We will just recall the most prominent features. The topic is studied in depth in Refs. [458, 459, 466, 467, 481, 482, 483]. The

[15] i.e., one assumes that the τ direction is given by their visible decay products: leptons or hadrons.

[16] In the CMS experiment the $H \to \gamma\gamma$ decay mode has a significance of one sigma more than $H \to \tau\tau$ in the energy range of interest [459]. Remarkably, the two photon mode at CMS and the two tau mode at $ATLAS$ have a similar significance at the discovery level in the mass range 115 GeV$\leftrightarrow$ 120 GeV with $30fb^{-1}$ of data.

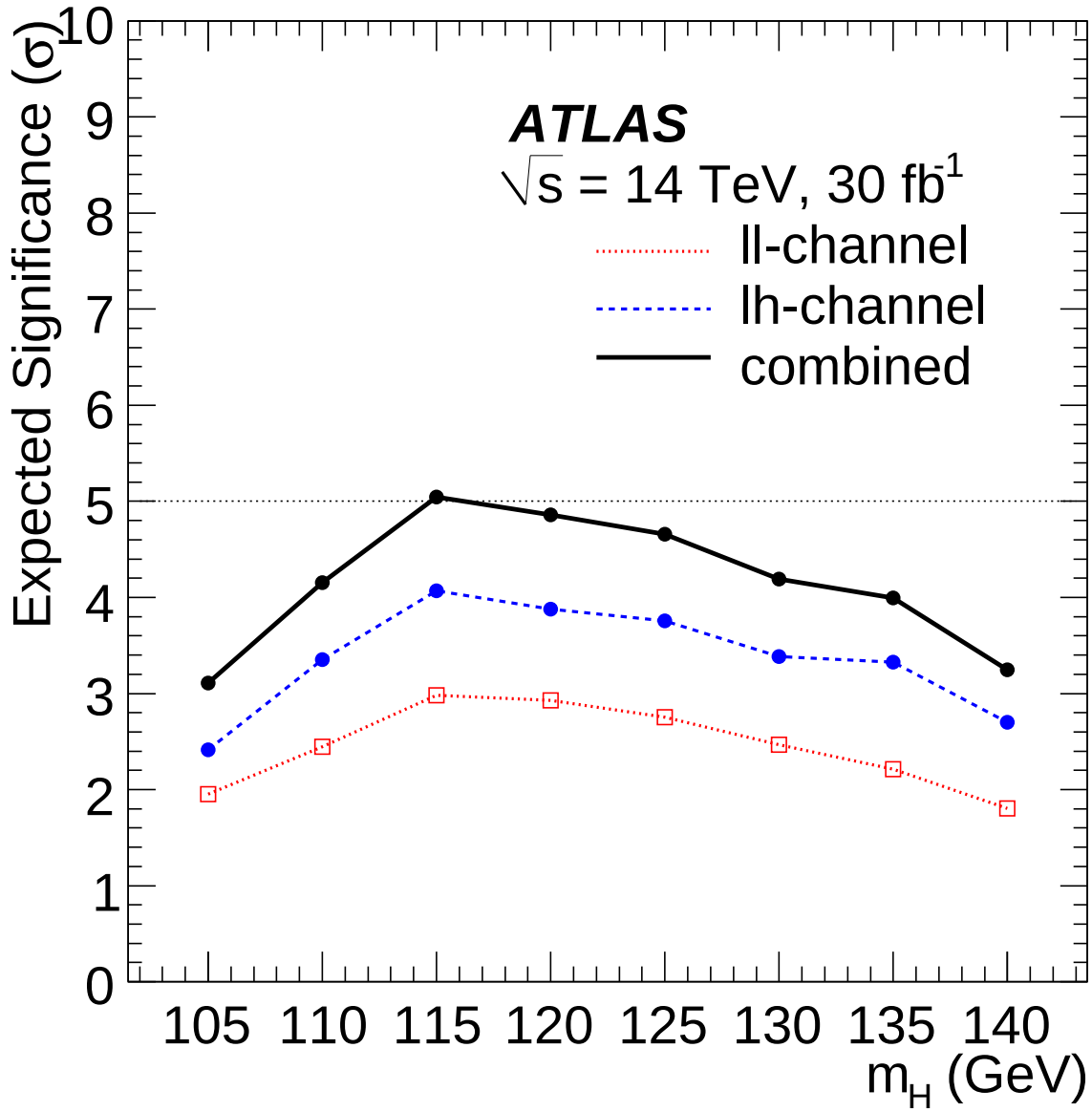

Figure 5.4: Expected signal significance for several masses based on fitting the $m_{\tau\tau}$ spectrum in $H^0 \to \tau^+\tau^-$ with $30 fb^{-1}$ of data (one year of data taking). From Ref. [458]. In the TAU10 Conference (13-19.09.2010), R.Goncalo reported on behalf of the *ATLAS* Coll. that the hh mode was at an advanced stage for being incorporated in these plots soon. However, figures were not available yet.

LHC has a large potential in the investigation of the *MSSM* Higgs sector. The Higgs couplings in the *MSSM* are different to those in the *SM*. In particular, for large Higgs masses ($m_H > 160$ GeV) its decays into weak gauge bosons are either suppressed or absent in the case of the pseudoscalar Higgs, A. On the other hand,

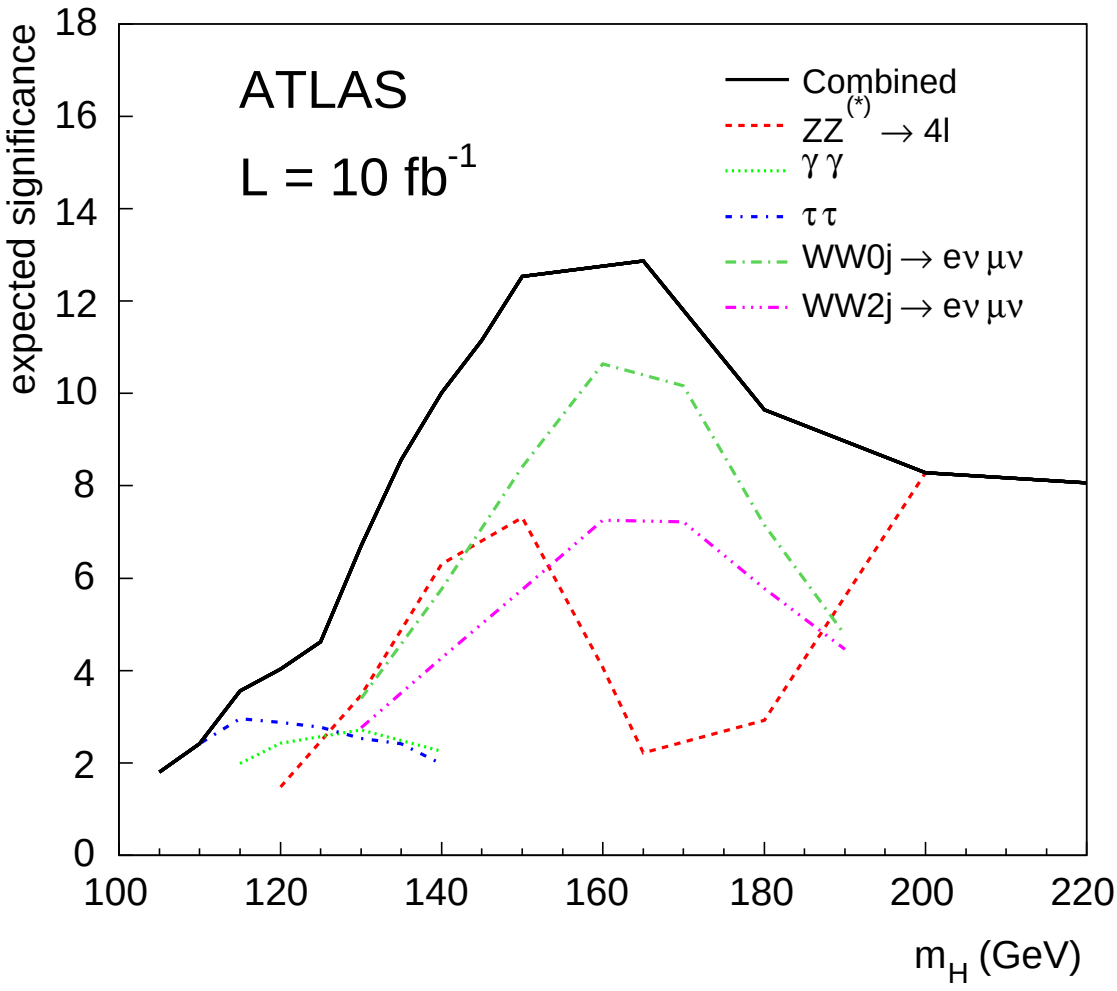

Figure 5.5: The median discovery significance for the SM Higs boson for the various channels as well as the combination for the integrated luminosity of $10 fb^{-1}$ for the lower mass range. From Ref. [458].

the coupling to third generation fermions is strongly enhanced for large regions of the parameter space which makes the decays into τ leptons even more interesting. The search for light neutral Higgs boson is based on the same channels as for the SM case, with more relevance of $H \to \tau\tau$ for larger masses in some subsets of the parameter space, due to enhanced couplings. In addition to this, $A \to \tau\tau$ is also relevant for large values of $\tan\beta$ [17]. In both decay channels, the ℓh detection mode would provide again the highest sensitivity. A final promising decay channel is $H^{\pm} \to \tau^{\pm}\nu_{\tau}$, that would unambiguously proof the existence of physics beyond the SM. For a high $SUSY$ mass scale this charged Higgs boson could be the first signal

[17] The ratio of the values of the two Higgs condensates.

of new physics (and indication for $SUSY$) discovered.

Chapter 6

$\tau^- \to (\pi\pi\pi)^-\nu_\tau$ decays

6.1 Introduction

In this chapter we will discuss the hadron form factors and related observables appearing in $\tau^- \to (\pi\pi\pi)^-\nu_\tau$ decays. These processes are a very clean scenario to learn about the axial-vector current, because the vector current contribution is forbidden by G-parity in the isospin limit. Moreover, the starring rôle of the lightest vector and axial-vector resonances will allow to study in detail the properties of the latter, since the first one is extremely well known from $e^+e^- \to \pi\pi$ and $\tau \to \pi\pi\nu_\tau$ decays. At the same time, this will be a stringent test of the joint consistency of the proposed width for a given definition of mass [386].

The $\tau \to \pi\pi\pi\nu_\tau$ decay is thus driven by the hadronization of the axial-vector current. Within the resonance chiral theory, and considering the large-N_C expansion, this process has been studied in Ref. [309]. In the light of later developments we revise here [322] this previous work by including a new off-shell width for the $a_1(1260)$ resonance that provides a good description of the $\tau \to \pi\pi\pi\nu_\tau$ spectrum and branching ratio. We also consider the rôle of the $\rho(1450)$ resonance in these observables. Thus we bring in an overall description of the $\tau \to \pi\pi\pi\nu_\tau$ process in excellent agreement with our present experimental knowledge.

The significant amount of experimental data on τ decays, in particular, $\tau \to \pi\pi\pi\nu_\tau$ branching ratios and spectra [78], encourages an effort to carry out a theoretical analysis within a model-independent framework capable to provide information on the hadronization of the involved QCD currents. A step in this direction has been done in Ref. [309], where the $\tau \to \pi\pi\pi\nu_\tau$ decays have been analyzed within the resonance chiral theory (RχT) [6, 7]. As explained in detail in earlier chapters, this procedure amounts to build an effective Lagrangian in which resonance states are treated as active degrees of freedom. Though the analysis in Ref. [309] allows to reproduce the experimental data on $\tau \to \pi\pi\pi\nu_\tau$ by fitting a few free parameters in this effective Lagrangian, it soon would be seen that the results of this fit are not compatible with theoretical expectations from short-distance QCD constraints [299]. We believe that the inconsistency can be attributed to the usage of an ansatz for the off-shell width of the $a_1(1260)$ resonance, which was introduced ad-hoc in

Ref. [309]. The aim of our work was to reanalyse $\tau \to \pi\pi\pi\nu_\tau$ processes within the same general scheme, now considering the energy-dependent width of the $a_1(1260)$ state within a proper RχT framework. The last issue, that is one of the major developments of our work is considered in detail in Section 6.3.1.

Although this chapter is based in Ref.[322], the material covered in Sects. 6.4.2, 6.4.3 and 6.4.4 is presented in this Thesis for the first time.

6.2 The axial-vector current in $\tau^- \to (\pi\pi\pi)^-\nu_\tau$ decays

Our effective Lagrangian will include the pieces given in Eqs. (3.66), (4.19) and (4.31) [1]. These decays are worked out considering exact isospin symmetry, so the corresponding hadron matrix elements will be

$$T_{\pm\mu}(p_1,p_2,p_3) \;=\; \langle \pi_1(p_1)\pi_2(p_2)\pi^{\pm}(p_3)|\, A_\mu\, e^{i\mathcal{L}_{QCD}}|0\rangle\,. \tag{6.1}$$

Outgoing states $\pi_{1,2}$ correspond here to π^- and π^0 for upper and lower signs in $T_{\pm\mu}$, respectively. The hadron tensor is written instead of three form factors following Eq. (5.51), with $F_4^V(Q^2,\, s_1,\, s_2) \,=\, 0$ since we have no vector current contribution. Since the contribution of $F_3^A(Q^2,\, s_1,\, s_2)$ -carrying pseudoscalar degrees of freedom- to the spectral function of $\tau \to \pi\pi\pi\nu_\tau$ goes like m_π^4/Q^4 and, accordingly, it is very much suppressed with respect to those coming from $F_1^A(Q^2,\, s_1,\, s_2)$ and $F_2^A(Q^2,\, s_1,\, s_2)$, we will not consider it in the following.

The evaluation of the form factors F_1 and F_2 within in the context of $R\chi T$ has been carried out in Ref. [309]. One has :

$$F_{\pm i} \;=\; \pm\left(F_i^{\chi} \,+\, F_i^{\rm R} \,+\, F_i^{\rm RR}\right)\;, \qquad i=1,2\;, \tag{6.2}$$

where the different contributions correspond to the diagrams in Figure 6.1. In terms of the Lorentz invariants Q^2, $s=(p_1+p_3)^2$, $t=(p_2+p_3)^2$ and $u=(p_1+p_2)^2$ (notice

[1] Notice that we only consider the effect of spin-one resonances. Given the vector character of the SM couplings of the hadron matrix elements in τ decays, form factors for these processes are ruled by vector and axial-vector resonances. Notwithstanding those form factors are given, in the $\tau \to PPP\nu_\tau$ decays, by a four-point Green function where other quantum numbers might play a role, namely scalar and pseudoscalar resonances [94, 484, 485, 486]. Among these, in the three pion tau decay modes, the lightest state -that one could expect to give the dominant contribution- is the σ or $f_0(600)$. As we assume the $N_C \to \infty$ limit, the nonet of scalars corresponding to the $f_0(600)$ is not considered. This multiplet is generated by rescattering of the ligthest pseudoscalars and then subleading in the $1/N_C$ expansion [487].

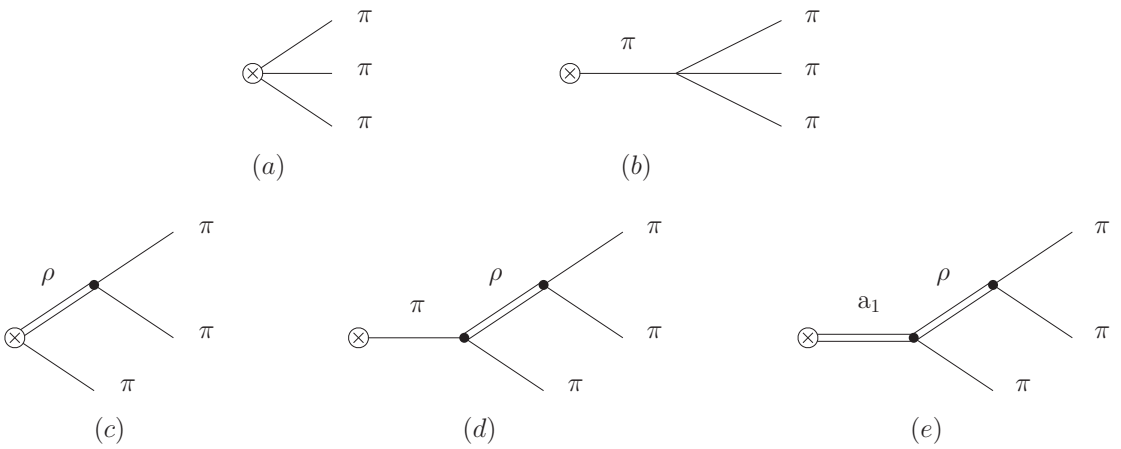

Figure 6.1: Diagrams contributing to the hadron axial-vector form factors F_i : (a) and (b) contribute to F_1^χ, (c) and (d) to F_1^R and (e) to F_1^{RR}.

that $u = Q^2 - s - t + 3m_\pi^2$) these contributions are given by [309]

$$\begin{aligned}
F_1^\chi(Q^2,s,t) &= -\frac{2\sqrt{2}}{3F} \\
F_1^{\rm R}(Q^2,s,t) &= \frac{\sqrt{2}\,F_V\,G_V}{3\,F^3}\left[\frac{3\,s}{s-M_V^2} - \left(\frac{2G_V}{F_V}-1\right)\left(\frac{2Q^2-2s-u}{s-M_V^2} + \frac{u-s}{t-M_V^2}\right)\right] \\
F_1^{\rm RR}(Q^2,s,t) &= \frac{4\,F_A\,G_V}{3\,F^3}\,\frac{Q^2}{Q^2-M_A^2}\left[-\,(\lambda'+\lambda'')\,\frac{3\,s}{s-M_V^2}\right. \\
&\qquad \left. +\,H(Q^2,s)\,\frac{2Q^2+s-u}{s-M_V^2} \,+\, H(Q^2,t)\,\frac{u-s}{t-M_V^2}\right],
\end{aligned} \tag{6.3}$$

where

$$H(Q^2,x) = -\,\lambda_0\,\frac{m_\pi^2}{Q^2} \,+\, \lambda'\,\frac{x}{Q^2} \,+\, \lambda''\,, \tag{6.4}$$

λ_0, λ' and λ'' being linear combinations of the λ_i couplings that can be read in Eq. (4.30). Bose symmetry under the exchange of the two identical pions in the final state implies that the form factors F_1 and F_2 are related by $F_2(Q^2,s,t) = F_1(Q^2,t,s)$.

The resonance exchange approximately saturates the phenomenological values of the $\mathcal{O}(p^4)$ couplings in the standard χPT Lagrangian. This allows to relate both schemes in the low energy region, and provides a check of our results in the limit $Q^2 \ll M_V^2$. This check has been performed [309], verifying the agreement between our expression Eq. (6.3) —two-resonance exchange terms do not contribute at this order— and the result obtained within χPT in Refs. [356, 428] coming from

saturation by vector meson resonances of the $\mathcal{O}(p^4)$ couplings :

$$T^{\chi PT}_{\pm\mu}\Big|_{1^+} = \mp\frac{2\sqrt{2}}{3F}\left[\left(1+\frac{3\,s}{2\,M_V^2}\right)V_{1\mu}+\left(1+\frac{3\,t}{2\,M_V^2}\right)V_{2\mu}\right]+\text{chiral loops }+\mathcal{O}(p^6)\ . \tag{6.5}$$

As an aside, it is worth to point out that this low–energy behaviour is not fulfilled by all phenomenological models proposed in the literature. In particular, in the widely used KS model [329] the hadron amplitude satisfies

$$T^{(KS)}_{\pm\mu} \stackrel{s,t\ll M_V^2}{\longrightarrow} \mp\frac{2\sqrt{2}}{3F}\left[\left(1+\frac{s}{M_V^2}\right)V_{1\mu}+\left(1+\frac{t}{M_V^2}\right)V_{2\mu}\right]\ . \tag{6.6}$$

Thus, while the lowest order behaviour is correct (it was constructed to be so), it is seen that the KS model fails to reproduce the χPT result at the next–to–leading order. Accordingly this model is not consistent with the chiral symmetry of QCD.

6.3 Short-distance constraints ruled by QCD

Besides the pion decay constant F, the above results for the form factors F_i depend on six combinations of the coupling constants in the Lagrangian $\mathcal{L}_{\mathrm{R}\chi\mathrm{T}}$, namely F_V, F_A, G_V, λ_0, λ' and λ'' and the masses M_V, M_A of the vector and axial-vector nonets. All of them are in principle unknown parameters. However, it is clear that $\mathcal{L}_{\mathrm{R}\chi\mathrm{T}}$ does not represent an effective theory of QCD for arbitrary values of the couplings. Though the determination of the effective parameters from the underlying theory is still an open problem, one can get information on the couplings by assuming that the resonance region —even when one does not include the full phenomenological spectrum— provides a bridge between the chiral and perturbative regimes [7]. This is implemented by matching the high energy behaviour of Green functions (or related form factors) evaluated within the resonance theory with asymptotic results obtained in perturbative QCD [7, 299, 310, 311, 314, 315, 323, 488]. In the $N_C \to \infty$ limit, and within the approximation of only one nonet of vector and axial-vector resonances, the analysis of the two-point Green functions $\Pi_{V,A}(q^2)$ and the three-point Green function VAP of QCD currents with only one multiplet of vector and axial-vector resonances lead to the following constraints [274] :

i) By demanding that the two-pion vector form factor vanishes at high momentum transfer one obtains the condition $F_V\,G_V = F^2$ [7].

ii) The first Weinberg sum rule [302] leads to $F_V^2 - F_A^2 = F^2$, and the second Weinberg sum rule gives $F_V^2\,M_V^2 = F_A^2\,M_A^2$ [6].

iii) The analysis of the VAP Green function [299] gives for the coupling combinations λ_0, λ' and λ'' entering the form factors in Eq. (6.3) the following results :

$$\lambda' \;=\; \frac{F^2}{2\sqrt{2}\,F_A\,G_V} \;=\; \frac{M_A}{2\sqrt{2}\,M_V}\,, \tag{6.7}$$

$$\lambda'' \;=\; \frac{2\,G_V\,-F_V}{2\sqrt{2}\,F_A} \;=\; \frac{M_A^2-2M_V^2}{2\sqrt{2}\,M_V\,M_A}\,, \tag{6.8}$$

$$4\,\lambda_0 \;=\; \lambda'+\lambda'' \;=\; \frac{M_A^2-M_V^2}{\sqrt{2}\,M_V\,M_A}\,, \tag{6.9}$$

where the second equalities in Eqs. (6.7) and (6.8) are obtained using the above relations i) and ii).

As mentioned above, M_V and M_A stand for the masses of the vector and axial-vector resonance nonets, in the chiral and large-N_C limits. A phenomenological analysis carried out in this limit [323] shows that M_V is well approximated by the $\rho(770)$ mass, where as for the axial-vector mass one gets $M_{\rm a_1}^{1/N_C} \equiv M_A = 998(49)$ MeV (which differs appreciably from the presently accepted value of $M_{\rm a_1}(1260)$= 1230±40 MeV).

In addition, one can require that the $J = 1$ axial-vector spectral function in $\tau \to \pi\pi\pi\nu_\tau$ vanishes for large momentum transfer. We consider the axial two–point function $\Pi_A^{\mu\nu}(Q^2)$, which plays in $\tau \to \pi\pi\pi\nu_\tau$ processes the same role than the vector–vector current correlator does in the $\tau \to \pi\pi\nu_\tau$ decays, driven by the vector form factor. The goal will be to obtain QCD–ruled constraints on the new couplings of the resonance Lagrangian. As these couplings do not depend on the Goldstone masses we will work in the chiral limit but our results will apply for non–zero Goldstone masses too. In the chiral limit the $\Pi_A^{\mu\nu}(Q^2)$ correlator becomes transverse, hence we can write

$$\Pi_A^{\mu\nu}(Q^2) = (Q^\mu Q^\nu - g^{\mu\nu}Q^2)\,\Pi_A(Q^2)\,. \tag{6.10}$$

As in the case of the pion and axial form factors, the function $\Pi_A(Q^2)$ is expected to satisfy an unsubtracted dispersion relation. This implies a constraint for the $J = 1$ spectral function ${\rm Im}\Pi_A(Q^2)$ in the asymptotic region, namely[297]

$${\rm Im}\Pi_A(Q^2) \;\stackrel{Q^2\to\infty}{\longrightarrow}\; \frac{N_C}{12\,\pi}\;. \tag{6.11}$$

Now, taking into account that each intermediate state carrying the appropriate quantum numbers yields a positive contribution to ${\rm Im}\Pi_A(Q^2)$, we have

$${\rm Im}\Pi_A(Q^2) \;\geq\; -\frac{1}{3\,Q^2}\int {\rm d}\Phi\;\left(T^\mu|_{1^+}\right)\left(T_\mu|_{1^+}\right)^*\,, \tag{6.12}$$

${\rm d}\Phi$ being the differential phase space for the three–pion state. The constraint in Eq. (6.11) then implies

$$\lim_{Q^2\to\infty}\int_0^{Q^2} ds\int_0^{Q^2-s} dt\;\frac{W_A}{(Q^2)^2} = 0\,, \tag{6.13}$$

where W_A is the structure function defined in Eq. (5.61) [2]. It can be seen that the condition in Eq. (6.13) is not satisfied in general for arbitrary values of the coupling constants in the chiral interaction Lagrangian. In fact, it is found that this constraint leads to the relations in Eqs. (6.7) and (6.8), showing the consistency of the procedure [3].

The above constraints allow in principle to fix all six free parameters entering the form factors F_i in terms of the vector and axial-vector masses M_V, M_A. However the form factors in Eq. (6.3) include zero–width $\rho(770)$ and $\mathrm{a}_1(1260)$ propagator poles, which lead to divergent phase–space integrals in the calculation of $\tau \to \pi\pi\pi\nu_\tau$ decay widths. As stated above, in order to regularize the integrals one should take into account the inclusion of resonance widths, which means to go beyond the leading order in the $1/N_C$ expansion. In order to account for the inclusion of NLO corrections we perform the substitutions :

$$\frac{1}{M_{R_j}^2 - q^2} \quad \longrightarrow \quad \frac{1}{M_j^2 - q^2 - i\, M_j\, \Gamma_j(q^2)}\,, \tag{6.14}$$

Here $R_j = V, A$, while the subindex $j = \rho, \mathrm{a}_1$ on the right hand side stands for the corresponding physical state.

The substitution in Eq. (6.14) implies the introduction of additional theoretical inputs, in particular, the behaviour of resonance widths off the mass shell. This issue is studied in detail in Appendix C and Section 6.3.1. In the following, we will compare it both to the popular width developed in the KS model [329] and to the proposal of the earlier study within $R\chi T$, where this off-shell width was added by hand.

6.3.1 Expressions for the off-shell width of the a_1 resonance

The definition we have given in Appendix C for the spin-one resonance width -and applied for the vector case- holds for axial-vector mesons as well, but it would amount to evaluate the axial-vector-axial-vector current correlator with absorptive cuts of three pGs (two-loops diagrams) within $R\chi T$. This motivated the chiral based off-shell behaviour proposal in Ref. [309], an oversimplified approach in which the a_1 width was written in terms of three parameters, namely the on-shell width $\Gamma_{\mathrm{a}_1}(M_{\mathrm{a}_1}^2)$, the mass M_{a_1} and an exponent α ruling the asymptotic behaviour :

$$\Gamma_{\mathrm{a}_1}(q^2) \,=\, \Gamma_{\mathrm{a}_1}(M_A^2)\, \frac{\phi(q^2)}{\phi(M_A^2)}\, \left(\frac{M_A^2}{q^2}\right)^{\alpha}\, \theta\left(q^2 \,-\, 9m_\pi^2\right) \tag{6.15}$$

[2] As expected from partial conservation of the axial-vector current ($PCAC$), the analogous relation is automatically fulfilled by W_{SA}.

[3] These results and those in Section 7.3 have been obtained using the program $MATHEMATICA$ [489].

where

$$\begin{aligned}\phi(q^2) &= q^2 \int \mathrm{d}s\,\mathrm{d}t\,\left\{V_1^2\,|\mathrm{BW}_\rho(s)|^2 + V_2^2\,|\mathrm{BW}_\rho(t)|^2\right. \\ &\left. +2(V_1\cdot V_2)\,\Re e\,[\mathrm{BW}_\rho(s)\,\mathrm{BW}_\rho(t)^*]\right\}\,, \end{aligned} \tag{6.16}$$

and

$$\mathrm{BW}_\rho(q^2) = \frac{M_V^2}{M_V^2 - q^2 - iM_V\,\Gamma_\rho(q^2)} \tag{6.17}$$

is the usual Breit-Wigner function for the $\rho\,(770)$ meson resonance shape, the energy-dependent width $\Gamma_\rho(q^2)$ is given by Eq. (C.8), and the integral extends over the 3π phase space. The vectors V_1 and V_2 and the Mandelstam variables s and t entering the function $\phi(x = q^2,\, M_A^2)$ are defined following the general conventions given in Sect. 5.4.1. One can check them explicitly in Ref. [309].

A fundamental result of this Thesis is the improvement in the description of the off-shell axial-vector widths. We will follow the paper [322] in our explanation.
We propose here a new parameterization of the $\mathrm{a}_1(1260)$ width that is compatible with the RχT framework used throughout our analysis. As stated, to proceed as in the ρ meson case, one faces the problem of dealing with a resummation of two-loop diagrams in the two-point correlator of axial-vector currents. However, it is still possible to obtain a definite result by considering the correlator up to the two-loop order only. The width can be defined in this way by calculating the imaginary part of the diagrams through the well-known Cutkosky rules.

Let us focus on the transversal component, $\Pi_T(Q^2)$, of the two-point Green function :

$$\begin{aligned}\Pi^{33}_{\mu\nu} &= i\int \mathrm{d}^4x\; e^{iQ\cdot x}\,\langle\,0|\,T[A^3_\mu(x)\,A^3_\nu(0)]\,|0\,\rangle \\ &= (Q^2\,g_{\mu\nu} - Q_\mu Q_\nu)\,\Pi_T(Q^2) + Q_\mu Q_\nu\,\Pi_L(Q^2)\,, \end{aligned} \tag{6.18}$$

where $A^i_\mu = \overline{q}\gamma_\mu\gamma_5\frac{\lambda^i}{2}q$. We will assume that the transversal contribution is dominated by the π^0 and the neutral component of the $\mathrm{a}_1(1260)$ triplet : $\Pi_T(Q^2) \simeq \Pi^{\pi^0}(Q^2) + \Pi^{\mathrm{a}_1}(Q^2)$. Following an analogous procedure to the one in Ref. [491], we write $\Pi^{\mathrm{a}_1}(Q^2)$ as the sum

$$\Pi^{\mathrm{a}_1}(Q^2) = \Pi^{\mathrm{a}_1}_{(0)} + \Pi^{\mathrm{a}_1}_{(1)} + \Pi^{\mathrm{a}_1}_{(2)} + \ldots\,, \tag{6.19}$$

where $\Pi^{\mathrm{a}_1}_{(0)}$ corresponds to the tree level amplitude, $\Pi^{\mathrm{a}_1}_{(1)}$ to a two-loop order contribution, $\Pi^{\mathrm{a}_1}_{(2)}$ to a four-loop order contribution, etc. The diagrams to be included are those which have an absorptive part in the s channel. The first two terms are represented by diagrams (a) and (b) in Figure 6.3.1, respectively, where effective vertices denoted by a square correspond to the sum of the diagrams in Figure 6.1. Solid lines in the diagram (b) of Figure 6.3.1 correspond to any set of light pseudoscalar mesons that carry the appropriate quantum numbers to be an intermediate state.

The first term of the expansion in Eq. (6.19) arises from the coupling driven by

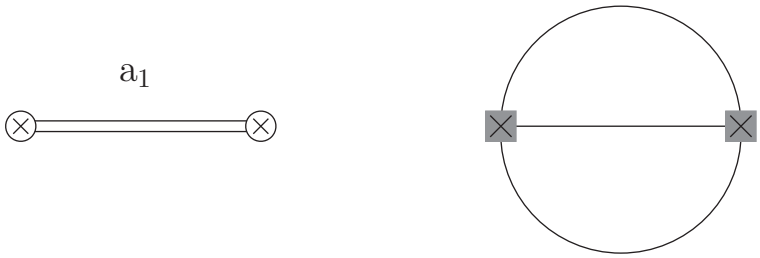

Figure 6.2: Diagrams contributing to the transverse part of the correlator of axial-vector currents in Eq. (6.19). Diagram (a) gives $\Pi^{a_1}_{(0)}$ and diagram (b) provides $\Pi^{a_1}_{(1)}$. The squared axial-vector current insertion in (b) corresponds to the sum of the diagrams in Figure 6.1. The double line in (a) indicates the a_1 resonance intermediate state. Solid lines in (b) indicate any Goldstone bosons that carry the appropriate quantum numbers.

F_A in the effective Lagrangian (4.19). We find

$$\Pi^{a_1}_{(0)} \;=\; -\,\frac{F_A^2}{M^2_{a_1}-Q^2}\;. \tag{6.20}$$

Thus, if the series in Eq. (6.19) can be resummed one should get

$$\Pi^{a_1}(Q^2) \;=\; -\,\frac{F_A^2}{M^2_{a_1}-Q^2+\Delta(Q^2)}\;, \tag{6.21}$$

and the energy dependent width of the $a_1(1260)$ resonance can be defined by

$$M_{a_1}\,\Gamma_{a_1}(Q^2) \;=\; -\,\mathrm{Im}\,\Delta(Q^2)\;. \tag{6.22}$$

Now if we expand $\Pi^{a_1}(Q^2)$ in powers of Δ and compare term by term with the expansion in Eq. (6.19), from the second term we obtain

$$\Delta(Q^2) \;=\; -\,\frac{(M^2_{a_1}-Q^2)}{\Pi^{a_1}_{(0)}}\;\Pi^{a_1}_{(1)}\;. \tag{6.23}$$

The off-shell width of the $a_1(1260)$ resonance will be given then by

$$\Gamma_{a_1}(Q^2) \;=\; \frac{(M^2_{a_1}-Q^2)}{M_{a_1}\,\Pi^{a_1}_{(0)}}\;\mathrm{Im}\,\Pi^{a_1}_{(1)}\;. \tag{6.24}$$

As stated, $\Pi^{a_1}_{(1)}$ receives the contribution of various intermediate states. These contributions can be calculated within our theoretical RχT framework from the

effective Lagrangian in Eqs. (4.19), (4.31), (4.33), (4.34), (4.43) and (4.44). In particular, for the intermediate $\pi^+\pi^-\pi^0$ state one has

$$\Pi^{\mathrm{a}_1}_{(1)}(Q^2) \;=\; \frac{1}{6Q^2}\int \frac{\mathrm{d}^4p_1}{(2\pi)^4}\,\frac{\mathrm{d}^4p_2}{(2\pi)^4}\,T^{\mu}_{1^+}\,T^{*}_{1^+\mu}\,\prod_{i=1}^{3}\frac{1}{p_i^2-m_\pi^2+i\epsilon}\;, \tag{6.25}$$

where $p_3 = Q - p_1 - p_2$, and T_{1^+} is the 1^+ piece of the hadron tensor in Eq. (6.1),

$$T^{\mu}_{1^+} \;=\; V_1^{\mu}\,F_1 \,+\, V_2^{\mu}\,F_2\;. \tag{6.26}$$

When extended to the complex plane, the function $\Pi^{\mathrm{a}_1}_{(1)}(z)$ has a cut in the real axis for $z \geq 9m_\pi^2$, where $\mathrm{Im}\,\Pi^{\mathrm{a}_1}_{(1)}(z)$ shows a discontinuity. The value of this imaginary part on each side of the cut can be calculated according to the Cutkosky rules as :

$$\mathrm{Im}\,\Pi^{\mathrm{a}_1}_{(1)}(Q^2\pm i\epsilon) = \mp\frac{i}{2}\,\frac{1}{6Q^2}\int \frac{\mathrm{d}^4p_1}{(2\pi)^4}\,\frac{\mathrm{d}^4p_2}{(2\pi)^4}\,T^{\mu}_{1^+}\,T^{*}_{1^+\mu}\,\prod_{i=1}^{3}(-2i\pi)\,\theta(p_i^0)\,\delta(p_i^2-m_\pi^2)\;, \tag{6.27}$$

with $p_3 = Q - p_1 - p_2$ and $Q^2 > 9m_\pi^2$. After integration of the delta functions one finds

$$\mathrm{Im}\,\Pi^{\mathrm{a}_1}_{(1)}(Q^2\pm i\epsilon) = \pm\,\frac{1}{192\,Q^4}\,\frac{1}{(2\pi)^3}\int \mathrm{d}s\,\mathrm{d}t\;T^{\mu}_{1^+}\,T^{*}_{1^+\mu}\;, \tag{6.28}$$

where the integrals extend over a three-pion phase space with total momentum squared Q^2. Therefore, the contribution of the $\pi^+\pi^-\pi^0$ state to the $\mathrm{a}_1(1260)$ width will be given by

$$\Gamma^{\pi}_{\mathrm{a}_1}(Q^2) \;=\; \frac{-1}{192(2\pi)^3F_A^2M_{\mathrm{a}_1}}\left(\frac{M^2_{\mathrm{a}_1}}{Q^2}-1\right)^2\int \mathrm{d}s\,\mathrm{d}t\;T^{\mu}_{1^+}\,T^{*}_{1^+\mu}\;. \tag{6.29}$$

In the same way one can proceed to calculate the contribution of the intermediate states $K^+K^-\pi^0$, $K^0\bar{K}^0\pi^0$, $K^-K^0\pi^+$ and $K^+\bar{K}^0\pi^-$. The corresponding hadron tensors $T^K_{1^+}$ can be obtained from Ref. [304]. Additionally one could consider the contribution of $\eta\pi\pi$ and $\eta\eta\pi$ intermediate states. However, the first one vanishes in the isospin limit because of G-parity (see Chapter 8) and the second one is suppressed by a tiny upper bound for the branching ratio [8, 490] and they will not be taken into account.

In this way we have [4]

$$\Gamma_{\mathrm{a}_1}(Q^2) \;=\; \Gamma^{\pi}_{\mathrm{a}_1}(Q^2)\,\theta(Q^2-9m_\pi^2) \;+\; \Gamma^{K}_{\mathrm{a}_1}(Q^2)\,\theta(Q^2-(2m_K+m_\pi)^2)\;, \tag{6.30}$$

where

$$\Gamma^{\pi,K}_{\mathrm{a}_1}(Q^2) \;=\; \frac{-S}{192(2\pi)^3F_A^2M_{\mathrm{a}_1}}\left(\frac{M^2_{\mathrm{a}_1}}{Q^2}-1\right)^2\int \mathrm{d}s\,\mathrm{d}t\;T^{\pi,K\mu}_{1^+}\,T^{\pi,K*}_{1^+\mu}\;. \tag{6.31}$$

[4] It is important to stress that we do not intend to carry out the resummation of the series in Eq. (6.19). In fact, our expression in Eq. (6.24) would correspond to the result of the resummation if this series happens to be geometric, which in principle is not guaranteed [491].

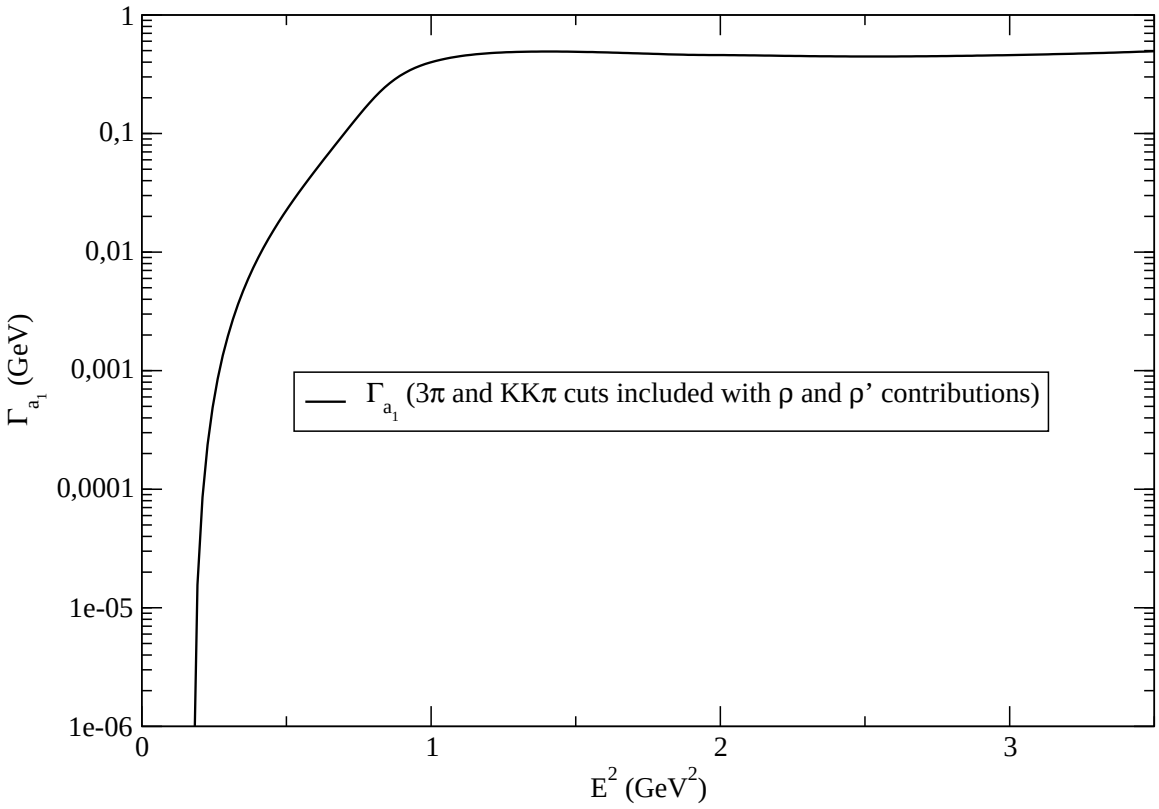

Figure 6.3: Plot of our expression for $\Gamma_{a_1}(Q^2)$ using the values of the couplings discussed in Sect. 6.4.

Here $\Gamma^{\pi}_{a_1}(Q^2)$ recalls the three pion contributions and $\Gamma^{K}_{a_1}(Q^2)$ collects the contributions of the $KK\pi$ channels. In Eq. (6.31) the symmetry factor $S = 1/n!$ reminds the case with n identical particles in the final state. It is also important to point out that, contrarily to the width we proposed in Ref. [309] [$\Gamma_{a_1}(Q^2)$, in Eq. (6.15)], the on-shell width $\Gamma_{a_1}(M^2_{a_1})$ is now a prediction and not a free parameter.

With this off-shell width a very accurate description of the related observables will be given in later sections. In other formalisms, like that of the hidden local symmetry chiral models [492] one needs to restore to a extremely unnatural off-shell width description that reaches the value of 10 GeV for $Q^2 \sim 2.5$ GeV^2. In Figure 6.3 our expression for Γ_{a_1} is plotted as a function of the invariant mass squared the hadron system has.

6.4 Phenomenology of the $\tau^- \to (\pi\pi\pi)^-\nu_\tau$ process

6.4.1 The contribution of the $\rho(1450)$

It turns out that, though some flexibility is allowed around the predicted values for the parameters, the region between $1.5 - 2.0$ GeV^2 of the three pion spectrum is still poorly described by the scheme we have proposed here. This is not surprising as the $\rho(1450)$, acknowledgeably rather wide, arises in that energy region. We find that it is necessary to include, effectively, the role of a $\rho' \equiv \rho(1450)$, in order to recover good agreement with the experimental data. The ρ' belongs to a second, heavier, multiplet of vector resonances that we have not considered in our procedure. Its inclusion would involve a complete new set of analogous operators to the ones already present in $\mathcal{L}_{R\chi T}$, Eqs. (4.19), (4.31), with the corresponding new couplings. This is beyond the scope of our analysis. However we propose to proceed by performing the following substitution in the $\rho(770)$ propagator :

$$\frac{1}{M_\rho^2 - q^2 - iM_\rho\Gamma_\rho(q^2)} \longrightarrow \frac{1}{1+\beta_{\rho'}}\left[\frac{1}{M_\rho^2 - q^2 - iM_\rho\Gamma_\rho(q^2)} + \frac{\beta_{\rho'}}{M_{\rho'}^2 - q^2 - iM_{\rho'}\Gamma_{\rho'}(q^2)}\right], \tag{6.32}$$

where as a first approximation the ρ' width is given by the decay into two pions :

$$\begin{aligned} \Gamma_{\rho'}(q^2) &= \Gamma_{\rho'}(M_{\rho'}^2)\,\frac{M_{\rho'}}{\sqrt{q^2}}\left(\frac{p(q^2)}{p(M_{\rho'}^2)}\right)^3 \theta(q^2 - 4\,m_\pi^2)\,, \qquad (6.33)\\ p(x) &= \frac{1}{2}\sqrt{x - 4m_\pi^2}\,. \end{aligned}$$

For the numerics we use the values $M_{\rho'} = 1.465$ GeV and $\Gamma_{\rho'}(M_{\rho'}^2) = 400$ MeV as given in Ref. [8]. We find that a good agreement with the spectrum, $d\Gamma/dQ^2$, measured by $ALEPH$ [78] is reached for the set of values :

$$\begin{aligned} F_V &= 0.180\,\text{GeV} \quad , \quad F_A = 0.149\,\text{GeV} \quad , \quad \beta_{\rho'} = -0.25\,,\\ M_V &= 0.775\,\text{GeV} \quad , \quad M_{K^*} = 0.8953\,\text{GeV} \quad , \quad M_{\text{a}_1} = 1.120\,\text{GeV}\,, \end{aligned} \tag{6.34}$$

that we call Set 1. The corresponding width is $\Gamma(\tau \to \pi\pi\pi\nu_\tau) = 2.09 \times 10^{-13}$ GeV, in excellent agreement with the experimental figure $\Gamma(\tau \to \pi\pi\pi\nu_\tau)|_{exp} = (2.11 \pm 0.02) \times 10^{-13}$ GeV [8]. From F_V and F_A in Eq. (6.34), and the second Weinberg sum rule we can also determine the value of $M_A = F_V M_V / F_A \simeq 0.94$ GeV, a result consistent with the one obtained in Ref. [323]. If, instead, we do not include the ρ' contribution, the best agreement with experimental data is reached for the values of Set 2 :

$$\begin{aligned} F_V &= 0.206\,\text{GeV} \quad , \quad F_A = 0.145\,\text{GeV} \quad , \quad \beta_{\rho'} = 0\,,\\ M_V &= 0.775\,\text{GeV} \quad , \quad M_{K^*} = 0.8953\,\text{GeV} \quad , \quad M_{\text{a}_1} = 1.115\,\text{GeV}\,, \end{aligned} \tag{6.35}$$

though the branching ratio is off by 15%. A comparison between the results for the $\tau \to \pi\pi\pi\nu_\tau$ spectra obtained from Sets 1, 2 and the data provided by $ALEPH$ is

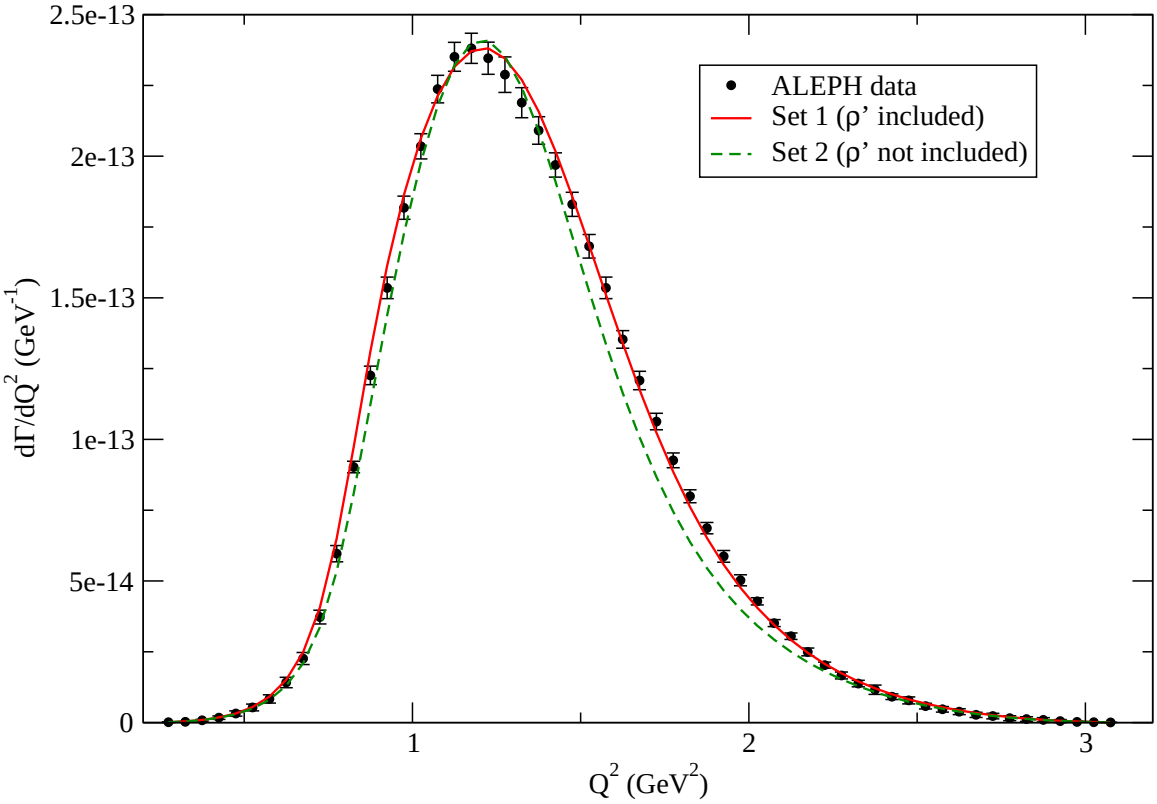

Figure 6.4: Comparison between the theoretical $M^2_{3\pi}$-spectra of the $\tau^- \to \pi^+\pi^-\pi^-\nu_\tau$ with *ALEPH* data [78]. Set 1 corresponds to the values of the parameters : $F_V = 0.180\,\text{GeV}$, $F_A = 0.149\,\text{GeV}$, $M_{a_1} = 1.120\,\text{GeV}$, $\beta_{\rho'} = -0.25$, $M_A \simeq 0.91\,\text{GeV}$. Set 2 corresponds to the values of the parameters : $F_V = 0.206\,\text{GeV}$, $F_A = 0.145\,\text{GeV}$, $M_{a_1} = 1.150\,\text{GeV}$, $\beta_{\rho'} = 0$, i.e. without the inclusion of the ρ'. In the case of Set 2 the overall normalization of the spectrum has been corrected by a 15% to match the experimental data.

shown in Figure 6.4. Notice that we have corrected the results provided by Set 2 by a normalization factor of 1.15 in order to compare the shapes of the spectra. Though it is difficult to assign an error to our numerical values, by comparing Set 1 and Set 2 we consider that a 15% should be on the safe side. Notice, however, that the error appears to be much smaller in the case of M_{a_1}.

For Set 1 the width of the $a_1(1260)$ is $\Gamma_{a_1}(M^2_{a_1}) = 0.483$ GeV, which, incidentally, is in agreement with the figure got in Ref. [309] from a fit to the data. The value of $\Gamma_{a_1}(M^2_{a_1})$ quoted in the *PDG* (2008) [8] goes from 250 MeV up to 600 MeV.

Our preferred set of values in Eq. (6.34) satisfies reasonably well all the short distance constraints pointed out in Sect. 6.3, with a deviation from Weinberg sum rules of at most 10%, perfectly compatible with deviations due to the single resonance approximation.

6.4.2 Low-energy description

After that, we take a closer look to the low-Q^2 region of the spectrum. In fact, in our approach we have assumed that $\mathcal{O}(p^4)$ corrections arising from chiral logs are small, hence the dominant contributions to hadron amplitudes arise from resonance exchange. In Figure 6.5, we can see that our expression fits the data remarkably well in the low-Q^2 without any need to improve it by adding the effect of the neglected chiral logs [5]. Our working hypothesis is thus confirmed. In this plot we also see that the form-factors proposed by the KS model induced a systematic departure of the data points increasing with the energy. It is interesting to note that -as we asserted in Chapter 5- that the wrong description at NLO in the chiral expansion is naturally carried on to higher energies, once the full expression is included. Indeed, the low-energy limits of the KS expressions for the form factors and ours [6] already show that the KS curve is systematically under ours getting farther as the energy increases.

In Figure 6.6 we can see that the shift induced at low-energies in the original KS-model [7] gets carried on naturally to higher energies. In the current $TAUOLA$ parameterization the agreement seems to be better by introducing a large on-shell a_1 width (0.6 GeV) that requires to adjust the normalization by a factor of order 40% (1.38 in the curve) that appears to be quite unnatural. Even doing so, the description between 1.5 and 1.8 GeV^2 is not good.

6.4.3 $\frac{d\Gamma}{ds_{ij}}$ distributions

Next, we will analyse the differential distributions in the invariant masses of pairs of pions, $s_{ij} \equiv (p_i + p_j)^2 = (Q - p_k)^2$ for $i \neq j \neq k$ and $i, j, k = 1, 2, 3$. Neither Ref. [78] nor any later publication made a dedicated study of these observables.

[5] Close to threshold (i.e. for $\sqrt{Q^2}$ well below M_V) one is able to explicitly calculate the contributions of $\mathcal{O}(p^4)$ chiral logs, therefore their impact can be numerically evaluated. In fact, Ref [309] considered this correction by using the results in Ref. [356] because the description at low-energies was not as good as the one we have achieved now. As we have already explained, the reason was that the choice of the off-shell width for the a_1 biased the determination of the parameters in the resonance Lagrangian and, particularly, affected some of the short-distance QCD relations involving parameters that have an impact close to threshold.

[6] As described in Eqs.(6.5) and (6.6).

[7] The original KS model used the following values for the parameters: $M_{a_1} = 1.251$ GeV and $\Gamma_{a_1}(M_{a_1}) = 0.475$ GeV. With these parameters, the description of the experimental data available at that time [493] was very good. However, as the experimental errors were reduced ten years later by $CLEO-II$ [403], $OPAL$ [494] and $ALEPH$ [78], one noticed that there was a need of including another parameter to keep such a good description. In order to keep the expression for the off-shell width the solution adopted in $TAUOLA$ was to modify the on-shell a_1 width and include a normalization factor to correct the branching ratio. The new width read $\Gamma_{a_1}(M_{a_1}) = 0.599$ GeV and the normalization factor enhances the decay rate by ~ 1.4.

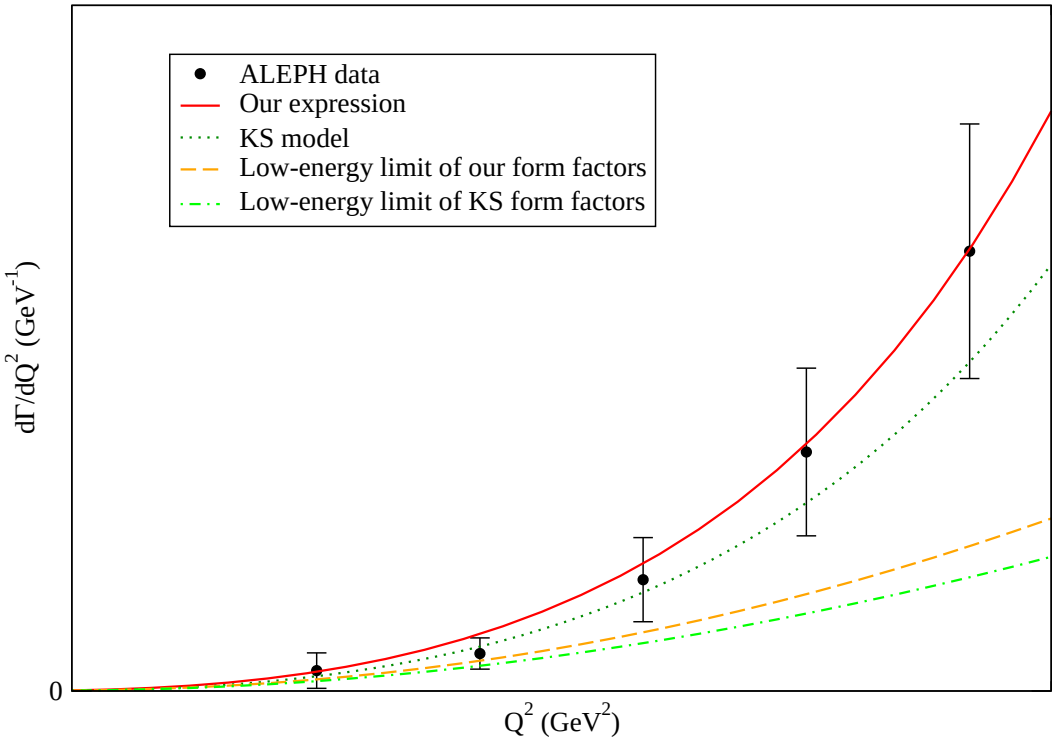

Figure 6.5: Comparison between the theoretical low-energy $M_{3\pi}^2$-spectra of the $\tau^- \to \pi^+\pi^-\pi^-\nu_\tau$ with *ALEPH* data [78]. Our results (red solid line) correspond to Set 1, Eq. (6.34), and its corresponding low-energy limit (orange dashed line) to Eq.(6.5). The green dotted line corresponds to the *KS* results [329] and its low-energy limit (green dashed-dotted line) is given in Eq. 6.6. We observe that the wrong *KS* description at *NLO* in the chiral expansion is naturally carried on to the whole expression for the spectrum. Moreover, the excellent agreement of our prediction with data shows that our working hypothesis of neglecting the effect of $\mathcal{O}(p^4)$ chiral logs is well-based.

Although we cannot compare our predictions to data now, it will be an interesting check to elucidate if our description is as accurate as Figure 6.4 indicates.

In Figure 6.7 we can see our prediction for $\mathrm{d}\Gamma/\mathrm{d}s$. The distribution starts to rise when $(p_\pi + \pi_\pi)^2$ reaches M_ρ^2 and then goes increasing smoothly goberned by the ρ and a_1 widths. The contribution of the configuration in which two of the three pions carry almost all the energy of the hadron system is negligible as one can see comparing the tail of the spectra with earlier fall off than the one seen in Figure 6.4. In this figure and in the next two the small bumps of the curves are due to the error associated to the integration that is larger in this case than in that of the spectral function.

Similarly, in Fig 6.8 we plot our prediction for the distribution with respect to u. Taking into account that s, t and u are related via $u = Q^2 - s - t + 3\,m_\pi^2$, that

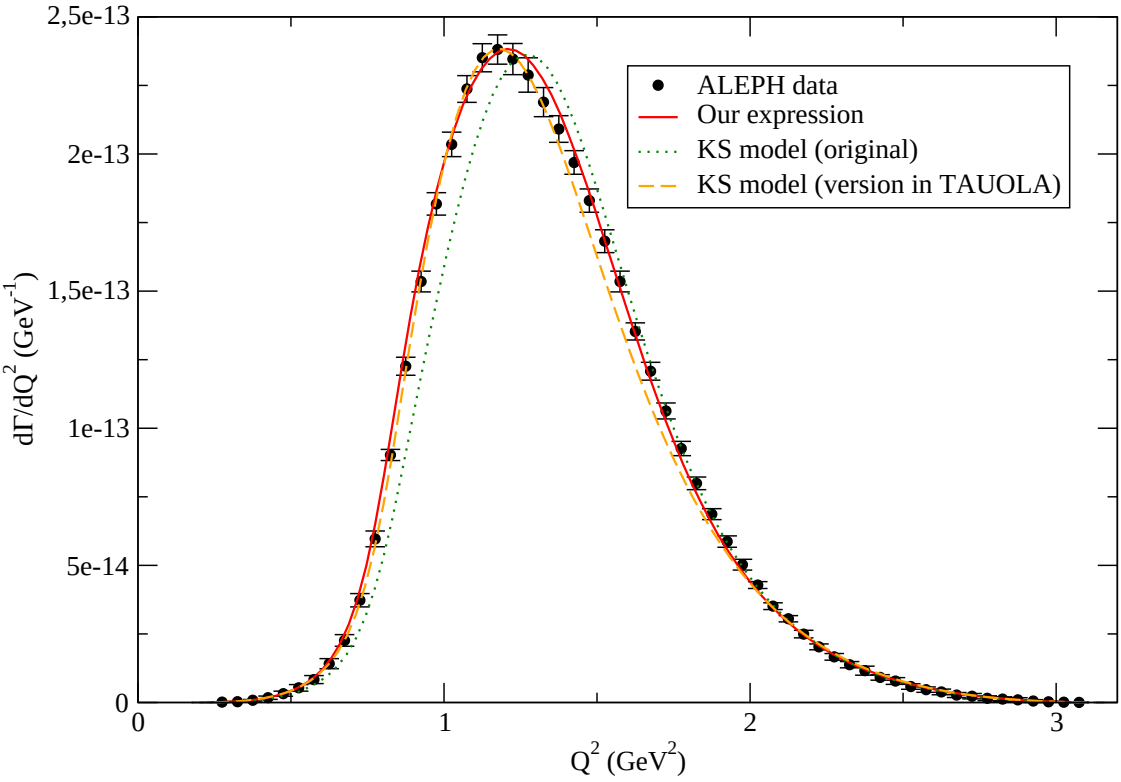

Figure 6.6: Comparison between the theoretical $M^2_{3\pi}$-spectra of the $\tau^- \to \pi^+\pi^-\pi^-\nu_\tau$ with *ALEPH* data [78]. Our results correspond to Set 1, Eq. (6.34), and they are also compared to the *KS* outcome, as they were given originally [329] as indicated in Eq. (6.6). We observe that the wrong *KS* description at *NLO* in the chiral expansion is naturally carried on as they are in *TAUOLA* right now. In the original parameterization one sees that the wrong description of the $\mathcal{O}(p^4)$ χPT terms is carried naturally to the rest of the spectrum. This is corrected in the updated parameterization in TAUOLA at the price of including a noticeably large on-shell a_1 width (0.6 GeV) and an unnaturally large normalization factor of 1.38.

form factors are symmetric under the exchange $\{1 \leftrightarrow 2,\ s \leftrightarrow t\}$ due to the identity of two pions one plot would be redundant. Since, moreover, we are working in the isospin conserved limit in which all pions are equivalent, one of the checks ($s_{ij} = s$ or $s_{ij} = t$) will suffice. We have verified that the s- and t- plots are identical. The plot in Figure 6.8 is noticeably different because the two pions of equal electric charge cannot couple to a spin-one resonance. We cannot forget that isospin symmetry breaking is not only induced by the difference of u and d quark masses compared to the value of the s quark mass, but also by the different electric charges of the $u-$ and $d-$type quarks. When this results in a selection rule, the effects are sizeable as we have observed.

We end this Section by noting that the dynamics encoded in the *KS* parame-

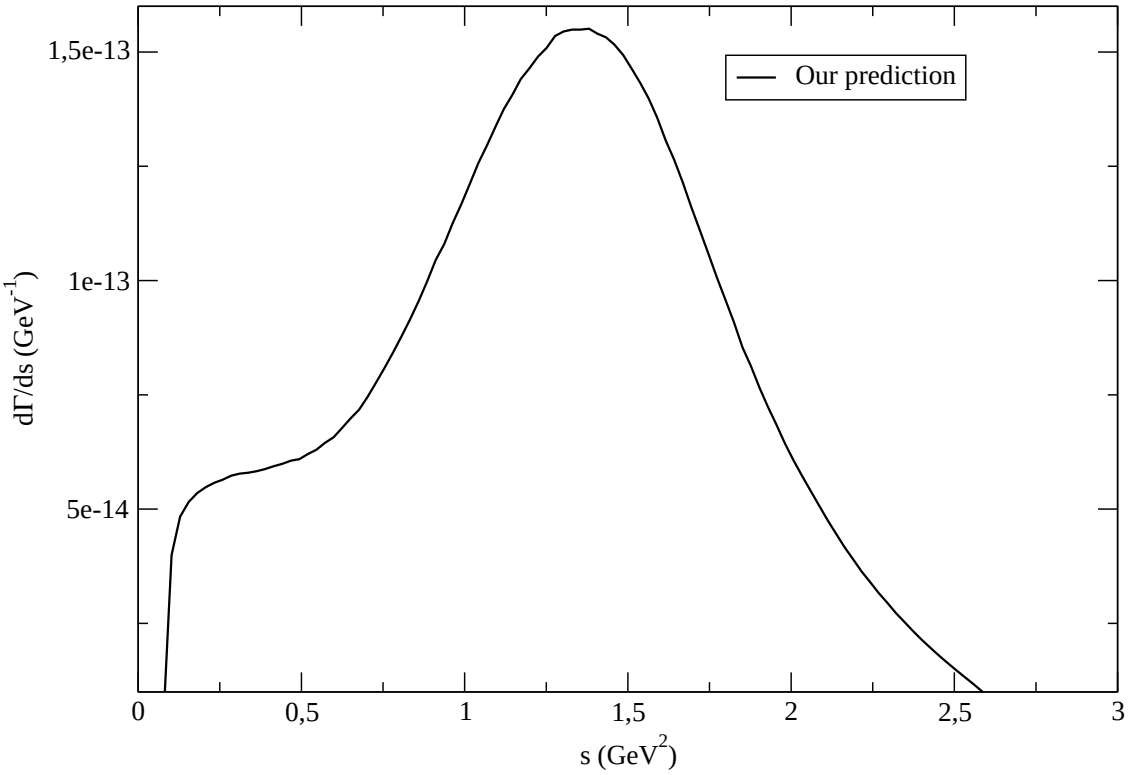

Figure 6.7: Our prediction for the s-spectra of the $\tau^- \to \pi^+\pi^-\pi^-\nu_\tau$ with the parameters of Set 1, Eq. (6.34).

terization and in our study is different. With this purpose we plot in Figure 6.9 the distributions for the s-spectra of the $\tau^- \to \pi^+\pi^-\pi^-\nu_\tau$ as given by the KS model in its original version and the one in $TAUOLA$ (the latter coveniently rescaled by 1.38). Similar differences can be observed in the t- and u-spectra.

6.4.4 Description of structure functions

Structure functions provide a full description of the hadron tensor $T_\mu T_\nu^*$ in the hadron rest frame. There are 16 real valued structure functions in $\tau^- \to (P_1P_2P_3)^-\,\nu_\tau$ decays (P_i is short for a pseudoscalar meson), most of which can be determined by studying angular correlations of the hadron system. Four of them carry information on the $J^P = 1^+$ transitions only : w_A, w_C, w_D and w_E (we refer to Ref. [346] and Eq. A.6 and to Appendix A for their precise definitions and discussion). Indeed, for the $\tau^- \to (\pi\pi\pi)^-\nu_\tau$ processes, other structure functions either vanish identically, or involve the pseudoscalar form factor F_3^A, which appears to be strongly suppressed above the very low–energy region due to its proportionality to the squared pion

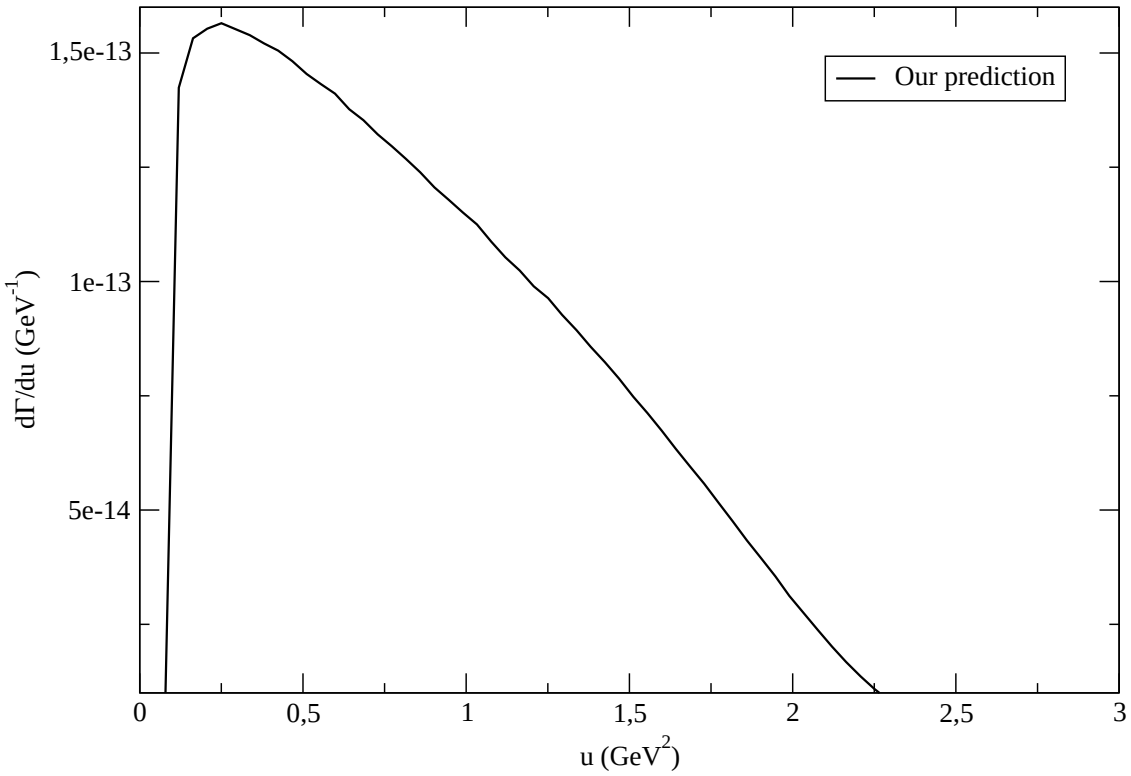

Figure 6.8: Our prediction for the u-spectra of the $\tau^- \to \pi^+\pi^-\pi^-\nu_\tau$ with the parameters of Set 1, Eq. (6.34).

mass.

Unfortunately the $ALEPH$ collaboration data [78] only allows to obtain w_A. However, both $CLEO-II$ [403] and $OPAL$ [494] studied all relevant structure functions. As a result, they have measured the four structure functions quoted above for the $\tau^- \to \pi^-\pi^0\pi^0\nu_\tau$ process, while concluding that other functions are consistent with zero within errors. Hence we can proceed to compare those experimental results with the description that provides our theoretical approach. In our expressions for the structure functions we input the values of the parameters of Set 1. This way we get the theoretical curves shown in Figs. 6.10, 6.11, 6.12 and 6.13. The latter are compared with the experimental data quoted by $CLEO$ and $OPAL$ [403, 494]. For w_C, w_D and w_E, it can be seen that we get a good agreement in the low Q^2 region, while for increasing energy the experimental errors become too large to state any conclusion (moreover, there seems to be a slight disagreement between both experiments at some points). It will be a task for the forthcoming experimental results from the B-factories to settle this issue.

On the other hand, in the case of the integrated structure function w_A, the quoted experimental errors are smaller, and the theoretical curve fits perfectly well

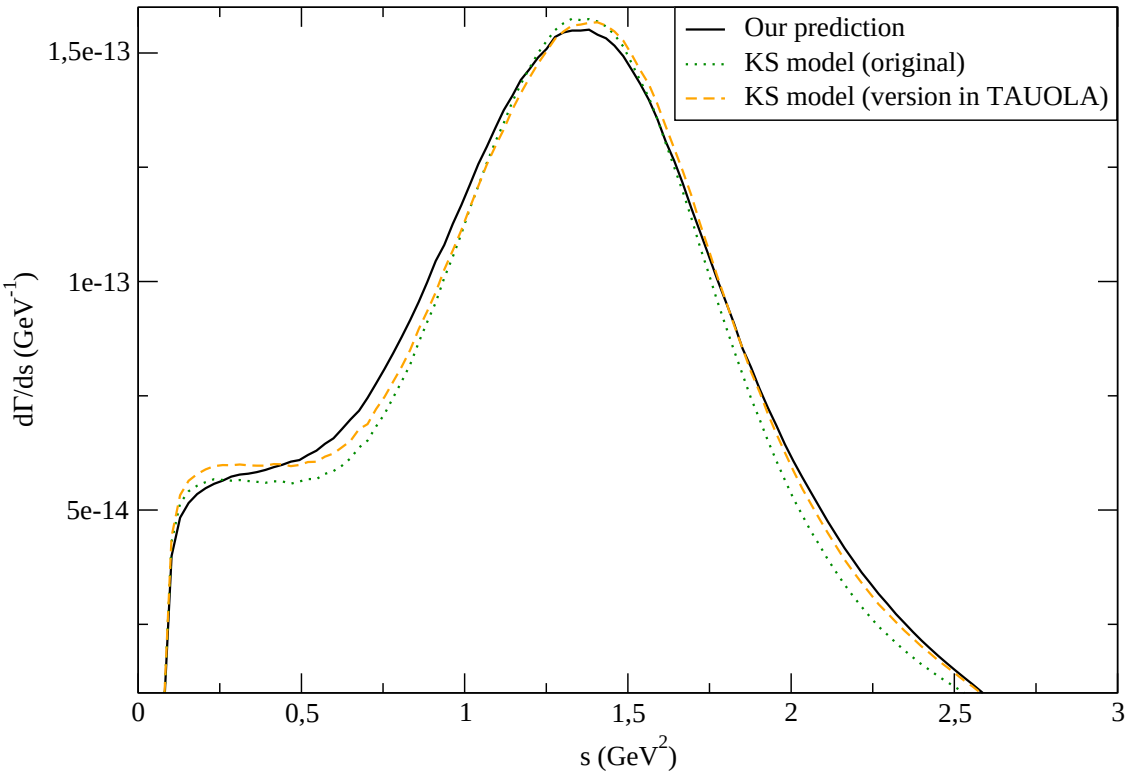

Figure 6.9: Comparison of our prediction and that of the KS model for the s-spectra of the $\tau^- \to \pi^+\pi^-\pi^-\nu_\tau$. Our parameters are fixed as indicated in Set 1, Eq. (6.34).

the $ALEPH$ data -that is clearly the one with smaller error bars- and seems to lie somewhat below the $CLEO$ and $OPAL$ data for $Q^2 \lesssim 1.5$ GeV^2. However, it happens that w_A contains essentially the same information about the hadron amplitude as the spectral function $d\Gamma/dQ^2$, so it should not surprise us the excellent agreement with $ALEPH$ data, considering the curve obtained with Set 1 in Fig 6.4. This relation becomes clear by looking at Eq. (5.59) if the scalar structure function W_{SA} is put to zero (remember that it should be suppressed by a factor $\mathcal{O}(m_\pi^2/Q^2)$). Taking into account that w_A is given by Eq. (5.60)

$$w_A(Q^2) = \int ds\, dt\, W_A(Q^2, s, t) \quad , \tag{6.36}$$

where W_A is the structure function previously introduced in Eq. (5.59), one simply has

$$\frac{d\Gamma}{dQ^2} = \frac{G_F^2\,|V_{ud}|^2}{384\,(2\pi)^5\,M_\tau} \left(\frac{M_\tau^2}{Q^2} - 1\right)^2 \left(1 + 2\,\frac{Q^2}{M_\tau^2}\right) \; w_A(Q^2) \quad . \tag{6.37}$$

In this way one can compare the measurements of w_A quoted by $CLEO-II$ and $OPAL$ with the data obtained by $ALEPH$ for the spectral function, conveniently translated into w_A. This is represented in Figure 6.10, where it can be seen

that some of the data from the different experiments do not agree with each other within errors. Notice that, due to phase space suppression, the factor of proportionality between $w_A(Q^2)$ and $\mathrm{d}\Gamma/\mathrm{d}Q^2$ in Eq. (6.37) goes to zero for $Q^2 \to M_\tau^2$, therefore the error bars in the $ALEPH$ points become enhanced toward the end of the spectrum. Notwithstanding, up to $Q^2 \lesssim 2.5$ GeV^2, it is seen that $ALEPH$ errors are still smaller than those corresponding to the values quoted by $CLEO-II$ and $OPAL$. On this basis, we have chosen to take the data obtained by $ALEPH$ to select the parameters as indicated in Set 1 to better describe the hadron amplitude. Finally, notice that a non vanishing contribution of W_{SA} (which is a positive quantity) cannot help to solve the experimental discrepancies, as it would go in the wrong direction. Anyway we have estimated that it is orders of magnitude smaller than the axial-vector contribution.

In the analysis of data carried out by the $CLEO$ Collaboration [401] onto their $\tau^- \to \pi^-\pi^0\pi^0\nu_\tau$ results it was concluded that the data was showing large contributions from intermediate states involving the isoscalar mesons $f_0(600)$, $f_0(1370)$ and $f_2(1270)$. Their analysis was done in a modelization of the axial–vector form factors that included Breit–Wigner functions in a Kühn and Santamaría inspired model. Our results in the Effective Theory framework show that, within the present experimental errors, there is no evidence of relevant contributions in $\tau^- \to (\pi\pi\pi)^-\nu_\tau$ decays beyond those of the $\rho(770)$, $\rho(1450)$ and $\mathrm{a}_1(1260)$ resonances.

6.5 Conclusions

The data available in $\tau \to \pi\pi\pi\nu_\tau$ decays provide an excellent benchmark to study the hadronization of the axial-vector current and, consequently, the properties of the $\mathrm{a}_1(1260)$ resonance. In this chapter we give a description of those decays within the framework of resonance chiral theory and the large-N_C limit of QCD that: 1) Satisfies all constraints of the asymptotic behaviour, ruled by QCD, of the relevant two and three point Green functions; 2) Provides an excellent description of the branching ratio and spectrum of the $\tau \to \pi\pi\pi\nu_\tau$ decays.

Though this work was started in Ref. [309], later achievements showed that a deeper comprehension of the dynamics was needed in order to enforce the available QCD constraints. To achieve a complete description we have defined a new off-shell width for the $\mathrm{a}_1(1260)$ resonance in Eq. (6.30), which is one of the main results of this work. Moreover we have seen that the inclusion of the $\rho(1450)$ improves significantly the description of the observables. In passing we have also obtained the mass value $M_{\mathrm{a}_1} = 1.120\,\mathrm{GeV}$ and the on-shell width $\Gamma_{\mathrm{a}_1}(M_{\mathrm{a}_1}^2) = 0.483\,\mathrm{GeV}$.

With the description of the off-shell width obtained in this work we can now consider that the hadronization of the axial-vector current within our scheme is complete and it can be applied in other hadron channels of tau decays.

The a_1 resonance, its off-shell width and its coupling to ρ-π, play an important role [495, 496, 497, 498, 499, 500, 501] in the evaluation of the dilepton and photon

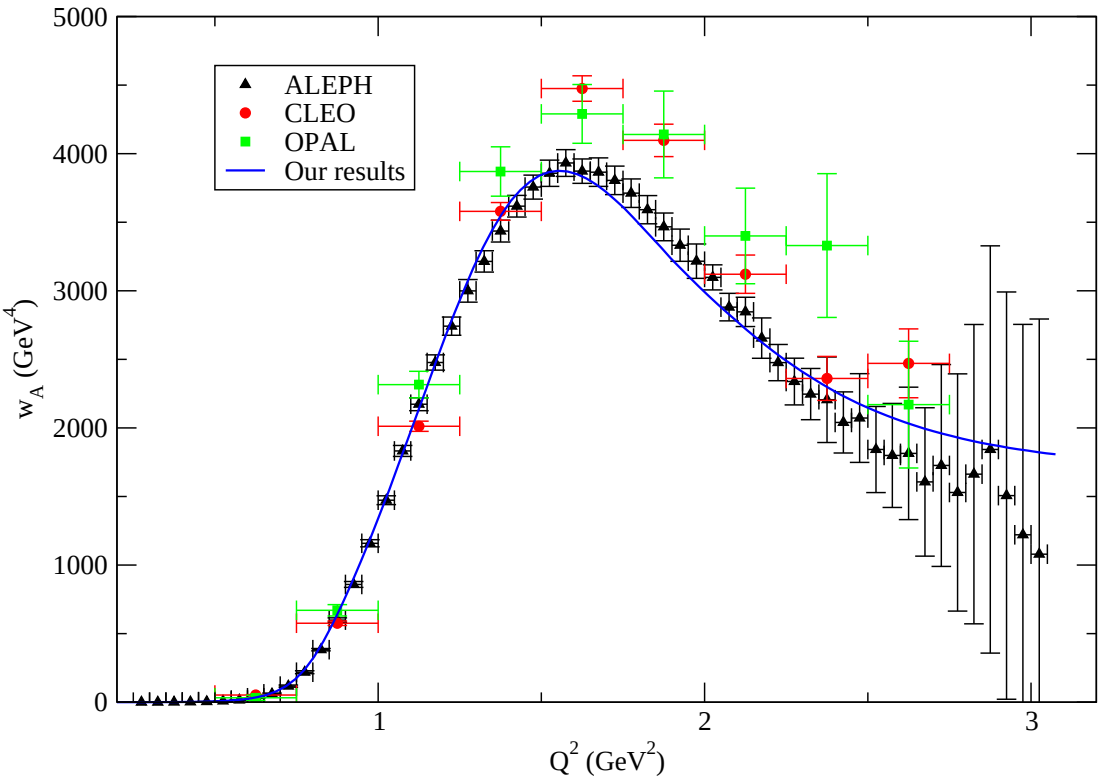

Figure 6.10: Comparison between the experimental data for w_A, from $\tau^- \to \pi^-\pi^0\pi^0\nu_\tau$, quoted by $CLEO-II$ and $OPAL$ [403, 494] and the values arising from $ALEPH$ measurements of $\tau^- \to \pi^-\pi^-\pi^+\nu_\tau$ spectral functions [78]. The solid line is obtained using the values of Set 1, Eq. (6.34).

production rates from a hadronic fireball assumed to be created in the relativistic heavy ion collisions. This would be important to be able to tell the electromagnetic radiation of the quark-gluon plasma from the hadronic sources, so that it could be regarded as an additional possible future application of our findings.

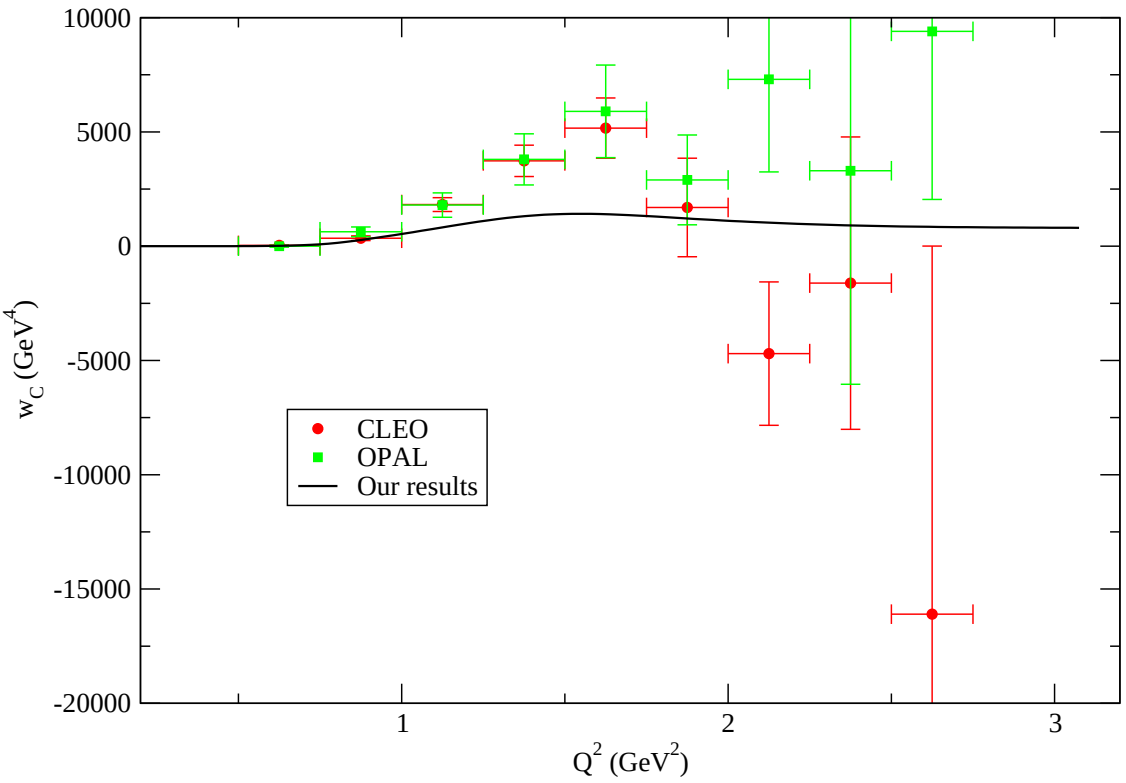

Figure 6.11: Comparison between the experimental data for w_C, from $\tau^- \to \pi^-\pi^0\pi^0\nu_\tau$, quoted by $CLEO-II$ and $OPAL$ [403, 494] and our results as obtained by using the values of Set 1, Eq. (6.34).

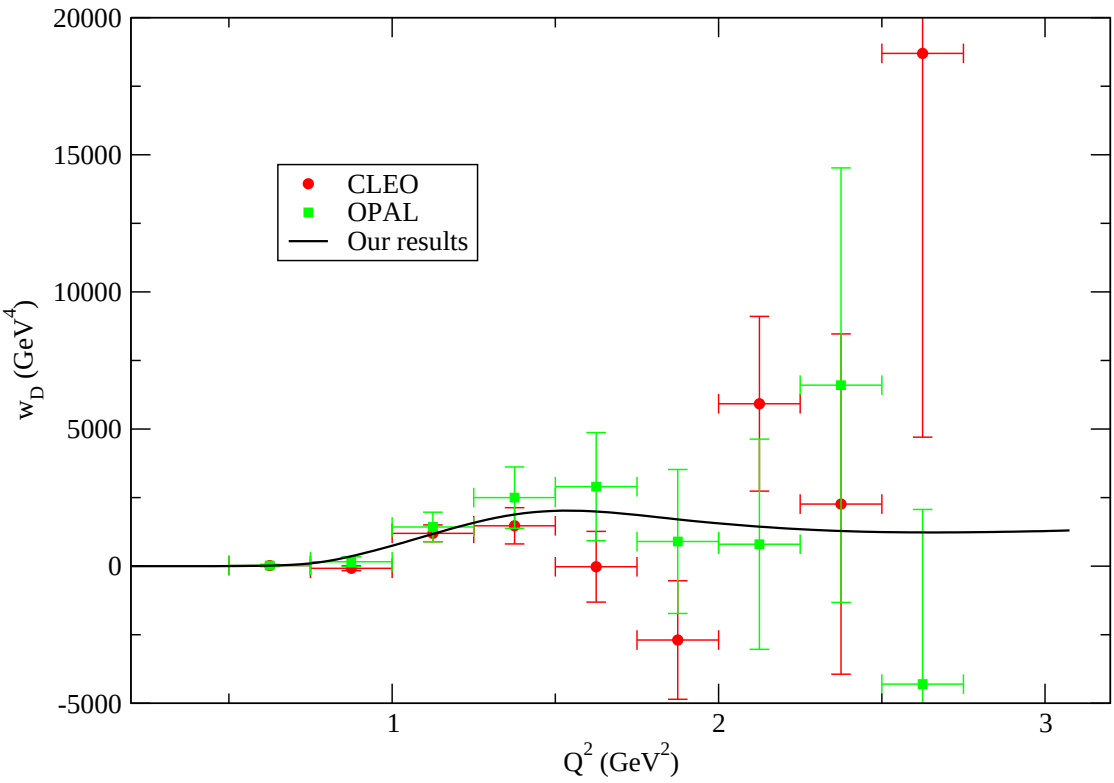

Figure 6.12: Comparison between the experimental data for w_D, from $\tau^- \to \pi^-\pi^0\pi^0\nu_\tau$, quoted by $CLEO-II$ and $OPAL$ [403, 494] and our results as obtained by using the values of Set 1, Eq. (6.34).

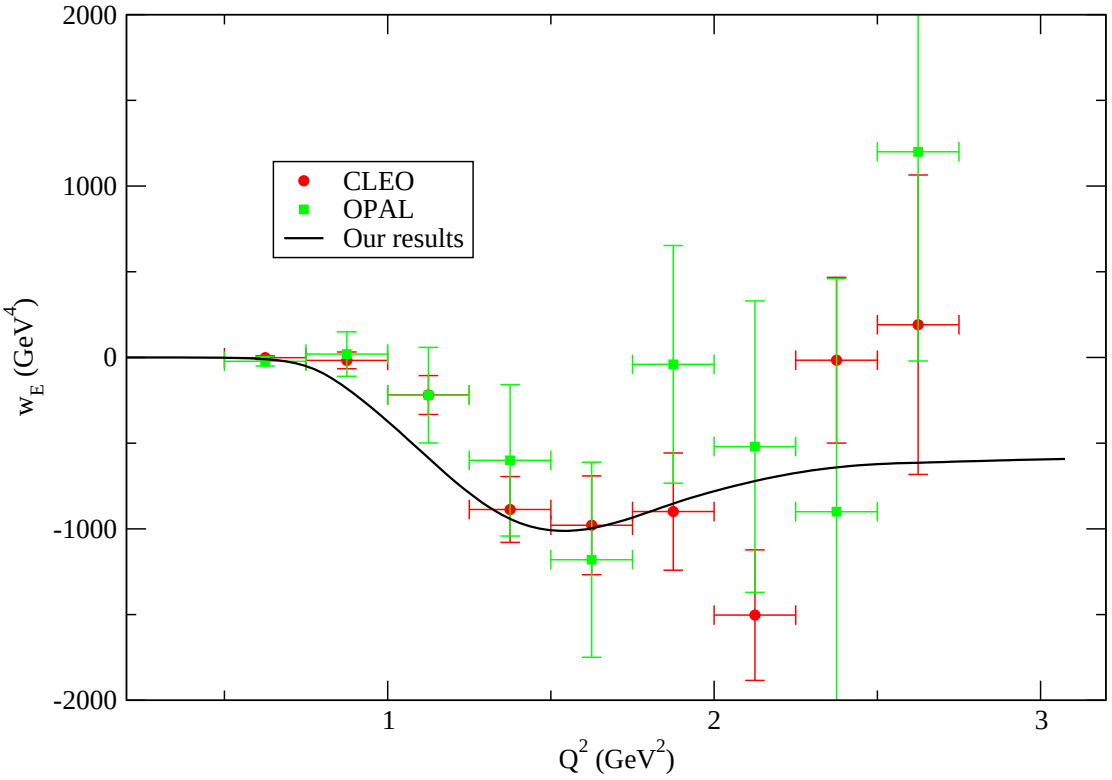

Figure 6.13: Comparison between the experimental data for w_E, from $\tau^- \to \pi^-\pi^0\pi^0\nu_\tau$, quoted by $CLEO-II$ and $OPAL$ [403, 494] and our results as obtained by using the values of Set 1, Eq. (6.34).

Chapter 7

$\tau^- \to (KK\pi)^-\nu_\tau$ decays

7.1 Introduction

In this chapter we will discuss the hadron form factors and related observables appearing in $\tau^- \to (KK\pi)^-\nu_\tau$ decays. Once the main features of the hadronization of the axial-vector current in these kind of decays have been fixed in the previous chapter, we can deal with these channels where both vector and axial-vector current contribute at, in principle, comparable rates. In fact, one of the purposes of our work is to analyze what is the relative relevance of each of them.

We thus analyse the hadronization structure of both vector and axial-vector currents leading to $\tau \to KK\pi\,\nu_\tau$ decays. At leading order in the $1/N_C$ expansion, and considering only the contribution of the lightest resonances, we work out, within the framework of the resonance chiral Lagrangian, the structure of the local vertices involved in those processes, that is richer that the one presented in previous chapters. The couplings in the resonance theory are constrained by imposing the asymptotic behaviour of vector and axial-vector spectral functions ruled by QCD. Noteworthy, the short-distance relations coming from QCD constraints are compatible in all with those found in Chapter 6 and to the ones we will find in Chapters 8 and 9 as well, a feature that highlights the consistency of the whole description. In this way we predict the hadron spectra and conclude that, contrarily to previous assertions, the vector contribution dominates by far over the axial-vector one in all $KK\pi$ charge channels.

Our study has a twofold significance. First, the study of branching fractions and spectra of those decays is a major goal of the asymmetric B factories ($BaBar$, $BELLE$). These are supplying an enormous amount of quality data owing to their large statistics, and the same is planned for the near future at tau-charm factories such as $BES-III$. Second, the required hadronization procedures involve QCD in a non-perturbative energy region ($E \lesssim M_\tau \sim 1.8$ GeV) and, consequently, these processes are a clean benchmark, not spoiled by an initial hadron state, where we can learn about the treatment of strong interactions when driven by resonances.

We recall that the analysis of these decays have to rely on a modelization of hadronization, as discussed in Chapter 5. A very popular approach is due to the

so-called Kühn-Santamaría model (KS) [327, 329] that, essentially, relies on the construction of form factors in terms of Breit-Wigner functions weighted by unknown parameters that are extracted from phenomenological analyses of data. This procedure, that has proven to be successful in the description of the $\pi\pi\pi$ final state, has been employed in the study of many two- and three-hadron tau decays [366, 378, 426, 427, 428, 440]. The ambiguity related with the choice of Breit-Wigner functions [327, 329, 330] is currently being exploited to estimate the errors in the determination of the free parameters. The measurement of the $KK\pi$ spectrum by the $CLEO$ Collaboration [404] has shown that the parameterization described by the KS model does not recall appropriately the experimental features keeping, at the same time, a consistency with the underlying strong interaction theory [324]. The solution provided by $CLEO$ based in the introduction of new parameters spoils the normalization of the Wess-Zumino anomaly, i.e. a specific prediction of QCD. Indeed, arbitrary parameterizations are of little help in the procedure of obtaining information about non-perturbative QCD. They may fit the data but do not provide us hints on the hadronization procedures. The key point in order to uncover the inner structure of hadronization is to guide the construction of the relevant form factors with the use of known properties of QCD.

The $TAUOLA$ library has been growing over the years [433, 434, 435, 436, 438, 448, 502, 503, 504] to be a complete library providing final state with full topology including neutrinos, resonances and lighter mesons and complete spin structure throughout the decay. In these works, the hadronization part of the matrix elements followed initially only assorted versions of the KS model. At present, the $TAUOLA$ library has become a key tool that handles analyses of tau decay data and it has been opened to the introduction of matrix elements obtained with other models. Hence it has become an excellent tool where theoretical models confront experimental data. This or analogous libraries [505, 506] are appropriate benchmarks where to apply the results of our research [429, 430, 431, 432].

We will be assisted in the presented task by the recent analysis of $e^+e^- \to KK\pi$ cross-section by $BABAR$ [507] where a separation between isoscalar and isovector channels has been performed. Hence we will be able to connect both processes through CVC. The general framework for these kind of analyses is discussed in Appendix C.3 and only the concrete application to this channel is included in this chapter. We have also used the process $\omega \to \pi^+\pi^-\pi^0$ to extract a given combination of Lagrangian couplings that will enter into the analysis. This computation constitutes Appendix C.3. Although this chapter is based on Ref. [304], the discussion of our predictions on the shape of the $\mathrm{d}\Gamma/\mathrm{d}s_{ij}$ and its comparison to the estimates of other models at the end of Sect. 7.4 are included in this Thesis for the first time.

7.2 Vector and axial-vector current form factors

7.2.1 Form factors in $\tau^- \to \left(K\overline{K}\right)\pi^-\nu_\tau$ decays

Our effective Lagrangian will include the pieces given in Eqs. (3.66), (3.86) -χPT contributions-, (4.19) [1], (4.33), (4.42) -operators with one resonance- (4.34) and (4.31) -operators with two resonances-.

We write the decay amplitude for the considered processes as

$$\mathcal{M} \,=\, -\,\frac{G_F}{\sqrt{2}}\,V_{ud}\,\overline{u}_{\nu_\tau}\,\gamma^\mu\,(1\,-\,\gamma_5)\;u_\tau\,T_\mu\;, \tag{7.1}$$

where the model dependent part is the hadron vector

$$T_\mu \,=\, \langle K(p_1)\,K(p_2)\,\pi(p_3)\,|\;(V_\mu - A_\mu)\,e^{i\mathcal{L}_{QCD}}\,|\,0\rangle\;, \tag{7.2}$$

that can be written in terms of four form factors F_1, F_2, F_3 and F_4, see Eq. (5.51). There are three different charge channels for the $KK\pi$ decays of the τ^- lepton, namely $K^+(p_+)\,K^-(p_-)\,\pi^-(p_\pi)$, $K^0(p_0)\,\overline{K}^0(\overline{p}_0)\,\pi^-(p_\pi)$ and $K^-(p_-)\,K^0(p_0)\,\pi^0(p_\pi)$. The definitions of Eq. (5.51) correspond to the choice $p_3 = p_\pi$ in all cases, and : $(p_1, p_2) = (p_+, p_-)$ for the $K^+\,K^-$ case, $(p_1, p_2) = (\overline{p}_0, p_0)$ for $K^0\,\overline{K}^0$ and $(p_1, p_2) = (p_-, p_0)$ for $K^-\,K^0$. In general, form factors F_i are functions of the kinematical invariants : Q^2, $s = (p_1 + p_2)^2$ and $t = (p_1 + p_3)^2$.

The general structure of the form factors, within our model, arises from the diagrams displayed in Figure 7.1. This provides the following decomposition :

$$F_i \,=\, F_i^\chi \,+\, F_i^{\rm R} \,+\, F_i^{\rm RR}\;,\quad i = 1,\,2,\,2,\,4\,; \tag{7.3}$$

where F_i^χ is given by the χPT Lagrangian [topologies a) and b) in Figure 7.1], and the rest are the contributions of one[Figure 1c), d) and e)] or two resonances [Figure 1f)].

In the isospin limit, form factors for the $\tau^- \to K^+K^-\pi^-\nu_\tau$ and $\tau^- \to K^0\overline{K^0}\pi^-\nu_\tau$

[1] Again, the fact that the SM coulings are of the type $V - A$ makes the spin-one resonances to rule hadron tau decays. The contribution of scalar and pseudoscalar resonances to the relevant four-point Green function should be minor for $\tau \to KK\pi\nu_\tau$. Indeed the lightest scalar, namely $f_0(980)$, couples dominantly to two pions, and therefore its role in the $K\overline{K}\pi$ final state should be negligible. Heavier flavoured or unflavoured scalars and pseudoscalars are at least suppressed by their masses, being heavier than the axial-vector meson $\mathrm{a}_1(1260)$ (like $K_0^*(1430)$ that couples to $K\pi$). The lightest pseudoscalar coupling to $K\pi$ is the K_0^* of $\kappa(800)$. As we assume the $N_C \to \infty$ limit, the nonet of scalars corresponding to the $\kappa(800)$ is not considered. This multiplet is generated by rescattering of the ligthest pseudoscalars and then subleading in the $1/N_C$ expansion [487]. In addition the couplings of unflavoured states to $K\overline{K}$ (scalars) and $K\overline{K}\pi$ (pseudoscalars) seem to be very small [8]. Thus in our description we include $J = 1$ resonances only. Nevertheless, if the study of these processes requires a more accurate description, additional resonances could also be included in our scheme.

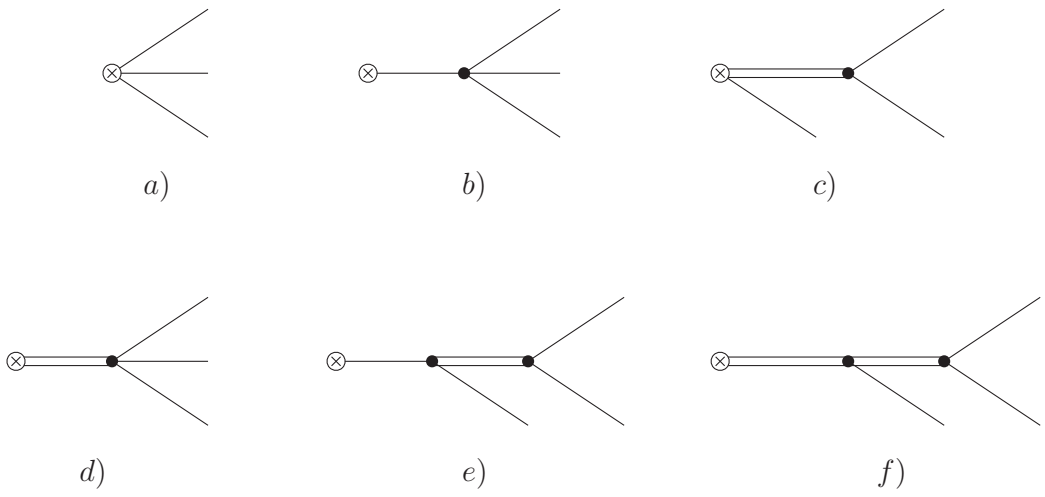

Figure 7.1: Topologies contributing to the final hadron state in $\tau \to KK\pi\,\nu_\tau$ decays in the $N_C \to \infty$ limit. A crossed circle indicates the QCD vector or axial-vector current insertion. A single line represents a pseudoscalar meson (K, π) while a double line stands for a resonance intermediate state. Topologies b) and e) only contribute to the axial-vector driven form factors, while diagram d) arises only (as explained in the text) from the vector current.

decays are identical. The explicit expressions for these are :

$$\begin{aligned}
F_1^{\chi} &= -\frac{\sqrt{2}}{3\,F}\,, \\
F_1^{\rm R}(s,t) &= -\frac{\sqrt{2}}{6}\,\frac{F_V\,G_V}{F^3}\,\left[\,\frac{A^{\rm R}(Q^2,s,u,m_K^2,m_\pi^2,m_K^2)}{M_\rho^2-s}\,+\,\frac{B^{\rm R}(s,u,m_K^2,m_\pi^2)}{M_{K^*}^2-t}\,\right], \\
F_1^{\mathcal{RR}}(s,t) &= \frac{2}{3}\,\frac{F_A G_V}{F^3}\,\frac{Q^2}{M_{\rm a_1}^2-Q^2}\,\left[\,\frac{A^{\mathcal{RR}}(Q^2,s,u,m_K^2,m_\pi^2,m_K^2)}{M_\rho^2-s}\right. \\
&\qquad\left. +\,\frac{B^{\rm RR}(Q^2,s,u,t,m_K^2,m_\pi^2,m_K^2)}{M_{K^*}^2-t}\,\right]\,,
\end{aligned} \tag{7.4}$$

where the functions $A^{\rm R}$, $B^{\rm R}$, $A^{\rm RR}$ and $B^{\rm RR}$ are

$$\begin{aligned}
A^{\rm R}(Q^2,x,y,m_1^2,m_2^2,m_3^2) &= 3\,x\,+m_1^2-m_3^2+\left(1-\frac{2G_V}{F_V}\right)\left[2\,Q^2-2\,x-y+m_3^2-m_2^2\right]\,, \\
B^{\rm R}(x,y,m_1^2,m_2^2) &= 2\,\left(m_2^2-m_1^2\right)\,+\left(1-\frac{2G_V}{F_V}\right)\left[y-x+m_1^2-m_2^2\right]\,,
\end{aligned} \tag{7.5}$$

$$
\begin{aligned}
A^{\rm RR}(Q^2,x,y,m_1^2,m_2^2,m_3^2) &= (\lambda'+\lambda'')\,(-3\,x+m_3^2-m_1^2) \\
&\quad + \left(2\,Q^2+x-y+m_1^2-m_2^2\right) F\left(\frac{x}{Q^2}\,,\,\frac{m_2^2}{Q^2}\right)\,, \\
B^{\rm RR}(Q^2,x,y,z,m_1^2,m_2^2,m_3^2) &= 2\,(\lambda'+\lambda'')\left(m_1^2-m_2^2\right) \\
&\quad + \left(y-x+m_2^2-m_1^2\right) F\left(\frac{z}{Q^2}\,,\,\frac{m_3^2}{Q^2}\right)\,.
\end{aligned}
$$

The dependence of the form factors with t follows from the relation $u = Q^2 - s - t + 2m_K^2 + m_\pi^2$. Moreover resonance masses correspond to the lowest states, $M_\rho = M_{\rho(770)}$, $M_{K^*} = M_{K^*(892)}$ and $M_{\rm a_1} = M_{\rm a_1(1260)}$. Resonance masses and widths within our approach are discussed in Appendix C.

Analogously the F_2 form factor is given by :

$$
\begin{aligned}
F_2^\chi &= F_1^\chi\,, \qquad (7.6)\\
F_2^{\rm R}(s,t) &= -\frac{\sqrt{2}}{6}\,\frac{F_V\,G_V}{F^3}\,\left[\frac{B^{\rm R}(t,u,m_K^2,m_K^2)}{M_\rho^2-s}+\frac{A^{\rm R}(Q^2,t,u,m_K^2,m_K^2,m_\pi^2)}{M_{K^*}^2-t}\right], \\
F_2^{\rm RR}(s,t) &= \frac{2}{3}\,\frac{F_A G_V}{F^3}\,\frac{Q^2}{M_{\rm a_1}^2-Q^2}\,\left[\frac{B^{\rm RR}(Q^2,t,u,s,m_K^2,m_K^2,m_\pi^2)}{M_\rho^2-s}\right. \\
&\quad \left. + \frac{A^{\rm RR}(Q^2,t,u,m_K^2,m_K^2,m_\pi^2)}{M_{K^*}^2-t}\right]\,.
\end{aligned}
$$

The F_3 form factor arises from the chiral anomaly and the non-anomalous odd-intrinsic-parity amplitude. We obtain :

$$
\begin{aligned}
F_3^\chi &= -\frac{N_C\,\sqrt{2}}{12\,\pi^2\,F^3}\,, \\
F_3^{\rm R}(s,t) &= -\frac{4\,G_V}{M_V\,F^3}\,\left[C^{\rm R}(Q^2,s,m_K^2,m_K^2,m_\pi^2)\,\left(\sin^2\theta_V\,\frac{1+\sqrt{2}\cot\theta_V}{M_\omega^2-s}\right.\right. \\
&\quad \left. + \cos^2\theta_V\,\frac{1-\sqrt{2}\tan\theta_V}{M_\phi^2-s}\right) + \frac{C^{\rm R}(Q^2,t,m_K^2,m_\pi^2,m_K^2)}{M_{K^*}^2-t} \\
&\quad \left. - \frac{2\,F_V}{G_V}\,\frac{D^{\rm R}(Q^2,s,t)}{M_\rho^2-Q^2}\right]\,, \qquad (7.7)\\
F_3^{\rm RR}(s,t) &= 4\sqrt{2}\frac{F_V\,G_V}{F^3}\,\frac{1}{M_\rho^2-Q^2}\,\left[C^{\rm RR}(Q^2,s,m_\pi^2)\,\left(\sin^2\theta_V\,\frac{1+\sqrt{2}\cot\theta_V}{M_\omega^2-s}\right.\right. \\
&\quad \left. \left. + \cos^2\theta_V\,\frac{1-\sqrt{2}\tan\theta_V}{M_\phi^2-s}\right) + \frac{C^{\rm RR}(Q^2,t,m_K^2)}{M_{K^*}^2-t}\right]\,,
\end{aligned}
$$

where $C^{\rm R}$, $D^{\rm R}$ and $C^{\rm RR}$ are defined as

$$\begin{aligned}
C^{\rm R}(Q^2,x,m_1^2,m_2^2,m_3^2) &= (c_1-c_2+c_5)\,Q^2-(c_1-c_2-c_5+2c_6)\,x \\
&\quad +(c_1+c_2+8c_3-c_5)\,m_3^2+8\,c_4\,(m_1^2-m_2^2)\,, \\
C^{\rm RR}(Q^2,x,m^2) &= d_3\,(Q^2+x)+(d_1+8\,d_2-d_3)\,m^2\,, \qquad (7.8)\\
D^{\rm R}(Q^2,x,y) &= (g_1+2\,g_2-g_3)\,(x+y)-2\,g_2\,(Q^2+m_K^2) \\
&\quad -(g_1-g_3)\,(3\,m_K^2+m_\pi^2)+2\,g_4\,(m_K^2+m_\pi^2)+2\,g_5\,m_K^2\,,
\end{aligned}$$

and θ_V is the mixing angle between the octet and singlet vector states ω_8 and ω_0 that defines the mass eigenstates $\omega(782)$ and $\phi(1020)$:

$$\begin{pmatrix} \phi \\ \omega \end{pmatrix} = \begin{pmatrix} \cos\theta_V & -\sin\theta_V \\ \sin\theta_V & \cos\theta_V \end{pmatrix} \begin{pmatrix} \omega_8 \\ \omega_0 \end{pmatrix}. \qquad (7.9)$$

For numerical evaluations we will assume ideal mixing, i.e. $\theta_V = \tan^{-1}(1/\sqrt{2})$. In this case the contribution of the $\phi(1020)$ meson to F_3 vanishes.

Finally, though we have not dwelled on specific contributions to the F_4 form factor, we quote for completeness the result obtained from our Lagrangian. Its structure is driven by the pion pole :

$$\begin{aligned}
F_4 &= F_4^\chi + F_4^{\rm R}\,, \qquad (7.10)\\
F_4^\chi(s,t) &= \frac{1}{\sqrt{2}\,F}\frac{m_\pi^2}{m_\pi^2-Q^2}\left(1+\frac{m_K^2-u}{Q^2}\right), \\
F_4^{\rm R}(s,t) &= \frac{G_V^2}{\sqrt{2}\,F^3}\frac{m_\pi^2}{Q^2(m_\pi^2-Q^2)}\left[\frac{s(t-u)}{M_\rho^2-s}+\frac{t(s-u)-(m_K^2-m_\pi^2)(Q^2-m_K^2)}{M_{K^*}^2-t}\right].
\end{aligned}$$

7.2.2 Form factors in $\tau^- \to K^-\,K^0\,\pi^0\,\nu_\tau$ decays

The diagrams contributing to the $\tau^- \to K^-\,K^0\,\pi^0\,\nu_\tau$ decay amplitude are also those in Figure 7.1, hence once again we can write $F_i = F_i^\chi + F_i^{\rm R} + F_i^{\rm RR} + \ldots$. However, the structure of the form factors for this process does not show the

symmetry observed in $\tau \to K\overline{K}\pi\nu_\tau$. We find :

$$
\begin{aligned}
F_1^\chi &= -\frac{1}{F}\,, \\
F_1^{\rm R}(s,t) &= -\frac{1}{6}\frac{F_V G_V}{F^3}\left[\frac{B^{\rm R}(s,u,m_K^2,m_\pi^2)}{M_{K^*}^2-t} + 2\,\frac{A^{\rm R}(Q^2,s,u,m_K^2,m_\pi^2,m_K^2)}{M_\rho^2-s}\right. \\
&\qquad \left. + \frac{A^{\rm R}(Q^2,u,s,m_\pi^2,m_K^2,m_K^2)}{M_{K^*}^2-u}\right], \\
F_1^{\rm RR}(s,t) &= \frac{\sqrt{2}}{3}\frac{F_A G_V}{F^3}\frac{Q^2}{M_{\rm a_1}^2-Q^2}\left[\frac{B^{\rm RR}(Q^2,s,u,t,m_K^2,m_\pi^2,m_K^2)}{M_{K^*}^2-t}\right. \\
&\qquad + 2\,\frac{A^{\rm RR}(Q^2,s,u,m_K^2,m_\pi^2,m_K^2)}{M_\rho^2-s} \\
&\qquad \left. + \frac{A^{\rm RR}(Q^2,u,s,m_\pi^2,m_K^2,m_K^2)}{M_{K^*}^2-u}\right], \qquad (7.11)
\end{aligned}
$$

$$
\begin{aligned}
F_2^\chi &= 0\,, \\
F_2^{\rm R}(s,t) &= -\frac{1}{6}\frac{F_V G_V}{F^3}\left[\frac{A^{\rm R}(Q^2,t,u,m_K^2,m_K^2,m_\pi^2)}{M_{K^*}^2-t} + 2\,\frac{B^{\rm R}(t,u,m_K^2,m_K^2)}{M_\rho^2-s}\right. \\
&\qquad \left. - \frac{A^{\rm R}(Q^2,u,t,m_K^2,m_K^2,m_\pi^2)}{M_{K^*}^2-u}\right], \\
F_2^{\rm RR}(s,t) &= \frac{\sqrt{2}}{3}\frac{F_A G_V}{F^3}\frac{Q^2}{M_{\rm a_1}^2-Q^2}\left[\frac{A^{\rm RR}(Q^2,t,u,m_K^2,m_K^2,m_\pi^2)}{M_{K^*}^2-t}\right. \\
&\qquad + 2\,\frac{B^{\rm RR}(Q^2,t,u,s,m_K^2,m_K^2,m_\pi^2)}{M_\rho^2-s} \\
&\qquad \left. - \frac{A^{\rm RR}(Q^2,u,t,m_K^2,m_K^2,m_\pi^2)}{M_{K^*}^2-u}\right]. \qquad (7.12)
\end{aligned}
$$

The form factor driven by the vector current is given by :

$$
\begin{aligned}
F_3^\chi &= 0 \\
F_3^{\rm R}(s,t) &= \frac{2\sqrt{2}\,G_V}{M_V\,F^3}\left[\frac{C^{\rm R}(Q^2,t,m_K^2,m_\pi^2,m_K^2)}{M_{K^*}^2-t} - \frac{C^{\rm R}(Q^2,u,m_K^2,m_\pi^2,m_K^2)}{M_{K^*}^2-u}\right. \\
&\qquad \left. - \frac{2F_V}{G_V}\frac{E^{\rm R}(t,u)}{M_\rho^2-Q^2}\right], \\
F_3^{\rm RR}(s,t) &= -4\frac{F_V G_V}{F^3}\frac{1}{M_\rho^2-Q^2}\left[\frac{C^{\rm RR}(Q^2,t,m_K^2)}{M_{K^*}^2-t} - \frac{C^{\rm RR}(Q^2,u,m_K^2)}{M_{K^*}^2-u}\right], \qquad (7.13)
\end{aligned}
$$

with $E^{\rm R}$ is defined as

$$E^{\rm R}(x,y) \,=\, (g_1 + 2\,g_2 - g_3)\,(x-y)\,. \tag{7.14}$$

Finally for the pseudoscalar form factor we have :

$$\begin{aligned} F_4^\chi(s,t) &= \frac{1}{2\,F}\frac{m_\pi^2\,(t-u)}{Q^2(m_\pi^2-Q^2)}\,, \\ F_4^{\rm R}(s,t) &= \frac{1}{2}\frac{G_V^2}{F^3}\frac{m_\pi^2}{Q^2(m_\pi^2-Q^2)}\left[\frac{t(s-u)-(m_K^2-m_\pi^2)(Q^2-m_K^2)}{M_{K^*}^2-t}+\frac{2\,s(t-u)}{M_\rho^2-s}\right. \\ &\qquad \left. -\frac{u(s-t)-(m_K^2-m_\pi^2)(Q^2-m_K^2)}{M_{K^*}^2-u}\right]\,. \end{aligned} \tag{7.15}$$

7.2.3 Features of the form factors

Several remarks are needed in order to understand our previous results for the form factors related with the vector and axial-vector QCD currents analysed above :

1/ Our evaluation corresponds to the tree level diagrams in Figure 7.1 that arise from the $N_C \to \infty$ limit of QCD. Hence the masses of the resonances would be reduced to $M_V = M_\rho = M_\omega = M_{K^*} = M_\phi$ and $M_A = M_{\rm a_1}$ as they appear in the resonance Lagrangian (4.18), i.e. the masses of the nonet of vector and axial-vector resonances in the chiral and large -N_C limit. However it is easy to introduce NLO corrections in the $1/N_C$ and chiral expansions on the masses by including the *physical* ones : M_ρ, M_{K^*}, M_ω, M_ϕ and $M_{\rm a_1}$ for the $\rho(770)$, $K^*(892)$, $\omega(782)$, $\phi(1020)$ and $\rm a_1(1260)$ states, respectively, as we have done in the expressions of the form factors. In this setting resonances also have zero width, which represents a drawback if we intend to analyse the phenomenology of the processes : Due to the high mass of the tau lepton, resonances do indeed resonate producing divergences if their width is ignored. Hence we will include energy-dependent widths for the $\rho(770)$, $\rm a_1(1260)$ and $K^*(892)$ resonances, that are rather wide, and a constant width for the $\omega(782)$. This issue is discussed in the Appendix C.

In summary, to account for the inclusion of NLO corrections we perform the substitutions :

$$\frac{1}{M_R^2-q^2} \;\longrightarrow\; \frac{1}{M_{phys}^2-q^2-\,i\,M_{phys}\,\Gamma_{phys}(q^2)}\,, \tag{7.16}$$

where $R = V, A$, and the subindex *phys* on the right hand side stands for the corresponding *physical* state depending on the relevant Feynman diagram.

2/ If we compare our results with those of Ref. [378], evaluated within the KS model, we notice that the structure of our form factors is fairly different and much more intricate. This is due to the fact that the KS model, i.e. a model resulting from combinations of *ad hoc* products of Breit-Wigner functions, does not meet higher order chiral constraints enforced in our approach.

3/ As commented above the pseudoscalar form factors F_4 vanishes in the chiral limit. Indeed the results of Eqs. (7.10, 7.15) show that they are proportional to m_π^2, which is tiny compared with any other scale in the amplitudes. Hence the contribution of F_4 to the structure of the spectra is actually marginal.

7.3 QCD constraints and determination of resonance couplings

Our results for the form factors F_i depend on several combinations of the coupling constants in our Lagrangian $\mathcal{L}_{R\chi T}$, most of which are in principle unknown parameters. Now, if our theory offers an adequate effective description of QCD at hadron energies, the underlying theory of the strong interactions should give information on those constants. Unfortunately the determination of the effective parameters from first principles is still an open problem in hadron physics.

A fruitful procedure when working with resonance Lagrangians has been to assume that the resonance region, even when one does not include the full phenomenological spectrum, provides a bridge between the chiral and perturbative regimes [7]. The chiral constraints supply information on the structure of the interaction but do not provide any hint on the coupling constants of the Lagrangian. Indeed, as in any effective theory [142], the couplings encode information from high energy dynamics. Our procedure amounts to match the high energy behaviour of Green functions (or related form factors) evaluated within the resonance theory with the asymptotic results of perturbative QCD. This strategy has proven to be phenomenologically sound [7, 299, 310, 311, 314, 315, 323, 488], and it will be applied here in order to obtain information on the unknown couplings.

Two-point Green functions of vector and axial-vector currents $\Pi_{V,A}(q^2)$ were studied within perturbative QCD in Ref. [297], where it was shown that both spectral functions go to a constant value at infinite transfer of momenta :

$$\Im m\, \Pi_{V,A}(q^2) \underset{q^2\to\infty}{\longrightarrow} \frac{N_C}{12\,\pi}\,. \tag{7.17}$$

By local duality interpretation the imaginary part of the quark loop can be understood as the sum of infinite positive contributions of intermediate hadron states. Now, if the infinite sum is going to behave like a constant at $q^2 \to \infty$, it is heuristically sound to expect that each one of the infinite contributions vanishes in that limit. This deduction stems from the fact that vector and axial-vector form factors should behave smoothly at high q^2, a result previously put forward from parton dynamics in Ref. [279, 280, 281, 282]. Accordingly in the $N_C \to \infty$ limit this result applies to our form factors evaluated at tree level in our framework.

Other hints involving short-distance dynamics may also be considered. The analyses of three-point Green functions of QCD currents have become a useful procedure to determine coupling constants of the intermediate energy (resonance) framework [314, 315, 310, 299, 311]. The idea is to use those functions (order parameters of

the chiral symmetry breaking), evaluate them within the resonance framework and match this result with the leading term in the OPE of the Green function.

In the following we collect the information provided by these hints on our coupling constants, attaching always to the $N_C \to \infty$ case [274] (approximated with only one nonet of vector and axial-vector resonances) :

i) By demanding that the two-pion vector form factor vanishes at high q^2 one obtains the condition $F_V\, G_V = F^2$ [7].

ii) The first Weinberg sum rule [302] leads to $F_V^2 - F_A^2 = F^2$, and the second Weinberg sum rule gives $F_V^2\, M_V^2 = F_A^2\, M_A^2$[6].

iii) The analysis of the VAP Green function [299] gives for the combinations of couplings defined in Eq. (4.32) the following results :

$$\begin{aligned} \lambda' &= \frac{F^2}{2\sqrt{2}\, F_A\, G_V} = \frac{M_A}{2\sqrt{2}\, M_V}\,, \\ \lambda'' &= \frac{2\, G_V - F_V}{2\sqrt{2}\, F_A} = \frac{M_A^2 - 2M_V^2}{2\sqrt{2}\, M_V\, M_A}\,, \\ 4\,\lambda_0 &= \lambda' + \lambda''\,, \end{aligned} \tag{7.18}$$

where, in the two first relations, the second equalities come from using relations i) and ii) above. Here M_V and M_A are the masses appearing in the resonance Lagrangian. Contrarily to what happens in the vector case where M_V is well approximated by the $\rho(770)$ mass, in Ref. [323] it was obtained $M_A = 998(49)$ MeV, hence M_A differs appreciably from the presently accepted value of M_{a_1}. It is worth to notice that the two first relations in Eq. (7.18) can also be obtained from the requirement that the $J = 1$ axial spectral function in $\tau \to 3\pi\nu_\tau$ vanishes for large momentum transfer [309].

iv) Both vector form factors contributing to the final states $K\overline{K}\pi^-$ and $K^-K^0\pi^0$ in tau decays, when integrated over the available phase space, should also vanish at high Q^2. Let us consider $H^3_{\mu\nu}(s,t,Q^2) \equiv T^3_\mu T^{3\,*}_\nu$, where T^3_μ can be inferred from Eq. (5.51). Then we define $\Pi_V(Q^2)$ by :

$$\int \mathrm{d}\Pi_3\, H^3_{\mu\nu}(s,t,Q^2) = \left(Q^2 g_{\mu\nu} - Q_\mu Q_\nu\right)\, \Pi_V(Q^2)\,, \tag{7.19}$$

where [2]

$$\begin{aligned} \int \mathrm{d}\Pi_3 &= \int \frac{d^3p_1}{2E_1}\frac{d^3p_2}{2E_2}\frac{d^3p_3}{2E_3}\delta^4\left(Q - p_1 - p_2 - p_3\right)\delta\left(s - (Q-p_3)^2\right)\delta\left(t - (Q-p_2)^2\right) \\ &= \frac{\pi^2}{4\,Q^2}\int ds\, dt\,. \end{aligned} \tag{7.20}$$

[2] See Section 5.4.1.

Hence we find that

$$\Pi_V(Q^2) \,=\, \frac{\pi^2}{12\,Q^4}\int \mathrm{ds\,dt}\; g^{\mu\nu}\, H^3_{\mu\nu}(s,t,Q^2)\,, \tag{7.21}$$

where the limits of integration can be obtained from Eq. (5.63), should vanish at $Q^2 \to \infty$. This constraint determines several relations on the couplings that appear in the F_3 form factor, namely :

$$\begin{aligned}
c_1 \,-\, c_2 \,+\, c_5 &= 0\,, &(7.22)\\
c_1 \,-\, c_2 \,-\, c_5 \,+\, 2c_6 &= -\,\frac{N_C}{96\,\pi^2}\,\frac{F_V\,M_V}{\sqrt{2}\,F^2}\,, &(7.23)\\
d_3 &= -\frac{N_C}{192\,\pi^2}\,\frac{M_V^2}{F^2}\,, &(7.24)\\
g_1 \,+\, 2g_2 \,-\, g_3 &= 0\,, &(7.25)\\
g_2 &= \frac{N_C}{192\,\sqrt{2}\,\pi^2}\,\frac{M_V}{F_V}\,. &(7.26)
\end{aligned}$$

If these conditions are satisfied, $\Pi_V(Q^2)$ vanishes at high transfer of momenta for both $K\overline{K}\pi^-$ and $K^-K^0\pi^0$ final states. We notice that the result in Eq. (7.22) is in agreement with the corresponding relation in Ref. [310], while Eqs. (7.23) and (7.24) do not agree with the results in that work. In this regard we point out that the relations in Ref. [310], though they satisfy the leading matching to the OPE expansion of the $\langle VVP\rangle$ Green function with the inclusion of one multiplet of vector mesons, do not reproduce the right asymptotic behaviour of related form factors. Indeed it has been shown [315, 323] that two multiplets of vector resonances are needed to satisfy both constraints. Hence we will attach to our results above, which we consider more reliable [3].

v) An analogous exercise to the one in iv) can be carried out for the axial-vector form factors F_1 and F_2. We have performed such an analysis and, using the relations in i) and ii) above, it gives us back the results provided in Eq. (7.18) for λ' and λ''. Hence both procedures give a consistent set of relations.

After imposing the above constraints, let us analyse which coupling combinations appearing in our expressions for the form factors are still unknown. We intend to write all the information on the couplings in terms of F, M_V and M_A. From the

[3] One of the form factors derived from the $\langle VVP\rangle$ Green function is $\mathcal{F}_{\pi\gamma^*\gamma}(q^2)$, that does not vanish at high q^2 with the set of relations in Ref. [310]. With our conditions in Eqs. (7.23,7.24) the asymptotic constraint on the form factor can be satisfied if the large-N_C masses, M_A and M_V, fulfill the relation $2M_A^2 = 3M_V^2$, that is again recovered in Chapter 9. It is interesting to notice the significant agreement with the numerical values for these masses mentioned above.

relations involving F_V, F_A and G_V we obtain :

$$\begin{aligned}
\frac{F_V^2}{F^2} &= \frac{M_A^2}{M_A^2 - M_V^2}\,, \\
\frac{F_A^2}{F^2} &= \frac{M_V^2}{M_A^2 - M_V^2}\,, \\
\frac{G_V^2}{F^2} &= 1 - \frac{M_V^2}{M_A^2}\,.
\end{aligned} \tag{7.27}$$

Moreover we know that F_V and G_V have the same sign, and we will assume that it is also the sign of F_A. Together with the relations in Eq. (7.18) this determines completely the axial-vector form factors $F_{1,2}$. Now from Eqs. (7.22-7.26) one can fix all the dominant pieces in the vector form factor F_3, i.e. those pieces that involve factors of the kinematical variables s, t or Q^2. The unknown terms, that carry factors of m_π^2 or m_K^2, are expected to be less relevant. They are given by the combinations of couplings : $c_1 + c_2 + 8\,c_3 - c_5$, $d_1 + 8\,d_2$, c_4 , g_4 and g_5. However small they may be, we will not neglect these contributions, and we will proceed as follows. Results in Ref. [310] determine the first and the second coupling combinations. As commented above the constraints in that reference do not agree with those we have obtained by requiring that the vector form factor vanishes at high Q^2. However, they provide us an estimate to evaluate terms that, we recall, are suppressed by pseudoscalar masses. In this way, from a phenomenological analysis of $\omega \to \pi^+\pi^-\pi^0$ (see Appendix C.3) it is possible to determine the combination $2\,g_4 + g_5$. Finally in order to evaluate c_4 and g_4 we will combine the recent analysis of $\sigma\,(e^+e^- \to KK\pi)$ by *BaBar* [507] with the information from the $\tau \to KK\pi\nu_\tau$ width.

7.3.1 Determination of c_4 and g_4

The separation of isoscalar and isovector components of the $e^+e^- \to KK\pi$ amplitudes, carried out by *BaBar* [507], provides us with an additional tool for the estimation of the coupling constant c_4 that appears in the hadronization of the vector current [508, 509]. Indeed, using $SU(2)_I$ symmetry alone one can relate the isovector contribution to $\sigma\,(e^+e^- \to K^-K^0\pi^+)$ with the vector contribution to $\Gamma\,(\tau^- \to K^0K^-\pi^0\nu_\tau)$ through the relation :

$$\frac{\mathrm{d}}{\mathrm{d}\,Q^2}\,\Gamma\left(\tau^- \to K^0K^-\pi^0\nu_\tau\right)\Big|_{F_3} = f(Q^2)\;\sigma_{I=1}\left(e^+e^- \to K^-K^0\pi^+\right)\,, \tag{7.28}$$

where $f(Q^2)$ and further relations are given in Appendix E. Another relation similar to Eq. (7.28) that has been widely used in the literature and the assumptions on which it relies are also discussed in this Appendix. In order not to lose the thread of our discourse, here we will complete the explanation of our methodology to determine c_4 and g_4.

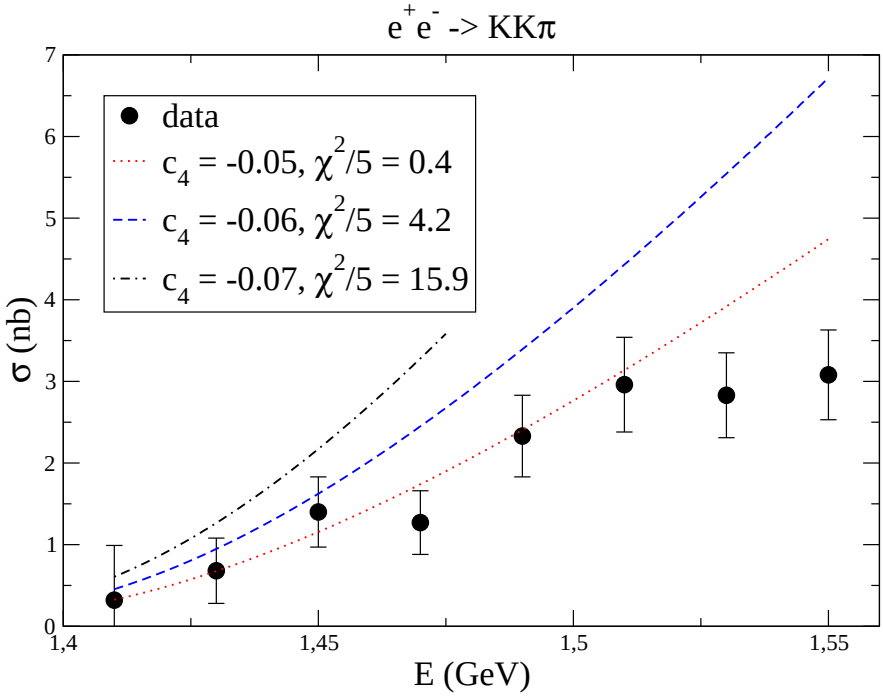

Figure 7.2: Comparison of the experimental data [507] with the theoretical prediction for the cross-section of the isovector component of $e^+e^- \to K^*(892)K \to K_S K^\pm \pi^\mp$ process, for different values of the c_4 coupling. The χ^2 values are associated to the first 6 data points only.

Hence we could use the isovector contribution to the cross-section for the process $e^+e^- \to K_S K^\pm \pi^\mp$ determined by *BaBar* and Eq. (7.28) to fit the c_4 coupling that is the only still undetermined constant in that process. However we have to take into account that our description for the hadronization of the vector current in the tau decay channel does not, necessarily, provide an adequate description of the cross-section. Indeed the complete different kinematics of both observables suppresses the high-energy behaviour of the bounded tau decay spectrum, while this suppression does not occur in the cross-section. Accordingly, our description of the latter away from the energy threshold can be much poorer. As can be seen in Figure 7.2 there is a clear structure in the experimental points of the cross-section that is not provided by our description.

Taking into account the input parameters quoted in Eq. (6.34) we obtain : $c_4 = -0.047 \pm 0.002$. The fit has been carried out for the first 6 bins (up to $E_{cm} \sim 1.52\,\text{GeV}$) using *MINUIT* [510]. This result corresponds to $\chi^2/dof = 0.3$ and the displayed error comes only from the fit.

We take into consideration now the measured branching ratios for the $KK\pi$ channels of Table 7.1 in order to extract information both from c_4 and g_4. We notice that it is not possible to reconcile a prediction of the branching ratios of $\tau \to K\overline{K}\pi\nu_\tau$ and $\tau \to K^- K^0 \pi^0 \nu_\tau$ in spite of the noticeable size of the errors shown in the Ta-

ble 7.1. Considering that the second process was measured long ago and that the $\tau^- \to K^+K^-\pi^-\nu_\tau$ decay has been focused by both $CLEO-III$ and $BaBar$ we intend to fit the branching ratio of the latter. For the parameter values :

$$\begin{aligned} c_4 &= -0.07 \pm 0.01\,, \\ g_4 &= -0.72 \pm 0.20\,, \end{aligned} \tag{7.29}$$

we find a good agreement with the measured widths $\Gamma(\tau^- \to K^+K^-\pi^-\nu_\tau)$ and $\Gamma(\tau \to K^-K^0\pi^0\nu_\tau)$ within errors (see Table 7.1). Notice that the value of $|c_4|$ is larger than that obtained from the fit to the $e^+e^- \to K_SK^\pm\pi^\mp$ data explained above. In Figure 7.2 we show the first 8 bins in the isovector component of $e^+e^- \to K_SK^\pm\pi^\mp$ and the theoretical curves for different values of the c_4 coupling. As our preferred result we choose the larger value of c_4 in Eq. (7.29), since it provides a better agreement with the present measurement of $\Gamma(\tau^- \to K^-K^0\pi^0\nu_\tau)$. Actually, one can expect an incertitude in the splitting of isospin amplitudes in the $e^+e^- \to K_SK^\pm\pi^\mp$ cross-section (as it is discussed in Appendix E). Taking into account this systematic error, it could be likely that the theoretical curve with $c_4 = -0.07$ falls within the error bars for the first data points.

Using $SU(2)_I$ symmetry, one can derive several relations between exclusive isovector hadron modes produced in e^+e^- collisions and those related with the vector current (F_3 form factor) in τ decays. One can read them in Appendix E, where other relations for the three meson decays of interest are also derived.

7.4 Phenomenology of $\tau \to KK\pi\nu_\tau$: Results and their analysis

Asymmetric B-factories span an ambitious τ programme that includes the determination of the hadron structure of semileptonic τ decays such as the $KK\pi$ channel. As commented in the Introduction the latest study of $\tau^- \to K^+K^-\pi^-\nu_\tau$ by the $CLEO-III$ Collaboration [404] showed a disagreement between the KS model, included in $TAUOLA$, and the data. Experiments with higher statistics such as $BABAR$ and $Belle$ should clarify the theoretical settings.

For the numerics in this section we use the following values

$$\begin{aligned} F &= 0.0924\,\text{GeV} \quad , \quad F_V = 0.180\,\text{GeV} \quad , \quad F_A = 0.149\,\text{GeV}\,, \\ M_V &= 0.775\,\text{GeV} \quad , \quad M_{K^*} = 0.8953\,\text{GeV} \quad , \quad M_{a_1} = 1.120\,\text{GeV}\,. \end{aligned} \tag{7.30}$$

Then we get λ', λ'' and λ_0 from the first equalities in Eq. (7.18).

At present no spectra for these channels is available and the determinations of the widths are collected in Table 7.1 [4].

We also notice that there is a discrepancy between the $BaBar$ measurement of

[4]The Belle Collaboration has compared recently [512] their spectra [345] with our parametrization [304]. Good agreement is seen at low-energies and a manifest deviation at $s \geq 2GeV^2$ is

Source	$\Gamma(\tau^- \to K^+K^-\pi^-\nu_\tau)$	$\Gamma(\tau^- \to K^0\overline{K}^0\pi^-\nu_\tau)$	$\Gamma(\tau^- \to K^-K^0\pi^0\nu_\tau)$
PDG [8]	3.103 (136)	3.465 (770)	3.262 (521)
BaBar [400]	3.049 (85)		
$CLEO-III$ [404]	3.511 (245)		
Belle [345]	3.465 (136)		
Our prediction	$3.4^{+0.5}_{-0.2}$	$3.4^{+0.5}_{-0.2}$	$2.5^{+0.3}_{-0.2}$

Table 7.1: Comparison of the measurements of partial widths (in units of 10^{-15} GeV) with our predictions for the set of values in Eq. (7.29). For earlier references see [8].

$\Gamma(\tau^- \to K^+K^-\pi^-\nu_\tau)$ and the results by *CLEO* and *Belle*. Within $SU(2)$ isospin symmetry it is found that $\Gamma(\tau^- \to K^+K^-\pi^-\nu_\tau) = \Gamma(\tau^- \to K^0\overline{K}^0\pi^-\nu_\tau)$, which is well reflected by the values in Table 7.1 within errors. Moreover, as commented above, the *PDG* data [8] indicate that $\Gamma(\tau^- \to K^-K^0\pi^0\nu_\tau)$ should be similar to $\Gamma(\tau^- \to K\overline{K}\pi\nu_\tau)$. It would be important to obtain a more accurate determination of the $\tau^- \to K^-K^0\pi^0\nu_\tau$ width (the measurements quoted by the *PDG* are rather old) in the near future.

In our analyses we include the lightest resonances in both the vector and axial-vector channels, namely $\rho(775)$, $K^*(892)$ and $a_1(1260)$. It is clear that, as it happens in the $\tau \to \pi\pi\pi\nu_\tau$ channel (see Chapter 6), a much lesser role, though noticeable, can be played by higher excitations on the vector channel. As experimentally only the branching ratios are available for the $KK\pi$ channel we think that the refinement of including higher mass resonances should be taken into account in a later stage, when the experimental situation improves.

In Figs. 7.3 and 7.4 we show our predictions for the normalized $M^2_{KK\pi}-$spectrum of the $\tau^- \to K^+K^-\pi^-\nu_\tau$ and $\tau^- \to K^-K^0\pi^0\nu_\tau$ decays, respectively. As discussed above we have taken $c_4 = -0.07 \pm 0.01$ and $g_4 = -0.72 \pm 0.20$ (notice that the second process does not depend on g_4). We conclude that the vector current contribution (Γ_V) dominates over the axial-vector one (Γ_A) in both channels :

$$\left.\frac{\Gamma_A}{\Gamma_V}\right|_{K\overline{K}\pi} = 0.16 \pm 0.05\,, \qquad \left.\frac{\Gamma_A}{\Gamma_V}\right|_{K^-K^0\pi} = 0.18 \pm 0.04\,,$$
$$\frac{\Gamma(\tau^- \to K^+K^-\pi^-\nu_\tau)}{\Gamma(\tau^- \to K^-K^0\pi^0\nu_\tau)} = 1.4 \pm 0.3\,, \tag{7.31}$$

observed. Their comparison shows our prediction for $c_4 = -0.04$ and $g_4 = -0.5$, that correspond to the values presented in Ref. [430]. This points to a lower value of c_4, as obtained in the fit to e^+e^- data (See Fig. 7.2) and also to a possible destructive interference of the higher-resonance states ρ' and K^*'. As soon as we can access definitive Belle data, we will investigate this issue in detail.

where the errors estimate the slight variation due to the range in c_4 and g_4. These ratios translate into a ratio of the vector current to all contributions of $f_v = 0.86 \pm 0.04$ for the $K\overline{K}\pi^-$ channel and $f_v = 0.85 \pm 0.03$ for $K^-K^0\pi^0$ one, to be compared with the result in Ref. [80], namely $f_v(K\overline{K}\pi) = 0.20 \pm 0.03$. Our results for the relative contributions of vector and axial-vector currents deviate strongly from most of the previous estimates, as one can see in Table 7.2. Only Ref. [440] pointed already to vector current dominance in these channels, although enforcing just the leading chiral constraints and using experimental data at higher energies.

We conclude that for all $\tau \to KK\pi\nu_\tau$ channels the vector component dominates

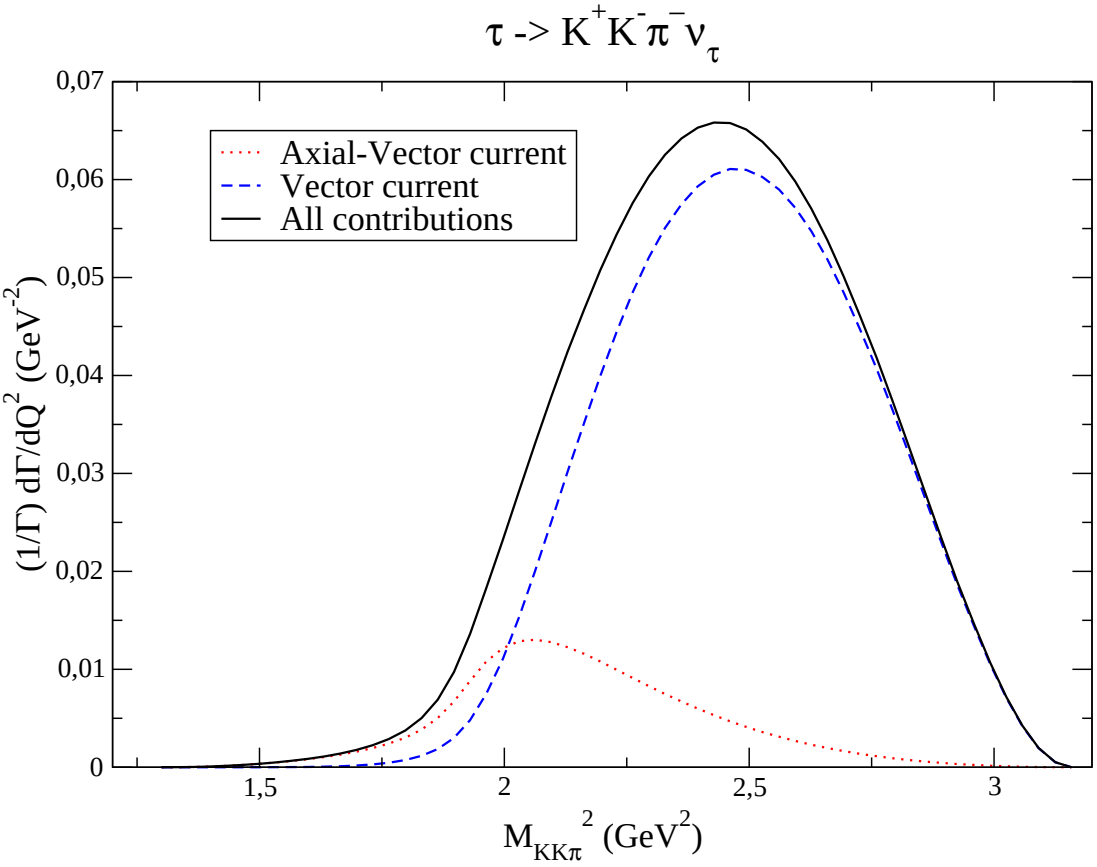

Figure 7.3: Normalized $M^2_{KK\pi}$-spectra for $\tau^- \to K^+K^-\pi^-\nu_\tau$. Notice the dominance of the axial-vector current at very low values of Q^2.

by far over the axial- vector one, though, as can be seen in the spectra in Figs. 7.3, 7.4, the axial- vector current is the dominant one in the very-low Q^2 regime.

Next we contrast our spectrum for $\tau^- \to K^+K^-\pi^-\nu_\tau$ with that one arising from the KS model worked out in Refs. [378, 511]. This comparison is by no means straight because in these references a second and even a third multiplet of resonances are included in the analysis. As we consider that the spectrum is dominated by the first multiplet, in principle we could start by switching off heavier resonances.

Source	Γ_V/Γ_A
Our result	6 ± 2
KS model [378]	$0.6 - 0.7$
KS model [511]	$0.4 - 0.6$
Breit-Wigner approach [440]	~ 9
CVC [80]	0.20 ± 0.03
Data analysis [404]	1.26 ± 0.35

Table 7.2: Comparison of the ratio of vector and axial-vector contribution for $\tau \to KK\pi\nu_\tau$ partial widths. The last two lines correspond to the $\tau^- \to K^+K^-\pi^-\nu_\tau$ process only. Results in Ref. [511] are an update of Ref. [378]. The result of Ref. [80] is obtained by connecting the tau decay width with the CVC related $e^+e^- \to K_S K^\pm \pi^\mp$ (see Appendix C.3). The analysis in [404] was performed with a parameterization that spoiled the chiral normalization of the form factors.

However we notice that, in the KS model, the $\rho(1450)$ resonance plays a crucial role in the vector contribution to the spectrum. This feature depends strongly on the value of the $\rho(1450)$ width, which has been changed from Ref. [378] to Ref. [511] [5]. In Figure 7.5 we compare our results for the vector and axial-vector contributions with those of the KS model as specified in Ref. [511] (here we have switched off the seemingly unimportant $K^*(1410)$). As it can be seen there are large differences in the structure of both approaches. Noticeably there is a large shift in the peak of the vector spectrum owing to the inclusion of the $\rho(1450)$ and $\rho(1700)$ states in the KS model together with its strong interference with the $\rho(770)$ resonance. In our scheme, including the lightest resonances only, the $\rho(1450)$ and $\rho(1700)$ information has to be encoded in the values of c_4 and g_4 couplings (that we have extracted in Subsection 7.3.1) and such an interference is not feasible. It will be a task for the experimental data to settle this issue.

In Figure 7.6 we compare the normalized full $M^2_{KK\pi}$ spectrum for the $\tau \to K\overline{K}\pi\nu_\tau$ channels in the KS model [511] and in our scheme. The most salient feature is the large effect of the vector contribution in our case compared with the leading role of the axial-vector part in the KS model, as can be seen in Figure 7.5. This is the main reason for the differences between the shapes of $M^2_{KK\pi}$ spectra observed in Figure 7.6. We see in Figures 7.7 and 7.8 that similar patterns are observed in the $K^-K^0\pi^0$ hadron mode.

As we have taken advantage of in Chapter 6, the plot of the differential distribution of the decay rate versus the Mandelstam variables s, t and u is a very

[5] Moreover within Ref. [378] the authors use two different set of values for the $\rho(1450)$ mass and width, one of them in the axial-vector current and the other in the vector one. This appears to be somewhat misleading.

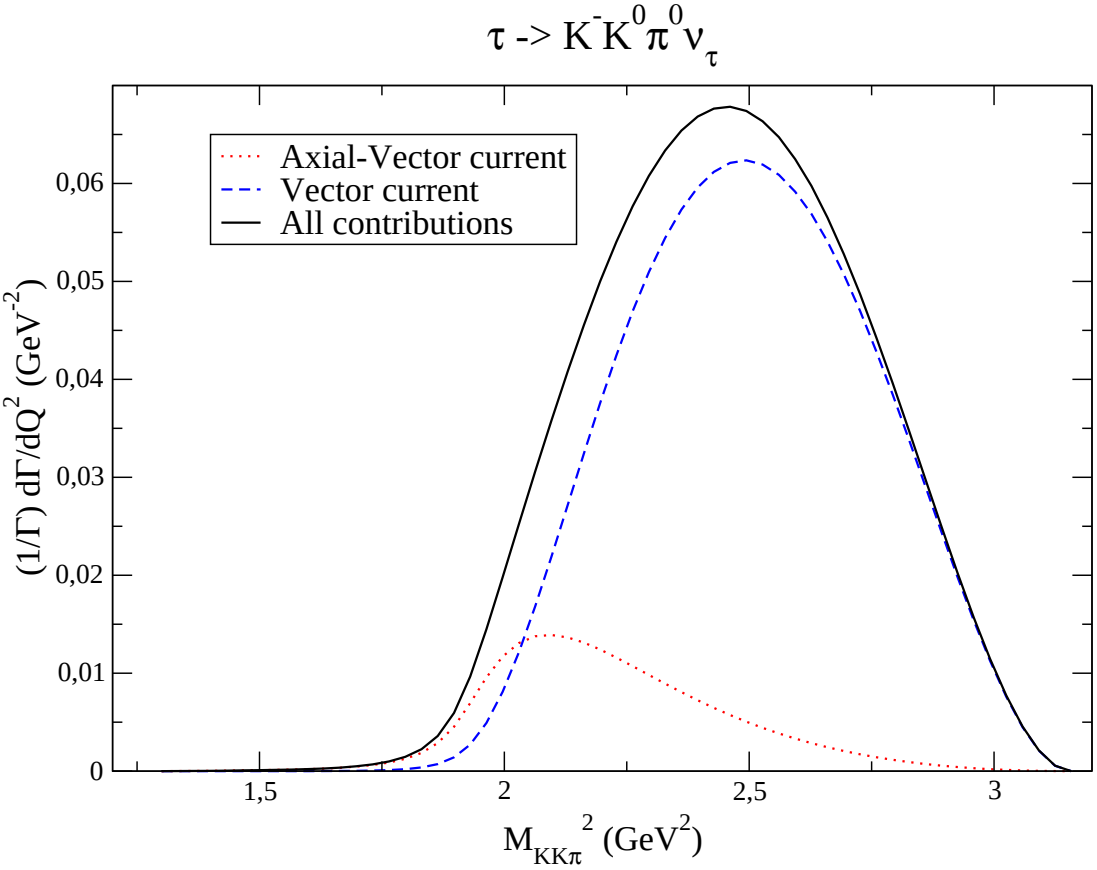

Figure 7.4: Normalized $M^2_{KK\pi}$-spectra for $\tau^- \to K^-K^0\pi^0\nu_\tau$. Notice the dominance of the axial-vector current at very low values of Q^2.

useful tool to learn about the dynamics of the process. In Figure 7.9 we represent $\mathrm{d}\Gamma/\mathrm{d}s$ for $\tau^- \to K^+K^-\pi^-\nu_\tau$, both for our prediction -there is no experimental data we can compare to- and the Finkemeier and Mirkes model. The latter has been normalized to give a branching ratio consistent with PDG by multiplying it by 0.8. Figure 7.9 makes clear how different the dynamics contained in the KS model and in our parameterization are.

Similarly, we present in Figs. 7.10 and 7.11 the analogous plots for the t- and u-spectra. Again, we observe that the physics contained in both approaches is pretty different. This shows up more neatly in Figure 7.10 that is thus another well-suited observable we have found to discriminate between both parameterizations. The observed pattern is analogous to that one shown in the s-, t- and u- spectra in the decays $\tau^- \to K^-K^0\pi^0\nu_\tau$. These are very interesting observables in which we expect data from the dedicated studies of B- and tau-charm-factories in the future.

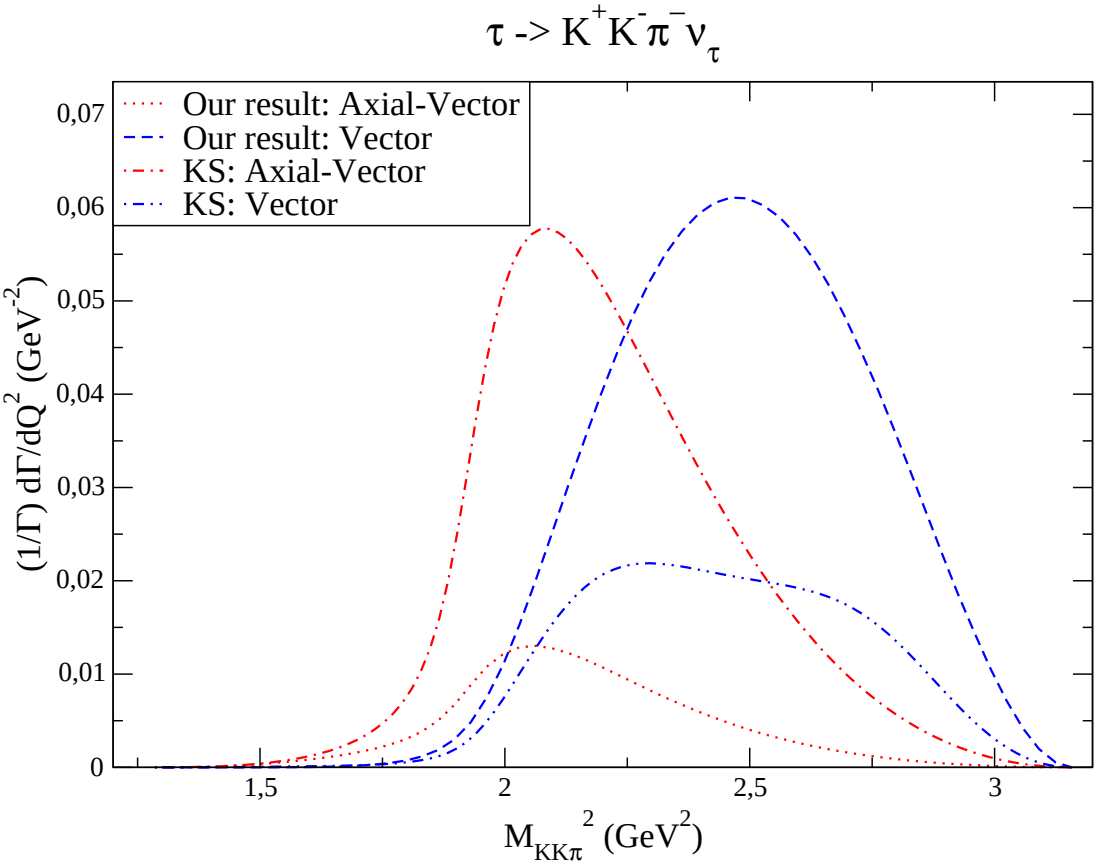

Figure 7.5: Comparison between the normalized $M^2_{KK\pi}$-spectra for the vector and axial-vector contributions to the $\tau^- \to K^+K^-\pi^-\nu_\tau$ channel in the KS model [511] and in our approach.

7.5 Conclusions

Hadron decays of the tau lepton are an all-important tool in the study of the hadronization process of QCD currents, in a setting where resonances play the leading role. In particular the final states of three mesons are the simplest ones where one can test the interplay between different resonance states. At present there are three parameterizations implemented in the $TAUOLA$ library to describe the hadronization process in tau decays. Two are based on experimental data. The other alternative, namely the KS model, though successfull in the account of the $\pi\pi\pi$ final state, has proven to be unsuitable [404] when applied to the decays into $KK\pi$ hadron states. Our procedure, guided by large N_C, chiral symmetry and the asymptotic behaviour of the form factors driven by QCD, was already employed in the analysis of $\tau \to \pi\pi\pi\nu_\tau$ in Refs. [309] and [322], which only concern the axial-vector current. Here we have applied our methodology to the analysis of the $\tau \to KK\pi\nu_\tau$ channels where the vector current may also play a significant role.

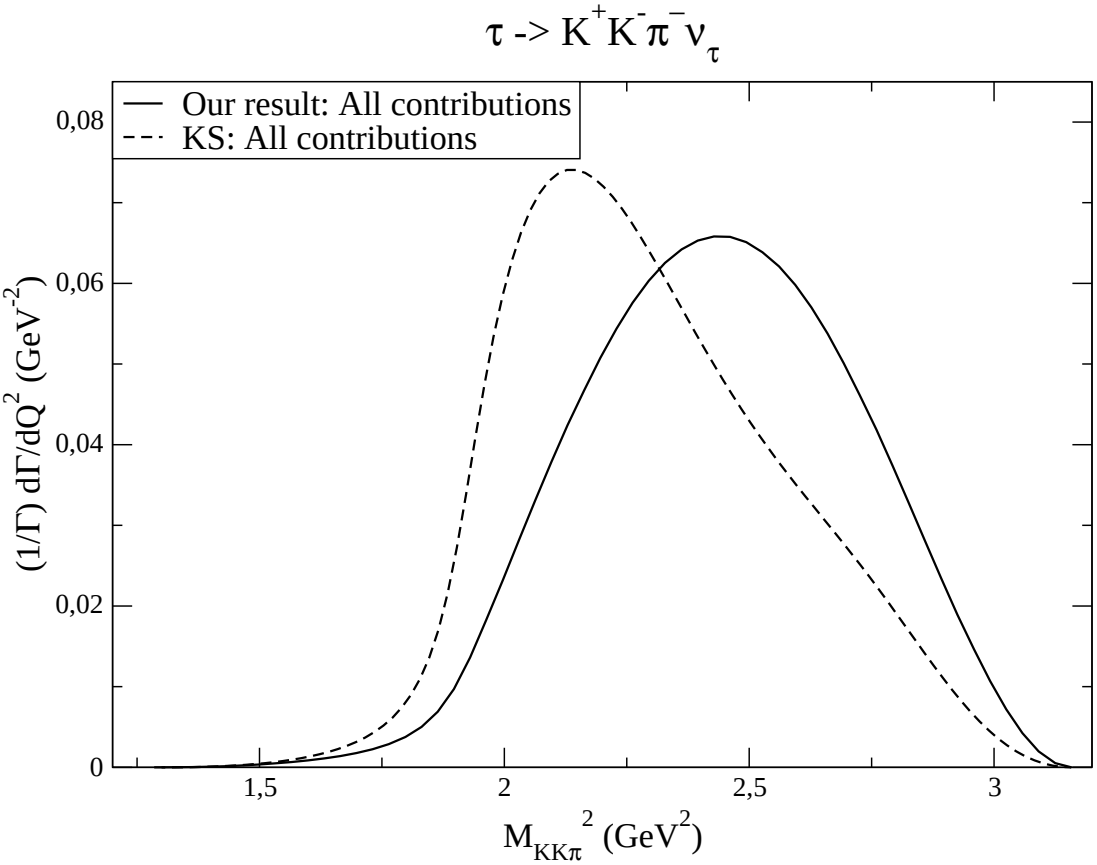

Figure 7.6: Comparison between the normalized $M^2_{KK\pi}$-spectra for $\tau^- \to K^+K^-\pi^-\nu_\tau$ in the KS model [511] and in our approach.

We have constructed the relevant Lagrangian involving the lightest multiplets of vector and axial-vector resonances. Then we have proceeded to the evaluation of the vector and axial-vector currents in the large-N_C limit of QCD, i.e. at tree level within our model. Though the widths of resonances are a next-to-leading effect in the $1/N_C$ counting, they have to be included into the scheme since the resonances do indeed resonate due to the high mass of the decaying tau lepton. We have been able to estimate the values of the relevant new parameters appearing in the Lagrangian with the exception of two, namely the couplings c_4 and g_4, which happen to be important in the description of $\tau \to KK\pi\nu_\tau$ decays. The range of values for these couplings has been determined from the measured widths $\Gamma(\tau^- \to K^+K^-\pi^-\nu_\tau)$ and $\Gamma(\tau^- \to K^-K^0\pi^0\nu_\tau)$.

In this way we provide a prediction for the —still unmeasured— spectra of both processes. We conclude that the vector current contribution dominates over the axial-vector current, in fair disagreement with the corresponding conclusions from the KS model [511] with which we have also compared our full spectra. On the other hand, our result is also at variance with the analysis in Ref. [80]. There are

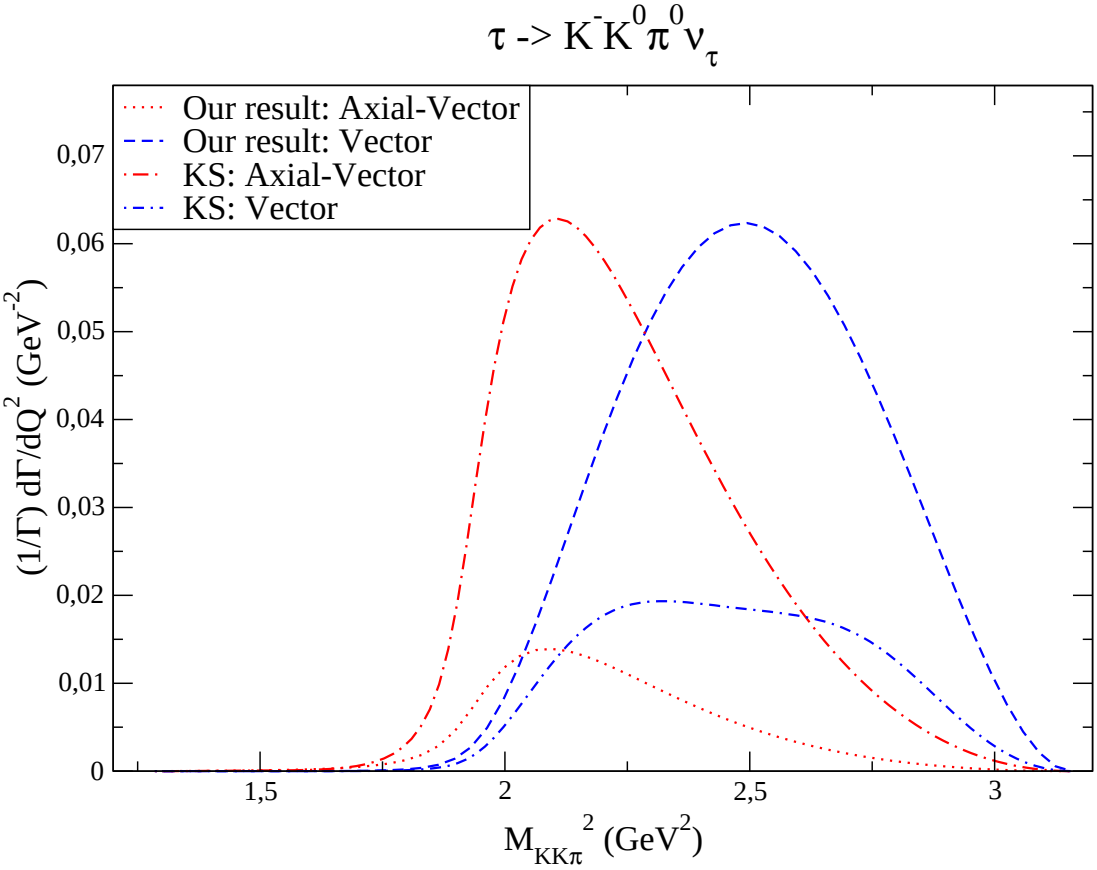

Figure 7.7: Comparison between the normalized $M^2_{KK\pi}$-spectra for the vector and axial-vector contributions to the $\tau^- \to K^- K^0 \pi^0 \nu_\tau$ channel in the KS model [511] and in our approach.

two all-important differences that come out from the comparison. First, while in the KS model the axial-vector contribution dominates the partial width and spectra, in our results the vector current is the one that rules both spectrum and width. Second, the KS model points out a strong interference between the $\rho(770)$, the $\rho(1450)$ and the $\rho(1700)$ resonances that modifies strongly the peak and shape of the $M_{KK\pi}$ distribution depending crucially on the included spectra. Not having a second multiplet of vector resonances in our approach, we cannot provide this feature. It seems strange to us the overwhelming role of the $\rho(1450)$ and $\rho(1700)$ states but it is up to the experimental measurements to settle this issue.

Even if our model provides a good deal of tools for the phenomenological analyses of observables in tau lepton decays, it may seem that our approach is not able to carry the large amount of input present in the KS model, as the later includes easily many multiplets of resonances. In fact, this is not the case, since the Lagrangian can be systematically extended to include whatever spectra of particles are needed. If such an extension is carried out the determination of couplings could be cumbersome

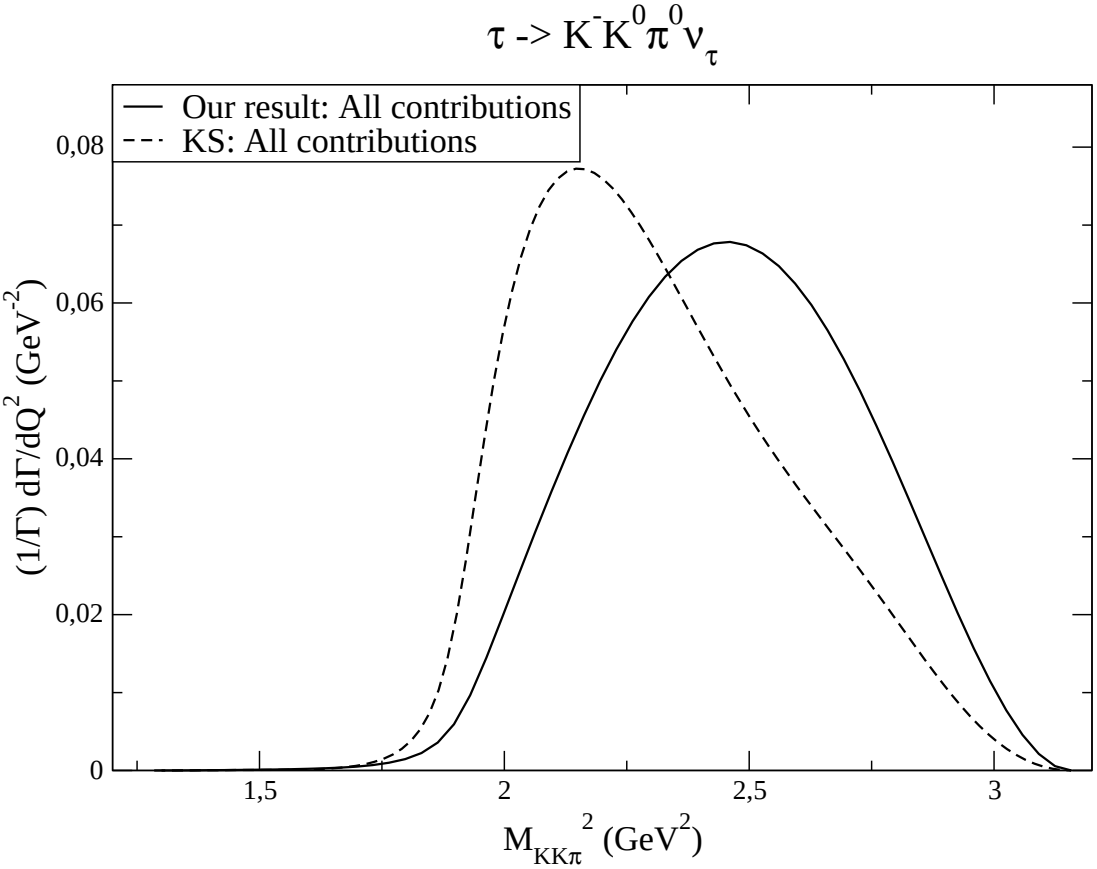

Figure 7.8: Comparison between the normalized $M^2_{KK\pi}$-spectra for $\tau^- \to K^-K^0\pi^0\nu_\tau$ in the KS model [511] and in our approach.

or just not feasible, but, on the same footing as the KS model, our approach would provide a parameterization to be fitted by the experimental data. The present stage, however, has its advantages. By including only one multiplet of resonances we have a setting where the procedure of hadronization is controlled from the theory. This is very satisfactory if our intention is to use these processes to learn about QCD and not only to fit the data to parameters whose relation with the underlying theory is unclear when not directly missing.

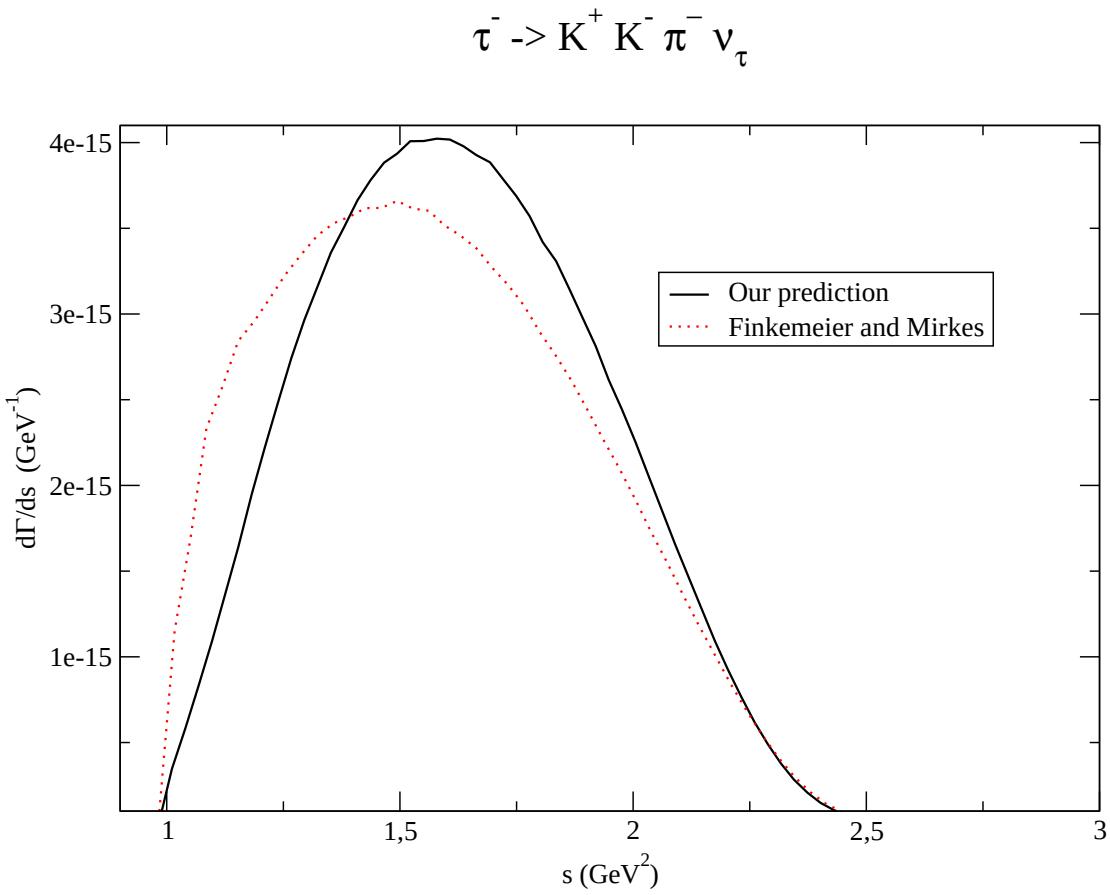

Figure 7.9: Comparison between the s-spectra for $\tau^- \to K^+K^-\pi^-\nu_\tau$ in the KS model [511] and in our approach. The Finkemeier and Mirkes form factors have been reweighted with a factor of 0.8 to match the experimental decay width of this process as reported by the PDG.

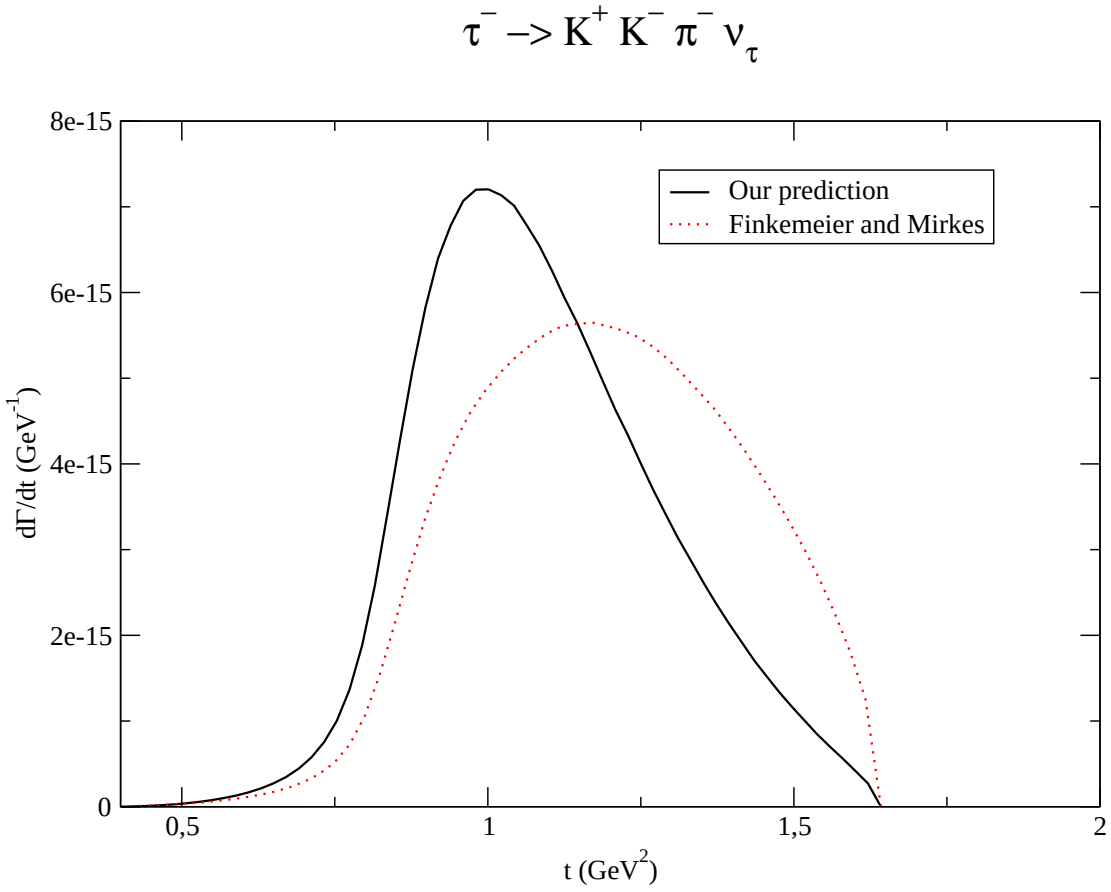

Figure 7.10: Comparison between the t-spectra for $\tau^- \to K^+K^-\pi^-\nu_\tau$ in the KS model [511] and in our approach. The Finkemeier and Mirkes form factors have been reweighted with a factor of 0.8 to match the experimental decay width of this process as reported by the PDG.

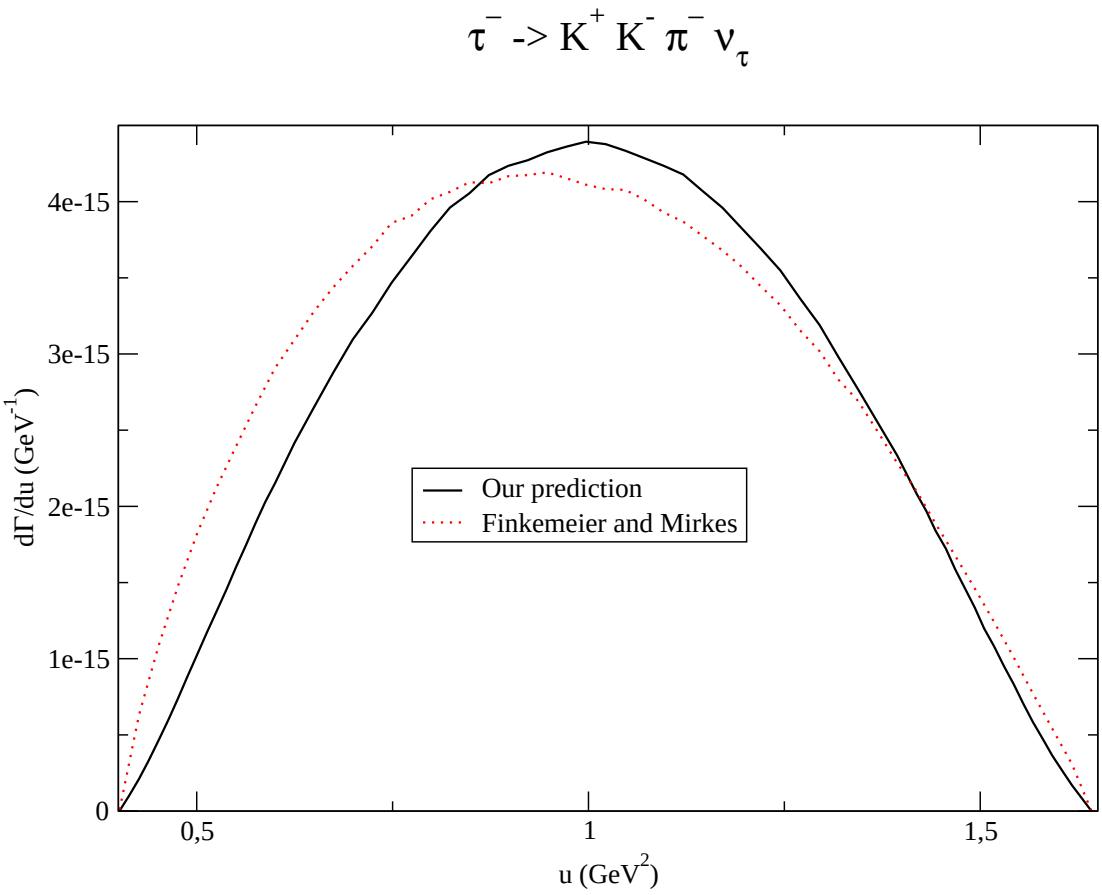

Figure 7.11: Comparison between the u-spectra for $\tau^- \to K^+K^-\pi^-\nu_\tau$ in the KS model [511] and in our approach. The Finkemeier and Mirkes form factors have been reweighted with a factor of 0.8 to match the experimental decay width of this process as reported by the PDG.

Chapter 8

$\tau^- \to \eta/\eta' \pi^- \pi^0 \nu_\tau$ and $\tau^- \to \eta/\eta' \eta \pi^- \nu_\tau$ decays

8.1 Introduction

In this chapter we present the study of the three-meson τ decay modes containing an η. These are the decays $\tau^- \to \eta\pi^-\pi^0\nu_\tau$ and $\tau^- \to \eta\eta\pi^-\nu_\tau$. They are really interesting: in the first one only the vector current participates allowing for a very precise study of it and the second one is a rare decay, in which all contributions from resonance exchange that we should consider within our formalism vanish, only the χPT part does not.

Although the computation of these modes is much simpler than that of the $2K\pi$ decay modes we can extract very precise information from them. As we advanced, the $\tau^- \to \eta\pi^-\pi^0\nu_\tau$ can only be produced via vector current. This mode is measured with an error $\sim 13\%$ [8] [1], therefore it should be an ideal benchmark to learn about the hadronization of the vector current in presence of QCD interactions [327] and, in particular, to test the determination of the couplings in the vector current resonance Lagrangian done in Chapter 7 and to confront it to the results in Chapter 9. However, the branching ratio for this mode in the PDG live disagrees with the value in the PDG 2008 within errors (the earlier value was $(1.81 \pm 0.24) \cdot 10^{-3}$ while the new one is $(1.39 \pm 0.10) \cdot 10^{-3}$), so one should be cautious about the strength of the conclusions we reach. On the other side, the decay $\tau^- \to \eta\eta\pi^-\nu_\tau$ is privileged. There are no vector current contributions and the axial-vector current carries only pseudoscalar degrees of freedom in this case, being suppressed as $F_4 \sim m_\pi^2/Q^2$, that is, as $\sim m_\pi^4/Q^4$ in the spectral function and branching ratios. This observation makes us to guess [2] a suppression at the level of four or five orders of magnitude with respect to the same observables in $\tau^- \to \eta\pi^-\pi^0\nu_\tau$. This estimate would yield a branching ratio of 10^{-7} or smaller, four orders of magnitude less than the current

[1] It is reduced to $\sim 7\%$ in the update on PDGlive, http://pdg.lbl.gov/2009/tables/rpp2009-sum-leptons.pdf.

[2] We take into account the relative contribution of the pseudoscalar form factor in the 3π and $KK\pi$ τ decay modes, where the relative suppression is identical.

lowest branching fraction obtained (See Table 5.1). If we are able to give the lowest order contribution to this decay and bound the value of the higher-order terms, this will be a very appealing channel to look for new physics.

8.2 Form factors in $\tau^- \to \eta\pi^-\pi^0\nu_\tau$

We consider [514] the process $\tau^- \to \eta(p_1)\,\pi^-(p_2)\,\pi^0(p_3)\,\nu_\tau$. The labeling of momenta corresponds to Eq. (5.52). The computation is made for $\eta = \eta_8$. The rest of definitions and normalizations are as usual.

Because of G-parity the axial-vector current form factors vanish

$$T^{\chi}_{A_{1,2}\mu} = T^{1R}_{A_{1,2}\mu} = T^{2R}_{A_{1,2}\mu} = 0\,. \tag{8.1}$$

In order to see this [327], one needs to consider the respective G-parities [3] of pion and eta: $G_\eta = +1$, $G_\pi = -1$, and of the (axial-)vector currents $G_{A_\mu} = -1$ and $G_{V_\mu} = +1$. Notwithstanding, one still has the contribution of the WZW term, Eq. (3.86) and the resonance exchange contributions in the odd-intrinsic parity sector in Eqs. (4.33), (4.34) and (4.42) without any suppression factor vanishing in the isospin limit. Since any isospin-correction to the G-parity forbidden terms would contribute much less than all others we neglect it, as we did in any application considered in this Thesis.

For the vector form factor one needs to consider the diagrams analogous to Figures 7.1.a), 7.1.c), 7.1.d) and 7.1.f), where the solid single lines now correspond to π and η mesons. The vector form factors read

$$T^{\chi}_{V\mu} = i\varepsilon_{\mu\nu\varrho\sigma}p_1^\nu p_2^\varrho p_3^\sigma \left[\frac{N_C}{6\sqrt{6}\,\pi^2\,F^3}\right], \tag{8.2}$$

$$\begin{aligned} T^{1R(1)}_{V\mu} &= i\varepsilon_{\mu\nu\varrho\sigma}p_1^\nu p_2^\varrho p_3^\sigma \frac{8\,G_V}{\sqrt{3}\,F^3\,M_V}\frac{1}{M_\rho^2-u}\left[(c_1-c_2+c_5)Q^2\,\times\right. \\ &\left. -(c_1-c_2-c_5+2c_6)u + (c_1+c_2+8c_3-c_5)m_\eta^2 + 8c_3\left(m_\pi^2-m_\eta^2\right)\right], \end{aligned} \tag{8.3}$$

$$\begin{aligned} T^{1R(2)}_{V\mu} &= -i\varepsilon_{\mu\nu\varrho\sigma}p_1^\nu p_2^\varrho p_3^\sigma \frac{16F_V}{\sqrt{3}\,M_V\,F^3}\frac{1}{M_V^2-Q^2}\left[(g_1+2g_2-g_3)\,u\right. \\ &\left. -g_2\left(Q^2+2m_\pi^2-m_\eta^2\right)-(g_1-g_3)\,2\,m_\pi^2+(2\,g_4+g_5)\,m_\pi^2\right]. \end{aligned} \tag{8.4}$$

$$\begin{aligned} T^{2R}_{V\mu} &= -i\varepsilon_{\mu\nu\varrho\sigma}p_1^\nu p_2^\varrho p_3^\sigma \left\{\frac{8\sqrt{2}}{\sqrt{3}}\frac{F_V G_V}{F^3}\frac{1}{M_V^2-Q^2}\times\right. \\ &\left.\frac{1}{M_\rho^2-u}\left(d_3(Q^2+u)+(d_1+8d_2-d_3)m_\eta^2+8d_2(m_\pi^2-m_\eta^2)\right)\right\}. \end{aligned} \tag{8.5}$$

[3] G-parity is only exact in the limit of conserved isospin.

To obtain the η_1 contribution one simply has to multiply the above amplitudes by $\sqrt{2}$ because we consider the single-angle mixing scheme. Although a detailed study would need the double-angle mixing framework between the mass eigenstates $|\eta\rangle$ and $|\eta'\rangle$ and the flavour eigenstates $|\eta_1\rangle$ and $|\eta_8\rangle$ [515, 516, 517, 518, 519], for our study this effect is irrelevant, so that we will simply use $|\eta\rangle = \cos\theta_P|\eta_8\rangle - \sin\theta_P|\eta_1\rangle$, $|\eta'\rangle = \sin\theta_P|\eta_8\rangle + \cos\theta_P|\eta_1\rangle$. We have

$$\begin{aligned} T_\eta &= \cos\theta_P T_{\eta_8} + \sin\theta_P T_{\eta_1} = \left(\cos\theta_P + \sin\theta_P\sqrt{2}\right) T \sim 0.600T \\ T_{\eta'} &= -\sin\theta_P T_{\eta_8} + \cos\theta_P T_{\eta_1} = \left(-\sin\theta_P + \cos\theta_P\sqrt{2}\right) T \sim 1.625T\,, \end{aligned} \tag{8.6}$$

where T stands for the amplitudes in Eqs. (8.2), (8.3), (8.4) and (8.5), calculated for $\eta = \eta_8$ for a value of $\theta_P \sim -15^\circ$.

8.3 Short-distance constraints on the couplings

Following the same procedure as in Sections 6.3 and 7.3 we have found the following constraints on the vector form factor:

$$\begin{aligned} c_{125} \equiv c_1 - c_2 + c_5 &= 0\,, \\ c_{1256} \equiv c_1 - c_2 - c_5 + 2c_6 &= -\frac{N_C}{96\pi^2}\frac{M_V F_V}{\sqrt{2}F^2}\,, \\ d_3 &= -\frac{N_C}{192\pi^2}\frac{M_V^2}{F^2}\,, \\ g_{123} \equiv g_1 + 2g_2 - g_3 &= 0\,, \\ g_2 &= \frac{N_C}{192\pi^2}\frac{M_V}{\sqrt{2}F_V}\,, \end{aligned} \tag{8.7}$$

that are consistent with the values found in the 3π and $2K\pi$ tau decay channels previously analyzed and also to those to be found in the $P^-\gamma$ decays in the next Chapter.

8.4 $\tau^- \to \eta\eta\pi^-\nu_\tau$

This mode is peculiar because in the chiral limit, it is not generated by the axial-vector current. This [327] can be understood by noticing that the axial-vector current coupling to three pGs is built up from the structure generating the two-meson vector coupling that can not give either $\eta\eta$ (because it vanishes due to the antisymmetric structure in momenta) or $\eta\pi$ that would have G-parity -1, while that of the vector current is $+1$. This feature is preserved when passing from χPT to $R\chi T$ because it only depends on the couplings of spin-one currents to pGs and

selection rules. Moreover, G-parity also forbids all contributions to F_4 including the exchange of a vector or axial-vector resonance.

That is why we only get a contribution in the pseudoscalar form factor F_4, that is nothing more than the χPT result at $\mathcal{O}(p^2)$. That is

$$T^{\chi PT}_{A_4\,\mu} \;=\; -i\frac{m_\pi^2}{3\sqrt{2}F(Q^2-m_\pi^2)}\,Q_\mu\,. \tag{8.8}$$

This channel offers us the possibility to evaluate our assumption of neglecting the effect of the exchange of spin-zero resonances. Since the χPT result at $\mathcal{O}(p^2)$ will give an irrelevantly small branching ratio, we can use this process to study in deep the relevance of scalar and pseudoscalar resonances in an appropriate environment where its rôle cannot be masked by any effect induced by vector or axial–vector resonances.

8.5 Phenomenological analyses

Unfortunately there is no available data for the spectra of any of the decays $\tau^- \to \eta(\eta')\pi^-\pi^0\nu_\tau$ and $\tau^- \to \eta(\eta')\eta\pi^-\nu_\tau$. We will be thus guided in our study only by the figures given by the PDG live, that are: $\Gamma\left(\tau^- \to \eta\pi^-\pi^0\nu_\tau\right) \;=\; 3.15(23)\cdot 10^{-15}$ GeV and $\Gamma\left(\tau^- \to \eta'\pi^-\pi^0\nu_\tau\right) \;\leq\; 1.81\cdot 10^{-16}$ GeV. The first one is dominated by the recent measurement made by the $BELLE$ collaboration [393], $3.06(07)\cdot 10^{-15}$ GeV with a high statistics 450 million τ-pair data sample. While this reference fixes an upper limit on the branching ratio for the mode $\tau^- \to \eta\eta\pi^-\nu_\tau$ consistent with the values given above, it does not provide any figure for the decay $\tau^- \to \eta'\pi^-\pi^0\nu_\tau$.

We will use the short-distance constraints obtained in Sect. 8.3 and complement them with information got in Ref. [310] as discussed in Chapters 6 and 7. We will employ the relevant values of the coupling constants fixed in Eq.(6.34) and also the determination of $2\,g_4 \,+\, g_5 \;=\; -0.60 \pm 0.02$ in Chapter 7. Notice that the determination of c_4 and g_4 in Sect. 7.3.1 does not play any rôle here.

This way we are left with only two unknowns: the coupling constants c_3 and d_2, so our phenomenological analyses will we aimed to gain some information on them and on their relevance in the spectra of the considered decays.

First of all we notice that it is not possible to reach the PDG branching fraction for the $\eta\pi\pi$ mode with these couplings set to zero, since in this case we have $\Gamma\left(\tau^- \to \eta\pi^-\pi^0\nu_\tau\right) \;\sim\; 6.970\cdot 10^{-16}$ GeV.

Then, a detailed study of the allowed region in parameter space for c_3 and d_2 yields that many possibilities are opened for $|c_3| \lesssim 0.06$ and $|d_2| \lesssim 0.5$, meaning that it is possible that one of them is zero while the other not and that it is possible that both do not vanish. In this last case, all possibilities of signs and relative signs are opened as we illustrate with the following eight benchmark points:

$$\begin{aligned}\{c_3,\,d_2\} \;=\; & \{0,\,-0.578\}\,,\;\{0,\,0.461\}\,,\;\{-0.0643,\,0\}\,,\;\{0.0560,\,0\}\,, \\ & \{-0.060,\,-0.040\}\,,\;\{-0.067,\,0.030\}\,,\;\{0.060,\,-0.038\}\,,\;\{0.055,\,0.011\}\;.\end{aligned} \tag{8.9}$$

For all of them we reproduce the PDG live value within less than one sigma.

We have checked that for all allowed values of the parameters we obtain a value for the decay channel $\Gamma\left(\tau^- \to \eta'\pi^-\pi^0\nu_\tau\right)$ that is above the PDG bound. We believe that the discovery of this mode will help to understand if that is a failure of our model or an issue in the detection of this mode. For this purpose, the analyses of the complete *BaBar* and *Belle* data samples will be useful. The values that we obtain for $\Gamma\left(\tau^- \to \eta'\pi^-\pi^0\nu_\tau\right)$ in units of 10^{-16} GeV for the eight benchmark points are: 10.92, 8.035, 16.36, 13.32, 15.90, 16.45, 13.65 and 13.31 (in the same order as given above).

In Figs. 8.1 and 8.2 we can see that the coupling that has a bigger impact in the features of the spectrum is c_3 while d_2 is only relevant when the former is close to zero. This is the reason why in Figs. 8.1 and 8.2 we are labeling only the curves with values of c_3 that are not close to each other and with d_2 only if $c_3 \sim 0$. Analyzing a spectrum it should be possible to determine which of the four labeled curves is preferred. And even lacking of that, a measurement of the branching ratio for the $\eta'\pi^-\pi^0$ mode will serve for this purpose as well.

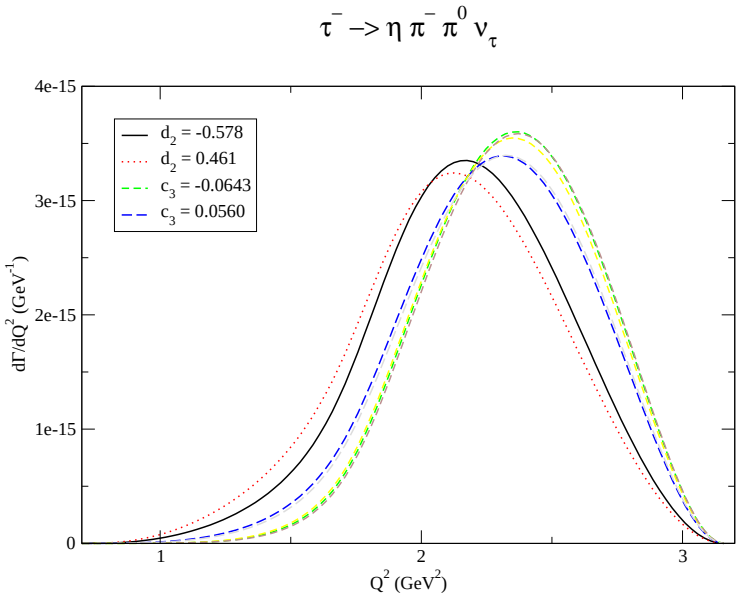

Figure 8.1: Spectral function for the decay $\tau^- \to \eta\pi^-\pi^0\nu_\tau$ using the values for the unknown couplings corresponding to the eight benchmark points as we define and explain in the text.

In Figure 8.3 we show the one-sigma contour for the pdg live branching ratio for the mode $\tau^- \to \eta\pi^-\pi^0\nu_\tau$ in the d_2-c_3 plane. In Figure 8.4 we check that the branching ratio that we obtain for the mode $\tau^- \to \eta'\pi^-\pi^0\nu_\tau$ is above the pdg bound for all allowed values of the parameters (labeled only by the parameter whose impact

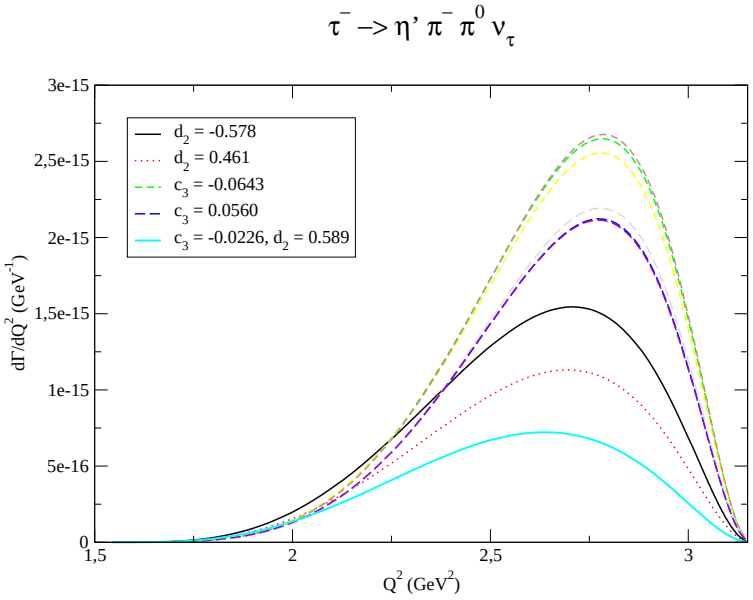

Figure 8.2: Spectral function for the decay $\tau^- \to \eta'\pi^-\pi^0\nu_\tau$ using the values for the unknown couplings corresponding to the eight benchmark points as we define and explain in the text.

is bigger, c_3).

Next, we have analyzed Belle data on the $\tau \to \eta\pi^-\pi^0\nu_\tau$ decay spectra. In Figure 8.5 we can see the results of our fit, which yields the values $d_2 = 0.585 \pm 0.006$ and $c_3 = -0.0213 \pm 0.0026$ that is also the one giving one of the smallest decay widths for the $\eta'\pi^-\pi^0$ mode, that is nevertheless a factor of three larger than the PDG upper bound (last curve in Fig. 8.2). Then, we conclude that the value of d_2 is much larger (in magnitude) than that of c_3 and the positive sign solution for d_2 is favoured by data. This could be confirmed by fitting the low-energy data on $\sigma(e^+e^- \to \eta\pi^+\pi^-)$ using the results in Appendix E [4] [5]. This possibility is illustrated in Figure 8.6, where we see that four representative benchmark points produce different predictions for this cross-section, probably enough to choose which scenario suits better if we had some experimental cross-section data to compare with. In addition, we consider also the curve obtained using the fit parameters for the spectrum of $\tau \to \eta\pi^-\pi^0\nu_\tau$. One observes that the latter curve has a clearly smoother behaviour in the highest-energy part of the figure, which is limited to $E \sim 1.5$ GeV since we cannot expect

[4] One can proceed conversely and use the data on e^+e^- annihilation into hadrons to predict the corresponding semileptonic tau decays [520, 521].

[5] Although the η' meson decays to $\eta\pi^+\pi^-$ about 45% of the time, there is no significant contamination from the chain $\sigma(e^+e^- \to \eta' \to \eta\pi^+\pi^-)$ since, because of C parity it must occur at NLO in the α-expansion.

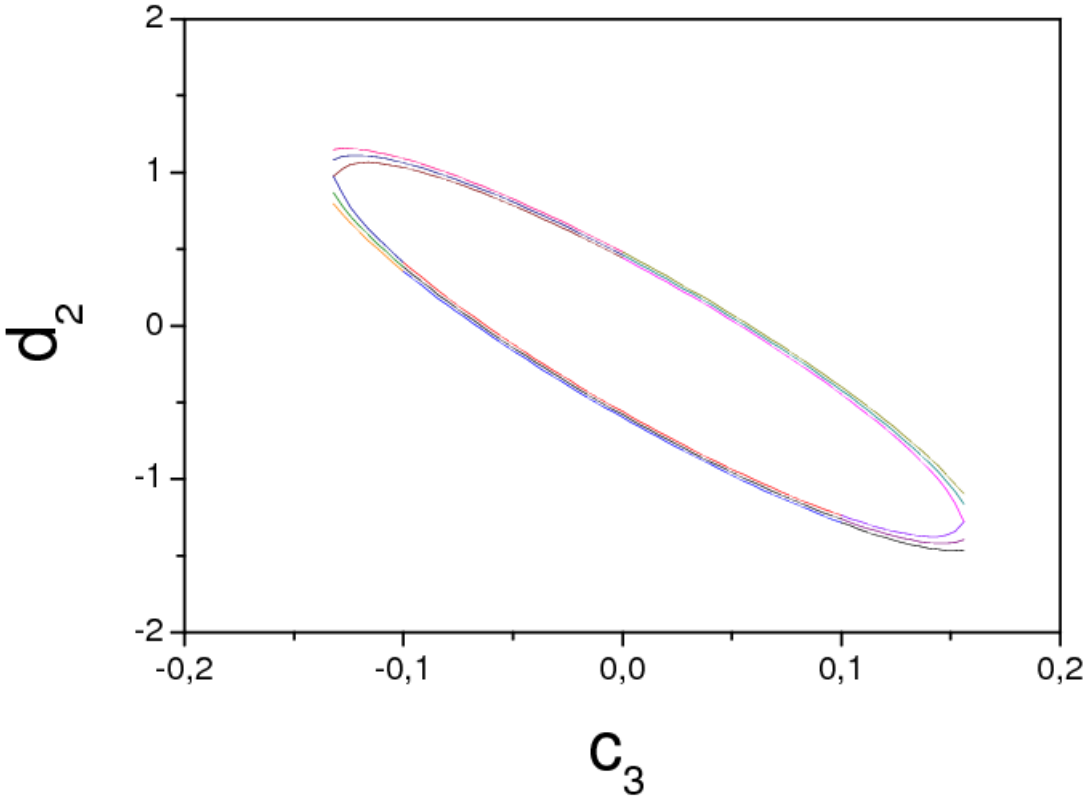

Figure 8.3: One-sigma contours for the branching ratio of the decay $\tau^- \to \eta\pi^-\pi^0\nu_\tau$ in the c_3-d_2 plane.

our parameterization to give a sensible description of the hadron e^+e^- cross-section much beyond this energy [304]. In Fig. 8.7 we compare our prediction to low-energy data from several experiments.

We will pursue in the the future a detailed analyses of the contributions from spin zero resonances to the process $\tau \to \eta\eta\pi^-\nu_\tau$ in order to exploit the possibility of searching for new Physics in this decay once it is discovered. This task is necessary since G-parity arguments do not forbid the contributions from the subprocesses with the axial-vector current coupled to the following hadron currents [6]: $\pi^* \to \eta\eta\pi$, $\pi^* \to f_0\pi \to \eta\eta\pi$ [7] and $\pi^* \to a_0\eta \to \eta\eta\pi$.

[6] A Lorentz index and the Dirac structure are omitted.

[7] Here we consider that the σ meson couples dominantly to two pions.

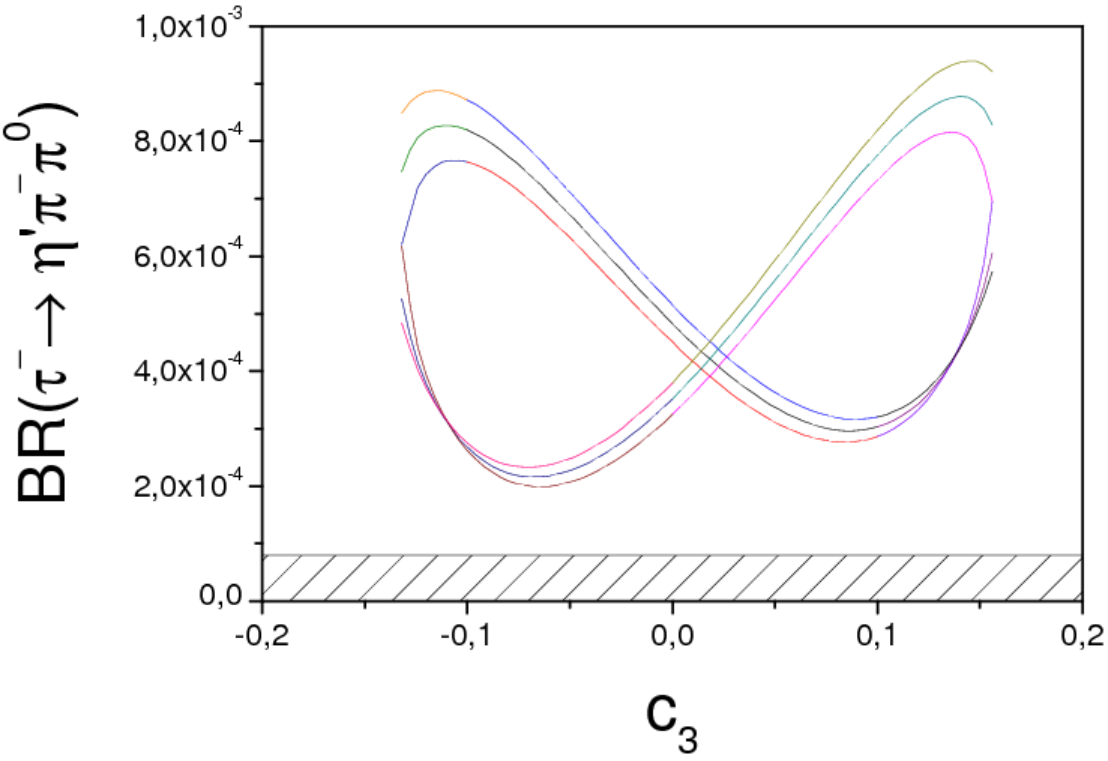

Figure 8.4: The branching ratio for the mode $\tau^- \to \eta'\pi^-\pi^0\nu_\tau$ is plotted versus the value of c_3 for all values of c_3 (and d_2, whose value is not plotted) that yield a branching ratio for the decay $\tau^- \to \eta\pi^-\pi^0\nu_\tau$ consistent within one sigma with the pdg live bound. The horizontal line for a $br = 0.8 \cdot 10^{-4}$ represents the current pdg bound and the dashed area to the allowed region that excludes all our curves.

8.6 Conclusions

We have worked out the decays $\tau^- \to \eta\pi^-\pi^0\nu_\tau$, $\tau^- \to \eta'\pi^-\pi^0\nu_\tau$ and $\tau^- \to \eta\eta\pi^-\nu_\tau$ within the framework of Resonance Chiral Theory guided by the large-N_C expansion of QCD, the low-energy limit given by χPT and the appropriate asymptotic behaviour of the form factors that helps to fix most of the initially unknown couplings. Indeed only two remain free after completing this procedure and having used information acquired in the previous chapter.

We have seen that it is not possible to reproduce the decay width given by the PDG on the former mode with both couplings vanishing. Then, we have observed that it is quite easy to do that for natural values of these couplings in such a way that there is a a whole zone of allowed values in the parameter space for them. Using isospin symmetry, we provide a prediction for the low-energy behaviour of $\sigma(e^+e^- \to \eta\pi^+\pi^-)$. For any allowed value of the two unknowns in the previous

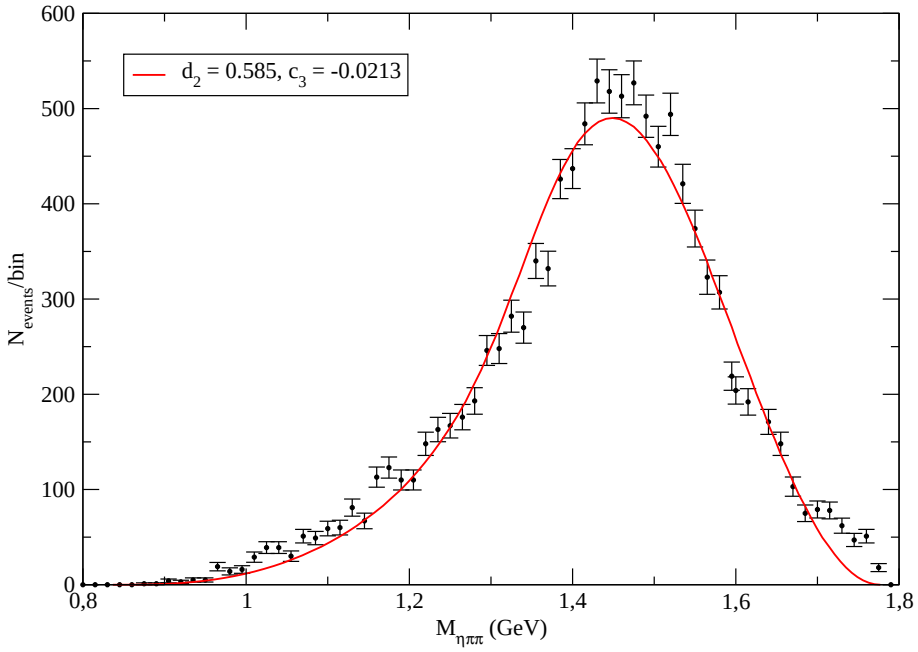

Figure 8.5: The two free parameters of our description of the $\tau^- \to \eta\pi^-\pi^0\nu_\tau$ decays are fitted to Belle data.

study we can not, however, reconcile our prediction for $\Gamma\left(\tau^- \to \eta'\pi^-\pi^0\nu_\tau\right)$ with the PDG upper bound. We conclude that maybe there was not enough statistics yet for it to be detected and that this can happen soon analyzing the data from *BaBar* and *Belle*. Finally, we find that until we characterize reliably the spin-zero contributions through resonance exchange to the process $\tau \to \eta\eta\pi^-\nu_\tau$ we cannot exploit the fact that the spin-one analogous contributions vanish, making then this channel a very promising place to search for new physics once it is first detected. We will tackle this task elsewhere.

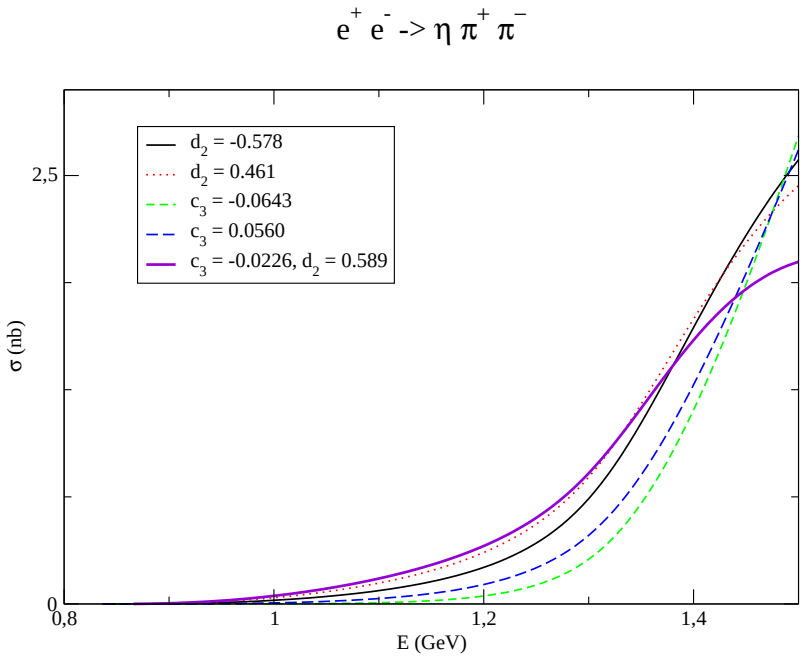

Figure 8.6: Having some cross-section data to compare with, one could tell which is the preferred scenario for $e^+e^- \to \eta\pi^+\pi^-$. Noticeably, the curve corresponding to the fit parameters obtained in $\tau \to \eta\pi^-\pi^0\nu_\tau$ gives the smoothest behaviour in energy.

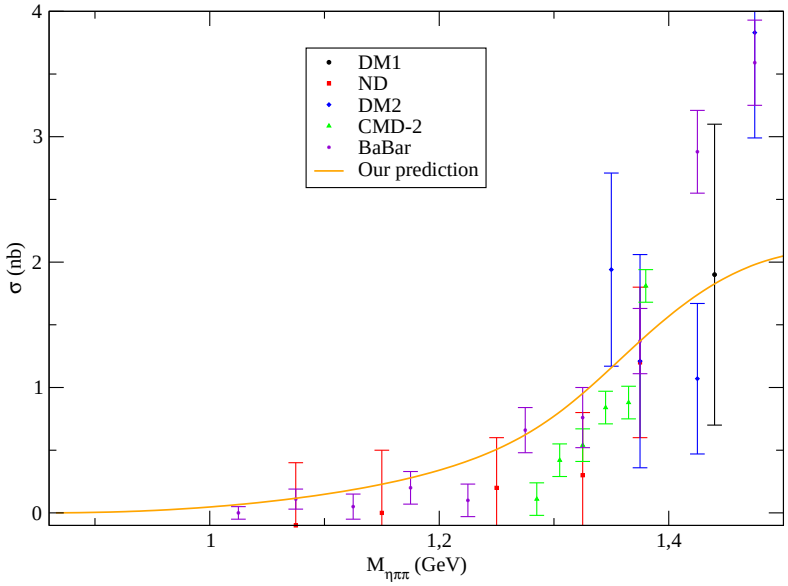

Figure 8.7: Prediction for the low-energy behaviour of $\sigma(e^+e^- \to \eta\pi^+\pi^-)$ based on the $\tau^- \to \eta\pi^-\pi^0\nu_\tau$ decays analysis compared to DM1 [522], ND [523], DM2 [524], CMD-2 [525] and BaBar [526] data.

Chapter 9

$\tau^- \to P^- \gamma \nu_\tau$ decays ($P = \pi,\, K$)

9.1 Introduction

In this chapter we will consider the structure dependent (SD) description of the processes $\tau^- \to P^- \gamma \nu_\tau$ decays ($P = \pi,\, K$) within the framework of $R\chi T$ as discussed in earlier chapters. Until today these channels have not been observed, which is strange according to the most nave expectations of their decay rates. To clarify this question is the main motivation of our study.

The structure independent part of the process has been discussed in Sect. 5.2.1. We will compute the SD depending part using the Lagrangians in Eqs. (3.66), (3.86), (4.19) [1], (4.31), (4.33) and (4.34). This chapter is based on Ref. [303].

As we recall in Sect. 5.2.2, the relative sign between the IB and SD dependent part motivated an addendum to [336]. This confusion was motivated by the fact that they did not used a Lagrangian approach for the SD part. In any Lagrangian approach this should not be an issue. In order to facilitate any independent check, we define the convention we follow as the one used by the PDG [8] in order to relate the external fields r_μ, ℓ_μ with the physical photon field

$$r_\mu = \ell_\mu = -e\, Q\, A_\mu + ..., \tag{9.1}$$

where e is the positron electric charge. Determining the relative sign between the model independent and dependent contributions is an added interest of our computation.

[1] We refer only to the part involving A and V resonances, as in any application in this Thesis. Given the vector character of the SM couplings of the hadron matrix elements in τ decays, form factors for these processes are ruled by vector and axial-vector resonances. In the $\tau \to P^- \gamma \nu_\tau$ decays the relevant form factors are given by a two-point Green function. The study of these [6] showed that other quantum numbers play a negligible rôle.

9.2 Structure dependent form factors in $\tau^- \to \pi^-\gamma\nu_\tau$

The Feynman diagrams, which are relevant to the vector current contributions to the SD part of the $\tau^- \to \pi^-\gamma\nu_\tau$ processes are given in Figure 9.1. The analytical result is found to be

$$i\mathcal{M}_{\mathrm{SD}_V} = iG_F\, V_{ud}\, e\, \overline{u}_{\nu_\tau}(q)\, \gamma^\mu(1-\gamma_5)\, u_\tau(s) \varepsilon_{\mu\nu\alpha\beta}\, \epsilon^\nu(k)\, k^\alpha p^\beta\, F_V^\pi(t)\,, \tag{9.2}$$

where the vector form-factor $F_V^\pi(t)$ is

$$\begin{aligned} F_V^\pi(t) \;=\; & -\frac{N_C}{24\pi^2 F_\pi} + \frac{2\sqrt{2}F_V}{3F_\pi M_V}\left[(c_2-c_1-c_5)t + (c_5-c_1-c_2-8c_3)m_\pi^2\right] \times \\ & \left[\frac{\cos^2\theta}{M_\phi^2}\left(1-\sqrt{2}\mathrm{tg}\theta\right) + \frac{\sin^2\theta}{M_\omega^2}\left(1+\sqrt{2}\mathrm{cotg}\theta\right)\right] \\ & + \frac{2\sqrt{2}F_V}{3F_\pi M_V}\, D_\rho(t)\left[(c_1-c_2-c_5+2c_6)t + (c_5-c_1-c_2-8c_3)m_\pi^2\right] \\ & + \frac{4F_V^2}{3F_\pi}\, D_\rho(t)\left[d_3 t + (d_1+8d_2-d_3)m_\pi^2\right] \times \\ & \left[\frac{\cos^2\theta}{M_\phi^2}\left(1-\sqrt{2}\mathrm{tg}\theta\right) + \frac{\sin^2\theta}{M_\omega^2}\left(1+\sqrt{2}\mathrm{cotg}\theta\right)\right]. \end{aligned} \tag{9.3}$$

Here we have defined $t = (k+p)^2 = (s-q)^2$ and $D_R(t)$ as

$$D_R(t) = \frac{1}{M_R^2 - t - iM_R\Gamma_R(t)}\,. \tag{9.4}$$

$\Gamma_R(t)$ stands for the decay width of the resonance R.

For the vector resonances ω and ϕ, we will assume the ideal mixing case for them in any numerical application:

$$\begin{aligned} \omega_1 &= \cos\theta\;\omega - \sin\theta\;\phi \;\sim \sqrt{\frac{2}{3}}\omega - \sqrt{\frac{1}{3}}\phi\,, \\ \omega_8 &= \sin\theta\;\omega + \cos\theta\;\phi \;\sim \sqrt{\frac{2}{3}}\phi + \sqrt{\frac{1}{3}}\omega\,. \end{aligned} \tag{9.5}$$

The Feynman diagrams related to the axial-vector current contribution to the SD part are given in Figure 9.2. The corresponding result is

$$i\mathcal{M}_{\mathrm{SD}_A} = G_F\, V_{ud}\, e\, \overline{u}_{\nu_\tau}(q)\, \gamma^\mu(1-\gamma_5)\, u_\tau(s)\, \epsilon^\nu(k)\left[(t-m_\pi^2)g_{\mu\nu} - 2k_\mu p_\nu\right] F_A^\pi(t)\,, \tag{9.6}$$

where the axial-vector form-factor $F_A^\pi(t)$ is

$$F_A^\pi(t) \;=\; \frac{F_V^2}{2F_\pi M_\rho^2}\left(1 - \frac{2G_V}{F_V}\right) - \frac{F_A^2}{2F_\pi} D_{\mathrm{a}_1}(t) + \frac{\sqrt{2}F_A F_V}{F_\pi M_\rho^2}\, D_{\mathrm{a}_1}(t)\left(-\lambda'' t + \lambda_0 m_\pi^2\right), \tag{9.7}$$

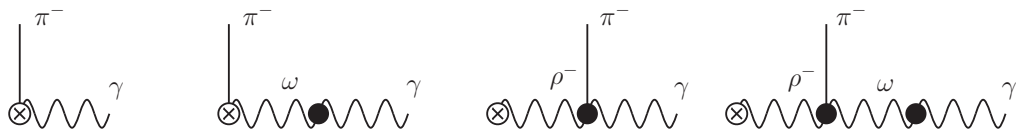

Figure 9.1: Vector current contributions to $\tau^- \to \pi^-\gamma\nu_\tau$.

where we have used the notation from Eq. (4.32) for the relevant combinations of the couplings in $\mathcal{L}_2^{VAP}$, Eq. (4.30).

Figure 9.2: Axial-vector current contributions to $\tau^- \to \pi^-\gamma\nu_\tau$.

9.3 Structure dependent form factors in $\tau^- \to K^-\gamma\nu_\tau$

Although one can read this from Eq.(5.12), let us emphasize that the model independent part $\mathcal{M}_{\mathrm{IB}_{\tau+K}}$ is the same as in the pion case by replacing the pion decay constant F_π with the kaon decay constant F_K. A brief explanation about this replacement is in order. The difference of F_π and F_K is generated by the low energy constants and the chiral loops in χPT [5], while in the large N_C limit of $R\chi T$ this difference is due to the scalar resonances in an implicit way. Due to the scalar tadpole, one can always attach a scalar resonance to any of the pG field, which will cause the pG wave function renormalization. A convenient way to count this effect is to make the scalar field redefinition before the explicit computation to eliminate the scalar tadpole effects. In the latter method, one can easily get the difference of F_π and F_K. For details, see Ref. [527] and references therein. For the model dependent parts, the simple replacements are not applicable and one needs to work out the corresponding form factors explicitly.

The vector current contributions to the SD part of the $\tau^- \to K^-\gamma\nu_\tau$ process are given in Figure 9.3. The analytical result is found to be

$$i\mathcal{M}_{\mathrm{SD}_V} = iG_F\, V_{us}\, e\, \overline{u}_{\nu_\tau}(q)\, \gamma^\mu(1-\gamma_5)\, u_\tau(s)\varepsilon_{\mu\nu\alpha\beta}\, \epsilon^\nu(k)\, k^\alpha p^\beta\, F_V^K(t)\,, \tag{9.8}$$

where the vector form-factor $F_V^K(t)$ is

$$\begin{aligned} F_V^K(t) &= -\frac{N_C}{24\pi^2 F_K} + \frac{\sqrt{2}F_V}{F_K M_V}\left[(c_2-c_1-c_5)t + (c_5-c_1-c_2-8c_3)m_K^2\right] \times \\ &\left[\frac{1}{M_\rho^2} - \frac{\sin^2\theta}{3M_\omega^2}\left(1-2\sqrt{2}\mathrm{cotg}\theta\right) - \frac{\cos^2\theta}{3M_\phi^2}\left(1+2\sqrt{2}\mathrm{tg}\theta\right)\right] \\ &+\frac{2\sqrt{2}F_V}{3F_K M_V}\, D_{K^*}(t)\left[(c_1-c_2-c_5+2c_6)t + (c_5-c_1-c_2-8c_3)m_K^2\right. \\ &\left.+24c_4(m_K^2-m_\pi^2)\right] + \frac{2F_V^2}{F_K}\, D_{K^*}(t)\left[d_3 t + (d_1+8d_2-d_3)m_K^2\right] \times \\ &\left[\frac{1}{M_\rho^2} - \frac{\sin^2\theta}{3M_\omega^2}\left(1-2\sqrt{2}\mathrm{cotg}\theta\right) - \frac{\cos^2\theta}{3M_\phi^2}\left(1+2\sqrt{2}\mathrm{tg}\theta\right)\right]. \end{aligned} \tag{9.9}$$

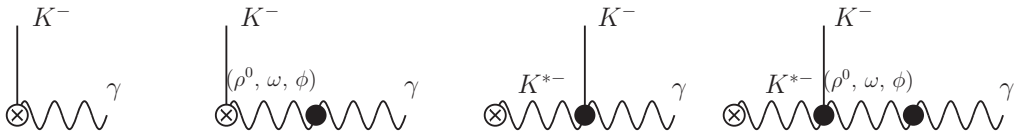

Figure 9.3: Vector current contributions to $\tau^- \to K^-\gamma\nu_\tau$.

The axial-vector current contributions to SD part are given in Figure 9.4. The corresponding analytical result is

$$i\mathcal{M}_{\mathrm{SD}_A} = G_F\, V_{us}\, e\, \overline{u}_{\nu_\tau}(q)\,\gamma^\mu(1-\gamma_5)\,u_\tau(s)\,\epsilon^\nu(k)\left[(t-m_K^2)g_{\mu\nu} - 2k_\mu p_\nu\right] F_A^K(t)\,, \tag{9.10}$$

where the axial-vector form-factor $F_A^K(t)$ is

$$\begin{aligned} F_A^K(t) &= \frac{F_V^2}{4F_K}\left(1-\frac{2G_V}{F_V}\right)\left(\frac{1}{M_\rho^2}+\frac{\cos^2\theta}{M_\phi^2}+\frac{\sin^2\theta}{M_\omega^2}\right) - \frac{F_A^2}{2F_K}\left[\cos^2\theta_A D_{K_{1H}}(t) + \sin^2\theta_A D_{K_{1L}}(t)\right] \\ &+\frac{F_A F_V}{\sqrt{2}F_K}\left[\cos^2\theta_A D_{K_{1H}}(t) + \sin^2\theta_A D_{K_{1L}}(t)\right] \\ &\times\left(\frac{1}{M_\rho^2}+\frac{\cos^2\theta}{M_\phi^2}+\frac{\sin^2\theta}{M_\omega^2}\right)\left(-\lambda'' t + \lambda_0 m_K^2\right). \end{aligned} \tag{9.11}$$

We have used the notations of K_{1H} and K_{1L} for the physical states of $K_1(1400)$ and $K_1(1270)$ respectively and the mixing angle θ_A is defined in Eq.(9.12) as we explain in the following.

The K_{1A} state appearing in Eq. (4.14) is related to the physical states $K_1(1270)$, $K_1(1400)$ through:

$$K_{1A} \,=\, \cos\theta_A\; K_1(1400) + \sin\theta_A\; K_1(1270)\,. \tag{9.12}$$

About the nature of $K_1(1270)$ and $K_1(1400)$, it has been proposed in Ref. [528] that they result from the mixing of the states K_{1A} and K_{1B}, where K_{1A} denotes the strange partner of the axial vector resonance a_1 with $J^{PC} = 1^{++}$ and K_{1B} is the corresponding strange partner of the axial vector resonance b_1 with $J^{PC} = 1^{+-}$. However in this work, we will not include the nonet of axial vector resonances with $J^{PC} = 1^{+-}$ [283]. As argued in Ref. [528], the contributions from these kind of resonances to tau decays are proportional to the $SU(3)$ symmetry breaking effects. Moreover, as one can see later, we will assume $SU(3)$ symmetry for both vector and axial-vector resonances in deriving the T-matrix always. For the pGs, physical masses will arise through the chiral symmetry breaking mechanism in the same way as it happens in QCD. For the (axial-)vector resonances, the experimental values will be taken into account in the kinematics.

Figure 9.4: Axial-vector current contributions to $\tau^- \to K^-\gamma\nu_\tau$.

9.4 Constraints from QCD asymptotic behavior

In this part, we will exploit the asymptotic results of the form factors from perturbative QCD to constrain the resonance couplings. When discussing the high energy constraints, we will work both in chiral and $SU(3)$ limits, which indicates we will not distinguish the form factors with pion and kaon, that are identical in this case.

For the vector form factor, the asymptotic result of perturbative QCD has been derived in Ref. [281, 298]

$$F_V^P(t \to -\infty) = \frac{F}{t}\,, \tag{9.13}$$

where F is the pion decay constant in the chiral limit. From the above asymptotic behavior, we find three constraints on the resonance couplings

$$c_1 - c_2 + c_5 \,=\, 0\,, \tag{9.14}$$

$$c_2 - c_1 + c_5 - 2c_6 \,=\, \frac{\sqrt{2}N_C M_V}{32\pi^2 F_V} + \frac{\sqrt{2}F_V}{M_V} d_3\,, \tag{9.15}$$

$$c_2 - c_1 + c_5 - 2c_6 \,=\, \frac{3\sqrt{2}F^2}{4F_V M_V} + \frac{\sqrt{2}F_V}{M_V} d_3\,, \tag{9.16}$$

where the constraints in Eqs.(9.14), (9.15) and (9.16) are derived from order of $\mathcal{O}(t^1)$, $\mathcal{O}(t^0)$ and $\mathcal{O}(t^{-1})$, respectively. Combining the above three constraints, we have

$$c_5 - c_6 = \frac{N_C M_V}{32\sqrt{2}\pi^2 F_V} + \frac{F_V}{\sqrt{2}M_V} d_3 \tag{9.17}$$

$$F = \frac{M_V\sqrt{N_C}}{2\sqrt{6}\pi}\,, \tag{9.18}$$

where the constraint of Eq.(9.18) has already been noticed in [281, 298, 336].

The high energy constraints on the resonance couplings c_i and d_i have been studied in different processes. The OPE analysis of the VVP Green Function gives [310]

$$c_5 - c_6 = \frac{N_C M_V}{64\sqrt{2}\pi^2 F_V}\,, \tag{9.19}$$

$$d_3 = -\frac{N_C M_V^2}{64\pi^2 F_V^2} + \frac{F^2}{8F_V^2}\,. \tag{9.20}$$

The constraint from $\tau^- \to (VP)^-\nu_\tau$ study leads to

$$c_5 - c_6 = -\frac{F_V}{\sqrt{2}M_V} d_3\,, \tag{9.21}$$

if one neglects the heavier vector resonance multiplet [529].

The results from the analysis of $\tau^- \to (KK\pi)^-\nu_\tau$ are [321, 508]

$$\begin{aligned} c_5 - c_6 &= \frac{N_C M_V F_V}{192\sqrt{2}\pi^2 F^2}\,, \\ d_3 &= -\frac{N_C M_V^2}{192\pi^2 F^2}\,. \end{aligned} \tag{9.22}$$

It is easy to check that the results of Eqs.(9.21) and (9.22) are consistent. Combining Eqs.(9.17) and (9.21) leads to

$$\begin{aligned} c_5 - c_6 &= \frac{N_C M_V}{64\sqrt{2}\pi^2 F_V}\,, \\ d_3 &= -\frac{N_C M_V^2}{64\pi^2 F_V^2}\,, \end{aligned} \tag{9.23}$$

where the constraint of $c_5 - c_6$ is consistent with the result from the OPE analysis of the VVP Green Function [310], while the result of d_3 is not [2].

By demanding the consistency of the constraints derived from the processes of $\tau^- \to P^-\gamma\nu_\tau$ and $\tau^- \to (VP)^-\nu_\tau$ given in Eq.(9.23) and the results form $\tau^- \to (KK\pi)^-\nu_\tau$ given in Eq.(9.22), we get the following constraint

$$F_V = \sqrt{3}F\,. \tag{9.24}$$

[2]However, the difference on the numerical value of both predictions is small, $\sim 16\%$ and the impact of such a difference in any observable in the considered processes is extremely tiny.

If one combines the high energy constraint from the two pion vector form factor [7]

$$F_V G_V = F^2 \,, \tag{9.25}$$

and the result of Eq.(9.24) we get here, the modified $KSRF$ will be derived

$$F = \sqrt{3} G_V \,, \tag{9.26}$$

which is also obtained in the partial wave dispersion relation analysis of $\pi\pi$ scattering [530] .

Although the branching ratios for the modes $\tau \to P\gamma\nu_\tau$ we are discussing should be higher than for some modes that have been already detected, they have not been observed yet. Lacking of experimental data, we will make some theoretically and phenomenologically based assumptions in order to present our predictions for the spectra and branching ratios.

Taking into account the previous relations one would have $F_V^\pi(t)$ in terms of $c_1 + c_2 + 8c_3 - c_5$ and $d_1 + 8d_2 - d_3$. For the first combination, $c_1 + c_2 + 8c_3 - c_5 = c_1 + 4c_3$ ($c_1 - c_2 + c_5 = 0$ has been used), the prediction for $c_1 + 4c_3$ in [310] yields $c_1 + c_2 + 8c_3 - c_5 = 0$. In Ref. [310] the other relevant combination of couplings is also restricted: $d_1 + 8d_2 - d_3 = \frac{F^2}{8F_V^2}$. In $F_V^\pi(t)$ c_4 appears, in addition. There is a phenomenological determination of this coupling in our work on the $KK\pi$ decay modes of the τ [508]: $c_4 = -0.07 \pm 0.01$.

Turning now to the axial-vector form factor, in both channels it still depends on four couplings: F_A, M_A, λ'' and λ_0. If one invokes the once subtracted dispersion for the axial vector form factor, as done in Ref. [336], one can not get any constraints on the resonance couplings from the axial vector form factors given in Eqs.(9.7) and (9.11). In fact by demanding the form factor to satisfy the unsubtracted dispersion relation, which guarantees a better high energy limit, we can get the following constraint

$$\lambda'' = \frac{2G_V - F_V}{2\sqrt{2}F_A} \,, \tag{9.27}$$

which has been already noted in [299].

In order to constrain the free parameters as much as possible, we decide to exploit the constraints from the Weinberg sum rules (WSR) [302]: $F_V^2 - F_A^2 = F^2$ and $M_V^2 F_V^2 - M_A^2 F_A^2 = 0$, yielding

$$F_A^2 = 2F^2 \;\;,\;\; M_A = \frac{6\pi F}{\sqrt{N_C}} \,. \tag{9.28}$$

For the axial vector resonance coupling λ_0, we use the result from Ref. [299, 322]

$$\lambda_0 = \frac{G_V}{4\sqrt{2}F_A} \,. \tag{9.29}$$

To conclude this section, we summarize the previous discussion on the high energy

constraints

$$F_V = \sqrt{3}F\,, \quad G_V = \frac{F}{\sqrt{3}}\,, \quad F_A = \sqrt{2}F\,, \quad M_V = \frac{2\sqrt{6}\pi F}{\sqrt{N_C}}\,, \quad M_A = \frac{6\pi F}{\sqrt{N_C}}\,,$$
$$\lambda_0 = \frac{1}{8\sqrt{3}}\,, \quad \lambda'' = -\frac{1}{4\sqrt{3}}\,, \quad c_5 - c_6 = \frac{\sqrt{N_C}}{32\pi}\,, \quad d_3 = -\frac{1}{8}\,. \tag{9.30}$$

In the above results, we have discarded the constraint in Eq.(9.20), which is the only inconsistent result with the others.

9.5 Phenomenological discussion

Apart from the parameters we mentioned in the last section, there is still one free coupling θ_A, which describes the mixing of the strange axial vector resonances in Eq.(9.12). The value of θ_A has already been determined in literature [528, 529, 531]. We recapitulate the main results in the following.

In Ref. [528], it is determined $\theta_A \sim 33°$. In Ref. [529], $|\theta_A| \sim 58.1°$ is determined through the considered decays $\tau^- \to (VP)^-\nu_\tau$. In Ref. [531], the study of $\tau \to K_1\nu_\tau$ gives $|\theta_A| =^{37°}_{58°}$ as the two possible solutions. The decay $D \to K_1\pi$ allows to conclude that θ_A must be negative and it is pointed out that the observation of $D^0 \to K_1^-\pi^+$ with a branching ratio $\sim 5\cdot 10^{-4}$ would imply $\theta_A \sim -58°$. However, a later analyses in Ref. [532] finds that the current measurement of $\bar{B}^0 \to K_1^-(1400)\pi^+$ [8] favors a mixing angle of $-37°$ over $-58°$. In this respect, the relation

$$\left|\Gamma\left(J/\Psi \to K_1^0(1400)\overline{K}^0\right)\right|^2 = \mathrm{tg}\theta_A^2 \left|\Gamma\left(J/\Psi \to K_1^0(1270)\overline{K}^0\right)\right|^2 \tag{9.31}$$

would be very useful to get θ_A, once these modes are detected.

9.5.1 Results including only the WZW contribution in the SD part

As it was stated in Sects. 5.2.2 and 9.1 it is strange that these modes have not been detected so far. The most nave and completely model independent estimate would just include the IB part and the WZW contribution to the VV part, as the latter is completely fixed by QCD. We know that doing this way we are losing the contribution of vector and axial-vector resonances, that should be important in the high-x region. However, even doing so one is able to find that the radiative decay $\tau^- \to \pi^-\gamma\nu_\tau$ has a decay probability larger than the mode $\tau^- \to K^+K^-K^-\nu_\tau$ [3]. For a reasonably low cut on the photon energy this conclusion holds for the $\tau^- \to K^-\gamma\nu_\tau$ as well.

[3] see Table 5.1, $\Gamma\left(\tau^- \to K^+K^-K^-\nu_\tau\right) = 3.579(66)\cdot 10^{-17}$ GeV.

Before seeing this, we will discuss briefly the meaning of cutting on the photon energy. A cut on the photon energy was introduced in Sect. 5.2.2. As it is well know [533, 534] the IR divergences due to the vanishing photon mass cancel when considering at the same time the non-radiative and the radiative decays. In practice, this translates into mathematical language the physical notion that the detectors have a limited angular resolution that defines a threshold detection angle for photons. If one considers a photon emitted with a smaller angle it should be counted together with the non-radiative decay as it is effectively measured this way. The sum is of course an IR safe observable. The splitting depends on the particular characteristics of the experimental setting. Obviously, the branching fraction for the radiative decay depends on this cut-off energy. We will consider here the case $E_{\gamma\,\mathrm{thr}} = 50$ MeV, that corresponds to $x = 0.0565$. In order to illustrate the dependence on this variable, we will also show the extremely conservative case of $E_{\gamma\,\mathrm{thr}} = 400$ MeV ($x = 0.45$). In Figure 9.5 we see the radiative π decay for a low value of x, while in Figure 9.6 we plot it for the high-x case. In the first case we obtain $\Gamma\left(\tau^- \to \pi^-\gamma\nu_\tau\right) = 3.182 \cdot 10^{-15}$ GeV, and in the second one we are still above the bound marked by the $3K$ decay, $\Gamma\left(\tau^- \to \pi^-\gamma\nu_\tau\right) = 3.615 \cdot 10^{-16}$ GeV. Proceeding analogously for the decays with a K^-, we find: $\Gamma\left(\tau^- \to K^-\gamma\nu_\tau\right) = 6.002 \cdot 10^{-17}$ GeV for $E_{\gamma\,\mathrm{thr}} = 50$ MeV (Figure 9.8), and $\Gamma\left(\tau^- \to K^-\gamma\nu_\tau\right) = 4.589 \cdot 10^{-18}$ GeV for $E_{\gamma\,\mathrm{thr}} = 400$ MeV. For any reasonable cut on E_γ these modes should have already been detected by the B-factories.

Already at this level of the phenomenological analysis, the question of the accuracy on the detection of soft photons at B-factories [535] arises. An error larger than expected (here and in some undetected particle interpreted as missing energy, in addition to a gaussian treatment of systematic errors) could enlarge the uncertainty claimed on the measurement of $B^- \to \tau^-\nu_\tau$ [8] when combining the $Belle$ [536] and $BaBar$ measurements [537, 538] taking it closer to the standard model expectations.

9.5.2 Results including resonance contributions in the π channel

Next we include also the model-dependent contributions. Since in the Kaon channel there are uncertainties associated to the strange axial-vector off-shell width and to the mixing of the corresponding light and heavy states we will present first the pion channel where there are not any uncertainty of these types and everything is fixed in an analogous fashion to what discussed in the preceding chapters.

In Figs. 9.9-9.12 the resulting photon spectrum in the process $\tau^- \to \pi^-\gamma\nu_\tau$ is displayed. In Figure 9.9, all contributions are shown for a cutoff on the photon energy of 50 MeV. For "soft" photons ($x_0 \lesssim 0.3$) the internal bremsstrahlung dominates completely. One should note that for very soft photons the multi-photon production

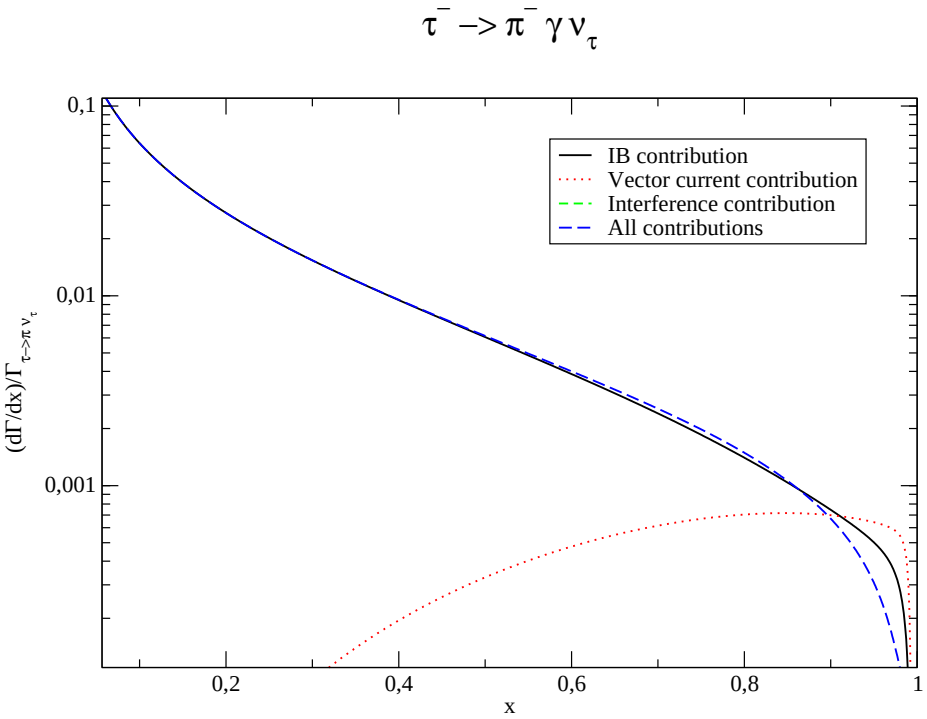

Figure 9.5: Differential decay width of the process $\tau^- \to \pi^-\gamma\nu_\tau$ including only the model independent contributions for a cut-off on the photon energy of 50 MeV. In the vector form factor only the WZW term is considered for this estimate. The interference contribution is negative. It can be appreciated in Fig. 9.6.

rate becomes important, thus making that our $\mathcal{O}(\alpha)$ results are not reliable too close to the IR divergence $x = 0$. We agree with the results in DF papers, for the same value of α to the three significant figures shown in Ref. [336].

The spectrum is significantly enhanced by SD contributions for hard photons ($x_0 \gtrsim 0.4$), as we can see in the close-up of Figure 9.9, in Figure 9.10. In Figure 9.11 we show that the vector current contribution mediated by vector resonances dominates the SD part, while in Figure 9.12 we plot the interference term between bremsstrahlung and SD part. If we compare the predicted curves to those in Ref. [336] we see that the qualitative behaviour is similar: the IB contribution dominates up to $x \sim 0.75$. For larger photon energies, the SD -that is predominantly due to the VV contribution- overcomes it. We confirm the peak and shoulder structure shown at $x \sim 1$ in the interference contribution, that is essentially due to $IB - V$ term, and also in the VA term, that is in any case tiny.

While the integration over the IB needs an IR cut-off, the SD part does not. We have performed the integration over the complete phase space, yielding (all

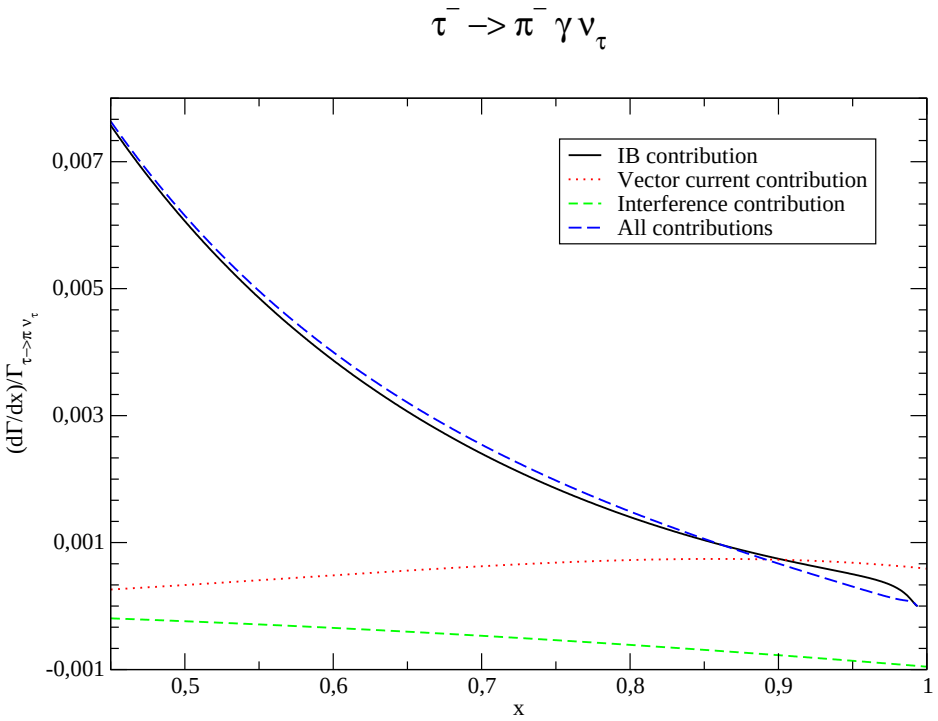

Figure 9.6: Differential decay width of the process $\tau^- \to \pi^-\gamma\nu_\tau$ including only the model independent contributions for a cut-off on the photon energy of 400 MeV. In the vector form factor only the WZW term is considered for this estimate.

contributions to the partial decay width are given in units of the non-radiative decay, here and in what follows):

$$\Gamma_{VV} = 0.99{\cdot}10^{-3}\,, \quad \Gamma_{VA} = 1.45{\cdot}10^{-9} \sim 0\,, \quad \Gamma_{AA} = 0.15{\cdot}10^{-3} \Rightarrow \Gamma_{SD} = 1.14{\cdot}10^{-3}\,. \tag{9.32}$$

Our number for Γ_{SD} lies between the results for the monopole and tripole parametrizations in Ref. [336]. However, they get a smaller(larger) $VV(AA)$ contribution than we do by $\sim 20\%(\sim 200\%)$. This last discrepancy is due to the off-shell a_1 width they use. In fact, if we use the constant width approximation we get a number very close to theirs for the AA contribution. With our understanding of the a_1 width in the $\tau \to 3\pi\nu_\tau$ observables, we can say that their (relatively) high AA contribution is an artifact of the ad-hoc off-shell width used. Since the numerical difference in varied vector off-shell widths is not that high, the numbers for VV are closer.

The numbers in Eq.(9.32) are translated into the following branching ratios

$$\mathrm{BR}_{VV}\,(\tau \to \pi\gamma\nu_\tau) = 1.05 \cdot 10^{-4}\,, \quad \mathrm{BR}_{AA}\,(\tau \to \pi\gamma\nu_\tau) = 0.15 \cdot 10^{-4}\,. \tag{9.33}$$

We can also compare the VV value with the narrow width estimate: taking into account the lowest lying resonance ρ we get

$$\begin{aligned} \mathrm{BR}_{VV}\,(\tau \to \pi\gamma\nu_\tau) &\sim BR(\tau \to \rho\nu_\tau) \times BR(\rho \to \pi\gamma) \sim BR(\tau \to \pi^-\pi^0\nu_\tau)BR(\rho \to \pi\gamma) \\ &\sim 25.52\% \times 4.5 \cdot 10^{-4} = 1.15 \cdot 10^{-4}\,, \end{aligned} \tag{9.34}$$

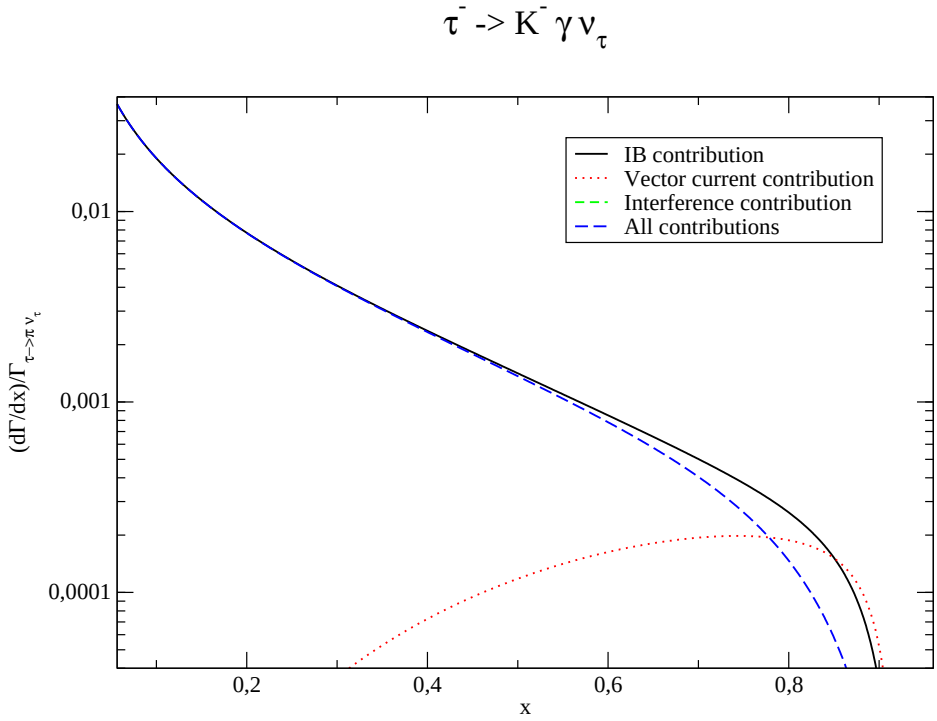

Figure 9.7: Differential decay width of the process $\tau^- \to K^-\gamma\nu_\tau$ including only the model independent contributions for a cut-off on the photon energy of 50 MeV. In the vector form factor only the WZW term (where the axial-vector contribution is absent) is considered for this estimate. The interference contribution is negative. It can be appreciated in Fig. 9.8.

which is quite a good approximation.
In Table 9.1 we give the display for two values of the photon energy cut-off how the different parts contribute to the total rate. For a low-energy cut-off the most of the rate comes from IB while for a higher-energy one the SD parts (and particularly the VV contribution) gains importance. While the VA contribution is always negligible, the $IB - V$, $IB - A$ and the SD parts VV and AA have some relevance for a higher-energy cut-off.

In Figs. 9.13-9.16 we show the pion-photon invariant spectrum. We find a much better separation between the IB and SD contributions as compared with the photon spectrum in the previous Figs. 9.9 to 9.12. Then, the pion-photon spectrum is better suited to study the SD effects. In this case, the VA is identically zero, since this interference vanishes in the invariant mass spectrum after integration over the other kinematic variable. Of course, in the VV spectrum we see the shape of the ρ contribution neatly, as one can see in Figure 9.15 where, on the contrary, the a_1 exchange in AA has a softer and broader effect. The $IB - SD$ radiation near the a_1 is dominated by $IB - A$, which gives the positive contribution to the decay rate. While near the energy region of the ρ resonance, we find the $IB - SD$ contribution

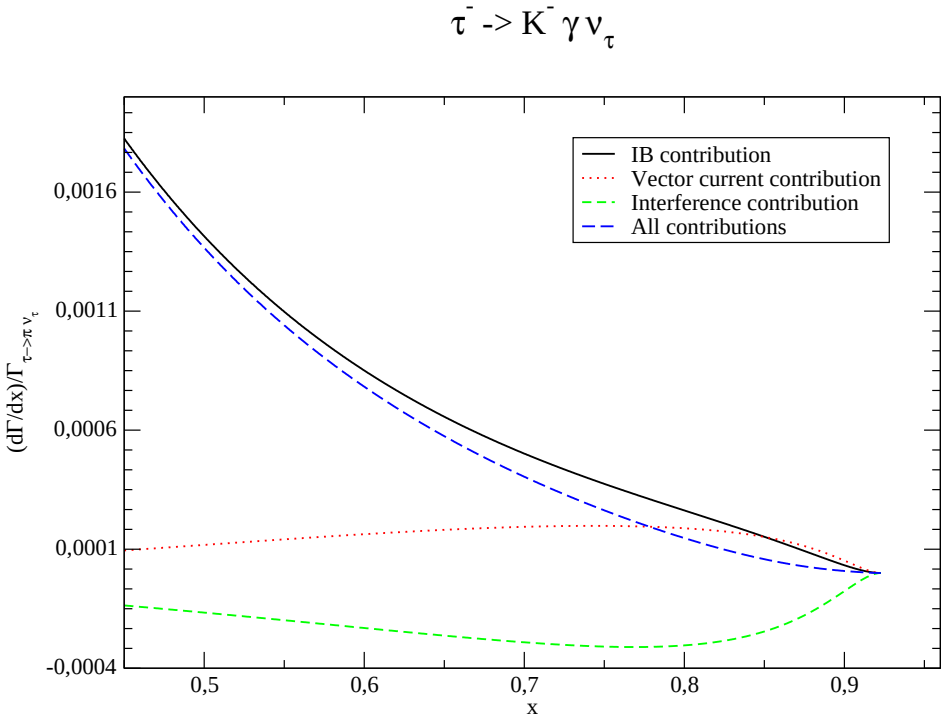

Figure 9.8: Differential decay width of the process $\tau^- \to K^-\gamma\nu_\tau$ including only the model independent contributions for a cut-off on the photon energy of 400 MeV. In the vector form factor only the WZW term (where the axial-vector contribution is absent) is considered for this estimate.

	$x_0 = 0.0565$	$x_0 = 0.45$
IB	$13.09 \cdot 10^{-3}$	$1.48 \cdot 10^{-3}$
$IB - V$	$0.02 \cdot 10^{-3}$	$0.04 \cdot 10^{-3}$
$IB - A$	$0.34 \cdot 10^{-3}$	$0.29 \cdot 10^{-3}$
VV	$0.99 \cdot 10^{-3}$	$0.73 \cdot 10^{-3}$
VA	~ 0	$0.02 \cdot 10^{-3}$
AA	$0.15 \cdot 10^{-3}$	$0.14 \cdot 10^{-3}$
ALL	$14.59 \cdot 10^{-3}$	$2.70 \cdot 10^{-3}$

Table 9.1: Contribution of the different parts to the total rate, using two different cut-offs for the photon energy: $E_\gamma = 50$ MeV ($x_0 = 0.0565$) and $E_\gamma = 400$ MeV ($x_0 = 0.45$).

to be negative as driven by $IB - V$ there. In the whole spectrum only the ρ resonance manifests as a peak and one can barely see the signal of the a_1, mainly due to its broad width and to the counter effect of interferences.

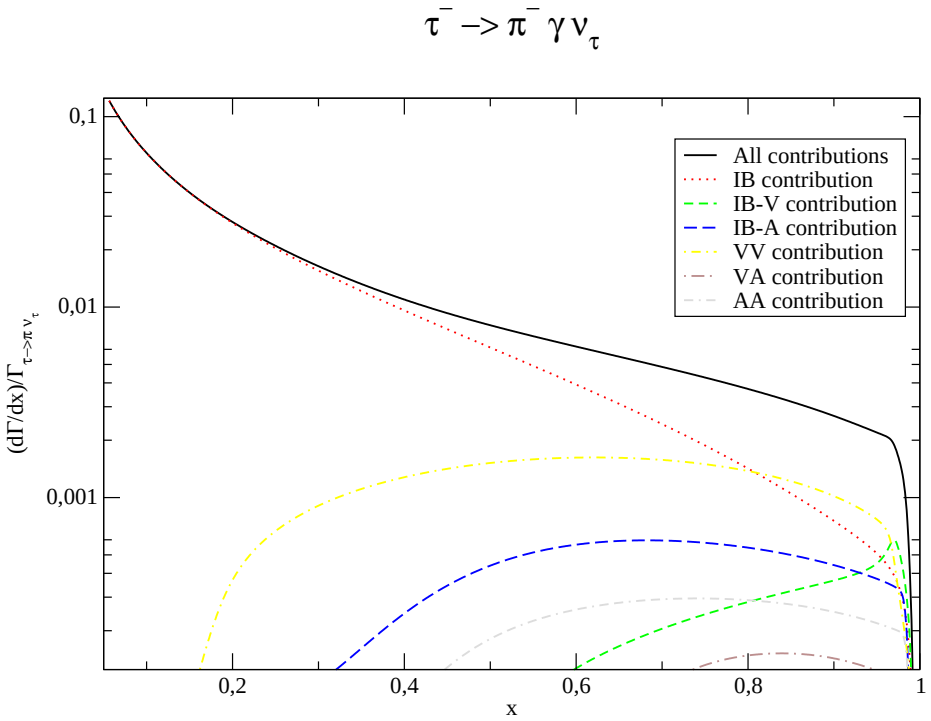

Figure 9.9: Differential decay width of the process $\tau^- \to \pi^-\gamma\nu_\tau$ including all contributions for a cut-off on the photon energy of 50 MeV.

9.5.3 Results including resonance contributions in the K channel

Next we turn to the $\tau^- \to K^-\gamma\nu_\tau$ channel. In this case, there are several sources of uncertainty that make our prediction less controlled than in the $\tau^- \to \pi^-\gamma\nu_\tau$ case. We comment them in turn.

Concerning the vector form factor contribution, there is no uncertainty associated to the vector resonances off-shell widths, that are implemented as done in previous applications and described in Appendix C. It turns out that the SD part is extremely sensitive to c_4. We have observed that the VV contribution is much larger (up to one order of magnitude, even for a low-energy cut-off) than the IB one for $c_4 \sim -0.07$, a feature that is unexpected. In this case, one would also see a prominent bump in the spectrum, contrary to the typical monotonous fall driven by the IB term. For smaller values of $|c_4|$ (which are suggested by the comparison to *Belle* data on $\tau \to KK\pi\nu_\tau$ decays) this bump reduces its magnitude and finally disappears. One should also not forget that the addition of a second multiplet of resonances may vary this conclusion.

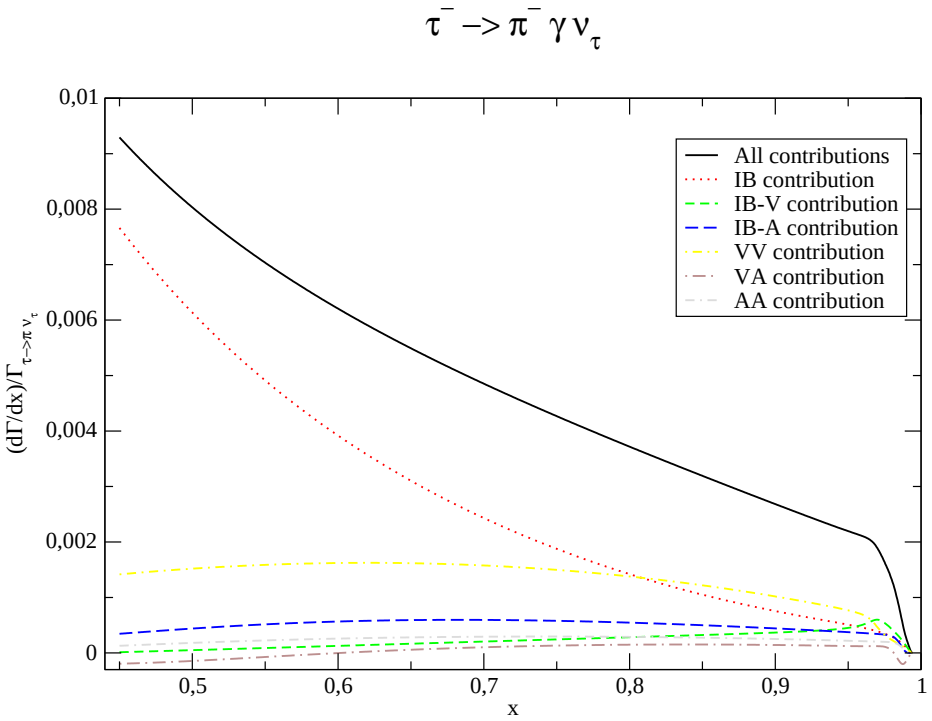

Figure 9.10: Differential decay width of the process $\tau^- \to \pi^-\gamma\nu_\tau$ including all contributions for a cut-off on the photon energy of 400 MeV.

The uncertainty in the axial-vector form factors is two-folded: on one side there is a broad band of allowed values for θ_A, as discussed at the beginning of this section. On the other hand, since we have not performed the analyses of the decay $\tau \to K\pi\pi\nu_\tau$ modes yet, we do not have an off-shell width derived from a Lagrangian for the K_{1A} resonances. In the $\tau \to 3\pi\nu_\tau$ decays, Γ_{a_1} has the starring role. Since the K_{1A} meson widths are much smaller (90 ± 20 MeV and 174 ± 13 MeV, for the $K_1(1270)$ and $K_1(1400)$, respectively) and they are hardly close to the on-shell condition, the rigorous description of the width is not an unavoidable ingredient for a reasonable estimate.

With respect to the two uncertainties just commented, we have checked that the branching ratio contribution by AA (that is subdominant) is $\sim 20\%$ higher for the $|\theta_A| \sim 37^\circ$ solution. In this case, the corresponding AA differential distribution peaks at a slightly larger x, and the curve is lower in the $0.40 \leftrightarrow 0.55$ region. In any case, different choices of $|\theta_A|$ can barely influence the final conclusions, as it is illustrated in Table 9.2.

For the K_{1A} off-shell widths we will follow Ref. [529] and use

$$\Gamma_{K_{1A}}(t) \;=\; \Gamma_{K_{1A}}(M^2_{K_{1A}})\,\frac{M^2_{K_{1A}}}{t}\,\frac{\sigma^3_{M_{K^*}m_\pi}(t)+\sigma^3_{M_\rho m_K}(t)}{\sigma^3_{M_{K^*}m_\pi}(M^2_{K_{1A}})+\sigma^3_{M_\rho m_K}(M^2_{K_{1A}})}\,, \tag{9.35}$$

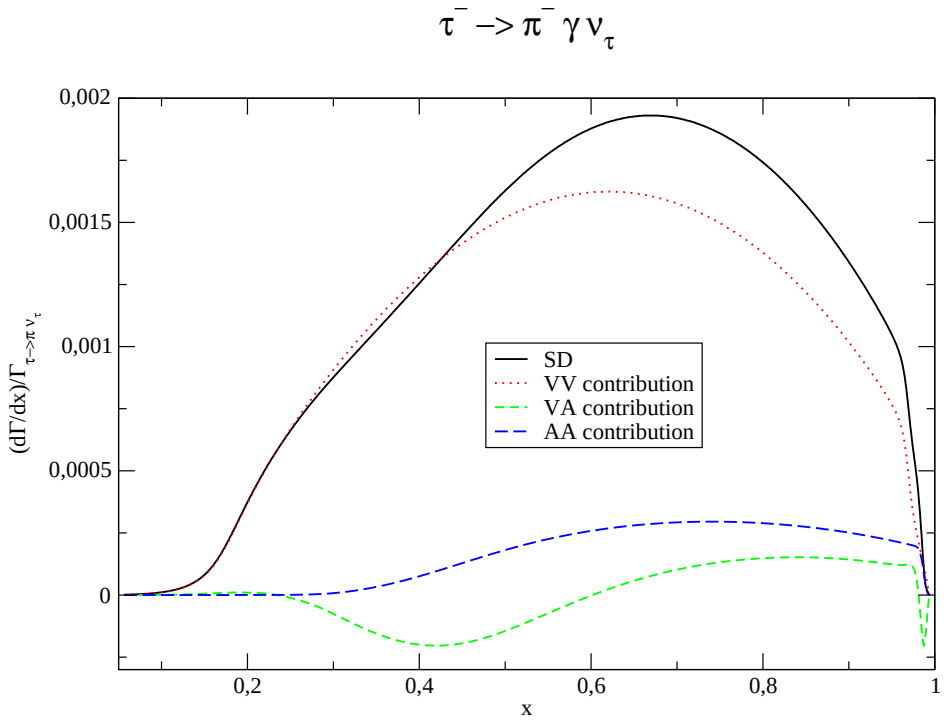

Figure 9.11: Differential decay width of the process $\tau^- \to \pi^-\gamma\nu_\tau$ including only the structure dependent contributions for a cut-off on the photon energy of 50 MeV.

	$x_0 = 0.0565$ $c_4 = -0.07$ $\lvert\theta_A\rvert = 58°(37°)$	$x_0 = 0.0565$ $c_4 = 0$ $\lvert\theta_A\rvert = 58°(37°)$	$x_0 = 0.45$ $c_4 = -0.07$ $\lvert\theta_A\rvert = 58°(37°)$	$x_0 = 0.45$ $c_4 = 0$ $\lvert\theta_A\rvert = 58°(37°)$
IB	$3.64 \cdot 10^{-3}$	$3.64 \cdot 10^{-3}$	$0.31 \cdot 10^{-3}$	$0.31 \cdot 10^{-3}$
$IB - V$	$0.69 \cdot 10^{-3}$	$0.10 \cdot 10^{-3}$	$0.83 \cdot 10^{-3}$	$0.12 \cdot 10^{-3}$
$IB - A$	$0.22(0.25) \cdot 10^{-3}$	$0.22(0.25) \cdot 10^{-3}$	$0.15(0.18) \cdot 10^{-3}$	$0.15(0.18) \cdot 10^{-3}$
VV	$58.55 \cdot 10^{-3}$	$1.30 \cdot 10^{-3}$	$29.04 \cdot 10^{-3}$	$0.66 \cdot 10^{-3}$
VA	$\sim 0(\sim 0)$	$\sim 0(\sim 0)$	$0.09(0.09) \cdot 10^{-3}$	$0.01(0.01) \cdot 10^{-3}$
AA	$0.13(0.16) \cdot 10^{-3}$	$0.13(0.16) \cdot 10^{-3}$	$0.12(0.15) \cdot 10^{-3}$	$0.12(0.15) \cdot 10^{-3}$
ALL	$63.23(63.29) \cdot 10^{-3}$	$5.39(5.45) \cdot 10^{-3}$	$30.54(30.60) \cdot 10^{-3}$	$1.37(1.43) \cdot 10^{-3}$

Table 9.2: Contribution of the different parts to the total rate in the decay $\tau^- \to K^-\gamma\nu_\tau$ (in unit of $\Gamma_{\tau\to K\nu}$), using two different cut-offs for the photon energy: $E_\gamma = 50$ MeV ($x_0 = 0.0565$) and $E_\gamma = 400$ MeV ($x_0 = 0.45$) and also different values of the resonance couplings. The numbers inside the parentheses denote the corresponding results with $|\theta_A| = 37°$, while the other numbers are obtained with $|\theta_A| = 58°$.

where

$$\sigma_{PQ}(x) \;=\; \frac{1}{x}\sqrt{(x-(P+Q)^2)\,(x-(P-Q)^2)}\theta\left[x-(P-Q)^2\right]\;. \qquad (9.36)$$

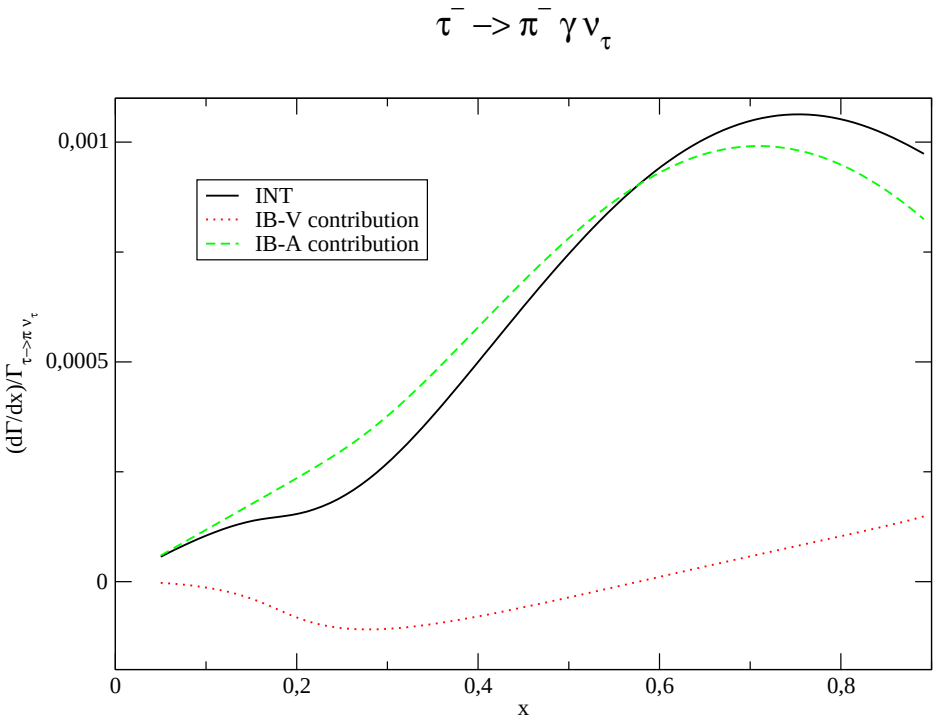

Figure 9.12: Differential decay width of the process $\tau^- \to \pi^-\gamma\nu_\tau$ including only the interference contributions for a cut-off on the photon energy of 50 MeV.

Considering all the sources of uncertainty commented, we will content ourselves with giving our predictions for the two limiting cases of $c_4 = -0.07$ and $c_4 = 0$. We present the analogous plots to those we discussed in the $\tau^- \to \pi^-\gamma\nu_\tau$ channel for both c_4 values.

9.6 Conclusions

In this chapter we have studied [303] the radiative one-meson decays of the τ: $\tau^- \to (\pi/K)^-\gamma\nu_\tau$. We have computed the relevant form factors for both channels and obtained the asymptotic conditions on the couplings imposed by the high-energy behaviour of these form factors, dictated by QCD. The relations that we have

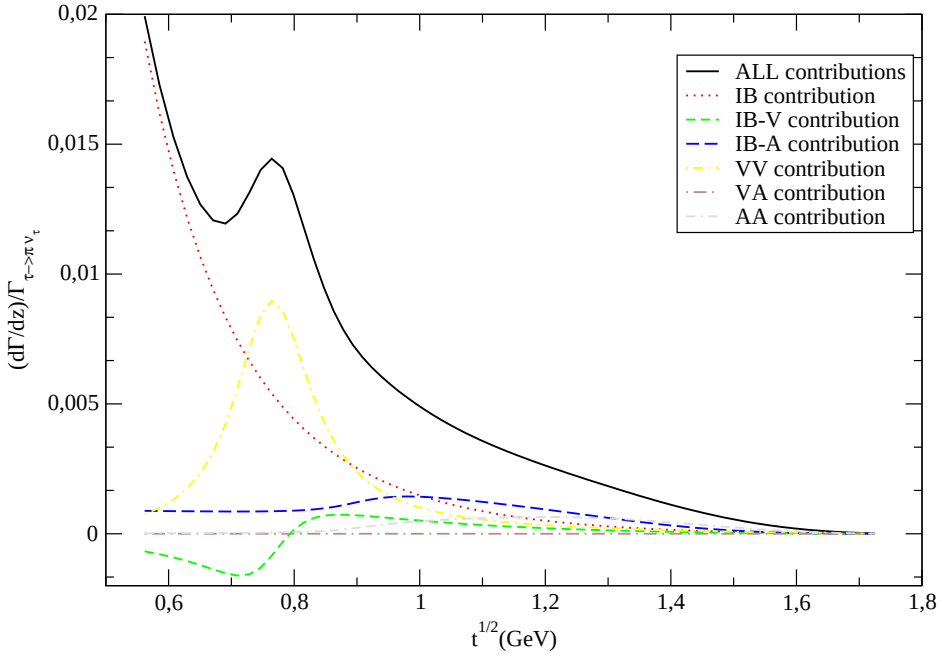

Figure 9.13: Pion-photon invariant mass spectrum of the process $\tau^- \to \pi^-\gamma\nu_\tau$ including all contributions. The VA contribution vanishes identically as explained in the main text.

found here are compatible with those obtained in previous chapters in the other phenomenological applications considered in this Thesis.

One of our motivations to examine these processes is that they have not been detected yet, according to naive estimates or to Breit-Wigner parametrizations. We have checked the existing computations for the IB part. Adding to it the WZW contribution, that is the LO contribution in χPT coming from the QCD anomaly, we have estimated the model independent contribution to both decays, that could be taken as a lower bound. The values that we obtain for the π channel are at least one order of magnitude above the already-observed $3K$ decay channel even for a high-energy cut-off on the photon energy. In the K channel, the model independent contribution gives a BR larger than that of the $3K$ decay channel, as well. Only imposing a large cut-off on E_γ one could understand that the latter mode has not been detected so far. We expect, then, that future measurements at B-factories will bring us the discovery of these tau decay modes in the near future.

We do not have any free parameter in the $\tau^- \to \pi^-\gamma\nu_\tau$ decay and that allowed us to make a complete study. Since the IB contribution dominates, it will require some statistics to study the SD effects. In this sense, the analysis of the $\pi - \gamma$ spectrum (t-spectrum) is more promising than that of the pure photon spectrum (x-spectrum), as we have shown. We are eager to see if the discovery of this mode confirms our findings, since we believe that the uncertainties of our study are small

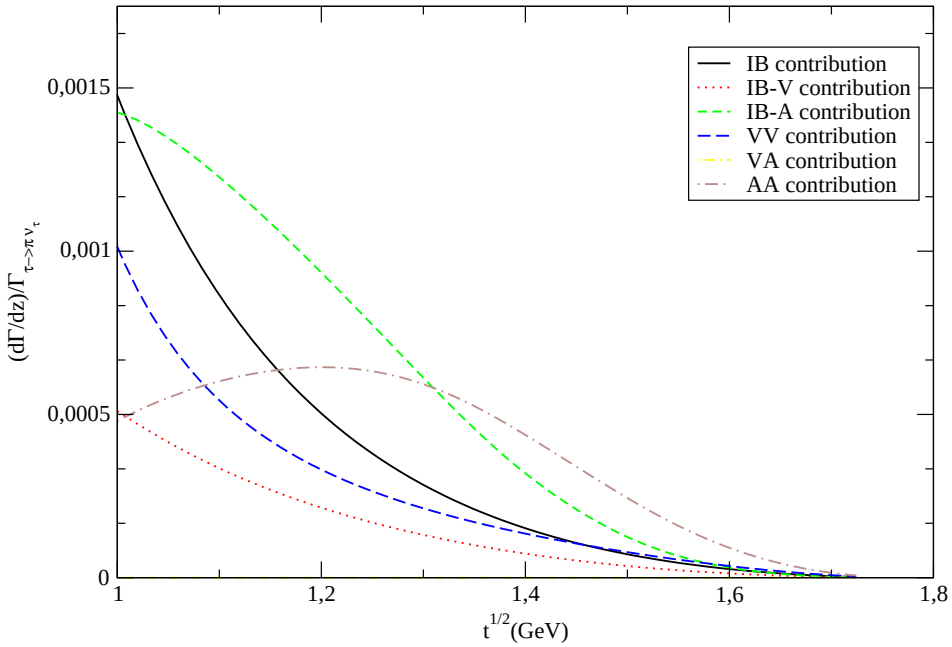

Figure 9.14: Close-up of the pion-photon invariant mass spectrum of the process $\tau^- \to \pi^-\gamma\nu_\tau$ including all contributions for $\sqrt{t} \gtrsim 1$ GeV. The VA contribution vanishes identically as explained in the main text.

for this channel.

As expected, the higher mass of the Kaon makes easier the observation of SD effects. However, there are several sources of uncertainty in the $\tau^- \to K^-\gamma\nu_\tau$ decays that prevent us from having done any quantitative analysis. The most important one either rises some doubts about the value of c_4, a parameter describing the $SU(3)$ breaking effect, obtained in Ref. [304] or on the sufficiency of one multiplet of vector resonances to describe this decay. As we have shown, the value of this coupling affects drastically the strength of the VV (and thus the whole SD) contribution. Besides, there is an uncertainty associated to the broad band of allowed values for θ_A. However since the AA contribution is anyway subleading, that one is negligible with respect to that on c_4. Even smaller is the error associated to the off-shell width behaviour of the axial-vector neutral resonance with strangeness, $K_{1H,L}$. Since we have not calculated the relevant three meson decay of the tau, we do not have this expression within $R\chi T$ yet. We took a simple parametrization including the on-shell cuts corresponding to the decay chains $K_{1H,L} \to (\rho K/K^*\pi)$. Since the effect of c_4 is so large, we expect that once it is discovered we will be able to bound this coupling.

As an application of this work, we are working out [303] the consequences of our study in lepton universality tests through the ratios $\Gamma(\tau^- \to \pi^-\nu_\tau\gamma)/\Gamma(\pi^- \to \mu^-\nu_\mu\gamma)$ and $\Gamma(\tau^- \to K^-\nu_\tau\gamma)/\Gamma(K^- \to \mu^-\nu_\mu\gamma)$ that were also considered by DF [342] and Marciano and Sirlin [30, 539, 540]. The ratio between the decays in the denomi-

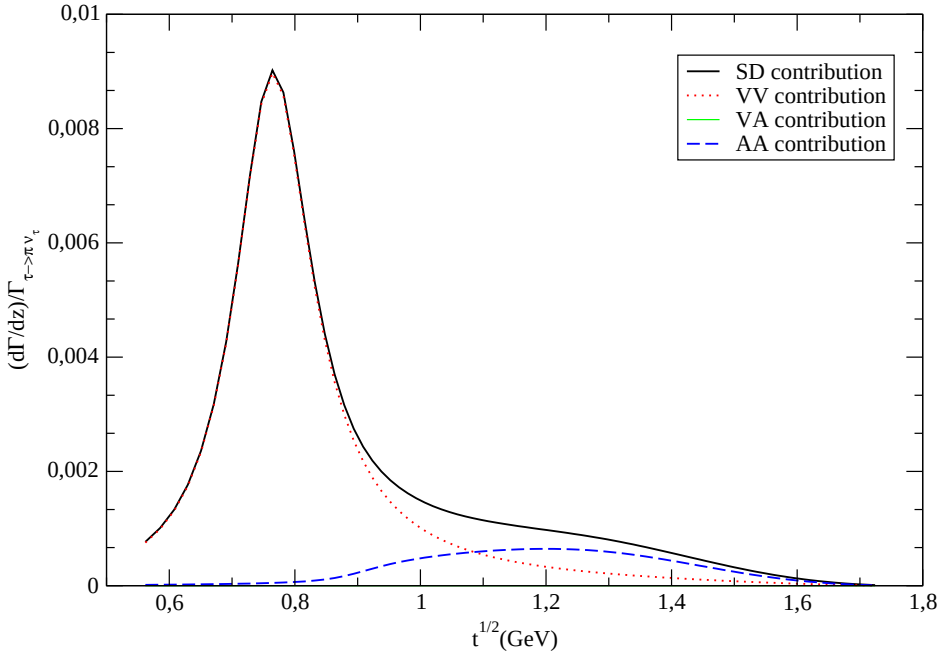

Figure 9.15: Pion-photon invariant mass spectrum of the process $\tau^- \to \pi^-\gamma\nu_\tau$ including only the SD contributions. The VA contribution vanishes identically as explained in the main text.

nators within χPT have been studied by Cirigliano and Rosell [541, 542] and the radiative pion decay within $R\chi T$ by Mateu and Portolés [323] recently.

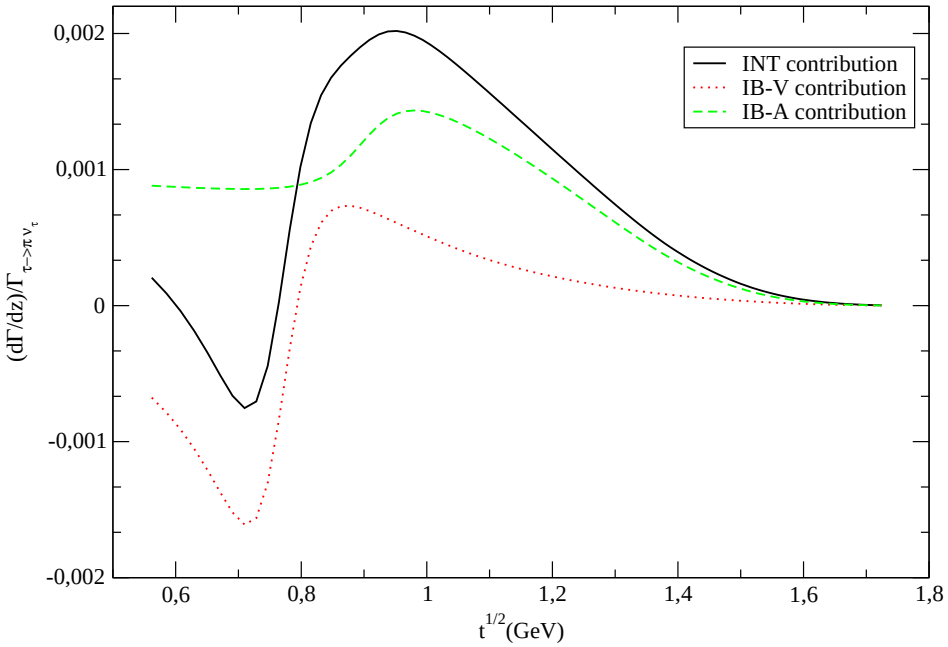

Figure 9.16: Pion-photon invariant mass spectrum of the process $\tau^- \to \pi^-\gamma\nu_\tau$ including only the interference contributions .

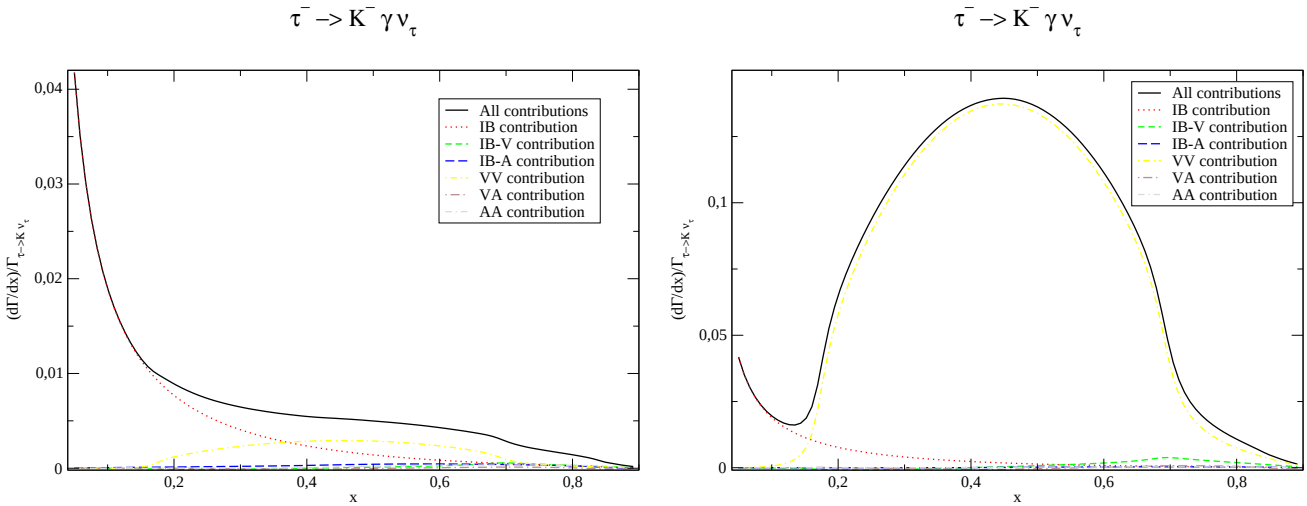

Figure 9.17: Differential decay width of the process $\tau^- \to K^-\gamma\nu_\tau$ including all contributions for a cut-off on the photon energy of 50 MeV and $c_4 = 0$ (left pane) and $c_4 = -0.07$ (right pane).

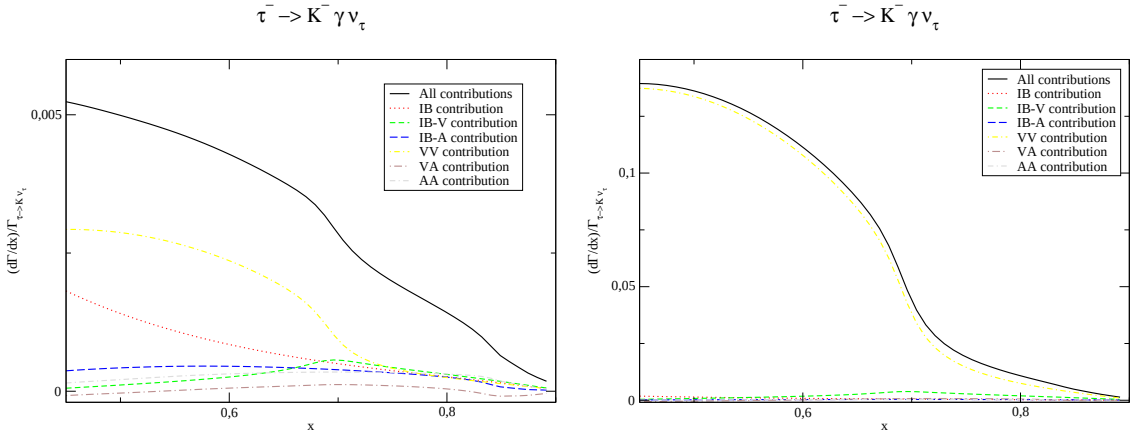

Figure 9.18: Differential decay width of the process $\tau^- \to K^-\gamma\nu_\tau$ including all contributions for a cut-off on the photon energy of 400 MeV and $c_4 = 0$ (left pane) and $c_4 = -0.07$ (right pane).

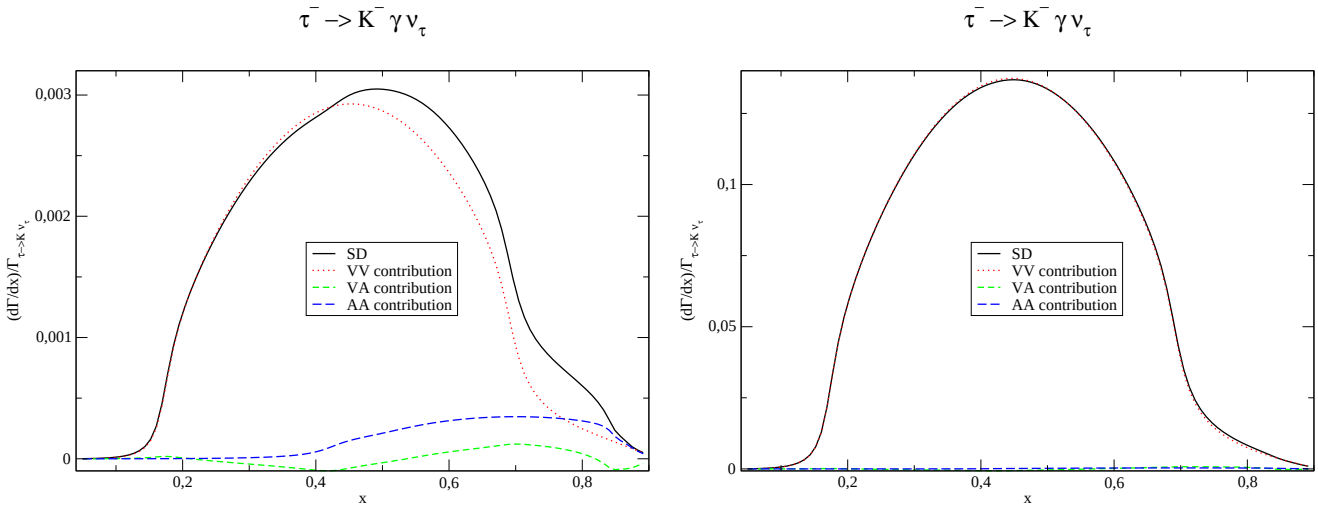

Figure 9.19: Differential decay width of the process $\tau^- \to K^-\gamma\nu_\tau$ including only the structure dependent contributions for a cut-off on the photon energy of 50 MeV and $c_4 = 0$ (left pane) and $c_4 = -0.07$ (right pane).

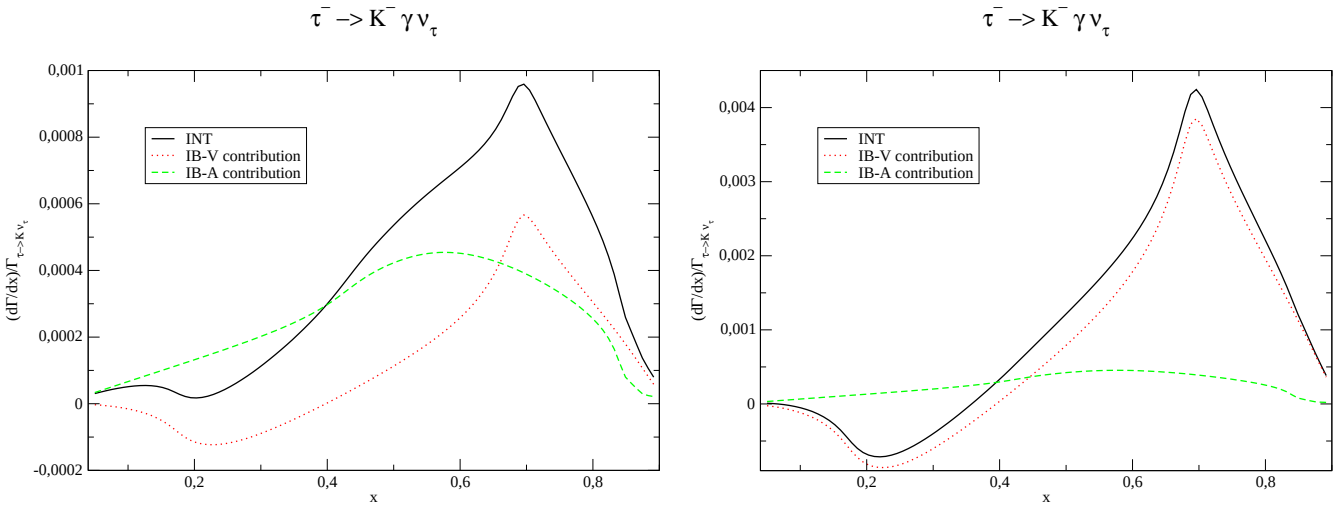

Figure 9.20: Differential decay width of the process $\tau^- \to K^-\gamma\nu_\tau$ including only the interference contributions for a cut-off on the photon energy of 50 MeV and $c_4 = 0$ (left pane) and $c_4 = -0.07$ (right pane).

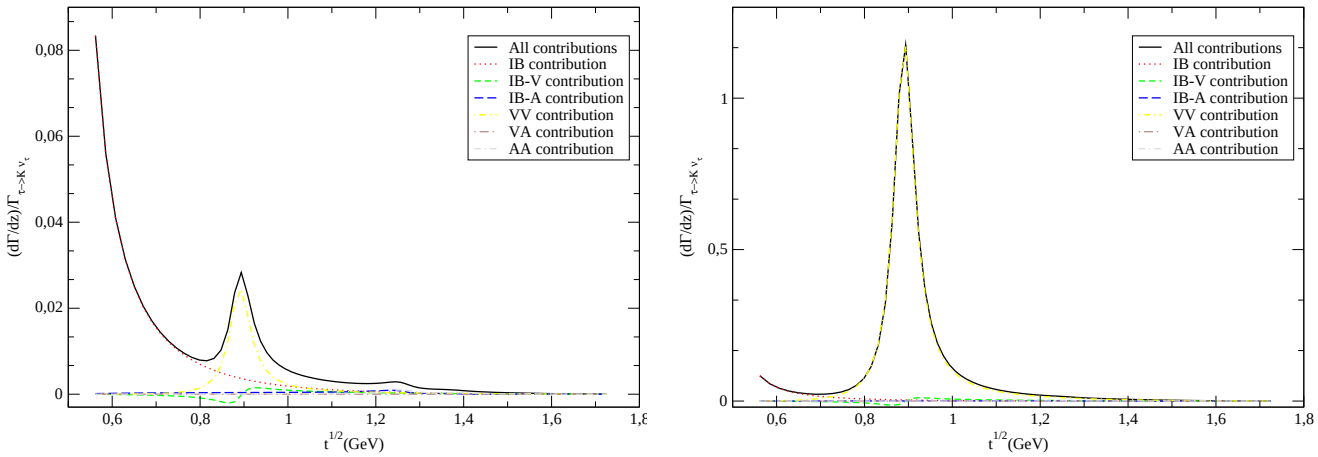

Figure 9.21: Kaon-photon invariant mass spectrum of the process $\tau^- \to K^-\gamma\nu_\tau$ including all contributions for $c_4 = 0$ (left pane) and $c_4 = -0.07$ (right pane). The VA contribution vanishes identically as explained in the main text.

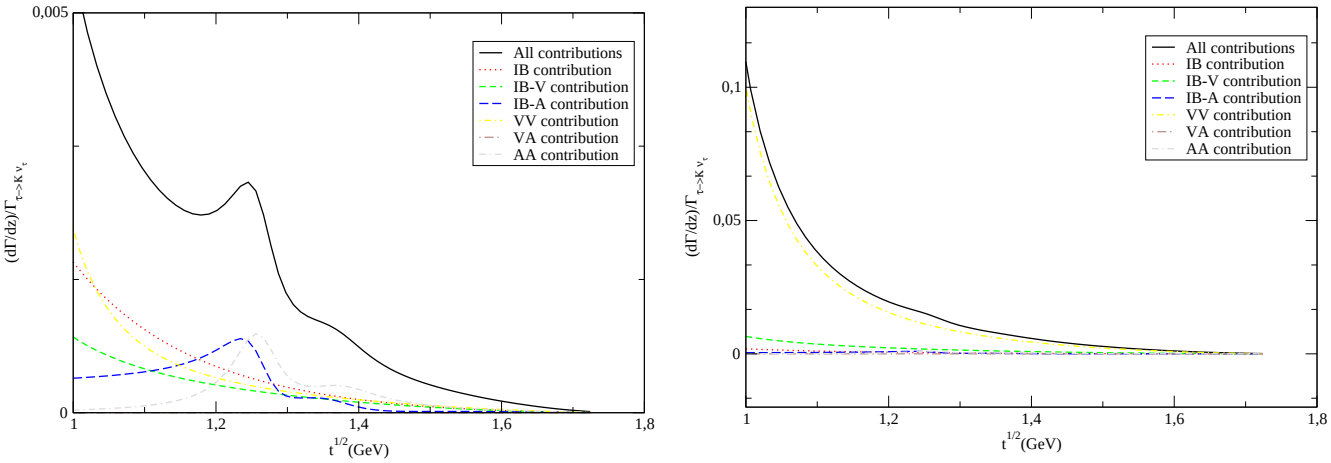

Figure 9.22: Close-up of the Kaon-photon invariant mass spectrum of the process $\tau^- \to K^-\gamma\nu_\tau$ including all contributions for $\sqrt{t} \gtrsim 1$ GeV and for $c_4 = 0$ (left pane) and $c_4 = -0.07$ (right pane). The VA contribution vanishes identically as explained in the main text.

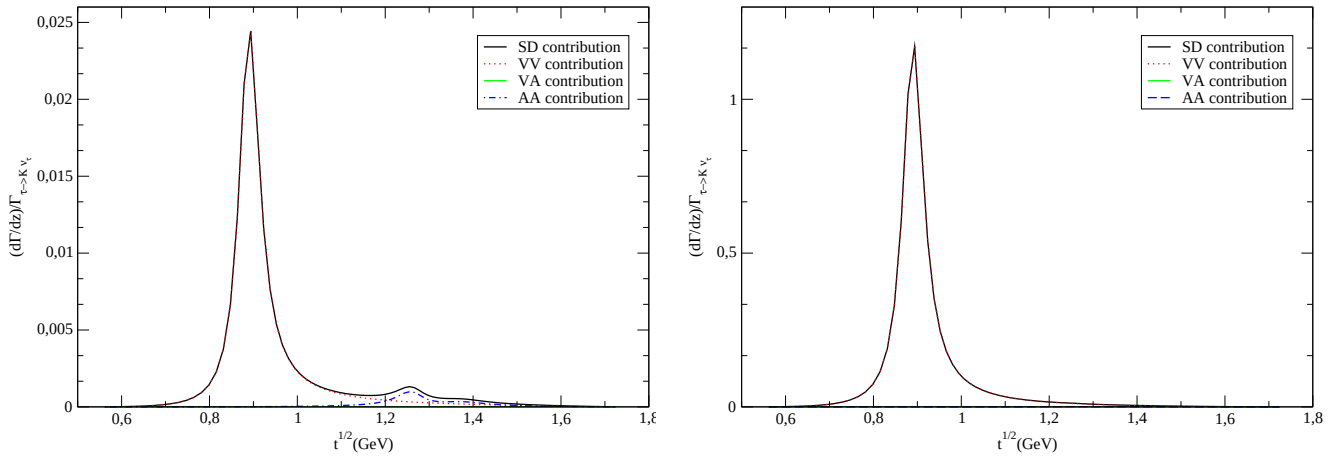

Figure 9.23: Kaon-photon invariant mass spectrum of the process $\tau^- \to K^-\gamma\nu_\tau$ including only the SD contributions for $c_4 = 0$ (left pane) and $c_4 = -0.07$ (right pane). The VA contribution vanishes identically as explained in the main text.

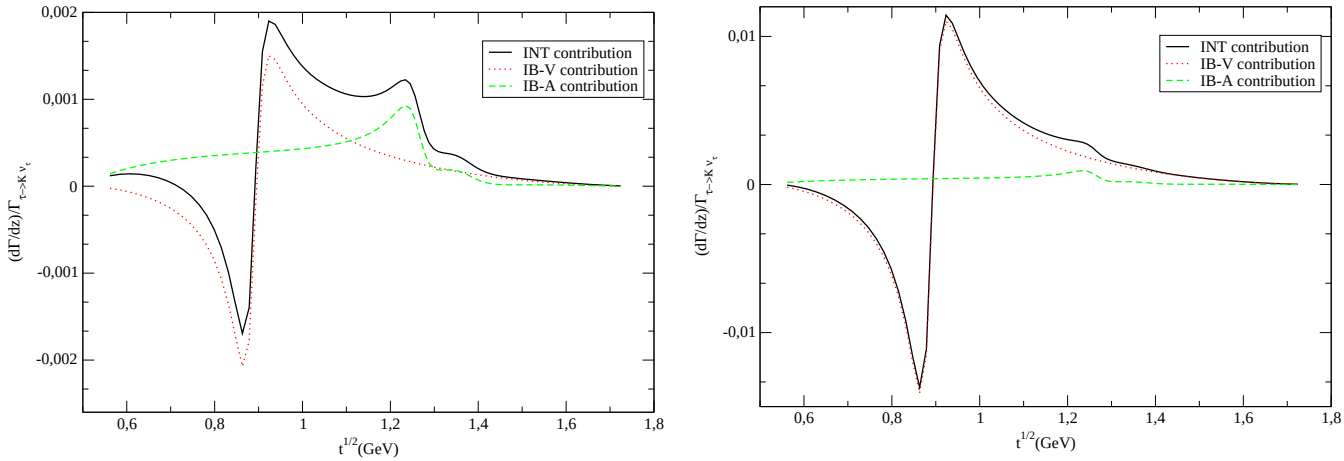

Figure 9.24: Kaon-photon invariant mass spectrum of the process $\tau^- \to \pi^-\gamma\nu_\tau$ including only the interference contributions for $c_4 = 0$ (left pane) and $c_4 = -0.07$ (right pane).

Conclusions

In this Thesis we have studied some decays of the τ into hadrons. Besides their intrinsic interest we were motivated by the possibility of learning about QCD hadronization in a clean environment provided by the $\tau - \nu_\tau - W$ coupling that keeps part of the process unpolluted from QCD. Moreover, since the resonances are not asymptotic states this kind of processes is an ideal tool to learn about their properties since its influence through exchange between the L^μ current and the final state mesons is sizable. Another target of our study was to provide the experimental community with an adequate theoretical tool to analyze these decays, in a time where there has been a lot of works from the B-factories $BaBar$ and $BELLE$ and the upgrade of the latter and the future results from $BES-III$ seem to point to an even more productive era. Since the description of hadron currents in the Monte Carlo generator $TAUOLA$ needed an improvement we wanted to work in this direction, as well. Finally, the low-energy e^+e^- cross section in the Monte Carlo generator $PHOKHARA$ [543] did not have all desirable low-energy constraints implemented for some modes [445, 544, 545, 546]. With the new efforts to measure with great precision this cross section exclusively in $VEPP$, $DA\Phi NE$ and the B-factories there was also a need to improve this low-energy interval of the form factors. We have worked in all these directions with the results that are summarized in the following.

Our task is rather non-trivial from the theoretical point of view since: first, the fundamental theory, QCD is written in terms of hadrons, while we measure mesons. Second, a perturbative expansion in the coupling constant of the QCD Lagrangian will not converge at the low and intermediate energies we are interested in so that we need to find an alternative expansion parameter to work in an EFT framework using the active fields in this range of energies as degrees of freedom and keeping the symmetries of the fundamental theory. Third, although it is clear how to build an EFT for low-energy QCD based on the approximate chiral symmetry of this subsector, it is not so when going to higher energies. Four, a promising parameter, as it is $1/N_C$, succeeds in explaining qualitatively the most salient features of meson phenomenology but it is difficult to apply it quantitatively since its predictions at lowest order are contradictory to the Weinberg's approach to $EFTs$: while LO in the $1/N_C$ expansion predicts an infinite tower of infinitely narrow resonances, the $EFTs$ require just the relevant fields. Besides, only a few excited resonances are known for every set of quantum numbers so there is no model independent way to satisfy the $N_C \to \infty$ requirements, either. As a conclusion on this point we must admit that it will be necessary to model the $1/N_C$ expansion. One realizes that we

have traded the problem of not having a suitable expansion parameter by having it, although lacking an unambiguous way to perform the expansion even cutting it at lowest order.

From the phenomenological point of view there are also some subtleties that require a caveat: while for some decay modes there is already a lot of very precise information that allow us to do a precision study ($\tau \to \pi\pi\nu_\tau$, $\tau \to K\pi\nu_\tau$, $\tau \to \pi\pi\pi\nu_\tau$), for other modes the situation is not that clear , like for instance the $\tau \to KK\pi\nu_\tau$ decays that would have helped to fix the vector current sector. Since that was not possible we turned to the channels $\tau \to \eta\pi\pi\nu_\tau$ where there is only vector current contribution in the isospin conserved limit that proved to be helpful. One should also bear in mind that the interplay between Monte Carlo generation and signal extraction is important and since the Monte Carlo relies on a given model for the signal to background splitting this brings in additional uncertainties, specially in the case where both currents can in principle contribute sizably to the decay as in $\tau \to KK\pi\nu_\tau$, or in rare decays where there can be an important background in some phase space corners from other modes. All this would suggest the following approach: The Monte Carlo generators having some variety of reasonable hadron currents and the fit to all relevant modes being made at a time. Since this is not possible yet, one should not take all conclusions from partial studies as definitive.

The considerations in the two previous paragraphs do not mean at all that there is no point in carrying these investigations on. The essential thing will be to recognize which conclusions are firm and which can be affected by any of the errors commented above. Our approach has as many QCD features as we have been able to capture and they are more than in other approaches which justifies our labor and brings in its interest. We will emphasize its virtues next.

Our approach includes the right low-energy behaviour inherited from χPT. This is essential because a mismatch there is carried on by the rest of the curves. It follows the ideas of the large-N_C limit of QCD and implements them in order to have a theory of mesons: including the lighter *pGbs* and the light-flavoured resonances. Therefore it has the relevant degrees of freedom to describe the problem. The theory built upon symmetries does not have yet all QCD features we can implement. To do so, we require a Brodsky-Lepage behaviour to the form factors. This warrants the right short-distance behaviour and determines some couplings which makes the theory more predictable. Our approach to the large-N_C limit of QCD is guided by simplicity on the spectrum (we include the least number of degrees of freedom that allow for a description of the data) and by the off-shell widths that are derived within $R\chi T$. In the remainder of the introduction we highlight the most relevant contributions we have made during our study.

First of all, we have fixed the axial-vector current sector making theoretical predictions and the description of observables compatible. There was an inconsistency between the relations obtained in the Green function $< VAP >$ and the description of the $\tau \to \pi\pi\pi\nu_\tau$ observables. We have found the way to understand both at a time and, remarkably, these relations do not only hold for all tau decays into three mesons and for the $\langle VAP \rangle$ Green function but also for the radiative decays $\tau \to (\pi/K)\gamma\nu_\tau$

which we take as a confirmation of our picture and of the assumptions we have made concerning the modelization of the large-N_C limit of QCD in a meson theory.

A fundamental result coming from both the $\tau \to \pi\pi\pi\nu_\tau$ and $\tau \to KK\pi\nu_\tau$ studies is the off-shell width of the axial-vector meson Γ_{a_1}. It incorporates all 3π and $KK\pi$ cuts and it neglects the $\eta\pi\pi$ cut that vanishes in the isospin limit because of G-parity and the $\eta\eta\pi$ cut whose upper br limit is tiny. $\Gamma_{a_1}(Q^2)$ and the $\tau \to \pi\pi\pi\nu_\tau$ form factors have been implemented in $TAUOLA$. The agreement is better than the error associated to the statistical sampling and at the level of few per thousand.

We provide our prediction for additional observables both for $\tau \to \pi\pi\pi\nu_\tau$ and $\tau \to KK\pi\nu_\tau$ that could be confronted to forthcoming data. On the latter channel there is however some ambiguity because in addition to the short-distance relations we obtained we borrowed two of them from the study of the $< VVP >$ Green function and this is an assumption. However lacking of a prediction for the spectra (we could not even digitize the published plots since they corresponded to raw mass data without the efficiency corrections implemented) we decided to make them since we have observed that the departure observed between short-distance relations affecting the vector current couplings in three-point Green functions and three-meson tau decays was small.

With this approach we have given our prediction for the relevant observables in the $KK\pi$ channels and we showed that, contrary to some previous determinations, the vector current contribution can not be neglected in these decays. Since we have convincing reasons to believe that the description of the axial-vector current is pretty accurate, we think that this conclusion is firm. On the contrary, there can be some changes in the shape of the curves due to the assumption commented in the previous paragraph. This only data will tell. Our parametrization for the hadron form factors in the $\tau \to KK\pi\nu_\tau$ has been implemented in $TAUOLA$ to a great level of precision. We have decided to allow for some freedom in the assumptions on the relations among couplings that we commented before.

The study of the decays $\tau \to \eta\pi\pi\nu_\tau$ has bring us information about two previously undetermined couplings. We have determined an allowed ellipse where they can be and illustrated with some benchmark points the impact of them on the spectra. The experimental data has allowed us to favour one of the benchmark scenarios that we considered and refine our determination fitting *Belle* data. If our description of the former process is correct we believe that the upper bound on the decay $\tau \to \eta'\pi\pi\nu_\tau$ is wrong, and should be detected with some five times more br. Finally we have worked out isospin constraints and provided a prediction for the low-energy cross section $e^+e^- \to \eta\pi^+\pi^-$ that compares well to data in these regime. We have provided with our codes to the $PHOKHARA$ team. Symmetries make the $\tau \to \eta\eta\pi\nu_\tau$ decay a wonderful scenario to test the dominance of the spin-one resonances over those of spin 0. All exchanges of vector and axial-vector resonances are forbidden and then one only has the contribution from χPT at $\mathcal{O}(p^2)$. The discovery of this mode would allow to estimate in a clean environment the effect of scalar and pseudoscalar resonances in the future.

Finally, we have studied the radiative decays $\tau \to (\pi/K)\gamma\nu_\tau$. Since the axial-

vector current is completely controlled we have very firm conclusions. First, we have confirmed the earlier estimations: this mode has much larger br than some that have indeed been measured. Second, we have obtained our predictions for the observables. We obtain a VV contribution similar to earlier works but we obtain a much smaller AA contribution as corresponds to the well- behaved Γ_{a_1} that we used.

If we assume that the IB contribution should dominate up to the hard photon region, it seems that the channel $\tau \to K\gamma\nu_\tau$ suggests that the value of c_4 that was obtained from $\tau \to KK\pi\nu_\tau$ decays is too large. Since this coupling does not appear in the $\tau \to \eta^{(\prime)}\pi\pi\nu_\tau$ decays one should wait to analyze experimental data on the $KK\pi$ mode to understand this issue.

Among the appendixes there is some technical material. For instance the formulae needed to obtain the distributions $d\Gamma/ds_{ij}$ that were requested by the $BELLE$ collaboration for an ongoing study they are doing on the substructure of the $\tau \to KK\pi\nu_\tau$ decays [547]. There are two other appendixes concerning the relation of theoretical formulae to the experimental measurements. One can also find the complete set of isospin relations for three meson modes between $\sigma(e^+e^-)$ and τ decays and the computation of the process $\omega \to \pi^+\pi^-\pi^0$ that allowed us to fix another combination of couplings in the Lagrangian. For this purpose we needed to derive a new piece for the Resonance Chiral Theory Lagrangian. The other appendixes summarize theoretical information that helps to understand better the contents of this Thesis.

As final conclusions we would like to say that we are satisfied for many reasons: we have fixed the couplings of the axial-vector current sector of the $R\chi T$ Lagrangian and we have provided a precise description of the $\tau \to \pi\pi\pi\nu_\tau$ observables. This includes a sound description of the a_1 resonance width. We have improved the knowledge on the odd-intrinsic parity sector of the Resonance Lagrangian and applied it to some processes of interest. Future experimental data from $BaBar$, $Belle$ and BES could help us to proceed further in this direction. We have also worked in the application of these findings to the Monte Carlo generators for low-energy Physics. In particular, for $TAUOLA$ in tau decays and $PHOKHARA$ in the e^+e^- cross-section. Ideally this will result in a global fit to all relevant channels with an adequate splitting of signal and background accounting well for the pollution from other channels. We hope to be able to accomplish this program.

Appendix A: Structure functions in tau decays

Hadron and lepton tensors are Hermitian and can be expanded in terms of a set of 16 independent elements:

$$\mathcal{L}_{\mu\nu}\mathcal{H}^{\mu\nu} \,=\, \mathcal{L}^{00}\mathcal{H}^{00} - \mathcal{L}^{i0}\mathcal{H}^{i0} - \mathcal{L}^{0j}\mathcal{H}^{0j} + \mathcal{L}^{ij}\mathcal{H}^{ij}\,. \tag{A.1}$$

In order to isolate the different angular dependencies, it is convenient to introduce 16 combinations of defined symmetry, the so-called lepton (L_X) and hadron (W_X) structure functions. This way,

$$\mathcal{L}_{\mu\nu}\mathcal{H}^{\mu\nu} \,=\, \sum_X L_X W_X \,=\, 2(M_\tau^2 - Q^2)\sum_X \overline{L}_X W_X\,, \tag{A.2}$$

where X stands for A, B, C, D, E, F, G, H and I -the structure functions that collect (axial-)vector contributions- and also for the ones including information on the pseudoscalar form factor: SA, SB, SC, SD, SE, SF and SG. All of them are obtained through [346]:

$$\begin{aligned}
L_A \,&=\, \frac{\mathcal{L}^{11}+\mathcal{L}^{22}}{2}\,, \quad W_A \,=\, \mathcal{H}^{11}+\mathcal{H}^{22}\,,\\
L_B \,&=\, \mathcal{L}^{33}\,, \quad W_B \,=\, \mathcal{H}^{33}\,,\\
L_C \,&=\, \frac{\mathcal{L}^{11}-\mathcal{L}^{22}}{2}\,, \quad W_C \,=\, \mathcal{H}^{11}-\mathcal{H}^{22}\,,\\
L_D \,&=\, \frac{\mathcal{L}^{12}+\mathcal{L}^{21}}{2}\,, \quad W_D \,=\, \mathcal{H}^{12}+\mathcal{H}^{21}\,,\\
L_E \,&=\, \frac{i}{2}(\mathcal{L}^{12}-\mathcal{L}^{21})\,, \quad W_E \,=\, -i(\mathcal{H}^{12}-\mathcal{H}^{21})\,,\\
L_F \,&=\, \frac{\mathcal{L}^{13}+\mathcal{L}^{31}}{2}\,, \quad W_F \,=\, \mathcal{H}^{13}+\mathcal{H}^{31}\,,\\
L_G \,&=\, \frac{i}{2}(\mathcal{L}^{13}-\mathcal{L}^{31})\,, \quad W_G \,=\, -i(\mathcal{H}^{13}-\mathcal{H}^{31})\,,\\
L_H \,&=\, \frac{\mathcal{L}^{23}+\mathcal{L}^{32}}{2}\,, \quad W_H \,=\, \mathcal{H}^{23}+\mathcal{H}^{32}\,,\\
L_I \,&=\, \frac{i}{2}(\mathcal{L}^{23}-\mathcal{L}^{32})\,, \quad W_I \,=\, -i(\mathcal{H}^{23}-\mathcal{H}^{32})\,;\\
L_{SA} \,&=\, \mathcal{L}^{00}\,, \quad W_{SA} \,=\, \mathcal{H}^{00}\,,
\end{aligned}$$

$$
\begin{aligned}
L_{SB} &= -\frac{\mathcal{L}^{10}+\mathcal{L}^{01}}{2}\,, \quad W_{SB} = H^{01}+\mathcal{H}^{10}\,,\\
L_{SC} &= -\frac{i}{2}(\mathcal{L}^{01}-\mathcal{L}^{10})\,, \quad W_{SC} = -i(\mathcal{H}^{01}-\mathcal{H}^{10})\,,\\
L_{SD} &= -\frac{\mathcal{L}^{02}+\mathcal{L}^{20}}{2}\,, \quad W_{SD} = \mathcal{H}^{02}+\mathcal{H}^{20}\,,\\
L_{SE} &= -\frac{i}{2}(\mathcal{L}^{02}-\mathcal{L}^{20})\, quad W_{SE} = -i(\mathcal{H}^{02}-\mathcal{H}^{20})\,,\\
L_{SF} &= -\frac{\mathcal{L}^{03}+\mathcal{L}^{30}}{2}\,, \quad W_{SF} = \mathcal{H}^{03}+\mathcal{H}^{30}\,,\\
L_{SG} &= -\frac{i}{2}(\mathcal{L}^{03}-\mathcal{L}^{30}) \quad , W_{SG} = -i(\mathcal{H}^{03}-\mathcal{H}^{30})\,.
\end{aligned}
\tag{A.3}
$$

In the hadron rest frame, with axis z and x aligned with the normal to the hadron plane and $\widehat{q}_3$, respectively; one has the relations:

$$
\begin{aligned}
&q_3^\mu = (E_3, q_3^x, 0, 0)\ ,\ q_2^\mu = (E_2, q_2^x, q_2^y, 0)\ ,\ q_1^\mu = (E_1, q_1^x, q_1^y, 0) \text{ with}\\
&E_i = \frac{Q^2 - s_i + m_i^2}{2\sqrt{Q^2}}\ ,\ q_3^x = \sqrt{E_3^2 - m_3^2}\,,\\
&q_2^x = \frac{2E_2E_3 - s_1 + m_2^2 + m_3^2}{2q_3^x}\ ,\ q_2^y = -\sqrt{E_2^2 - (q_2^x)^2 - m_2^2}\,,\\
&q_1^x = \frac{2E_1E_3 - s_2 + m_1^2 + m_3^2}{2q_3^x}\ ,\ q_1^y = \sqrt{E_1^2 - (q_1^x)^2 - m_1^2} = -q_2^y\,.
\end{aligned}
\tag{A.4}
$$

If we introduce the following variables:

$$
x_1 = V_1^x = q_1^x - q_3^x\ ,\ x_2 = V_2^x = q_2^x - q_3^x\ ,\ x_3 = V_1^y = q_1^y = -q_2^y\ ,\ x_4 = V_3^z = \sqrt{Q^2}x_3q_3^x\,,
\tag{A.5}
$$

it is straightforward to see that both descriptions either in terms of form factors [4] or structure functions are completely equivalent:

$$
\begin{aligned}
W_A &= (x_1^2+x_3^2)^2|F_1^A|^2 + (x_2^2+x_3^2)^2|F_2^A|^2 + 2(x_1x_2 - x_3^2)\Re e(F_1^AF_2^{A*})\,,\\
W_B &= x_4^2|F_4^V|^2\,,\\
W_C &= (x_1^2-x_3^2)^2|F_1^A|^2 + (x_2^2-x_3^2)^2|F_2^A|^2 + 2(x_1x_2 + x_3^2)\Re e(F_1^AF_2^{A*})\,,\\
W_D &= 2\left[x_1x_3|F_1^A|^2 - x_2x_3|F_2^A|^2 + x_3(x_2-x_1)\Re e(F_1^AF_2^{A*})\right]\,,\\
W_E &= -2x_3(x_1+x_2)\Im m(F_1^AF_2^{A*})\,,\\
W_F &= 2x_4\left[x_1\Im m(F_1^AF_4^{V*}) + x_2\Im m(F_2^AF_4^{V*})\right]\,,\\
W_G &= -2x_4\left[x_1\Re e(F_1^AF_4^{V*}) + x_2\Re e(F_2^AF_4^{V*})\right]\,,
\end{aligned}
$$

[4] As defined in Eq. (5.51).

$$
\begin{aligned}
W_H &= 2x_3x_4\left[\Im m(F_1^A F_4^{4*}) - \Im m(F_2^A F_4^{V*})\right] ,\\
W_I &= -2x_3x_4\left[\Re e(F_1^A F_4^{V*}) - \Re e(F_2^A F_4^{V*})\right] ;\\
W_{SA} &= Q^2|F_3^A|^2 ,\\
W_{SB} &= 2\sqrt{Q^2}\left[x_1\Re e(F_1^A F_3^{A*}) + x_2\Re e(F_2^A F_3^{A*})\right] ,\\
W_{SC} &= -2\sqrt{Q^2}\left[x_1\Im m(F_1^A F_3^{A*}) + x_2\Im m(F_2^A F_3^{A*})\right] ,\\
W_{SD} &= 2\sqrt{Q^2}x_3\left[\Re e(F_1^A F_3^{A*}) - \Re e(F_2^A F_3^{A*})\right] ,\\
W_{SE} &= -2\sqrt{Q^2}x_3\left[\Im m(F_1^A F_3^{A*}) - \Im m(F_2^A F_3^{A*})\right] ,\\
W_{SF} &= -2\sqrt{Q^2}x_4\left[\Im m(F_4^V F_3^{A*})\right] ,\\
W_{SG} &= -2\sqrt{Q^2}x_4\left[\Re e(F_4^V F_3^{A*})\right] .
\end{aligned}
\tag{A.6}
$$

The corresponding formulae for the two-meson decays of the tau can be found in Eq. (5.47) and for the decays into one pG and a spin-one resonance in Ref. [347].

Appendix B: $\frac{\mathrm{d}\Gamma}{\mathrm{d}s_{ij}}$ in three-meson tau decays

In this appendix we start from the expressions for the structure functions in three-meson tau decays derived in Sec. 5.4.1 and derive from them the formulae for the differential decay width with respect to the invariant masses of the different meson pairs, $\frac{\mathrm{d}\Gamma}{\mathrm{d}s_{ij}}$.

We will obtain expressions allowing to exchange at will the role of the Mandelstam variables s, t and u, Eqs. (B.10) and (B.11).

Clearly, one cannot exchange the orders of integration for the variables s and Q^2 in Eq. (5.63), since $s^{max} = s^{max}(Q^2)$.

Therefore, it is useful to perform a change in the integration variables so that any dependence in them is erased from the integration limits. It is the following:

$$\int_a^b dx = \int_0^1 (b-a)dy \longleftrightarrow x \equiv a + y(b-a)\,, dx = (b-a)dy\,. \tag{B.1}$$

In our case, this would be $\left(s \equiv (m_1+m_2)^2 + y\left[(\sqrt{Q^2}-m_3)^2 - (m_1+m_2)^2\right]\right)$:

$$\int_{(m_1+m_2)^2}^{(\sqrt{Q^2}-m_3)^2} ds = \int_0^1 dy \left[(\sqrt{Q^2}-m_3^2)^2 - (m_1+m_2)^2\right]\,, \tag{B.2}$$

so we will have:

$$\Gamma = \int_{(m_1+m_2+m_3)^2}^{(M_\tau-m_\nu)^2} dQ^2 \int_0^1 dy \int_{t_-(Q^2,y)}^{t^+(Q^2,y)} \left[(\sqrt{Q^2}-m_3)^2 - (m_1+m_2)^2\right] F(Q^2,y,t)\,, \tag{B.3}$$

and we can exchange the y and Q^2 integrations to write:

$$d\Gamma = \int_0^1 dy \int_{(m_1+m_2+m_3)^2}^{(M_\tau-m_\nu)^2} dQ^2 \int_{t_-(Q^2,y)}^{t^+(Q^2,y)} \tag{B.4}$$

whence:

$$\frac{d\Gamma}{dy} = \int_{(m_1+m_2+m_3)^2}^{(M_\tau-m_\nu)^2} dQ^2 \int_{t_-(Q^2,y)}^{t^+(Q^2,y)} \left[(\sqrt{Q^2}-m_3)^2 - (m_1+m_2)^2\right] F(Q^2,y,t)\,. \tag{B.5}$$

In order to have for y the physical limits s has, we perform a second change of variable, so that $s_{min} = (m_1 + m_2)^2$, but $s_{max} = (M_\tau - m_\nu - m_3)^2$, that is: $y \equiv \frac{s-(m_1+m_2)^2}{(M_\tau - m_\nu - m_3)^2 - (m_1+m_2)^2}$. Explicitly:

$$\begin{aligned}
&\int_{(m_1+m_2+m_3)^2}^{(M_\tau - m_\nu)^2} dQ^2 \int_{(m_1+m_2)^2}^{(\sqrt{Q^2}-m_3^2)^2} ds \int_{t_-(Q^2,s)}^{t^+(Q^2,s)} F(Q^2,s,t) = \\
&= \int_0^1 dy \int_{(m_1+m_2+m_3)^2}^{(M_\tau - m_\nu)^2} dQ^2 \int_{t_-(Q^2,y)}^{t^+(Q^2,y)} \left[(\sqrt{Q^2}-m_3^2)^2 - (m_1+m_2)^2\right] F(Q^2,y,t) = \\
&= \int_{(m_1+m_2)^2}^{(M_\tau - m_\nu - m_3)^2} ds \int_{(m_1+m_2+m_3)^2}^{(M_\tau - m_\nu)^2} dQ^2 \int_{t_-(Q^2,s)}^{t^+(Q^2,s)} F(Q^2,s,t) \times \\
&\frac{\left[(\sqrt{Q^2}-m_3^2)^2 - (m_1+m_2)^2\right]}{(M_\tau - m_\nu - m_3)^2 - (m_1+m_2)^2} \,. \qquad \text{(B.6)}
\end{aligned}$$

If one is interested in obtaining $\mathrm{d}\Gamma/\mathrm{d}s$, for instance, one may use the following expression:

$$\begin{aligned}
\frac{d\,\Gamma}{d\,s} \;=\; & \frac{G_F^2\,|V_{ij}^{CKM}|^2}{128\,(2\pi)^5\,M_\tau} \int dQ^2\,dt\,\left(\frac{M_\tau^2}{Q^2}-1\right)^2 J(Q^2)\left[W_{SA}(Q^2,\overline{s},t) + \frac{1}{3}\left(1+2\frac{Q^2}{M_\tau^2}\right)\right. \\
& \left.\left(W_A(Q^2,\overline{s},t) + W_B(Q^2,\overline{s},t)\right)\right] , \qquad \text{(B.7)}
\end{aligned}$$

where $\overline{s}$ is defined as [5]

$$\overline{s}(s,Q^2) \equiv (m_1+m_2)^2 + \frac{s-(m_1+m_2)^2}{(M_\tau - m_\nu - m_3)^2 - (m_1+m_2)^2}\left[\left(\sqrt{Q^2}-m_3\right)^2 - (m_1+m_2)^2\right] , \qquad \text{(B.8)}$$

and the factor $J(Q^2)$ is:

$$J(Q^2) \equiv \frac{\left(\sqrt{Q^2}-m_3\right)^2 - (m_1+m_2)^2}{(M_\tau - m_\nu - m_3)^2 - (m_1+m_2)^2} \,. \qquad \text{(B.9)}$$

The limits for the Q^2 remain unchanged, and t_{min}^{max} remain the same, provided one uses $\overline{s}$: $t_{min}^{max} = t_{min}^{max}(Q^2,\overline{s})$. In case one is interested in a projection different from the s-one, the indices 1,2,3 can be permuted ciclically and one can use the integration limits:

$${s_{ij}}_{min}^{max} \;=\; \frac{1}{4s_{jk}}\left\{\left(Q^2 - m_k^2 - m_i^2 + m_j^2\right)^2 - \left[\lambda^{1/2}\left(Q^2,s_{jk},m_i^2\right) \mp \lambda^{1/2}\left(m_j^2,m_k^2,s_{jk}\right)\right]^2\right\} , \qquad \text{(B.10)}$$

$$\begin{aligned}
{s_{jk}}_{min} \;=\; (m_j+m_k)^2 \;, {s_{jk}}^{max} \;=\; (\sqrt{Q^2}-m_i)^2 \;; \\
Q^2_{min} \;=\; (m_1+m_2+m_3)^2 \;, {Q^2}^{max} \;=\; (M_\tau - m_\nu)^2 \,. \qquad \text{(B.11)}
\end{aligned}$$

[5] From the following Eq. it is evident how to proceed with just one change of variables. However, I preferred to present it in two steps because of the general usefulness of the change in Eq. (B.1).

It may be convenient to use

$$\frac{d\,\Gamma}{d\,\sqrt{s}} \,=\, 2\,\sqrt{s}\frac{d\,\Gamma}{d\,s}\,. \tag{B.12}$$

It is worth to notice that the proposed expression (B.7) is efficient and fast when computing the integration, even with rather ellaborated structures for the form factors and realistic off-shell widths for the resonances.

Appendix C: Off-shell width of Vector resonances

C.1 Introduction

Resonance widths have a big importance in any process whose energy is able to reach its on-mass shell, specially if they are rather wide. Any sensible modelization of the process must take this into account. Masses and widths of particles depend on the conventions one employs and on the chosen formalism. We will explain in this appendix the approach we use and show that it is consistent with $R\chi T$ and general field theory arguments.

Since our work only includes spin-one resonances, we will not consider the case of scalar and pseudoscalar resonances. We will start by the easier case of vector resonances that involves, at lowest order, two-particle intemediate states. Then, we will consider the case of axial-vector resonances, where the three particle cuts give the first contribution.

C.2 Definition of a hadron off-shell width for vector resonances

In the antisymmetric tensor formulation [6] the bare propagator of vector mesons is given by

$$\langle\, 0|T\left\{V_{\mu\nu}(x),\, V_{\rho\sigma}(y)\right\}|0\,\rangle \,=\, \int \frac{\mathrm{d}^4k}{(2\pi)^4} e^{-ik(x-y)} \left\{ \frac{2i}{M^2-q^2}\,\Omega^{L}_{\mu\nu,\rho\sigma} \,+\, \frac{2i}{M^2}\,\Omega^{T}_{\mu\nu,\rho\sigma} \right\}, \tag{C.1}$$

with $\Omega^{L(T)}_{\mu\nu,\rho\sigma}$ the projectors over longitudinal (transverse) polarizations.

There is no doubt that physical observables are insensitive to the field representation. But here we are concerned about the off-shell behaviour of resonances so, in principle, the issue of independence on field redefinitions should be studied for the proposed width.

Ref. [491] proposes to define the spin-1 meson width as the imaginary part of the pole generated by resuming those diagrams, with an absorptive contribution in

[6] For further details, see Appendix E.2.

the s channel, that contribute to the two-point function of the corresponding vector current. That is, the pole of

$$\Pi^{jk}_{\mu\nu} \,=\, i \int \mathrm{d}^4x e^{iqx} \langle\, 0|T\left[V^j_\mu(x) V^k_\nu(0)\right]|0\,\rangle\,, \tag{C.2}$$

with

$$V^j_\mu \,=\, \frac{\delta S_{R\chi T}}{\delta v^\mu_j}\,, \tag{C.3}$$

where $S_{R\chi T}$ is the action that generates the Lagrangian of RχT.

The widths obtained in this way are shown to satisfy the requirements of analyticity, unitarity and chiral symmetry prescribed by QCD.

C.1 ρ off-shell width

In order to construct the dressed propagator of the ρ^0 (770) meson, we should consider -for a definite intermediate state- all the contributions carrying the appropriate quantum numbers. In this case, the first cut corresponds to a two-pGs absorptive contribution that happens to saturate its width. We will neglect the contribution of higher multiplicity states that is suppressed by phase space and ordinary chiral counting. The procedure will not reduce to the computation of self-energy diagrams. The counting in the EFT will rule what effective vertices are to be used to obtain the relevant contributions to the off-shell width.

The effective vertices that will contribute to $\pi\,\pi$ scattering and to the pion vector form factor, are those corresponding to an external vector current coupled to two pGs, and to a vector transition in the s channel contributing to the four pGs-vertex. The construction of the effective vertices goes as sketched in Figure C.1 where, at the lowest chiral order, the local vertices on the RHS of the equivalence are provided by the $\mathcal{O}(p^2)$ χPT Lagrangian. The diagrams contributing to the physical observables will be constructed taking into account all possible combinations of these two effective vertices.

In Ref. [491], it was proposed to construct a Dyson-Schwinger-like equation through a perturbative loop expansion. At tree level, one has to take into account the amplitude provided by Figs.C.2(a) and C.2(b) , that is, the effective vertex in Figure C.1 . For the one-loop corrections, we are only interested in those contributions with absorptive parts in the s channel, generated by inserting a pG-loop using the two effectives vertices in Figure C.1 which leads to the four contributions in Figs. C.2(c), C.2(d), C.2(e) and C.2(f). In this way the computation is complete up to two loops. The resulting infinite series happens to be geometric and its resummation gives

$$F_V(q^2) \,=\, \frac{M_V^2}{M_V^2\left[1\,+\,2\frac{q^2}{F^2}\Re e\overline{B_{22}}\right]\,-\,q^2\,-\,i\,M_V\,\Gamma_\rho(q^2)}\,, \tag{C.4}$$

where M_V is the common mass for all the multiplet of vector mesons in the chiral limit,

$$\overline{B_{22}} \equiv B_{22}\,(q^2,\, m_\pi^2,\, m_\pi^2) \,+\, \frac{1}{2}\, B_{22}(q^2,\, m_K^2,\, m_K^2)\,, \tag{C.5}$$

and $B_{22}(q^2,\, m_K^2,\, m_K^2)$ is defined through

$$\int \frac{\mathrm{d}^D\ell}{i(2\pi)^D}\, \frac{\ell_\mu \ell_\nu}{[\ell^2 \,-\, m_K^2]\,[(\ell-q)^2 \,-\, m_K^2]} \,\equiv\, q_\mu q_\nu\, B_{21} \,+\, q^2 g_{\mu\nu}\, B_{22}\,, \tag{C.6}$$

as

$$\begin{aligned} B_{22}\,(q^2,\, m_\pi^2,\, m_\pi^2) \;&=\; \frac{1}{192\pi^2}\,\left[\left(1 \,-\, 6\frac{m_\pi^2}{q^2}\right)\left[\lambda_\infty \,+\, \ln\left(\frac{m_\pi^2}{\mu^2}\right)\right]\right. \\ &\left. +\, 8\frac{m_\pi^2}{q^2} \,-\, \frac{5}{3} \,+\, \sigma_\pi^3 \ln\left(\frac{\sigma_\pi \,+\, 1}{\sigma_\pi \,-\, 1}\right)\right]\,, \end{aligned} \tag{C.7}$$

where $\sigma_P \,=\, \sqrt{1 - \frac{4m_P^2}{q^2}}$ and $\lambda_\infty \,=\, \left[\frac{2}{D-4}\right]\mu^{D-4} \,-\, [\Gamma'(1) \,+\, \ln(4\pi) \,+\, 1]$.

The q^2-dependent width of the ρ^0 (770) meson is given by

$$\begin{aligned} \Gamma_\rho(q^2) \;&=\; -2M_V \frac{q^2}{F^2}\, \Im m\, \overline{B_{22}} \\ &=\; \frac{M_V\, q^2}{96\,\pi\, F^2}\left[\sigma_\pi^3\, \theta(q^2 \,-\, 4m_\pi^2) \,+\, \frac{1}{2}\,\sigma_K^3\, \theta(q^2 \,-\, 4m_K^2)\right]\,, \end{aligned} \tag{C.8}$$

in complete agreement with the expression in Ref. [359].

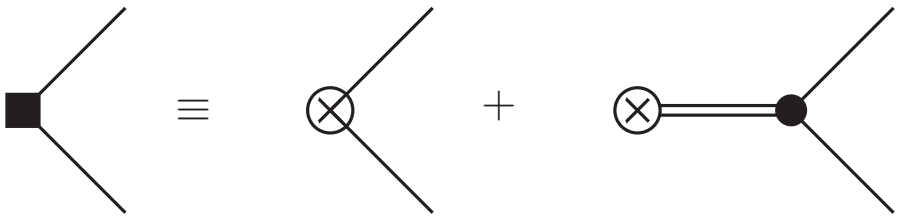

$(s - channel)$

Figure C.1: Effective vertices contributing to vector transitions in the s channel that are relevant for the vector form factor of the pion . The crossed circle stands for an external vector current insertion. A double line indicates the vector meson and a single one the pG. Local vertices on the RHS are provided, at LO, by $\mathcal{L}_\chi$ at $\mathcal{O}(p^2)$.

The real part of the pole of $F_V(q^2)$ in Eq. (C.4) needs still to be regulated through wave function and mass renormalization of the vector field. The local part of $\Re e B_{22}$ can be fixed by matching Eq. (C.4) with the $\mathcal{O}(p^4)$ χPT result.

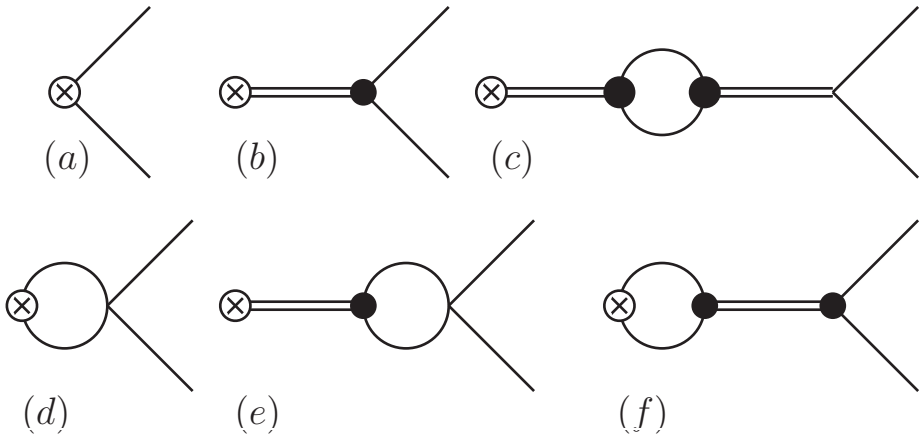

Figure C.2: Diagrams contributing to the vector form factor of the pion up to one loop within $R\chi T$ that have an absorptive part in the s channel.

An analogous procedure can be applied to the study of the vector component of $\pi\,\pi$ scattering. We will be concerned about the s-channel amplitude of $\pi^+\,\pi^- \to \pi^+\pi^-$, that is dominated by ρ exchange, so that one can construct a Dyson-Schwinger equation as in the case of the pion form factor. Consequently, analogous diagrams to those in Figure C.2 are considered, replacing external vector current insertions by two pion legs, according to all possible contributions in Figure C.1 . Projecting the p wave, it is found a geometric series, which can be resummed to give

$$\begin{aligned}\mathcal{A}(\pi^+\,\pi^- \,\to\, \pi^+\pi^-)|_{J=1} \;&=\; \frac{-i}{2F^2}\,(u-t) \\ &\times \frac{M_V^2}{M_V^2\left[1\,+\,2\frac{q^2}{F^2}\Re e\overline{B_{22}}\right]\,-\,q^2\,-\,i\,M_V\,\Gamma_\rho(q^2)}\,,\end{aligned} \tag{C.9}$$

where u and t are the usual Mandelstam variables ($q^2 \,=\, s$). Remarkably, the pole of the amplitude coincides with the one obtained for the vector form factor of pion and, therefore, gives the same width for the ρ^0 meson.

When one applies the definition proposed at the beginning of the section for spin-one meson widths to the case of the ρ^0 (770), its quantum numbers correspond to $j \,=\, k \,=\, 3$ for the flavour index. Lorentz covariance and current conservation allow to define the two-point function of the considered vector current in terms of an invariant function of q^2 through

$$\begin{aligned}\Pi^{33}_{\mu\nu} \;&=\; (q^2\,g_{\mu\nu}\,-\,q_\mu\,q_\nu)\,\Pi^\rho(q^2)\,, \\ \Pi^\rho(q^2) \;&=\; \Pi^\rho_{(0)}\,+\,\Pi^\rho_{(1)}\,+\,\Pi^\rho_{(2)}\,,\,\ldots\,,\end{aligned} \tag{C.10}$$

where $\Pi^\rho_{(0)}$ corresponds to the tree level contribution of Figure C.3 (a), $\Pi^\rho_{(1)}$ to the one-loop amplitudes and so forth. Up to one loop, and considering again the two-particle absorptive contributions only, all the diagrams generated by the effective

vertices in Figure C.1 are shown in Figure C.3. One finds, in the isospin limit,

$$\Pi^{\rho}_{(0)} = \frac{F_V^2}{M_V^2 - q^2}\,, \tag{C.11}$$

$$\Pi^{\rho}_{(1)} = \Pi^{\rho}_{(0)}\left[-\frac{M_V^2}{F_V^2}\,\frac{M_V^2}{M_V^2 - q^2}\,4\overline{B_{22}}\right]\,. \tag{C.12}$$

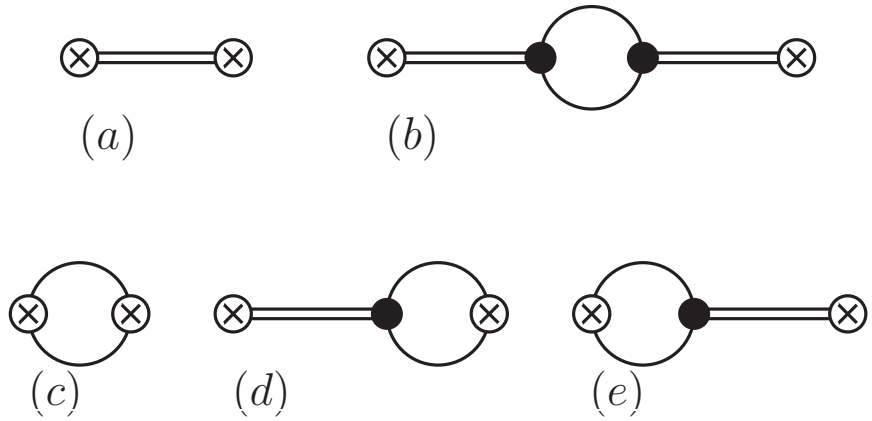

Figure C.3: Diagrams contributing to the vector-vector correlator $\Pi^{33}_{\mu\nu}$ up to one loop within $R\chi T$.

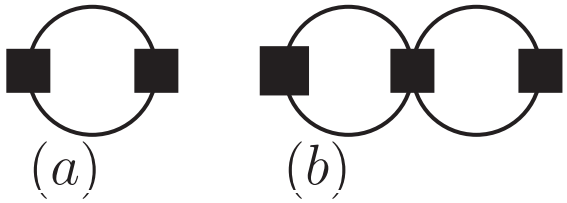

Figure C.4: One- and two-loop diagrams leading to $\Pi^{\rho}_{(1)}$ (a) and $\Pi^{\rho}_{(2)}$ (b). The effective squared vertices are given in Figure C.1.

At this point, one realizes that the resummation procedure cannot consist only of self-energy diagrams. QCD predicts the two-point spectral function of vector currents to go to a constant value as $q^2 \to \infty$ [297]. The loop diagram in Figure C.3 (b) behaves itself as a constant value in this limit, which is against of expectations because it corresponds to only one of the infinite number of possible intermediate states. In order to satisfy the QCD-ruled behaviour, one would foresee that all the individual (positive) contributions from the intermediate states should vanish in the infinite q^2 limit. Indeed, this is achieved when one adds the diagrams depicted in Figs.C.3(c), C.3(d) and C.3(e). The requirement of vanishing at $q^2 \to \infty$ for the Π^{ρ}_i is also fulfilled for $i \geq 2$ provided one considers, at a given order, all possible

diagrams with absorptive contributions in the s-channel, and not just self-energies.

Iterating in all possible ways the one-loop diagrams in Figure C.3, one obtains all possible contributions to the two-loop computation, as sketched in Figure C.4. The result of the calculation was found to be

$$\Pi^{\rho}_{(2)} \,=\, \Pi^{\rho}_{(1)} \left[-\frac{q^2}{F_V^2}\,\frac{M_V^2}{M_V^2\,-\,q^2}\,4\overline{B_{22}} \right] . \tag{C.13}$$

In Ref. [491], it was checked explicitly up to three loops that the invariant two-point function $\Pi^{\rho}(q^2)$, generated by resuming effective loop diagrams with an absorptive amplitude in the s channel [7] is perturbatively given by

$$\begin{aligned} \Pi^{\rho}(q^2) \;&=\; \Pi^{\rho}_{(0)} \,+\, \Pi^{\rho}_{(1)} \sum_{n=0}^{\infty} \left[-\frac{q^2}{F_V^2}\,\frac{M_V^2}{M_V^2\,-\,q^2}\,4\overline{B_{22}} \right]^n \\ &= \Pi^{\rho}_{(0)} \left[1 \,+\, \omega \sum_{n=0}^{\infty} \left(\frac{q^2}{M_V^2}\,\omega \right)^n \right] , \end{aligned} \tag{C.14}$$

where

$$\omega \,=\, -\frac{M_V^2}{F_V^2}\,\frac{M_V^2}{M_V^2\,-\,q^2}\,4\overline{B_{22}}\,. \tag{C.15}$$

Using that $F_V^2 \,=\, 2F^2$, and substituting (C.15) for performing the resummation, one finally gets

$$\begin{aligned} \Pi^{\rho}(q^2) \;&=\; \frac{2F^2}{M_V^2\left[1\,+\,2\frac{q^2}{F^2}\Re e\overline{B_{22}}\right]\,-\,q^2\,-\,i\,M_V\,\Gamma_{\rho}(q^2)} \\ &\quad \times \left[1 \,-\, 2\frac{M_V^2}{F^2}\overline{B_{22}} \right] , \end{aligned} \tag{C.16}$$

where the off-shell ρ^0 width $\Gamma_{\rho}(q^2)$ is given by (C.4). The consistency of the resummation procedure shows up neatly because the residue in $\Pi^{\rho}(q^2)$ satisfies the required unitarity condition

$$\begin{aligned} \Im m\Pi^{\rho}(q^2) \;&=\; \frac{1}{48\pi}\left[\sigma_{\pi}^3\,\theta(q^2\,-\,4m_{\pi}^2) \,+\, \frac{1}{2}\,\sigma_K^3\,\theta(q^2\,-\,4m_K^2) \right] \\ &\quad \times |F_V(q^2)|^2 , \end{aligned} \tag{C.17}$$

with $F_V(q^2)$ given by (C.4).

The last comment to be made concerns the independence of the definition of the spin-one meson width on the chosen representation for the fields. To see this, it is enough to realize that the effective vertices in Figure C.1 are universal. Different theoretical descriptions of the spin-one mesons lead to resonance-exchange contributions that differ by local terms. Since the physical amplitudes are required to satisfy

[7] Note that the procedure employed implies that the only significant result of $\Pi^{\rho}(q^2)$ is its imaginary part.

the QCD-ruled behaviour at short distances, this difference is necessarily counterbalanced by explicit local terms [7]. Including these local terms in the local vertices of Figure C.1 , the resulting effective vertices (which are the building blocks of the described resummation) are formulation independent and thus, the whole procedure is.

C.2 K^* off-shell width

Being the definition of spin-one resonance width completely general, what is left now is simply to employ it for any resonance we are interested in. In particular, for the case of the K^* resonance, we have

$$\begin{aligned}\Gamma_{K^*}(q^2) &= \frac{M_{K^*}\, q^2}{128\pi F^2}\left[\lambda^{3/2}\left(1,\, \frac{m_K^2}{q^2},\, \frac{m_\pi^2}{q^2}\right)\theta\left(q^2 - (m_K + m_\pi)^2\right)\right. \\ &\left. + \lambda^{3/2}\left(1,\, \frac{m_K^2}{q^2},\, \frac{m_\eta^2}{q^2}\right)\theta\left(q^2 - (m_K + m_\eta)^2\right)\right], \end{aligned} \tag{C.18}$$

in agreement with [380].

C.3 ω-ϕ off-shell width

The full widths PDG [8] reports for the vector resonances we are interested in are: $\Gamma_\rho = 149.4 \pm 1.0$ MeV, $\Gamma_\omega = 8.49 \pm 0.8$ MeV, $\Gamma_\Phi =$ MeV, and $\Gamma_{K^*} \sim 50.5 \pm 1.0$ MeV. Based on this, we have decided to neglect the off-shell width of the isospin zero resonances ω (782) and $\Phi(1020)$, because it is a tiny effect compared both to that of the ρ (770) and K^* (892) widths and to the uncertainties we still have in the determination of the coupling constants or the error introduced by other approximations. We have used the values reported as the constant ω (782) and Φ (1020) widths in our study.

Appendix D: $\omega \to \pi^+\pi^-\pi^0$ within $R\chi T$

The decay of the $\omega(782)$ into three pions, $\omega \to \pi^+(k_1)\,\pi^-(k_2)\,\pi^0(k_3)$, has been a useful source of information on the odd-intrinsic parity couplings. Within the framework of $R\chi T$ it was first studied in Ref. [310], where the contribution of the VVP vertices was already found and the need to account for $VPPP$ vertices was put forward.

We will denote the polarization vector of the ω as $\varepsilon_\omega^\sigma$ and use the kinematic invariants $s_{ij} = (k_i + k_j)^2$. In our work we have included for the first time the contribution of the decay via a direct vertex.

The amplitude associated to the diagram of Figure D.1 -that should be the leading one according to vector meson dominance- including cyclic permutations among k_1, k_2 and k_3, reads

$$i\,\mathcal{M}^{\rm VMD}_{\omega\to 3\pi} = i\,\epsilon_{\alpha\beta\rho\sigma}\,k_1^\alpha k_2^\beta k_3^\rho \epsilon_\omega^\sigma \frac{8\,G_V}{M_\omega F^3}\left[\frac{m_\pi^2(d_1+8d_2-d_3)+(M_\omega^2+s_{12})\,d_3}{M_V^2-s_{12}} + \{s_{12}\to s_{13}\}+\{s_{12}\to s_{23}\}\right]. \qquad \text{(D.1)}$$

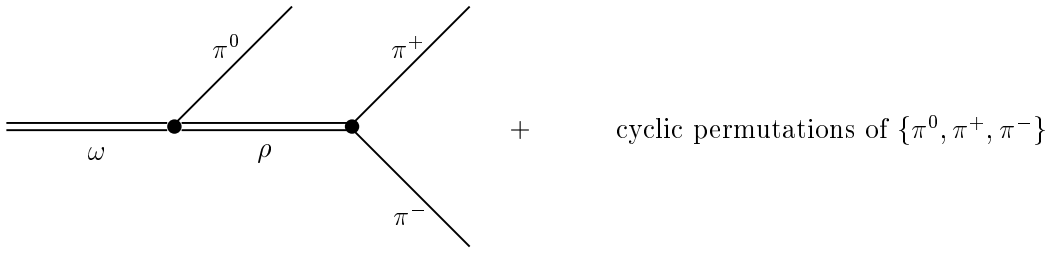

Figure D.1: The $\omega \to \pi^+\pi^-\pi^0$ decay amplitude via an intermediate ρ exchange.

Now, the contribution via a direct vertex $VPPP$ yields

$$i\,\mathcal{M}^{VPPP}_{\omega\to\pi^+\pi^-\pi^0} \,=\, i\,\varepsilon_{\alpha\beta\rho\sigma}k_1^\alpha k_2^\beta k_3^\rho \varepsilon_\omega^\sigma \qquad \left\{ \frac{8G_V}{M_\omega F^3}\frac{8\sqrt{2}}{F^3 M_\omega M_V}\left[(g_1 \,-\, g_2 \,-\, g_3)(M_\omega^2 \,-\, 3\,m_\pi^2)\right.\right. \\ \left.\left. +\,3\,m_\pi^2(2\,g_4 \,+\, g_5)\right]\right\}\,. \tag{D.2}$$

In the above expression, we have assumed ideal mixing between the states $|\,\omega_8\rangle$ and $|\,\omega_1\rangle$:

$$|\,\omega\rangle \,=\, \sqrt{\frac{2}{3}}\,|\,\omega_1\rangle + \sqrt{\frac{1}{3}}\,|\,\omega_8\rangle\,, \tag{D.3}$$

and

$$|\,\phi\rangle \,=\, -\sqrt{\frac{1}{3}}\,|\,\omega_1\rangle + \sqrt{\frac{2}{3}}\,|\,\omega_8\rangle\,. \tag{D.4}$$

The relation between the amplitudes of the singlet and octet states is the following one:

$$\mathcal{M}_{\omega_1\to\pi^+\pi^-\pi^0} \,=\, \sqrt{2}\,\mathcal{M}_{\omega_8\to\pi^+\pi^-\pi^0}\,. \tag{D.5}$$

The decay width is then obtained as

$$\Gamma(\omega\to\pi^+\pi^-\pi^0) \;=\; \frac{G_V^2}{4\,\pi^3\,M_\omega^5\,F^6}\int_{4m_\pi^2}^{(M_\omega-m_\pi)^2} ds_{13}\int_{s_{23}^{min}}^{s_{23}^{max}} ds_{23}\,\mathcal{P}(s_{13},s_{23})\,\times \tag{D.6}$$

$$\times\left[\frac{m_\pi^2(d_1+8d_2-d_3)+(M_\omega^2+s_{12})\,d_3}{M_V^2-s_{12}} + \{s_{12}\to s_{13}\}+\{s_{12}\to s_{23}\}\right.$$

$$\left.+\frac{8\sqrt{2}}{F^3M_\omega M_V}\left[(g_1 \,-\, g_2 \,-\, g_3)(M_\omega^2 \,-\, 3\,m_\pi^2) \,+\, 3\,m_\pi^2(2\,g_4 \,+\, g_5)\right]\right]^2,$$

where the function $\mathcal{P}$ is the polarization average of the tensor structure of $\mathcal{M}_{\omega\to 3\pi}$,

$$\mathcal{P}(s_{13},s_{23}) = \frac{1}{12}\left\{-m_\pi^2(m_\pi^2-M_\omega^2)^2 - s_{13}s_{23}^2 + (3m_\pi^2+M_\omega^2-s_{13})s_{13}s_{23}\right\}\,. \tag{D.7}$$

With $G_V = F/\sqrt{2}$ and the relations obtained by the short-distance matching. In the analyses of the VVP Green function all couplings appearing in Eq. (D.1) were predicted

$$\begin{aligned} d_1 + 8\,d_2 \;&=\; -\frac{N_C}{64\pi^2}\frac{M_V^2}{F_V^2} \,+\, \frac{F^2}{4F_V^2} \quad , \\ d_3 \;&=\; -\frac{N_C}{64\pi^2}\frac{M_V^2}{F_V^2} \,+\, \frac{F^2}{8F_V^2}\,. \end{aligned} \tag{D.8}$$

Taking just this piece of the amplitude into account, one obtains a decay width that is only one fifth [310] of the experimental value.

Additionally, the following relations were obtained studying the decays $\tau^- \to (KK\pi)^-\nu_\tau$ [304, 321]:

$$\begin{aligned} d_3 &= -\frac{N_C}{192\pi^2}\frac{M_V^2}{F_V\,G_V}\,, \\ g_1 + 2\,g_2 - g_3 &= 0\,, \\ g_2 &= \frac{N_C}{192\pi^2}\,\frac{M_V}{\sqrt{2}\,F_V}\,. \end{aligned} \tag{D.9}$$

As explained in Chapter 7 we find more reliable the determination of the coupling d_3 in Eq. (D.9), that we will follow. Taking all these information into account we are able to match the experimental value reported by the *PDG* [8] $\Gamma(\omega \to \pi^+\pi^-\pi^0)|_{\rm exp} = (7.57 \pm 0.06)\,\text{MeV}$ with $2g_4 + g_5 = -0.60 \pm 0.02$ that has been used in the hadron tau decays studied in this Thesis.

Appendix E: Isospin relations between τ^- and e^+e^- decay channels

E.1 Introduction

In this appendix we provide the derivation of several relations between τ^- and e^+e^- decay channels that are related by an isospin rotation. Since $SU(2)$ is a very accurate symmetry whose violations are smaller than the typical errors of the experimental measurements and our theoretical assumptions, the conclusions we draw should hold. At the low energies we are interested in, one can safely neglect the Z contributions to the hadron e^+e^- cross-section. In this limit, the process will only be due to vector current via photon exchange. Therefore, the relations that we obtain will relate $\sigma_{e^+e^-\to\text{hadrons}}$ to the vector current contribution in the corresponding tau decay. Depending on the channel, the importance of the latter will vary from being the only one to be forbidden by symmetry arguments, like G-parity. Thus this study will be interesting for some of the channels and irrelevant for others [8].

In this introduction we will first give the conventions we follow for the relations between one-particle charge and isospin states and the ladder operators. Then we will recall the general formula for the tau decay width into a given final state of three mesons and the tau neutrino and give the derivation of the analogous expression for the e^+e^- cross-section into a three-hadron system. We will finish this section with the projection of the weak and electromagnetic currents into its isospin components. Charge conjugated relations are understood and most of the times not written.

The triplet of pions is related to the isospin states, $|I, I_3\rangle$, in the following way:

$$\pi^+ \sim \overline{d}u \sim -|1,+1\rangle\,, \quad \pi^0 \sim \frac{\overline{u}u - \overline{d}d}{\sqrt{2}} \sim |1,0\rangle\,, \quad \pi^- \sim \overline{u}d \sim |1,-1\rangle\,. \tag{E.1}$$

[8] As two immediate examples of this we quote the three pion tau decay channel where there is no vector current contribution because of G-parity and the 3η state that cannot be a decay product of the τ.

It is important to understand that the four kaon states group into two doublets according to its strangeness:

$$K^+ \sim \overline{s}u \sim \left|\frac{1}{2}, +\frac{1}{2}\right\rangle, \quad K^0 \sim \overline{s}d \sim \left|\frac{1}{2}, -\frac{1}{2}\right\rangle, \tag{E.2}$$

and

$$\overline{K}^0 \sim \overline{d}s \sim -\left|\frac{1}{2}, +\frac{1}{2}\right\rangle, \quad K^- \sim \overline{u}s \sim \left|\frac{1}{2}, -\frac{1}{2}\right\rangle. \tag{E.3}$$

Defining the isospin operators $T_\pm = \frac{T_1 \pm i T_2}{\sqrt{2}}$, we get the following relations:

$$[T_+, T_-] \,=\, T_3, \qquad [T_+, u] \,=\, -\frac{d}{\sqrt{2}}, \qquad \left[T_+, d^\dagger\right] \,=\, \frac{u^\dagger}{\sqrt{2}}, \tag{E.4}$$

$$T_+|I, +I\,\rangle = T_-|I, -I\,\rangle = 0\ , \tag{E.5}$$

$$T^+\overline{d}u|0\,\rangle = \left[T_+, \overline{d}u\right]|0\,\rangle = \frac{\overline{u}u - \overline{d}d}{\sqrt{2}}|0\,\rangle\ , \tag{E.6}$$

that will allow to relate the neutral and charged current weak decays.

Before analysing the most interesting channels, we will need Eq. (5.62) for the tau decay width into a given three meson and a tau-neutrino final state and the analogous formula for the e^+e^- cross-section into a three hadron final state. The latter is obtained in the following.

We consider the decay $e^+(\ell_1, s_1)e^-(\ell_2, s_2) \to h_1(p_1)h_2(p_2)h_3(p_3)$. The amplitude of the process is splitted into its lepton and hadron tensors as in Chapter 5.One has

$$\mathcal{L}_{\mu\nu} = \sum_{s_1, s_2} \overline{v}(\ell_2, s_2)\gamma_\mu u(\ell_1, s_1)\overline{u}(\ell_1, s_1)\gamma_\nu v(\ell_2, s_2)\,. \tag{E.7}$$

Its transverse projection reads ($Q \,=\, p_1 + p_2 + p_3 \,=\, \ell_1 + \ell_2$)

$$\left(g^{\mu\nu} - \frac{Q^\mu Q^\nu}{Q^2}\right)\mathcal{L}_{\mu\nu} = -4\,(Q^2 \,+\, 2\,m_e^2)\,. \tag{E.8}$$

On the other hand, the hadron tensor is decomposed as

$$\mathcal{H}^{\mu\nu} = S\left(Q^2,\, s,\, t\right)\frac{Q^\mu Q^\nu}{Q^2} + \left(g^{\mu\nu} - \frac{Q^\mu Q^\nu}{Q^2}\right)V\left(Q^2,\, s,\, t\right)\ . \tag{E.9}$$

Since the process is mediated by vector current only the scalar component vanishes ($S = 0$) and we have

$$V\left(Q^2,\, s,\, t\right) = \frac{\mathcal{H}^{\mu\nu}}{3}\left(g^{\mu\nu} - \frac{Q^\mu Q^\nu}{Q^2}\right)\ . \tag{E.10}$$

Using the expression for $\int \mathrm{d}\Pi_3$ in Eq. (5.58) one immediately has

$$\begin{aligned}\sigma_{e^+e^-\to h_1h_2h_3}(Q^2) &= \frac{1}{2^2}\left(\frac{e^2}{Q^2}\right)^2 \frac{1}{2\lambda^{1/2}(Q^2,m_e^2,m_e^2)}\,\frac{1}{32\pi^3}\,\frac{1}{4Q^2}\int \mathrm{d}s\mathrm{d}t\,\times \\ &\quad \frac{4}{3}\,(Q^2+2\,m_e^2)\,|F_3|^2\,(-V_{3\mu}V_3^{\mu *}) \\ &\sim \frac{\alpha^2}{48\pi}\,\frac{1}{Q^6}\int \mathrm{d}s\mathrm{d}t\,|F_3|^2\,(-V_{3\mu}V_3^{\mu *})\,. \end{aligned} \tag{E.11}$$

So that the e^+e^- cross-section into three hadrons is given by

$$\sigma_{e^+e^-\to h_1h_2h_3}(Q^2) = \frac{e^4}{768\,\pi^3}\frac{1}{Q^6}\int \mathrm{d}s\mathrm{d}t|F_3|^2\,(-V_{3\mu}V_3^{\mu *})\,. \tag{E.12}$$

This way one ends up with the desired relation

$$\frac{\mathrm{d}\Gamma\,(\tau^-\to (3h)^-\nu_\tau)}{\mathrm{d}Q^2} = f(Q^2)\,\sigma_{e^+e^-\to (3h)^0}(Q^2)|_{I=1}\,, \tag{E.13}$$

where $(3h)^-$ and $(3h)^0$ are related via an isospin rotation and

$$f(Q^2) = \frac{G_F^2|V_{ij}^{CKM}|^2}{384(2\pi)^5 M_\tau}\left(\frac{M_\tau^2}{Q^2}-1\right)^2\left(1+2\frac{Q^2}{M_\tau^2}\right)\left(\frac{\alpha^2}{96\pi}\right)^{-1} Q^6\,. \tag{E.14}$$

The W bosons can couple to $\overline{u}s$, $\overline{s}u$ (that are two components of different multiplets with $I=1/2$), and to $\overline{d}u$, $\overline{u}d$. Both have $I=1$ and differ by a relative global sign.

The Z boson can couple to the $I=0,1$ combinations that are $\frac{\overline{u}u\mp\overline{d}d}{\sqrt{2}}$ where the upper signs correspond to the neutral component of $I=1$.

Now let us consider the electromagnetic current. One can decompose it into its $I=0$ and $I=1$ pieces:

$$\Gamma^\mu = \frac{1}{3}\left(2\overline{u}\gamma^\mu u - \overline{d}\gamma^\mu d - \overline{s}\gamma^\mu s\right) = \Gamma^\mu_{(0)} + \Gamma^\mu_{(1)}\,, \tag{E.15}$$

where

$$\Gamma^\mu_{(0)} = \frac{1}{6}\left(\overline{u}\gamma^\mu u + \overline{d}\gamma^\mu d - 2\overline{s}\gamma^\mu s\right)\,,\quad \Gamma^\mu_{(1)} = \frac{1}{2}\left(\overline{u}\gamma^\mu u - \overline{d}\gamma^\mu d\right)\,. \tag{E.16}$$

As it is well-known, there are no tree level $FCNC$. Moreover, the electromagnetic current conserves strangeness. This implies that the strangeness changing channels $K\pi\pi$, $K\pi\eta$, $K\eta\eta$, KKK can only be reached via $W^\pm$-mediated loops. Therefore, they are very much suppressed -even more at the low-energies we are interested in- and it makes no sense to analyze them in this context [9]. This short-hand writing

[9] A complementary reasoning in terms of isospin can also be made: Neither the Z nor the γ couple to $I=1/2$. This prevents a study of this type for the $|\eta\eta K\rangle \sim |K\rangle$ state -with $I=1/2$- because there is only one accesible state in τ^- decays, in addition, so that no relation can be established. Similarly, the three kaon state has half-integer I, so it can only be produced in τ decays. There is only a trivial isospin relation $A_{+--} = A_{0\overline{0}-}$ in this case. The notation employed uses as subscripts the electric charges of the particles involved for a given mode. In this case, for instance, this would correspond to $A_{K^+K^-K^-} = A_{K^0\bar{K}^0K^-}$.

will be used in the remainder of the chapter.

E.2 $KK\pi$ channels

One must realize that in all charge channels both kaons belong to different isospin multiplets because they have opposite strangeness. At the practical level this implies that there is an additional label implying that the ordering when writing the states is irrelevant. We give an example to illustrate this: $|\pi^+\pi^-\rangle$ and $|\pi^-\pi^+\rangle$ are different isospin states corresponding to $|1,+1\rangle \otimes |1,-1\rangle$ and $|1,-1\rangle \otimes |1,+1\rangle$, respectively. However, K^-K^0 is $|-1,\frac{1}{2},-\frac{1}{2}\rangle \otimes |1,\frac{1}{2},-\frac{1}{2}\rangle$, where the first label is the strangeness of the state (-1 for s) making manifest that they belong to different subspaces.

We will consider first the product of the two kaons states. This can give either the isoscalar channel 'ω' or the isovector channel 'ρ'. Then we will consider the product of the produced states with the remaining π. Some signs may vary by considering first the product of one of the kaons to the pion and then that of the resulting states with the kaon left. However, the relations we will find are independent of the procedure we follow.

The pair of kaons can couple as

$$\begin{aligned}
\frac{1}{\sqrt{2}}\left(K^+K^- + K^0\overline{K}^0\right) \qquad & I=0\,, \\
-K^+\overline{K}^0 \qquad & I=1,\, I_3=+1\,, \\
\frac{1}{\sqrt{2}}\left(K^+K^- - K^0\overline{K}^0\right) \qquad & I=1,\, I_3=0\,, \\
K^0K^- \qquad & I=1,\, I_3=-1\,.
\end{aligned} \tag{E.17}$$

Now we consider the direct product of the 'ρ' and 'ω' states with the appropriate pion. We will have $I=1$ in 'ω' channel and $I=0$, 1, 2 in 'ρ' channel. One has

$$\begin{aligned}
\frac{1}{\sqrt{2}}\left(K^+K^-\pi^+ + K^0\overline{K}^0\pi^+\right) \qquad & I=1,\, I_3=+1\,, \\
\frac{1}{\sqrt{2}}\left(K^+K^-\pi^0 + K^0\overline{K}^0\pi^0\right) \qquad & I=1,\, I_3=0\,, \\
\frac{1}{\sqrt{2}}\left(K^+K^-\pi^- + K^0\overline{K}^0\pi^-\right) \qquad & I=1,\, I_3=-1\,,
\end{aligned} \tag{E.18}$$

in ω channel, while the states produced in ρ channel are

$$\begin{aligned}
\frac{1}{\sqrt{3}}\left[K^0K^-\pi^+ - \frac{1}{\sqrt{2}}\left(K^+K^-\pi^0 - K^0\overline{K}^0\pi^0\right) - K^+\overline{K}^0\pi^-\right] \qquad & I=0,\, I_3=0\,,\\
\frac{1}{\sqrt{2}}\left[-K^+\overline{K}^0\pi^0 + \frac{1}{\sqrt{2}}\left(K^+K^-\pi^+ - K^0\overline{K}^0\pi^+\right)\right] \qquad & I=1,\, I_3=+1\,,\\
\frac{1}{\sqrt{2}}\left[-K^+\overline{K}^0\pi^- - K^0K^-\pi^+\right] \qquad & I=1,\, I_3=0\,,\\
\frac{1}{\sqrt{2}}\left[\frac{1}{\sqrt{2}}\left(K^+K^-\pi^- - K^0\overline{K}^0\pi^-\right) - K^0K^-\pi^0\right] \qquad & I=1,\, I_3=-1\,,\\
- K^+\overline{K}^0\pi^+ \qquad & I=2,\, I_3=+2\,,\\
\frac{1}{2}\left(-\sqrt{2}K^+\overline{K}^0\pi^0 + K^+K^-\pi^+ - K^0\overline{K}^0\pi^+\right) \qquad & I=2,\, I_3=+1\,,\\
\frac{1}{\sqrt{6}}\left(-K^+\overline{K}^0\pi^- + \sqrt{2}K^+K^-\pi^0 - \sqrt{2}K^0\overline{K}^0\pi^0 + K^0K^-\pi^+\right) \qquad & I=2,\, I_3=0\,,\\
\frac{1}{2}\left(K^+K^-\pi^- - K^0\overline{K}^0\pi^- + \sqrt{2}K^0K^-\pi^0\right) \qquad & I=2,\, I_3=-1\,,\\
K^0K^-\pi^- \qquad & I=2,\, I_3=-2\,.
\end{aligned} \tag{E.19}$$

Since the operator $\overline{d}\,\Gamma^\mu\, u$ has $I=1$ we have [10]

$$_{(2,-1)}\langle\, KK\pi|\overline{d}\Gamma_\mu u|0\,\rangle \;=\; 0\,, \tag{E.20}$$

for the charged weak current. Thus

$$\langle\, K^+K^-\pi^- - K^0\overline{K}^0\pi^- + \sqrt{2}K^0K^-\pi^0|\overline{d}\,\Gamma_\mu\, u|0\,\rangle \;=\; 0\,. \tag{E.21}$$

If we denote the correponding hadron amplitudes as A_μ^{+--}, A_μ^{00-} and A_μ^{0-0}, Eq. (E.21) implies

$$A_\mu^{+--} - A_\mu^{00-} \;=\; -\sqrt{2}A_\mu^{0-0}\,. \tag{E.22}$$

One can proceed analogously for the neutral current weak operator $\frac{\overline{u}\Gamma_\mu u - \overline{d}\Gamma_\mu d}{\sqrt{2}}$. Since it carries isospin $I=1$, we have the relations

$$_{(2,0)}\langle\, KK\pi|\overline{u}u - \overline{d}d|0\,\rangle \;=\; _{(0,0)}\langle\, KK\pi|\overline{u}u - \overline{d}d|0\,\rangle \;=\; 0\,. \tag{E.23}$$

[10] $\Gamma^\mu = \gamma^\mu, \gamma^\mu\gamma_5$. Since the spinor structure is unrelated to isospin, one has separate relations holding for both for the vector ans axial-vector currents. This will be understood in what follows.

Therefore, writing the isospin states in terms of charge states one has

$$\begin{aligned} A_\mu^{0-+} - A_\mu^{+0-} &= -\frac{1}{\sqrt{2}}\left(A_\mu^{000} - A_\mu^{+-0}\right) = 0\,, \\ A_\mu^{0-+} - A_\mu^{+0-} &= -\sqrt{2}\left(A_\mu^{+-0} - A_\mu^{000}\right) = 0\,, \end{aligned} \tag{E.24}$$

where the respective amplitudes were denoted using the same convention for the indices as before.

Finally, the relations (E.4), (E.5), (E.6) allow to write

$${}_{(1,-1)}\langle\, KK\pi|\overline{d}\Gamma_\mu u|0\,\rangle = -_{(1,0)}\left\langle KK\pi\right|\frac{\overline{u}\Gamma_\mu u - \overline{d}\Gamma_\mu d}{\sqrt{2}}\left|0\right\rangle. \tag{E.25}$$

This yields relations for the hadron amplitudes in 'ρ' and 'ω' channels, between the charged and neutral current weak processes:

$$\begin{aligned} A_\mu^{0-0} = A_\mu^{+0-} = A_\mu^{0-+} &= \frac{1}{\sqrt{2}}\left(A_\mu^{00-} - A_\mu^{+--}\right), \\ A_\mu^{+--} + A_\mu^{00-} &= 2A_\mu^{+-0} = 2A_\mu^{000}\,. \end{aligned} \tag{E.26}$$

Now we consider also the electromagnetic processes with $I = 1$. We will factor out the Lorentz structure in the hadron matrix elements:

$$\begin{aligned} A_\mu^- &\equiv \langle\,(KK\pi)^-|\overline{d}\gamma_\mu u|0\,\rangle = A^-\epsilon_{\mu\nu\rho\sigma}p_1^\nu p_2^\rho p_3^\sigma\,, \\ A_\mu^0 &\equiv \left\langle(KK\pi)^0\right|\frac{\overline{u}\gamma_\mu u - \overline{d}\gamma_\mu d}{\sqrt{2}}\left|0\right\rangle = A^0\epsilon_{\mu\nu\rho\sigma}p_1^\nu p_2^\rho p_3^\sigma\,. \end{aligned} \tag{E.27}$$

In general we will have

$$\langle\,(KK\pi)^-| = \frac{a_1}{\sqrt{2}}\langle\,K^+K^-\pi^- + K^0\overline{K}^0\pi^-| + \frac{a_2}{\sqrt{2}}\langle\,K^+K^-\pi^- - K^0\overline{K}^0\pi^-| + a_3\langle\,K^0K^-\pi^0|\,, \tag{E.28}$$

in such a way that

$$A^- = a_1A_1^- + a_2A_2^- + a_3A_3^- = \frac{a_1+a_2}{\sqrt{2}}A^{+--} + \frac{a_1-a_2}{\sqrt{2}}A^{00-} + a_3A^{0-0}\,. \tag{E.29}$$

Since

$$\frac{A^{+--} - A^{00-}}{\sqrt{2}} = -A^{0-0} \Rightarrow A_2^- = -A^{0-0}\,, \tag{E.30}$$

we can easily solve for the A_i^-:

$$A_1^- = \frac{A^{+--} + A^{00-}}{\sqrt{2}}\,, \quad A_2^- = \frac{A^{+--} - A^{00-}}{\sqrt{2}}\,, \quad A_3^- = A^{0-0}\,. \tag{E.31}$$

Following Eq. (E.27) for naming the amplitudes of the different charge channels we have finally

$$A^{+0-} = A^{0-+} = A^{0-0}\,, \quad A^{+-0} = A^{000} = \frac{1}{2}\left(A^{+--} + A^{00-}\right) = \frac{1}{\sqrt{2}}\,A_1^-\,. \tag{E.32}$$

Summing over all τ^- charge channels one has

$$|A^{+--}|^2 + |A^{00-}|^2 + |A^{0-0}|^2 \,=\, |A_1^-|^2 + |A_2^-|^2 + |A_3^-|^2 \,=\, 2|A_3^-|^2 + |A_1^-|^2\,, \quad \text{(E.33)}$$

whereas doing it over the four neutral channels reached in e^+e^- annihilations with $I = 1$ we have

$$|A^{+0-}|^2+|A^{0-+}|^2+|A^{+-0}|^2+|A^{000}|^2 \,=\, 2|A^{0-0}|^2+2\left(\frac{1}{2}\right)^2|A^{+--}+A^{00-}|^2 \,=\, 2|A_3^-|^2+|A_1^-|^2\,. \quad \text{(E.34)}$$

Using the above relations one can obtain the isovector component of the process $e^+e^- \to K^0K^-\pi^+$ using the form factors computed for $\Gamma\left(\tau^- \to K^0K^-\pi^0\nu_\tau\right)$.

$$\frac{\mathrm{d}\Gamma\left(\tau^- \to K^0K^-\pi^0\nu_\tau\right)}{\mathrm{d}Q^2}|_{\text{Vector}} \,=\, f(Q^2)\,\sigma|_{I=1}\left(e^+e^- \to K^0K^-\pi^+\right)\,, \quad \text{(E.35)}$$

where $f(Q^2)$ was defined in Eq. (E.14). One can also establish a similar relation including linear combinations of decay channels. Namely

$$\frac{\mathrm{d}\Gamma\left(\tau^- \to K^0K^-\pi^0\nu_\tau\right)}{\mathrm{d}Q^2}|_{\text{Vector}} \,+\, \frac{\mathrm{d}\Gamma\left(\tau^- \to K^0K^-\pi^0\nu_\tau\right)}{\mathrm{d}Q^2}|_{\text{Vector}} \,=$$
$$f(Q^2)\,\left[\sigma|_{I=1}\left(e^+e^- \to K^0K^-\pi^+\right) + 2\sigma|_{I=1}\left(e^+e^- \to K^0K^-\pi^+\right)\right]\,. \quad \text{(E.36)}$$

Summing all charge channels one finds

$$\sum_{i=1}^{3}\frac{\mathrm{d}\Gamma\left(\tau^- \to (KK\pi)^-\nu_\tau\right)}{\mathrm{d}Q^2}|_{\text{Vector}} \,=\, f(Q^2)\,\sum_{i=1}^{4}\sigma|_{I=1}\left(e^+e^- \to (KK\pi)^0\right)\,. \quad \text{(E.37)}$$

As a byproduct we have obtained the relations

$$F_i\left(\tau^- \to K^+K^-\pi^-\nu_\tau\right) - F_i\left(\tau^- \to K^0\overline{K}^0\pi^-\nu_\tau\right) \,=\, -\sqrt{2}F_i\left(\tau^- \to K^0K^-\pi^0\nu_\tau\right)\,. \quad \text{(E.38)}$$

We have checked that our form factors in Chapter 7 satisfy this constraint.

We emphasize that isospin symmetry alone is not able to relate the isovector component of $\sigma\left(e^+e^- \to K_SK^\pm\pi^\mp\right)$ with the sum of all $KK\pi$ $I = 1$ contributions of the e^-e^+ cross section. For that, the experimental collaborations use to employ the relation

$$\sigma\left(e^+e^- \to KK\pi\right) \,=\, 3\,\sigma\left(e^+e^- \to K_SK^\pm\pi^\mp\right)\,. \quad \text{(E.39)}$$

However, even using all available isospin relations it is not possible to express $\sigma\left(e^+e^- \to KK\pi\right)$ in terms of the corresponding cross section for a single charge channel. However, Eq. (E.39) can be justified following the arguments that we explain at the end of this section.

For this we will need to take into account not only the $I = 1$ component of the electromagnetic current -as before- but also the isoscalar part. The application of

the corresponding current, $\Gamma^\mu_{(0)}$ in Eq. (E.16), on the $|2,0\rangle$ and $|1,0\rangle$ states allows to obtain nontrivial relations between the corresponding isoscalar ($^{(0)}$) electromagnetic amplitudes:

$$A^{(0)}_{+-0} = -A^{(0)}_{0\bar{0}0}\,, \quad A^{(0)}_{+\bar{0}-} = -A^{(0)}_{0-+}\,, \quad \sqrt{2}(A^{(0)}_{+-0} - A^{(0)}_{0\bar{0}0}) = A^{(0)}_{+\bar{0}-} - A^{(0)}_{0-+}\,, \tag{E.40}$$

which yields

$$\sqrt{2}A^{(0)}_{+-0} = A^{(0)}_{+\bar{0}-} = -A^{(0)}_{0-+} = -\sqrt{2}A^{(0)}_{0\bar{0}0}\,. \tag{E.41}$$

Adding this information to the relations found previously one is still unable to reproduce Eq. (E.39).

However, now we proceed in a different way. We do not consider the $KK\pi$ state as a $1/2 \times 1/2 \times 1$ isospin state in our reasoning. Since the K^* contribution dominates over that of the ρ, ω and ϕ in the hadronic matrix elements of interest, we can consider the composition $K \times \pi$ and then keep only its $I = 1/2$ component, corresponding to the K^*. In addition, the processes with charged and neutral pions can be distinguished at detection, which makes that the following amplitudes should be considered independently [507] (we will be writing the $K\pi$ pair making the K^* as the last two particles until the end of this section): $K^+K^-\pi^0$, $K^0\bar{K}^0\pi^0$, $K^0K^-\pi^+$ and $K^+\bar{K}^0\pi^-$. In addition, we will considered the C-parity conjugated decays. Proceeding this way one finds the following amplitudes (we call B_0 and B_1 the participating isoscalar and isovector amplitudes):

$$\begin{aligned} A\left(K^+K^-\pi^0\right) &= -\frac{B_0+B_1}{\sqrt{6}}\,, \quad A\left(K^0\bar{K}^0\pi^0\right) = \frac{B_0-B_1}{\sqrt{6}}\,, \\ A\left(K^0K^-\pi^+\right) &= \frac{B_1-B_0}{\sqrt{3}}\,, \quad A\left(K^+\bar{K}^0\pi^-\right) = -\frac{B_0+B_1}{\sqrt{3}}\,, \end{aligned} \tag{E.42}$$

while for the C-conjugated amplitudes one finds (we introduce the amplitudes C_0 and C_1):

$$\begin{aligned} A\left(K^-K^+\pi^0\right) &= \frac{C_1-C_0}{\sqrt{6}}\,, \quad A\left(\bar{K}^0K^0\pi^0\right) = \frac{C_0+C_1}{\sqrt{6}}\,, \\ A\left(\bar{K}^0K^+\pi^-\right) &= -\frac{C_1+C_0}{\sqrt{3}}\,, \quad A\left(K^-K^0\pi^+\right) = \frac{C_1-C_0}{\sqrt{3}}\,, \end{aligned} \tag{E.43}$$

Summing up the first, second, third and four relations in Eqs. (E.42) and (E.43) in pairs one obtains the relations

$$\begin{aligned} \sigma\left(e^+e^- \to K^+\bar{K}^0\pi^- + e^+e^- \to K^-K^+\pi^0\right) &= \frac{1}{6}\left|A_0 - A_1\right|^2\,, \\ \sigma\left(e^+e^- \to K^0\bar{K}^0\pi^0 + e^+e^- \to \bar{K}^0K^0\pi^0\right) &= \frac{1}{6}\left|A_0 + A_1\right|^2\,, \\ \sigma\left(e^+e^- \to K^0K^-\pi^+ + e^+e^- \to \bar{K}^0K^+\pi^-\right) &= \frac{1}{3}\left|A_0 + A_1\right|^2\,, \\ \sigma\left(e^+e^- \to \bar{K}^0K^+\pi^- + e^+e^- \to K^-K^0\pi^+\right) &= \frac{1}{3}\left|A_0 - A_1\right|^2\,, \end{aligned} \tag{E.44}$$

where $A_0 \equiv B_0 + C_0$ and $A_1 \equiv B_1 + C_1$ have been introduced. Summing up all Eqs. in (E.44) gives

$$\sigma\left(e^+e^- \to KK\pi\right) = |A_0|^2 + |A_1|^2\,, \tag{E.45}$$

and adding the last two Eqs. in (E.44) yields

$$\sigma\left(e^+e^- \to KK\pi^\pm\right) = \frac{2}{3}\left(|A_0|^2 + |A_1|^2\right) \tag{E.46}$$

and using that $K_S = \left(K^0 - \bar{K}^0\right)/\sqrt{2}$ one gets finally

$$3\,\sigma\left(e^+e^- \to K_S K^\pm\pi^\mp\right) = |A_0|^2 + |A_1|^2 = \sigma\left(e^+e^- \to KK\pi\right)\,, \tag{E.47}$$

which is Eq. (E.39). Since *BaBar* [507] manages to split the $I = 0$ and $I = 1$ components of $\sigma\left(e^+e^- \to K_S K^\pm\pi^\mp\right)$, and thus to measure $|A_0|^2/3$ and $|A_1|^2/3$, it is straightforward to obtain $\sigma|_{I=1}\left(e^+e^- \to KK\pi\right)$.
What are the approximations employed in order to get this relation? In addition to the well supported $SU(2)$ symmetry and K^* dominance, there is a source of error given by the definition employed for the K^*. To give an example, and as commented at the beginning of this section, the states $K^+K^-\pi^0$ and $K^-K^+\pi^0$ are the same in a $KK\pi$ analysis while this is not the case in a KK^* study. One could argue that since the K^* is quite narrow, this approximation is justified.

E.3 $\eta\pi\pi$ channels

Since both the η_8 and the η_1 are $SU(2)$-singlets, we can compute the isospin relations between $\eta_{1,8}\pi\pi$ channels just by taking into account the isospin of the $\pi\pi$ states. We will use η to denote either state irrespectively. The first study of isospin relations for this and related modes was carried out in Ref. [490]. Our results are, to our knowledge, new.

The different states $\eta_{1,8}\pi\pi$ that can be produced in τ decays and e^+e^- collisions

are the following:

$$
\begin{aligned}
|\pi^+\pi^-\rangle &= |1,+1\rangle \otimes |1,-1\rangle = \frac{1}{\sqrt{6}}|2,0\rangle + \frac{1}{\sqrt{2}}|1,0\rangle + \frac{1}{\sqrt{3}}|0,0\rangle\,, \\
|\pi^-\pi^+\rangle &= |1,-1\rangle \otimes |1,+1\rangle = \frac{1}{\sqrt{6}}|2,0\rangle - \frac{1}{\sqrt{2}}|1,0\rangle + \frac{1}{\sqrt{3}}|0,0\rangle, \\
|\pi^0\pi^0\rangle &= |1,0\rangle \otimes |1,0\rangle = \sqrt{\frac{2}{3}}|2,0\rangle - \frac{1}{\sqrt{3}}|0,0\rangle, \\
|\pi^-\pi^0\rangle &= |1,-1\rangle \otimes |1,0\rangle = \frac{1}{\sqrt{2}}\left(|2,-1\rangle - |1,-1\rangle\right), \\
|\pi^0\pi^-\rangle &= |1,0\rangle \otimes |1,-1\rangle = \frac{1}{\sqrt{2}}\left(|2,-1\rangle + |1,-1\rangle\right), \\
|\pi^+\pi^0\rangle &= |1,+1\rangle \otimes |1,0\rangle = \frac{1}{\sqrt{2}}\left(|2,+1\rangle + |1,+1\rangle\right), \\
|\pi^0\pi^+\rangle &= |1,0\rangle \otimes |1,+1\rangle = \frac{1}{\sqrt{2}}\left(|2,+1\rangle - |1,+1\rangle\right). \qquad \text{(E.48)}
\end{aligned}
$$

Solving for the $|I,I_3\rangle$ states yields:

$$
\begin{aligned}
|2,0\rangle &= \frac{1}{\sqrt{6}}\left(|\pi^+\pi^-\rangle + |\pi^-\pi^+\rangle + 2|\pi^0\pi^0\rangle\right), \\
|1,0\rangle &= \frac{1}{\sqrt{2}}\left(|\pi^+\pi^-\rangle - |\pi^-\pi^+\rangle\right), \\
|0,0\rangle &= \frac{1}{\sqrt{3}}\left(|\pi^+\pi^-\rangle + |\pi^-\pi^+\rangle - |\pi^0\pi^0\rangle\right), \\
|2,-1\rangle &= \frac{1}{\sqrt{2}}\left(|\pi^-\pi^0\rangle + |\pi^0\pi^-\rangle\right), \\
|1,-1\rangle &= \frac{1}{\sqrt{2}}\left(|\pi^0\pi^-\rangle - |\pi^-\pi^0\rangle\right), \\
|2,+1\rangle &= \frac{1}{\sqrt{2}}\left(|\pi^+\pi^0\rangle + |\pi^0\pi^+\rangle\right), \\
|1,+1\rangle &= \frac{1}{\sqrt{2}}\left(|\pi^+\pi^0\rangle - |\pi^0\pi^+\rangle\right). \qquad \text{(E.49)}
\end{aligned}
$$

Using Eqs. (E.4), (E.5), (E.6) one has:

$$
{}_{(I,-1)}\langle\,\eta\pi\pi|\overline{d}\,\Gamma_\mu\,u|0\,\rangle = -{}_{(I,0)}\Big\langle\eta\pi\pi\Big|\frac{\overline{u}\,\Gamma_\mu\,u\,-\,\overline{d}\,\Gamma_\mu\,d}{\sqrt{2}}\Big|0\Big\rangle\,. \qquad \text{(E.50)}
$$

Now if we denote by $T_{-0}, T_{0-}, T_{+-}, T_{-+}, T_{00}$ the amplitudes $\langle\, \eta\pi\pi|\overline{d}\Gamma_\mu u|0\,\rangle$ and $\left\langle \eta\pi\pi\left|\frac{\overline{u}\Gamma_\mu u-\overline{d}\Gamma_\mu d}{\sqrt{2}}\right|0\right\rangle$ for charge $\eta\pi\pi$ states, we obtain the following relations

$$\begin{aligned}
&\frac{1}{\sqrt{2}}\,(T_{-0}+T_{0-}) = -\frac{1}{\sqrt{6}}\,(T_{+-}+T_{-+}-2T_{00}) = 0\,,\\
&\frac{1}{\sqrt{2}}\,(T_{0-}-T_{-0}) = -\frac{1}{\sqrt{2}}\,(T_{-+}-T_{+-})\ ,\\
&\sqrt{3}\,(T_{+-}+T_{-+}-T_{00}) = 0\,,
\end{aligned} \tag{E.51}$$

which lead to

$$T_{00} = 0\ \ , T_{+-} = -T_{-+} = T_{0-} = -T_{-0}\,. \tag{E.52}$$

Now let us consider the electromagnetic current. One can decompose it into $I=0$ and $I=1$ pieces:

$$\Gamma^\mu = \frac{1}{3}\left(2\overline{u}\gamma^\mu u - \overline{d}\gamma^\mu d - \overline{s}\gamma^\mu s\right) = \Gamma^\mu_{(0)} + \Gamma^\mu_{(1)}\,, \tag{E.53}$$

where

$$\Gamma^\mu_{(0)} = \frac{1}{6}\left(\overline{u}\gamma^\mu u + \overline{d}\gamma^\mu d - 2\overline{s}\gamma^\mu s\right)\ ,\ \Gamma^\mu_{(1)} = \frac{1}{2}\left(\overline{u}\gamma^\mu u - \overline{d}\gamma^\mu d\right)\ . \tag{E.54}$$

In general we will have

$$\langle\,(\eta\pi\pi)^0| = A_{+-}\langle\,\eta\pi^+\pi^-| + A_{-+}\langle\,\eta\pi^-\pi^+| + A_{00}\langle\,\eta\pi^0\pi^0|\,. \tag{E.55}$$

Using the decomposition in Eq. (E.48) one can relate the amplitudes $\langle\,\eta\pi\pi|\Gamma^\mu|0\,\rangle$ for charge and isospin $|\eta\pi\pi\,\rangle$ states as:

$$A_{+-} = \frac{1}{\sqrt{2}}A_1 + \frac{1}{\sqrt{3}}A_0\,,\quad A_{-+} = -\frac{1}{\sqrt{2}}A_1 + \frac{1}{\sqrt{3}}A_0\,,\quad A_{00} = -\frac{1}{\sqrt{3}}A_0\,. \tag{E.56}$$

Moreover the vanishing of the amplitude A_2 implies

$$2A_{00} + A_{+-} + A_{-+} = 0\,. \tag{E.57}$$

In this way one obtains the following relations:

$$\begin{aligned}
&A_{+-} + A_{00} = \frac{1}{\sqrt{2}}A_1\,,\ A_{-+} + A_{00} = -\frac{1}{\sqrt{2}}A_1\,,\ A_1 = \frac{A_{+-}-A_{-+}}{\sqrt{2}}\,,\\
&A_0 = \frac{A_{+-}+A_{-+}-A_{00}}{\sqrt{3}} = -\sqrt{3}A_{00} = \frac{\sqrt{3}}{2}\,(A_{+-}+A_{-+})\ ,
\end{aligned} \tag{E.58}$$

which lead to

$$|A_{+-}+A_{-+}|^2 + |A_{+-}-A_{-+}|^2 = 2\left(|A_{+-}|^2+|A_{-+}|^2\right) = 4|A_{00}|^2 + 2|A_1|^2\,, \tag{E.59}$$

$$|A_1|^2 = |A_{+-}|^2 + |A_{-+}|^2 - 2|A_{00}|^2\,. \tag{E.60}$$

The corresponding cross sections are related by [11]

$$\begin{aligned}\sigma\left(e^+e^-\to\eta\pi\pi\right)|_{I=1} &= \sigma\left(e^+e^-\to\eta\pi^+\pi^-\right)+\sigma\left(e^+e^-\to\eta\pi^-\pi^+\right)\\ &\quad -2\times 2\,\sigma\left(e^+e^-\to\eta\pi^0\pi^0\right),\\ &= 2\,\sigma\left(e^+e^-\to\eta\pi^+\pi^-\right)-4\,\sigma\left(e^+e^-\to\eta\pi^0\pi^0\right)\sim\\ &\sim 2\,\sigma\left(e^+e^-\to\eta\pi^+\pi^-\right), \end{aligned} \tag{E.61}$$

where the additional factor of 2 in the above relation comes from the identity of particles in the final state, introducing a factor of 1/2 in the angular integration. For the isoscalar part we have

$$\sigma\left(e^+e^-\to\eta\pi\pi\right)|_{I=0} = 6\,\sigma\left(e^+e^-\to\eta\pi^0\pi^0\right)\sim 0\,. \tag{E.62}$$

Finally, one has

$$\frac{1}{\sqrt{2}}\left(T^{0-}-T^{-0}\right)=\sqrt{2}T^{0-}=-\langle 1,0|\frac{\bar{u}u-\bar{d}d}{\sqrt{2}}|0\rangle=-\sqrt{2}A_1\,. \tag{E.63}$$

Taking into account Eq. (E.12) the cross-sections for the different modes read ($|A_{+-}|^2=\frac{|A_1|^2}{2}=\frac{|A_{-0}|^2}{2}$)

$$\begin{aligned}\sigma\left(e^+e^-\to\eta\pi^+\pi^-\right) &= \frac{\alpha^2}{96\pi}\frac{1}{Q^6}\int \mathrm{d}s\;\mathrm{d}t\;|T_{-0}|^2\left(V_{3\mu}V^{3\mu *}\right),\\ \sigma\left(e^+e^-\to\eta\pi^0\pi^0\right) &= \frac{\alpha^2}{48\pi}\frac{1}{Q^6}\int \mathrm{d}s\;\mathrm{d}t\;\frac{1}{2}|T_{00}|^2\left(V_{3\mu}V^{3\mu *}\right)\sim 0\,, \end{aligned} \tag{E.64}$$

where the additional factor of 1/2 in the second line comes from having identical particles in the final state.

Using the former isospin relations one finally obtains

$$\begin{aligned}\frac{d\Gamma(\tau\to\eta\pi^-\pi^0\nu_\tau)}{\mathrm{d}Q^2} &= f(Q^2)\,\sigma(e^+e^-\to\eta\pi\pi)|_{I=1}\\ &= f(Q^2)\left[\sigma(e^+e^-\to\eta\pi^+\pi^-)-2\,\sigma(e^+e^-\to\eta\pi^0\pi^0)\right]\\ &\sim f(Q^2)\,\sigma(e^+e^-\to\eta\pi^+\pi^-) \end{aligned} \tag{E.65}$$

where $f(Q^2)$ is given in Eq. (E.14).

E.4 Other channels

E.1 $\eta\eta\pi$ channels

Since the $\eta_{1,8}$ are $SU(2)$ singlets it is as if it was just $\eta\eta\pi\sim\pi$, where η will be referring either to the singlet or the octet state here and in following sections.

[11] Because of C-parity, $\sigma\left(e^+e^-\to\eta\pi^0\pi^0\right)=0$ to $\mathcal{O}(\alpha)$, since $C_\gamma=-$ and $C_{\pi^0,\eta,\eta'}=+$. Although it is non-vanishing at higher orders, it can be safely neglected in all the low-energy applications we are considering.

Here we are concerned with the processes $e^+e^- \to \eta\eta\pi^0 \sim |1,0\rangle$ and $\tau^- \to \eta\eta\pi^-\nu_\tau \sim |1,-1\rangle$. Considering that

$$ {}_{(1,-1)}\langle\, \eta\eta\pi|\overline{d}\,\Gamma_\mu\, u|0\,\rangle \,=\, -{}_{(1,0)}\Big\langle \eta\eta\pi\Big|\frac{\overline{u}\,\Gamma_\mu\, u - \overline{d}\,\Gamma_\mu\, d}{\sqrt{2}}\Big|0\Big\rangle\,, \tag{E.66} $$

the respective amplitudes (T_0 and T_-) are the same up to a sign. Using also that there is only isovector component in the considered e^+e^- cross section we have

$$ \frac{\mathrm{d}\Gamma\left(\tau \to \eta\eta\pi^-\nu_\tau\right)}{\mathrm{d}Q^2} \,=\, f(Q^2)\,\sigma\left(e^+e^- \to \eta\eta\pi^0\right)\,. \tag{E.67} $$

E.2 ηKK channels

Again, the η can be ignored as far as isospin is concerned, so that we have $e^+e^- \to K^+K^-\eta \sim |K^+K^-\rangle$, $e^+e^- \to K^0\overline{K}^0\eta \sim |K^0\overline{K}^0\rangle$ and $\tau \to \eta K^-K^0 \sim |K^-K^0\rangle$. Note that both kaons belong to different isospin multiplets, so the order is not important. Using the results in Eq. (E.17) we see that

$$ |0,0\,\rangle \,=\, \Big|\frac{K^+K^- + K^0\overline{K}^0}{\sqrt{2}}\Big\rangle\,, \quad |1,0\,\rangle \,=\, \Big|\frac{K^+K^- - K^0\overline{K}^0}{\sqrt{2}}\Big\rangle\,, \quad |1,-1\,\rangle \,=\, |K^-K^0\,\rangle\,. \tag{E.68} $$

Using that

$$ {}_{(I,-1)}\langle\, KK\pi|\overline{d}\,\Gamma_\mu\, u|0\,\rangle \,=\, -{}_{(I,0)}\Big\langle KK\pi\Big|\frac{\overline{u}\,\Gamma_\mu\, u - \overline{d}\,\Gamma_\mu\, d}{\sqrt{2}}\Big|0\Big\rangle\,, \tag{E.69} $$

one gets

$$ T_{-0} \,=\, \frac{1}{\sqrt{2}}\left(T_{0\overline{0}} \,-\, T_{+-}\right)\,, \tag{E.70} $$

for the weak amplitudes. Since the quark operators carry $I = 1$, the amplitude associated to the production of $|0,0\,\rangle$ vanishes, so that $T_{+-} + T_{0\overline{0}} = 0$ and we have the following relations between the weak amplitudes

$$ T_{-0} \,=\, -\sqrt{2}T_{+-} \,=\, \sqrt{2}T_{0\overline{0}}\,, \tag{E.71} $$

that one can use to obtain the low-energy description of $e^+e^- \to \eta KK$ using the vector form factor computed in the CVC-related τ decay, $\tau \to \eta K^-K^0$, with amplitude T_{-0}.

Now we consider the electromagnetic current. The isospin amplitudes are

$$ A_1 \,=\, \frac{A_{+-} \,-\, A_{0\overline{0}}}{\sqrt{2}}\,, \quad A_0 \,=\, \frac{A_{+-} \,+\, A_{0\overline{0}}}{\sqrt{2}}\,. \tag{E.72} $$

The isoscalar piece vanishes and we are only left with the isovector one. We have thus

$$ \sigma\left(e^+e^- \to KK\eta\right) \,=\, 2\sigma\left(e^+e^- \to K^+K^-\eta\right)\,. \tag{E.73} $$

Appendix F: Antisymmetric tensor formalism for meson resonances

The antisymmetric tensor formalism for spin-one fields was already developed in the sixties [548, 549], although its generalization needed to wait until Gasser and Leutwyler proposed it to introduce the starring ρ resonance in the chiral Lagrangian [4] and a few years later, Ecker *et al.* [6] took adventage of it for including the resonances in $R\chi T$. These benefits will be explained throughout this Appendix together with the main features of the formalism.

A crucial understanding was that -provided consistency with QCD asymptotic behaviour- the physics given by the EFT does not depend on the chosen formalism [7], which authorizes us to choose the tensor formalism for convenience.

In Ref. [550, 551] it was proved that for massive antisymmetric tensor fields there are (up to multiplicative factors and a total divergence) only two possible Lagrangians of second order in derivatives, if one assumes the existence of a Klein-Gordon divisor. They correspond to having either the Lorentz condition or else the Bianchi identity satisfied by the fields. In the case of spin-1 particles one has the following two options ($W_{\mu\nu} = -W_{\nu\mu}$),

1. The subsidiary condition is the Bianchi identity, i.e. $\epsilon^{\mu\lambda\rho\sigma}\partial_\lambda W_{\rho\sigma}$, and W_{ik} are frozen, so the three dynamical degrees of freedom are W_{i0}, where $i = 1, 2, 3$.

2. The subsidiary condition is the Lorentz condition, $\partial^\rho W_{\rho\nu} = 0$ and W_{i0} are frozen, so the degrees of freedom are W_{ij}.

For historical reasons the first option was chosen, as we will see in the following. We consider a Lagrangian quadratic in the antisymmetric tensor field $W_{\mu\nu}$,

$$\mathcal{L} \,=\, a\,\partial^\mu W_{\mu\nu}\partial_\rho W^{\rho\nu} \,+\, b\,\partial^\rho W_{\mu\nu}\partial_\rho W^{\mu\nu} \,+\, c\,W_{\mu\nu}W^{\mu\nu}\,, \tag{F.1}$$

where a, b and c are arbitrary constants. The field $W^{\mu\nu}$ contains six degrees of freedom. To describe massive spin-one particle we must reduce them to three corresponding to the physical polarizations these particles have. This can be done with a clever choice of a and b. Indeed, consider the EOM

$$a\,(\partial^\mu\partial_\sigma W^{\sigma\nu} \,-\, \partial^\nu\partial_\sigma W^{\sigma\mu}) \,+\, 2b\,\partial^\sigma\partial_\sigma W^{\mu\nu} \,-\, 2c\,W^{\mu\nu} \,=\, 0\,, \tag{F.2}$$

that can be splitted up into the time-spatial and spatial-spatial components:

$$\begin{aligned}(a+2b)\ddot{W}^{0i} + a\partial_l\dot{W}^{li} - a\partial^i\partial_l W^{l0} - 2(b\Box + c)W^{0i} = 0\,,\\ 2b\ddot{W}^{ik} + a\left[\partial^i(\dot{W}^{0k} + \partial_l W^{lk})\right] - 2(b\Box + c)W^{ik} = 0\,,\end{aligned} \tag{F.3}$$

where the dots denote time derivatives and $\Box$ stands for the Dalembertian operator. For $a + 2b = 0$, the three fields W^{0i} do not propagate ($b = 0$ freezes the spatial-spatial components, on the contrary). The $W^{\mu\nu}$ propagator, defined to be the inverse of the differential operator in (F.1) contains poles in $k^2 = -c/b$ and $k^2 = -2c/(a+2b)$, which disappear for $b = 0$, or $a + 2b = 0$, respectively. To maintain only one pole and reduce the number of degrees of freedom to three, we must choose among these two options. In [6], it was preferred to fix $b = 0$, and to choose a and c for the pole to correspond to the particle mass, that is, $a = -1/2$, and $c = M^2/4$. Then, the Lagrangian (F.1) becomes

$$\mathcal{L} = -\frac{1}{2}\partial^\mu W_{\mu\nu}\partial_\rho W^{\rho\nu} + \frac{1}{4}M^2 W_{\mu\nu}W^{\mu\nu}\,, \tag{F.4}$$

from which the free-case EOM is

$$\partial^\mu\partial_\sigma W^{\sigma\nu} - \partial^\nu\partial_\sigma W^{\sigma\mu} + M^2 W^{\mu\nu} = 0\,, \tag{F.5}$$

where only three degrees of freedom corresponding to a spin-one particle resonance of mass M are described. Notice that the definition

$$W_\mu = \frac{1}{M}\,\partial^\nu W_{\nu\mu}\,, \tag{F.6}$$

allows to recover from (F.5) the familiar Proca equation

$$\partial_\rho(\partial^\rho W^\mu - \partial^\mu W^\rho) + M^2 W^\mu = 0\,. \tag{F.7}$$

From the Lagrangian (F.4), one can derive the explicit expression for the resonance propagator

$$\langle\, 0|T\left\{W_{\mu\nu}(x),\, W_{\rho\sigma}(y)\right\}|0\,\rangle = \int \frac{\mathrm{d}^4k}{(2\pi)^4}e^{-ik(x-y)}\left\{\frac{2i}{M^2-q^2}\,\Omega^L_{\mu\nu,\rho\sigma} + \frac{2i}{M^2}\,\Omega^T_{\mu\nu,\rho\sigma}\right\}, \tag{F.8}$$

where the antisymmetric tensors

$$\begin{aligned}\Omega^L_{\mu\nu,\rho\sigma}(q) &= \frac{1}{2q^2}\left(g_{\mu\rho}q_\nu q_\sigma - g_{\rho\nu}q_\mu q_\sigma - (\rho\leftrightarrow\sigma)\right),\\ \Omega^T_{\mu\nu,\rho\sigma}(q) &= -\frac{1}{2q^2}\left(g_{\mu\rho}q_\nu q_\sigma - g_{\rho\nu}q_\mu q_\sigma - q^2 g_{\mu\rho}g_{\nu\sigma} - (\rho\leftrightarrow\sigma)\right),\end{aligned} \tag{F.9}$$

have been defined. Upper-indices mean longitudinal or transversal polarizations. In order to identify the preceding operators with projectors over these polarizations, one needs to consider as a generalized identity in this space the tensor $\mathcal{I}_{\mu\nu,\rho\sigma}$,

$$\mathcal{I}_{\mu\nu,\rho\sigma} = \frac{1}{2}\left(g_{\mu\rho}g_{\nu\sigma} - g_{\mu\sigma}g_{\nu\rho}\right), \tag{F.10}$$

because any antisymmetric tensor, $\mathcal{A}_{\mu\nu} = -\mathcal{A}_{\nu\mu}$, fulfills

$$\mathcal{A}\cdot\mathcal{I} = \mathcal{I}\cdot\mathcal{A} = \mathcal{A}\,, \tag{F.11}$$

and therefore the $\Omega^{L(T)}$ indeed verify projector properties

$$\begin{aligned}\Omega^T + \Omega^L = \mathcal{I}\,,\;\; \Omega^T\cdot\Omega^L = \Omega^L\cdot\Omega^T = 0\,,\\ \Omega^T\cdot\Omega^T = \Omega^T\,,\;\; \Omega^L\cdot\Omega^L = \Omega^L\,.\end{aligned} \tag{F.12}$$

The propagator (F.8) corresponds to the normalization

$$\langle\, 0|\, W_{\mu\nu}\,|W,p\,\rangle = \frac{i}{M}[p_\mu\epsilon_\nu(p) - p_\nu\epsilon_\mu(p)]\,. \tag{F.13}$$

Once we have seen the general properties of the antisymmetric tensor formalism and how it works, let us move to the second important issue: What is the advantage of using it instead of the more familiar Proca formalism? Working with the antisymmetric tensor formalism there is no need to consider $\mathcal{L}_4$ from χPT to give the EFT the asymptotic behaviour ruled by QCD.

As an example of that, I will consider the same taken in [7]: the vector form factor of the pion.

Tree-level computation with (4.19) -with antisymmetric tensor formalism, thengives:

$$\mathcal{F}(q^2) = 1 + \frac{F_V G_V}{F^2}\frac{q^2}{M_V^2 - q^2}\,. \tag{F.14}$$

Let us consider now the corresponding Lagrangian written in the Proca formalism that describes meson resonances [552, 553],

$$\mathcal{L}^{\rm Proca} = \mathcal{L}^{\rm Proca}_{\rm kin} + \mathcal{L}^{\rm Proca}_2\,, \tag{F.15}$$

where it has been defined

$$\begin{aligned}\mathcal{L}^{\rm Proca}_{\rm kin} &= -\frac{1}{4}\langle\, \hat{V}_{\mu\nu}\hat{V}^{\mu\nu} - 2M_V^2\hat{V}_\mu\hat{V}^\mu\,\rangle\,,\\ \Delta L^{\rm Proca}_2 &= -\frac{1}{2\sqrt{2}}\Big(f_V\langle\,\hat{V}^{\mu\nu}f^+_{\mu\nu}\,\rangle + ig_V\langle\,\hat{V}_{\mu\nu}[u^\mu,u^\nu]\,\rangle\Big)\,,\\ \hat{V}_{\mu\nu} &= \nabla_\mu\hat{V}_\nu - \nabla_\nu\hat{V}_\mu\,,\end{aligned} \tag{F.16}$$

and the hat identifies Proca formalism. For simplicity, only that part of the Lagrangian contributing to the considered form factor has been written. The result (F.16) gives for the vector form factor of the pion is

$$\widetilde{\mathcal{F}}^{\rm Proca}(q^2) = 1 + \frac{f_V g_V}{F^2}\frac{(q^2)^2}{M_V^2 - q^2}\,. \tag{F.17}$$

QCD short-distance behaviour ($q^2 \to \infty$) dictates that the pion form factor must vanish in this limit [12]. For (F.14) this relates three $LECs$ as in Eq. (4.21), $F_V G_V = F^2$, but for (F.17) this behaviour is not possible unless we add to (F.16) a local term. This one must have the structure of the term whose coefficient is L_9 in Eq. (3.77). One then needs at the same time that $L_9^{\rm Proca} = \frac{1}{2} f_V g_V$ and $f_V g_V = F^2/M_V^2$ happen

$$\begin{aligned} \mathcal{F}^{\rm Proca}(q^2) &= 1 + \frac{f_V g_V}{F^2} \frac{(q^2)^2}{M_V^2 - q^2} + \frac{2}{F^2} L_9^{\rm Proca} q^2 \,, \\ L_9^{\rm Proca} &= \frac{1}{2} f_V g_V \,, \end{aligned} \tag{F.18}$$

where the tilde over the form factor has been removed because it has been corrected by the needed local terms discussed previously to guarantee the right asymptotic behaviour.

It can be shown [7] that this finding in the case of the pion vector form factor is a general fact: Working with the tensor formalism there is no need to include the terms of $\mathcal{L}_4$ from χPT,

$$L_i = 0 \qquad i = 1, 2, 3, 9, 10 \,, \tag{F.19}$$

whereas for the Proca case we must include them fulfilling

$$\begin{aligned} L_1^{\rm Proca} = \frac{1}{8} g_V^2 \,, \qquad L_2^{\rm Proca} = \frac{1}{4} g_V^2 \,, \qquad L_3^{\rm Proca} = -\frac{3}{4} g_V^2 \,, \\ L_9^{\rm Proca} = \frac{1}{2} f_V g_V \,, \qquad L_{10}^{\rm Proca} = -\frac{1}{4} f_V^2 \,, \end{aligned} \tag{F.20}$$

for vector resonances. Something similar [7] happens for the axial-vectors, the other resonances that dominate phenomenology whenever they can be involved. Then, it is clear we can choose the formalism for describing resonances, and justify that it is more convenient to take the antisymmetric tensor formalism.

For completeness, I mention that there is another way of treating resonances: the so-called hidden-gauge formalism [554, 555, 556, 557]. This method is based on the freedom that exists to choose the representative of the coset G/H of the chiral group G over the vector subgroup. In the Hidden Local Symmetry model, vector mesons are regarded as authentic gauge bosons of a hidden symmetry of the Lagrangian that relates the different possible choices of the coset representative. However, it is not clear at all that vector mesons stand out from axial-vectors (in fact, VMD involves both), nor the gauge nature of resonances is not an artifact. At the end of the day, (pseudo)scalar resonances do exist and there is no natural procedure to

[12] Formally, this comes from the analysis of the spectral function $\Im\mathrm{m}\ \Pi_V(q^2)$ of the $I = 1$ vector current two-point function. In the framework of QCD, one finds [297] $\Im m\, \Pi_V(q^2) \to$ constant as $q^2 \to \infty$, from which it follows that $F(q^2)$ obeys a dispersion relation with at most one subtraction. In the narrow-width approximation for the exchanged ρ, all this drives directly to $\mathcal{F}(q^2) = 1 + \frac{\text{const.} \times q^2}{M_V^2 - q^2}$, as (F.14).

include them in this model. The loop corrections in these theories [558, 559] give an ultraviolet behaviour that is much simpler than the one found in $R\chi T$ [192].

Appendix G: Successes of the large-N_C limit of QCD

G.1 Introduction

In this appendix we will review the most important phenomenological successes of the large-N_C limit of QCD. First we will consider the results obtained in the limit $N_C \to \infty$ limit of QCD to understand some characteristic features of meson phenomenology. After that, we will review the rle of the $1/N_C$ expansion in the effective theories of QCD for low and intermediate energies: χPT and $R\chi T$. They come to complement the most relevant success of the large-N_C limit of QCD for us, namely that it provides us with a framework able to describe exclusive hadron decays of the τ as we have seen in this Thesis.

G.2 Phenomenological successes of the large-N_C expansion

- There is a supression in hadron physics of the sea quark pairs, $\overline{q}\,q$. Therefore, mesons are pure $\overline{q}\,q$ states, thus exotic states such as $\overline{q}\,q\,\overline{q}\,q$ are eliminated in practice. In short, this is due to the fact that there are much more gluon than quark states. In the large-N_C limit sea quarks are negligible. Apart from that, in this limit, mesons do not interact, so any candidate to an exotic state must be, in fact, a set of ordinary states. Being exotic requires interaction for the state to be seen as a composite one; but mesons do not interact in the $N_C \to \infty$ limit.

- Confinement restricts hadron states to be singlets of colour. From the group theoretical point of view, it is clear [560] that a quark -antiquark state can be decomposed into a direct sum in the following way (all representations are in colour space):

$$\underline{3} \otimes \overline{\underline{3}} = \underline{1} \oplus \underline{8}\,. \tag{G.1}$$

  Of course, the octet $\underline{8}$ cannot live as meson non-singlet of colour state. Still,

it can combine with a partner to become $\underline{1}$:

$$\underline{8} \otimes \underline{8} = \underline{27} \oplus \underline{10} \oplus \overline{\underline{10}} \oplus \underline{8} \oplus \underline{8} \oplus \underline{1}\,. \tag{G.2}$$

Zweig rule [561] states that this possibility is strongly suppressed, being greatly exceeded by one-gluon exchange among a meson and a sea quark-antiquark pair. For instance, this together with the conservation of all internal quantum numbers explains why the J/Ψ has such a narrow decay width: six strong vertices are required for its decay. Zweig rule has the consequence that mesons are better described, in the large-N_C limit, as flavour $U(3)$-nonets, rather than as singlets plus octets, because this splitting involves annihilation diagrams among them that are suppressed in this limit [13]. To conclude, gluon states decoupling is a result of all that: because they cannot be produced at LO in $1/N_C$ as a product of reactions starting from hadrons or electroweak currents. Therefore, these states are not seen experimentally.

- Meson decays are mostly of two-body type, because many final-state particle processes are less probable than those resonant decays into two intermediate particles. This is a natural consequence in the $1/N_C$-expansion. For a particle decaying into three mesons both processes are globally $\mathcal{O}(1/N_C)$; the point is that decaying directly is $\mathcal{O}(1/N_C)$, while the first vertex in the two-step process is $\mathcal{O}(1/\sqrt{N_C})$, and thus the two-body intermediate decay dominates over the direct one.

- At first sight, it seemed a strange feature that the number of resonances becomes infinite in this limit. The big number of resonances that has been discovered and their relatively thin width can be taken as another phenomenological support of the large-N_C arguments.

- Last but not least, the success of phenomenology describing strong interaction in the intermediate-energy region in terms of tree-level Feynman diagrams with hadrons as degrees of freedom, that is, the success of $EFTs$ -and particularly of $R\chi T$-, based on large$-N_C$ arguments; is a recognition of the $1/N_C$ -expansion. NLO corrections correspond to loop diagrams involving hadrons and provide the resonances with a finite width.

G.3 $1/N_C$ expansion for χPT

The $1/N_C$ expansion provides a well-defined counting scheme for $EFTs$ of QCD, exactly what we needed to develop an EFT of the strong interaction in the intermediate-energy region involving light quarks. Although we do not need $1/N_C$ as an expansion

[13] For $N_C \to \infty$, the axial anomaly disappears and $U(n_f)_L \otimes U(n_f)_R$ is restored. Moreover, under very general assumptions, it can be shown that in the large-N_C limit, $U(n_f)_L \otimes U(n_f)_R$ is broken down to $U(n_f)_V$ [562].

parameter at very-low energies, it is justified to apply it to χPT, to check the consistency of the expansion with a theory known to be successful. After that, we will have a strong test for any new EFT extending to higher energies. As we will see, for $R\chi T$ one gets reasonable results when subjected to this exam.

The main features of the effective theory relevant for the meson sector of QCD in the large-N_C limit were discovered long ago [271, 270, 563, 564, 565]. The systematic analysis in the framework of χPT was taken up in Ref. [5], where the Green functions of QCD were studied by means of a simultaneous expansion in powers of momenta, quark masses and $1/N_C$ (with $1/N_C \sim p^2 \sim m_q$).

The dominant terms should be $\mathcal{O}(N_C)$, as they are the corresponding correlation functions among quark bilinears. A quark loop means a trace in Dirac, colour and flavour space. The last one supresses these kind of terms with respect to those without quark loops. One quark loop is needed to provide the quantum numbers of a meson, but each additional quark loop will be suppressed by a $1/N_C$ factor.

In the large-N_C limit of QCD the axial anomaly disappears, so that the spectrum does not correspond to $SU(3)$-multiplets anymore (octet and singlet, each one on its own), but to $U(3)$-multiplets, that is, nonets.

Therefore, at LO in $1/N_C$ the axial anomaly vanishes and the eta singlet becomes the ninth pG:

$$\begin{aligned} \Phi(x) &= \frac{1}{\sqrt{2}} \sum_{a=0}^{8} \lambda_a \Phi^a \qquad (G.3) \\ &= \begin{pmatrix} \frac{1}{\sqrt{2}}\pi^0 + \frac{1}{\sqrt{6}}\eta_8 + \frac{1}{\sqrt{3}}\eta_1 & \pi^+ & K^+ \\ \pi^- & -\frac{1}{\sqrt{2}}\pi^0 + \frac{1}{\sqrt{6}}\eta_8 + \frac{1}{\sqrt{3}}\eta_1 & K^0 \\ K^- & \overline{K}^0 & -\frac{2}{\sqrt{6}}\eta_8 + \frac{1}{\sqrt{3}}\eta_1 \end{pmatrix}, \end{aligned}$$

where the set of Gell-Mann matrices that are the generators of $SU(3)$ in the fundamental representation, has been enlarged by including the extra-generator of $U(3)$ proportional to the identity matrix: $\lambda_0 = \sqrt{\frac{2}{3}} I_3$ [14].

At LO in the chiral expansion, $\mathcal{L}_2$ has only two $LECs$: F and B. The first one was defined in (3.53), and it is the analogue of f_n in the above discussion, so it is $F \sim \mathcal{O}(\sqrt{N_C})$. B was defined in (3.55). Both the LHS and the RHS [15] are $\mathcal{O}(N_C)$, so $B \sim \mathcal{O}(1)$. With these dependencies, we can check that scattering amplitudes behave as explained before. For instance, for $\pi\,\pi$ scattering, we have:

$$T = \frac{s - m_\pi^2}{F^2} \sim \frac{1}{N_C}, \qquad (G.4)$$

$s = (p_{\pi,1} + p_{\pi,2})^2$, and has the right dependence. We conclude also that $\mathcal{L}_2$ has a global dependence of $\mathcal{O}(N_C)$ due to the common factor $\frac{F^2}{4}$. Each Goldstone field

[14] One can work however the large-N_C limit either for a $SU(3) \otimes SU(3)$ theory [5] of for a $U(3) \otimes U(3)$ theory [566]. The first approach is taken in what follows. The matching between both was studied in Refs. [275, 567].

[15] The matrix element is of order $\mathcal{O}\left(\sqrt{N_C}^2\right)$, exactly the same as F^2.

we add comes from the exponential divided by a factor F, giving thus the expected suppresion of $\mathcal{O}(\sqrt{N_C})$ for every additional pG. m-meson interaction vertices go with F^{2-m}, so they are $\mathcal{O}(N_C^{1-n/2})$. Because of the global N_C factor in $\mathcal{L}_2$ and the independence of the exponential on N_C, the expansion in $1/N_C$ is equivalent to a semiclassical expansion for an EFT whose degrees of freedom are hadrons [16]. Quantum corrections computed with this Effective Lagrangian are suppressed by $1/N_C$ for each loop.

The ten phenomenologically relevant $LECs$ at this chiral order are not expected to be of the same order in this expansion, because there are terms with only one trace in flavour space, and others with two; as it has been explained, each additional loop receives a supression of $1/N_C$. Therefore, L_3, L_5, L_8, L_9 and L_{10} would be $\mathcal{O}(N_C)$, whereas L_1, L_2, L_4, L_6 and L_7 would be $\mathcal{O}(1)$ -see Eq. (3.77)-. There is, however, a relation holding for traces of 3×3 matrices that modifies this naïve reasoning warning us that although L_1 and L_2 are, separately, $\mathcal{O}(1)$; when considering the relation mentioned before, they get modified by δL_i:

$$2\delta L_1 \sim \delta L_2 \sim -\frac{1}{2}\delta L_3 \sim \mathcal{O}(N_C)\,. \tag{G.5}$$

Deciding not to consider the new term, both L_1 and L_2 become $\mathcal{O}(N_C)$, but their combination $2L_1 - L_2$ persists to be $\mathcal{O}(1)$. Table G.3 displays how the experimental values obtained for the $\mathcal{O}(p^4)$ $LECs$ do agree with large-N_C predictions [143, 274].

Summing up, all the $LECs$ appearing at LO and NLO in the chiral Lagrangians obey the following $1/N_C$ counting (the case of L_7 will be commented later on):

$$\begin{aligned} B_0,\, \mathcal{M},\, m_{\pi,K,\eta},\, 2L_1 - L_2,\, L_4,\, L_6 &\sim \mathcal{O}(1)\,, \\ L_1,\, L_2,\, L_3,\, L_5,\, L_8,\, L_9,\, L_{10} &\sim \mathcal{O}(N_C)\,, \\ F &\sim \mathcal{O}\left(\sqrt{N_C}\right)\,. \end{aligned} \tag{G.6}$$

The LO chiral Lagrangian in the odd-intrinsic parity sector does not introduce any new LEC, but it has a global factor of N_C generated by the triangular quark loop over which the different number of colours run.

G.4 $1/N_C$ expansion for $R\chi T$

There are three kinds of checks we can perform for $R\chi T$. On the one hand, we can restore to phenomenology to fit the couplings entering its Lagrangian and predict another observables with the obtained values. This way has been exploited

[16] At first glance, (4.4) seems to imply -because of the global N_C factor- that QCD also reduces to a semiclassical theory in terms of quark and gluon fields in the large-N_C limit, but this is not true, because the number of them increases as N_C and $\sim N_C^2$, respectively. This is not the case for χPT. As commented, the exponential including the pGs does not introduce additional factors of N_C as we include more and more of them.

i	$L_i^r(M_\rho)$	$\mathcal{O}(N_C)$	source	$L_i^{N_C\to\infty}$
$2L_1 - L_2$	-0.6 ± 0.6	$\mathcal{O}(1)$	K_{e4}, $\pi\pi \to \pi\pi$	0.0
L_2	1.4 ± 0.3	$\mathcal{O}(N_C)$	K_{e4}, $\pi\pi \to \pi\pi$	1.8
L_3	-3.5 ± 1.1	$\mathcal{O}(N_C)$	K_{e4}, $\pi\pi \to \pi\pi$	-4.3
L_4	-0.3 ± 0.5	$\mathcal{O}(1)$	Zweig's rule	0.0
L_5	1.4 ± 0.5	$\mathcal{O}(N_C)$	$F_K : F_\pi$	2.1
L_6	-0.2 ± 0.3	$\mathcal{O}(1)$	Zweig's rule	0.0
L_7	-0.4 ± 0.2	$\mathcal{O}(1)$	GMO, L_5, L_8	-0.3
L_8	0.9 ± 0.3	$\mathcal{O}(N_C)$	M_ϕ, L_5	0.8
L_9	6.9 ± 0.7	$\mathcal{O}(N_C)$	$\langle r^2 \rangle_V^\pi$	7.1
L_{10}	-5.5 ± 0.7	$\mathcal{O}(N_C)$	$\pi \to e\nu\gamma$	-5.4

Table G.1: Experimental values of the coupling constants $L_i^r(M_\rho)$ from the Lagrangian $\mathcal{L}_4$ in units of 10^{-3} [274]. The fourth column shows the experimental source employed. The fifth column shows the predictions that are obtained in the large-N_C limit using the one-resonance approximation.

throughout the Thesis with optimistic results. On the other hand, as we have derived the $1/N_C$ expansion for QCD, we can apply it to $R\chi T$ in much the same way we did it for χPT and verify that large-N_C estimates are not at variance with phenomenology. Finally, one can also explicitly check the convergence of the expansion by comparing the leading and next-to-leading orders in $1/N_C$, whenever the latter are available.

First of all, we will see the $1/N_C$ expansion for $R\chi T$ and the relations that are derived among $R\chi T$ couplings in (4.18), (4.19). The theory built upon the symmetries of $QCD^{n_f=3}$ that reproduces its low-energy behaviour is still not complete. A capital step is the matching procedure, as we have explained in Sec. 3.5. We must enforce the theory to yield the asymptotic behaviour of the underlying theory, as it has been done repeatedly throughout this Thesis.

We aim to characterize the couplings appearing in $\mathcal{L}_R$. One can work with (4.18), (4.19) written in a way that splits the singlet and the octet terms [6]. The obtained result is in complete agreement with convergence of octet plus singlet into nonet.

First of all, and according to the fact that meson decay constants are $\mathcal{O}\left(\sqrt{N_C}\right)$, and decay processes are given at LO by tree level amplitudes, it is clear that couplings creating a resonance from the vacuum will be $\mathcal{O}\left(\sqrt{N_C}\right)$: F_V, F_A, c_m, $\tilde{c}_m$, d_m and $\tilde{d}_m$.

The other kind of processes we need to consider for completing the study are decays of resonances into pGs. Again, the decay of one vector or scalar resonance into two pGs is $\mathcal{O}\left(\sqrt{N_C}\right)$, so G_V, c_d and $\tilde{c}_d$ will be also of this order.

It was shown that masses have smooth limits in the large-N_C limit: they are $\mathcal{O}(1)$.

In summary, the couplings entering $R\chi T$ Lagrangian are:

$$F_V,\, G_V,\, F_A,\, c_d,\, \tilde{c}_d,\, c_m,\, \tilde{c}_m,\, d_m, \tilde{d}_m \;\sim\; \mathcal{O}\left(\sqrt{N_C}\right), \qquad M_i \,\sim\, \mathcal{O}(1)\,. \tag{G.7}$$

At LO in $1/N_C$ Zweig rule becomes exact, the axial anomaly disappears and $U(3)_L \otimes U(3)_R$ is restored. For hadron spectroscopy this implies that particles fill nonet representations of $U(3)$ instead of octet plus singlet of $SU(3)$. In the large-N_C limit one has the relations

$$M_{S_1} \,=\, M_S\,, \quad |\tilde{c}_d| \,=\, \frac{|c_d|}{\sqrt{3}}\,, \quad |\tilde{c}_m| \,=\, \frac{|c_m|}{\sqrt{3}}\,, \quad M_{P_1} \,=\, M_P\,, \quad |\tilde{d}_m| \,=\, \frac{|d_m|}{\sqrt{3}}\,. \tag{G.8}$$

Now, I turn to examine how (axial-)vector contributions to $\mathcal{O}(p^4)$ saturate the $LECs$ L_i when integrated out, reproducing the notion of Vector meson dominance, proposed long ago [318]. In fact, independent large-N_C analyses of χPT and $R\chi T$ yielded that most of the L_i were $\mathcal{O}(N_C)$ and those in $\mathcal{L}_R$ were $\mathcal{O}(\sqrt{N_C})$. Because resonance exchange is then giving an $\mathcal{O}(N_C)$ contribution coming from the two vertices, it is plausible that in the large-N_C limit $R\chi T$ $LECs$ saturate χPT couplings.

Considering the sra, the obtained contributions are all $\mathcal{O}(N_C)$

$$\begin{aligned}
L_1 \;&=\; \frac{G_V^2}{8M_V^2} \,-\, \frac{c_d^2}{6M_S^2} \,+\, \frac{\tilde{c}_d^2}{2M_{S_1}^2}\,,\; L_2 \,=\, \frac{G_V^2}{4M_V^2}\,,\; L_3 \,=\, -\frac{3G_V^2}{4M_V^2} \,+\, \frac{c_d^2}{2M_S^2}\,,\\
L_4 \;&=\; -\frac{c_d c_m}{3M_S^2} \,+\, \frac{\tilde{c}_d \tilde{c}_m}{M_{S_1}^2}\,,\; L_5 \,=\, \frac{c_d c_m}{M_S^2}\,,\; L_6 \,=\, -\frac{c_m^2}{6M_S^2} \,+\, \frac{\tilde{c}_m^2}{2M_{S_1}^2}\,,\\
L_7 \;&=\; \frac{d_m^2}{6M_P^2} - \frac{\tilde{d}_m^2}{2M_{P_1}^2}\,,\; L_8 \,=\, \frac{c_m^2}{2M_S^2} \,-\, \frac{d_m^2}{2M_P^2}\,,\; L_9 \,=\, \frac{F_V G_V}{2M_V^2}\,,\\
L_{10} \;&=\; -\frac{F_V^2}{4M_V^2} \,+\, \frac{F_A^2}{4M_A^2}\,,\; H_1 \,=\, -\frac{F_V^2}{8M_V^2} - \frac{F_A^2}{8M_A^2}\,,\; H_2 \,=\, \frac{c_m}{M_S^2} \,+\, \frac{d_m^2}{M_P^2}\,.
\end{aligned} \tag{G.9}$$

Taking into account the large-N_C relations (G.8); L_4, L_6 and L_7 contributions vanish, while for L_1 only that coming from vectors survives. The suppresion of these $LECs$ and the saturation of all L_i by (axial-)vector contributions are shown in Table G.2.

Due to the $U(1)$ anomaly, even in the chiral limit, the η_1 has -apart from the common contribution coming from the trace anomaly [569]- the anomalous extra-term which motivates that commonly it is also integrated out from the standard χPT Lagrangian. Using the same notation for this coupling both in χPT and in its large-N_C limit we can say that this provokes a change in L_7 due to pseudoscalar η_1-exchange. With the notation introduced before, we can simply write

$$L_7 \,=\, -\frac{\tilde{d}_{\eta_1}^2}{2M_{\eta_1}^2}\,, \qquad \tilde{d}_{\eta_1} \,=\, -\frac{F}{\sqrt{24}}\,: \tag{G.10}$$

i	$L_i^r\,(M_\rho)$	V	A	S	η_1	Total	Total^b	Total^c
1	0.4 ± 0.3	0.6	0.0	0.0	0.0	0.6	0.9	0.9
2	1.4 ± 0.3	1.2	0.0	0.0	0.0	1.2	1.8	1.8
3	-3.5 ± 1.1	-3.6	0.0	0.6	0.0	-3.0	-4.9	$\{-3.2, -4.3, -5.0\}$
4	-0.3 ± 0.5	0.0	0.0	0.0	0.0	0.0	0.0	0.0
5	1.4 ± 0.5	0.0	0.0	1.4^a	0.0	1.4	1.4	2.2
6	-0.2 ± 0.3	0.0	0.0	0.0	0.0	0.0	0.0	0.0
7	-0.4 ± 0.2	0.0	0.0	0.0	-0.3	-0.3	-0.3	$\{-0.2, -0.3, -0.3\}$
8	0.9 ± 0.3	0.0	0.0	0.9^b	0.0	0.9	0.9	$\{0.6, 0.8, 1.5\}$
9	6.9 ± 0.7	6.9^a	0.0	0.0	0.0	6.9	7.3	7.2
10	-5.5 ± 0.7	-10.0	4.0	0.0	0.0	-6.0	-5.5	-5.4

Table G.2: Comparison between phenomenological values of the coupling constants $L_i^r(M_\rho)$ in units of 10^{-3} and the contributions given by resonance exchange [135]. For scalar resonances it is considered a nonet and the contribution of pseudoscalar resonances is neglected with respect to the η_1 contribution. ^{a} stands for inputs and ^{b},^{c} means that short-distance QCD corrections have been taken into account. The last column corresponds to the reanalysis of Ref.[319], where three different values for the parameter d_m are considered. Essentially this is possible because there are less restrictions from high-energy QCD behaviour in the spin-zero sector than in that with spin-one [274, 568].

being the extra contribution to $M_{\eta_1} \sim \mathcal{O}(1/N_C)$, L_7 -that is $\mathcal{O}(1)$ in $1/N_C$- grows to reach the value $\mathcal{O}(N_C^2)$ for what we have written as L_7 in the previous equation. Still, the $1/N_C$-counting is not so clear at this point [570]: I have explained how out of the chiral limit M_{η_1} receives three comparable contributions: from explicit chiral symmetry breaking, from the singlet-axial anomaly and from the trace anomaly. To integrate the η_1 out amounts to admit that the axial anomaly contribution is much greater than the other two and this does not seem to be the case. For further discussions on η_1/η_8 and their mixings η/η', see [515, 516, 517, 518, 571, 572].

In Table G.2 the experimental value of these couplings and the contributions got from resonance exchange [135] are presented. We see that there is good agreement between them and that Vector meson dominance emerges as a natural result of the analyses. There is no reason to include additional multiplets of resonances looking only at χPT at $\mathcal{O}(p^4)$. The comparison has been made at a renormalization scale $\mu = M_\rho$ -for the χPT loops-, but similar results are found for any value belonging to the region of interest: 0.5 GeV $\leq \mu \leq$ 1 GeV.

Finally, we can see how these conclusions change when considering the evaluations of the L_i at NLO in $1/N_C$ within $R\chi T$. The most important acquaintance we gain is that now one keeps full control of the renormalization scale dependence of these $LECs$. References [287, 288, 290, 292] constitute the study of this question within $R\chi T$. By imposing QCD short-distance constraints, the chiral couplings can

be written in terms of the resonance masses and couplings and do not depend explicitly on the coefficients of the chiral operators in the Goldstone boson sector of $R\chi T$. This is the counterpart formulation of the resonance saturation statement in the context of the resonance lagrangian. As an illustration, the values of the couplings L_8 and L_{10} at NLO in $1/N_C$ evaluated at $\mu = M_\rho$ are given: $L_8^r(M_\rho) = 0.6 \pm 0.4$, $L_{10}^r(M_\rho) = -4.4 \pm 0.9$ (always in units of 10^{-3}). We see that the corrections of the NLO term amount to a reasonable $(20 \leftrightarrow 30)\,\%$.

Appendix H: Comparing theory to data

We include a brief note on how we have normalized our theoretical spectrum in order to compare it with experimental measurements. Let P be the process $\tau^- \to (\pi\pi\pi)^-\nu_\tau$ and x (an energy) the variable in which the spectrum is given. The experiment provides us with the total number of events of process P, N_P, and its spectrum in x, i.e., $\frac{Events}{bin}$ versus x, where $bin = \Delta x$.

Our theoretical computation yields $\frac{\mathrm{d}\Gamma_P}{\mathrm{d}x}$, whose integral over the whole x-spectrum gives the partial width of process P:

$$\int_{x_{max}}^{x_{min}} \mathrm{d}x \frac{\mathrm{d}\Gamma_P}{\mathrm{d}x} \;=\; \Gamma_P \longleftrightarrow \int_{x_{max}}^{x_{min}} \mathrm{d}x \frac{1}{\Gamma_P}\frac{\mathrm{d}\Gamma_P}{\mathrm{d}x} \;=\; 1\,, \tag{H.1}$$

and this allow us to compare with the experiment provided

$$\int_{x_{max}}^{x_{min}} \mathrm{d}x \frac{Events}{\Delta x} \;=\; N_P \tag{H.2}$$

and therefore

$$N_P \int_{x_{max}}^{x_{min}} \mathrm{d}x \frac{1}{\Gamma_P}\frac{\mathrm{d}\Gamma_P}{\mathrm{d}x} \;=\; \int_{x_{max}}^{x_{min}} \mathrm{d}x \frac{Events}{\Delta x}\,, \tag{H.3}$$

or in differential form:

$$\underbrace{N_P}_{exp}\left[\frac{1}{\Gamma_P}\frac{\mathrm{d}\Gamma_P}{\mathrm{d}x}\right]_{th} \;=\; \left[\frac{Events}{\Delta x}\right]_{exp}\,, \tag{H.4}$$

where exp and th are a reminder of the source of each term: either the experiment, or the theoretical computation.

Usually, x is a dimensionful variable, so we can write $\Delta x = n\,[x]$, where the x in square brackets stands for the dimensions of Δx. Thus, the LHS of (H.4) has dimension x^{-1} and, finally:

$$\underbrace{N_P\, n}_{exp}\left[\frac{1}{\Gamma_P}\frac{\mathrm{d}\Gamma_P}{\mathrm{d}x}\right]_{th} \;=\; \left[\frac{Events}{\Delta x}\right]_{exp}\,, \tag{H.5}$$

and n is chosen according to the experimental information as we will see next.

Our computation yields $\frac{\mathrm{d}\Gamma_{\tau^-\to\pi^+\pi^-\pi^-\nu_\tau}}{\mathrm{d}Q^2}$, so what we have for comparing with the

experiment is

$$\frac{1}{\Gamma_{\tau^-\to(\pi\pi\pi)^-\nu_\tau}}\frac{\mathrm{d}\Gamma_{\tau^-\to(\pi\pi\pi)^-\nu_\tau}}{\mathrm{d}Q^2} = \sum_{i=SA,\,A,}\frac{\mathrm{d}\Gamma_i}{\mathrm{d}Q^2}\,. \tag{H.6}$$

One can reason similarly for other three meson modes and for other observables, like $d\Gamma/ds_{ij}$.

Bibliography

Bibliography

[1] S. L. Glashow, "Partial Symmetries Of Weak Interactions," Nucl. Phys. **22**, 579 (1961).
S. Weinberg, "A Model Of Leptons," Phys. Rev. Lett. **19**, 1264 (1967).
A. Salam, in Elementary Particle Theory, ed. N. Svartholm (Almquist and Wiksells, Stockholm, 1969), p.367.
S. L. Glashow, J. Iliopoulos and L. Maiani, "Weak Interactions with Lepton-Hadron Symmetry," Phys. Rev. D **2**, 1285 (1970).

[2] H. Fritzsch and M. Gell-Mann, "Current Algebra: Quarks And What Else?," Proc. XVI Int. Conf. on High Energy Physics, eds. J. D. Jackson and A. Roberts, Fermilab **2** (1972) 135. arXiv:hep-ph/0208010.
H. Fritzsch, M. Gell-Mann and H. Leutwyler, "Advantages Of The Color Octet Gluon Picture," Phys. Lett. B **47** (1973) 365.

[3] S. Weinberg, "Phenomenological Lagrangians," Physica A **96**, 327 (1979).

[4] J. Gasser and H. Leutwyler, "Chiral Perturbation Theory To One Loop," Annals Phys. **158**, 142 (1984).

[5] J. Gasser and H. Leutwyler, "Chiral Perturbation Theory: Expansions In The Mass Of The Strange Quark," Nucl. Phys. B **250**, 465 (1985).

[6] G. Ecker, J. Gasser, A. Pich and E. de Rafael, "The Role Of Resonances In Chiral Perturbation Theory," Nucl. Phys. B **321** (1989) 311.

[7] G. Ecker, J. Gasser, H. Leutwyler, A. Pich and E. de Rafael, "Chiral Lagrangians for Massive Spin 1 Fields," Phys. Lett. B **223** (1989) 425.

[8] C. Amsler *et al.* [Particle Data Group], "Review of particle physics," Phys. Lett. B **667**, 1 (2008).

[9] E. Komatsu *et al.* [$WMAP$ Collaboration], "Five-Year Wilkinson Microwave Anisotropy Probe ($WMAP$) Observations:Cosmological Interpretation," Astrophys. J. Suppl. **180** (2009) 330. [arXiv:0803.0547 [astro-ph]].

[10] M. L. Perl *et al.*, "Evidence for anomalous lepton production in e^+e^- annihilation," Phys. Rev. Lett. **35**, 1489 (1975).

[11] M. Kobayashi and T. Maskawa, "CP Violation In The Renormalizable Theory Of Weak Interaction," Prog. Theor. Phys. **49**, 652 (1973).

[12] J. H. Christenson, J. W. Cronin, V. L. Fitch and R. Turlay, "Evidence For The 2 Π Decay Of The $K(2)^0$ Meson," Phys. Rev. Lett. **13**, 138 (1964).

[13] N. Cabibbo, "Unitary Symmetry and Leptonic Decays," Phys. Rev. Lett. **10**, 531 (1963).

[14] D. N. Spergel *et al.* [$WMAP$ Collaboration], "First Year Wilkinson Microwave Anisotropy Probe ($WMAP$) Observations: Determination of Cosmological Parameters," Astrophys. J. Suppl. **148** (2003) 175. [arXiv:astro-ph/0302209].

[15] M. Kowalski *et al.* [Supernova Cosmology Project Collaboration], "Improved Cosmological Constraints from New, Old and Combined Supernova Datasets," Astrophys. J. **686** (2008) 749. [arXiv:0804.4142 [astro-ph]].

[16] J. Chang *et al.*, "An Excess Of Cosmic Ray Electrons At Energies Of 300.800 Gev," Nature **456** (2008) 362.

[17] O. Adriani *et al.*, "A new measurement of the antiproton-to-proton flux ratio up to 100 GeV in the cosmic radiation," Phys. Rev. Lett. **102** (2009) 051101. [arXiv:0810.4994 [astro-ph]].

[18] O. Adriani *et al.* [$PAMELA$ Collaboration], "An anomalous positron abundance in cosmic rays with energies 1.5.100 GeV," Nature **458** (2009) 607. [arXiv:0810.4995 [astro-ph]].

[19] A. A. Abdo *et al.* [The Fermi LAT Collaboration], "Measurement of the Cosmic Ray e^+ plus e^- spectrum from 20 GeV to 1 TeV with the Fermi Large Area Telescope," Phys. Rev. Lett. **102** (2009) 181101. [arXiv:0905.0025 [astro-ph.HE]].

[20] M. L. Perl *et al.*, "Properties Of The Proposed Tau Charged Lepton," Phys. Lett. B **70** (1977) 487.

[21] S. W. Herb *et al.*, "Observation of a dimuon resonance at 9.5-GeV in 400-GeV proton - nucleus collisions," Phys. Rev. Lett. **39** (1977) 252.

[22] F. Abe *et al.* [CDF Collaboration], "Observation of top quark production in $\bar{p}p$ collisions," Phys. Rev. Lett. **74** (1995) 2626. [arXiv:hep-ex/9503002].

[23] S. Abachi *et al.* [$D0$ Collaboration], "Observation of the top quark," Phys. Rev. Lett. **74** (1995) 2632. [arXiv:hep-ex/9503003].

[24] A. Pich, I. Boyko, D. Dedovich and I. I. Bigi, "Tau decays," Int. J. Mod. Phys. A **24** (2009) 715.

[25] A. Pich, "Tau Physics: Theory Overview," Nucl. Phys. Proc. Suppl. **181-182** (2008) 300. [arXiv:0806.2793 [hep-ph]].

[26] A. Pich, "Tau physics: Theoretical perspective," Nucl. Phys. Proc. Suppl. **98** (2001) 385. [arXiv:hep-ph/0012297].

[27] B. C. Barish and R. Stroynowski, "The Physics of the tau Lepton," Phys. Rept. **157** (1988) 1.

[28] A. Stahl, "Physics with tau leptons," Springer Tracts Mod. Phys. **160** (2000) 1.

[29] M. Davier, A. Hocker and Z. Zhang, "The physics of hadronic tau decays," Rev. Mod. Phys. **78**, 1043 (2006). [arXiv:hep-ph/0507078].

[30] W. J. Marciano and A. Sirlin, "Electroweak Radiative Corrections to tau Decay," Phys. Rev. Lett. **61** (1988) 1815.

[31] E. Braaten and C. S. Li, "Electroweak radiative corrections to the semihadronic decay rate of the tau lepton," Phys. Rev. D **42** (1990) 3888.

[32] J. Erler, "Electroweak radiative corrections to semileptonic tau decays," Rev. Mex. Fis. **50** (2004) 200. [arXiv:hep-ph/0211345].

[33] K. Abe *et al.* [*Belle* Collaboration], "Measurement of the mass of the tau-lepton and an upper limit on the mass difference between τ^+ and τ^-," Phys. Rev. Lett. **99** (2007) 011801. [arXiv:hep-ex/0608046].

[34] V. V. Anashin *et al.*, "Measurement of the tau lepton mass at the $KEDR$ detector," JETP Lett. **85** (2007) 347.

[35] D. M. Asner *et al.*, "Physics at BES-III," arXiv:0809.1869 [hep-ex].

[36] A. Pich, "Tau physics," in *Proc. of the 19th Intl. Symp. on Photon and Lepton Interactions at High Energy LP99* ed. J.A. Jaros and M.E. Peskin, *In the Proceedings of 19th International Symposium on Lepton and Photon Interactions at High-Energies (LP 99), Stanford, California, 9-14 Aug 1999, pp 157-173.* [arXiv:hep-ph/9912294].

[37] L. Michel, "Interaction Between Four Half Spin Particles And The Decay Of The Mu Meson," Proc. Phys. Soc. A **63** (1950) 514.

[38] C. Bouchiat and L. Michel, "Theory of mu-Meson Decay with the Hypothesis of Nonconservation of Parity," Phys. Rev. **106** (1957) 170.

[39] T. Kinoshita and A. Sirlin, "Muon Decay with Parity Nonconserving Interactions and Radiative Corrections in the Two-Component Theory," Phys. Rev. **107** (1957) 593.

[40] T. Kinoshita and A. Sirlin, "Polarization of Electrons in Muon Decay with General Parity-Nonconserving Interactions," Phys. Rev. **108** (1957) 844.

[41] W. Fetscher, H. J. Gerber and K. F. Johnson, "Muon Decay: Complete Determination of the Interaction and Comparison with the Standard Model," Phys. Lett. B **173** (1986) 102.

[42] A. Pich and J. P. Silva, "Constraining new interactions with leptonic τ decays," Phys. Rev. D **52** (1995) 4006. [arXiv:hep-ph/9505327].

[43] R. P. Feynman and M. Gell-Mann, "Theory of the Fermi interaction," Phys. Rev. **109** (1958) 193.

[44] A. G. Shamov *et al.* [$KEDR$ Collaboration], "Tau mass measurement at $KEDR$, Nucl. Phys. Proc. Suppl. **181-182** (2008) 311.

[45] C. Athanassopoulos *et al.* [$LSND$ Collaboration], "Evidence for $\bar{\nu}_\mu \to \bar{\nu_e}$ oscillation from the $LSND$ experiment at the Los Alamos Meson Physics Facility," Phys. Rev. Lett. **77** (1996) 3082. [arXiv:nucl-ex/9605003].

[46] A. Aguilar *et al.* [$LSND$ Collaboration], "Evidence for neutrino oscillations from the observation of $\bar{\nu_e}$ appearance in a $\bar{\nu}_\mu$ beam," Phys. Rev. D **64** (2001) 112007. [arXiv:hep-ex/0104049].

[47] Q. R. Ahmad *et al.* [SNO Collaboration], "Measurement of the charged current interactions produced by $B-8$ solar neutrinos at the Sudbury Neutrino Observatory," Phys. Rev. Lett. **87** (2001) 071301. [arXiv:nucl-ex/0106015].

[48] Q. R. Ahmad *et al.* [SNO Collaboration], "Direct evidence for neutrino flavor transformation from neutral-current interactions in the Sudbury Neutrino Observatory," Phys. Rev. Lett. **89** (2002) 011301. [arXiv:nucl-ex/0204008].

[49] K. S. Hirata *et al.* [Kamiokande-II Collaboration], "Observation of a small atmospheric ν_μ/ν_e ratio in Kamiokande," Phys. Lett. B **280** (1992) 146.

[50] Y. Fukuda *et al.* [Super-Kamiokande Collaboration], "Evidence for oscillation of atmospheric neutrinos," Phys. Rev. Lett. **81** (1998) 1562. [arXiv:hep-ex/9807003].

[51] B. Aubert *et al.* [$BABAR$ Collaboration], "Searches for Lepton Flavor Violation in the Decays $\tau \to e\gamma$ and $\tau \to \mu\gamma$," Phys. Rev. Lett. **104** (2010) 021802. [arXiv:0908.2381 [hep-ex]].

[52] B. Aubert *et al.* [$BABAR$ Collaboration], "Search for Lepton Flavor Violating Decays $\tau^\pm \to \ell^\pm\omega$ $(\ell = e, \mu)$," Phys. Rev. Lett. **100** (2008) 071802. [arXiv:0711.0980 [hep-ex]].

[53] B. Aubert *et al.* [*BABAR* Collaboration], "Improved limits on the lepton-flavor violating decays $\tau^- \to \ell^-\ell^+\ell^-$," Phys. Rev. Lett. **99** (2007) 251803. [arXiv:0708.3650 [hep-ex]].

[54] B. Aubert *et al.* [*BABAR* Collaboration], "Search for Lepton Flavor Violating Decays $\tau^\pm \to \ell^\pm\pi^0$, $\ell^\pm\eta$, $\ell^\pm\eta'$," Phys. Rev. Lett. **98** (2007) 061803. [arXiv:hep-ex/0610067].

[55] B. Aubert *et al.* [*BABAR* Collaboration], "Search for lepton flavor violation in the decay $\tau^\pm \to e^\pm\gamma$," Phys. Rev. Lett. **96** (2006) 041801. [arXiv:hep-ex/0508012].

[56] B. Aubert *et al.* [*BaBar* Collaboration], "Search for lepton-flavor and lepton-number violation in the decay $\tau^- \to \ell^\mp h^\pm h'^-$," Phys. Rev. Lett. **95** (2005) 191801. [arXiv:hep-ex/0506066].

[57] B. Aubert *et al.* [*BABAR* Collaboration], "Search for lepton flavor violation in the decay $\tau^- \to \ell^-\ell^+\ell^-$," Phys. Rev. Lett. **92** (2004) 121801. [arXiv:hep-ex/0312027].

[58] K. Hayasaka *et al.* [*Belle* Collaboration], "New search for $\tau \to \mu\gamma and \tau \to e\gamma$ decays at *Belle*," Phys. Lett. B **666** (2008) 16. [arXiv:0705.0650 [hep-ex]].

[59] Y. Nishio *et al.* [*Belle* Collaboration], "Search for lepton-flavor-violating $\tau \to \ell V^0$ decays at *Belle*," Phys. Lett. B **664** (2008) 35. [arXiv:0801.2475 [hep-ex]].

[60] Y. Miyazaki *et al.* [*Belle* Collaboration], "Search for Lepton Flavor Violating tau Decays into Three Leptons," Phys. Lett. B **660** (2008) 154. [arXiv:0711.2189 [hep-ex]].

[61] Y. Miyazaki *et al.* [*BELLE* Collaboration], "Search for lepton flavor violating τ^- decays into $l^-\eta$, $l^-\eta'$ and $l^-\pi^0$," Phys. Lett. B **648** (2007) 341. [arXiv:hep-ex/0703009].

[62] Y. Yusa *et al.* [*BELLE* Collaboration], "Search for neutrinoless decays $\tau \to \ell hh$ and $\tau \to \ell V^0$," Phys. Lett. B **640** (2006) 138. [arXiv:hep-ex/0603036].

[63] Y. Enari *et al.* [*Belle* Collaboration], "Search for lepton flavor violating decays $\tau^- \to \ell^-\pi^0$, $\ell^-\eta$, $\ell^-\eta'$," Phys. Lett. B **622** (2005) 218. [arXiv:hep-ex/0503041].

[64] Y. Enari *et al.* [*Belle* Collaboration], "Search for the lepton flavor violating decay $\tau^- \to \mu^-\eta$ at *Belle*," Phys. Rev. Lett. **93** (2004) 081803. [arXiv:hep-ex/0404018].

[65] K. Abe *et al.* [*Belle* Collaboration], "An upper bound on the decay $\tau \to \mu\gamma$ from *Belle*," Phys. Rev. Lett. **92** (2004) 171802. [arXiv:hep-ex/0310029].

[66] Y. Miyazaki, "Search for Lepton Flavor Violating τ^- Decays into $\ell^- K^0_S$ and $\ell^- K^0_S K^0_S$," arXiv:1003.1183 [hep-ex].

[67] K. Kodama *et al.* [*DONUT* Collaboration], "Observation of tau-neutrino interactions," Phys. Lett. B **504** (2001) 218. [arXiv:hep-ex/0012035].

[68] R. Barate *et al.* [*ALEPH* Collaboration], "An upper limit on the tau neutrino mass from three- and five-prong tau decays," Eur. Phys. J. C **2** (1998) 395.

[69] A. Pich, "Recent Progress on Tau Lepton Physics," Nucl. Phys. Proc. Suppl. **186** (2009) 187. [arXiv:0811.1347 [hep-ph]].

[70] K. G. Wilson, "Nonlagrangian models of current algebra," Phys. Rev. **179** (1969) 1499.

[71] K. G. Wilson and W. Zimmermann, "Operator Product Expansions And Composite Field Operators In The General Framework Of Quantum Field Theory," Commun. Math. Phys. **24** (1972) 87.

[72] W. Zimmermann, "Normal products and the short distance expansion in the perturbation theory of renormalizable interactions," Annals Phys. **77** (1973) 570. [Lect. Notes Phys. **558** (2000) 278].

[73] E. Braaten, S. Narison and A. Pich, "QCD analysis of the tau hadronic width," Nucl. Phys. B **373** (1992) 581.

[74] P. A. Baikov, K. G. Chetyrkin and J. H. Kühn, "Order α_s^4 QCD Corrections to Z and τ Decays," Phys. Rev. Lett. **101** (2008) 012002. [arXiv:0801.1821 [hep-ph]].

[75] F. Le Diberder and A. Pich, "The Perturbative QCD Prediction To R_τ Revisited," Phys. Lett. B **286** (1992) 147.

[76] A. Pich, "QCD predictions for the tau hadronic width: Determination of $\alpha_s(M_\tau^2)$," Nucl. Phys. Proc. Suppl. **39BC** (1995) 326. [arXiv:hep-ph/9412273].

[77] A. A. Pivovarov, "Renormalization group analysis of the tau-lepton decay within QCD," Z. Phys. C **53** (1992) 461 [Sov. J. Nucl. Phys. **54** (1991 YAFIA,54,1114.1991) 676]. [arXiv:hep-ph/0302003].

[78] R. Barate *et al.* [*ALEPH* Collaboration], "Measurement of the spectral functions of axial-vector hadronic tau decays and determination of $\alpha_S(M_\tau^2)$," Eur. Phys. J. C **4** (1998) 409.

[79] K. Ackerstaff *et al.* [*OPAL* Collaboration], "Measurement of the strong coupling constant α_S and the vector and axial-vector spectral functions in hadronic tau decays," Eur. Phys. J. C **7** (1999) 571. [arXiv:hep-ex/9808019].

[80] M. Davier, S. Descotes-Genon, A. Höcker, B. Malaescu and Z. Zhang, "The Determination of α_s from τ Decays Revisited," Eur. Phys. J. C **56** (2008) 305. [arXiv:0803.0979 [hep-ph]].

[81] A. Pich, "α_S Determination from Tau Decays: Theoretical Status," arXiv:1001.0389 [hep-ph].

[82] G. Rodrigo, A. Pich and A. Santamaría, "$\alpha_S(M_Z)$ from tau decays with matching conditions at three loops," Phys. Lett. B **424**, 367 (1998). [arXiv:hep-ph/9707474].

[83] E. C. Poggio, H. R. Quinn and S. Weinberg, "Smearing The Quark Model," Phys. Rev. D **13** (1976) 1958.

[84] M. A. Shifman, "Quark-hadron duality," arXiv:hep-ph/0009131.

[85] O. Catà, M. Golterman and S. Peris, "Duality violations and spectral sum rules," JHEP **0508** (2005) 076. [arXiv:hep-ph/0506004].

[86] M. González-Alonso, "Estimación de los condensados de QCD del correlador $V - A$ de quarks ligeros," Valéncia Univ. Masther Thesis (2007).

[87] O. Catà, M. Golterman and S. Peris, "Unraveling duality violations in hadronic tau decays," Phys. Rev. D **77** (2008) 093006. [arXiv:0803.0246 [hep-ph]].

[88] O. Catà, M. Golterman and S. Peris, "Possible duality violations in tau decay and their impact on the determination of α_S," Phys. Rev. D **79** (2009) 053002. [arXiv:0812.2285 [hep-ph]].

[89] M. Gonzalez-Alonso, A. Pich and J. Prades, "Violation of Quark-Hadron Duality and Spectral Chiral Moments in QCD," arXiv:1001.2269 [hep-ph].

[90] A. Pich and J. Prades, "Perturbative quark mass corrections to the tau hadronic width," JHEP **9806** (1998) 013. [arXiv:hep-ph/9804462].

[91] A. Pich and J. Prades, "Strange quark mass determination from Cabibbo-suppressed tau decays," JHEP **9910** (1999) 004. [arXiv:hep-ph/9909244].

[92] P. A. Baikov, K. G. Chetyrkin and J. H. Kühn, "Strange quark mass from tau lepton decays with $\mathcal{O}(\alpha_S^3)$) accuracy," Phys. Rev. Lett. **95** (2005) 012003. [arXiv:hep-ph/0412350].

[93] E. Gamiz, M. Jamin, A. Pich, J. Prades and F. Schwab, "V_{us} and m_s from hadronic tau decays," Phys. Rev. Lett. **94** (2005) 011803. [arXiv:hep-ph/0408044].

[94] M. Jamin, J. A. Oller and A. Pich, "Scalar $K\pi$ form factor and light quark masses," Published in Phys.Rev.D74:074009,2006. arXiv:hep-ph/0605095.

[95] E. Gamiz, M. Jamin, A. Pich, J. Prades and F. Schwab, "Theoretical progress on the V_{us} determination from tau decays," PoS **KAON** (2008) 008. [arXiv:0709.0282 [hep-ph]].

[96] B. Sciascia [FlaviaNet Kaon Working Group], "Precision tests of the SM with leptonic and semileptonic kaon decays," Nucl. Phys. Proc. Suppl. **181-182** (2008) 83. [arXiv:0812.1112 [hep-ex]].

[97] E. D. Bloom *et al.*, "High-Energy Inelastic $e^- - p$ Scattering At 6-Degrees And 10-Degrees," Phys. Rev. Lett. **23** (1969) 930.

[98] M. Breidenbach *et al.*, "Observed Behavior Of Highly Inelastic Electron-Proton Scattering," Phys. Rev. Lett. **23** (1969) 935.

[99] Y. Ne'eman, "Derivation of strong interactions from a gauge invariance," Nucl. Phys. **26** (1961) 222.

[100] M. Gell-Mann, "The Eightfold Way: A Theory Of Strong Interaction Symmetry,"

[101] M. Gell-Mann, "A Schematic Model Of Baryons And Mesons," Phys. Lett. **8** (1964) 214.

[102] C. N. Yang and R. L. Mills, "Conservation Of Isotopic Spin And Isotopic Gauge Invariance," Phys. Rev. **96** (1954) 191.

[103] G. 't Hooft, "The Birth Of Asymptotic Freedom," Nucl. Phys. B **254** (1985) 11.

[104] A. Pich, "Aspects Of Quantum Chromodynamics," Lectures given at ICTP Summer School in Particle Physics, Trieste, Italy, 7 Jun - 9 Jul, 1999. Published in 'Trieste 1999, Particle physics' 53-102.

[105] L. D. Faddeev and V. N. Popov, "Feynman Diagrams For The Yang-Mills Field," Phys. Lett. B **25** (1967) 29.

[106] F. Wilczek, "Problem Of Strong P And T Invariance In The Presence Of Instantons," Phys. Rev. Lett. **40** (1978) 279.

[107] E. C. G. Stueckelberg and A. Petermann, "Normalization of constants in the quanta theory," Helv. Phys. Acta **26** (1953) 499.

[108] M. Gell-Mann and F. E. Low, "Quantum electrodynamics at small distances," Phys. Rev. **95** (1954) 1300.

[109] L. P. Kadanoff, "Scaling laws for Ising models near T_C," Physics **2** (1966) 263.

[110] C. G. . Callan, "Broken Scale Invariance In Scalar Field Theory," Phys. Rev. D **2** (1970) 1541.

[111] K. Symanzik, "Small Distance Behavior In Field Theory And Power Counting," Commun. Math. Phys. **18** (1970) 227.

[112] K. G. Wilson, "The Renormalization Group And Strong Interactions," Phys. Rev. D **3** (1971) 1818.

[113] D. J. Gross and F. Wilczek, "Ultraviolet Behavior Of Non-Abelian Gauge Theories," Phys. Rev. Lett. **30** (1973) 1343.

[114] D. J. Gross and F. Wilczek, "Asymptotically Free Gauge Theories. 1," Phys. Rev. D **8** (1973) 3633.

[115] D. J. Gross and F. Wilczek, "Asymptotically Free Gauge Theories. 2," Phys. Rev. D **9** (1974) 980.

[116] H. D. Politzer, "Reliable Perturbative Results For Strong Interactions?," Phys. Rev. Lett. **30** (1973) 1346.

[117] H. D. Politzer, "Asymptotic Freedom: An Approach To Strong Interactions," Phys. Rept. **14** (1974) 129.

[118] S. A. Larin and J. A. M. Vermaseren, "The Three Loop QCD Beta Function And Anomalous Dimensions," Phys. Lett. B **303** (1993) 334. [arXiv:hep-ph/9302208].

[119] T. van Ritbergen, J. A. M. Vermaseren and S. A. Larin, "The four-loop beta function in quantum chromodynamics," Phys. Lett. B **400** (1997) 379. [arXiv:hep-ph/9701390].

[120] K. G. Wilson, "CONFINEMENT OF QUARKS," Phys. Rev. D **10** (1974) 2445.

[121] A. M. Polyakov, "Quantum geometry of bosonic strings," Phys. Lett. B **103** (1981) 207.

[122] J. Goldstone, "Field Theories With 'Superconductor' Solutions," Nuovo Cim. **19** (1961) 154.

[123] S. R. Coleman, J. Wess and B. Zumino, "Structure Of Phenomenological Lagrangians. 1," Phys. Rev. **177** (1969) 2239.

[124] C. G. Callan, S. R. Coleman, J. Wess and B. Zumino, "Structure Of Phenomenological Lagrangians. 2," Phys. Rev. **177** (1969) 2247.

[125] G. 't Hooft, "A Planar Diagram Theory For Strong Interactions," Nucl. Phys. B **72** (1974) 461.

[126] G. 't Hooft, "A Two-Dimensional Model For Mesons," Nucl. Phys. B **75** (1974) 461.

[127] E. Witten, "Baryons In The $1/N$ Expansion," Nucl. Phys. B **160** (1979) 57.

[128] V. Cirigliano, G. Ecker, M. Eidemüller, R. Kaiser, A. Pich and J. Portolés, "Towards a consistent estimate of the chiral low-energy constants," Nucl. Phys. B **753** (2006) 139. arXiv:hep-ph/0603205.

[129] H. Georgi and S. L. Glashow, "Unity Of All Elementary Particle Forces," Phys. Rev. Lett. **32** (1974) 438.

[130] G. Senjanovic and R. N. Mohapatra, "Exact Left-Right Symmetry And Spontaneous Violation Of Parity," Phys. Rev. D **12** (1975) 1502.

[131] S. Dimopoulos and H. Georgi, "Softly Broken Supersymmetry And $SU(5)$," Nucl. Phys. B **193** (1981) 150.

[132] T. Kaluza, "On The Problem Of Unity In Physics," Sitzungsber. Preuss. Akad. Wiss. Berlin (Math. Phys.) **1921** (1921) 966.

[133] O. Klein, "Quantum theory and five-dimensional theory of relativity," Z. Phys. **37** (1926) 895 [Surveys High Energ. Phys. **5** (1986) 241].

[134] L. Randall and R. Sundrum, "A large mass hierarchy from a small extra dimension," Phys. Rev. Lett. **83** (1999) 3370. [arXiv:hep-ph/9905221].

[135] A. Pich, "Effective Field Theory," Talk given at Les Houches Summer School in Theoretical Physics, Session 68: Probing the Standard Model of Particle Interactions, Les Houches, France, 28 Jul - 5 Sep 1997. Published in 'Les Houches 1997, Probing the standard model of particle interactions, Pt. 2' 949-1049.

[136] A. V. Manohar, "Effective Field Theories," Lectures given at 35th Internationale Universitatswochen fuer Kern- und Teilchenphysik (International University School of Nuclear and Particle Physics): Perturbative and Nonperturbative Aspects of Quantum Field Theory, Schladming, Austria, 2-9 Mar 1996. Published in 'Schladming 1996, Perturbative and nonperturbative aspects of quantum field theory' 311-362.

[137] A. Dobado, A. Gómez-Nicola, A. L. Maroto and J. R. Peláez, "Effective lagrangians for the standard model," *N.Y., Springer-Verlag, 1997. (Texts and Monographs in Physics).*

[138] H. Georgi, "Effective field theory," Ann. Rev. Nucl. Part. Sci. **43** (1993) 209.

[139] A. Manohar and H. Georgi, "Chiral Quarks And The Nonrelativistic Quark Model," Nucl. Phys. B **234** (1984) 189.

[140] D. B. Kaplan, "Effective field theories," arXiv:nucl-th/9506035.

[141] D. B. Kaplan, "Five lectures on effective field theory," arXiv:nucl-th/0510023.

[142] H. Georgi, "On-Shell Effective Field Theory," Nucl. Phys. B **361** (1991) 339.

[143] G. Ecker, "Chiral Perturbation Theory," Prog. Part. Nucl. Phys. **35** (1995) 1 [arXiv:hep-ph/9501357].

[144] T. Appelquist and J. Carazzone, "Infrared Singularities And Massive Fields," Phys. Rev. D **11** (1975) 2856.

[145] J. C. Taylor, "Ward Identities And Charge Renormalization Of The Yang-Mills Field," Nucl. Phys. B **33** (1971) 436.

[146] G. 't Hooft and M. J. G. Veltman, "Regularization And Renormalization Of Gauge Fields," Nucl. Phys. B **44** (1972) 189.

[147] A. A. Slavnov, "Ward Identities In Gauge Theories," Theor. Math. Phys. **10** (1972) 99. [Teor. Mat. Fiz. **10** (1972) 153].

[148] C. Becchi, A. Rouet and R. Stora, "Renormalization Of Gauge Theories," Annals Phys. **98** (1976) 287.

[149] E. Fermi, "Trends To A Theory Of Beta Radiation. (In Italian)," *Nuovo Cim.* **11** (1934) 1.

[150] S. Weinberg, "Baryon And Lepton Nonconserving Processes," Phys. Rev. Lett. **43** (1979) 1566.

[151] G. D'Ambrosio, G. F. Giudice, G. Isidori and A. Strumia, "Minimal flavour violation: An effective field theory approach," Nucl. Phys. B **645** (2002) 155. [arXiv:hep-ph/0207036].

[152] E. E. Salpeter and H. A. Bethe, "A Relativistic equation for bound state problems," Phys. Rev. **84** (1951) 1232.

[153] G. P. Lepage, "Analytic Bound State Solutions In A Relativistic Two-Body Formalism With Applications In Muonium And Positronium," Phys. Rev. A **16** (1977) 863.

[154] R. Barbieri and E. Remiddi, "Solving The Bethe-Salpeter Equation For Positronium," Nucl. Phys. B **141** (1978) 413.

[155] S. R. Coleman, "Quantum Sine-Gordon Equation As The Massive Thirring Model," Phys. Rev. D **11** (1975) 2088.

[156] W. E. Thirring, "A soluble relativistic field theory," Annals Phys. **3** (1958) 91.

[157] M. J. G. Veltman, "Radiative Corrections To Vector Boson Masses," Phys. Lett. B **91** (1980) 95.

[158] J. Bernabéu, A. Pich and A. Santamaría, "$\Gamma(Z \to b\bar{b})$: A Signature Of Hard Mass Terms For A Heavy Top," Phys. Lett. B **200** (1988) 569.

[159] J. Bernabéu, A. Pich and A. Santamaría, "Top Quark Mass From Radiative Corrections To The $Z \to b\bar{b}$ Decay," Nucl. Phys. B **363** (1991) 326.

[160] J. Prades, E. de Rafael and A. Vainshtein, "Hadronic Light-by-Light Scattering Contribution to the Muon Anomalous Magnetic Moment," arXiv:0901.0306 [hep-ph].

[161] F. Jegerlehner and A. Nyffeler, "The Muon $g-2$," Phys. Rept. **477** (2009) 1. [arXiv:0902.3360 [hep-ph]].

[162] S. Actis *et al.*, "Quest for precision in hadronic cross sections at low energy: Monte Carlo tools vs. experimental data," arXiv:0912.0749 [hep-ph].

[163] D. Hanneke, S. Fogwell and G. Gabrielse, "New Measurement of the Electron Magnetic Moment and the Fine Structure Constant," Phys. Rev. Lett. **100** (2008) 120801. [arXiv:0801.1134 [physics.atom-ph]].

[164] G. Gabrielse, D. Hanneke, T. Kinoshita, M. Nio and B. C. Odom, "New Determination of the Fine Structure Constant from the Electron g Value and QED," Phys. Rev. Lett. **97** (2006) 030802. [Erratum-ibid. **99** (2007) 039902].

[165] A. Sirlin, "Radiative Corrections In The $SU(2)_L \otimes U(1)$ Theory: A Simple Renormalization Framework," Phys. Rev. D **22** (1980) 971.

[166] A. Sirlin, "Role of $\sin^2\theta_W(m_Z)$ at the Z^0 Peak," Phys. Lett. B **232** (1989) 123.

[167] W. J. Marciano and A. Sirlin, "Radiative Corrections To Neutrino Induced Neutral Current Phenomena In The $SU(2)_L \otimes U(1)$ Theory," Phys. Rev. D **22** (1980) 2695. [Erratum-ibid. D **31** (1985) 213].

[168] S. Schael *et al.* [$ALEPH$ Collaboration], "Branching ratios and spectral functions of tau decays: Final $ALEPH$ measurements and physics implications," Phys. Rept. **421** (2005) 191. [arXiv:hep-ex/0506072].

[169] [$ALEPH$ Collaboration and $DELPHI$ Collaboration and $L3$ Collaboration and $OPAL$ Collaboration], "Precision electroweak measurements on the Z resonance," Phys. Rept. **427** (2006) 257. [arXiv:hep-ex/0509008].

[170] M. Passera, W. J. Marciano and A. Sirlin, "The Muon $g-2$ and the bounds on the Higgs boson mass," Phys. Rev. D **78** (2008) 013009. [arXiv:0804.1142 [hep-ph]].

[171] N. Cabibbo and R. Gatto, "Electron Positron Colliding Beam Experiments," Phys. Rev. **124** (1961) 1577.

[172] S. Eidelman and F. Jegerlehner, "Hadronic contributions to $g-2$ of the leptons and to the effective fine structure constant $\alpha(M_Z^2)$," Z. Phys. C **67** (1995) 585. [arXiv:hep-ph/9502298].

[173] M. Davier and A. Hocker, "Improved determination of $\alpha(M_Z^2)$ and the anomalous magnetic moment of the muon," Phys. Lett. B **419** (1998) 419. [arXiv:hep-ph/9711308].

[174] H. Burkhardt and B. Pietrzyk, "Update Of The Hadronic Contribution To The QED Vacuum Polarization," Phys. Lett. B **513** (2001) 46.

[175] F. Jegerlehner, "Hadronic contributions to the photon vacuum polarization and their role in precision physics," J. Phys. G **29** (2003) 101. [arXiv:hep-ph/0104304].

[176] F. Jegerlehner, "Hadronic vacuum polarization effects in $\alpha_{em}(M_Z)$," arXiv:hep-ph/0308117.

[177] F. Jegerlehner, "Theoretical precision in estimates of the hadronic contributions to $(g-2)_\mu$ and $\alpha_{QED}(M_Z)$," Nucl. Phys. Proc. Suppl. **126** (2004) 325. [arXiv:hep-ph/0310234].

[178] F. Jegerlehner, "The role of $\sigma(e^+e^- \to hadrons)$ in precision tests of the standard model," Nucl. Phys. Proc. Suppl. **131** (2004) 213. [arXiv:hep-ph/0312372].

[179] F. Jegerlehner, "Precision measurements of $\sigma(hadronic)$ for $\alpha(eff)(E)$ at ILC energies and $(g-2)_\mu$," Nucl. Phys. Proc. Suppl. **162** (2006) 22. [arXiv:hep-ph/0608329].

[180] F. Jegerlehner, "The running fine structure constant $\alpha(E)$ via the Adler function," Nucl. Phys. Proc. Suppl. **181-182** (2008) 135. [arXiv:0807.4206 [hep-ph]].

[181] K. Hagiwara, A. D. Martin, D. Nomura and T. Teubner, "The SM prediction of $g-2$ of the muon," Phys. Lett. B **557** (2003) 69. [arXiv:hep-ph/0209187].

[182] K. Hagiwara, A. D. Martin, D. Nomura and T. Teubner, "Predictions for $g-2$ of the muon and $\alpha_{QED}(M_Z^2)$," Phys. Rev. D **69** (2004) 093003. [arXiv:hep-ph/0312250].

[183] K. Hagiwara, A. D. Martin, D. Nomura and T. Teubner, "Improved predictions for $g-2$ of the muon and $\alpha_{\rm QED}(M_Z^2)$," Phys. Lett. B **649** (2007) 173. [arXiv:hep-ph/0611102].

[184] M. Gourdin and E. De Rafael, "Hadronic contributions to the muon g-factor," Nucl. Phys. B **10** (1969) 667.

[185] M. Davier, A. Hoecker, B. Malaescu, C. Z. Yuan and Z. Zhang, "Reevaluation of the hadronic contribution to the muon magnetic anomaly using new $e^+e^- \to \pi^+\pi^-$ cross section data from $BABAR$," arXiv:0908.4300 [hep-ph].

[186] S. I. Eidelman, "Standard Model Predictions for the Muon $(g-2)/2$," arXiv:0904.3275 [hep-ex].

[187] J. Prades, "Standard Model Prediction of the Muon Anomalous Magnetic Moment," arXiv:0909.2546 [hep-ph].

[188] M. Passera, W. J. Marciano and A. Sirlin, "The muon $g-2$ discrepancy: new physics or a relatively light Higgs?," arXiv:1001.4528 [hep-ph].

[189] C. Bini and G. Venanzoni, "PhiPsi08, Proceedings Of The International Workshop On e^+e^- Collisions From Φ To Ψ, Frascati (Rome) Italy, 7-10 April 2008,"

[190] A. Bondar and S. Eidelman, "Tau 2008, proceedings of the 10th International Workshop on Tau Lepton Physics, Novosibirsk, Russia, 22-25 September 2008,"

[191] M. Davier *et al.*, "The Discrepancy Between τ and e^+e^- Spectral Functions Revisited and the Consequences for the Muon Magnetic Anomaly," arXiv:0906.5443 [hep-ph].

[192] I. Rosell, "Quantum Corrections in the Resonance Chiral Theory," arXiv:hep-ph/0701248.

[193] G. Colangelo, J. Gasser and H. Leutwyler, "$\pi\pi$ scattering," Nucl. Phys. B **603** (2001) 125 [arXiv:hep-ph/0103088].

[194] I. Caprini, G. Colangelo and H. Leutwyler, "Mass and width of the lowest resonance in QCD," Phys. Rev. Lett. **96** (2006) 132001 [arXiv:hep-ph/0512364].

[195] J. Goldstone, A. Salam and S. Weinberg, "Broken Symmetries," Phys. Rev. **127** (1962) 965.

[196] F. Englert and R. Brout, "BROKEN SYMMETRY AND THE MASS OF GAUGE VECTOR MESONS," Phys. Rev. Lett. **13** (1964) 321.

[197] P. W. Higgs, "Broken Symmetries, Massless Particles And Gauge Fields," Phys. Lett. **12** (1964) 132.

[198] P. W. Higgs, "Broken Symmetries And The Masses Of Gauge Bosons," Phys. Rev. Lett. **13** (1964) 508.

[199] P. W. Higgs, "Spontaneous Symmetry Breakdown Without Massless Bosons," Phys. Rev. **145** (1966) 1156.

[200] T. W. B. Kibble, "Symmetry Breaking In Non-Abelian Gauge Theories," Phys. Rev. **155** (1967) 1554.

[201] C. Vafa and E. Witten, "Restrictions On Symmetry Breaking In Vector - Like Gauge Theories," Nucl. Phys. B **234** (1984) 173.

[202] A. Pich, "Chiral Perturbation Theory," Rept. Prog. Phys. **58** (1995) 563 [arXiv:hep-ph/9502366].

[203] S. Scherer, "Introduction to Chiral Perturbation Theory," edited by J. W. Negele and E.Vogt in Negele, W. *et al.*: "Advances in Nuclear Physics," **27** 277-538. [arXiv:hep-ph/0210398]. "Chiral Dynamics I + II," Courses given at the Johannes-Gutenberg Universität, Mainz.

[204] H. Leutwyler, "On the foundations of Chiral Perturbation Theory," Annals Phys. **235** (1994) 165. [arXiv:hep-ph/9311274].

[205] J. Bijnens, "Chiral perturbation theory and anomalous processes," Int. J. Mod. Phys. A **8** (1993) 3045.

[206] J. F. Donoghue, E. Golowich and B. R. Holstein, "Dynamics Of The Standard Model," Camb. Monogr. Part. Phys. Nucl. Phys. Cosmol. **2** (1992) 1.

[207] S. Weinberg, "Pion Scattering Lengths," Phys. Rev. Lett. **17** (1966) 616.

[208] S. Weinberg, "Dynamical Approach To Current Algebra," Phys. Rev. Lett. **18** (1967) 188.

[209] S. Weinberg, "Nonlinear Realizations Of Chiral Symmetry," Phys. Rev. **166**, 1568 (1968).

[210] J. Gasser and H. Leutwyler, "Low-Energy Expansion Of Meson Form-Factors," Nucl. Phys. B **250** (1985) 517.

[211] O. Catà and V. Mateu, "Chiral Perturbation Theory with tensor sources," JHEP **0709** (2007) 078. [arXiv:0705.2948 [hep-ph]].

[212] M. Gell-Mann, R. J. Oakes and B. Renner, "Behavior Of Current Divergences Under $SU(3) \otimes SU(3)$," Phys. Rev. **175** (1968) 2195.

[213] S. Weinberg, "A New Light Boson?," Phys. Rev. Lett. **40**, (1978) 223226.

[214] M. Gell-Mann, "Model of Strong Couplings," Phys. Rev. **106**, (1957) 1296.

[215] S. Okubo, "Note On Unitary Symmetry In Strong Interactions," Prog. Theor. Phys. **27** (1962) 949.

[216] N. H. Fuchs, H. Sazdjian and J. Stern, "How to probe the scale of $(\overline{q}q)$ in Chiral Perturbation Theory," Phys. Lett. B **269** (1991) 183.

[217] J. Stern, H. Sazdjian and N. H. Fuchs, "What π - π scattering tells us about Chiral Perturbation Theory," Phys. Rev. D **47** (1993) 3814. [arXiv:hep-ph/9301244].

[218] M. Knecht, H. Sazdjian, J. Stern and N. H. Fuchs, "A Possible experimental determination of $M_s/(M_u + M_d)$ decays," Phys. Lett. B **313** (1993) 229. [arXiv:hep-ph/9305332].

[219] L. Giusti, F. Rapuano, M. Talevi and A. Vladikas, "The QCD chiral condensate from the lattice," Nucl. Phys. B **538** (1999) 249. [arXiv:hep-lat/9807014].

[220] P. Hernández, K. Jansen and L. Lellouch, "Finite-size scaling of the quark condensate in quenched lattice QCD," Phys. Lett. B **469** (1999) 198. [arXiv:hep-lat/9907022].

[221] T. W. Chiu and T. H. Hsieh, "Light quark masses, chiral condensate and quark-gluon condensate in quenched lattice QCD with exact chiral symmetry," Nucl. Phys. B **673** (2003) 217. [Nucl. Phys. Proc. Suppl. **129** (2004) 492]. [arXiv:hep-lat/0305016].

[222] D. Becirevic and V. Lubicz, "Estimate of the chiral condensate in quenched lattice QCD," Phys. Lett. B **600** (2004) 83. [arXiv:hep-ph/0403044].

[223] V. Giménez, V. Lubicz, F. Mescia, V. Porretti and J. Reyes, "Operator product expansion and quark condensate from $LQCD$ in coordinate space," PoS **LAT2005** (2006) 081. [arXiv:hep-lat/0510090].

[224] C. McNeile, "An estimate of the chiral condensate from unquenched lattice QCD," Phys. Lett. B **619** (2005) 124. [arXiv:hep-lat/0504006].

[225] T. DeGrand, R. Hoffmann, S. Schaefer and Z. Liu, "Quark condensate in one-flavor QCD," arXiv:hep-th/0605147.

[226] *et al.* [$JLQCD$ collaboration], "Determination of the chiral condensate from $2+1$-flavor lattice QCD," arXiv:0911.5555 [hep-lat].

[227] V. P. Spiridonov and K. G. Chetyrkin, "Nonleading Mass Corrections And Renormalization Of The Operators $M\overline{\Psi}\Psi$ And $G^2_{\mu\nu}$)," Sov. J. Nucl. Phys. **47** (1988) 522 [Yad. Fiz. **47** (1988) 818].

[228] K. G. Chetyrkin, C. A. Domínguez, D. Pirjol and K. Schilcher, "Mass singularities in light quark correlators: The Strange quark case," Phys. Rev. D **51** (1995) 5090 [arXiv:hep-ph/9409371].

[229] K. G. Chetyrkin, D. Pirjol and K. Schilcher, "Order-α_s^3 determination of the strange quark mass," Phys. Lett. B **404** (1997) 337 [arXiv:hep-ph/9612394].

[230] H. G. Dosch and S. Narison, "Direct extraction of the chiral quark condensate and bounds on the light quark masses," Phys. Lett. B **417** (1998) 173 [arXiv:hep-ph/9709215].

[231] M. Jamin, "Flavour-symmetry breaking of the quark condensate and chiral corrections to the Gell-Mann-Oakes-Renner relation," Phys. Lett. B **538** (2002) 71 [arXiv:hep-ph/0201174].

[232] C. A. Domínguez, N. F. Nasrallah and K. Schilcher, "Strange quark condensate from QCD sum rules to five loops," JHEP **0802** (2008) 072 [arXiv:0711.3962 [hep-ph]].

[233] J. Bordes, C. A. Domínguez, P. Moodley, J. Peñarrocha and K. Schilcher, "Chiral corrections to the $SU(2) \times SU(2)$ Gell-Mann-Oakes-Renner relation," arXiv:1003.3358 [hep-ph].

[234] S. Descotes-Genon, L. Girlanda and J. Stern, "Paramagnetic effect of light quark loops on chiral symmetry breaking," JHEP **0001** (2000) 041. [arXiv:hep-ph/9910537].

[235] S. Descotes-Genon and J. Stern, "Finite-volume analysis of N_f-induced chiral phase transitions," Phys. Rev. D **62** (2000) 054011. [arXiv:hep-ph/9912234].

[236] S. Descotes-Genon and J. Stern, "Vacuum fluctuations of $\bar{q} - q$ and values of low-energy constants," Phys. Lett. B **488** (2000) 274. [arXiv:hep-ph/0007082].

[237] S. Descotes-Genon, N. H. Fuchs, L. Girlanda and J. Stern, "Analysis and interpretation of new low-energy $\pi\pi$ scattering data," Eur. Phys. J. C **24** (2002) 469. [arXiv:hep-ph/0112088].

[238] S. Descotes-Genon, L. Girlanda and J. Stern, "Chiral order and fluctuations in multi-flavour QCD," Eur. Phys. J. C **27** (2003) 115. [arXiv:hep-ph/0207337].

[239] S. Descotes-Genon, N. H. Fuchs, L. Girlanda and J. Stern, "Resumming QCD vacuum fluctuations in three-flavour chiral perturbation theory," Eur. Phys. J. C **34** (2004) 201. [arXiv:hep-ph/0311120].

[240] S. Descotes-Genon, "Low-energy $\pi\pi$ and πK scatterings revisited in three-flavour resummed chiral perturbation theory," Eur. Phys. J. C **52** (2007) 141. [arXiv:hep-ph/0703154].

[241] J. Wess and B. Zumino, "Consequences Of Anomalous Ward Identities," Phys. Lett. B **37** (1971) 95.

[242] E. Witten, "Global Aspects Of Current Algebra," Nucl. Phys. B **223** (1983) 422.

[243] S. L. Adler, "Axial-vector vertex in spinor electrodynamics," Phys. Rev. **177** (1969) 2426.

[244] J. S. Bell and R. Jackiw, "A $PCAC$ puzzle: $\pi^0 \to \gamma\gamma$ in the sigma model," Nuovo Cim. A **60** (1969) 47.

[245] S. L. Adler and W. A. Bardeen, "Absence of higher order corrections in the anomalous axial-vector divergence equation," Phys. Rev. **182** (1969) 1517-1536.

[246] K. Fujikawa, "Path Integral Measure For Gauge Invariant Fermion Theories," Phys. Rev. Lett. **42** (1979) 1195.

[247] K. Fujikawa, "Path Integral For Gauge Theories With Fermions," Phys. Rev. D **21** (1980) 2848. [Erratum-ibid. D **22** (1980) 1499].

[248] J. Bijnens, G. Ecker and J. Gasser, "Chiral Perturbation Theory," arXiv:hep-ph/9411232.

[249] C. G. Callan and E. Witten, "Monopole Catalysis Of Skyrmion Decay," Nucl. Phys. B **239** (1984) 161.

[250] H. W. Fearing and S. Scherer, "Extension of the chiral perturbation theory meson Lagrangian to order p^6," Phys. Rev. D **53** (1996) 315 [arXiv:hep-ph/9408346].

[251] J. Bijnens, G. Colangelo and G. Ecker, "The Mesonic Chiral Lagrangian Of Order p^6," JHEP **9902** (1999) 020. [arXiv:hep-ph/9902437].

[252] J. Bijnens, G. Colangelo and G. Ecker, "Renormalization Of Chiral Perturbation Theory To Order p^6," Annals Phys. **280** (2000) 100. [arXiv:hep-ph/9907333].

[253] J. Bijnens, L. Girlanda and P. Talavera, "The anomalous chiral Lagrangian of order p^6," Eur. Phys. J. C **23** (2002) 539. [arXiv:hep-ph/0110400].

[254] N. Isgur and M. B. Wise, "Weak Transition Form-Factors Between Heavy Mesons," Phys. Lett. B **237** (1990) 527.

[255] N. Isgur and M. B. Wise, "Weak Decays Of Heavy Mesons In The Static Quark Approximation," Phys. Lett. B **232** (1989) 113.

[256] E. Eichten and B. R. Hill, "An Effective Field Theory for the Calculation of Matrix Elements Involving Heavy Quarks," Phys. Lett. B **234** (1990) 511.

[257] H. Georgi, "An Effective Field Theory for Heavy Quarks at Low-Energies," Phys. Lett. B **240** (1990) 447.

[258] B. Grinstein, "The Static Quark Effective Theory," Nucl. Phys. B **339** (1990) 253.

[259] A. V. Manohar and M. B. Wise, "Heavy quark physics," Camb. Monogr. Part. Phys. Nucl. Phys. Cosmol. **10** (2000) 1.

[260] W. E. Caswell and G. P. Lepage, "Effective Lagrangians For Bound State Problems In QED, QCD, And Other Field Theories," Phys. Lett. B **167** (1986) 437.

[261] G. P. Lepage, L. Magnea, C. Nakhleh, U. Magnea and K. Hornbostel, "Improved nonrelativistic QCD for heavy quark physics," Phys. Rev. D **46** (1992) 4052. [arXiv:hep-lat/9205007].

[262] G. T. Bodwin, E. Braaten and G. P. Lepage, "Rigorous QCD analysis of inclusive annihilation and production of heavy quarkonium," Phys. Rev. D **51** (1995) 1125. [Erratum-ibid. D **55** (1997) 5853]. [arXiv:hep-ph/9407339].

[263] A. Pineda and J. Soto, "Effective field theory for ultrasoft momenta in $NRQCD$ and $NRQED$," Nucl. Phys. Proc. Suppl. **64** (1998) 428. [arXiv:hep-ph/9707481].

[264] N. Brambilla, A. Pineda, J. Soto and A. Vairo, "The infrared behaviour of the static potential in perturbative QCD," Phys. Rev. D **60** (1999) 091502. [arXiv:hep-ph/9903355].

[265] M. E. Luke, A. V. Manohar and I. Z. Rothstein, "Renormalization group scaling in nonrelativistic QCD," Phys. Rev. D **61** (2000) 074025. [arXiv:hep-ph/9910209].

[266] N. Brambilla, A. Pineda, J. Soto and A. Vairo, "Potential $NRQCD$: An effective theory for heavy quarkonium," Nucl. Phys. B **566** (2000) 275. [arXiv:hep-ph/9907240].

[267] N. Brambilla, A. Pineda, J. Soto and A. Vairo, "Effective field theories for heavy quarkonium," Rev. Mod. Phys. **77** (2005) 1423. [arXiv:hep-ph/0410047].

[268] N. Brambilla *et al.* [Quarkonium Working Group], "Heavy quarkonium physics," arXiv:hep-ph/0412158.

[269] E. Witten, "Instantons, The Quark Model, And The $1/N$ Expansion," Nucl. Phys. B **149** (1979) 285.

[270] P. Di Vecchia and G. Veneziano, "Chiral Dynamics In The Large-N Limit," Nucl. Phys. B **171** (1980) 253.

[271] E. Witten, "Large-N Chiral Dynamics," Annals Phys. **128** (1980) 363.

[272] S. R. Coleman, "$1/N$" in "Aspects of Symmetry," Selected Erice Lectures of S. R. Coleman. C.U.P., Harvard (1984).

[273] A. V. Manohar, "Large-N QCD," Talk given at the Les Houches Summer School in Theoretical Physics, Session 68: Probing the Standard Model of Particle Interactions, Les Houches, France, 28 Jul - 5 Sep 1997. Published in 'Les Houches 1997, Probing the standard model of particle interactions, Pt. 2' 1091-1169. arXiv:hep-ph/9802419.

[274] A. Pich, "Colourless Mesons In A Polychromatic World," Published in 'Tempe 2002, Phenomenology of large N_C QCD' 239-258. arXiv:hep-ph/0205030.

[275] R. Kaiser and H. Leutwyler, "Large N_C In Chiral Perturbation Theory," Eur. Phys. J. C **17** (2000) 623. [arXiv:hep-ph/0007101].

[276] R. F. Dashen, E. E. Jenkins and A. V. Manohar, "The $1/N_C$ expansion for baryons," Phys. Rev. D **49** (1994) 4713. [Erratum-ibid. D **51** (1995) 2489]. [arXiv:hep-ph/9310379].

[277] R. F. Dashen, E. E. Jenkins and A. V. Manohar, "Spin-Flavor Structure of Large-N Baryons," Phys. Rev. D **51** (1995) 3697. [arXiv:hep-ph/9411234].

[278] E. E. Jenkins, "Large-N_c Baryons," Ann. Rev. Nucl. Part. Sci. **48** (1998) 81. [arXiv:hep-ph/9803349].

[279] S. J. Brodsky and G. R. Farrar, "Scaling Laws At Large Transverse Momentum," Phys. Rev. Lett. **31** (1973) 1153.

[280] S. J. Brodsky and G. R. Farrar, "Scaling Laws For Large Momentum Transfer Processes," Phys. Rev. D **11** (1975) 1309.

[281] G. P. Lepage and S. J. Brodsky, "Exclusive Processes In Quantum Chromodynamics: Evolution Equations For Hadronic Wave Functions And The Form-Factors Of Mesons," Phys. Lett. B **87** (1979) 359.

[282] G. P. Lepage and S. J. Brodsky, "Exclusive Processes In Perturbative Quantum Chromodynamics," Phys. Rev. D **22** (1980) 2157.

[283] G. Ecker and C. Zauner, "Tensor meson exchange at low energies," Eur. Phys. J. C **52** (2007) 315. [arXiv:0705.0624 [hep-ph]].

[284] B. Moussallam, "Analyticity constraints on the strangeness changing vector current and applications to $\tau \to K\pi\nu_\tau$, $\tau \to K\pi\pi\nu_\tau$," Eur. Phys. J. C **53** (2008) 401. [arXiv:0710.0548 [hep-ph]].

[285] I. Rosell, J. J. Sanz-Cillero and A. Pich, "Quantum loops in the resonance chiral theory: The vector form factor," JHEP **0408** (2004) 042. [arXiv:hep-ph/0407240].

[286] I. Rosell, P. Ruiz-Femenía and J. Portolés, "One-loop renormalization of resonance chiral theory: Scalar and pseudoscalar resonances," JHEP **0512** (2005) 020. [arXiv:hep-ph/0510041].

[287] I. Rosell, J. J. Sanz-Cillero and A. Pich, "Towards a determination of the chiral couplings at NLO in $1/N_C$: $L_8^r(\mu)$," JHEP **0701** (2007) 039. [arXiv:hep-ph/0610290].

[288] J. Portolés, I. Rosell and P. Ruiz-Femenía, "Vanishing chiral couplings in the large-N_C resonance theory," Phys. Rev. D **75** (2007) 114011. [arXiv:hep-ph/0611375].

[289] J. J. Sanz-Cillero, "On the structure of two-point Green functions at next-to-leading order in $1/N_C$," Phys. Lett. B **649** (2007) 180. [arXiv:hep-ph/0702217].

[290] A. Pich, I. Rosell and J. J. Sanz-Cillero, "Form-factors and current correlators: chiral couplings $L_10(\mu)$ and $C_87(\mu)$ at NLO in $1/N_C$," JHEP **0807** (2008) 014. [arXiv:0803.1567 [hep-ph]].

[291] J. J. Sanz-Cillero, "Renormalization group equations in resonance chiral theory," Phys. Lett. B **681** (2009) 100. [arXiv:0905.3676 [hep-ph]].

[292] I. Rosell, P. Ruiz-Femenía and J. J. Sanz-Cillero, "Resonance saturation of the chiral couplings at NLO in $1/N_C$," Phys. Rev. D **79** (2009) 076009. [arXiv:0903.2440 [hep-ph]].

[293] J. J. Sanz-Cillero and J. Trnka, "High energy constraints in the octet $SS-PP$ correlator and resonance saturation at NLO in $1/N_C$," Phys. Rev. D **81** (2010) 056005. [arXiv:0912.0495 [hep-ph]].

[294] J. J. Sanz-Cillero, "One loop predictions for the pion VFF in Resonance Chiral Theory," arXiv:1009.6012 [hep-ph].

[295] M. A. Shifman, A. I. Vainshtein and V. I. Zakharov, "QCD And Resonance Physics. Sum Rules," Nucl. Phys. B **147** (1979) 385.

[296] M. A. Shifman, A. I. Vainshtein and V. I. Zakharov, "QCD And Resonance Physics: Applications," Nucl. Phys. B **147** (1979) 448.

[297] E. G. Floratos, S. Narison and E. de Rafael, "Spectral Function Sum Rules In Quantum Chromodynamics. 1. Charged Currents Sector," Nucl. Phys. B **155** (1979) 115.

[298] S. J. Brodsky and G. P. Lepage, "Large Angle Two Photon Exclusive Channels In Quantum Chromodynamics," Phys. Rev. D **24** (1981) 1808.

[299] V. Cirigliano, G. Ecker, M. Eidemüller, A. Pich and J. Portolés, "The $\langle VAP \rangle$ Green function in the resonance region," Phys. Lett. B **596** (2004) 96. [arXiv:hep-ph/0404004].

[300] K. Kawarabayashi and M. Suzuki, "Partially conserved axial vector current and the decays of vector mesons," Phys. Rev. Lett. **16** (1966) 255.

[301] Riazuddin and Fayyazuddin, "Algebra of current components and decay widths of ρ and K^* mesons," Phys. Rev. **147** (1966) 1071.

[302] S. Weinberg, "Precise Relations Between The Spectra Of Vector And Axial Vector Mesons," Phys. Rev. Lett. **18** (1967) 507.

[303] Z. H. Guo and P. Roig, "One meson radiative tau decays," arXiv:1009.2542 [hep-ph]; "Lepton universality tests through ratios involving the one meson radiative decays of the tau," work in progress.

[304] D. G. Dumm, P. Roig, A. Pich and J. Portolés, "Hadron structure in $\tau \to KK\pi\nu_\tau$ decays," Phys. Rev. D **81** (2010) 034031 [arXiv:0911.2640 [hep-ph]].

[305] S. Peris, M. Perrottet and E. de Rafael, "Matching long and short distance in large N_C QCD," JHEP **9805** (1998) 011.

[306] M. Knecht, S. Peris, M. Perrottet and E. de Rafael, "Decay of pseudoscalars into lepton pairs and large N_C QCD," Phys. Rev. Lett. **83** (1999) 5230. [arXiv:hep-ph/9908283].

[307] S. Peris, B. Phily and E. de Rafael, "Tests of large N_C QCD from hadronic tau decays," Phys. Rev. Lett. **86** (2001) 14-17.

[308] E. de Rafael, "Analytic approaches to kaon physics," Nucl. Phys. Proc. Suppl. **119** (2003) 71-83.

[309] D. Gómez Dumm, A. Pich and J. Portolés, "$\tau \to \pi\ \pi\ \pi\ \nu_\tau$ decays in the resonance effective theory," Phys. Rev. D **69** (2004) 073002. [arXiv:hep-ph/0312183].

[310] P. D. Ruiz-Femenía, A. Pich and J. Portolés, "Odd-intrinsic-parity processes within the resonance effective theory of QCD," JHEP **0307** (2003) 003. [arXiv:hep-ph/0306157]. "Phenomenology of the Green's function within the resonance chiral theory," Nucl. Phys. Proc. Suppl. **133** (2004) 215.

[311] V. Cirigliano, G. Ecker, M. Eidemüller, R. Kaiser, A. Pich and J. Portolés, "The Green function and $SU(3)$ breaking in $K_{\ell 3}$ decays," JHEP **0504** (2005) 006. [arXiv:hep-ph/0503108].

[312] E. Pallante and R. Petronzio, "Anomalous effective Lagrangians and vector resonance models," Nucl. Phys. B **396** (1993) 205.

[313] B. Moussallam, "Chiral sum rules for parameters of the order six Lagrangian in the W-Z sector and application to π^0, η, η' decays," Phys. Rev. D **51** (1995) 4939. [arXiv:hep-ph/9407402].

[314] B. Moussallam, "A sum rule approach to the violation of Dashen's theorem," Nucl. Phys. B **504** (1997) 381. [arXiv:hep-ph/9701400].

[315] M. Knecht and A. Nyffeler, "Resonance estimates of $\mathcal{O}(p^6)$ low-energy constants and QCD short-distance constraints," Eur. Phys. J. C **21** (2001) 659. [arXiv:hep-ph/0106034].

[316] J. Bijnens, E. Gamiz, E. Lipartia and J. Prades, "QCD short-distance constraints and hadronic approximations," JHEP **0304** (2003) 055. [arXiv:hep-ph/0304222].

[317] J. Prades, "Massive spin-1 field chiral Lagrangian from an extended Nambu-Jona-Lasinio model of QCD," Z. Phys. C **63** (1994) 491. [Erratum-ibid. C **11** (1999) 571]. [arXiv:hep-ph/9302246].

[318] J. J. Sakurai, "Currents and mesons," Univ. Chicago Press, Chicago IL (1969).

[319] R. Kaiser, "Large N_C in chiral resonance Lagrangians," arXiv:hep-ph/0502065.

[320] P. Roig, "Hadronic decays of the tau lepton: $\tau \to K\bar{K}\pi\nu_\tau$ channels," Valéncia Univ. Masther Thesis (2006).

[321] P. Roig, "Hadronic decays of the tau lepton into K K pion modes within Resonance Chiral Theory," AIP Conf. Proc. **964** (2007) 40. [arXiv:0709.3734 [hep-ph]].

[322] D. G. Dumm, P. Roig, A. Pich and J. Portolés, "$\tau \to \pi\pi\pi\nu_\tau$ decays and the $a_1(1260)$ off-shell width revisited," Phys. Lett. B **685** (2010) 158. arXiv:0911.4436 [hep-ph].

[323] V. Mateu and J. Portolés, "Form Factors in radiative pion decay," Eur. Phys. J. C **52** (2007) 325. [arXiv:0706.1039 [hep-ph]].

[324] J. Portolés, "Hadronic decays of the tau lepton: Theoretical overview," Nucl. Phys. Proc. Suppl. **144** (2005) 3. [arXiv:hep-ph/0411333].

[325] R. Fischer, J. Wess and F. Wagner, "Decays Of The Heavy Lepton Tau And Chiral Dynamics," Z. Phys. C **3** (1979) 313.

[326] H. K. Kühn and F. Wagner, "Semileptonic Decays Of The Tau Lepton," Nucl. Phys. B **236** (1984) 16.

[327] A. Pich, "'Anomalous' η production in τ decay," Phys. Lett. B **196** (1987) 561.

[328] A. Pich, "QCD Tests From Tau Decay Data," FTUV/89-22 *Talk given at Tau Charm Factory Workshop, Stanford, Calif., May 23-27, 1989.* Proceedings: 'Study of tau, charm and J/Ψ physics development of high luminosity e^+e^-, Ed. L. V. Beers, SLAC (1989).

[329] J. H. Kühn and A. Santamaría, "Tau Decays To Pions," Z. Phys. C **48** (1990) 445.

[330] G. J. Gounaris, J. J. Sakurai, "Finite width corrections to the vector meson dominance prediction for $\rho \to e^+e^-$," Phys. Rev. Lett. **21**, 244 (1968).

[331] R. Barate *et al.* [*ALEPH* Collaboration], "Measurement of the spectral functions of vector current hadronic tau decays," Z. Phys. C **76** (1997) 15.

[332] S. Anderson *et al.* [*CLEO* Collaboration], "Hadronic structure in the decay $\tau^- \to \pi^-\pi^0\nu_\tau$," Phys. Rev. D **61** (2000) 112002. [arXiv:hep-ex/9910046].

[333] M. Athanas *et al.* [*CLEO* Collaboration], "Limit on tau-neutrino mass from $\tau^- \to \pi^-\pi^+\pi^-\pi^0\nu_\tau$," Phys. Rev. D **61** (2000) 052002. [arXiv:hep-ex/9906015].

[334] A. Pich, "Flavourdynamics," Published in Spanish Fund.Phys.1995:0001-54 (QCD161:I92:1995). arXiv:hep-ph/9601202.

[335] A. Pich, "The Standard model of electroweak interactions," arXiv:0705.4264 [hep-ph].

[336] R. Decker and M. Finkemeier, "Radiative tau decays with one pseudoscalar meson," Phys. Rev. D **48** (1993) 4203 [Addendum-ibid. D **50** (1994) 7079] [arXiv:hep-ph/9302286].

[337] S. G. Brown and S. A. Bludman, "Further Analysis Of The Decay $\pi \to e\nu\gamma$," Phys. Rev. **136** (1964) B1160.

[338] P. de Baenst and J. Pestieau, Nuovo Cimento 53A, 407 (1968).

[339] E. Bycling, K. Kajantie "Particle Kinematics" John Wiley and Sons Ltd. (April 30, 1973).

[340] J.Kim and L.Resnick, "Tau radiative decays", Phys. Rev. D **21**, (1980) 1330.

[341] C. Q. Geng and C. C. Lih, "Tau radiative decays in the light front quark model," Phys. Rev. D **68** (2003) 093001 [arXiv:hep-ph/0310161].

[342] R. Decker and M. Finkemeier, "Radiative corrections to the decay $\tau \to \pi/K\nu_\tau$," Phys. Lett. B **316** (1993) 403 [arXiv:hep-ph/9307372].

[343] R. Decker and M. Finkemeier, "Short And Long Distance Effects In The Decay $\tau \to \pi\nu_\tau(\gamma)$," Nucl. Phys. B **438** (1995) 17 [arXiv:hep-ph/9403385].

[344] R. Decker and M. Finkemeier, "Radiative corrections to the decay $\tau \to \pi/K\nu_\tau$," Phys. Lett. B **334** (1994) 199.

[345] M. J. Lee *et al.* [*Belle* Collaboration], "Measurement of the branching fractions and the invariant mass distributions for $\tau^- \to h^-h^+h^-\nu_\tau$ decays," Phys. Rev. D **81** (2010) 113007 [arXiv:1001.0083 [hep-ex]].

[346] J. H. Kühn and E. Mirkes, "Structure functions in tau decays," Z. Phys. C **56** (1992) 661. [Erratum-ibid. C **67** (1995) 364].

[347] R. Decker and E. Mirkes, "Angular distributions in the $\tau^- \to \nu_\tau\omega\pi^-$ decay mode," Z. Phys. C **57** (1993) 495.

[348] R. R. Akhmetshin *et al.* [$CMD-2$ Collaboration], "Reanalysis of Hadronic Cross Section Measurements at $CMD-2$," Phys. Lett. B **578** (2004) 285 [arXiv:hep-ex/0308008].

[349] V. M. Aulchenko *et al.* [$CMD-2$ Collaboration], "Measurement of the pion form factor in the energy range 1.04-GeV - 1.38-GeV with the $CMD-2$ detector," JETP Lett. **82** (2005) 743 [Pisma Zh. Eksp. Teor. Fiz. **82** (2005) 841] [arXiv:hep-ex/0603021].

[350] R. R. Akhmetshin *et al.* [$CMD-2$ Collaboration], "High-statistics measurement of the pion form factor in the rho-meson energy range with the $CMD-2$ detector," Phys. Lett. B **648** (2007) 28. [arXiv:hep-ex/0610021].

[351] M. N. Achasov *et al.*, "Update of the $e^+e^- \to \pi^+\pi^-$ cross section measured by SND detector in the energy region 400 MeV $< s^(1/2) <$ 1000 MeV," J. Exp. Theor. Phys. **103** (2006) 380. [Zh. Eksp. Teor. Fiz. **130** (2006) 437]. [arXiv:hep-ex/0605013].

[352] A. Aloisio, et al., ($KLOE$ Collaboration) "Measurement of $\sigma(e^+e^- \to \pi^+\pi^-\gamma)$ and extraction of $\sigma(e^+e^- \to \pi^+\pi^-)$ below 1 GeV with the $KLOE$ detector," Published in Phys. Lett. B**606** (2005) 12-24. [arXiv hep-ex/0407048].

[353] F. Ambrosino *et al.* [$KLOE$ Collaboration], "Measurement of $\sigma(e^+e^- \to \pi^+\pi^-\gamma(\gamma))$ and the dipion contribution to the muon anomaly with the $KLOE$ detector," Phys. Lett. B **670** (2009) 285. [arXiv:0809.3950 [hep-ex]].

[354] B. Aubert *et al.* [$BABAR$ Collaboration], "Precise measurement of the $e^+e^- \to \pi^+\pi^-(\gamma)$ cross section with the Initial State Radiation method at BABAR," Phys. Rev. Lett. **103** (2009) 231801 [arXiv:0908.3589 [hep-ex]].

[355] M. Fujikawa *et al.* [Belle Collaboration], "High-Statistics Study of the $\tau^- \to \pi^-\pi^0\nu_\tau$ Decay," Phys. Rev. D **78** (2008) 072006 [arXiv:0805.3773 [hep-ex]].

[356] G. Colangelo, M. Finkemeier and R. Urech, "Tau Decays and Chiral Perturbation Theory," Phys. Rev. D **54** (1996) 4403. [arXiv:hep-ph/9604279].

[357] J. Bijnens, G. Colangelo and P. Talavera, "The vector and scalar form factors of the pion to two loops," JHEP **9805** (1998) 014. [arXiv:hep-ph/9805389].

[358] J. Bijnens and P. Talavera, "Pion and kaon electromagnetic form factors," JHEP **0203** (2002) 046. [arXiv:hep-ph/0203049].

[359] F. Guerrero and A. Pich, "Effective field theory description of the pion form factor," Phys. Lett. B **412** (1997) 382. [arXiv:hep-ph/9707347].

[360] R. Omnés, "On The Solution Of Certain Singular Integral Equations Of Quantum Field Theory," Nuovo Cim. **8** (1958) 316.

[361] J. A. Oller, E. Oset and J. E. Palomar, "Pion and kaon vector form factors," Phys. Rev. D **63** (2001) 114009. [arXiv:hep-ph/0011096].

[362] A. Pich and J. Portolés, "The vector form factor of the pion from unitarity and analyticity: A model-independent approach," Phys. Rev. D **63** (2001) 093005. [arXiv:hep-ph/0101194].

[363] A. Pich and J. Portolés, "Vector form factor of the pion: A model-independent approach," Nucl. Phys. Proc. Suppl. **121** (2003) 179. [arXiv:hep-ph/0209224].

[364] J. F. De Trocóniz and F. J. Yndurain, "Precision determination of the pion form factor and calculation of the muon $g-2$," Phys. Rev. D **65** (2002) 093001. [arXiv:hep-ph/0106025].

[365] J. J. Sanz-Cillero and A. Pich, "Rho meson properties in the chiral theory framework," Eur. Phys. J. C **27** (2003) 587. [arXiv:hep-ph/0208199].

[366] C. Bruch, A. Khodjamirian and J. H. Kühn, "Modeling the pion and kaon form factors in the timelike region," Eur. Phys. J. C **39** (2005) 41. [arXiv:hep-ph/0409080].

[367] C. A. Domínguez, "Pion form factor in large-N_C QCD," Phys. Lett. B **512** (2001) 331 [arXiv:hep-ph/0102190].

[368] M. Benayoun, P. David, L. Del Buono, O. Leitner and H. B. O'Connell, "The Dipion Mass Spectrum In e^+e^- Annihilation and tau Decay: A Dynamical (ρ^0, ω, ϕ) Mixing Approach," Eur. Phys. J. C **55** (2008) 199 [arXiv:0711.4482 [hep-ph]].

[369] P. Masjuan, S. Peris and J. J. Sanz-Cillero, "Vector Meson Dominance as a first step in a systematic approximation: the pion vector form factor," Phys. Rev. D **78** (2008) 074028 [arXiv:0807.4893 [hep-ph]].

[370] P. Masjuan, "A Rational Approach to the Resonance Region," Nucl. Phys. Proc. Suppl. **186** (2009) 149 [arXiv:0809.2704 [hep-ph]].

[371] V. Cirigliano, G. Ecker and H. Neufeld, "Radiative tau decay and the magnetic moment of the muon," JHEP **0208** (2002) 002. [arXiv:hep-ph/0207310].

[372] F. Flores-Baez, A. Flores-Tlalpa, G. López Castro and G. Toledo Sánchez, "Long-distance radiative corrections to the di-pion tau lepton decay," Phys. Rev. D **74** (2006) 071301 [arXiv:hep-ph/0608084].

[373] R. Appel *et al.* [E865 Collaboration], "A new measurement of the properties of the rare decay $K^+ \to \pi^+ e^+ e^-$," Phys. Rev. Lett. **83** (1999) 4482. [arXiv:hep-ex/9907045].

[374] T. K. Pedlar *et al.* [*CLEO* Collaboration], "Precision measurements of the timelike electromagnetic form factors of pion, kaon, and proton," Phys. Rev. Lett. **95** (2005) 261803. [arXiv:hep-ex/0510005].

[375] B. Aubert *et al.* [*BABAR* Collaboration], "Measurement of the $\tau^- \to K^-\pi^0\nu_\tau$ branching fraction," Phys. Rev. D **76** (2007) 051104 [arXiv:0707.2922 [hep-ex]].

[376] D. Epifanov *et al.* [*Belle* Collaboration], "Study of $\tau^- \to K_S\pi^-\nu_\tau$ decay at Belle," Phys. Lett. B **654** (2007) 65 [arXiv:0706.2231 [hep-ex]].

[377] J. Lowe and M. D. Scadron, "The pion and kaon electromagnetic form factors," arXiv:hep-ph/0503100.

[378] M. Finkemeier and E. Mirkes, "Tau decays into kaons," Z. Phys. C **69** (1996) 243. [arXiv:hep-ph/9503474].

[379] M. Finkemeier and E. Mirkes, "The scalar contribution to $\tau \to K\pi\nu_\tau$," Z. Phys. C **72** (1996) 619. [arXiv:hep-ph/9601275].

[380] M. Jamin, A. Pich and J. Portolés, "Spectral distribution for the decay $\tau \to \nu_\tau$ K π," Published in Phys. Lett. B **640** (2006) 176-181. arXiv:hep-ph/0605096.

[381] M. Jamin, A. Pich and J. Portolés, "What can be learned from the *Belle* spectrum for the decay $\tau^- \to \nu_\tau K_S\pi^-$," Phys. Lett. B **664** (2008) 78. [arXiv:0803.1786 [hep-ph]].

[382] M. Jamin, J. A. Oller and A. Pich, "Order p^6 chiral couplings from the scalar $K\pi$ form factor," JHEP **0402** (2004) 047 [arXiv:hep-ph/0401080].

[383] D. R. Boito, R. Escribano and M. Jamin, "$K\pi$ vector form factor, dispersive constraints and $\tau \to \nu_\tau K\pi$ decays," Eur. Phys. J. C **59** (2009) 821 [arXiv:0807.4883 [hep-ph]].

[384] V. Bernard and E. Passemar, "Matching Chiral Perturbation Theory and the Dispersive Representation of the Scalar $K\pi$ Form Factor," Phys. Lett. B **661** (2008) 95 [arXiv:0711.3450 [hep-ph]].

[385] V. Bernard and E. Passemar, "Chiral Extrapolation of the Strangeness Changing $K\pi$ Form Factor," JHEP **1004** (2010) 001 [arXiv:0912.3792 [hep-ph]].

[386] D. R. Boito, R. Escribano and M. Jamin, "$K\pi$ vector form factor, dispersive constraints and $\tau \to \nu_\tau K\pi$ decays," Eur. Phys. J. C **59** (2009) 821 [arXiv:0807.4883 [hep-ph]].

[387] D. R. Boito, R. Escribano and M. Jamin, "$K\pi$ vector form factor constrained by $\tau \to K\pi\nu_\tau$ and $K_{\ell 3}$ decays," JHEP **1009** (2010) 031 [arXiv:1007.1858 [hep-ph]].

[388] F. Guerrero, "Extensión de χPT a energías superiores," Tesis doctoral. Universitat de Valéncia, 1998.

[389] D. M. Asner *et al.* [*CLEO* Collaboration], "Analysis of $D^0 \to K\bar{K}X$ decays," Phys. Rev. D **54** (1996) 4211.

[390] R. Barate *et al.* [*ALEPH* Collaboration], "One prong tau decays with kaons," Eur. Phys. J. C **10** (1999) 1. [arXiv:hep-ex/9903014].

[391] G. Abbiendi *et al.* [*OPAL* Collaboration], "Tau decays with neutral kaons," Eur. Phys. J. C **13** (2000) 213. [arXiv:hep-ex/9911029].

[392] Talk given by K.Hayasaka at the EPS 09 Conference in Cracow. Available at through the corresponding link at http://www.slac.stanford.edu/xorg/hfag/tau/index.html.

[393] K. Inami *et al.* [*Belle* Collaboration], "Precise measurement of hadronic tau-decays with an eta meson," Phys. Lett. B **672** (2009) 209 [arXiv:0811.0088 [hep-ex]].

[394] N. Paver and D. Treleani, "Tau Decay Into $\eta\pi$ And Abnormal Currents," Lett. Nuovo Cim. **31** (1981) 364.

[395] N. Paver and Riazuddin, "On meson dominance in the 'second class' $\tau \to \eta\pi\nu_\tau$ decay," arXiv:1005.4001 [hep-ph].

[396] C. K. Zachos and Y. Meurice, "Review of Theoretical Expectations for $\tau \to \eta\pi\nu$," Mod. Phys. Lett. A **2** (1987) 247.

[397] A. Bramon, S. Narison and A. Pich, "The $\tau \to \nu_\tau\eta\pi$ Process in and beyond QCD," Phys. Lett. B **196** (1987) 543.

[398] H. Neufeld and H. Rupertsberger, "Isospin breaking in chiral perturbation theory and the decays $\eta \to \pi\ell\nu$ and $\tau \to \eta\pi\nu$," Z. Phys. C **68** (1995) 91.

[399] G. Colangelo, M. Finkemeier, E. Mirkes and R. Urech, "Structure functions in semihadronic tau decays," Nucl. Phys. Proc. Suppl. **55C** (1997) 325. [arXiv:hep-ph/9611329].

[400] B. Aubert *et al.* [*BABAR* Collaboration], "Exclusive branching fraction measurements of semileptonic tau decays into three charged hadrons, $\tau^- \to \phi\pi^-\nu_\tau$ and $\tau^- \to \phi K^-\nu_\tau$," Phys. Rev. Lett. **100** (2008) 011801 [arXiv:0707.2981 [hep-ex]].

[401] D. M. Asner *et al.* [*CLEO* Collaboration], "Hadronic structure in the decay $\tau^- \to \nu_\tau\pi^-\pi^0\pi^0$ and the sign of the tau neutrino helicity," Phys. Rev. D **61** (2000) 012002 [arXiv:hep-ex/9902022].

[402] P. Abreu *et al.* [$DELPHI$ Collaboration], "A Study of the hadronic resonance structure in the decay $\tau \to 3\pi + \nu_\tau$," Phys. Lett. B **426** (1998) 411.

[403] K. Ackerstaff *et al.* [$OPAL$ Collaboration], "A measurement of the hadronic decay current and the ν_τ helicity in $\tau^- \to \pi^-\pi^-\pi^+\nu_\tau$," Z. Phys. C **75** (1997) 593.

[404] F. Liu, "$\tau^- \to K^+K^-\pi^-\nu_\tau$ at $CLEO - III$," Nucl. Phys. B (Proc. Suppl.) **123** (2003) 66.

[405] T. E. Coan *et al.* [$CLEO$ Collaboration], "Wess-Zumino current and the structure of the decay $\tau^- \to K^-K^+\pi^-\nu_\tau$," Phys. Rev. Lett. **92** (2004) 232001. [arXiv:hep-ex/0401005].

[406] J. E. Duboscq [$CLEO$ Collaboration], "Recent $CLEO$ results on tau hadronic decays," Nucl. Phys. Proc. Suppl. **144** (2005) 40. [arXiv:hep-ex/0412023].

[407] K. Inami *et al.* [*Belle* Collaboration], "First observation of the decay $\tau^- \to \Phi K^-\nu_\tau$," Phys. Lett. B **643** (2006) 5 [arXiv:hep-ex/0609018].

[408] Y. S. Tsai, "Decay Correlations Of Heavy Leptons In $e + e^- \to \text{Lepton}^+ \text{Lepton}^-$," Phys. Rev. D **4** (1971) 2821 [Erratum-ibid. D **13** (1976) 771].

[409] H. B. Thacker and J. J. Sakurai, "Lifetimes and branching ratios of heavy leptons," Phys. Lett. B **36** (1971) 103.

[410] F. J. Gilman and S. H. Rhie, "Calculation Of Exclusive Decay Modes Of The Tau," Phys. Rev. D **31** (1985) 1066.

[411] T. Berger, "An Effective Chiral Lagrangian Model For The Tau Decay Into Three Charged Pions," Z. Phys. C **37** (1987) 95.

[412] N. Isgur, C. Morningstar and C. Reader, "The a_1 in tau Decay," Phys. Rev. D **39** (1989) 1357.

[413] E. Braaten, R. J. Oakes and S. M. Tse, "An Effective Lagrangian Calculation of the $\pi^-\pi^0\eta$ Decay Mode of the Tau Lepton," Phys. Rev. D **36** (1987) 2188.

[414] E. Braaten, R. J. Oakes and S. M. Tse, "An Effective Lagrangian Calculation of the Semileptonic Decay Modes of the Tau Lepton," Int. J. Mod. Phys. A **5** (1990) 2737.

[415] M. Feindt, "Measuring hadronic currents and weak coupling constants in $\tau \to 3\pi\nu$," Z. Phys. C **48** (1990) 681.

[416] B. A. Li, "$U(2)_L \otimes U(2)_R$ chiral theory of mesons," Phys. Rev. D **52** (1995) 5165. [arXiv:hep-ph/9504304].

[417] B. A. Li, "$U(3)_L \otimes U(3)_R$ chiral theory of mesons," Phys. Rev. D **52** (1995) 5184. [arXiv:hep-ph/9505235].

[418] B. A. Li, "Theory of tau mesonic decays," Phys. Rev. D **55** (1997) 1436. [arXiv:hep-ph/9606402].

[419] B. A. Li, "tau mesonic decays and strong anomaly of $PCAC$," Phys. Rev. D **55** (1997) 1425. [arXiv:hep-ph/9607354].

[420] B. A. Li, "$\tau \to \eta(\eta')2\pi\nu$, $3\pi\nu$ and the WZW anomaly," Phys. Rev. D **57** (1998) 1790. [arXiv:hep-ph/9702316].

[421] S. N. Biswas, A. Goyal and J. N. Passi, "Determination Of $\tau^- \to (K\pi\pi)^-\nu_\tau$ Weak Decay Structure Functions From Current Algebra," Phys. Rev. D **22** (1980) 2915.

[422] L. Beldjoudi and T. N. Truong, "Application of current algebra in three pseudoscalar meson decays of tau lepton," Phys. Lett. B **344** (1995) 419 [arXiv:hep-ph/9411424].

[423] J. Portolés, "Exclusive hadronic tau decays in the resonance effective action of QCD," Nucl. Phys. Proc. Suppl. **98** (2001) 210. [arXiv:hep-ph/0011303].

[424] L. Girlanda and J. Stern, "The decay $\tau \to 3\pi\nu_\tau$ as a probe of the mechanism of dynamical chiral symmetry breaking," Nucl. Phys. B **575** (2000) 285. [arXiv:hep-ph/9906489].

[425] M. Vojik, P. Lichard, S. U. i. Opava and C. T. U. Prague, "Three-pion decays of the tau lepton, the $a_1(1260)$ properties, and the $a_1 - \rho - \pi$ Lagrangian," arXiv:1006.2919 [hep-ph].

[426] R. Decker, E. Mirkes, R. Sauer and Z. Was, "Tau decays into three pseudoscalar mesons," Z. Phys. C **58** (1993) 445.

[427] R. Decker and E. Mirkes, "Measuring the Wess-Zumino anomaly in tau decays," Phys. Rev. D **47** (1993) 4012. [arXiv:hep-ph/9301203].

[428] R. Decker, M. Finkemeier and E. Mirkes, "Pseudoscalar Mass Effects In Decays Of Taus With Three Pseudoscalar Mesons," Phys. Rev. D **50** (1994) 6863. [arXiv:hep-ph/9310270].

[429] P. Roig, "A proposal for improving the hadronization of QCD currents in $TAUOLA$," Nucl. Phys. Proc. Suppl. **181-182** (2008) 319. [arXiv:0810.1255 [hep-ph]].

[430] P. Roig, "Hadronic matrix elements for $TAUOLA$: 3π and $KK\pi$ channels," arXiv:0810.5764 [hep-ph].

[431] P. Roig, "Improving the Hadronization of QCD currents in $TAUOLA$ and $PHOKHARA$," Nucl. Phys. Proc. Suppl. **186** (2009) 167. [arXiv:0810.2187 [hep-ph]].

[432] P. Roig, "Hadronic tau decays into two and three meson modes within Resonance Chiral Theory," Published in XLVIII First Young Researchers Workshop 'Physics Challenges in the LHC Era' 2009 Ed. E. Nardi Frascati, May 11th and May 14th, 2009 ISBN 978-88-86409-57-5. Also in *Frascati 2009, Physics challenges in the LHC era* 19-24. arXiv:0907.5540 [hep-ph].

[433] S. Jadach and Z. Was, "$KORALB$ version 2.1: An Upgrade with $TAUOLA$ library of tau decays," Comput. Phys. Commun. **64** (1991) 267.

[434] S. Jadach, J. H. Kühn and Z. Was, "$TAUOLA$: A Library of Monte Carlo programs to simulate decays of polarized tau leptons," Comput. Phys. Commun. **64** (1990) 275.

[435] M. Jezabek, Z. Was, S. Jadach and J. H. Kuhn, "The tau decay library $TAUOLA$, update with exact $\mathcal{O}(\alpha)$ QED corrections in $\tau \to \mu(e)\nu\bar{n}u$ decay modes," Comput. Phys. Commun. **70** (1992) 69.

[436] S. Jadach, Z. Was, R. Decker and J. H. Kühn, "The tau decay library $TAUOLA$: Version 2.4," Comput. Phys. Commun. **76** (1993) 361.

[437] P. Golonka, B. Kersevan, T. Pierzchala, E. Richter-Was, Z. Was and M. Worek, "The tauola-photos-F environment for the $TAUOLA$ and $PHOTOS$ packages, release II," Comput. Phys. Commun. **174** (2006) 818 [arXiv:hep-ph/0312240].

[438] A. E. Bondar, S. I. Eidelman, A. I. Milstein, T. Pierzchala, N. I. Root, Z. Was and M. Worek, "Novosibirsk hadronic currents for $\tau \to 4\pi$ channels of tau decay library $TAUOLA$," Comput. Phys. Commun. **146** (2002) 139 [arXiv:hep-ph/0201149].

[439] Work in progress with O. Shekhovtsova and Z. Was

[440] J. J. Gómez-Cadenas, M. C. González-García and A. Pich, "The Decay $\tau^- \to K^- K^+ \pi^-$ And The Tau-Neutrino Mass," Phys. Rev. D **42** (1990) 3093.

[441] G. Kramer and W. F. Palmer, "A Chiral Anomaly Channel In Tau Decay," Z. Phys. C **25** (1984) 195.

[442] G. Kramer and W. F. Palmer, "A chiral anomaly channel in Tau channel. 2," Z. Phys. C **39** (1988) 423.

[443] R. Decker, M. Finkemeier, P. Heiliger and H. H. Jonsson, "Tau decays into four pions," Z. Phys. C **70** (1996) 247 [arXiv:hep-ph/9410260].

[444] J. H. Kühn, "The tau lepton: Particle physics in a nutshell," Nucl. Phys. Proc. Suppl. **76** (1999) 21 [arXiv:hep-ph/9812399].

[445] H. Czyz and J. H. Kühn, "Four Pion Final States with Tagged Photons at Electron Positron Colliders," Eur. Phys. J. C **18** (2001) 497 [arXiv:hep-ph/0008262].

[446] A. Rougé, "Isospin and the tau hadronic decay modes," Z. Phys. C **70** (1996) 65.

[447] A. Rougé, "Isospin constraints on the $\tau \to K\bar{K}(n)\pi\nu_\tau$ decay mode," Eur. Phys. J. C **4** (1998) 265. [arXiv:hep-ph/9708473].

[448] J. H. Kühn and Z. Was, "tau decays to five mesons in $TAUOLA$," Acta Phys. Polon. B **39** (2008) 147 [arXiv:hep-ph/0602162].

[449] D. Buskulic *et al.* [$ALEPH$ Collaboration], "A study of tau decays involving eta and omega mesons," Z. Phys. C **74** (1997) 263.

[450] K. W. Edwards *et al.* [$CLEO$ Collaboration], "Resonant structure of $\tau \to 3\pi\pi^0\nu_\tau$ and $\tau \to \omega\pi\nu_\tau$ decays," Phys. Rev. D **61** (2000) 072003 [arXiv:hep-ex/9908024].

[451] K. Arms *et al.* [$CLEO$ Collaboration], "Study of tau decays to four-hadron final states with kaons," Phys. Rev. Lett. **94** (2005) 241802. [arXiv:hep-ex/0501042].

[452] B. Aubert *et al.* [$BaBar$ Collaboration], "Measurement of the $\tau^- \to \eta\pi^-\pi\pi^-\nu_{tau}$ Branching Fraction and a Search for a Second-Class Current in the $\tau^- \to \eta'(958)\ \pi^-\nu_{tau}$ Decay," Phys. Rev. D **77** (2008) 112002 [arXiv:0803.0772 [hep-ex]].

[453] I. Adachi *et al.* [$BelleCollaboration$], "Precise measurement of Br($\tau^- \to K^{*0}(892)K^-\nu_\tau$) and the mass and width of the $K^{*0}(892)$ meson," arXiv:0808.1059 [hep-ex].

[454] B. Aubert *et al.* [the $BABAR$ Collaboration], "Study of the $\tau^- \to 3h^-2h^+\nu_\tau$ decay," Phys. Rev. D **72** (2005) 072001 [arXiv:hep-ex/0505004].

[455] D. Gibaut *et al.* [$CLEO$ Collaboration], "Study of the five charged pion decay of the tau lepton," Phys. Rev. Lett. **73** (1994) 934.

[456] A. Anastassov *et al.* [$CLEO$ Collaboration], "Study of tau decays to six pions and neutrino," Phys. Rev. Lett. **86** (2001) 4467 [arXiv:hep-ex/0010025].

[457] R. J. Sobie, "Branching ratios of multi-pion tau decays," Phys. Rev. D **60** (1999) 017301.

[458] G. Aad *et al.* [$ATLAS$ Collaboration], "The $ATLAS$ Experiment at the CERN Large Hadron Collider," JINST **3** (2008) S08003.

[459] G. L. Bayatian *et al.* [CMS Collaboration], "CMS technical design report, volume II: Physics performance," J. Phys. G **34** (2007) 995.

[460] R. Barate *et al.* [LEP Working Group for Higgs boson searches and $ALEPH$ Collaboration and], "Search for the standard model Higgs boson at LEP," Phys. Lett. B **565** (2003) 61 [arXiv:hep-ex/0306033].

[461] [CDF Collaboration and $D0$ Collaboration], "Combined CDF and $DZero$ Upper Limits on Standard Model Higgs-Boson Production with up to 4.2 fb$^-$1 of Data," arXiv:0903.4001 [hep-ex].

[462] C. Quigg, "Unanswered Questions in the Electroweak Theory," Ann. Rev. Nucl. Part. Sci. **59** (2009) 505 [arXiv:0905.3187 [hep-ph]].

[463] T. Plehn, D. L. Rainwater and D. Zeppenfeld, "Determining the structure of Higgs couplings at the LHC," Phys. Rev. Lett. **88** (2002) 051801 [arXiv:hep-ph/0105325].

[464] M. Duhrssen, S. Heinemeyer, H. Logan, D. Rainwater, G. Weiglein and D. Zeppenfeld, "Extracting Higgs boson couplings from LHC data," Phys. Rev. D **70** (2004) 113009 [arXiv:hep-ph/0406323].

[465] C. Ruwiedel, N. Wermes and M. Schumacher, "Prospects for the measurement of the structure of the coupling of a Higgs boson to weak gauge bosons in weak boson fusion with the $ATLAS$ detector," Eur. Phys. J. C **51** (2007) 385.

[466] G. Aad *et al.* [The $ATLAS$ Collaboration], "Expected Performance of the $ATLAS$ Experiment - Detector, Trigger and Physics," arXiv:0901.0512 [hep-ex].

[467] E. Richter-Was [$ATLAS$ Collaboration], "Prospect for the Higgs searches with the $ATLAS$ detector," Acta Phys. Polon. B **40** (2009) 1909 [arXiv:0903.4198 [hep-ex]].

[468] J. D'Hondt [CMS Collaboration], "Potential of standard model measurements with CMS," PoS **HEP2005** (2006) 295.

[469] T. Sjostrand, S. Mrenna and P. Z. Skands, "$PYTHIA$ 6.4 Physics and Manual," JHEP **0605** (2006) 026 [arXiv:hep-ph/0603175].

[470] N. Davidson, P. Golonka, T. Przedzinski and Z. Was, "MC-TESTER v. 1.23: a universal tool for comparisons of Monte Carlo predictions for particle decays in high energy physics," arXiv:0812.3215 [hep-ph].

[471] N. Davidson, G. Nanava, T. Przedzinski, E. Richter-Was and Z. Was, "Universal Interface of TAUOLA Technical and Physics Documentation," arXiv:1002.0543 [hep-ph].

[472] K. A. Assamagan and Y. Coadou, "The hadronic tau decay of a heavy $H^\pm$ in $ATLAS$," Acta Phys. Polon. B **33** (2002) 707.

[473] K. A. Assamagan and A. Deandrea, "The hadronic tau decay of a heavy charged Higgs in models with singlet neutrino in large extra dimensions," Phys. Rev. D **65** (2002) 076006 [arXiv:hep-ph/0111256].

[474] T. Pierzchala, E. Richter-Was, Z. Was and M. Worek, "Spin effects in tau-lepton pair production at LHC," Acta Phys. Polon. B **32** (2001) 1277 [arXiv:hep-ph/0101311].

[475] G. R. Bower, T. Pierzchala, Z. Was and M. Worek, "Measuring the Higgs boson's parity using $\tau \to \rho\nu_\tau$," Phys. Lett. B **543** (2002) 227 [arXiv:hep-ph/0204292].

[476] K. Desch, A. Imhof, Z. Was and M. Worek, "Probing the CP nature of the Higgs boson at linear colliders with tau spin correlations: The case of mixed scalar-pseudoscalar couplings," Phys. Lett. B **579** (2004) 157 [arXiv:hep-ph/0307331].

[477] E. Richter-Was and T. Szymocha, "Hadronic τ identification with track based approach: the $Z \to \tau\tau$, $W \to \tau\nu_\tau$ and dijet events from $DC1$ data samples," $ATLAS$ Note ATL-PHYS-PUB-2005-005, http://cdsweb.cern.ch/record/813002.

[478] M. Heldmann and D. Cavalli, "An improved τ-identification for the $ATLAS$ experiment," $ATLAS$ Note ATL-PHYS-PUB-2006-008, http://cdsweb.cern.ch/record/923980.

[479] D. L. Rainwater, D. Zeppenfeld and K. Hagiwara, "Searching for $H \to \tau\tau$ in weak boson fusion at the LHC," Phys. Rev. D **59** (1999) 014037 [arXiv:hep-ph/9808468].

[480] S. Asai *et al.*, "Prospects for the search for a standard model Higgs boson in $ATLAS$ using vector boson fusion," Eur. Phys. J. C **32S2** (2004) 19 [arXiv:hep-ph/0402254].

[481] S. Abdullin *et al.* [CMS Collaboration], "Discovery potential for supersymmetry in CMS," J. Phys. G **28** (2002) 469 [arXiv:hep-ph/9806366].

[482] M. S. Carena, S. Heinemeyer, C. E. M. Wagner and G. Weiglein, "Suggestions for benchmark scenarios for $MSSM$ Higgs boson searches at hadron colliders," Eur. Phys. J. C **26** (2003) 601 [arXiv:hep-ph/0202167].

[483] M. Schumacher, "Investigation of the discovery potential for Higgs bosons of the minimal supersymmetric extension of the standard model ($MSSM$) with $ATLAS$," arXiv:hep-ph/0410112.

[484] M. Jamin, J. A. Oller and A. Pich, "S-wave $K\pi$ scattering in chiral perturbation theory with resonances," Nucl. Phys. B **587** (2000) 331 [arXiv:hep-ph/0006045].

[485] P. Buettiker, S. Descotes-Genon and B. Moussallam, "A re-analysis of πK scattering à la Roy and Steiner," Eur. Phys. J. C **33** (2004) 409 [arXiv:hep-ph/0310283].

[486] S. Descotes-Genon and B. Moussallam, "The $K^{0*}(800)$ scalar resonance from Roy-Steiner representations of πK scattering," Eur. Phys. J. C **48** (2006) 553 [arXiv:hep-ph/0607133].

[487] V. Cirigliano, G. Ecker, H. Neufeld and A. Pich, "Meson resonances, large N_C and chiral symmetry," JHEP **0306** (2003) 012 [arXiv:hep-ph/0305311].

[488] G. Amorós, S. Noguera and J. Portolés, "Semileptonic decays of charmed mesons in the effective action of QCD," Eur. Phys. J. C **27** (2003) 243. [arXiv:hep-ph/0109169].

[489] S. Wolfram *et al.*, Version Number 7.1.0, © 1988-2010 Wolfram Research, Inc. [http:\\www.wolfram.com].

[490] F. J. Gilman, "TAU DECAYS INVOLVING THE ETA MESON," Phys. Rev. D **35** (1987) 3541.

[491] D. Gómez Dumm, A. Pich and J. Portolés, "The hadronic off-shell width of meson resonances," Phys. Rev. D **62** (2000) 054014. [arXiv:hep-ph/0003320].

[492] N. N. Achasov and A. A. Kozhevnikov, "Confronting generalized hidden local symmetry chiral model with the $ALEPH$ data on the decay $\tau^- \to \pi^+\pi^-\pi^-\nu_\tau$," arXiv:1005.0720 [hep-ph].

[493] H. Albrecht *et al.* [$ARGUS$ Collaboration], "Measurement of tau Decays Into Three Charged Pions," Z. Phys. C **33** (1986) 7.

[494] T. E. Browder *et al.* [$CLEO$ Collaboration], "Structure functions in the decay $\tau^\mp \to pi^\mp pi^0 pi^0 \nu_\tau$," Phys. Rev. D **61** (2000) 052004 [arXiv:hep-ex/9908030].

[495] L. Xiong, E. V. Shuryak and G. E. Brown, "Photon production through A1 resonance in high-energy heavy ion collisions," Phys. Rev. D **46** (1992) 3798 [arXiv:hep-ph/9208206].

[496] C. Song, "Photon emission from hot hadronic matter described by an effective chiral Lagrangian," Phys. Rev. C **47** (1993) 2861.

[497] C. Song, C. M. Ko and C. Gale, "Role Of The A1 Meson In Dilepton Production From Hot Hadronic Matter," Phys. Rev. D **50** (1994) 1827 [arXiv:nucl-th/9401011].

[498] K. Haglin, "Photons from axial vector radiative decay in a hadron gas," Phys. Rev. C **50** (1994) 1688 [arXiv:nucl-th/9406026].

[499] J. K. Kim, P. Ko, K. Y. Lee and S. Rudaz, "$a_1(1260)$ contribution to photon and dilepton productions from hot hadronic matter : Revisited," Phys. Rev. D **53** (1996) 4787 [arXiv:hep-ph/9602293].

[500] S. Gao and C. Gale, "Off-shell effects in dilepton production from hot interacting mesons," Phys. Rev. C **57** (1998) 254 [arXiv:nucl-th/9711006].

[501] S. Turbide, R. Rapp and C. Gale, "Hadronic production of thermal photons," Phys. Rev. C **69** (2004) 014903 [arXiv:hep-ph/0308085].

[502] P. Golonka, E. Richter-Was and Z. Was, "The tauola-photos-F environment for versioning the $TAUOLA$ and $PHOTOS$ packages," arXiv:hep-ph/0009302.

[503] P. Golonka, B. Kersevan, T. Pierzchala, E. Richter-Was, Z. Was and M. Worek, "The tauola-photos-F environment for the $TAUOLA$ and $PHOTOS$ packages, release II," Comput. Phys. Commun. **174** (2006) 818 [arXiv:hep-ph/0312240].

[504] N. Davidson, G. Nanava, T. Przedzinski, E. Richter-Was and Z. Was, "Universal Interface of $TAUOLA$ Technical and Physics Documentation," arXiv:1002.0543 [hep-ph].

[505] T. Gleisberg, S. Hoche, F. Krauss, A. Schalicke, S. Schumann and J. C. Winter, "SHERPA 1.alpha, a proof-of-concept version," JHEP **0402** (2004) 056 [arXiv:hep-ph/0311263].

[506] T. Laubrich, "Implementation of τ-lepton Decays into the Event-Generator $SHERPA$," Diplomarbeit zur Erlangung des akademischen Grades. Diplom-Physiker. Institut für Theoretische Physik. Technische Universitt Dresden.

[507] B. Aubert *et al.* [*BaBar* Collaboration], "Measurements of $e^+e^- \to K^+K^-\eta$, $K^+K^-\pi^0$ and $K^0_sK^\pm\pi^\mp$ cross- sections using initial state radiation events," Phys. Rev. D **77** (2008) 092002 [arXiv:0710.4451 [hep-ex]].

[508] P. Roig, "Hadronization in $\tau \to KK\pi\nu_\tau$ decays," Proceedings of 43rd Rencontres de Moriond on QCD and High Energy Interactions, La Thuile, Italy, 8-15 Mar 2008. arXiv:0809.4977 [hep-ph].

[509] P. Roig, "Hadronization in three meson channels at τ decays and e^+e^- cross-section," Proceedings of Science PoS (EFT09) 056. arXiv:0907.5101 [hep-ph].

[510] F. James and M. Roos, "Minuit: A System For Function Minimization And Analysis Of The Parameter Errors And Correlations," Comput. Phys. Commun. **10** (1975) 343.

[511] M. Finkemeier, J. H. Kuhn and E. Mirkes, "Theoretical aspects of $\tau \to Kh(h)\nu_\tau$ decays and experimental comparisons," Nucl. Phys. Proc. Suppl. **55C** (1997) 169 [arXiv:hep-ph/9612255].

[512] M. J. Lee for the *Belle* Collaboration, "Study of the hadronic three-prong decays of the tau lepton in the Belle experiment," To appear in the Proceedings of the Conference TAU 10. To be published in Nucl. Phys. Proc. Suppl.

[513] I. Adachi *et al.* [*Belle* Collaboration], "Study of the $tau^- \to K^- pi^+ pi^- nu_t au$ decay," arXiv:0812.0480 [hep-ex].

[514] P. Roig, "$\tau^- \to \eta\pi^-\pi^0\nu_\tau$ and $\sigma(e^+e^- \to \eta\pi^+\pi^-)$ at low energies," arXiv:1010.0224 [hep-ph]. D. G. Dumm, P. Roig and A. Pich, to appear.

[515] A. Bramon and M. D. Scadron, "Pseudoscalar $\eta-\eta'$ Mixing And $SU(3)$ Breaking," Phys. Lett. B **234** (1990) 346.

[516] A. Bramon, R. Escribano and M. D. Scadron, "Mixing of $\eta - \eta'$ mesons in J/Ψ decays into a vector and a pseudoscalar meson," Phys. Lett. B **403** (1997) 339. [arXiv:hep-ph/9703313].

[517] A. Bramon, R. Escribano and M. D. Scadron, "The $\eta - \eta'$ mixing angle revisited," Eur. Phys. J. C **7** (1999) 271. [arXiv:hep-ph/9711229].

[518] A. Bramon, R. Escribano and M. D. Scadron, "Radiative $V \to P\gamma$ transitions and $\eta - \eta'$ mixing," Phys. Lett. B **503** (2001) 271. [arXiv:hep-ph/0012049].

[519] R. Escribano and J. M. Frere, "Study of the $\eta - \eta'$ system in the two mixing angle scheme," JHEP **0506** (2005) 029 [arXiv:hep-ph/0501072].

[520] S. I. Eidelman and V. N. Ivanchenko, Phys. Lett. B **257** (1991) 437.

[521] V. A. Cherepanov and S. I. Eidelman, JETP Lett. **89** (2009) 429 [Pisma Zh. Eksp. Teor. Fiz. **89** (2009) 515].

[522] B. Delcourt, D. Bisello, J. C. Bizot, J. Buon, A. Cordier and F. Mane, Phys. Lett. B **113** (1982) 93 [Erratum-ibid. B **115** (1982) 503].

[523] V. P. Druzhinin *et al.*, Phys. Lett. B **174** (1986) 115.

[524] A. Antonelli *et al.* [DM2 Collaboration], Phys. Lett. B **212** (1988) 133.

[525] R. R. Akhmetshin *et al.* [CMD-2 Collaboration], Phys. Lett. B **489** (2000) 125 [arXiv:hep-ex/0009013].

[526] B. Aubert *et al.* [BABAR Collaboration], Phys. Rev. D **76** (2007) 092005 [Erratum-ibid. D **77** (2008) 119902] [arXiv:0708.2461 [hep-ex]].

[527] J. J. Sanz-Cillero, "Pion and kaon decay constants: Lattice vs. resonance chiral theory," Phys. Rev. D **70** (2004) 094033 [arXiv:hep-ph/0408080].

[528] M. Suzuki, "Strange axial-vector mesons," Phys. Rev. D **47** (1993) 1252.

[529] Z. H. Guo, "Study of $\tau^- \to VP^-\nu_\tau$ in the framework of resonance chiral theory," Phys. Rev. D **78** (2008) 033004 [arXiv:0806.4322 [hep-ph]].

[530] Z. H. Guo, J. J. Sanz Cillero and H. Q. Zheng, "Partial waves and large N_C resonance sum rules," JHEP **0706** (2007) 030 [arXiv:hep-ph/0701232].

[531] H. Y. Cheng, "Hadronic charmed meson decays involving axial vector mesons," Phys. Rev. D **67** (2003) 094007 [arXiv:hep-ph/0301198].

[532] H. Y. Cheng and K. C. Yang, "Hadronic charmless B decays $B \to AP$," Phys. Rev. D **76** (2007) 114020 [arXiv:0709.0137 [hep-ph]].

[533] T. Kinoshita, "Mass Singularities Of Feynman Amplitudes," J. Math. Phys. **3** (1962) 650.

[534] M. E. Peskin and D. V. Schroeder, "An Introduction To Quantum Field Theory," SPIRES entry *Reading, USA: Addison-Wesley (1995) 842 p.*

[535] D. Becirevic, B. Haas and E. Kou, Phys. Lett. B **681** (2009) 257

[536] K. Ikado *et al.* [*Belle* Collaboration], "Evidence of the purely leptonic decay $B^- \to \tau^- \bar{\nu}_\tau$," Phys. Rev. Lett. **97** (2006) 251802 [arXiv:hep-ex/0604018].

[537] B. Aubert *et al.* [*BABAR* Collaboration], "A Search for $B^+ \to \tau^+\nu_\tau$," Phys. Rev. D **76** (2007) 052002 [arXiv:0705.1820 [hep-ex]].

[538] B. Aubert *et al.* [*BABAR* Collaboration], "A Search for $B^+ \to \tau^+\nu_\tau$ with Hadronic B tags," Phys. Rev. D **77** (2008) 011107 [arXiv:0708.2260 [hep-ex]].

[539] A. Sirlin, "Large M_W, M_Z Behavior Of The $\mathcal{O}(\alpha)$ Corrections To Semileptonic Processes Mediated By W," Nucl. Phys. B **196**, 83 (1982).

[540] W. J. Marciano and A. Sirlin, "Radiative corrections to $\pi_{\ell 2}$ decays," Phys. Rev. Lett. **71** (1993) 3629.

[541] V. Cirigliano and I. Rosell, "Two-loop effective theory analysis of $\pi(K) \to e\bar{\nu}_e[\gamma]$ branching ratios," Phys. Rev. Lett. **99** (2007) 231801.

[542] V. Cirigliano and I. Rosell, "$\pi/K \to e\nu_e$ branching ratios to $\mathcal{O}(e^2p^4)$ in Chiral Perturbation Theory," JHEP **0710** (2007) 005.

[543] G. Rodrigo, H. Czyz, J. H. Kühn and M. Szopa, "Radiative return at *NLO* and the measurement of the hadronic cross-section in electron positron annihilation," Eur. Phys. J. C **24** (2002) 71 [arXiv:hep-ph/0112184].

[544] H. Czyz, A. Grzelinska, J. H. Kühn and G. Rodrigo, "Electron positron annihilation into three pions and the radiative return," Eur. Phys. J. C **47** (2006) 617 [arXiv:hep-ph/0512180].

[545] H. Czyz, J. H. Kühn and A. Wapienik, "Four-pion production in τ decays and e^+e^- annihilation: an update," Phys. Rev. D **77** (2008) 114005 [arXiv:0804.0359 [hep-ph]].

[546] H. Czyz, S. Eidelman, A. Grzelinska, $e^+e^- \to \eta\pi^+\pi^-$ in $PHOKHARA$. Work in progress. Private communication.

[547] K. Hayasaka, H. Hayashii. Private communication.

[548] E. Kyriakopoulos, "Vector-Meson Interaction Hamiltonian," Phys. Rev. **183** (1969) 1318.

[549] Y. Takahashi and R. Palmer, "Gauge-Independent Formulation Of A Massive Field With Spin One," Phys. Rev. D **1** (1970) 2974.

[550] A. Z. Capri, S. Kamefuchi and M. Kobayashi, "Lagrangians For Massive Totally Antisymmetric Tensor Fields," Prog. Theor. Phys. **74** (1985) 368.

[551] A. Z. Capri, M. Kobayashi and Y. Ohnuki, "THE SECOND RANK TENSOR FIELD, A SYSTEMATIC STUDY: CLASSIFICATION OF THE SECOND RANK TENSOR FIELD THEORIES," Prog. Theor. Phys. **77** (1987) 1484.

[552] U. G. Meissner, "Low-energy hadron physics from effective chiral lagrangians with vector mesons," Phys. Rep. **161** (1988) 213-362.

[553] J. F. Donoghue, C. Ramírez and G. Valencia, "Spectrum of QCD and chiral lagrangian of the strong and weak interactions," Phys. Rev. D **39,7** (1989) 1947-1955.

[554] M. Bando, T. Kugo, S. Uehara, K. Yamawaki and T. Yanagida, "Is Rho Meson A Dynamical Gauge Boson Of Hidden Local Symmetry?," Phys. Rev. Lett. **54** (1985) 1215.

[555] T. Fujiwara, T. Kugo, H. Terao, S. Uehara and K. Yamawaki, "Nonabelian Anomaly And Vector Mesons As Dynamical Gauge Bosons Of Hidden Local Symmetries," Prog. Theor. Phys. **73** (1985) 926.

[556] M. Bando, T. Kugo and K. Yamawaki, "On The Vector Mesons As Dynamical Gauge Bosons Of Hidden Local Symmetries," Nucl. Phys. B **259** (1985) 493.

[557] M. Bando, T. Kugo and K. Yamawaki, "Nonlinear Realization And Hidden Local Symmetries," Phys. Rept. **164** (1988) 217.

[558] M. Harada and K. Yamawaki, "Hidden local symmetry at one loop," Phys. Lett. B **297** (1992) 151 [arXiv:hep-ph/9210208].

[559] M. Harada and K. Yamawaki, "Hidden local symmetry at loop: A new perspective of composite gauge boson and chiral phase transition," Phys. Rept. **381** (2003) 1. [arXiv:hep-ph/0302103].

[560] H. Georgi, "Lie Algebras in Particle Physics," Perseus Books (1999).

[561] H. J. Lipkin, "Triality, Exotics And The Dynamical Basis Of The Quark Model," Phys. Lett. B **45** (1973) 267.

[562] S. R. Coleman and E. Witten, "Chiral Symmetry Breakdown In Large N Chromodynamics," Phys. Rev. Lett. **45** (1980) 100.

[563] C. Rosenzweig, J. Schechter and C. G. Trahern, "Is The Effective Lagrangian For QCD A Sigma Model?," Phys. Rev. D **21**, 3388 (1980).

[564] K. Kawarabayashi and N. Ohta, "The Problem Of Eta In The Large N Limit: Effective Lagrangian Approach," Nucl. Phys. B **175**, 477 (1980).

[565] P. Di Vecchia, F. Nicodemi, R. Pettorino and G. Veneziano, "Large N, Chiral Approach To Pseudoscalar Masses, Mixings And Decays," Nucl. Phys. B **181**, 318 (1981).

[566] P. Herrera-Siklody, J. I. Latorre, P. Pascual and J. Tarón, "Chiral effective Lagrangian in the large-N_C limit: The nonet case," Nucl. Phys. B **497** (1997) 345 [arXiv:hep-ph/9610549].

[567] P. Herrera-Siklody, "Matching of $U(3)_L \otimes U(3)_R$ and $SU(3)_L \otimes SU(3)_R$ chiral perturbation theories," Phys. Lett. B **442** (1998) 359 [arXiv:hep-ph/9808218].

[568] M. F. L. Golterman and S. Peris, "The 7/11 rule: An estimate of M_ρ/F_π," Phys. Rev. D **61** (2000) 034018 [arXiv:hep-ph/9908252].

[569] S. L. Adler, J. C. Collins and A. Duncan, "Energy-Momentum-Tensor Trace Anomaly In Spin 1/2 Quantum Electrodynamics," Phys. Rev. D **15** (1977) 1712.

[570] S. Peris and E. de Rafael, "On the large N_C behavior of the L_7 coupling in χPT," Phys. Lett. B **348** (1995) 539 [arXiv:hep-ph/9412343].

[571] P. Herrera-Siklody, J. I. Latorre, P. Pascual and J. Taron, "$\eta - \eta'$ mixing from $U(3)_L \otimes U(3)_R$ chiral perturbation theory," Phys. Lett. B **419** (1998) 326 [arXiv:hep-ph/9710268].

[572] P. Herrera-Siklody, "η and η' hadronic decays in $U(3)_L \otimes U(3)_R$ chiral perturbation theory," arXiv:hep-ph/9902446.

Acknowledgements

Llega el momento más deseado de la escritura de la Tesis, en el que no quedan ni siquiera pequeos retoques y uno se decide a escribir por fin los agradecimientos y dejar caer el punto y final.

Vull agrair-li a Jorge Portolés, el director d'aquesta Tesi, el haver pogut treballar amb ell aquestos anys, en un tema que des del començament m'ha semblat molt interessant (percepció que s'ha anat afiançant amb el temps). Agraix de la seua direcció que estimulara la meua independència i que en les discussions mai no em donara la raó fins no estar totalment segur si la tenia (aspecte on hi ha hagut sana reciprocitat, val a dir-ho). Sense la seua revisió aquesta Tesi contindria infinitament més errates de les que hagen pogut quedar després del seu esforçat recorregut sobre un document que –cal reconèixer-lo– ha eixit un pèl llarg. Li done també les gràcies per haver-me donat llibertat per emprendre altres projectes durant aquesta Tesi i molt especialment, que sempre haja estat disposat a donar un bon consell i a ajudar-me.

A Toni Pich, el meu tutor, li dec la entrada al grup d'investigació PARSIFAL, primer que res. Les excepcionals classes, seues i de Jorge, de Teoria Quàntica de Camps van ser un motiu de pes per entrar a aquest grup, eren un autèntic desperta-vocacions, des del meu punt de vista. Li agraïsc també que m'haja guiat en algunes decissions difícils, sobre les estades finals de la Tesi i que sempre haja tingut un moment, malgrat tots els seus compromisos, per les cosses importants. Tant a Toni com a Jorge els hi dec el haver-me donat suport a l'hora d'encetar projectes i col-laboracions internacionals que han de resultar molt profitosos.

A Daniel Gómez Dumm le agradezco su colaboración a lo largo de estos años. Fue un placer. Especial mención requiere su revisión del apéndice sobre relaciones de isospín y gran parte del material del capítulo octavo y por supuesto todo su esfuerzo para entender qué aproximaciones hacían los experimentales (y cuáles nosotros) al aplicar CVC en los canales $KK\pi$.

I thank Zhi-Hui Guo for the collaboration giving rise to the material included in chapter nine of this Thesis. I do not expect that many people understand this, but I remember how great it was to achieve very accurate agreement in the numerics while sitting on the floor in a corridor outside the last Flavianet meeting (of course during a coffee break).

I wish to thank Nora Brambilla and Antonio Vairo, whom I have visited in two different long periods. One while in Milano and the other one in München. We also enjoyed time of collaboration in Valencia, where they came for some time as well.

Our study of the lineshape in $J/\Psi \to \gamma\eta_c$ revealed as very interesting and offer me the oportunity to learn a lot about radiative transitions of Quarkonia.

I would like to thank Sébastien Descotes-Genon for his time and interest in our study of duality violations in tau decays and e^+e^- annihilation into hadrons while I was in Orsay, from which I have learnt a lot.

I have been enjoying the collaboration with Olga Shekhovtsova and Zbigniew Was for two years. I am happy with the results that we are obtaining and I hope that the project can extend for long since we will need it in order to complete a global description of the most important tau decay channels in TAUOLA.

It is a pleasure to thank Simon Eidelman for useful discussions and comments that made me learn a lot and for his help in accessing data and understanding its suitable interpretation (which was always the most difficult part).

Two years and a half ago I became member of the Working Group on Monte Carlo Generators and Radiative Corrections for Low-Energy Physics and since the first meeting I have felt like in a family (one of those in which peaceful harmony reins, I mean). I thank all more faith participants for the interesting and participative discussions that were held and especially the WG convenors Henryk Czyz, Guido Montagna and Graziano Venanzoni for their always kind invitation to attend every meeting (despite the icelandic volcano) and Germán Rodrigo, who helped my adaptation at the beginning.

I want to thank some people in PARSIFAL: Vicent Mateu, con el que compartí despacho tres años y con el que extraamente nunca llegué a hablar en Valenciano pues a las pocas palabras saltábamos inevitablemente al castellano. Con él sostuve muchísimas discusiones muy interesantes en ese tiempo. También agradezco las discusiones con otro ex-miembros del grupo: Pedro Ruiz Femenía, Juanjo Sanz Cillero y Natxo Rosell. Con todos ellos he tenido la ocasión de seguir debatiendo diversas cuestiones de Teorías Quiral, de Resonancias y de QCD no relativistas a lo largo de los años. I remember with gratitude all the efforts Frédéric Jugeau made in order to help me prepare my first presentation in front of the group.

I also ackowledge the following researchers by useful advices and illuminating conversations at different conferences: Bogdan Malaescu, Ximo Prades -God rest his soul-, Matthias Jamin, Gabriel López Castro, Kim Maltman, Hisaki Hayashii, Alberto Lusiani, George Lafferty, Michel Davier, Kenji Inami, Rafel Escribano, Jaroslav Trnka, Hans Kühn, Maurice Benayoun, Bachir Moussallam, Gerard Ecker, Heiri Leutwyler, Eduardo de Rafael, Santi Peris, Joan Soto, Antonio Pineda, Gino Isidori, Jimmy MacNaughton, Kiyoshi Hayasaka, Ryan Mitchell, Yu Jia, Miguel Ángel Sanchís, Damir Becirevic, T. N. Pham, Stefan Narison, Wolfram Weiβe and Roland Kaiser.

Hay muchas otra gente a la que quiero agradecer su presencia a mi lado a lo largo de este periplo, creo que a todos les debo alguna ayuda inestimable o conversación valiosa (probablemente más de una en cada caso): Miguel Nebot, Patricia Aguar, Josep Canet, Emma Torró, Mercedes Miñano, Loli Jordán, Neus López, Joan Català, Carlos Escobar, Paco Salesa, María Moreno, Avelino Vicente, Alberto Aparici, Pere Masjuan, Oscar Catá, Francisco Flores, Miguel Ángel Escobedo, Max

Stahlhofen, Xavier Garcia i Tormo, Emilie Passemar, Fabio Bernardoni, Alberto Filipuzzi, Paula Tuzón, David Greynat, David Palao, Alfredo Vega, Pancho Molina, Joel Jones, Jacopo Ghiglieri, Guillaume Toucas, Pablo Arnalte, José Cuenca, Pepe Ródenas, David Ruano, Juan Carlos Algaba, Javier Ors, Brian Martínez, Sergio Fernández, Carlos Navarrete, Julia Garayoa, Iván Agulló, Jacobo Díaz, Enrique Fernández, Ana Cámara, Elena Fernández, Antonio Lorenzo, Ginés Pérez, Lorena Marset, Beatriz Sarrià, Guillermo Ríos, Rubén García, José Miguel No y Dani Peña (a ellos tres no voy a incluirlos después en el apartado dedicado al Colegio de España, para evitar double counting), Diogo Boito, Alberto Ramos, Jorge Mondéjar, Xian-Wei Kang, Yoko Usuki, Ian Nugent, Anna Vinokurova, Tomasz Przedzinski, Houssine El-Mezoir y Thomas Laubrich.

Agradezco también a Carlos Martínez que resucitara mi portátil en un par ocasiones para evitar pérdida de documentos y que consiguiera hacer funcionar el cañón del proyector tras un fallo inesperado previo a la presentación de mi Tesina. También le doy las gracias a Lauren por revivir mi portátil la última vez, con una quinta parte de la Tesis dentro y sin copias de seguridad hechas.

Agradezco mi buena formación a los Profesores del Colegio Salesiano San Juan Bosco de la Avenida de la Plata y a los del Instituto Extensión del San Vicente Ferrer (actual Blasco Ibáñez). Muy especialmente a los buenos profesores que he tenido en la carrera (sin repetir nombres ya mencionados) que supieron recuperar mi interés después de un inicio muy rutinario y aburrido: José Bernabéu, Benito Gimeno, José Adolfo de Azcárraga, José Navarro Salas (con quien disfruté una beca de introducción a la investigación), Nuria Rius y Arcadi Santamaría. A Günter Werth y Alexandros Drakoudis, con quienes tuve mi primera experiencia de iniciación a la investigación, en Mainz, a nuestros *monis* entonces, a toda la gente querida que se quedó por allí, por Milán, por Munich y por Orsay.

Por supuesto una parte importante de mis agradecimientos van para quienes no tienen nada que ver con la Física (más allá de lo que les haya salpicado indirectamente por conocerme). Lo primero agradecerle a mi madre (y a mi abuela, que en paz descanse) la buena educación que me dieron. Nada marca tan decisivamente a una persona y siempre agradecer el que se me educara para serlo integralmente, tanto en conocimientos y habilidades como emocionalmente y en ser humano.

A Maru le agradezco que sea exactamente como es, hermosa *flod* que perfectamente acopla con su arbolito, amorosos ellos.

Y, por supuesto, a todos mis amigos de la falla y de Salesianos, los que me han visto evolucionar y crecer, ser el Boig de las primeras salidas, el Tanque de las pachangas o Tarik el emigrante: Nacho, Manolo, Morgan, Dobi, Goti, Rafa, Boro, María, María (el lector atento podrá observar que la diferente grafía denota dos personas distintas), Zalo, Gonzalo (nada que ver con la puntualización anterior), Taribo, Pablo, Carmen, Elena, Virgi, María, Inma, Josep, Bea, Falo, Vicent, Juanma, Ángela, Pons, Virginia, Capi, Luque, Paco, Toni, Primo, Dani, Cubatas (cómo poner Ángel?).

La experiencia del Colegio de España ha sido maravillosamente enriquecedora (al margen de haber conocido a Maru en él, acontecimiento que se sale de la escala).

Agradezco a su Director, Javier de Lucas, su implicación en la jornada divulgativa que allí coordiné y a Stephanie Mignot, por nuestra colabración en la organización de charlas a cargo de los residentes durante todo el año. También agradezco el trato recibido de Ramón Solé y Víctor Matamoro. Por supuesto agradezco a Juanjo Rué, Jadra Mosa, Jovi Siles, María José López, Mercedes Sánchez, Juliana Saliba, Paloma Palau, Paloma Gutiérrez y Santi Rello (se ha mantenido la política de eliminar el doble agradecimiento) nuestra experiencia en el Comité de Residentes del Colegio. Aunque hubo mucho trabajo, lo hicimos bien y lo pasamos mejor. También quiero tener un recuerdo especial para Gerardo, Ana, Sergio, Idoia-Idoia (una sola persona en este caso), Evita, Joaquín, Marta, Laura, Geles, Estrella, los Patitos, Roberto, Ricard, el Cordobés, Rocío, Marta, Neus, Betlem, Mourad, Elipe, Chus, Javi, ...

A todos, gracias.